NEW THERAPEUTIC OPTIONS FOR RARE DISEASES

EDITED BY: Sascha Meyer, Juergen Brunner, Oliver Semler, E. Ann Yeh and Andrea Lynne Gropman

PUBLISHED IN: Frontiers in Pediatrics and Frontiers in Genetics

frontiers Research Topics

frontiers

ISSN 1664-8714
ISBN 978-2-88974-174-8
DOI 10.3389/978-2-88974-174-8

About Frontiers

Frontiers is more than just an open-access publisher of scholarly articles: it is a pioneering approach to the world of academia, radically improving the way scholarly research is managed. The grand vision of Frontiers is a world where all people have an equal opportunity to seek, share and generate knowledge. Frontiers provides immediate and permanent online open access to all its publications, but this alone is not enough to realize our grand goals.

Frontiers Journal Series

The Frontiers Journal Series is a multi-tier and interdisciplinary set of open-access, online journals, promising a paradigm shift from the current review, selection and dissemination processes in academic publishing. All Frontiers journals are driven by researchers for researchers; therefore, they constitute a service to the scholarly community. At the same time, the Frontiers Journal Series operates on a revolutionary invention, the tiered publishing system, initially addressing specific communities of scholars, and gradually climbing up to broader public understanding, thus serving the interests of the lay society, too.

Dedication to Quality

Each Frontiers article is a landmark of the highest quality, thanks to genuinely collaborative interactions between authors and review editors, who include some of the world's best academicians. Research must be certified by peers before entering a stream of knowledge that may eventually reach the public - and shape society; therefore, Frontiers only applies the most rigorous and unbiased reviews.
Frontiers revolutionizes research publishing by freely delivering the most outstanding research, evaluated with no bias from both the academic and social point of view. By applying the most advanced information technologies, Frontiers is catapulting scholarly publishing into a new generation.

What are Frontiers Research Topics?

Frontiers Research Topics are very popular trademarks of the Frontiers Journals Series: they are collections of at least ten articles, all centered on a particular subject. With their unique mix of varied contributions from Original Research to Review Articles, Frontiers Research Topics unify the most influential researchers, the latest key findings and historical advances in a hot research area! Find out more on how to host your own Frontiers Research Topic or contribute to one as an author by contacting the Frontiers Editorial Office: frontiersin.org/about/contact

NEW THERAPEUTIC OPTIONS FOR RARE DISEASES

Topic Editors:
Sascha Meyer, Saarland University Hospital, Germany
Juergen Brunner, Innsbruck Medical University, Austria
Oliver Semler, University Hospital of Cologne, Germany
E. Ann Yeh, Hospital for Sick Children, Canada
Andrea Lynne Gropman, Children's National Hospital, United States

Citation: Meyer, S., Brunner, J., Semler, O., Yeh, E. A., Gropman, A. L., eds. (2022). New Therapeutic Options for Rare Diseases. Lausanne: Frontiers Media SA.
doi: 10.3389/978-2-88974-174-8

Table of Contents

frontiers in Pediatrics

EDITORIAL
published: 24 January 2022
doi: 10.3389/fped.2021.832395

Editorial: New Therapeutic Options for Rare Diseases

Sascha Meyer[1]*, *E. Ann Yeh*[2], *Jürgen Brunner*[3,4], *Oliver Semler*[5] and *Andrea Gropman*[6]

[1] Department General Pediatrics, Neonatology, and Neuropediatrics, University Hospital of Saarland, Homburg, Germany, [2] Division of Neurology, Department of Pediatrics, Neurosciences and Mental Health, SickKids Research Institute, Hospital for Sick Children, University of Toronto, Toronto, ON, Canada, [3] Department of Pediatrics, Innsbruck Medical University, Innsbruck, Austria, [4] Danube Private University, Krems, Austria, [5] Department of Pediatrics, Faculty of Medicine and University Hospital Cologne, University of Cologne, Cologne, Germany, [6] Neurogenetics and Neurodevelopmental Pediatrics, George Washington School of Medicine and Health Sciences, Washington, DC, United States

Keywords: rare diseases, children, pediatrics, diagnostics, new drug therapies, genetics, therapy

Editorial on the Research Topic

New Therapeutic Options for Rare Diseases

INTRODUCTION

A rare disease is defined as a disease with <5 affected individuals in 10.000 people (1, 2). However, as a whole, rare diseases are not as rare as one might think. Rare diseases comprise roughly some 6,000–8,000 different clinical entities with genetic causes accounting for ∼80% of rare diseases. In Europe, some 30 million people are estimated to be affected by a rare disease.

Due to advances in molecular diagnosis and early metabolic testing, many individuals are being diagnosed in infancy or early childhood. Of note, nowadays individuals with a rare disease may even be diagnosed *in utero*—as commonly seen in tuberous sclerosis complex disease (3). Nevertheless, in real life, it can often be quite challenging for affected people to find a physician with specific expertise in this field, thus leading to a delay in establishing a correct diagnosis and initiation of early, adequate treatment if available. Therefore, expert centers for rare diseases have been established by many university and tertiary hospitals. The aim of these centers is to create a network to facilitate diagnosis and optimize treatment and to generate and coordinate research activities. Treating rare diseases requires close cooperation between experts of various medical disciplines in a truly interdisciplinary setting (4). If a specific drug therapy is available, this is often associated with substantial costs for the health care system.

In this collection of up-to-date, cutting edge articles, several important aspects are addressed, most importantly novelties in diagnostics and new therapies with regard to rare diseases in children. In doing so, specific new insights into genetics, pathophysiology, and pharmacology are provided. While new promising therapeutic options are on the horizon (including genome editing), still many issues remain to be resolved, most importantly long-term outcome and survival. Thus, in addition to these new and potentially effective, individually tailored therapies, no definite cure can be provided for many children with rare and life-limiting diseases. Therefore, the role of palliative services must be stressed as well.

OPEN ACCESS

Edited and reviewed by:
Jordi Pérez-Tur,
Institute of Biomedicine of Valencia, Spanish National Research Council (CSIC), Spain

***Correspondence:**
Sascha Meyer
sascha.meyr@uks.eu

Specialty section:
This article was submitted to Genetics of Common and Rare Diseases, a section of the journal Frontiers in Pediatrics

Received: *09 December 2021*
Accepted: *10 December 2021*
Published: *24 January 2022*

Citation:
Meyer S, Yeh EA, Brunner J, Semler O and Gropman A (2022) Editorial: New Therapeutic Options for Rare Diseases. Front. Pediatr. 9:832395. doi: 10.3389/fped.2021.832395

Due to the great number of rare diseases, this collection cannot be comprehensive in its coverage; it does, however, intent to shed light on new important and promising approaches for these highly vulnerable patients.

DIAGNOSTICS

Li, Jia et al. describe two rare novel gross deletion mutations in the neurotrophic tyrosine kinase receptor type 1 gene (NTRK1) associated with congenital insensitivity to pain with anhidrosis in two unrelated families, employing whole exome sequencing, thus expanding the mutational spectrum of NRTK1 mutations. In their study, Qiu et al. identified 11 hub genes that may play critical roles in idiopathic pulmonary arterial hypertension (IPAH) by integrated bioinformatics analyses. The authors conclude that in addition to modifying the clinical course and progression of IPAH, they may also be candidate targets for IPAH treatment. Hu et al. report employed whole exome sequencing (WES) to describe a novel PAX3 mutation associated with Waardenburg syndrome type 1 (WS), thus expanding the understanding of (WS) Hu et al. Yang J.O. et al.also used whole-exome sequencing to provide new important insights into the spectrum of genetic variations associated with Lennox-Gastaut syndrome (LGS), a very severe type of childhood-onset epilepsy characterized by multiple types of seizures, specific discharges on EEG, and intellectual disability, in 17 unrelated Korean families by. In doing so, they were able to identify 14 mutations in 14 genes as causes for LGS or LGS-like epilepsy. Chen M. et al. report a case report with an unusual late-onset carnitine-acylcarnitine translocase deficiency with SLC25A20 c.199-10T>G variation, and they stress the importance of early recognition of symptoms and timely and appropriate treatment in improving outcome as mandatory for most rare diseases.

Murillo-Cuesta et al. for/on behalf of the Working group on Animal Models of Rare Diseases review examples of current advances in preclinical research in rare diseases using mouse models, and they discuss their perspective on future directions and challenges in this important diagnostic field.

Li L. et al. report on the role of high-throughput sequencing in revealing the loss-of-function mutation in GALT cause recessive classical galactosemia, thus expanding the phenotypic and mutational spectrum of GALT. Their findings could be helpful/informative in providing evidence for prenatal counseling/interventions and individually-tailored pharmacological treatments Li L. et al.

Tenembaum et al. describe the current state of knowledge with regard to clinical manifestations, diagnosis, and therapies for children with Neuromyelitis Optica Spectrum Disorders (NMOSD). They also provide insights with regard to the importance of auto-antibodies to aquaporin (AQP4-IgG) and myelin oligodendrocyte glycoprotein (MOG-IgG) in NMSOD (Tenembaum et al.) Chen Y. et al. studied the genetic and clinical features of Dopa-responsive dystonia (DRD) in 31 patients with DRD (1). Based on their results, DRD can be divided into classic DRD and DRD-plus disease. Interestingly, fever was the most important inducing factor of DRD, while L-Dopa exhibited sustained and stable effects in patients with classic DRD. In DRD-plus patients, treatment with L-Dopa ameliorated most of the clinical symptoms (Chen Y. et al.).

THERAPY

In their randomized-controlled study (28 patients: interventional group, 28 patients: control group), Wang et al.conclude that sirolimus may play a role in the treatment of systemic lupus erythematosus (SLE) by increasing the level of autophagy in peripheral blood lymphocytes. A major shortcoming, as in many clinical studies, was the fact that the authors did not assess long-term outcome in their study cohort (Wang et al.)

Liu et al. provide a systematic review on liver transplantation for glycogen storage disease type I (GSD) in 24 patients, a rare autosomal recessive disorder. While extra-hepatic manifestations, most importantly cardiac involvement may still progress, liver transplantation remains the only therapeutic option to increase both quantity and quality of life in children with GSD type 1 (Liu and Sun). Grant et al. report on cerebral revascularization surgery in a child with mucopolysaccharidosis type I, a rare lysosomal storage disorder, with overt stroke, infarction and bilateral terminal carotid artery stenosis with no further neurological events at a 3-year follow-up.

Flotats-Bastardas and Hahn present a succinct overview of new therapeutic options for patients with neuromuscular disorders, a genetically heterogeneous group of diseases. With the advent of new drugs in this field—either by ameliorating secondary pathophysiological consequences or by modifying the underlying genetic defect itself—treatment has changed fundamentally in recent years (5, 6).

Matsoukas provides a state-of-the art perspective on genome editing for rare genetic diseases without double-strand breaks or donor DNA, concluding that the development of prime editing provides a significant and important addition to the genome editing toolbox.

Sherzai et al. report on HMTase inhibitors as a potential epigenetic-based therapeutic approach for Friedreich's ataxia in FRDA fibroblasts, demonstrating that a combination therapy of G9a-inhibitor and EZH2-inhibitor [two histone methyltransferase (HMTase) inhibitor compounds] significantly increased frataxin (FXN) gene expression levels, but did not increase in frataxin protein levels.

Hully et al. provide on behalf of Neuromuscular Commission of the Societé Francaise de Neuropédiatrie the results from a prospective multicenter French study based on parents' reports about palliative care in 80 children with SMA type I (2012–2016). While their data confirmed previous reports on the natural history of this fatal disease, their study also demonstrated that palliative care has become an active approach involving a multidisciplinary team, and this has led to more home-hospital settings. The implementation of integrated palliative supportive care has played an important role in enabling more coordinated medical support (Hully et al.) Hully et al. also emphasize the importance of taking into consideration the advent of new drug therapies in patients with SMA with the potential to

positively impact on life expectancy and quality of life. These new therapeutic avenues will also entail important medical, financial, and ethical issues. In that context, parents need to be clearly informed on the different therapeutic options with the remaining unknowns before they can consent to new treatment modalities (Hully et al.).

CONCLUDING REMARKS

This article collection of the Research Topic provides the reader with an up-to-date overview on important progress in both diagnostic and therapeutic modalities in children with rare diseases. Despite new and promising diagnostic—probably most importantly the wide use of whole exome sequencing in clinical practice—and therapeutic avenues in these rare clinical entities, a definite cure for a substantial number of patients will not be at hand any time soon, thus stressing the importance of supportive and palliative care services (Hully et al.).

In the near future, it will be important to assess the efficacy of new drugs in high-quality clinical trials, including medium- and long-term outcome. To do so, robust epidemiological data with regard to incidence and prevalence of these rare diseases is of great importance (1–3). But, considering the very low incidence and prevalence of rare diseases, other important avenues to generate new and relevant data include both animal research models (Murillo-Cuesta et al.) as well as high-quality case reports as provided in this Special Issue (Chen M. et al.; Hu et al.; Grant et al.). Moreover, collaboration between experts throughout the world will have to be intensified.

We hope that this Special Issue on Rare Diseases in children will serve this purpose, and will be helpful in bringing together worldwide experts from many different fields (basic research, biology, genetics, biochemistry, medicine, nursing, palliative care, etc.), thus providing a basis to improve both diagnostic and treatment modalities for these very susceptible young patients.

AUTHOR CONTRIBUTIONS

This editorial was jointly conceptualized and written by all authors.

REFERENCES

1. Ebrahimi-Fakhari D, Zemlin M, Sauer H, Poryo M, Graf N, Meyer S. 25 years of ESPED as a surveillance tool for rare diseases in children in Germany: a critical analysis. *Klin Padiatr*. (2018) 230:215–24. doi: 10.1055/a-0586-4365
2. Disse SC, Toelle SP, Schroeder S, Theiler M, Weibel L, Broser P, et al. Epidemiology, clinical features, and use of early supportive measures in PHACE syndrome: a European multinational observational study. *Neuroepidemiology*. (2020) 54:383–39. doi: 10.1159/000508187
3. Ebrahimi-Fakhari D, Mann LL, Poryo M, Graf N, von Kries R, Heinrich B, et al. Incidence of tuberous sclerosis and age at first diagnosis: new data and emerging trends from a national, prospective surveillance study. *Orphanet J Rare Dis*. (2018) 13:117. doi: 10.1186/s13023-018-0870-y
4. Ebrahimi-Fakhari D, Poryo M, Graf N, Zemlin M, Flotats-Bastardas M, Heine G, et al. Optimized care in patients with rare diseases: TSC at the Center for Rare Diseases (ZSEUKS) at Saarland University Medical Center, Germany. *Klin Padiatr*. (2017) 229:311–5. doi: 10.1055/s-0043-120069
5. Flotats-Bastardas M, Hahn A, Schwartz O, Linsler S, Meyer S, Kolodziej M, et al. Multicenter experience with nusinersen application via an intrathecal port and catheter system in spinal muscular atrophy. *Neuropediatrics*. (2020) 51:401–6. doi: 10.1055/s-0040-1715481
6. Ebrahimi-Fakhari D, Dillmann U, Flotats-Bastardas M, Poryo M, Abdul-Khaliq H, Shamdeen MG, et al. Off-label use of ataluren in four non-ambulatory patients with nonsense mutation duchenne muscular dystrophy: effects on cardiac and pulmonary function and muscle strength. *Front Pediatr*. (2018) 6:316. doi: 10.3389/fped.2018.00316

Conflict of Interest: The authors declare that the research was conducted in the absence of any commercial or financial relationships that could be construed as a potential conflict of interest.

frontiers in Pediatrics

ORIGINAL RESEARCH
published: 18 February 2020
doi: 10.3389/fped.2020.00004

Palliative Care in SMA Type 1: A Prospective Multicenter French Study Based on Parents' Reports

Marie Hully[1,2], Christine Barnerias[1], Delphine Chabalier[1], Sophie Le Guen[3], Virginie Germa[2], Elodie Deladriere[2], Catherine Vanhulle[4], Jean-Marie Cuisset[5], Brigitte Chabrol[6], Claude Cances[7], Carole Vuillerot[8], Caroline Espil[9], Michele Mayer[10], Marie-Christine Nougues[10], Pascal Sabouraud[11], Jeremie Lefranc[12], Vincent Laugel[13], Francois Rivier[14], Ulrike Walther Louvier[15], Julien Durigneux[16], Sylvia Napuri[17], Catherine Sarret[18], Michel Renouil[19], Alice Masurel[20], Marcel-Louis Viallard[21,22], and Isabelle Desguerre[1] on behalf of Neuromuscular Commission of the Societe Française de Neuropédiatrie*

[1] Pediatric Neurology Department, Necker–Enfants Malades Hospital, APHP, Paris, France, [2] Physical Rehabilitation Department, Necker–Enfants Malades Hospital, APHP, Paris, France, [3] Clinical Research Department, Necker–Enfants Malades Hospital, APHP, Paris, France, [4] Neonatal Department, Charles Nicolle Hospital, Rouen, France, [5] Pediatric Neurology Department and Neuromuscular Diseases Reference Center, CHU, Lille, France, [6] Pediatric Neurology Department, La Timone Hospital, APHM, Marseille, France, [7] Pediatric Neurology Department, Enfants Hospital, Toulouse, France, [8] Pediatric Physical Rehabilitation Department, Femme Mère Enfants Hospital, Bron, France, [9] Pediatric Neurology Department, Pellegrin Hospital, Bordeaux, France, [10] Pediatric Neurology Department, Armand Trousseau Hospital, APHP, Paris, France, [11] Pediatric Department, American Memorial Hospital, Reims, France, [12] Pediatric Neurology Department, Morvan Hospital, Brest, France, [13] Pediatric Neurology Department, Hautepierre Hospital, Strasbourg, France, [14] Pediatric Neurology Department & Neuromuscular Diseases Reference Center AOC, CHU Montpellier, PhyMedExp, University of Montpellier, INSERM, CNRS, Montpellier, France, [15] Pediatric Neurology Department & Neuromuscular Diseases Reference Center AOC, CHU Montpellier, Montpellier, France, [16] Pediatric Neurology Department, University Hospital, Angers, France, [17] Pediatric Department, South Hospital, Rennes, France, [18] Pediatric Department, CHU Clermont-Ferrand, Clermont-Ferrand, France, [19] Pediatric Department, St-Pierre Hospital, Saint-Denis, France, [20] Genetic Department, Children Hospital, CHU Dijon, Dijon, France, [21] Palliative Care Team, Necker–Enfants Malades Hospital, APHP, Paris, France, [22] Research Team "ETRES", UMR des Cordeliers, Université de Paris, Paris, France

OPEN ACCESS

Edited by:
Oliver Semler, Universitätsklinikum Köln, Germany

Reviewed by:
Maurizio Elia, Oasi Research Institute (IRCCS), Italy
Juan Dario Ortigoza-Escobar, Pediatric Research Hospital Sant Joan de Déu, Spain

***Correspondence:**
Marie Hully
marie.hully@aphp.fr

Specialty section:
This article was submitted to Pediatric Neurology, a section of the journal Frontiers in Pediatrics

Received: *09 October 2019*
Accepted: *07 January 2020*
Published: *18 February 2020*

Citation:
Hully M, Barnerias C, Chabalier D, Le Guen S, Germa V, Deladriere E, Vanhulle C, Cuisset J-M, Chabrol B, Cances C, Vuillerot C, Espil C, Mayer M, Nougues M-C, Sabouraud P, Lefranc J, Laugel V, Rivier F, Louvier UW, Durigneux J, Napuri S, Sarret C, Renouil M, Masurel A and Viallard M-L and Desguerre I (2020) Palliative Care in SMA Type 1: A Prospective Multicenter French Study Based on Parents' Reports. Front. Pediatr. 8:4. doi: 10.3389/fped.2020.00004

Spinal muscular atrophy type 1 (SMA-1) is a severe neurodegenerative disorder, which in the absence of curative treatment, leads to death before 1 year of age in most cases. Caring for these short-lived and severely impaired infants requires palliative management. New drugs (nusinersen) have recently been developed that may modify SMA-1 natural history and thus raise ethical concerns about the appropriate level of care for patients. The national Hospital Clinical Research Program (PHRC) called "Assessment of clinical practices of palliative care in children with Spinal Muscular Atrophy Type 1 (SMA-1)" was a multicenter prospective study conducted in France between 2012 and 2016 to report palliative practices in SMA-1 in real life through prospective caregivers' reports about their infants' management. Thirty-nine patients were included in the prospective PHRC (17 centers). We also studied retrospective data regarding management of 43 other SMA-1 patients (18 centers) over the same period, including seven treated with nusinersen, in comparison with historical data from 222 patients previously published over two periods of 10 years (1989–2009). In the latest period studied, median age at diagnosis was 3 months [0.6–10.4]. Seventy-seven patients died at a median 6 months of age[1–27]: 32% at home and 8% in an intensive care unit. Eighty-five percent of patients received enteral nutrition, some through a gastrostomy (6%). Sixteen percent

had a non-invasive ventilation (NIV). Seventy-seven percent received sedative treatment at the time of death. Over time, palliative management occurred more frequently at home with increased levels of technical supportive care (enteral nutrition, oxygenotherapy, and analgesic and sedative treatments). No statistical difference was found between the prospective and retrospective patients for the last period. However, significant differences were found between patients treated with nusinersen vs. those untreated. Our data confirm that palliative care is essential in management of SMA-1 patients and that parents are extensively involved in everyday patient care. Our data suggest that nusinersen treatment was accompanied by significantly more invasive supportive care, indicating that a re-examination of standard clinical practices should explicitly consider what treatment pathways are in infants' and caregivers' best interest. This study was registered on clinicaltrials.gov under the reference NCT01862042 (https://clinicaltrials.gov/ct2/show/study/NCT01862042?cond=SMA1&rank=8).

Keywords: SMA, palliative care, caregivers, ethics, standard of care

INTRODUCTION

Homozygous deletion of exon 7 or other mutations in the *SMN1* gene on chromosome 5q13, resulting in survival motor neuron (SMN) protein deficiency (1), causes classic proximal spinal muscular atrophy (SMA), one of the most frequently occurring neuromuscular diseases with an incidence of about 1/10,000 live births (2). SMA phenotype relies on the amount of functional SMN protein produced (3), related to the number of copies of the *SMN2* gene present in one patient (4). Distinct SMA subtypes have thus been categorized according to the age of onset and severity of the disease (5) from SMA type 0, in which onset is *in utero* with reduced or absent movements, to cases of onset in adult life (SMA type 4). The most frequent presentation remains the severe SMA type 1 [60% (6)] in which infants develop generalized progressive muscle weakness and atrophy before 6 months of age and cannot achieve independent head support nor ability to sit upright, without cognitive involvement. Associated with generalized paralysis, development of chronic respiratory failure and bulbar dysfunction in infants leads to death before 2 years of age without ventilatory support (7, 8), with recent data suggesting available simple tools to evaluate respiratory function in those infants (9). Published in 2007, the Consensus Statement for standard of Care in SMA [recently revised (10, 11)] reported different care pathways across countries and cultures, especially concerning respiratory and nutritional management (7, 8, 10–14). For the past 20 years, the French national pediatric neuromuscular network has considered a palliative care-centered approach the most ethical choice of treatment. This leads, most of the time, to an end of life before 1 year of age (7). On the other hand, in the USA, a more proactive approach with early non-invasive ventilation (NIV) and gastrostomy (GS) has been reported, leading to a more prolonged survival (12, 13, 15–17), but with an ever-increasing load of complementary and more invasive care.

In the last 5 years, drugs have been developed and reached phase I–III clinical trials (18–21): a targeted treatment has been developed with the antisense oligonucleotides (nusinersen), which alters splicing of SMN2 pre-mRNA and thus increases production of functional SMN protein. Over the last years, nusinersen has shown some clinical efficacy in well-controlled clinical trials with prolonged survival beyond 2 years of age in different populations of SMA patients, including severe SMA-1 patients (19). However, data suggest that those surviving patients require a number of technical medical supports (GS and NIV). The ethical considerations implicit in parents' and medical teams' decisions about whether or not to treat severely affected babies with nusinersen warrant a fulsome consideration of the complementary supportive care which then needs to be provided and could also modify our medical practice.

We thus intended to evaluate the evolution of our practice in palliative care, before the nusinersen era, with the active collaboration of parents, as compared with French historical data. We thus performed a prospective multicentric study over 4 years (2012–2016) about palliative care in newly diagnosed SMA-1 patients, including for the first time parents' prospective reports about care given to their child in real time until death. Parents were thus asked to give their own evaluation of the care and treatments provided to their child by a medical team, with insights on the quality of life for their child and themselves.

METHODS

From June 2012 to June 2016, patients from all pediatric neuromuscular centers in France ($n = 17$) with a genetically confirmed SMA-1 were included in a prospective study after parents signed the informed consent in accordance with national guidelines.

First, after inclusion, parents were given a specific health book (HB), developed by a multidisciplinary team that manages SMA-1 patients (physiotherapists, occupational therapists, physicians involved in neuromuscular pediatric disorders, and a pediatric palliative team). This HB contained information about the

disease, advice about care (nutrition, installation, etc.), and activities adapted to infants with SMA-1. Parents were asked to fill in, at minimum every month but in fact as often as they wanted, some questionnaires about everyday care for their child. These questionnaires included both multiple-choice questions and open-ended questions requiring written free answers. The questionnaires were split into four parts: respiratory management, nutritional management, installation and physiotherapy, and aspects about pain and comfort. Parents were also encouraged to give each of their child's physician or caregiver the HB so that they could also add information about their contributions to the child's care, with specific questions for the referent physician [age at diagnosis, SMN1 deletion, number of SMN2 copies, vaccinations, weight, height, cranial and thoracic perimeters, and use of any medically related public assistance programs (medical insurance and disabled children's allowance)] and for the physiotherapist (frequency and duration of respiratory and motor interventions, use of a suction aspiration system, and physiotherapy technique used). Any other physicians and paramedics such as nurses and occupational therapists could also write any information about their involvement in that child's multidisciplinary care. After the child's death, a copy of this complete HB was obtained from the parents, and data were extracted and analyzed.

Quantitative data (responses to multiple-choice questions) were manually reported in tables using Microsoft Excel version 2010, in which medians, means, and standard deviations were then calculated. Qualitative data (open-ended questions and any comments from parents and caregivers) were manually reported, word by word, without orthographic correction, using Microsoft Word version 2010, and additional information concerning the child's care was extracted and filled in dedicated tables to enhance the accuracy of the parent-reported information. We also recorded and report which professionals wrote in the HB and the number of interventions for each child by each professional.

We also present in the article data concerning patients with SMA-1 not included in the PHRC but followed in France over the same time (retrospective study), receiving or not receiving nusinersen therapy.

Those anonymous data were retrospectively collected through the French Pediatric Neuromuscular Network: physicians of the network filled in a dedicated questionnaire containing information about age at diagnosis of SMA-1, current age or age at which death occurred, place of death, use of an enteral nutrition with or without GS, use of NIV or tracheostomy, use of analgesic or sedative medicines, and use of nusinersen therapy.

We compared our population to the historical French studies over the last 20 years. The flowchart (**Figure 1**) summarizes the different populations studied in the current paper.

We then compared data between prospective and retrospective studies' patients using Fisher exact tests to compare proportions and Student *t*-test or Wilcoxon test to compare means or medians, when necessary.

Because of the beginning use of nusinersen therapy during the time of the prospective study, we chose to analyze those treated patients separately and thus also compared data between patients treated or not by nusinersen using Fisher exact and Wilcoxon tests.

Statistical analyses were performed using R version 3.3.1 software.

In a second part of the study, after the child's death, the physician filled in a specific questionnaire about care and medications during the last 48 h before death, with information about possible life-sustaining treatment limitation decision and the opportunity for parents to meet a psychologist. This questionnaire contained also both multiple-choice questions and open-ended questions, which were reported and analyzed as data from the HB.

For the third part of the study, at least 6 months after the child's death, parents were encouraged to perform a semi-directed interview with a trained psychologist. Those interviews were recorded and transcribed verbatim. Then data were qualitatively analyzed via a grounded theory framework, using NVivo version 9 software. Those data are not presented in the current article but are currently processed.

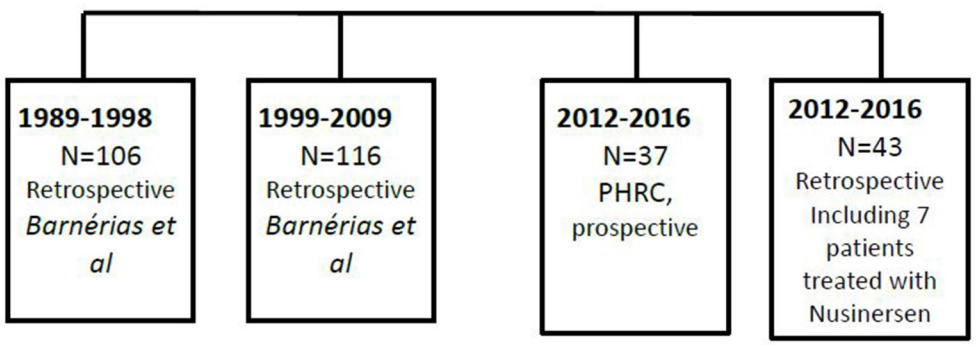

FIGURE 1 | Flowchart of the patients involved in the prospective and retrospective studies (2012–2016), as well as data from previous published French study (1989–2009).

This multicentric prospective French study was financed by the Ministry of Health (PHRC AOM11183) and received approval from the ethical board *Comité de Protection des Personnes* (CPP) *Ile de France II* on April 3, 2012, and registered on clinicaltrials.gov (NCT01862042).

RESULTS

Population's Description

Patients Enrolled in the PHRC

Thirty-nine patients were included in the prospective study from 17 centers all over France during a 4-year period. Among them, two were secondarily excluded, as one patient was in fact a type 1-bis SMA, i.e., without bulbar involvement, and one was rapidly lost on follow-up. We thus report data here about only 37 SMA-1 French patients, 20 girls and 17 boys. The diagnosis was genetically confirmed, and patients were thereafter included at a median age of 3 months [0.6–10.4]. Median age reported at first signs (data available for 31 patients) was 1 month [0–4]. All the patients died, at a median age of 5.5 months [1.5–16.4], i.e., a median of 2 months [0.2–12.8] after diagnosis.

All but three HBs were retrieved, but two of them had not been filled in by the parents or the medical or paramedical therapists. We thus report the number of patients for whom the information was available for each item in our description of the population.

Table 1 presents global care used for the patients (involved in the PHRC and others over the same period of time) and reports the results available from the previous retrospective published French study (7).

Comparison Between Patients Involved in the Prospective Study and Other French Patients Over the Same Period (Retrospective Study)

We collected retrospective data concerning 43 more patients with SMA-1 not included in the prospective study presented above but followed in France (18 centers) over the same period of time. Among those patients, seven received nusinersen intrathecal therapy. At the time of the study, five patients were still alive [median age 38 months (36–59)] including four receiving nusinersen. Mean age at diagnosis (3.5 months, $SD = 1.64$) was not different from that of patients presented before (3.95 months, $SD = 2.59$) ($p = 0.95$), neither was age at the time of death (8.3 months, $SD = 5.8$ vs. 6.64 months, $SD = 3.85$, $p = 0.15$). There was no statistical difference in the number of surviving infants between the two groups ($p = 0.06$).

Data regarding the place of death were also available for those patients: 10 died at home, 6 in a regional community hospital, and 22 in a university hospital, including four in intensive care units (not different from the data presented below, $p = 0.17$).

TABLE 1 | Presentation of the population and care use in the current prospective study as compared to the previous retrospective published French data over 20 years from Barnérias et al.

	1989–1998 ($n = 106$)	1999–2009 ($n = 116$)	2012–2016			
			Prospective ($n = 37$)	Retrospective ($n = 43$)	p (test)	Total ($n = 80$)
Median age at first signs	NA	2 m [0–5]	1 m [0–4]	NA		NA
Median age at diagnostic	3 m [0.5–7]	4 m [0.5–8]	3 m [0.6–10]	3 m [2–6] ($n = 6$)	0.95 (Wilcoxon)	3 m [0.6–10.4]
Motor physiotherapy	NA	109 (90%)	26/30 (87%)	NA		NA
Respiratory physiotherapy	NA	111 (93%)	29/32 (91%)	NA		NA
Enteral feeding	36 (34%)	59 (52%)	34/37 (92%)	34/43 (79%)	0.13 (Fisher)	68/80 (85%)
Gastrostomy	2 (1.8%)	4 (3.4%)	1/37 (3%)	4/43 (9%)	0.37 (Fisher)	5/80 (6%)
Installation	28 (26%)	63 (61%)	18/20 (90%)	NA		NA
Suction aspiration system	44 (41%)	65 (64%)	25/28 (89%)	NA		NA
Oxygenotherapy	NA	10 (8%)	21/27 (78%)	NA		NA
Non-invasive ventilation at home	0	8 (7%)	4/37 (11%)	9/43 (21%), 1 tracheo	0.30 (Fisher)	13/80 (16%, 1 tracheo)
			1/37 (1%)	9/43 (21%), 1 tracheo	**0.01** (Fisher)	10/80 (1 tracheo, 12.5%)
Home hospitalization setting	35 (33%)	30 (26%)	16/26 (62%)	NA		NA
Pediatric palliative care team	NA	11%	17/23 (74%)	NA		NA
Home health nurse	NA	NA	18/24 (75%)	NA		NA
Median age at death	6 m [1–13]	7.5 m [1–24]	5.5 m [1.5–16.4]	6 m [1–27]	0.15 (t-test)	6 m [1–27]
Use of sedation and analgesia at the time of death	15 (18%)	65 (60%)	30/37 (81%)	27/37 (73%)	0.58 (Fisher)	57/74 (77%)

We summarized for the current study the availability of the information, as reported in the health book by parents and caregivers. Tracheo, tracheostomy.
Bold value represents statistically significant values.

Data regarding the use of an enteral nutrition, a GS, and NIV are reported in **Table 1**. No statistical differences were found comparing these two populations for enteral nutrition ($p = 0.13$), GS ($p = 0.37$), and NIV ($p = 0.30$), but the use of an NIV at home was different between the prospective ($n = 1$) and the retrospective ($n = 9$ and 1 tracheostomy) studies ($p = 0.01$).

We also compared the use of sedation (use of anxiolytics and/or grade III analgesics) for those two groups of patients. Altogether, 52 patients received sedation and 22 did not: 24 patients included in the prospective study (eight did not) and 28 patients in the retrospective study (14 did not), without reaching statistical difference ($p = 0.61$). At the time of death, 57 patients were under a sedative treatment (including 30 in the prospective study and 27 in the retrospective study), 17 were not (7 vs. 10), without reaching statistical difference ($p = 0.58$).

We then compared data between patients receiving nusinersen or not. Data are presented in **Table 2**, where comparisons reaching statistically significant differences are bold. We found no statistical differences in the management of patents not receiving nusinersen between the prospective and the retrospective studies. On the contrary, despite a small group of patients receiving nusinersen ($n = 7$), we found statistical differences with more patients alive in the nusinersen group, more nusinersen patients with a GS ($p = 0.004$) and an NIV ($p = 0.016$) especially at home ($p = 0.0058$), and less prescription of an analgesic treatment in the same group ($p = 0.002$).

Supportive Care Evolution, Data From a Prospective (PHRC) Study

Respiratory Management

Concerning respiratory management, most patients (29/32, 91%) received respiratory physiotherapy—at home in most cases (26/29, 90%), from a median age of 4 months (0.9–12.2), most of them (20/25, 80%) at least three times a week to everyday and the others once a week, each session lasting usually around 10 min. One patient was provided with a cough assist and an intermittent positive pressure breathing device; the latter was also used by two additional patients.

Most patients (25/28, 89%) had a suction aspiration system at home; their parents had been trained to use it (21/25, 84%) and used it at home (22/25, 88%).

Most patients (30/37, 81%) received oxygenotherapy during their follow-up, including seven patients for whom the information was available only at the time of death. Many parents (21/27, 78%) reported using oxygenotherapy at home starting at a median age of 5 months (1.3–16.4).

Four patients were provided with NIV during the follow-up, but only one at home at 6.6 months (he died while on NIV). For the remaining patients, NIV use was of short duration during hospitalization, including one patient who died while on NIV. In these cases, parents reported an improvement in their child's comfort while on NIV but cited increased restriction in motion, limiting the ability to play with or cradle the treated child.

Figure 2 presents parents' opinions about respiratory management concerning oxygenotherapy and respiratory physiotherapy.

Nutritional Management

Most parents (27/29, 93%) reported difficulties in feeding their child at a median of 4.7 (0.8–12.2) months of age. Parents reported prolonged meal duration at a median of 6.4 months (0.8–12.2) (17/27, 63%), eating-induced fatigue at a median 5.3 months (0.8–12.2) (21/27, 78%), restricted intakes at a median of 5.3 months (1.4–12.2) (19/27, 70%), or even food refusal at a median of 5.7 months (2.4–11.8) (12/27, 44%). Parents also reported gastroesophageal reflux (GOR) in 8/27 (30%) of cases at a median age of 5.4 months (1.8–8) and food being swallowed

TABLE 2 | Comparison of patients not receiving nusinersen between prospective and retrospective studies and comparison between patients receiving nusinersen and those not receiving nusinersen.

	No nusinersen				Nusinersen	*p* (test)
	Prospective study ($n = 37$)	**Retrospective study ($n = 36$)**	***p* (test)**	**Total ($n = 73$)**	**Retrospective study ($n = 7$)**	
Median age at diagnosis	3 m [0.6–10]	3 m [2–6] ($n = 6$)	0.95 (Wilcoxon)	3 m [0.6–10]	NA	NA
Number of alive patients (median age)	0/37	1/36 (NA)	0.49 (Fisher)	1/73 (1%)	4/7 (57%) (38 m [36–59])	**1.1×10^{-4}** (Fisher)
Median age at death	5.5 m [1.5–16.4]	6 m [1–27]	0.25 (*t* test)	6 m [1–27]	10 m [8–16]	0.11 (Wilcoxon)
Enteral feeding	34/37 (92%)	28/36 (78%)	0.11 (Fisher)	62/73 (85%)	6/7 (86%)	1 (Fisher)
Gastrostomy	1/37 (3%)	1/36 (3%)	1 (Fisher)	2/73 (3%)	3/7 (43%)	**0.004** (Fisher)
Non-invasive ventilation (NIV)	4/37 (11%)	5/36 (14%) and 1 tracheostomy (3%)	0.60 (Fisher)	9/73 (12%) and 1 tracheostomy (1%)	4/7 (57%)	**0.016** (Fisher)
NIV at home	1/37 (1%)	5/36 (14%) and 1 tracheostomy (3%)	0.06 (Fisher)	6/73 (8%) and 1 tracheostomy (1%)	4/7 (57%)	**0.0058** (Fisher)
Sedation	24/32 (75%)	27/35 (77%)	1 (Fisher)	51/67 (76%)	1/7 (14%)	**0.002** (Fisher)
Sedation at the time of death	30/37 (81%)	26/34 (76%)	0.77 (Fisher)	56/71 (79%)	1/3 (33%)	0.13 (Fisher)

Bold values represent statistically significant values.

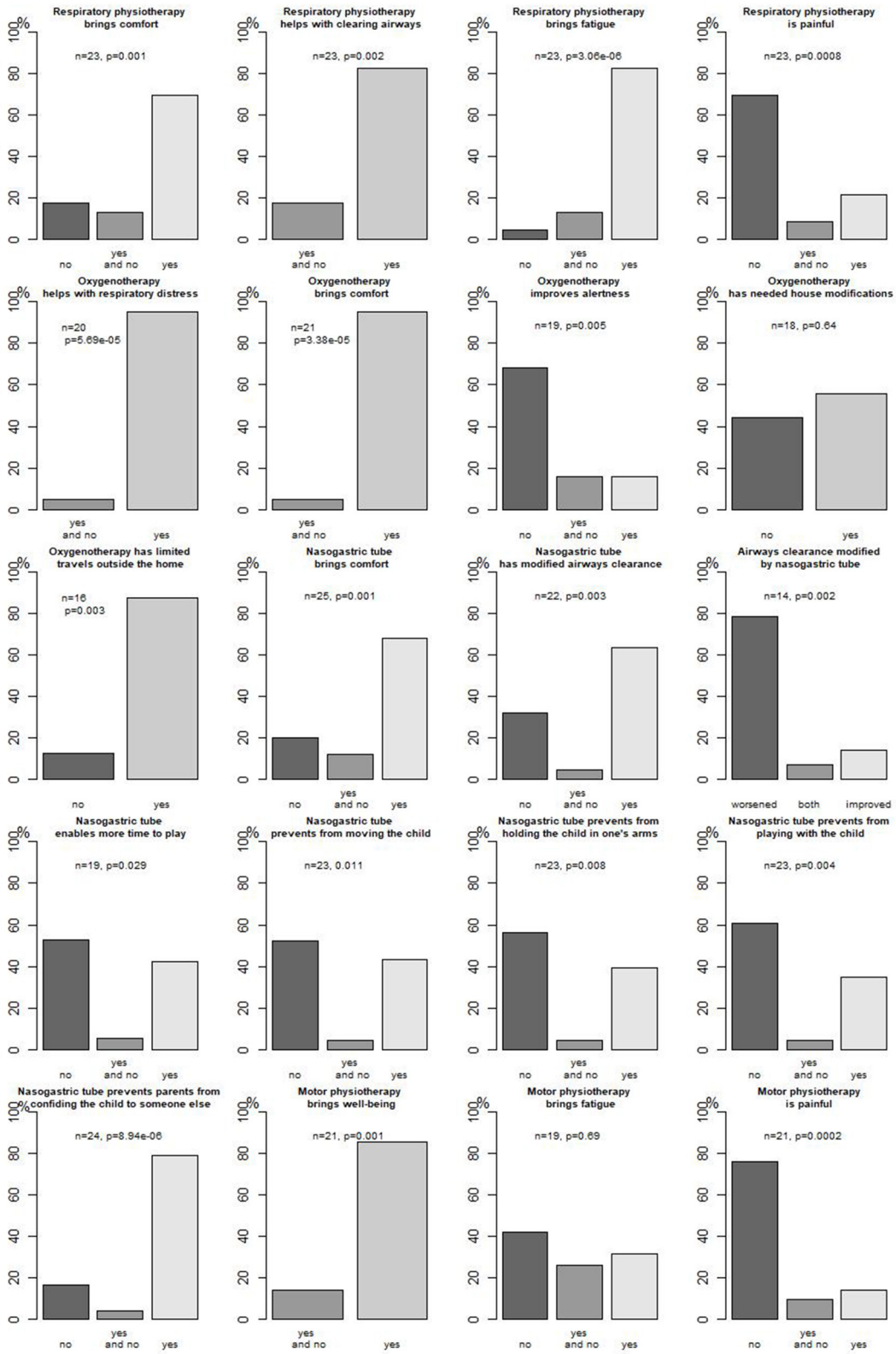

FIGURE 2 | Parents' opinion about their child's technical care.

the wrong way in 14/27 (52%) of cases at a median of 4.9 months (1.4–7.6). Constipation was also reported in 22/27 (81%) of cases.

As a result, 15/37 (41%) of patients received a treatment for GOR (six of eight patients whose parents reported GOR were treated), and 16/22 (73%) for constipation (either oral treatment or suppository or rectal enema).

Those difficulties resulted in an enteral nutrition for 34/37 (92%) of patients at a median age of 5 months (0.8–16.4), including four for whom the information was available only at the time of death. The enteral nutrition was administered through a nasogastric tube (NGT) in most cases; only one patient had a GS performed at 6.5 months of age. Enteral nutrition was begun in hospital for most (24/26, 92%) patients, and 23/26 (88%) of parents were taught how to use it, either in a hospital (20/23, 87%) or at home. While on enteral nutrition, children were delivered either homemade food (20/24, 83%) or ready-to-use therapeutic food (13/23, 57%).

Parents' opinion about enteral feeding through an NGT is presented in **Figure 2**.

Installation and Motor Management

Of 30 patients, 26 (78%) received motor physiotherapy since a median age of 3.8 months (0.9–12.2); 21/25 (84%) patients received it at home. Different techniques were used, mostly performing (11/12, 92%) postures. Parents' opinion about motor physiotherapy is presented in **Figure 2**.

Pain and Comfort Management

When reported ($n = 27$), all parents described their child as "comfortable" at a median age of 4 months (0.8–11.8). Among them, three parents first reported their child as comfortable at a median age of 4.2 months (2.5–4.4), but then as not comfortable at a median age of 5.2 months (3.5–6.8).

Parents evaluated their child's comfort during different activities and in different positions (significant results, $p < 0.05$), reported in **Figure 3** with most patients being comfortable in side decubitus and no patient being comfortable in a prone position for instance. They also mentioned that their child seemed comfortable during strolls ($n = 2$), during hugs ($n = 7$), at play ($n = 5$), and while placed in adapted equipment ($n = 4$).

Of 33 patients, 28 (85%) reported using medicine(s) to ensure their child's comfort at a median age of 4.3 months (0.7–11.2). Those medicines included grade I analgesics (mostly paracetamol) in 19/31 (61%) since a median age of 5.2 months (0.7–12.2), grade III analgesics (mostly oral morphine) in 11/32 (34%) since a median age of 5.2 months (1.8–7.9),

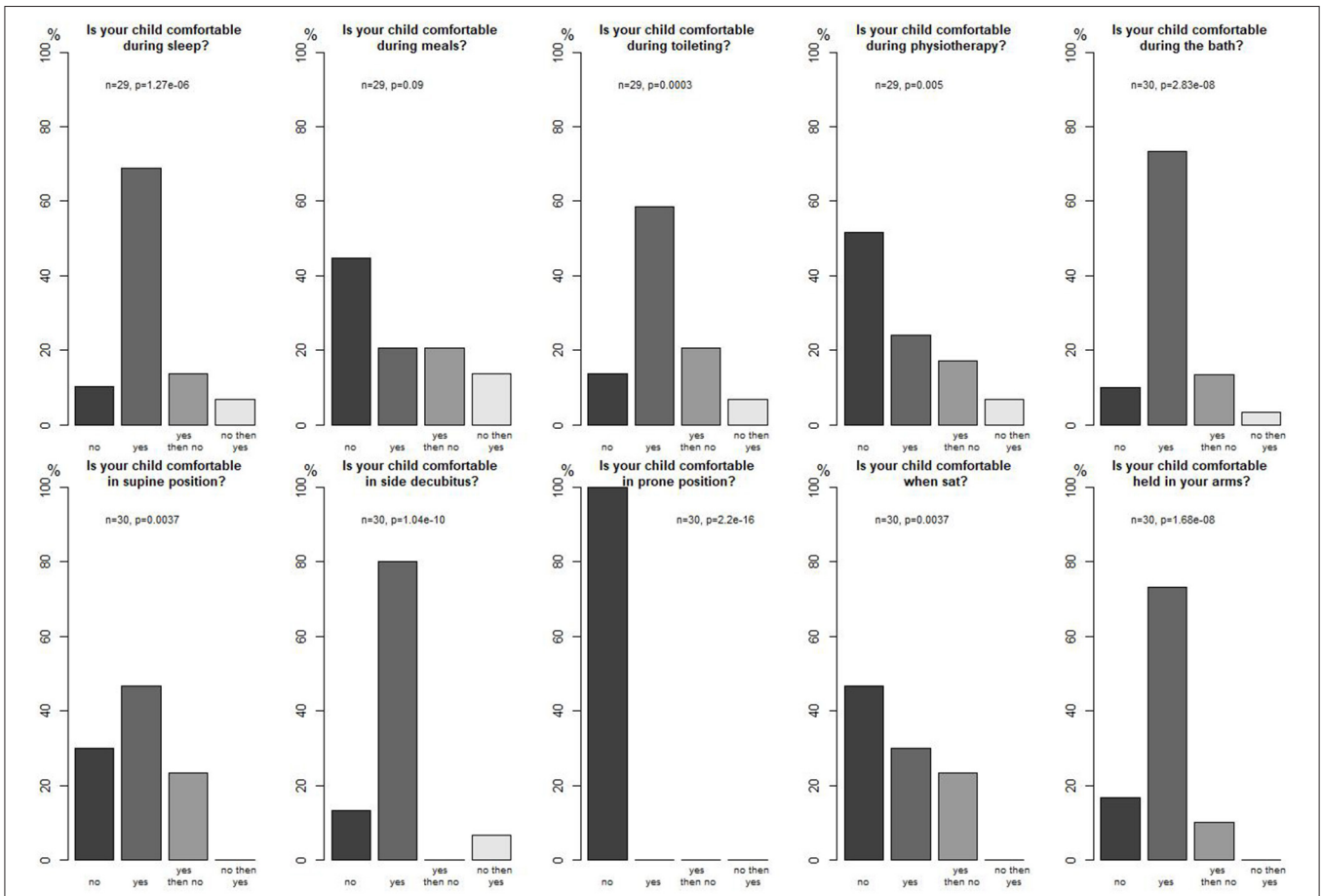

FIGURE 3 | Parents' opinion about their child's comfort.

benzodiazepines in 8/31 (26%) since a median age of 6 months (1.8–7.9), and amitriptyline in 10/32 (31%) since 5 months of age (2–9). Parents also mentioned here the use of transdermic scopolamine in 6/31 (19%) at a median age of 7 months (5.6–9), hydroxyzine in 2 patients, and antibiotics for pulmonary infections in 11.

Care at the Time of Death, Data From the PHRC Study

We analyzed data from a specific questionnaire about care and medications during the last 48 h before death filled in by the physician in charge of the infant, after the child's death ($n = 37$). Most patients (31/37, 84%) died because of chronic respiratory insufficiency, the others because of abrupt bulbar dysfunction leading to cardiac arrest (5/37, 14%), and for one patient, the physician was not able to identify one or another of the mechanisms. Fourteen (38%) of the 37 patients died at home, and 17 (46%) in the local university hospital (where the neuromuscular center is located) including two patients who died in the intensive care unit, and one in a public space.

Of 37 patients, 22 (59%) received grade I analgesics (paracetamol) at the time of death, and 21 (57%) received grade III analgesics (morphine), which were associated with grade I analgesics in 11 cases. Five (14%) did not receive any conventional analgesics. Fifteen (41%) patients received benzodiazepines (mostly midazolam) at the time of death, associated with grade III analgesics for 10 (27%) of them. Fifteen (41%) received amitriptyline at the time of death, one received ketamine, two (5%) received hydroxyzine, and two (5%) received scopolamine. Altogether, seven (19%) patients did not receive any sedation or grade III analgesics, and three (8%) patients did not receive any analgesic or sedative treatment (even grade I analgesic) at the time of death. Medicines were given through an NGT in most patients (31/37, 84%).

During the last 48 h before death, two patients were under NIV (2/37, 5%), 28 (28/37, 76%) received oxygenotherapy (26 through nasal cannula and two through a nasobuccal mask), and 7 (7/37, 19%) patients did not receive any specific respiratory treatment. Children were monitored on clinical examination alone for 24 patients (24/37, 65%), using a pulse oximeter for five (5/37, 14%) and a cardiorespiratory electronic scope for eight (8/37, 22%).

Do-not-resuscitate anticipated decisions were discussed with the parents for all but one patient, and a written document of the final decision was available for 32 of the patients. Three additional physicians reported that the final decision had been communicated orally (no data available for the remaining patient). The decision had been taken after a collaborative multidisciplinary discussion for 28 patients and assumed by the sole physician in eight cases.

Caregivers' Implication and Evaluation

Caregivers Implicated

Data concerning the professional caregivers who provided services within the patients' home were available for 28/37 (76%) patients. A nurse provided care in the patient's home in 18 cases: as the sole care provider in two cases, in association with an in-home hospitalization service for five patients, with a palliative care team for six, and in addition to an in-home hospitalization service and a palliative care team both in five cases. In-home hospitalization service was involved in 16 cases—as the sole professional service provider in three cases and in association with a palliative care team for three. A palliative care team was involved in 17 cases, three of which were the only in-home care service for the patients.

Parents were encouraged to meet with a psychologist in 36/37 (97%) cases. Twenty-six families agreed to meeting a psychologist while their child was alive, and finally, 29 of them met a psychologist immediately before or after their child's death.

No parent reported seeking the services of a homeopath, and three reported consulting an osteopath, one an acupuncturist, three a magnetizer, and two a healer.

Medical and Paramedical Staff's Implication in the PHRC Study

We then reported which caregivers wrote in the specific HB for each patient. A neuropediatrician wrote commentaries in 24/37 (65%) cases, a median of 3 times for each patient (1–12). A general practitioner wrote in 19/37 (51%) HBs, a median of 1 time (1–5). For six patients, another physician (pneumopediatrician, physician in the emergency department, or physician from in-home hospitalization) wrote a median of 1 time (1–2). Of 37 physiotherapists, 22 (59%) filled in their specific questionnaire with a median of 2 free-written commentaries (1–17). Occupational therapists wrote in 4/37 (11%) HBs, a median of 4 times (2–6). Nurses wrote commentaries in 14/37 (38%) cases, a median of 2 times (1–8). The palliative care team wrote a median of 3 times (1–8) for 11/37 (30%) patients. Psychologists wrote a median of 1 comment (1–5) in 6/37 (16%) cases. Lastly, isolated comments from a social worker, psychometrician, speech therapist, midwife, and head nurse were found.

Parents' Implication and Opinion

As mentioned before, parents evaluated oxygenotherapy, respiratory physiotherapy, and enteral feeding (**Figure 2**).

Of 22 parents, 16 (73%) found the information about nutrition and feeding provided in the HB helpful. Concerning constipation, 16/22 (73%) considered it uncomfortable for their child and thus modified their child's alimentation and massaged their child's abdomen in order to improve bowel function.

Of 28 parents, 22 (79%) found the information about positioning provided in the HB helpful.

Of 27 parents, 10 (37%) also evaluated their child as being in pain, 12 (44%) as being not in pain, and 5 as being not originally in pain but becoming so at a median of 4.6 months of age (1.5–7.6). In that context, most parents (18/24, 75%) found that pain was properly rated by the medical team in charge of their child, and 20/23 (87%) found their care plan relevant to their child's needs.

Sleep was considered as not disturbed in 18/28 (64%) of patients [however, they reported more than one nocturnal awakening per night in 12/18 (67%)] and disturbed in 6/28 (21%), and for 4/28 (14%), sleep became an issue (when sleep was

considered disturbed, all parents reported more than one and up to more than five nocturnal awakenings per night). Nocturnal awakenings were explained by the need for a change in position (19/28, 68%), need for massage (6/28, 21%), loss of pacifier (17/28, 61%), need for a feeding (13/28, 46%), need to be held (19/28, 68%), and need for upper-airway suction (6/28, 21%).

We also reported whether parents wrote written-free answers in the dedicated questions of the HB and also reported when they made spontaneous (i.e., not solicited by a question) comments. Only six parents did not write any solicited written-free answer; others wrote solicited written-free answers a median of 9 times (0–50). Moreover, 24/37 parents wrote spontaneous comments a median of 2 times (0–61).

DISCUSSION

We here report on 80 infants with severe SMA-1, followed in France between 2012 and 2016. Our data confirm previous reports on natural history for this fatal disease with a median diagnosis at 3 months (range 0.6–10.4 months) and a median age at the time of death of 6 months (range 1–27) (7). This homogeneity over the last 20 years emphasizes the ethical choice that has been made by French pediatric physicians involved in neuromuscular disorders not to implement long-term ventilation (NIV or tracheostomy) for those severe patients whose motor evolution is not modified by proactive ventilation (12, 16). However, our study confirms that palliative care is an active approach involving a multidisciplinary team, and the development of palliative care in France since 2005 (Law No. 2005-370, promulgated on April 22, 2005, and Law No. 2016-87 promulgated on February 2, 2016, regarding end of life and patients' right) has led to the implication of more home-hospital settings (26–62%) and involvement of dedicated pediatric palliative care teams (11–74%) in the management of those severe patients. If there was no evolution in NIV use over the period studied, oxygenotherapy, suction aspiration system, and enteral feeding through an NGT were used in most patients, as reported in other studies (8, 15, 22, 23) and recommended in the recently revised consensus statement on standards of care in SMA (5, 10).

Our study also collected information about medical conditions at the time of death, which occurred at home for 38% of patients vs. 17 and 23% in the previous periods reported in France (7). While there are little data among studies to enable robust comparison across countries (8, 22–24), evidence as is collectively suggests that there is an increasing consideration for parents' wishes about their child's death conditions. Morphine and benzodiazepines were used more (77%) over the last period than during the two previous ones studied in France (18 and 60%, respectively), but less than that in other studies when reported (8, 22, 23), and use of analgesics and/or sedative treatments has not been ruled yet in the last standards of care (5, 10). However, pain and dyspnea were the main symptoms reported during the last 48 h in a recent retrospective study (22), underscoring the need to prioritize comfort for those infants. Of note, amitriptyline has also been used to ensure well-being and diminish anxiety due to chronic respiratory insufficiency but needs further evaluation. Do-not-resuscitate anticipated decisions had been made for all but one patient, written in most cases (89%) and after a collaborative multidisciplinary discussion (78%), which is in accordance with current French law.

The implementation of specific pediatric palliative care in the context of SMA-1 patients needs active collaboration and coordination between the different actors involved to ensure the child's and family's best quality of life. This need for coordination has recently been supported in qualitative studies (25, 26), as well as the importance of parents' input about their wishes for their child's treatments and end-of-life conditions (22, 24, 25, 27–29).

In our study, an attempt was made to cross-validate sources to ensure the best possible description and evaluation in real life for those infants. Indeed, most technical treatments were evaluated in real life by the parents, giving insights on both benefits and disadvantages of such treatments. For instance, both respiratory and motor physiotherapy, oxygenotherapy, and NGT significantly bring comfort to the infants according to most parents without major adverse events, but for instance, an NGT was considered to worsen airway ($p = 0.002$) clearance in most cases, and especially oxygenotherapy and an NGT modified family organization [house modifications (not significant), activities, and travels]. Parents also evaluated comfort, pain, and sleep, which clearly are part of quality of life for their infants. To our knowledge, there are few studies reporting parents' opinions on specific treatments in SMA-1 patients: for instance, Davis et al. reported caregivers' opinion on nutritional management, confirming high prevalence of GOR and constipation among those children (15). As many professionals are involved in the management of those children, parents as caregivers play a major role in transmitting information, ensuring a continuum of care as no home hospitalization settings enables constant nurse or medical staff presence. This empowerment of parents in their child's care has been claimed in recent studies (24, 25, 28, 29) and seems a key point to ensure the best care for the child in real life. In our study, not only did parents report as "Clinical Research Assistant" their child's symptoms and treatments in the HB, but they also spontaneously evaluated the treatments and recommendations made by care providers, and most of all they made propositions on everyday management of a child with SMA-1 (plays, installation, and feeding), enlightening that in addition to being a caregiver, they take care of their child as every parent does.

During our study occurred the phase I–III trials with nusinersen, which since its approval by the Food and Drug Administration (FDA) at the end of 2016 has led to major hopes in the community of scientists dealing with this devastating disease. However, as mentioned above, as discrepancies existed among countries concerning nutritional and mostly respiratory management for SMA-1 patients, we chose to isolate data concerning nusinersen-treated patients in our study. Despite a small number ($n = 7$) of patients included, we found major differences in medical practice for those patients in comparison

with the rest of our population study (more GS, more NIV, less analgesia and sedation, and more alive patients). This need for standardization of care has been claimed (30) to ensure better controlled studied and further analysis, especially concerning nusinersen, which remains a new drug, with lacking evidence on its long-term efficacy and tolerance profile. Moreover, major issues concerning medico-economic evaluation of orphan drugs emerge (31–34), not only of the drug itself but also of the medical organization needed to ensure appropriate deliverance and monitoring, prolonged life with potential prolonged need for technical care (enteral nutrition, respiratory support, orthopedic installation, etc.) (35, 36), or, on the contrary, improvement of respiratory function with less hospitalizations, for instance (37). In that context, not only medical costs are taken into account but also social costs for families since one parent usually needs to reduce or discontinue external employment (38). So far, no treatment cures SMA-1, and if new drugs have shown benefits on respiratory function and prolonged life (19), with improvement on motor function (21) for later-onset SMA patients, long-term evolution and especially need for long-term ventilation (even non-invasive), technical care, have to be measured. Such technical support clearly has to be evaluated in real life by the day-to-day caregivers that parents are (and of course children if possible), to ensure that their benefits overcome their burden in the condition of a still motor- and respiratory-impaired child.

CONCLUSION

Whereas, natural history has not evolved since 1989 in France for SMA-1 patients, improvements concerning integrated palliative supportive care have been made, enabling more coordinated medical support, as well as more well-defined implication of parents as everyday-life caregivers to their child. However, new therapies are emerging that raise hopes but also ethical issues not only about care access and drug availability in a limited medico-economic context but also and above all about defining the child's best interest. In that context, parents need to be clearly informed on the different existing options with the remaining unknowns, before they consent to any treatment option, including their mandatory implication in their child's care and evaluation.

DATA AVAILABILITY STATEMENT

The procedures carried out with the French data privacy authority (CNIL, Commission nationale de l'informatique et des libertés) do not provide for the transmission of the database, nor do the information and consent documents signed by the patients. Consultation by the editorial board or interested researchers may nevertheless be considered, subject to prior determination of the terms and conditions of such consultation and in respect for compliance with the applicable regulations.

ETHICS STATEMENT

This multicentric prospective French study received approval from the ethical board Comité de Protection des Personnes (CPP) Ile de France II on April 3, 2012. Information and consent forms for the participation of the child and his/her parents in the study and publication of the results were included in that approval. This study was registered on clinicaltrials.gov under the reference NCT01862042.

AUTHOR CONTRIBUTIONS

MH was responsible for reporting the quantitative and qualitative data, analyzed them, performed the statistical analysis, and drafted and revised the manuscript for intellectual content. MH had full access to all the data in the study and takes responsibility for the integrity of the data and the accuracy of the data analysis. CB was responsible for the study conceptualization and design, collected data, and revised portions of the manuscript for intellectual content. DC was responsible for collecting and reporting qualitative and quantitative data and revised portions of the manuscript for intellectual content. SL was responsible for collecting data, managed them, and ensured the conduct of the study. VG and ED were involved in the specific health book conception and collected data. They revised portions of the manuscript for intellectual content. CVa, J-MC, BC, CC, CVu, MM, M-CN, PS, JL, VL, FR, UL, JD, SN, CS, MR, and AM collected data and revised portions of the manuscript for intellectual content. M-LV was responsible for the study conceptualization and design and revised portions of the manuscript for intellectual content. ID was responsible for the study conceptualization and design, collected data, and drafted and revised portions of the manuscript for intellectual content. All authors read and approved the final manuscript.

FUNDING

This study was financed by the Ministry of Health (Programme Hospitalier de Recherche Clinique, PHRC, AOM11183).

ACKNOWLEDGMENTS

We want to acknowledge Dr. Aude Ledivenah, who participated in the study conceptualization. We acknowledge Beatrice Barbier who participated in the financial management of the study. We acknowledge Mariesa Ho who revised the manuscript for appropriate English language. We also want to acknowledge the ECLAS association who is involved in family support and has developed useful tools to inform and help families and children. This study could not have been done without the families' participation, and we acknowledge them for that, especially in the context of this severe fatal disorder.

REFERENCES

1. Lefebvre S, Burglen L, Reboullet S, Clermont O, Burlet P, Viollet L, et al. Identification and characterization of a spinal muscular atrophy-determining gene. *Cell*. (1995) 80:155–65. doi: 10.1016/0092-8674(95)90460-3
2. Verhaart IEC, Robertson A, Wilson IJ, Aartsma-Rus A, Cameron S, Jones CC, et al. Prevalence, incidence and carrier frequency of 5q–linked spinal muscular atrophy – a literature review. *Orphanet J Rare Dis*. (2017) 12:124. doi: 10.1186/s13023-017-0671-8
3. Lefebvre S, Burlet P, Liu Q. Bertrandy S, Clermont O, Munnich A, et al. Correlation between severity and SMN protein level in spinal muscular atrophy. *Nat Genet*. (1997) 16:265–69. doi: 10.1038/ng0797-265
4. Wirth B, Brichta L, Schrank B, Lochmuller H, Blick S, Baasner A. Mildly affected patients with spinal muscular atrophy are partially protected by an increased SMN2 copy number. *Hum Genet*. (2006) 119:422–8. doi: 10.1007/s00439-006-0156-7
5. Mercuri E, Finkel RS, Muntoni F, Wirth B, Montes J, Main M, et al. Diagnosis and management of spinal muscular atrophy: part 1: recommendations for diagnosis, rehabilitation, orthopedic and nutritional care. *Neuromuscul Disord*. (2018) 28:103–15. doi: 10.1016/j.nmd.2017.11.005
6. Lunn MR, Wang CH. Spinal muscular atrophy. *Lancet*. (2008) 371:2120–33. doi: 10.1016/S0140-6736(08)60921-6
7. Barnérias C, Quijano S, Mayer M, Estournet B, Cuisset J-M, Sukno S, et al. Amyotrophie spinale type 1: enquête multicentrique des pratiques de soins et d'accompagnement palliatif sur deux périodes successives de 10ans. *Arch Pédiatrie*. (2014) 21:347–54. doi: 10.1016/j.arcped.2014.01.017
8. Tassie B, Isaacs D, Kilham H, Kerridge I. Management of children with spinal muscular atrophy type 1 in Australia: audit of spinal muscular atrophy type 1. *J Paediatr Child Health*. (2013) 49:815–9. doi: 10.1111/jpc.12291
9. Ropars J, Barnerias C, Hully M, Chabalier D, Peudenier S, Barzic A, et al. Thoracic circumference: a new outcome measure in spinal muscular atrophy type 1? *Neuromuscul Disord*. (2019) 29:415–21. doi: 10.1016/j.nmd.2019.03.003
10. Finkel RS, Mercuri E, Meyer OH, Simonds AK, Schroth MK, Graham RJ, et al. Diagnosis and management of spinal muscular atrophy: part 2: pulmonary and acute care; medications, supplements and immunizations; other organ systems; and ethics. *Neuromuscul Disord*. (2018) 28:197–207. doi: 10.1016/j.nmd.2017.11.004
11. Wang CH, Finkel RS, Bertini ES, Schroth M, Simonds A, Wong B, et al. Consensus statement for standard of care in spinal muscular atrophy. *J Child Neurol*. (2007) 22:1027–49. doi: 10.1177/0883073807305788
12. Finkel RS, McDermott MP, Kaufmann P, Darras BT, Chung WK, Sproule DM, et al. Observational study of spinal muscular atrophy type I and implications for clinical trials. *Neurology*. (2014) 83:810–87. doi: 10.1212/WNL.0000000000000741
13. Oskoui M, Levy G, Garland CJ, Gray JM, O'hagen J, De Vivo DC, et al. The changing natural history of spinal muscular atrophy type 1. *Neurology*. (2007) 69:1931–6. doi: 10.1212/01.wnl.0000290830.40544.b9
14. Ryan MM. The use of invasive ventilation is appropriate in children with genetically proven spinal muscular atrophy type 1: the motion against. *Paediatr Respir Rev*. (2008) 9:51–4. doi: 10.1016/j.prrv.2007.10.002
15. Davis RH, Godshall BJ, Seffrood E, Marcus M, LaSalle BA, Wong B, et al. Nutritional practices at a glance: spinal muscular atrophy type i nutrition survey findings. *J Child Neurol*. (2014) 29:1467–72. doi: 10.1177/0883073813503988
16. De Sanctis R, Coratti G, Pasternak A, Montes J, Pane M, Mazzone ES, et al. Developmental milestones in type I spinal muscular atrophy. *Neuromuscul Disord*. (2016) 26:754–9. doi: 10.1016/j.nmd.2016.10.002
17. Lemoine TJ, Swoboda KJ, Bratton SL, Holubkov R, Mundorff M, Srivastava R. Spinal muscular atrophy type 1: are proactive respiratory interventions associated with longer survival? *Pediatr Crit Care Med*. (2012) 13:e161–5. doi: 10.1097/PCC.0b013e3182388ad1
18. Chiriboga CA, Swoboda KJ, Darras BT, Iannaccone ST, Montes J, Darryl C, et al. Results from a phase 1 study of nusinersen (ISIS-SMNRx) in children with spinal muscular atrophy. *Neurology*. (2016) 86:890–7. doi: 10.1212/WNL.0000000000002445
19. Finkel RS, Mercuri E, Darras BT, Connolly AM, Kuntz NL, Kirschner J, et al. Nusinersen versus sham control in infantile-onset spinal muscular atrophy. *N Engl J Med*. (2017) 377:1723–32. doi: 10.1056/NEJMoa1702752
20. Finkel RS, Chiriboga CA, Vajsar J, Day JW, Montes J, De Vivo DC, et al. Treatment of infantile-onset spinal muscular atrophy with nusinersen: a phase 2, open-label, dose-escalation study. *Lancet*. (2016) 388:3017–26. doi: 10.1016/S0140-6736(16)31408-8
21. Mercuri E, Darras BT, Chiriboga CA, Day JW, Campbell C, Connolly AM, et al. Nusinersen versus sham control in later-onset spinal muscular atrophy. *N Engl J Med*. (2018) 378:625–35. doi: 10.1056/NEJMoa1710504
22. Di Pede C, Agosto C, De Tommasi V, De Gregorio A, Benini F. Symptom management and psychological support for families are the cornerstones of end-of-life care for children with spinal muscular atrophy type 1. *Acta Paediatr*. (2018) 107:140–4. doi: 10.1111/apa.14086
23. García-Salido A, de Paso-Mora MG, Monleón-Luque M, Martino-Alba R. Palliative care in children with spinal muscular atrophy type I: what do they need? *Palliat Support Care*. (2015) 13:313–7. doi: 10.1017/S1478951514000042
24. Lövgren M, Sejersen T, Kreicbergs U. Information and treatment decisions in severe spinal muscular atrophy: a parental follow-up. *Eur J Paediatr Neurol*. (2016) 20:830–8. doi: 10.1016/j.ejpn.2016.08.008
25. Higgs EJ, McClaren BJ, Sahhar MA, Ryan MM, Forbes R. "A short time but a lovely little short time": Bereaved parents' experiences of having a child with spinal muscular atrophy type 1: Bereaved parents' experiences of SMA 1. *J Paediatr Child Health*. (2016) 52:40–6. doi: 10.1111/jpc.12993
26. Hjorth E, Kreicbergs U, Sejersen T, Lövgren M. Parents' advice to healthcare professionals working with children who have spinal muscular atrophy. *Eur J Paediatr Neurol*. (2018) 22:128–34. doi: 10.1016/j.ejpn.2017.10.008
27. Beernaert K, Lövgren M, Jeppesen J, Werlauff U, Rahbek J, Sejersen T, et al. Parents' experiences of information and decision making in the care of their child with severe spinal muscular atrophy: a population survey. *J Child Neurol*. (2019) 34:210–5. doi: 10.1177/0883073818822900
28. Lövgren M, Sejersen T, Kreicbergs U. Parents' experiences and wishes at end of life in children with spinal muscular atrophy types I and II. *J Pediatr*. (2016) 175:201–5. doi: 10.1016/j.jpeds.2016.04.062
29. Murrell DV, Crawford CA, Jackson CT, Lotze TE, Wiemann CM. Identifying opportunities to provide family-centered care for families with children with type 1 spinal muscular atrophy. *J Pediatr Nurs*. (2018) 43:111–9. doi: 10.1016/j.pedn.2018.09.007
30. Finkel RS, Bishop KM, Nelson RM. Spinal muscular atrophy type i: is it ethical to standardize supportive care intervention in clinical trials? *J Child Neurol*. (2017) 32:155–60. doi: 10.1177/0883073816671236
31. Burgart AM, Magnus D, Tabor HK, Paquette ED-T, Frader J, Glover JJ, et al. Ethical challenges confronted when providing nusinersen treatment for spinal muscular atrophy. *JAMA Pediatr*. (2018) 172:188. doi: 10.1001/jamapediatrics.2017.4409
32. King NMP, Bishop CE. New treatments for serious conditions: ethical implications. *Gene Ther*. (2017) 24:534–8. doi: 10.1038/gt.2017.32
33. Luzzatto L, Hyry HI, Schieppati A, Costa E, Simoens S, Schaefer F, et al. Outrageous prices of orphan drugs: a call for collaboration. *Lancet*. (2018) 392:791–4. doi: 10.1016/S0140-6736(18)31069-9

34. Vukovic S, McAdam L, Zlotnik-Shaul R, Amin R. Putting our best foot forward: clinical, treatment-based and ethical considerations of nusinersen therapy in Canada for spinal muscular atrophy: spinal muscular atrophy and nusinersen. *J Paediatr Child Health*. (2019) 55:18–24. doi: 10.1111/jpc.14226
35. Farrar MA, Park SB, Vucic S, Carey KA, Turner BJ, Gillingwater TH, et al. Emerging therapies and challenges in spinal muscular atrophy: therapies and Challenges in SMA. *Ann Neurol*. (2017) 81:355–68. doi: 10.1002/ana.24864
36. Zuluaga-Sanchez S, Teynor M, Knight C, Thompson R, Lundqvist T, Ekelund M, et al. Cost effectiveness of nusinersen in the treatment of patients with infantile-onset and later-onset spinal muscular atrophy in Sweden. *Pharmacoeconomics*. (2019) 37:845–65. doi: 10.1007/s40273-019-00769-6
37. Lee M, França UL, Graham RJ, McManus ML. Pre-nusinersen hospitalization costs of children with spinal muscular atrophy. *Pediatr Neurol*. (2019) 92:3–5. doi: 10.1016/j.pediatrneurol.2018.11.002
38. Klug C, Schreiber-Katz O, Thiele S, Schorling E, Zowe J, Reilich P, et al. Disease burden of spinal muscular atrophy in Germany. *Orphanet J Rare Dis*. (2016) 11:58. doi: 10.1186/s13023-016-0424-0

Conflict of Interest: J-MC: conference participation fees paid by Biogen and AveXis. CVu: PI for Roche studies, consultancy agreements with Roche and Biogen. VL: member of the advisory board for Biogen, AveXis, and Roche.

The remaining authors declare that the research was conducted in the absence of any commercial or financial relationships that could be construed as a potential conflict of interest.

frontiers in Pediatrics

SYSTEMATIC REVIEW
published: 27 February 2020
doi: 10.3389/fped.2020.00028

The Efficacy and Safety of Topiramate in the Prevention of Pediatric Migraine: An Update Meta-Analysis

Xinwei Wu[1], *Yan Zhang*[2], *Mei Lu*[1], *Xiaolin Yu*[1], *Xiang Ye*[1], *Xingbang Wang*[1]* *and Peiyan Shan*[1]*

[1] Department of Geriatrics, Qilu Hospital of Shandong University, Jinan, China, [2] Department of Gastroenterology, Qilu Hospital of Shandong University, Jinan, China

Background: Migraine is the most common acute primary headache in children and adolescents. In 2014, topiramate became the first preventive drug for migraine, approved by the Food and Drug Administration (FDA) for adolescents. This meta-analysis was aimed to evaluate the efficacy and safety of topiramate in the prevention of pediatric migraine.

Methods: We searched the PubMed, EMBASE, Cochrane Library, and Chinese National Knowledge Infrastructure (CNKI) databases up to June 2019 for eligible randomized controlled trials (RCTs). The primary outcomes were mean migraine days per month, ≥50% reduction rate, and Pediatric Migraine Disability Assessment Scale (PedMIDAS) scores. RevMan5.3 software was performed for statistical analysis.

Results: Overall, 5 RCTs recruiting 531 patients (6–17 years of age) were included in the meta-analysis. The target dose of topiramate was 2 mg/kg (the maintenance phase was 12 weeks), 2–3 mg/kg, 50 mg/day, and 100 mg/day (maintaining for 16 weeks), respectively, in the included studies. Our results demonstrate that participants receiving topiramate had a significant advantage in remitting the monthly migraine days than those receiving placebo, with a mean difference (MD) of −0.78 ($n = 531$; 95% CI, −1.23 to −0.32; $Z = 3.37$; $P = 0.0008$). Topiramate could also reduce the mean PedMIDAS scores ($n = 238$; 95% CI, −16.53 to −0.49; $Z = 2.43$; $P = 0.04$). However, there was no significant difference in the percentage of patients experiencing a ≥50% reduction in monthly headache days between topiramate and placebo groups ($n = 531$; 95% CI, 0.94–1.77; $Z = 1.58$; $P = 0.11$). Topiramate was associated with higher rates of side effects such as weight decrease ($n = 395$; 95% CI, 2.73–22.98; $Z = 3.81$; $P < 0.01$) and paresthesia ($n = 531$; 95% CI, 3.05–13.18; $Z = 4.94$; $P < 0.01$).

Conclusions: Topiramate can significantly decrease monthly headache days and migraine-related burden in migraine patients <18 years old. However, it failed to increase 50% response rate. Adverse events seem to be more frequent in topiramate-treated children.

Keywords: topiramate, pediatric, migraine, prevention, meta-analysis

OPEN ACCESS

Edited by:
Oliver Semler,
Universitätsklinikum Köln, Germany

Reviewed by:
Michele Roccella,
University of Palermo, Italy
Francesco Domenico Pisani,
University of Messina, Italy

***Correspondence:**
Xingbang Wang
208937923@qq.com
Peiyan Shan
804745293@qq.com

Specialty section:
This article was submitted to Pediatric Neurology, a section of the journal Frontiers in Pediatrics

Received: *10 October 2019*
Accepted: *20 January 2020*
Published: *27 February 2020*

Citation:
Wu X, Zhang Y, Lu M, Yu X, Ye X, Wang X and Shan P (2020) The Efficacy and Safety of Topiramate in the Prevention of Pediatric Migraine: An Update Meta-Analysis. Front. Pediatr. 8:28. doi: 10.3389/fped.2020.00028

INTRODUCTION

Headache is the third cause of school absence among the pediatric population (1), and migraine is the most common acute primary headache in children and adolescents (2). Epidemiological studies have reported that migraine affects 3–5% of children, and the prevalence increases to 10–20% among adolescents (3–5). There is a slight male predominance before puberty; however, it is reversed after puberty (5). Unlike adults, pediatric migraine tends to manifest atypical clinical symptoms like episodic nausea, vomiting, nystagmus, vertigo, and so on (6).

Although ∼20% of children with migraine can effectively get relieved before 25 years old, most of them still experience headache attacks through older ages (7). Pediatric migraine, which can affect the children's school performances and quality of life (8, 9), has become a significant problem for children. Most researchers (10) believe that if migraine has more than three to four episodes per month or the attack causes significant disability, which can be measured by the Pediatric Migraine Disability Assessment Scale (PedMIDAS) (11, 12), then preventive treatment for migraine needs to be initiated (13). Management of pediatric migraine includes treatment of acute headache attack and preventive treatment. The preventive treatment can be divided into pharmaceutical and non-pharmaceutical interventions (14). Drug treatment for pediatric migraine mainly consists of abortive and prophylactic medications.

Topiramate, an antiepileptic drug, which is widely used in the prevention of migraine in adults, was the first preventive drug approved by the Food and Drug Administration (FDA) for migraine in 12–18 years old adolescents (15). It is a neuromodulator with neuron-stabilizing properties (16), and its exact mechanism of effectiveness in migraine is unclear yet. Several randomized, double-blind trials have reported discordant results in the efficacy of topiramate for the pediatric migraine prevention, and these RCT trials have yielded disproportionate results (17, 18). In 2017, a meta-analysis (19) showed topiramate failed to decrease the monthly headache days or decrease the percentage of patients experiencing a ≥50% reduction in migraine days per month. However, the results seemed to be disputable because it had the following problems: (1) In one included study, topiramate was divided into two groups of 50 and 100 mg/day, so it was more reasonable to consider it as two RCT trials; and (2) the data of the meta-analysis were not accurate. For example, in the study of Powers et al., there were 66 patients in the placebo group, which was misclassified as 33 in the previous meta-analysis. To investigate whether topiramate treatment is beneficial compared to placebo for migraine prevention in children, we designed this meta-analysis of randomized controlled trials including four studies with a total of 531 patients.

METHODS

Data Sources and Search Strategy

We searched the PubMed, EMBASE, Cochrane Library, and Chinese National Knowledge Infrastructure (CNKI) databases for eligible studies published up to June 2019 without language restrictions. The following keywords were used in our search strategies: ("topiramate" or "topamax"), AND ("pediatric migraine" or "pediatric headache" or "child/children/childhood migraine" or "child/children headache" or "adolescent/adolescents migraine" or "adolescent/adolescents headache"). Conference abstracts, references of related studies, and reviews were also searched to avoid omitting relevant RCTs.

Selection Criteria

The study was performed according to the Preferred Reporting Items for Systematic Reviews and Meta-Analyses (PRISMA) guidelines (20). Studies were considered eligible if they met the following criteria: (i) double-blind, randomized, and placebo-controlled trials that evaluated topiramate in migraine prevention; (ii) participants were children and adolescents (≤18 years old) with the clinical diagnosis of migraine according to the International Classification of Headache Disorders II (ICHD-II); and (iii) trials reported complete efficacy outcome. The exclusion criteria included reviews, animal trials, duplicate secondary analyses, studies comparing two or more interventions with each other but no contrast with placebo, and studies with incomplete or unavailable outcome data.

Outcome Measures

According to the International Headache Society (IHS) recommendations (21), migraine days or days of migraine episodes were recommended as the primary efficacy outcomes. Headache index, intensity of headache, headache duration, and responder rates were used as the secondary evaluation for efficacy. In this study, mean migraine days per month post-treatment, ≥50% reduction rate, and PedMIDAS scores were extracted from the included literatures to estimate efficacy of topiramate treatment. When headache days was reported in some other unit of time, we adjusted all to be days of headaches per month. For feasibility analysis, it was assessed both by the proportion of patients who discontinued the study for any reason and by the proportion of patients dropout because of adverse effects.

Data Extraction and Quality Assessment

Two experienced authors (Wu X. and Wang X.) screened the titles and abstracts of each literature independently to verify all potentially suitable trials that met the above inclusion criteria. Then, the study designs, participant characteristics, and outcomes were abstracted from the RCTs. Disagreements were resolved by discussion or following arbitration by the corresponding author. We used the "Risk of Bias" tool developed by the Cochrane Collaboration to assess the methodological quality of the trials.

Data Analysis

We performed all statistical tests using RevMan5.3 software (Cochrane Information Management System). Continuous variables were analyzed with mean differences (MDs) along with 95% confidence intervals (CIs), and dichotomous outcomes were calculated of risk ratios (RRs) along with 95% CIs. Statistical

significance was set at 0.10 for heterogeneity tests and 0.05 for all others. Heterogeneity was evaluated with I^2. If I^2 was >50%, heterogeneity of the enrolled trials was considered unacceptable and analyzed using random-effect model. If I^2 was ≤50%, a fixed-effect model was chosen. RevMan5.3 software was performed for all statistical analysis. When there were more than 10 trials reporting the same outcome, the funnel plot analysis was used to evaluate publication bias.

RESULTS

Search Findings

Overall, 710 relevant articles were initially identified for the analysis, with 230 being duplicates resulting in exclusion. After screening the titles and abstracts of the remaining records, 437 papers were excluded. We reviewed 43 possibly relevant articles in full text, of which there were 24 reviews, 6 non-RCTs, 2 letters, and 1 case report, which were all excluded. In addition, two studies compared the efficacy between topiramate and propranolol, one study on topiramate and cinnarizine, along with two RCTs on dose comparison of topiramate, and one RCT did provide the precise outcome above even though it compared topiramate with placebo (**Figure 1**). At last, we identified four studies including five RCTs that met our inclusion criteria (**Table 1**).

Characteristics of Included Studies

Four papers containing 5 trials (22–25) recruiting 531 patients were included in the meta-analysis. The sample size in each study ranged from 46 to 217 (topiramate and placebo participants only), with one study (23) recruiting <50 patients. All the four papers reported the criteria for pediatric migraine diagnosis. The mean age of the study population was 12.5 years old, and 57.9% of the participants were girls. The predominant ethnic groups represented were Caucasian, as well as African, Asian, and others. One study (22) had three arms: topiramate, placebo, and a third treatment group—amitriptyline. The data of amitriptyline group was not included in this review. One of the studies included two dose treatments of topiramate (50 and 100 mg/day), and therefore, it was considered as two separate trials. All the included studies reported the duration of topiramate treatment ranging from 16 to 31 weeks. Washout and screening phases, weaning period, and follow-up were also incorporated into the studies. The dose of topiramate was gradually increased in all the included studies.

All the selected literatures reported days of headache and ≥50% reduction rate as trial outcomes. Two studies also reported difference in PedMIDAS scores between topiramate and placebo groups.

Quality Assessment and Publication Bias

The methodological quality of the trials was assessed by Cochrane Collaboration "Risk of Bias" tool. All the included trials described methods of random sequence generation and allocation concealment. Detailed information about blinding of participants and outcome assessment was reported in all studies. The outcome data were complete. The studies were at low risk of bias (**Figure 2**).

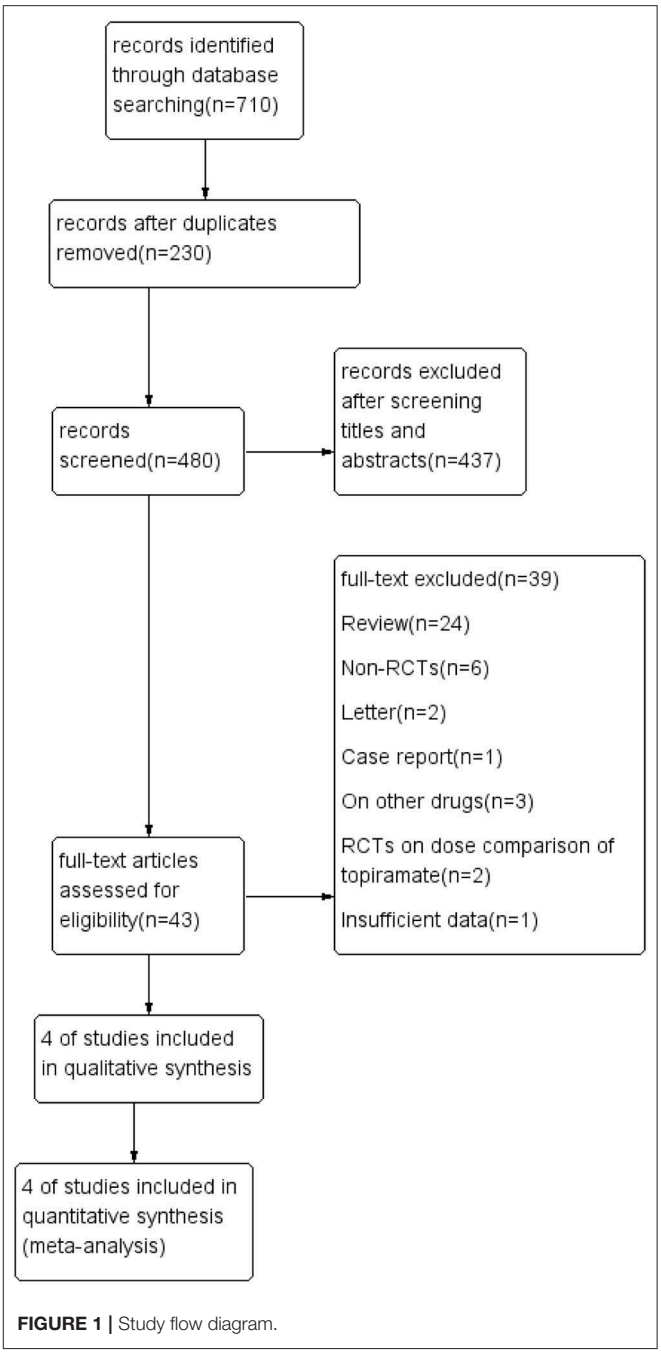

FIGURE 1 | Study flow diagram.

Efficacy Outcomes

Primary Outcome

All the five selected trials reported monthly days of headache as a trial outcome. Our results demonstrated that participants receiving topiramate had a significant advantage in remitting the monthly migraine days than those receiving placebo, with an MD of −0.78 ($n = 531$; 95% CI, −1.23 to −0.32; $Z = 3.37$; $P = 0.0008$).

TABLE 1 | Characteristics of included randomized controlled trials.

Study	Sample size	Mean age (years)	Girls (%)	Dropout (%)	Treatment groups	Dose range (mg/day)	Topiramate titration phase (week)	Topiramate maintenance phase (week)	Study design	Trial outcomes
Powers et al. (22)	217	14.2 ± 2.4	69.1	9.7	Topiramate vs. placebo	2 mg/kg	8	16	Parallel	Mean headache days, reduction in monthly headache attacks, ≥50% responder rate, headache disability (PedMIDAS score)
Lakshmi et al. (23)	46	10.6 ± 1.4	31	8.7	Topiramate vs. placebo	100	4	12	Parallel	Mean headache days, ≥50% responder rate, reduction in mean migraine frequency and severity, headache disability (PedMIDAS score + school absenteeism), times of analgesics use
Winner et al. (24)	162	11.1 ± 2.5	48.4	19.1	Topiramate vs. placebo	2–3 mg/kg	8	12	Parallel	Mean headache days, reduction in monthly headache days, ≥50, ≥75, and 100% responder rate
Lewis et al. (25)	106	14.2 ± 1.6	61	17	Topiramate vs. placebo	50, 100	4	12	Parallel	Percent reduction in monthly migraine attack rate, mean headache days, ≥50% responder rate, rate of analgesics use

The data selected in the analysis showed low heterogeneity ($I^2 = 18\%$; $P = 0.30$), and fixed-effects model was used. Z test for overall effect was statistically significant ($P = 0.0008$) (**Figure 3**).

Secondary Outcomes

All the five trials included reported the rate of patients experiencing a ≥50% reduction in the number of headache days. This meta-analysis revealed that there was no significant difference in the percentage of patients experiencing a ≥50% reduction in monthly headache days between topiramate and placebo groups ($n = 531$; 95% CI, 0.94–1.77; $Z = 1.58$; $P = 0.11$). Random-effects model was used because the data showed heterogeneity ($I^2 = 71\%$; $P = 0.003$) (**Figure 4**). In addition, two studies reported headache-related disability as the outcome. Our results showed that there was significant difference between the two groups in the mean PedMIDAS scores ($n = 238$; 95% CI, −16.53 to −0.49; $Z = 2.43$; $P = 0.04$). The data selected in the analysis showed heterogeneity ($I^2 = 59\%$; $P = 0.12$), and random-effects model was used (**Figure 5**).

Side Effects and Adverse Reactions

All studies mentioned side effects and adverse reactions. The overall incidence of adverse events was more frequent in topiramate-treated group than that in placebo. Serious adverse event like suicide attempt was only reported in one incidence treated with topiramate. Adverse events occurring more frequently in topiramate group than that in placebo included paresthesia, loss of weight, upper respiratory tract infection, paresthesia, anorexia, fatigue, and so on (**Figure 6**). Numbers of withdrawals for any reason in the topiramate group significantly increased than those in the placebo group ($n = 531$; 95% CI, 1.07–4.44; $Z = 2.14$; $P = 0.03$) with low heterogeneity ($I^2 = 0\%$; $P = 0.98$) (**Figure 7**). We then carried out the meta-analysis of each common side effect that reported in the trials. As shown in **Table 2**, weight decrease ($n = 395$; 95% CI, 2.73–22.98; $Z = 3.81$, $P < 0.01$) and paresthesia ($n = 531$; 95% CI, 3.05–13.18; $Z = 4.94$; $P < 0.01$) significantly increased in patients with topiramate.

DISCUSSION

Topiramate became the first and only drug approved by FDA for migraine prevention in children of 12–17 years old in 2014. Although studies have proved that topiramate can reduce migraine frequency and improve quality of life in adults (17), evidence for topiramate to prevent migraine in children and adolescent was insufficient. A meta-analysis published in 2017 found that topiramate failed to decrease the number or increase 50% response rate. However, there were several serious defects in this analysis (as was mentioned in *Introduction*). In this study, we have corrected these flaws and evaluated the efficacy and safety of topiramate in the prevention of pediatric migraine. The results demonstrated that topiramate had a significant advantage in reducing the migraine days and PedMIDAS scores than placebo; however, it still failed to increase 50% response rate. It meant that topiramate could significantly decrease headache days and migraine-related burden. In the included studies, three trials

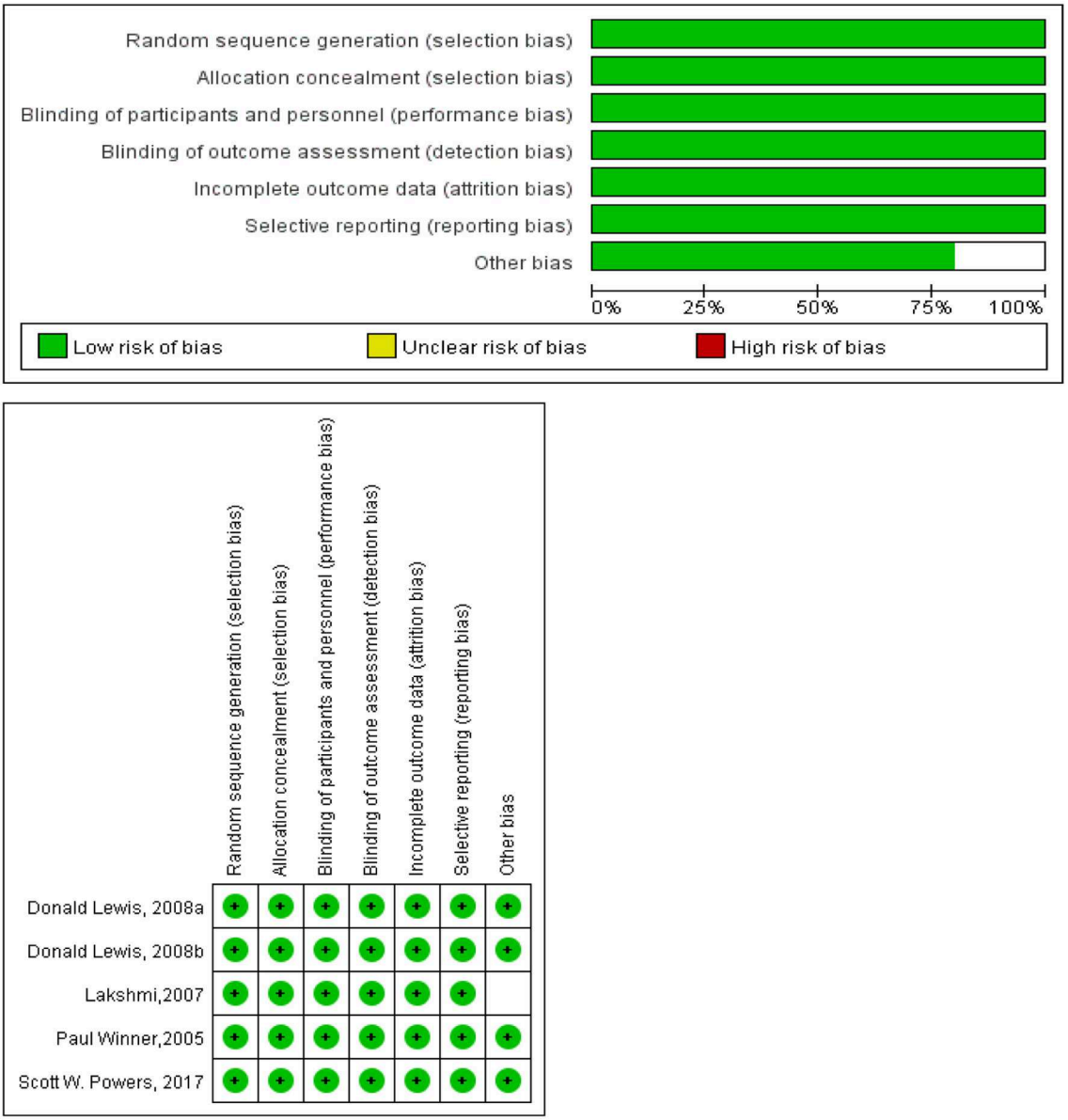

FIGURE 2 | Risk of bias graph and summary.

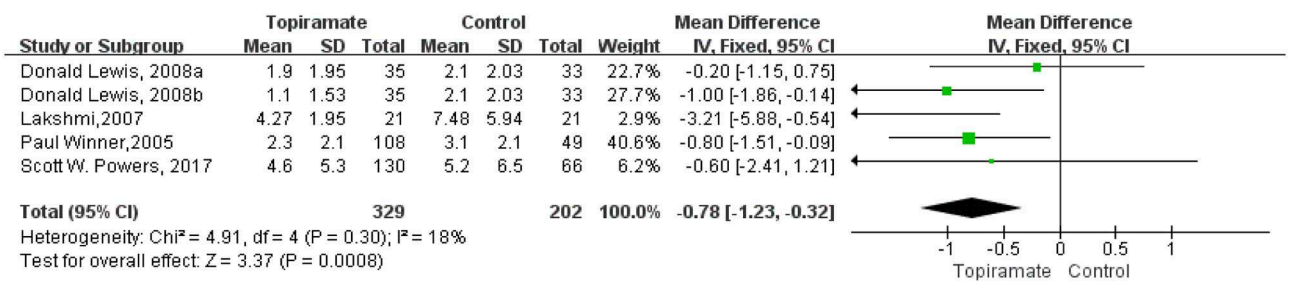

FIGURE 3 | Comparison of the monthly migraine days between topiramate and placebo groups.

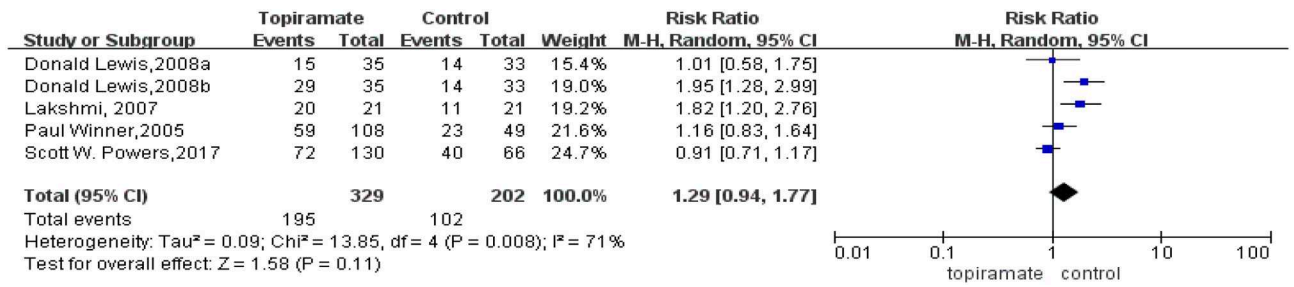

FIGURE 4 | Comparison of ≥50% response rate monthly migraine days between topiramate and placebo groups.

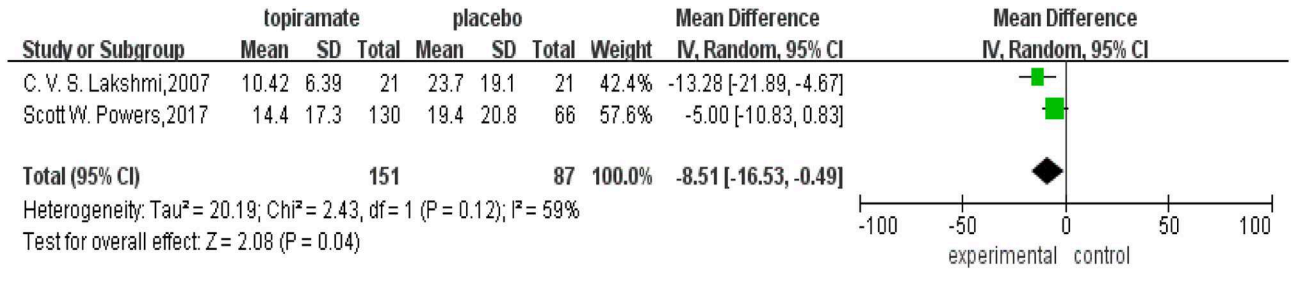

FIGURE 5 | Comparison of Pediatric Migraine Disability Assessment Scale (PedMIDAS) scores between topiramate and placebo groups.

(23–25) found that the decrease in monthly migraine days in the topiramate group was significantly greater compared with the placebo group. As for response rate, one study showed ≥50% response rate favored topiramate at 100 mg/day, not 50 mg/day (25). In the two studies in which patients were treated with topiramate at 2–3 mg/kg/day, one (23) found that topiramate achieved statistical significance in ≥50% responder rate. However, the other study (24) revealed ≥75% responder rate, rather than the 50% responder rate, was significantly higher in topiramate group than the placebo group. There were two researches reporting PedMIDAS changes, and one found that patients treated with topiramate experienced significant decrease in the PedMIDAS scores (23). One study measuring school absenteeism reported that the decrease in school absenteeism was significant among topiramate-treated children (23). Numbers of acute analgesic medications were evaluated in only one study, and no significant difference was found between the two groups (23).

Of particular note is that in the Donald Lewis, research, different dosages (50 and 100 mg/day) of topiramate were studied (25). Donald Lewis found that topiramate at 100 mg/day, instead of 50 mg/day, resulted in a statistically significant reduction in monthly migraine days and a greater percentage of patients experiencing a ≥50% reduction. Although this paper made the conclusion that topiramate at 50 mg/day had no efficacy in the prevention of pediatric migraine, a double-blind, dose comparison study of topiramate demonstrated that in both the 25 and 100 mg/day topiramate-treated groups, headache days per month decreased significantly (26). There were 100% of 25-mg patients responding with a ≥50% reduction in migraine days and 71% of 100-mg patients, which implied that low dosage of topiramate could also help to prevent pediatric migraine. Thus, in our opinion, it is not appropriate to include only topiramate at 100 mg/day in the previous meta-analysis, which is probably the main reason for our different results.

Furthermore, there is also an RCT with topiramate at 50, 100, and 200 mg to prevent migraine in children (27). However, the trial used the median percentage reductions in monthly migraine days as the main outcome. It demonstrated that compared with placebo, topiramate at 100 and 200 mg/day could reduce median percentage reductions in migraine days. All dosage of topiramate failed to significantly decrease the days of acute medication use compared with placebo.

This study illustrated that there was no significant difference in the percentage of patients experiencing a ≥50% reduction in monthly headache days between topiramate and placebo groups. The result may be due to the high placebo response rate of children (28). While placebo effects have been predicted ∼35% in migraine studies of adults, the placebo effects of pediatric migraine trials can reach to 50% or higher (29). In our study, the percentage of patients responding with a ≥50% reduction in migraine days was 50.50 vs. 59.27% in the topiramate group. The difference between topiramate and placebo groups was too small to demonstrate the drug efficacy (30).

Although topiramate was reported to be well-tolerated in most studies, our results showed that numbers of withdrawals were more in the topiramate group. Like other antiepileptic drugs, topiramate has many adverse events, and some of them were serious. Migraine patients seem to be more sensitive to topiramate-associated side effects than those with epilepsy (31).

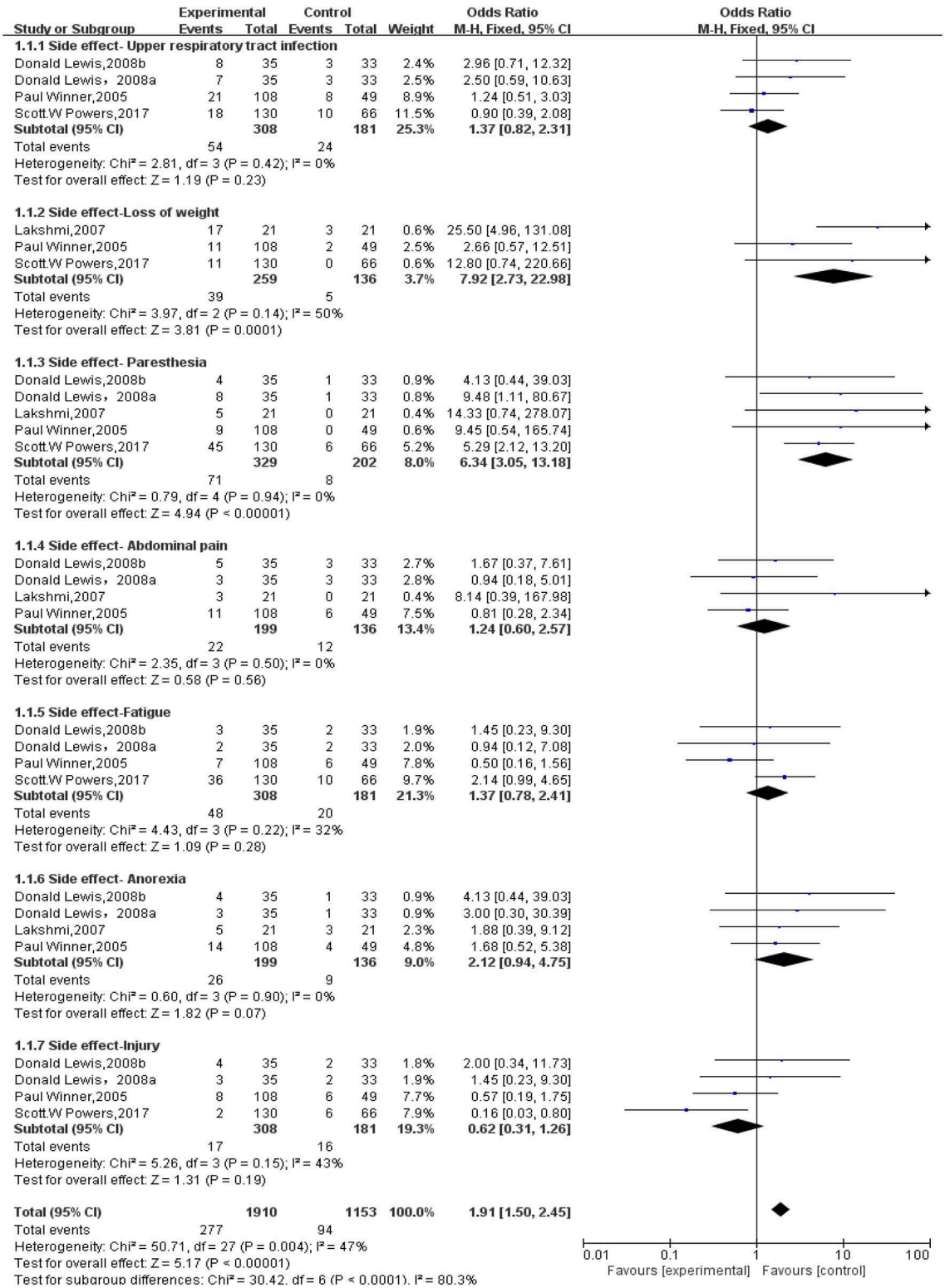

FIGURE 6 | Comparison of side effects and adverse reactions between topiramate and placebo groups.

All the four included studies reported that the topiramate group was associated with higher rate than the placebo group. Most of the side effects were mild to moderate and seemed to be related with the dosage of topiramate (27). The most common side effects in this meta-analysis were paresthesia, weight loss, fatigue, somnolence, upper respiratory tract infection, memory

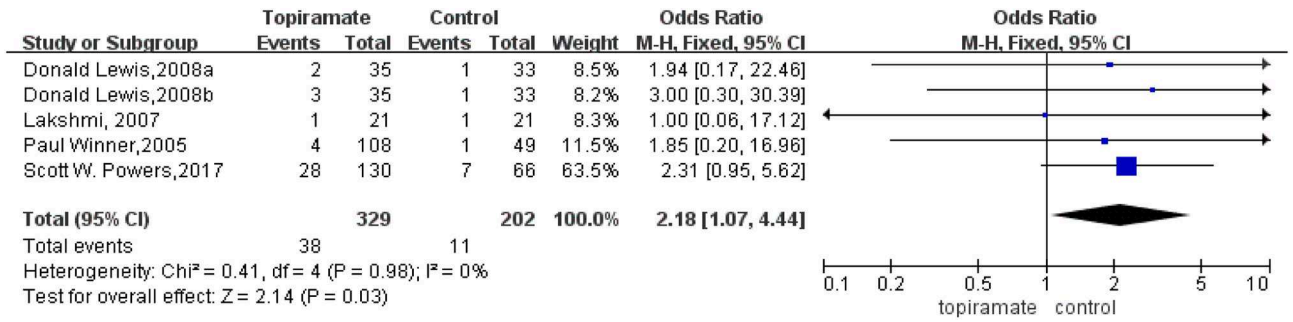

FIGURE 7 | Withdrawals for any reason between topiramate and placebo groups.

TABLE 2 | Side effects and adverse reactions of topiramate vs. placebo.

Side effects	Topiramate placebo No. of events/No. of participants		Relative risk (95% CI)	*Z*	*P*	Heterogeneity		
						Z	*df*	I^2%
Loss of weight	39/259	5/136	7.92 (2.73–22.98)	3.81	<0.01	3.97	2	50
Paresthesia	71/329	8/202	6.34 (3.05–13.18)	4.94	<0.01	0.79	4	0
Upper respiratory tract infection	54/308	24/181	1.37 (0.82–2.31)	1.19	0.23	2.81	3	0
Abdominal pain	22/199	12/136	1.24 (0.60–2.57)	0.58	0.56	2.35	3	0
Fatigue	48/308	20/181	1.37 (0.78–2.41)	1.09	0.28	4.43	3	32
Anorexia	26/199	9/136	2.12 (0.94–4.75)	1.82	0.07	0.60	3	0
Injury	17/308	16/181	0.62 (0.31–1.26)	1.31	0.19	5.26	3	43

impairment, aphasia, and cognitive disorder, which were similar with the previous clinical trials in adults and children (17, 32). Rare but serious suicide attempt was observed when patients were treated with topiramate other than placebo (33). In 2008, the association between suicidality and antiepileptic drugs (AEDs), especially topiramate, was issued by FDA. Screening for psychiatric comorbidities before and during the treatment is suggested in patients with topiramate.

There were also RCTs evaluating the efficiency of topiramate vs. other drugs. Powers et al. (22) also evaluated the efficiency of topiramate vs. amitriptyline for pediatric migraine. No difference was found between topiramate and amitriptyline in migraine days and headache-related disability. Ashrafi et al. (34) also reported that there was no statistically significant difference between topiramate and cinnarizine in preventing pediatric migraine. However, another RCT (35) showed that topiramate at 50 mg/day produced better efficacy to reduce monthly headache days compared with propranolol 80 mg/day.

This meta-analysis followed rigorous data extraction procedures and credible data for analysis, and the included studies were all with high quality and at low risk of bias. However, there are several limitations that must be addressed here. First, after rigorous screening, our analysis only included four papers including five studies, and one of them involved a relatively small sample size. Second, in this meta-analysis, some outcome measures showed significant heterogeneity, such as ≥50% reduction in monthly headache days (I^2 = 71%) and PedMIDAS score (I^2 = 59%). However, only five trials were included in this analysis, and no variables could explain it. Third, migraine had a relative long course and chronic tendency for both children and adults, so a longer treatment duration than 12–20 weeks was reported in the included papers. Thus, the optimal therapeutic response and long-term drug efficacy should be evaluated further. Finally, there were only three measuring indexes in our results. Indexes evaluating quality of life and the use of analgesic medications were reported in few studies. More useful efficacy parameters should be measured and reported as recommended by the IHS.

CONCLUSION

In conclusion, the current evidence demonstrates that topiramate shows greater beneficial effects for the prophylaxis of pediatric migraine than placebo. It can significantly decrease monthly headache days and migraine-related burden in migraine patients <18 years old. However, it failed to increase 50% response rate. Adverse events seem to be more frequent in topiramate-treated children. As for the limitations of the present study, more high-quality placebo-controlled RCTs are needed.

DATA AVAILABILITY STATEMENT

All datasets generated for this study are included in the article/supplementary material.

AUTHOR CONTRIBUTIONS

XWu: study conception, design and organization, acquisition of data, analysis and interpretation of data, drafting of the manuscript, critical revision of the manuscript for important intellectual content, statistical analysis, administrative, technical, material support, and study supervision. YZ: study conception, design, organization, and acquisition of data. ML: acquisition of data, analysis and interpretation of data, and statistical analysis. XYu: acquisition of data and analysis and interpretation of data. XYe: acquisition of data, and analysis and interpretation of data. XWa: study conception, design and organization, acquisition of data, analysis of data, critical revision of the manuscript for important intellectual content, administrative, technical, and material support, and study supervision. PS: acquisition of data, analysis and interpretation of data, statistical analysis, administrative, technical, and material support, and study supervision.

REFERENCES

1. Newacheck PW, Taylor WR. Childhood chronic illness: prevalence, severity, and impact. *Am J Public Health*. (1992) 82:364–71. doi: 10.2105/AJPH.82.3.364
2. Camarda R, Monastero R, Santangelo G, Raimondo D, Puma D, Pipia C, et al. Migraine headaches in adolescents: a five-year follow-up study. *Headache*. (2002) 42:1000–5. doi: 10.1046/j.1526-4610.2002.02229.x
3. Hamalainen ML. Migraine in children and adolescents: a guide to drug treatment. *CNS Drugs*. (2006) 20:813–20. doi: 10.2165/00023210-200620100-00003
4. Bugdayci R, Ozge A, Sasmaz T, Kurt AO, Kaleagasi H, Karakelle A, et al. Prevalence and factors affecting headache in Turkish schoolchildren. *Pediatr Int*. (2005) 47:316–22. doi: 10.1111/j.1442-200x.2005.02051.x
5. Laurell K, Larsson B, Eeg-Olofsson O. Prevalence of headache in Swedish schoolchildren, with a focus on tension-type headache. *Cephalalgia*. (2004) 24:380–8. doi: 10.1111/j.1468-2982.2004.00681.x
6. Landy S. Migraine throughout the life cycle: treatment through the ages. *Neurology*. (2004) 62:S2–8. doi: 10.1212/WNL.62.5_suppl_2.S2
7. Guidetti V, Galli F. Evolution of headache in childhood and adolescence: an 8-year follow-up. *Cephalalgia*. (1998) 18:449–54. doi: 10.1046/j.1468-2982.1998.1807449.x
8. Powers SW, Patton SR, Hommel KA, Hershey AD. Quality of life in paediatric migraine: characterization of age-related effects using PedsQL 4.0. *Cephalalgia*. (2004) 24:120–7. doi: 10.1111/j.1468-2982.2004.00652.x
9. Hershey AD. Current approaches to the diagnosis and management of paediatric migraine. *Lancet Neurol*. (2010) 9:190–204. doi: 10.1016/S1474-4422(09)70303-5
10. Lewis DW, Scott D, Rendin V. Treatment of paediatric headache. *Expert Opin Pharmacother*. (2002) 3:1433–42. doi: 10.1517/14656566.3.10.1433
11. Hershey AD, Winner PK. Pediatric migraine: recognition and treatment. *J Am Osteopath Assoc*. (2005) 105:2S—8S.
12. Topcu Y, Hiz KS, Bayram E, Sozmen K, Yis U. The Paediatric migraine disability assessment score is a useful tool for evaluating prophylactic migraine treatment. *Acta Paediatr*. (2014) 103:e484–9. doi: 10.1111/apa.12752
13. Lagman-Bartolome AM, Lay C. Pediatric migraine variants: a review of epidemiology, diagnosis, treatment, and outcome. *Curr Neurol Neurosci Rep*. (2015) 15:34. doi: 10.1007/s11910-015-0551-3
14. Gelfand AA, Qubty W, Goadsby PJ. Pediatric migraine prevention-first, do no harm. *JAMA Neurol*. (2017) 74:893–4. doi: 10.1001/jamaneurol.2017.1011
15. FDA approves Topamax for migraine prevention in adolescents. *J Pain Palliat Care Pharmacother*. (2014) 28:191.
16. Sakulchit T, Meckler GD, Goldman RD. Topiramate for pediatric migraine prevention. *Can Fam Physician*. (2017) 63:529–31.
17. Silberstein SD. Topiramate in migraine prevention: a 2016 perspective. *Headache*. (2017) 57:165–78. doi: 10.1111/head.12997
18. Ferraro D, Di Trapani G. Topiramate in the prevention of pediatric migraine: literature review. *J Headache Pain*. (2008) 9:147–50. doi: 10.1007/s10194-008-0030-1
19. Le K, Yu D, Wang J, Ali AI, Guo Y. Is topiramate effective for migraine prevention in patients less than 18 years of age? A meta-analysis of randomized controlled trials. *J Headache Pain*. (2017) 18:69. doi: 10.1186/s10194-017-0776-4
20. Moher D, Liberati A, Tetzlaff J, Altman DG. Preferred reporting items for systematic reviews and meta-analyses: the PRISMA statement. *Int J Surg*. (2010) 8:336–41. doi: 10.1016/j.ijsu.2010.02.007
21. Silberstein S, Tfelt-Hansen P, Dodick DW, Limmroth V, Lipton RB, Pascual J, et al. Guidelines for controlled trials of prophylactic treatment of chronic migraine in adults. *Cephalalgia*. (2008) 28:484–95. doi: 10.1111/j.1468-2982.2008.01555.x
22. Powers SW, Coffey CS, Chamberlin LA, Ecklund DJ, Klingner EA, Yankey JW, et al. Trial of amitriptyline, topiramate, and placebo for pediatric migraine. *N Engl J Med*. (2017) 376:115–24. doi: 10.1056/NEJMoa1610384
23. Lakshmi CV, Singhi P, Malhi P, Ray M. Topiramate in the prophylaxis of pediatric migraine: a double-blind placebo-controlled trial. *J Child Neurol*. (2007) 22:829–35. doi: 10.1177/0883073807304201
24. Winner P, Pearlman EM, Linder SL, Jordan DM, Fisher AC, Hulihan J. Topiramate for migraine prevention in children: a randomized, double-blind, placebo-controlled trial. *Headache*. (2005) 45:1304–12. doi: 10.1111/j.1526-4610.2005.00262.x
25. Lewis D, Winner P, Saper J, Ness S, Polverejan E, Wang S, et al. Randomized, double-blind, placebo-controlled study to evaluate the efficacy and safety of topiramate for migraine prevention in pediatric subjects 12 to 17 years of age. *Pediatrics*. (2009) 123:924–34. doi: 10.1542/peds.2008-0642
26. Lewis D, Paradiso E. A double-blind, dose comparison study of topiramate for prophylaxis of basilar-type migraine in children: a pilot study. *Headache*. (2007) 47:1409–17. doi: 10.1111/j.1526-4610.2007.00867.x
27. Winner P, Gendolla A, Stayer C, Wang S, Yuen E, Battisti WP, et al. Topiramate for migraine prevention in adolescents: a pooled analysis of efficacy and safety. *Headache*. (2006) 46:1503–10. doi: 10.1111/j.1526-4610.2006.00610.x
28. El-Chammas K, Keyes J, Thompson N, Vijayakumar J, Becher D, Jackson JL. Pharmacologic treatment of pediatric headaches: a meta-analysis. *JAMA Pediatr*. (2013) 167:250–8. doi: 10.1001/jamapediatrics.2013.508
29. Lewis DW, Winner P, Wasiewski W. The placebo responder rate in children and adolescents. *Headache*. (2005) 45:232–9. doi: 10.1111/j.1526-4610.2005.05050.x
30. Faria V, Linnman C, Lebel A, Borsook D. Harnessing the placebo effect in pediatric migraine clinic. *J Pediatr*. (2014) 165:659–65. doi: 10.1016/j.jpeds.2014.06.040
31. Luykx J, Mason M, Ferrari MD, Carpay J. Are migraineurs at increased risk of adverse drug responses? A meta-analytic comparison of topiramate-related adverse drug reactions in epilepsy and migraine. *Clin Pharmacol Ther*. (2009) 85:283–8. doi: 10.1038/clpt.2008.203
32. Silberstein SD, Dodick DW, Lindblad AS, Holroyd K, Harrington M, Mathew NT, et al. Randomized, placebo-controlled trial of propranolol

added to topiramate in chronic migraine. *Neurology*. (2012) 78:976–84. doi: 10.1212/WNL.0b013e31824d5846
33. Kanner AM. Are antiepileptic drugs used in the treatment of migraine associated with an increased risk of suicidality? *Curr Pain Headache Rep*. (2011) 15:164–9. doi: 10.1007/s11916-011-0199-x
34. Ashrafi MR, Najafi Z, Shafiei M, Heidari K, Togha M. Cinnarizine versus topiramate in prophylaxis of migraines among children and adolescents: a randomized, double-blind clinical trial. *Iran J Child Neurol*. (2014) 8:18–27.
35. Ashtari F, Shaygannejad V, Akbari M. A double-blind, randomized trial of low-dose topiramate vs propranolol in migraine prophylaxis. *Acta Neurol Scand*. (2008) 118:301–5. doi: 10.1111/j.1600-0404.2008.01087.x

Conflict of Interest: The authors declare that the research was conducted in the absence of any commercial or financial relationships that could be construed as a potential conflict of interest.

frontiers in Pediatrics

ORIGINAL RESEARCH
published: 28 February 2020
doi: 10.3389/fped.2020.00083

Clinical and Genetic Heterogeneity in a Cohort of Chinese Children With Dopa-Responsive Dystonia

Yan Chen, Xinhua Bao, Yongxin Wen, Jiaping Wang, Qingping Zhang and Jiayou Yan*

Department of Pediatric, Peking University First Hospital, Beijing, China

Background: The aim of this study was to investigate the genetic and clinical features of dopa-responsive dystonia (DRD) in China.

Method: Characteristics of gene mutations and clinical manifestations of 31 patients diagnosed with DRD were analyzed retrospectively.

Result: From January 2000 to January 2019, 31 patients were diagnosed with DRD. Twenty (64.5%) were male, and 11 (35.5%) were female. Ten patients (32.3%) had classic DRD, 19 (61.3%) had DRD-plus, and 2 (6.4%) patients had mutations in the dopamine synthetic pathway (*PTS* gene mutation) without a typical phenotype (not DRD or DRD-plus). Twenty-eight (90.3%) patients underwent genetic testing. Homozygous or compound heterozygous *TH* gene mutations were found in 22 patients. *GCH1* and *PTS* gene mutations were found in 2 patients. Heterozygous *TH* mutation and genetic testing were negative in 1 patient. They took different doses of L-dopa, ranging from 0.4 to 8.7 mg/kg/d. Patients with classic DRD responded well. In patients with DRD-plus, 94.7% (18/19) responded well with residual symptoms. One patient (5.3%) did not show any improvement.

Conclusion: DRD can be divided into classic DRD and DRD-plus. In this cohort, the most common pathogenic gene was *TH*. Fever was the important inducing factor of the disease. L-dopa has sustained and stable effects on patients with classic DRD. In patients with DRD-plus, treatment with L-dopa could ameliorate most of the symptoms.

Keywords: dopa-responsive dystonia, L-dopa, genetic test, clinical and genetic heterogeneity, prognosis of dopa-responsive dystonia

OPEN ACCESS

Edited by:
Andrea Gropman, Children's National Hospital, United States

Reviewed by:
Francesco Nicita, Bambino Gesù Children Hospital (IRCCS), Italy
Juan Dario Ortigoza-Escobar, Pediatric Research Hospital Sant Joan de Déu, Spain

****Correspondence:***
Xinhua Bao
zwhang@pku.edu.cn

Specialty section:
This article was submitted to Pediatric Neurology, a section of the journal Frontiers in Pediatrics

Received: *28 October 2019*
Accepted: *19 February 2020*
Published: *28 February 2020*

Citation:
Chen Y, Bao X, Wen Y, Wang J, Zhang Q and Yan J (2020) Clinical and Genetic Heterogeneity in a Cohort of Chinese Children With Dopa-Responsive Dystonia. Front. Pediatr. 8:83. doi: 10.3389/fped.2020.00083

INTRODUCTION

Dopa-responsive dystonia (DRD) is clinically defined as a kind of hereditary progressive dystonia with marked diurnal fluctuation in tradition. However, with the recognition of the disease, many atypical manifestations have been reported. These issues caused confusion as to what DRD is. For this reason, Jeon et al. suggested that DRD should be genetically defined as a syndrome of selective nigrostriatal dopamine deficiency caused by genetic defects in the dopamine synthetic pathway without nigral cell loss (1). The estimated prevalence of the disease is 0.5–1 per million (2, 3). DRD was first described by Segawa et al. (4). Thereafter, classic DRD has been well-recognized. In recent years, patients with atypical manifestations have been reported. The onset of the disease could be as early as the neonatal period. Some patients had psychomotor retardation, convulsion, and parkinsonism, which may be accompanied by vegetative and fluctuating extrapyramidal symptoms (5–7). For this reason, Jeon et al. proposed the term "DRD-plus" to cover patients with features

that were not seen in classic DRD in 1988 (1, 8). Classic DRD is described as childhood- or adolescent-onset dystonia associated with diurnal fluctuation, parkinsonism, and a good response to a small dosage of L-dopa (9). However, no relationship has been found between genotype and phenotype. Genes involved in DRD include *GCH1*, *TH*, *PTS*, *SPR*, *QDPR,* and *PCBD*. Tyrosine hydroxylase (TH EC 1.14.16.2; gene symbol *TH* OMIM 191290) makes dopamine from tyrosine. Tetrahydrobiopterin (BH4) is a cofactor of tyrosine hydroxylase. The enzymes involved in the *de novo* biosynthesis of BH4 include GTP cyclohydrolase 1 (GCH1 EC 3.5.4.16), encoded by the *GCH1* gene (OMIM 600225); pyruvoyl-tetrahydropterin synthase (PTPS EC 4.6.1.10), encoded by the *PTS* gene (OMIM 612719); and sepiapterin reductase (SR EC 1.1.1.153), encoded by the *SPR* gene (OMIM 182125). In addition to the enzymes related to the biosynthesis of BH4, there are two enzymes related to the regeneration of BH4, pterin-4a-carbinolamine dehydratase (PCD EC 4.2.1.96), encoded by the gene *PCBD* (OMIM 126090), and dihydropterin reductase (DHPR EC 1.6.99.7), encoded by the gene *QDPR* (OMIM 612676). Thus, in theory, the deficiency of any of the above enzymes related to the biosynthesis and recycling of BH4 could be the cause of DRD. Furthermore, BH4 is also an essential cofactor for the activity of other enzymes, such as nitric oxide synthases, phenylalanine and tryptophane hydroxylases (10). These enzymes have many functions, which may explain the clinical heterogeneity.

However, very few reports have published the frequency of gene mutations and the relationship between the genotype and phenotype of DRD. In this study, a cohort of 31 Chinese patients diagnosed with DRD was investigated clinically or genetically. Their clinical characteristics and related mutated genes are reported here.

PATIENTS AND METHODS

Patients

Inclusion Criteria

Patients with dystonia who visited the Department of Pediatrics, Peking University First Hospital between January 2000 and 2019 were recruited. A low dose of L-dopa was administered. We used Burke-Fahn-Marsden (BFM) to measure patients' dystonia and its variation after L-dopa. Patients who met either clinical criteria or genetic criteria were diagnosed with DRD. Clinical criteria refers to patients whose dystonia improved by at least 50% after the treatment. Genetic criteria refers to patients whose genetic analysis showed mutation of the *GCH1*, *PTS*, *SPR*, *TH*, *PCBD,* or *QDPR* genes. All patients were divided into classic DRD or DRD-plus clinically. Classic DRD referred to the patients who had isolated dystonia without other neurological manifestations and a sustained response to a low dose of L-dopa. DRD-plus referred to the patients with the following phenotypes: (1) earlier onset than classic DRD, such as neonatal onset; (2) more severe motor phenotypes, such as poor sucking, swallowing difficulties, and severe hypotonia; and (3) non-motor features (extra-nigrostriatal dopaminergic dysfunctions), such as convulsions (generalized convulsion or myoclonic seizures), psychomotor retardation, mental retardation, drowsiness, irritability, recurrent hyperthermia without infections, and ptosis (9).

Exclusion Criteria

All patients were re-evaluated regardless of their previous diagnosis. Patients who had neither clinical criteria nor genetic criteria were excluded from our cohort.

Clinical Data

The clinical data were carefully collected, including family history, gender, age of onset, age of diagnosis, clinical manifestations of dystonia, and additional features at the time of onset, diurnal fluctuation, neurological signs, treatment and prognosis. The end of follow-up was June 2019.

Genetic Analysis

Genomic DNA was extracted using standard methods from the peripheral blood of the patients and their parents. Polymerase chain reaction (PCR) analysis of *TH* and *GCH1* was performed before 2016. After 2016, patients were analyzed by a targeted next-generation sequencing (NGS) panel containing 20 genes, including *ANO3*, *ATP1A3*, *CACNAA1B*, *GCH1*, *GNAL*, *HPCA*, *PCBD1*, *PNKD*, *PRKRA*, *PRRT2*, *PTS*, *QDPR*, *SGCE*, *SLC2A1*, *SPR*, *TAF1*, *TH*, *THAP1*, *TOR1A*, and *TUBB4A,* or by whole-exome sequencing. MLPA was performed in case 23 in 2019 because the patient had one point mutation that could not explain his disease. Library preparation was carried out following a standard Ion AmpliSeq library preparation protocol (pub. no. MAN0006735). The enriched libraries were sequenced on the Illumina HiSeq 2500 platform (CA, USA) to generate 100 bp paired-end reads. Raw reads were aligned to UCSC hg19 with BWA software. Aligned reads were processed with SAMtools and Picard following the best practice guidelines of the Genome Analysis Toolkit (GATK). Single-nucleotide variants (SNVs) and small insertion-deletions (indels) were detected with the GATK Haplotype Caller.

Multiplex ligation-dependent probe amplification (MLPA) was performed to evaluate large deletions and duplications using the SALSA MLPA Probemix P099 GCH-1-TH-SGCE. The obtained *TH* and *GCH1* gene products were separated and analyzed using the ABI Prism 3100 Genetic Analyser and GeneScan software according to the manufacturer's instructions.

Variants were annotated with ANNOVAR (http://annovar.openbioinformatics.org/en/latest/). Common sites with a population allele frequency above 5% according to the dbSNP 138, 1000 Genomes Project, ESP6500 or ExAC databases were excluded. Variant pathogenicity was interpreted according to the ACMG Standards and Guidelines of 2015. The pathogenic variants were validated by Sanger sequencing.

RESULTS

In total, thirty-one patients were diagnosed with DRD. Among 31 patients, 10 (32.3%) were diagnosed with classic DRD, 19 (61.3%) with DRD-plus, and 2 (6.4%) with 6-pyruvoyl-tetrahydropterin synthase deficiency but without a typical phenotype. Twenty (64.5%) were male, and 11 (35.5%) were female (**Figure 1**).

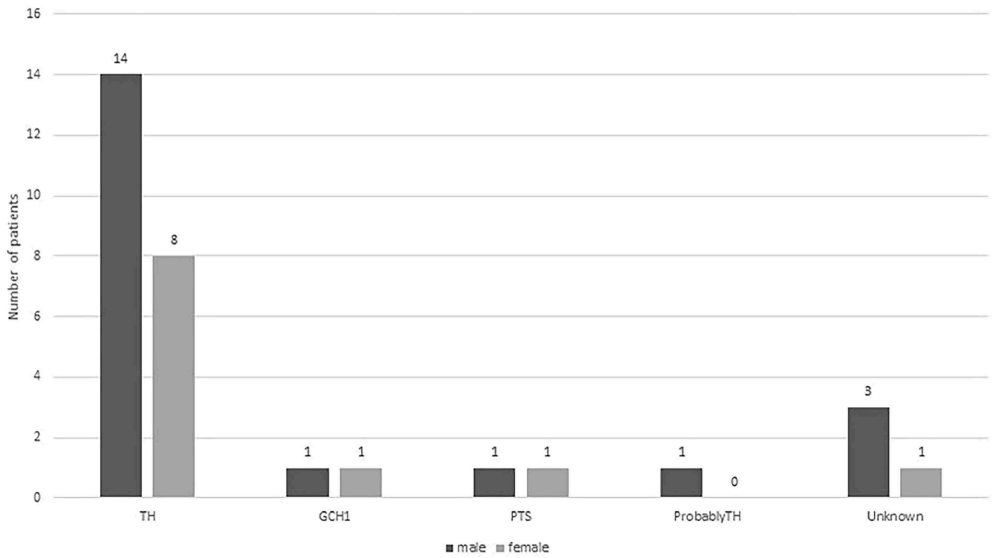

FIGURE 1 | Distributions of boys (dark gray bar) and girls (light gray bars) with different gene mutation.

Eleven of them had a family history of DRD, 10 of them were siblings, and 1 was a daughter and father. Twenty-nine had brain MRI, one (case 11) showed delayed myelination, one showed delayed white matter development, and others were normal. Twenty-eight (90.3%) underwent genetic testing. Twenty-two patients, six of whom were diagnosed with classic DRD and 16 with DRD-plus, had homozygous or compound heterozygous mutations in the *TH* gene. A heterozygous mutation in the *TH* gene was detected in one patient with DRD-plus. Two patients had *GCH-1* mutations and were diagnosed with classic DRD. Two patients had *PTS* gene mutations, and they did not have the clinical features of DRD. Genes related to dopa-responsive dystonia were not detected in one patient. Three patients did not have a genetic test. All patients received different doses of L-dopa, and most responded well, except for 1 patient with DRD-plus caused by *TH* mutation and two patients with 6-pyruvoyl-tetrahydropterin synthase deficiency caused by *PTS* gene mutation.

Unfortunately, cerebrospinal fluid (CSF) neurotransmitters are also very important for the diagnosis of DRD, but we failed to perform these tests. The possible reasons are as follows: (1) many patients came to our hospital many years ago, and although they had lumbar puncture, it was difficult to analyse CSF neurotransmitters at that time; (2) most parents think lumbar puncture injury is very large, and they refused this examination; and (3) compared with lumbar puncture to obtain CSF, parents think genetic testing is more valuable. Once genetic testing has told them the disease of their children, they do not want to have any other tests.

Patients With Mutations of the TH Gene

Homozygous or compound heterozygous mutations in the *TH* gene were found in 22 (78.6%) patients, which is consistent with autosomal recessive inheritance. There were 20 different mutations, including 11 missense mutations, four non-sense mutations, three intron codon site mutations or splicing site mutations, one promoter region mutation and one deletion (frameshift). Among them, 10 mutations were previously unreported, including c.734G>T/p.R245M, c.767C>T/p.T256I, c.1039C>T/p.H347Y, c.668C>T/p.P223L, c.1471G>C/p.D491H, c.738-2A>G, c.1045T>C/p.S349P, c.737+8_c.737+9delGCinsTT, c.1070+1G>T, and c.978-1_c.1019del. All missense mutations were predicted as disease-causing by MutationTaster and Polyphen 2. Mutations c.1070+1G>T, c.738-2A>G and c.737+8_c.737+9delGCinsTT are intron codons in close proximity to exons. Mutation c.978-1_c.1019del is frameshift mutation. The most common point mutation was c.698G>A/p.R233H, with a mutation frequency of 9/44 (20.5%) found in five patients with heterozygous mutations and 2 with homozygous mutations. The second most common mutation was c.739G>A/p.G247S, which was found in seven patients from five families with a mutation frequency of 15.9% (7/44). The mutations c.734C>T/p.R245M, c.694C>T/p.Q232X, c.943G>A/p.G315S, and c.457C>T/p.R153X were found in three patients from two families with a genetic frequency of 3/44 (6.8%). Protein TH consists of four subunits. Each subunit is composed of a regulatory ACT domain with an unstructured N-terminal tail of different lengths (11), a catalytic domain and an oligomerization domain (12). In this cohort, 71.1% (32/45, including the heterozygous mutation reported later) of the mutations were located in the catalytic domain (**Figure 2**). Mutations are detailed in **Table 1**. Eight patients were siblings from four families, including six sisters and one brother from three families and two brothers from one family. One patient with a homozygous *TH* mutation was a child of consanguineous parents. Six patients were diagnosed with classic DRD and 16 DRD-plus. The average age of onset was 12.1 months. Nine patients were misdiagnosed with cerebral palsy, two with

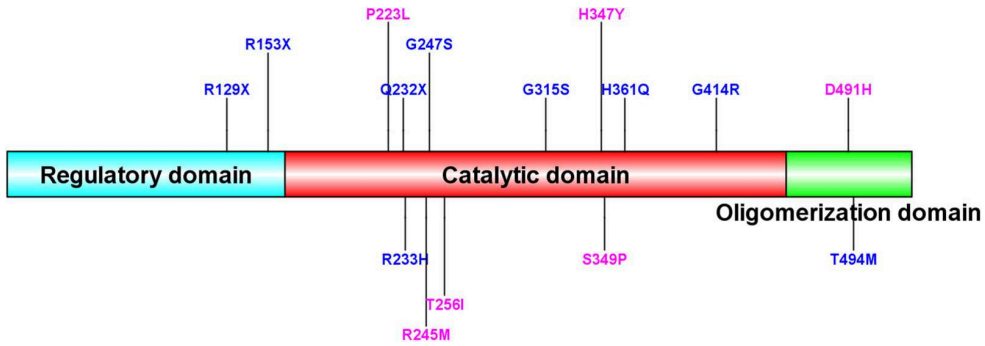

FIGURE 2 | Sequence alignment of human TH (isoform 1) and mutation site of our patients. New TH mutations were drawed in pink color. The protein consists of four subunits. Each subunit is made up of a regulatory ACT domain with an unstructured N-terminal tail of different length, a catalytic domain and an oligomerization domain.

epilepsy, one with muscular dystrophy, and one with metabolic disease. Ten patients had diurnal fluctuations or improvement by sleep or rest. Eight patients had parkinsonism in the course of the disease.

Patients Diagnosed With Classic DRD With TH Mutation

Six patients were diagnosed with classic DRD. The average onset age was 34.5 months, ranging from 15 to 87 months. They could control their heads at an average age of 3 months, ranging from 2 to 4 months old; turn over at an average age of 4.2 months old, ranging from 4 to 5 months old; sit independently at an average age of 6.8 months, ranging from 6 to 8 months; and walk independently 17 months, ranging from 13 to 25 months. Dystonia, as the main symptom, started from the lower limbs in five patients and from the right arm in one patient. Additionally, four patients had diurnal fluctuations, three had parkinsonism, and one had fever before the onset of dystonia. Three were misdiagnosed with cerebral palsy, and one was misdiagnosed with muscular dystrophy. They had taken an average dosage of 3.0 mg/kg/d (range 2.1–5.0 mg/kg/d) of L-dopa for 47.3 months (range 8–120 months). All of them achieved complete remission without obvious side effects.

Interestingly, three boys with *TH* mutations were diagnosed with classic DRD, and their sisters, who had the same mutations, were diagnosed with DRD-plus.

Patients Diagnosed With DRD-plus With TH Mutation

Sixteen patients were diagnosed with DRD-plus, including two brothers from one family. The onset age of the patients ranged from neonate to 13 months old, and the average age was 3.8 months old. Six patients were misdiagnosed with cerebral palsy, and two were misdiagnosed with epilepsy. Six patients had diurnal fluctuations or improvement by sleep or rest. Five patients had parkinsonism in the course of the disease.

Among them, seven were born with generalized dystonia and severe developmental delay. Five of the seven patients could control their heads at an average age of 19.4 months, ranging from 4 to 6 years old; turn over at the average age of 13 months, ranging from 7 to 2 years old; and sit independently at the average age of 22.3 months, ranging from 11 to 4 years old. Only one patient (case 16) could walk with support at the age of 20 months old. Two of the seven patients were never able to control their heads; they could roll and sit when they were diagnosed with DRD-plus at the age of 11 years old and 15 months old, respectively. Three of the seven patients had fever-induced encephalopathy with manifestation of lethargy and severe hypotonia, losing all motor function, including head control, turning over, and sitting.

Six patients had relatively normal development before the onset of the disease. All of them could control the head, five could sit independently, 4 could climb or roll over, and two could stand with support. The onset age ranged from 4 to 13 months, with an average age of 9 months. The patients became severely hypotonic and lost almost all the acquired motor function quickly, including head control and sitting. The regression was induced by fever in three patients. Among them, one patient had fever-induced generalized hypotonia and tremors twice. The other three patients did not have any obvious inducing factors.

Three patients had episodic abnormalities, such as oculogyric crises, hypersalivation, tremor, irritability, repeated vomiting, and rigidity, with an early-onset age of 1–4 months. The symptoms were induced by fever in one patient, and there were no obvious causative factors in the other two patients.

All patients had taken L-dopa 1.0 to 6.7 mg/kg/d (average 3.7 mg/kg/d) for 49.9 months (range 9 months to 11 years). Fifteen patients had a dramatic response; however, only two of these patients became completely normal, two patients retained abnormal posture because of delayed treatment, and 11 patients still had symptoms such as concentration deficiency, dysarthria, poor coordination, lethargy, fatigue, and abnormal gait. No improvement was achieved in one patient. The patient (case 12) had poor sucking and repeated vomiting accompanied by episodic head backward, limb stiffness and staring when she was 1 month old. Genetic testing was performed in China and Japan

TABLE 1 | Clinical manifestations of patients with *TH* mutation.

	Diagnosed year	Gender	Family history	Age of onset	Diurnal fluctuation	Site of onset	Diagnosis	Gene locus	Amino acid alteration	L-dopa mg/kg/d	Misdiagnosed	Outcome
1	2005	M	No	7m	No	Generalized	DRD-plus	c.698G>A c.385C>T	p.R233H p.R129X	3.3		Concentration deficiency, easily tired
2	2008	F	Yes	8m	No	Generalized	DRD-plus	c.734G>T c.457C>T	p.R245M p.R153X	3.0	Cerebral palsy	Abnormal posture
3	2008	M	Yes	15m	Yes	LL	Classic DRD	c.734G>T c.457C>T	p.R245M p.R153X	2.5	Cerebral palsy	Normal
4	2011	M	Yes	0m	No	Generalized	DRD-plus	c.739G>A c.1045T>c	p.G247S p.S349P	5.7	Cerebral palsy	Concentration deficiency
5	2011	M	Yes	0m	No	Generalized	DRD-plus	c.739G>A c.1045T>c	p.G247S p.S349P	4.0	Cerebral palsy	Concentration deficiency
6	2012	M	No	12m	Yes	Generalized	DRD-plus	c.698G>A c.698G>A	p.R233H p.R233H	1.3	Cerebral palsy	Concentration deficiency, i Poor coordination
7	2013	M	No	4m	No		DRD-plus	c.698G>A c.1070+1G>T	p.R233H	6.7	Epilepsy	Normal
8	2013	M	No	4m	Yes	Generalized	DRD-plus	c.698G>A c.943G>A	p.R233H p.G315S	4.7	Metabolic disease	Normal
9	2014	F	No	18m	No	LL	Classic DRD	c.767C>T IVS9-1_c.1019del	p.T256I	3.0	Cerebral palsy	Normal
10	2015	M	No	10m	Yes	Generalized	DRD-plus	c.698G>A (G-A)-70 to initiation codon	p.R233H	2.5		Drowsiness, easily tired, poor coordination
11	2015	F	No	0m	No	Generalized	DRD-plus	c.1471G>C c.739G>A	p.D491H p.G247S	3.4		Wide-based gait, Poor coordination
12	2015	F	No	1m	No		DRD-plus	c.1039C>T c.738-2A>G	p.H347Y	1.0	Epilepsy	Sever hypotonia, drooling, Mental retardation
13	2016	M	Yes	48m	Yes	LL	Classic DRD	c.1481C>T c.943G>A	p.T494M p.G315S	3.0		Normal
14	2016	F	Yes	0m	No	Generalized	DRD-plus	c.1481C>T c.943G>A	p.T494M p.G315S	6.5	Cerebral palsy	Abnormal postures
15	2016	M	No	19m	Yes	LL	Classic DRD	c.1240G>A c.1083C>G	p.G414R p.H361Q	5.0	Cerebral palsy	Normal
16	2016	F	No	0m	No	Generalized	DRD-plus	c.739G>A c.694C>T	p.G247S p.Q232X	3.0	Cerebral palsy	Wide-based gait
17	2016	M	No	1m	No		DRD-plus	c.698G>A c.457C>T	p.R233H p.R153X	6.3		Wide-based gait
18	2017	M	No	0m	Yes	Generalized	DRD-plus	c.734G>T c.668C>T	p.R245M p.P223L	4.2		Concentration deficiency
19	2017	F	Yes	0m	Yes	Generalized	DRD-plus	c.739G>A c.694C>T	p.G247S; p.Q232X	2.6		Abnormal posture
20	2017	M	Yes	20m	Yes	LL	Classic DRD	c.739G>A c.694C>T	p.G247S p.Q232X	2.1	Muscular dystrophy	Normal
21	2018	F	No	13m	Yes	Generalized	DRD-plus	c.698G>A c.698G>A	p.R233H p.R233H	1.1		Poor coordination
22	2018	M	No	87m	No	UL	Classic DRD	c.739G>A c.737+8_c.737+9delGCinsTT	p.G247S	2.5		Normal
23	2017	M	No	4.5m	Yes	Generalized	DRD-plus	c.1481C>T heterozygous mutation	p.T494M	4.6		Wide-based gait, drooling

LL, lower limbs; UL, upper limbs.

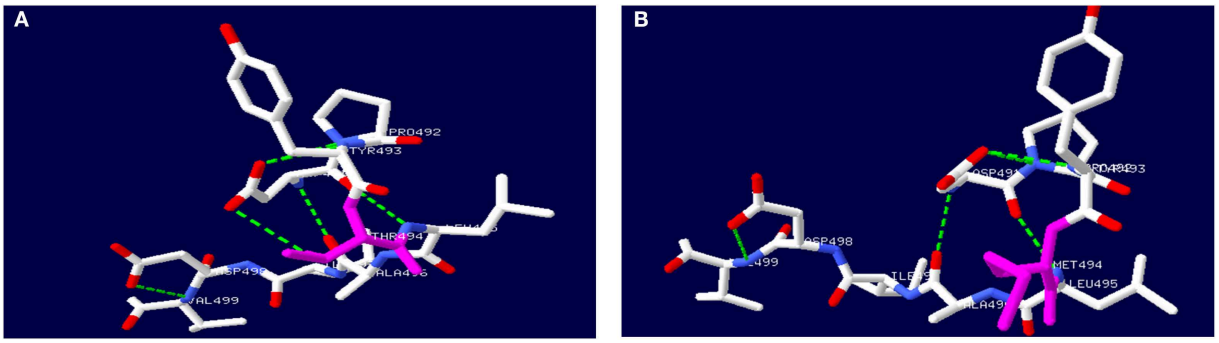

FIGURE 3 | Secondary structure prediction of TH protein by Swiss PDB software. **(A)** showed wild-type TH protein. **(B)** showed mutated TH protein with c.1481C>T, p.T494M gene mutation.

and found the same TH mutations of c.1039C>T/p.347H>Y and c.738-2A>G. The symptoms worsened after L-dopa was added.

Patient Disease Is Probably Caused by TH Mutation

In one patient (case 23), a heterozygous *TH* gene mutation in c.1481C>T/ p.T494M inherited from his asymptomatic mother was found. The mutation test was repeated several times by different companies using whole-exome sequencing, Sanger sequencing and MLPA testing of *TH* and *GCH1* genes. No mutations, including large fragment deletions, were found in the other allele of the *TH* gene. According to his clinical manifestation, DRD-plus was diagnosed. He could control his head at 3 months old, turn over and had eye contact before the onset of the disease. At 4.5 months of age, generalized hypotonia and tremors presented after fever. He lost the ability to control his head and turn over within several days. A low dose of L-dopa (4.6 mg/kg/d) was used for 19.5 months. The tremors disappeared, and the hypotonia improved dramatically 3 days after the treatment. He could sit independently at 6 months old, walk at 1 year and 5 months old, and verbally communicate at 1 year and 7 months old. However, he still had wide-based gait and drooling at 2 years of age. He had diurnal fluctuation and parkinsonism in the course of the disease.

The *TH* gene mutation of c.1481C>T/p.T494M is located in the oligomerization domain. Secondary structure prediction of TH protein with this mutation by Swiss PDB software is shown in **Figure 3**. The mutation causes the hydrogen bond between aspartic acid (491) and methionine (494) to break. No large deletion was found after MLPA. His parents refused other tests, including CSF, blood or urine, because these tests had no use for treatment.

Mutations in the GCH1 Gene or PTS Gene

Two patients (6.5%) had *GCH1* gene mutations and were diagnosed with classic DRD, with dystonia beginning in the lower limbs, diurnal fluctuation, improvement by sleep or rest and a sustained response to L-dopa. One patient (a girl, case 24) with a family history of dystonia had dystonia that started from her right toes when she was 2 years old after fever. Her father had the same *GCH1* gene mutation of c.631_632delAT (p.Met211ValfsTer38). He had parkinsonism after extensive writing when he was 27 years old. After taking L-dopa, his symptoms disappeared. Detailed information is shown in **Table 2**.

Two patients had *PTS* gene mutations. The main symptoms included drowsiness, sleeping 15–16 h daily, episodic abnormal behavior and movement such as tremor, stiffness, bradykinesia, drooling, stereotyped movement, involuntary smile, and difficulty talking. Both had diurnal fluctuations or improvement by sleep or rest. The symptoms were induced by fever in one patient. These symptoms presented when they were tired or emotionally stressed at the beginning and became increasingly frequent. They were prone to tiring. All of them were believed to be epileptic. There was no response to antiepileptic drugs such as valproate sodium, topiramate and levetiracetam and no epileptic discharge on EEG during the attacks. They underwent urinary pterin spectrum analysis, and they both had decreased biopterin concentrations and normal neopterin concentrations. After confirming the diagnosis of pyruvoyl-tetrahydropterin synthase deficiency, L-dopa was given at doses of 1 and 1.9 mg/kg/d with no response. The symptoms were significantly improved only after administration of tetrahydrobiopterin (1.88 mg/kg/d). To date, none of the patients had obvious side effects after treatment for 3 and 5 years. Detailed information is shown in **Table 2**.

Patients Without Mutation or Without Genetic Testing

In 1 patient (case 28) with classic DRD, no mutation was found by whole-exome sequencing, Sanger sequencing or MLPA of the *TH* and *GCH1* genes. Three patients did not have a gene test. One patient (case 28) had fever before dystonia began. Two patients were misdiagnosed with cerebral palsy, and one was misdiagnosed with epilepsy. Two patients (case 28 and case 31) had typical symptoms of classic DRD, such as dystonia beginning from the lower limbs, mild parkinsonism, diurnal fluctuation and improvement after sleep or rest, and sustained response to low doses of L-dopa. The other two cases (case 29 and case 30) were older brothers and younger sisters.

TABLE 2 | Clinical manifestations of Patients with *GCH1* and *PTS* mutations.

	Diagnosed year	Gender	Age of onset	Diurnal fluctuation	Family history	Diagnosis	Urine biopterin	Urine neopterin	Gene	Gene locus	Amino acid alteration	L-dopa mg/kg/d	Outcome
24	2002	F	2y	Yes	Yes	Classic DRD			GCH-1	c.631_632delAT	p.Met211Valfs Ter38	0.4	Normal
25	2016	M	5y	Yes		Classic DRD			GCH-1	c.548A>C	p.E183A	1.8	Normal
26	2014	M	10y11m	Yes			Decreased	Normal	PTS	c.166G>A c.286G>A	p.V56M p.D96N	1.9	Wide-based gait
27	2016	F	3y	Yes			Decreased	Normal	PTS	c.272A>G c.286G>A	p.K91R p.D96N	1.0	Wide-based gait

TABLE 3 | Clinical manifestations of patients without mutation or without test.

	Diagnosed year	Gender	Age of onset	Site of onset	Diurnal fluctuation	Family history	Diagnosis	Gene locus	L-dopa mg/kg/d	Outcome
28	2012	M	7y5m	LL	Yes	No	Classic DRD	Negative	8.7	Normal
29	2009	F	3m		Yes	Yes	DRD-plus	No test	3.5	Normal
30	2009	M	3m		Yes	Yes	DRD-plus	No test	2.3	Normal
31	2010	M	1y	LL	Yes	No	Classic DRD	No test	3.5	Normal

LL, lower limbs.

They had similar symptoms, such as early onset at 3 months old, diurnal fluctuation, parkinsonism and episodic staring, head tilting, and gnathospasmus. A low dose of L-dopa was administered after the diagnosis of DRD-plus, and the patient achieved quick remission. Detailed information is shown in **Table 3**.

DISCUSSION

DRD is a disease with typical manifestations of childhood or adolescent onset, marked diurnal fluctuations and improvement by L-dopa. With the recognition of the disease, various atypical presentations and variable onset ages have been reported. DRD-plus can be diagnosed as patients with dystonia and other atypical symptoms, such as convulsion, ptosis, severe dystonia and autonomic symptoms. Clot et al. (13) reported 64 patients, of whom 57 (89.1%) had classic DRD, and 7 (10.9%) had DRD-plus. The subtype distribution is different from this cohort of 31 patients, in whom 10 patients (32.3%) had classic DRD, 19 (61.3%) had DRD-plus, and two had 6-pyruvoyl-tetrahydropterin synthase deficiency (6.4%). With the development of next-generation sequencing (NGS), more patients with atypical symptoms of DRD had been diagnosed (**Figure 4**). There was also a difference in gender distribution between this cohort and the reported cohort of Nygaard. In his report, females were affected 2.5–4 times more than males (13, 14). In this cohort, males were 1.9 times more common than females. In classic DRD, the ratio of males to females is 4:1, and in DRD-plus, the ratio of males to females is 11:8. Moreover, the GCH1 mutation was the most common gene mutation; however, in this cohort, the *TH* gene mutation was the most common. The ratio of *TH* to *GCH1* mutation was 11:1. We suppose these differences may be attributed to racial background. Unfortunately, no reports were found to support this supposition.

Genes related to tyrosine hydroxylase, biosynthesis and recycling of BH4, including *GCH1*, *TH*, *PTS*, *SPR*, *PCBD,* and *QDPR,* were thought to be the causative genes of DRD. In Clot's report, the most common pathogenic gene is *GCH1* (13), with autosomal dominant heredity (2, 13, 15–17). The diseases related to the *GCH1* mutation were classified into three different types (18): (1) autosomal dominant heredity characterized by classical DRD and always accompanied with no hyperphenylalaninemia (HPA) because the autosomal dominant *GCH1* mutation has selective defect expression in the brain and not in the liver (9). (2) Autosomal recessive *GCH1* deficient with HPA. The patients always have severe neurologic disorders, such as psychomotor retardation and convulsions. (3) Compound heterozygous mutation displayed between the above. In Clot's report (13), 47 patients (73.4%, 47/64) carried a heterozygous mutation in *GCH1*. However, in our cohort, there were only two patients (7.1%, 2/28) with heterozygous *GCH1* mutations, in accordance with autosomal dominant inheritance. The manifestations belonged to classic DRD without HPA. Clinical heterogeneity presented in a family (case 24). Males have a later onset age, milder phenotype, and lower penetrance than females, which has also been previously reported (19, 20). Twenty-two patients (78.6%, 22/28) had compound heterozygous mutations or homozygous mutations of the *TH* gene in accordance with autosomal recessive inheritance, which was the most common genetic mutation in this cohort. TH is the limiting enzyme of catecholamine neurotransmitters (21). The phenotypes caused by *TH* gene

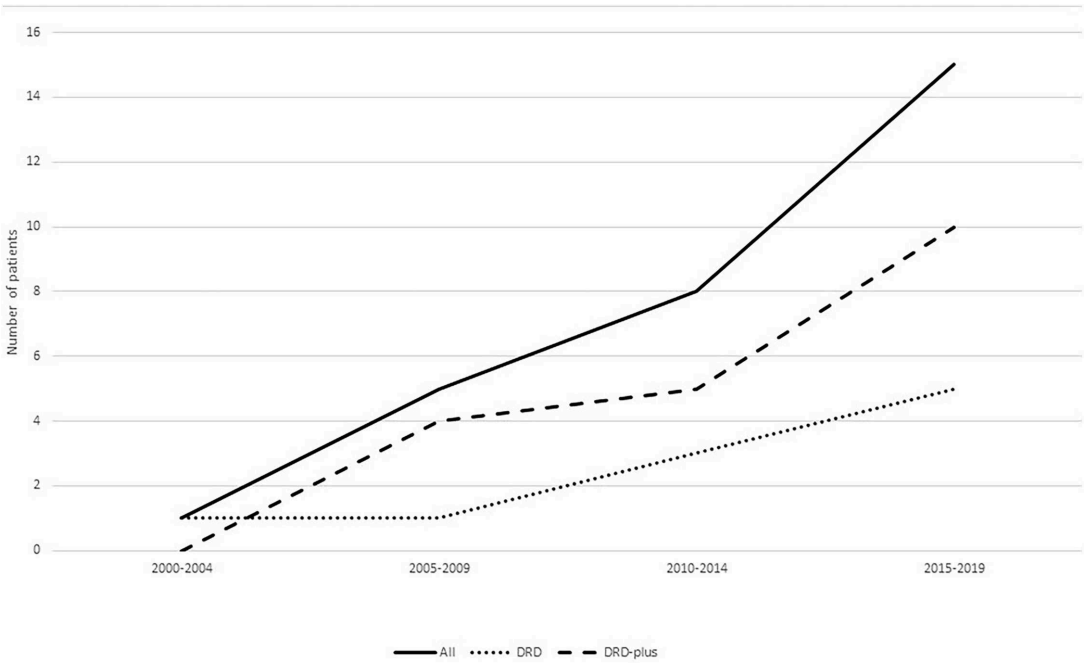

FIGURE 4 | Patients diagnosed with DRD in different years. With the recognition of the disease, more and more patients were diagnosed especially patients diagnosed with DRD-plus.

mutation have been summarized as follows: (1) progressive infantile encephalopathy (22, 23), which refers to patients who mainly showed motor retardation, fluctuating extrapyramidal and autonomic symptoms that treatment with L-dopa could ameliorate symptoms but usually does not normalize (23), (2) classic DRD (24–26), and (3) L-dopa-responsive infantile parkinsonism with good response to L-dopa that was limited by dyskinesia, which refers to patients who had early-onset severe motor problems, including parkinsonism and myoclonic jerks (27). The first and third types were classified as DRD-plus. In the largest published study of 36 patients with TH mutations, the phenotype was classified into two major types (28): type A: progressive hypokinetic-rigid syndrome with dystonia; and type B: complex encephalopathy. The onset age of type A is usually before 1 year of age (range 2 months−5 years old) (13, 22, 26, 29–33), with slowly progressive paroxysmal dystonia and rare additional symptoms (tremor, ptosis, oculogyric crises). The onset age of type B is usually earlier (at birth or within a few weeks of birth) and develops more quickly than type A (23, 34, 35). The onset symptoms are complicated, but they finally develop into marked hypokinesia, bradykinesia and dystonic symptoms. Type B might be accompanied by mental retardation and autonomic functions (36). Type A was similar to classic DRD, and type B was similar to classic DRD-plus in this study.

In this cohort, 72.7% (16/22) of the patients with homozygous or compound heterozygous *TH* gene mutations were DRD-plus. Only 27.3% (6/22) were classic DRD. Fourteen of them were boys, and 8 were girls, with a male to female ratio of 1.75:1. Eight patients had a family history. Six patients were older sisters and younger brothers from three families. However, all the older sisters were DRD-plus, and the younger brothers were classic DRD. This means that the same mutation can result in different manifestations, and females had more severe symptoms than males. The causes of these results need further study. The other two patients were brothers. They had similar manifestations and were diagnosed with DRD-plus.

Only a heterozygous mutation of the *TH* gene was found in a patient with DRD-plus by an extensive gene mutational test, which was inherited from his asymptomatic mother. The mutation c.1481C>T/p.T494M was first reported by Swaans et al. (26). In his report, the mutation was found in two patients with classic DRD from the same family, which were compound heterozygous mutations of c.1010G>A/p.R337H and c.1481C>T/p.T494M. However, only a heterozygous mutation was found in our patient. Whether there is a mutation in the non-coding region of the other allele or there are other mechanisms is unknown. No data about incomplete penetrance have been reported to date. TH belongs to BH4-dependent aromatic amino acid hydroxylases and consists of four identical subunits, with each subunit consisting of three domains (11). TH needs an enzyme-bound non-heme ferrous iron (Fe^{2+}), 6R-tetrahydrobiopterin (BH_4) as a cofactor, and molecular oxygen (O_2) as an additional substrate for catalysis. Functional characterization and *in silico* analysis showed that the mutation c.1481C>T caused the hydrophilic threonine

substituted by a hydrophobic methionine, which led to the breaking of the hydrogen bond and the changing of the α-helix. Finally, tetramer formation was influenced (**Figure 3**). Whether the severely damaged TH protein structure alone through heterozygous mutation causes the disease needs further study. However, this could not explain why the mother with the same mutation had no symptoms. We presumed that there may be a mutation in the promoter, enhancer, or intron in the other allele.

Generalized dystonia with marked diurnal fluctuation or dystonia presented in the eyelids, mandibular region, trunk, and extremities was observed in patients with *PTS* gene mutations. Other clinical features, such as severe hypotonia, bedridden status, dysphagia, lack of eye contact, small for gestational age, failure to thrive, microcephaly, odd smell, blond hair, frequent pneumonia, hyperthermia, and HPA, were reported (37). PTS mutations are often accompanied by HPA and can be diagnosed early and treated with dopamine and/or BH4, which prevents DRD-like symptoms (13, 38). Only 7.1% of patients (2/28) were found to have compound heterozygous mutation *PTS* mutations in this cohort. They did not have a good response to L-dopa and required BH4 to normalize the symptoms and phenylalanine concentration, as reported in the literature (37). They were included because of *PTS* mutations. Disease caused by *PTS* mutation was recently categorized as dopa-reactive dystonia, but a low dose of L-dopa could not ameliorate patients' symptoms. Dystonia caused by *PTS* mutation requires the treatment of both L-dopa and BH4, which do not meet the clinical diagnosis of DRD. Therefore, whether the disease caused by *PTS* mutation should be classified as dopa-responsive dystonia is debatable. Other gene mutations were not found in this cohort because these enzyme deficiencies result in HPA, which can be detected and treated early to prevent the onset of the disease.

DRD has broad clinical heterogeneity that is often misdiagnosed as diplegic cerebral palsy or hereditary spastic paraplegia due to the brisk lower limb tendon reflexes, increased lower limb tone and spurious striatal plantar response (39). DRD can also be misdiagnosed as epilepsy because of episodic dystonia and abnormal behavior (40). In this study, 11 patients had been misdiagnosed with cerebral palsy, and five patients had been misdiagnosed with epilepsy. Compared with DRD, cerebral palsy is a static disease other than a progressive disease, does not respond to L-dopa administration and has characteristic patterns in neuroimaging that are not observed in DRD. Overall, once dystonia is displayed in patients, we should let patients take a low dose of L-dopa to avoid misdiagnosis. With regard to the differential diagnosis with epilepsy, it is known that interictal and specially ictal EEG are useful to identify epileptic seizures; additionally, ictal and post-ictal epileptic manifestations may have specific features which are not encountered in DRD.

According to the literature, DRD can always be treated with L-dopa, but residual symptoms can be observed. A low dose of L-dopa (1–5 mg/kg/d) treatment had a significant effect, especially on the symptoms of dystonia. L-dopa should be started at 1 mg/kg/day, and it is advisable to add 1 mg/kg over several days or weeks. A higher dose of dopamine, 20 mg/kg/d in children or 1,000 mg/day in adults, could be used in patients diagnosed with classic DRD or DRD-plus (41, 42). The response of L-dopa is usually stable; it is rare for patients to develop dyskinesia, but dance-like movements or athetosis occasionally appear (41), and the rate is not known. Although a dramatic response can be observed in patients with *GCH1* mutations, some still have residual motor symptoms (females are more common), such as dystonia and parkinsonism (43, 44). L-dopa used to treat autosomal recessive GCH1 deficiency requires high doses in childhood (45). Patients with autosomal recessive *GCH1* mutations might need to be treated with BH4 and 5-hydroxytryptophan (the precursor of 5-HT) in addition to L-dopa (46). In patients with *TH* mutations, the response to L-dopa is different, which is contrary to the severity of symptoms (28). For the symptoms of the non-motor system presented in DRD-plus, the response to L-dopa is not as good (31). However, there have been reports of L-dopa-related dyskinesia in patients with *TH* mutations in the early stages of treatment (47, 48). The pathophysiological basis of dyskinesia in DRD is unclear (49). When these situations occur, reducing L-dopa and oral amantadine may be helpful (41, 47). Hwang et al. reported patients with dyskinesia after taking L-dopa 11.6 years (0.5–25 years), with a daily mean L-dopa dose of 343.8 mg/d (range 100–600 mg/d). The amount of L-dopa should be gradually reduced over time if taking the drug over a prolonged period to avoid dyskinesia and recurrent DRD symptoms (41). In this study, the dosage of L-dopa ranged from 0.4 to 8.7 mg/kg/d. Normal posture and movement were achieved in 10 patients diagnosed with classic DRD after a low dose of L-dopa for 8 months to 16 years without obvious side effects. In 19 patients with DRD-plus, L-dopa was used for 9 months to 10 years; four recovered completely, and 14 responded well, though they still had problems such as imbalance, abnormal posture, wide-based gait, concentration deficiency, fatigue, excessive drooling, hypotonia, drowsiness, and mental retardation. Only one patient had no response, and the reason was unknown. Patients in this cohort did not have obvious side effects.

In conclusion, there is broad genetic and clinical heterogeneity in DRD. In recent years, the disease has been diagnosed more easily since NGS has been commonly used, and the atypical manifestations have been recognized more clearly. Several gene mutations could cause DRD. In our study, the most common mutation was in the *TH* gene. Patients with classic DRD have good and sustained responses to low doses of L-dopa. In patients with DRD-plus, although most of them had a good response, some non-motor symptoms remained. Delays in diagnosis and treatment can lead to irreversible abnormalities, so enhancing clinicians' knowledge about DRD is very important.

DATA AVAILABILITY STATEMENT

The data used and/or analyzed are available from the corresponding author.

ETHICS STATEMENT

This study was approved by the Clinical Research Ethics Committee, Peking University. Written informed consent was obtained from parents of participants or participants of the study.

AUTHOR CONTRIBUTIONS

XB designed and conceptualized the study and revised the manuscript. YC designed the study, collected patient information, and drafted the manuscript. YW, JW, QZ, and JY provided help in the genetic analysis and collection of patient information. All authors have approved the publication of the manuscript.

FUNDING

This study was financially supported by 985 Peking University and Clinical Hospital Cooperation Project (2013-1-06) and Wu Jieping Medical Fund (320.6750.17091).

ACKNOWLEDGMENTS

We thank the patients and their parents for their support in this study.

REFERENCES

1. Jeon BS, Jeong JM, Park SS, Lee MC. Dopa-responsive dystonia: a syndrome of selective nigrostriatal dopamine deficiency. *Adv Neurol.* (1998) 78:309–17. doi: 10.3346/jkms.1997.12.4.269
2. Zirn B, Steinberger D, Troidl C, Brockmann K, von der Hagen M, Feiner C, et al. Frequency of GCH1 deletions in Dopa-responsive dystonia. *J Neurol Neurosurg Psychiatry*. (2008) 79:183–6. doi: 10.1136/jnnp.2007.128413
3. Nygaard TG. Dopa-responsive dystonia. Delineation of the clinical syndrome and clues to pathogenesis. *Adv Neurol.* (1993) 60:577–85.
4. Segawa M, Hosaka A, Miyagawa F, Nomura Y, Imai H. Hereditary progressive dystonia with marked diurnal fluctuation. *Adv Neurol*. (1976) 14:215–33.
5. Nygaard TG, Takahashi H, Heiman GA, Snow BJ, Fahn S, Calne DB. Long-term treatment response and fluorodopa positron emission tomographic scanning of parkinsonism in a family with dopa-responsive dystonia. *Ann Neurol.* (1992) 32:603–8. doi: 10.1002/ana.410320502
6. Chaila EC, McCabe DJ, Delanty N, Costello DJ, Murphy RP. Broadening the phenotype of childhood-onset dopa-responsive dystonia. *Arch Neurol.* (2006) 63:1185–8. doi: 10.1001/archneur.63.8.1185
7. Furukawa Y, Kish SJ, Bebin EM, Jacobson RD, Fryburg JS, Wilson WG, et al. Dystonia with motor delay in compound heterozygotes for GTP-cyclohydrolase I gene mutations. *Ann Neurol.* (1998) 44:10–6. doi: 10.1002/ana.410440107
8. Jeon BS, Jeong JM, Park SS, Kim JM, Chang YS, Song HC, et al. Dopamine transporter density measured by [123I]beta-CIT single-photon emission computed tomography is normal in dopa-responsive dystonia. *Ann Neurol.* (1998) 43:792–800. doi: 10.1002/ana.410430614
9. Lee WW, Jeon BS. Clinical spectrum of dopa-responsive dystonia and related disorders. *Curr Neurol Neurosci Rep.* (2014) 14:461. doi: 10.1007/s11910-014-0461-9
10. Thony B, Auerbach G, Blau N. Tetrahydrobiopterin biosynthesis, regeneration and functions. *Biochem J.* (2000) 347(Pt 1):1–16. doi: 10.1042/bj3470001
11. Bezem MT, Baumann A, Skjaerven L, Meyer R, Kursula P, Martinez A, et al. Stable preparations of tyrosine hydroxylase provide the solution structure of the full-length enzyme. *Sci Rep*. (2016) 6:30390. doi: 10.1038/srep30390
12. Fitzpatrick PF. Structural insights into the regulation of aromatic amino acid hydroxylation. *Curr Opin Struct Biol.* (2015) 35:1–6. doi: 10.1016/j.sbi.2015.07.004
13. Clot F, Grabli D, Cazeneuve C, Roze E, Castelnau P, Chabrol B, et al. Exhaustive analysis of BH4 and dopamine biosynthesis genes in patients with Dopa-responsive dystonia. *Brain J Neurol.* (2009) 132:1753–63. doi: 10.1093/brain/awp084
14. Nygaard TG. Dopa-responsive dystonia. *Curr Opin Neurol.* (1995) 8:310–3. doi: 10.1097/00019052-199508000-00011
15. Horvath GA, Stockler-Ipsiroglu SG, Salvarinova-Zivkovic R, Lillquist YP, Connolly M, Hyland K, et al. Autosomal recessive GTP cyclohydrolase I deficiency without hyperphenylalaninemia: evidence of a phenotypic continuum between dominant and recessive forms. *Mol Genet Metab*. (2008) 94:127–31. doi: 10.1016/j.ymgme.2008.01.003
16. Furukawa Y, Guttman M, Sparagana SP, Trugman JM, Hyland K, Wyatt P, et al. Dopa-responsive dystonia due to a large deletion in the GTP cyclohydrolase I gene. *Ann Neurol.* (2000) 47:517
17. Huang CL, Lan MY, Chang YY, Hsu CY, Lai SC, Chen RS, et al. Large SGCE deletion contributes to Taiwanese myoclonus-dystonia syndrome. *Parkinsonism Relat. Disord.* (2010) 16:585–9. doi: 10.1016/j.parkreldis.2010.06.016
18. Hahn H, Trant MR, Brownstein MJ, Harper RA, Milstien S, Butler IJ. Neurologic and psychiatric manifestations in a family with a mutation in exon 2 of the guanosine triphosphate-cyclohydrolase gene. *Arch Neurol.* (2001) 58:749–55. doi: 10.1001/archneur.58.5.749
19. Trender-Gerhard I, Sweeney MG, Schwingenschuh P, Mir P, Edwards MJ, Gerhard A, et al. Autosomal-dominant GTPCH1-deficient DRD: clinical characteristics and long-term outcome of 34 patients. *J Neurol Neurosurg Psychiatry*. (2009) 80:839–45. doi: 10.1136/jnnp.2008.155861
20. Goodchild RE, Grundmann K, Pisani A. New genetic insights highlight "old" ideas on motor dysfunction in dystonia. *Trends Neurosci.* (2013) 36:717–25. doi: 10.1016/j.tins.2013.09.003
21. Rilstone JJ, Alkhater RA, Minassian BA. Brain dopamine-serotonin vesicular transport disease and its treatment. *N Engl J Med*. (2013) 368:543–50. doi: 10.1056/NEJMoa1207281
22. Ribases M, Serrano M, Fernandez-Alvarez E, Pahisa S, Ormazabal A, Garcia-Cazorla A, et al. A homozygous tyrosine hydroxylase gene promoter mutation in a patient with dopa-responsive encephalopathy: clinical, biochemical and genetic analysis. *Mol Genet Metab*. (2007) 92:274–7. doi: 10.1016/j.ymgme.2007.07.004
23. Hoffmann GF, Assmann B, Brautigam C, Dionisi-Vici C, Haussler M, de Klerk JB, et al. Tyrosine hydroxylase deficiency causes progressive encephalopathy and dopa-nonresponsive dystonia. *Ann Neurol.* (2003) 54(Suppl.6):S56–65. doi: 10.1002/ana.10632
24. Schiller A, Wevers RA, Steenbergen GC, Blau N, Jung HH. Long-term course of L-dopa-responsive dystonia caused by tyrosine hydroxylase deficiency. *Neurology*. (2004) 63:1524–6. doi: 10.1212/01.WNL.0000142083.47927.0A
25. Ludecke B, Dworniczak B, Bartholome K. A point mutation in the tyrosine hydroxylase gene associated with Segawa's syndrome. *Hum Genet*. (1995) 95:123–5. doi: 10.1007/bf00225091
26. Swaans RJ, Rondot P, Renier WO, van Den Heuvel LP, Steenbergen-Spanjers GC, Wevers RA. Four novel mutations in the tyrosine hydroxylase gene in patients with infantile parkinsonism. *Ann Hum Genet*. (2000) 64:25–31. doi: 10.1046/j.1469-1809.2000.6410025.x
27. Ludecke B, Knappskog PM, Clayton PT, Surtees RA, Clelland JD, Heales SJ, et al. Recessively inherited L-DOPA-responsive parkinsonism in infancy caused by a point mutation (L205P) in the tyrosine hydroxylase gene. *Hum Mol Genet*. (1996) 5:1023–8. doi: 10.1093/hmg/5.7.1023
28. Willemsen MA, Verbeek MM, Kamsteeg EJ, de Rijk-van Andel JF, Aeby A, Blau N, et al. Tyrosine hydroxylase deficiency: a treatable disorder

of brain catecholamine biosynthesis. *Brain J Neurol.* (2010) 133:1810–22. doi: 10.1093/brain/awq087
29. Furukawa Y, Graf WD, Wong H, Shimadzu M, Kish SJ. Dopa-responsive dystonia simulating spastic paraplegia due to tyrosine hydroxylase (TH) gene mutations. *Neurology*. (2001) 56:260–3. doi: 10.1212/wnl.56.2.260
30. Wu ZY, Lin Y, Chen WJ, Zhao GX, Xie H, Murong SX, et al. Molecular analyses of GCH-1, TH, and parkin genes in Chinese dopa-responsive dystonia families. *Clin Genet*. (2008) 74:513–21. doi: 10.1111/j.1399-0004.2008.01039.x
31. Giovanniello T, Leuzzi V, Carducci C, Carducci C, Sabato ML, Artiola C, et al. Tyrosine hydroxylase deficiency presenting with a biphasic clinical course. *Neuropediatrics*. (2007) 38:213–5. doi: 10.1055/s-2007-991151
32. Diepold K, Schutz B, Rostasy K, Wilken B, Hougaard P, Guttler F, et al. Levodopa-responsive infantile parkinsonism due to a novel mutation in the tyrosine hydroxylase gene and exacerbation by viral infections. *Mov Disord*. (2005) 20:764–7. doi: 10.1002/mds.20416
33. de Rijk-Van Andel JF, Gabreels FJ, Geurtz B, Steenbergen-Spanjers GC, van Den Heuvel LP, Smeitink JA, et al. L-dopa-responsive infantile hypokinetic rigid parkinsonism due to tyrosine hydroxylase deficiency. *Neurology*. (2000) 55:1926–8. doi: 10.1212/wnl.55.12.1926
34. P DEL, Nassogne MC, van Gennip AH, van Cruchten AC, Billatte de Villemeur T, Cretz M, et al. Tyrosine hydroxylase deficiency unresponsive to L-dopa treatment with unusual clinical and biochemical presentation. *J Inherit Metab Dis*. (2000) 23:819–25. doi: 10.1023/A:1026760602577
35. Zafeiriou DI, Willemsen MA, Verbeek MM, Vargiami E, Ververi A, Wevers R. Tyrosine hydroxylase deficiency with severe clinical course. *Mol Genet Metab*. (2009) 97:18–20. doi: 10.1016/j.ymgme.2009.02.001
36. Wijemanne S, Jankovic J. Dopa-responsive dystonia–clinical and genetic heterogeneity. *Nat Rev Neurol*. (2015) 11:414–24. doi: 10.1038/nrneurol.2015.86
37. Niu DM. Disorders of BH4 metabolism and the treatment of patients with 6-pyruvoyl-tetrahydropterin synthase deficiency in Taiwan. *Brain Dev*. (2011) 33:847–55. doi: 10.1016/j.braindev.2011.07.009
38. Hanihara T, Inoue K, Kawanishi C, Sugiyama N, Miyakawa T, Onishi H, et al. 6-Pyruvoyl-tetrahydropterin synthase deficiency with generalized dystonia and diurnal fluctuation of symptoms: a clinical and molecular study. *Mov Disord*. (1997) 12:408–11. doi: 10.1002/mds.870120321
39. Malek N, Fletcher N, Newman E. Diagnosing dopamine-responsive dystonias. *Practical Neurol*. (2015) 15:340–5. doi: 10.1136/practneurol-2015-001101
40. Jan MM. Misdiagnoses in children with dopa-responsive dystonia. *Pediatr Neurol*. (2004) 31:298–303. doi: 10.1016/j.pediatrneurol.2004.03.017
41. Hwang WJ, Calne DB, Tsui JK, de la Fuente-Fernandez R. The long-term response to levodopa in dopa-responsive dystonia. *Parkinsonism Relat Disord*. (2001) 8:1–5. doi: 10.1016/S1353-8020(00)00084-5
42. Hyland K. Clinical utility of monoamine neurotransmitter metabolite analysis in cerebrospinal fluid. *Clin Chem*. (2008) 54:633–41. doi: 10.1373/clinchem.2007.099986
43. Tadic V, Kasten M, Bruggemann N, Stiller S, Hagenah J, Klein C. Dopa-responsive dystonia revisited: diagnostic delay, residual signs, and non-motor signs. *Arch Neurol*. (2012) 69:1558–62. doi: 10.1001/archneurol.2012.574
44. Tassin J, Durr A, Bonnet AM, Gil R, Vidailhet M, Lucking CB, et al. Levodopa-responsive dystonia. GTP cyclohydrolase I or parkin mutations? *Brain J Neurol*. (2000) 123 :1112–21. doi: 10.1093/brain/123.6.1112
45. Bruggemann N, Spiegler J, Hellenbroich Y, Opladen T, Schneider SA, Stephani U, et al. Beneficial prenatal levodopa therapy in autosomal recessive guanosine triphosphate cyclohydrolase 1 deficiency. *Arch Neurol*. (2012) 69:1071–5. doi: 10.1001/archneurol.2012.104
46. Thony B, Blau N. Mutations in the BH4-metabolizing genes GTP cyclohydrolase I, 6-pyruvoyl-tetrahydropterin synthase, sepiapterin reductase, carbinolamine-4a-dehydratase, and dihydropteridine reductase. *Hum Mutation*. (2006) 27:870–8. doi: 10.1002/humu.20366
47. Pons R, Syrengelas D, Youroukos S, Orfanou I, Dinopoulos A, Cormand B, et al. Levodopa-induced dyskinesias in tyrosine hydroxylase deficiency. *Mov Disord: Official J Mov Disord Society*. (2013) 28:1058–63. doi: 10.1002/mds.25382
48. Asmus F, Gasser T. Dystonia-plus syndromes. *Eur J Neurol*. (2010) 17(Suppl. 1):37–45. doi: 10.1111/j.1468-1331.2010.03049.x
49. Hong JY, Oh JS, Lee I, Sunwoo MK, Ham JH, Lee JE, et al. Presynaptic dopamine depletion predicts levodopa-induced dyskinesia in *de novo* Parkinson disease. *Neurology*. (2014) 82:1597–604. doi: 10.1212/WNL.0000000000000385

Conflict of Interest: The authors declare that the research was conducted in the absence of any commercial or financial relationships that could be construed as a potential conflict of interest.

frontiers in Genetics

ORIGINAL RESEARCH
published: 05 June 2020
doi: 10.3389/fgene.2020.00584

HMTase Inhibitors as a Potential Epigenetic-Based Therapeutic Approach for Friedreich's Ataxia

*Mursal Sherzai[1], Adamo Valle[2,3], Nicholas Perry[4], Ester Kalef-Ezra[1], Sahar Al-Mahdawi[1], Mark Pook[1] and Sara Anjomani Virmouni[1]**

[1] Ataxia Research Group, Division of Biosciences, Department of Life Sciences, College of Health and Life Sciences, Brunel University London, Uxbridge, United Kingdom, [2] Energy Metabolism and Nutrition, Research Institute of Health Sciences (IUNICS) and Health Research Institute of Balearic Islands (IdISBa), University of Balearic Islands, Palma de Mallorca, Spain, [3] Biomedical Research Networking Center for Physiopathology of Obesity and Nutrition (CIBERobn), Instituto de Salud Carlos III, Madrid, Spain, [4] Division of Cancer Biology, The Institute of Cancer Research, London, United Kingdom*

Friedreich's ataxia (FRDA) is a progressive neurodegenerative disorder caused by a homozygous GAA repeat expansion mutation in intron 1 of the frataxin gene (*FXN*), which instigates reduced transcription. As a consequence, reduced levels of frataxin protein lead to mitochondrial iron accumulation, oxidative stress, and ultimately cell death; particularly in dorsal root ganglia (DRG) sensory neurons and the dentate nucleus of the cerebellum. In addition to neurological disability, FRDA is associated with cardiomyopathy, diabetes mellitus, and skeletal deformities. Currently there is no effective treatment for FRDA and patients die prematurely. Recent findings suggest that abnormal GAA expansion plays a role in histone modification, subjecting the *FXN* gene to heterochromatin silencing. Therefore, as an epigenetic-based therapy, we investigated the efficacy and tolerability of two histone methyltransferase (HMTase) inhibitor compounds, BIX0194 (G9a-inhibitor) and GSK126 (EZH2-inhibitor), to specifically target and reduce H3K9me2/3 and H3K27me3 levels, respectively, in FRDA fibroblasts. We show that a combination treatment of BIX0194 and GSK126, significantly increased *FXN* gene expression levels and reduced the repressive histone marks. However, no increase in frataxin protein levels was observed. Nevertheless, our results are still promising and may encourage to investigate HMTase inhibitors with other synergistic epigenetic-based therapies for further preliminary studies.

Keywords: FRDA, Friedreich ataxia, frataxin, FXN, GAA repeat, HMTase inhibitor

OPEN ACCESS

Edited by:
Oliver Semler, Universitätsklinikum Köln, Germany

Reviewed by:
Theodora Katsila, National Hellenic Research Foundation, Greece
Joel M. Gottesfeld, The Scripps Research Institute, United States

****Correspondence:***
Sara Anjomani Virmouni
sara.anjomani-virmouni@brunel.ac.uk

Specialty section:
This article was submitted to Genetic Disorders, a section of the journal Frontiers in Genetics

Received: *03 December 2019*
Accepted: *14 May 2020*
Published: *05 June 2020*

Citation:
Sherzai M, Valle A, Perry N, Kalef-Ezra E, Al-Mahdawi S, Pook M and Anjomani Virmouni S (2020) HMTase Inhibitors as a Potential Epigenetic-Based Therapeutic Approach for Friedreich's Ataxia. Front. Genet. 11:584. doi: 10.3389/fgene.2020.00584

INTRODUCTION

Friedreich ataxia (FRDA) is the most common autosomal recessive ataxia. It is caused by homozygous GAA repeat expansion mutation within intron 1 of the frataxin (*FXN*) gene (Campuzano et al., 1996), which induces *FXN* gene silencing and hence reduced expression of the essential mitochondrial protein frataxin (Campuzano et al., 1997). Frataxin insufficiency leads to iron-sulfur cluster protein deficits, increased oxidative stress, mitochondrial iron accumulation, and ultimately cell death, with primary sites of pathology being the large sensory neurons of the dorsal root ganglia (DRG) and the dentate nucleus of the cerebellum (Koeppen, 2011). Clinically,

the outcome is progressive spinocerebellar neurodegeneration, hypertrophic cardiomyopathy and a high prevalence of diabetes due to pancreatic β-cell dysfunction (Cnop et al., 2012), with premature death occurring in early adulthood (Pandolfo, 2009). Although there is currently no effective treatment for FRDA, advances in research of its pathogenesis have led to a wide range of therapeutic strategies that are being tested in clinical trials. These include the use of antioxidants such as idebenone, EPI-A0001 and pioglitazone; iron chelators such as deferiprone; and frataxin-increasing compounds such as erythropoietin (EPO) and histone deacetylase (HDAC) inhibitors (Schulz et al., 2009). Of these, the synthetic coenzyme Q10 analog, idebenone, has undergone the most intensive testing of any compound, including two large Phase III clinical trials, placebo-controlled NICOSIA (National Institutes of Health Collaboration with Santhera in Ataxia) study of 48 children (Lynch et al., 2010) and IONIA (Idebenone Effects on Neurological ICARS Assessments) study of 70 pediatric participants (Lagedrost et al., 2011) over 6 months. While a positive effect was observed in the secondary outcome of left ventricular heart mass in one study (Mariotti et al., 2003), these trials have failed to show alleviation of the neurological symptoms associated with FRDA (Kearney et al., 2012). Therefore, there is still a high unmet clinical need to develop effective FRDA therapies.

Novel epigenetic-based frataxin-increasing therapies are considered to be among the most promising approaches. Although DNA methylation is considered to be a stable epigenetic modification, post-translational modifications of histone proteins play more flexible roles in transcriptional regulation. Acetylation and methylation of histones at lysine (and arginine) residues are highly dynamic and are involved in several neurological disorders (Ziemka-Nalecz et al., 2018; Wang and Liu, 2019). Histone acetylation at lysine residues is regulated by two distinct families of enzymes with opposing action, histone acetyltransferases (HATs) and histone deacetylases (HDACs). Similarly, histone lysine methylation is controlled by histone methyltransferases (HMTases) and histone demethylases (e.g., LSD1 and JmjC), which have been linked to a number of cellular processes including DNA repair, replication, transcriptional activation, and repression (Kouzarides, 2007). Transcriptional repression of genes is associated with hypoacetylation of certain histone residues, primarily H3K9, together with increased methylation of histone residues, such as H3K9me3, H3K27me3, and H4K20me3 (Kourmouli et al., 2004; Martin and Zhang, 2005; Jenuwein, 2006).

In FRDA cells, such histone modifications have been identified within the *FXN* gene, predominantly at the region immediately upstream of the expanded GAA repeats, indicating that the *FXN* gene is subject to heterochromatin silencing (reviewed in Sandi et al., 2013). These findings have encouraged the investigation of epigenetic-based therapies, in particular the use of histone deacetylase (HDAC) inhibitors, to reverse *FXN* gene silencing (reviewed in Gottesfeld et al., 2013; Sandi et al., 2013). In fact, several compounds, such as the 2-aminobenzamide HDAC inhibitor 109 and nicotinamide, have shown interesting outcomes reversing the *FXN* gene silencing in cell and mouse models of FRDA (Sandi et al., 2011; Chutake et al., 2016). Subsequently, RG2833 – the formulated form of 109 – has been taken forward to a phase I clinical trial showing increased levels of *FXN* mRNA and H3K9 acetylation in peripheral blood mononuclear cells from FRDA patients (Soragni et al., 2014). Although targeting histone acetylation marks appears promising, no studies have yet explored the therapeutic potential of targeting histone methylation. The class III HDAC inhibitor, nicotinamide – which is able to increase *FXN* expression in FRDA cell and mouse models – has also been shown to decrease the levels of H3K9me3 and H3K27me3 at the *FXN* locus (Chan et al., 2013).

As an additional epigenetic-based therapeutic approach for FRDA therapy, we chose to investigate the use of HMTase inhibitors to improve *FXN* expression in FRDA. HMTase enzymes are lysine- or arginine-specific and usually modify only one particular histone residue. On the basis of pharmacological outcome and efficacy in other diseases such as cancer (Kubicek et al., 2007; McCabe et al., 2012), we chose two HMTase inhibitors, BIX0194 (G9a-inhibitor) and GSK126 (EZH2-inhibitor) to specifically target and reduce H3K9me2/3 and H3K27me3 levels, respectively, in FRDA human primary fibroblasts.

MATERIALS AND METHODS

Cell Lines and Culture Conditions

FRDA and healthy control fibroblasts were grown in DMEM medium with 10% FBS and 1% penicillin-streptomycin (all from Invitrogen) in 5% CO_2 at 37°C. Human and mouse primary cell lines were treated with 1 nM–10 μM of BIX01294 and GSK126 alone or in combination in triplicate for 72 h. Mouse fibroblast cell lines were established from YG8sR FRDA and Y47R control mouse models as previously described (Anjomani Virmouni et al., 2015).

PrestoBlue® Cell Viability Assay

Cells were cultured in a 24 well culture plate for 24 h and washed once with PBS followed by adding fresh medium containing 1 nM–10 μM of BIX01294 and/or GSK126 (in DMSO, final concentration 0.1% v/v) in triplicates for 72 h. Control cells were also cultured and treated simultaneously with the equivalent volume of DMSO at 0.1% finalconcentration (v/v). Cells were incubated for 72 h and PrestoBlue® reagent (Invitrogen) was added to a 1x final concentration followed by incubating the cells for further 3 h. Upon entering a living cell, PrestoBlue® reagent is reduced from resazurin, a blue compound with no intrinsic fluorescent value, to resorufin which is red in color and highly fluorescent. Conversion is proportional to the number of metabolically active cells and therefore can be measured quantitatively. The fluorescence intensity was then measured using xMark™ Microplate Absorbance Spectrophotometer (Bio-Rad) with an excitation wavelength of 570 nm and emission wavelength of 600 nm.

Quantitative RT-PCR

Total RNA was isolated from cells using the Trizol (Invitrogen) method and cDNA was then prepared by using AMV reverse

transcriptase (Invitrogen) with oligo$(dT)_{20}$ primers following the manufacturer's instructions. Levels of *FXN* and *HPRT* mRNA expression were assessed by quantitative RT–PCR using a QuantStudio 7 Flex Real-Time PCR instrument and SYBR® Green (Applied Biosystems) with the following primers: *FXN*-h-forward 5′-CAGAGGAAACGCTGGACTCT-3′, *FXN*-h-reverse 5′ AGCCAGATTTGCTTGTTTGGC-3′, *HPRT*-h-forward 5′-GGTGAAAAGGACCCCACGA-3′, *HPRT* -h-reverse 5′-TCAAGGGCATATCCTACAACA-3′, *Fxn*-m-forward 5′-TTGAAGACCTTGCAGACAAG-3′, *Fxn*-m-reverse 5′-AGCCAGATTTGCTTGTTTGG-3′, *Hprt*-m-forward 5′-ATGAAGGAGATGGGAGGCCA-3′, *Hprt*-m-reverse 5′- TCCA GCAGGTCAGCAAAGAA -3′. Assays were performed in triplicate in at least two independent experiments. Human Endogenous Control Gene Panel was used to assess the off-target effects of the HMTase inhibitors on global gene expression by qRT-PCR using specific Primer sets (TATAAbiocenter).

Immunoblot Analysis

Cells were treated with 100 nM BIX01294, 2 μM GSK126 or combination of both for 72 h. Cells were washed with ice-cold PBS and lysed on ice for 30 min with cell lysis buffer (Cell Signaling Technology, 9803) supplemented with 400 μM PMSF protease inhibitor (Cell Signaling Technology, 8553). Lysates were subjected to centrifugation at 12,000 g for 30 min at 4°C and protein concentrations were determined using the BCA protein assay reagent (Thermo Scientific). 50 μg of protein lysates were boiled for 10 min and subjected to SDS-PAGE electrophoresis using 4–15% precast gels (Bio-Rad, 567-1084). Densitometry was calculated using the Image Lab Software 5.2.1 (Bio-Rad). Antibodies used in this study are as follows: anti-frataxin (1:250, ab113691, Abcam), β-actin (1:1000, A2066, Sigma), goat anti-Rabbit HRP (1:5000, P0448, Dako) and goat anti-Mouse HRP (1:5000, P0447, Dako).

Frataxin Dipstick Assay

Protein concentration was quantified by BCA assay and levels of frataxin protein were measured by lateral flow immunoassay with the Frataxin Protein Quantity Dipstick Assay Kit (MitoSciences, Eugene, OR, United States) according to the manufacturer's instructions (Willis et al., 2008). Signal intensity was measured with a Hamamatsu ICA-1000 Immunochromatographic Reader (MitoSciences).

Histone Methyltransferase Activity Assay

Cells were treated with 100 nM BIX01294, 2 μM GSK126 or combination of both for 72 h, followed by nuclear extract preparations using the EpiQuik™ Nuclear Extraction Kit (Epigentek), according to the manufacturer's instructions. Subsequently, HMTase activities were evaluated using the EpiQuik™ HMTase activity assay kits (for H3K9, P-3003-96 and for H3K27, P-3005-96, Epigentek) according to the manufacturer's instructions. This assay is based on the principle that the HMTase enzyme G9a and EZH2, transfers a methyl group from S-Adenosyl methionine (Adomet) to lysine 9 and 27 of histone H3, respectively. The level of methylated histone H3K9/H3K27 is then recognized with a high-affinity antibody, which is directly proportional to enzyme activity. This was quantified through horseradish peroxidase (HRP) conjugated secondary antibody-color development system. The resulting absorbance was measured at 450 nm using the xMark™ Microplate reader (Bio-Rad).

Chromatin Immunoprecipitation-qPCR Assay

Histone modifications at the 5′UTR promoter of *FXN* gene were detected by ChIP analysis in FRDA and control cells. This procedure was performed by using ChIP qPCR kit (Chromatrap) with an acetylated H3 (Lys9) (06-942, Merck Millipore), trimethyl-H3 (Lys9) (07-442, Merck Millipore), and trimethyl-H3 (Lys27) (07-449, Merck Millipore), antibody on formaldehyde cross-linked samples. DNA was then sheared by sonication, followed by immunoprecipitation. For each experiment, normal rabbit serum (SIGMA) was used as a negative control. After reversal of cross-linking, quantitative RT–PCR amplification of the resultant co-immunoprecipitated DNA was carried out with SYBR® Green in a QuantStudio 7 Flex Real-Time PCR instrument (Applied Biosystems) using the following primers; h-*FXN*-pro-forward 5′-AAGCAGGCTCTCCATTTTTG-3′ and h-*FXN*-pro-reverse 5′- CGAGAGTCCACATGCTGCT-3′. The data were from three independent chromatin preparations, with each experiment done in triplicate.

Statistical Analyses

For statistical analysis, the unpaired two-tailed Student's *t*-test were used to assess the significance of the differences between group data with a significance value set at $P < 0.05$.

RESULTS

Effects of HMTase Inhibitors on Primary Fibroblasts Viability

The safety and cellular tolerability of BIX01294 and GSK126 treatment were determined by cell viability assay. Human and mouse primary cell lines were treated with BIX01294 (1 nM–10 μM) and GSK126 (1 nM–10 μM) in triplicate for 72 h. Fibroblast cells tolerated BIX01294 treatment with concentrations ranging from 1 to 100 nM, whereas, higher concentrations significantly decreased their viability (**Figure 1A** and **Supplementary Figure 1A**). In comparison to BIX01294 treatment, cells were generally less sensitive to GSK126 treatment (**Figure 1B** and **Supplementary Figure 1B**). Both normal and FRDA human fibroblasts indicated no significant change in viability with 1 nM to 2 μM GSK126 treatment (**Figure 1B**), although cell viability was significantly reduced following treatment with 10 μM GSK126. A similar pattern was also observed in mouse fibroblasts treated with GSK126, however, FRDA cells showed reduced tolerance with 2 μM GSK126 ($P < 0.05$) (**Supplementary Figure 1B**). These results gave a valuable indication of the optimal

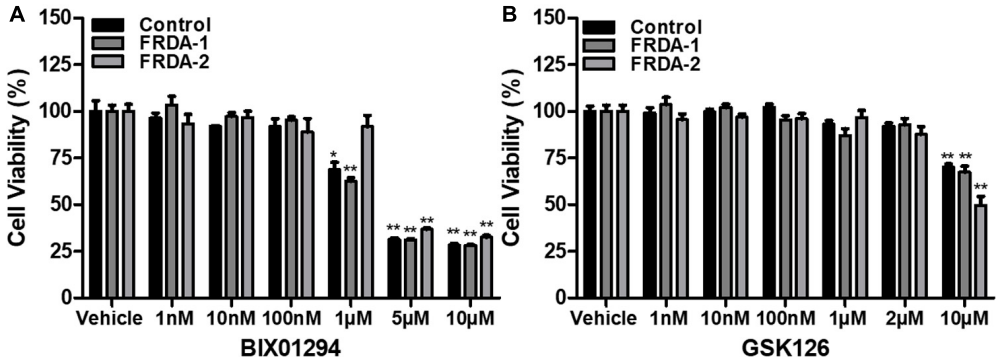

FIGURE 1 | Cell viability analysis following 72 h HMTase inhibitor treatment. **(A)** BIX01294 and **(B)** GSK126 treatment analysis in human FRDA (GM03816 and GM04078) and normal fibroblasts (GM07492). The mean value of all data was normalized to the PrestoBlue reduction of vehicle treated cells (set at 100%). Error bars indicate SEM and values represent mean ± SEM ($n = 3$). Asterisks indicate statistically significant differences between drug and vehicle treated cell lines, assessed by unpaired two-tailed Student's *t*-test (*$P < 0.05$, **$P < 0.01$).

compound dosing *in vitro* required for subsequent molecular analysis to determine the efficacy of BIX01294 and GSK125 for FRDA therapy.

The Effect of HMTase Inhibitors on Frataxin Expression

In order to test the effects of BIX01294 and GSK126 on *FXN* gene reactivation, normal and FRDA human primary fibroblasts were treated with 100 nM, 500 nM, and 1 μM of BIX01294 and 1 and 2 μM of GSK126. The cells were treated with the drug(s) either individually or in combination over a period of 72 h. *FXN* mRNA levels in control cells were generally unaffected by treatments, whether alone or in combination. In FRDA cells, treatment with BIX01294 did not significantly increase *FXN* gene expression levels, except for 500 nM concentrations, which induced a modest increase of 19% ($P < 0.05$) (**Figure 2**). Similarly, individual treatments of GSK126 did not have a substantial effect on *FXN* mRNA expression levels in FRDA cells, where in fact a significant decrease is seen with 1 μM (22%, $P < 0.05$) and 2 μM (38%, $P < 0.01$) concentrations. However, all combination treatments of BIX01294 and GSK126 in FRDA cell lines were shown to significantly increase *FXN* mRNA levels. The highest significant increase of 88% ($P < 0.01$) was observed with combination treatment of 100 nM BIX01294 and 2 μM GSK126, followed by 34% ($P < 0.01$) increase with 1 μM BIX01294 and 1 μM GSK126 treatment, then 26% ($P < 0.01$) increase with 500 nM BIX01294 and 1 μM GSK126 treatment. This suggests that simultaneous inhibition of both H3K9me2/3 and H3K27me3 with BIX01294 and GSK126, respectively, is beneficial in reversing the histone modifications and in activating the *FXN* gene. These results were confirmed in an additional FRDA cell line, however, interestingly this effect was more predominant in this cell line showing higher level of *FXN* expression compared to the control when treated with the combination of both inhibitors (**Supplementary Figure 2**). Similar to human fibroblasts, the mouse primary fibroblasts were treated either individually or in combination with 1 and 100 nM of BIX01294 and 100 nM and 1 μM of GSK126 for 72 h. Generally, no significant changes in *FXN* gene expression levels were observed in FRDA mouse cells after individual treatments with BIX01294 and GSK126 (**Supplementary Figure 1C**). However, similar to human FRDA fibroblasts, combination treatments of 100 nM BIX01294 with 100 nM GSK126 and 100 nM BIX01294 with 1 μM GSK126, both have significantly increased the *FXN* mRNA expression levels in FRDA mouse cells by 16% ($P < 0.01$) and 37% ($P < 0.01$), respectively (**Supplementary Figure 1C**).

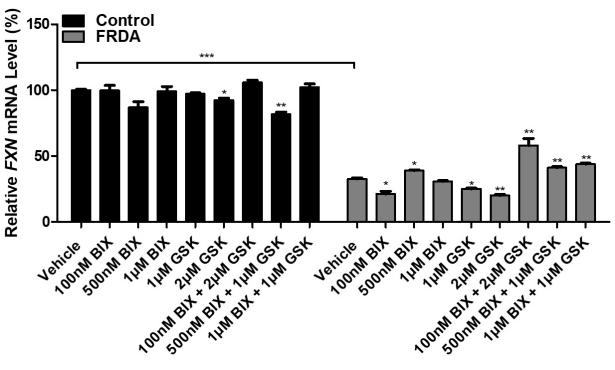

FIGURE 2 | qRT-PCR analysis indicating the relative *FXN* mRNA levels following treatment with BIX01294 and GSK126 alone or in combination in human primary fibroblasts (FRDA, GM03816 and normal, GM07492). Each result displayed is the mean of two independent experiments and the *FXN* mRNA levels of each sample were normalized to *HPRT* gene as an endogenous control. The values were expressed as a ratio to the vehicle treated samples of normal fibroblasts. Error bars indicate SEM and values represent mean ± SEM ($n = 3$). Asterisks indicate significant differences between drug and vehicle treated cell lines, assessed by unpaired two-tailed Student's *t*-test (*$P < 0.05$, **$P < 0.01$, ***$P < 0.001$).

After determining the synergistic effect with 100 nM BIX01294 and 2 μM GSK126 as the optimum drug dosing, we then investigated the effect of this combination treatment on *FXN* gene expression levels with different time

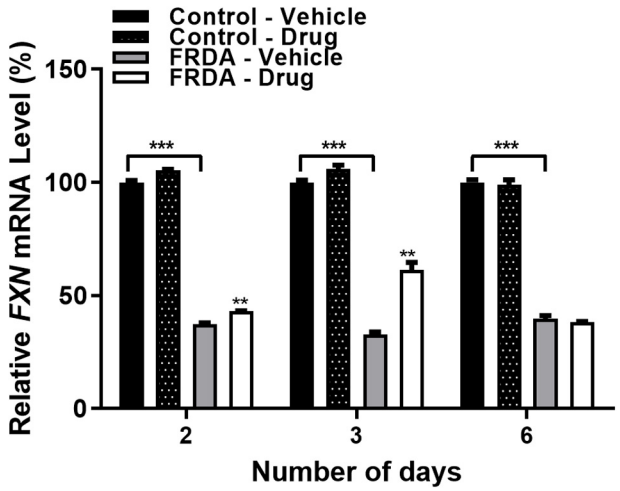

FIGURE 3 | qRT-PCR analysis indicating the relative *FXN* mRNA levels following combination treatment with BIX01294 (100 nM) and GSK126 (2 μM) in human primary fibroblasts (FRDA, GM03816 and normal, GM07492) for different time points. For this treatment, the cell culture medium was replaced with fresh medium supplemented with the drug every 3 days. Mean *FXN* mRNA levels of each sample were normalized to *HPRT* gene as an endogenous control. Values were expressed as a ratio to the vehicle treated samples of normal fibroblasts at the corresponding time point. Error bars indicate SEM and values represent mean ± SEM ($n = 3$). Asterisks indicate significant differences between drug and vehicle treated cell lines, assessed by unpaired two-tailed Student's *t*-test (**$P < 0.01$, ***$P < 0.001$).

points (2, 3, and 6-day) in FRDA cell lines (**Figure 3** and **Supplementary Figure 1D**). We noted a gradual increase in *FXN* transcription after 2 and 3-day treatments by 15% ($P < 0.01$) and 88% ($P < 0.01$) in human FRDA cell lines, respectively. Consistent with our results in the human cell lines, 3-day treatment indicated an increase in the *FXN* gene expression by 37% ($P < 0.001$) in FRDA mouse cell lines (**Supplementary Figure 1D**).

To determine the change in frataxin protein expression, combination treatments were carried out with 100 nM BIX01294 and 2 μM GSK126 for different time points (2–6 days). The levels of frataxin protein were determined by dipstick assay. As expected, FRDA cells show significantly reduced frataxin protein levels compared to healthy counterparts, but no significant change was observed after drug treatment at any time point (**Figure 4A** and **Supplementary Figure 1E**). Western blot analysis further confirmed our dipstick assay results (**Figure 4B**), suggesting that other post-translational mechanisms may be playing a role in regulation of frataxin protein levels.

Inhibition of the HMTase G9a and EZH2 by BIX01294 and GSK126

To assess the inhibitory effects of BIX01294 and GSK126, we investigated the enzymatic activity levels of EZH2 and G9a, respectively, following treatment in human primary fibroblasts. We treated the cells with 100 nM BIX01294 and 2 μM GSK126 either individually or in combination for 72 h. Consistently, the EZH2 activity was significantly higher by 53% ($P < 0.01$) in vehicle treated FRDA fibroblasts as compared to normal fibroblasts (**Figure 5A**). However, 2 μM GSK and a combination treatment of 2 μM GSK126 + 100 nM BIX01294 in FRDA fibroblasts have shown to significantly reduce the EZH2 activity by 28% ($P < 0.05$) and 20% ($P < 0.05$), respectively. Similarly, FRDA fibroblasts were shown to have a 59% significantly higher G9a enzymatic activity as compared to normal fibroblasts (**Figure 5B**). This activity was significantly reduced by 25% ($P < 0.01$) and 20% ($P < 0.01$) with 100 nM BIX01294 and combination treatment of 2 μM GSK126 + 100 nM BIX01294, respectively. There was no significant change in EZH2 and G9a activity levels between individual and synergistic drug treatment in FRDA cells. This suggest that the combination treatment of BIX01294 and GSK126 does not interfere with or potentiate the drugs' specific inhibitory effects. Furthermore, a similar change in EZH2 and G9a enzymatic activity was also observed in normal fibroblasts after treatment, suggesting that BIX01294 and GSK126 might have a non-disease specific inhibitory effect.

Treatment With HMTase Inhibitors Decreases Repressive H3K9/H3K27 Marks at FXN Promoter

To examine the effects of BIX01294 and GSK126 on histone modifications, human primary fibroblasts were treated with a combination of 100 nM BIX01294 and 2 μM GSK126 for 72 h, followed by performing ChIP assay, to determine the histone modification changes in the *FXN* 5′UTR promoter region. Immunoprecipitation with anti-H3K9ac antibody revealed a significant reduction ($P < 0.01$) in FRDA fibroblasts treated with vehicle as compared to normal fibroblasts (**Figure 6**). Interestingly, the combination treatment with BIX01294 and GSK126 increased H3K9ac in both FRDA and control cell lines ($P < 0.001$). Along with histone hypoacetylation, both lysine 9 and lysine 27 of histone H3 were highly methylated in FRDA cell lines (H3K9me3 and H3K27me3, $P < 0.01$). However, after drug treatment, the methylation levels significantly decreased in H3K9me3 ($P < 0.01$) and H3K27me3 ($P < 0.01$). Nonetheless, an increase in H3K9ac and decrease in H3K9me3 and H3K27me3 levels is also observed in normal fibroblasts after drug treatment, which correlates well with the change in EZH2 and G9a enzymatic activity (**Figure 6**). Overall, the change in histone modification after drug treatment in FRDA fibroblasts did not reach the regular levels seen in normal fibroblasts.

Off-Target Effects of HMTase Inhibitors on Gene Expression

Like any epigenetic-based therapies, HMTase inhibitors are expected to induce a widespread effect on gene expression by altering global histone modification levels, and thus have a potential off-target effects. Therefore, to evaluate the possibility of BIX01294 and GSK126 off-target effects in FRDA, we treated human fibroblasts with a combination treatment of the two drugs (100 nM BIX01293 and 2 μM GSK126), which had

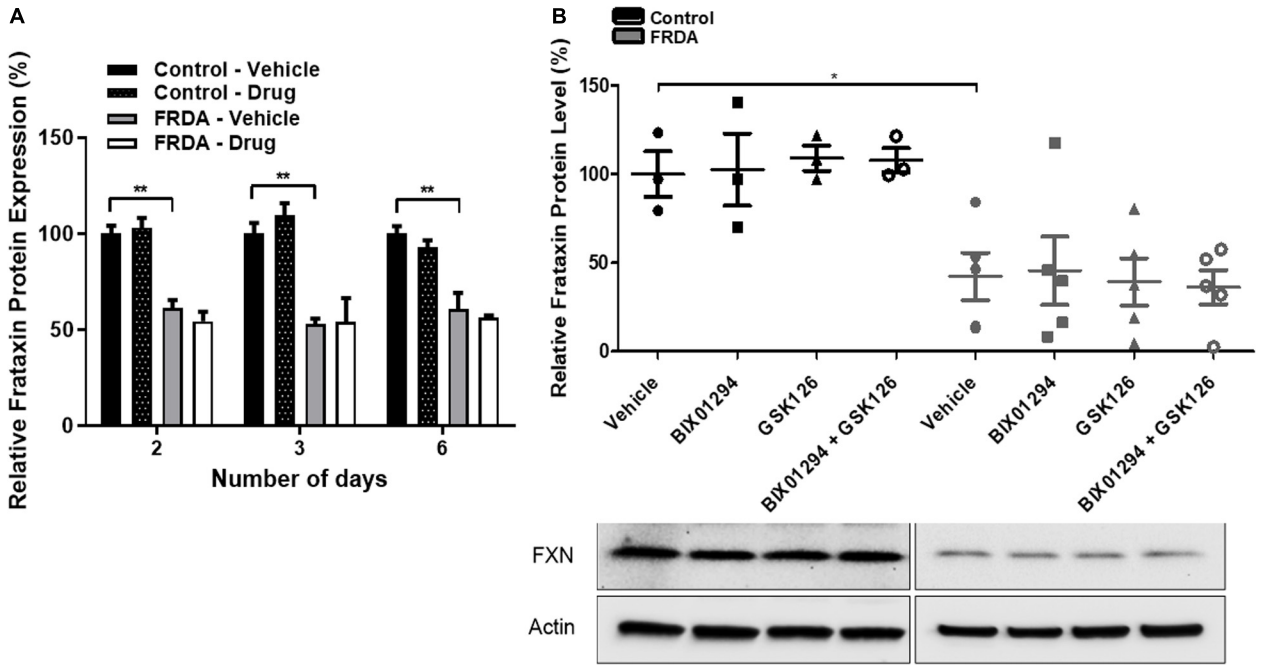

FIGURE 4 | Frataxin expression levels. **(A)** Dipstick immunoassay of frataxin protein in primary fibroblasts (FRDA, GM03816 and normal, GM07492) following synergistic treatment with BIX01294 (100 nM) and GSK126 (2 μM) for different time points. Values are expressed as percentage of the vehicle treated samples of normal fibroblasts at the corresponding time point. **(B)** Western blot analysis indicating the relative frataxin protein expression levels in human fibroblasts (FRDA, GM04078 and FA3, and normal GM08399 and GM08333) following synergistic treatment with BIX01294 (100 nM) and GSK126 (2 μM) for 3 days. Values were normalized to actin levels and were expressed as percentage of the vehicle treated samples of normal fibroblasts. Representative Immunoblots are shown. Error bars indicate SEM and values represent mean ± SEM ($n = 3$). Asterisks indicate significant differences between drug and vehicle treated cell lines, assessed by unpaired two-tailed Student's *t*-test (*$P < 0.05$, **$P < 0.01$).

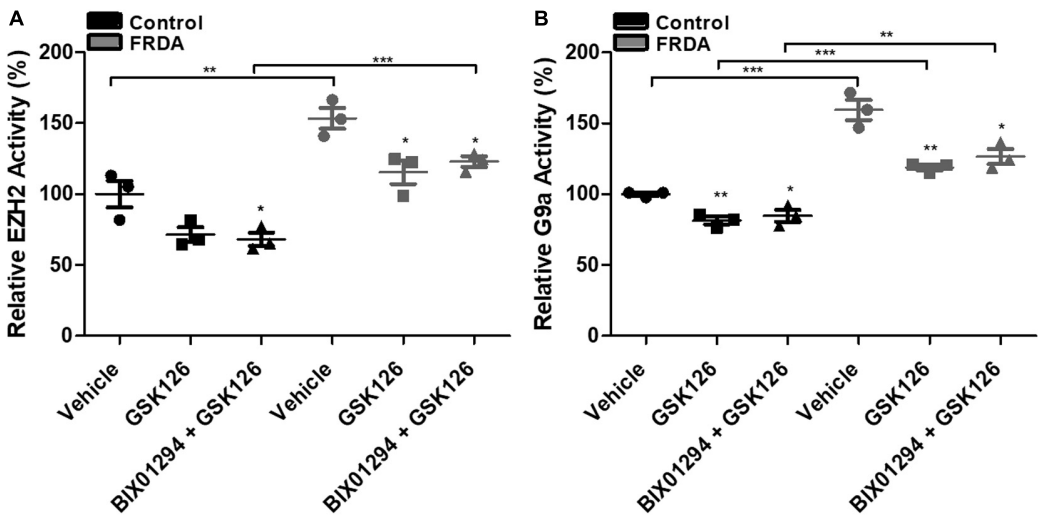

FIGURE 5 | HMTase enzymatic activity analysis in human fibroblasts (FRDA, GM03816 and normal, GM07492) treated individually and in combination with BIX01294 (100 nM) and GSK126 (2 μM). **(A)** EZH2 and **(B)** G9a activity levels. The values were expressed as a ratio to the vehicle treated samples of normal fibroblasts. Error bars indicate SEM and values represent mean ± SEM ($n = 3$). Asterisks indicate significant differences between drug and vehicle treated cell lines, assessed by unpaired two-tailed Student's *t*-test (*$P < 0.05$, **$P < 0.01$, ***$P < 0.001$).

exerted a change in *FXN* gene expression levels (**Figures 3**, **4**), for 72 h. We then quantitatively measured changes in the expression of a panel of endogenous control genes by qRT-PCR in human fibroblasts. The results obtained show that there is no significant change in any of the genes explored in human fibroblasts after treatment (**Figure 7**). This suggests that

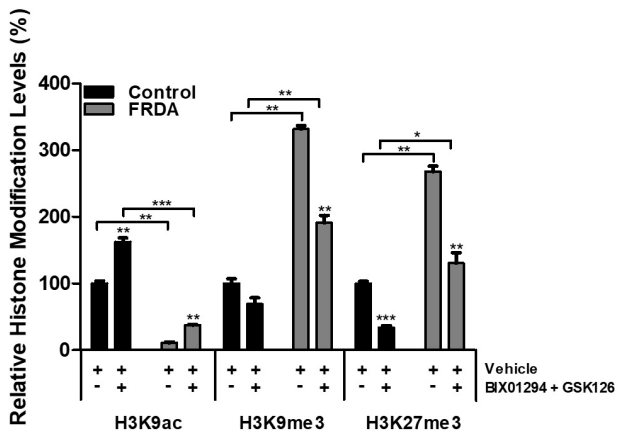

FIGURE 6 | Histone modification changes in the *FXN* 5′UTR promoter region, after synergistic treatment with BIX01294 (100 nM) and GSK126 (2 μM) for 72 h in human FRDA (GM03816) and normal (GM07492) fibroblasts. The values were expressed as a ratio to the vehicle treated samples of normal fibroblasts. Error bars indicate SEM and values represent mean ± SEM ($n = 3$). Asterisks indicate significant differences between drug and vehicle treated cell lines, assessed by unpaired two-tailed Student's *t*-test (*$P < 0.05$, **$P < 0.01$, ***$P < 0.001$).

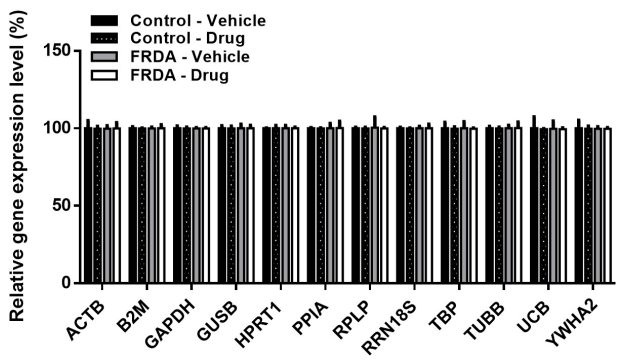

FIGURE 7 | Relative change in the expression of a panel of human endogenous control genes in primary fibroblasts (FRDA, GM03816 and normal, GM07492), following BIX01294 (100 nM) and GSK126 (2 μM) combination treatment. Values were expressed as a ratio to the vehicle treated samples of normal fibroblasts. Error bars indicate SEM and values represent mean ± SEM ($n = 3$). ACTB, beta-actin; B2M, beta-2-microglobulin; GAPDH, glyceraldehyde-3-phosphate dehydrogenase; GUSB, beta-glucuronidase; HPRT1, hypoxanthine-guanine phosphoribosyltransferase; PPIA, cyclophillin A; RPLP, 60S acidic ribosomal protein P0; RRN18S, 18S rRNA; TBP, TATAA-box binding protein, TUBB, beta-tubulin, UCB, ubiquitin C; YWHA2, tyrosine 3/tryptophan 5-monooxygenase activation protein zeta.

BIX01294 and GSK126 exerts minimal off-target effects outside of *FXN* gene regulation.

DISCUSSION

It has been reported that 98% of FRDA patients have a homozygous GAA trinucleotide repeat expansion within the first intron of the *FXN* gene, leading to reduced expression of frataxin (Campuzano et al., 1996). Although the mechanism by which the GAA repeat expansion leads to decreased levels of frataxin are currently unknown, it is generally accepted that FRDA may be caused by a heterochromatin-mediated silencing effect of the *FXN* gene (Saveliev et al., 2003; Festenstein, 2006). In support of this hypothesis, differential DNA methylation in FRDA patients accompanied by various histone modifications have been identified within the vicinity of the expanded GAA repeats and near the promoter region of the *FXN* gene. This includes elevated methylation of histone residues, such as H3K9me2/3 and H3K27me3, with hypoacetylation of H3K9 (Herman et al., 2006; Greene et al., 2007; Al-Mahdawi et al., 2008; De Biase et al., 2009). Such DNA and histone modifications can be reversed, representing a suitable target for epigenetic-based therapy. Moreover, since the expanded GAA repeat in FRDA does not alter the amino acid sequence of frataxin, gene reactivation would be of therapeutic benefit (Sandi et al., 2014a). In this study, we have demonstrated the *in vitro* feasibility of two HMTase inhibitors, BIX01294 (G9a-inhibitor) and GSK126 (EZH2-inhibitor), to potentially increase frataxin expression, by reducing histone methylation levels at the *FXN* locus. Notably, 72 h treatment with BIX01294 or GSK126 alone did not significantly enhance *FXN* gene expression in FRDA fibroblasts. In fact, a dose-dependent decrease in *FXN* gene expression level is seen with GSK126 treatments. Previously, it was reported that chemical inhibition of G9a with BIX01294 treatment showed to decrease H3K9 methylation at the *FXN* locus but failed to up-regulate *FXN* to a significant high level (Punga and Buhler, 2010). A possible explanation for this could be that H3K9 methylation may have a redundant role or it may cooperate with another heterochromatin mark in silencing the *FXN* gene. It is interesting to note, that on the silenced *FXN* locus there is presence of both H3K9 and H3K27 methylation at high levels. H3K9 methylation is associated with HP1 mediated silencing of highly heterochromatinised satellite repeats, whereas H3K27 is linked to polycomb-mediated silencing of formerly euchromatin genes. Typically, these two marks do not overlap in the mammalian genome (Yandim et al., 2013). Therefore, it can be hypothesized that there is a cooperation between the H3K9 and H3K27 methylation marks on the *FXN* locus. Indeed, a study in 2003 reported an accumulation of H3K27me3 in SUV39H double null cells may partially substitute for lack H3K9me3 histone marks (Peters et al., 2003).

In accordance with this, combination treatment with BIX01294 and GSK126 was shown to promote a safe induction of *FXN* mRNA expression levels in FRDA fibroblasts, predominantly after a 3-day treatment period. This indicates that simultaneous inhibition of G9a and EZH2, which targets H3K9me2/3 and H3K27me3 repressive histone marks, may have beneficial effect, to some extent, in increasing *FXN* gene expression levels in FRDA. However, frataxin dipstick and western blot analyses revealed that frataxin protein expression levels remained unaffected after combined treatment with BIX01294 and GSK126. This suggests that there may be other post-translational mechanisms at play, affecting either the *FXN*

mRNA stability or frataxin protein translation, stability or degradation that will require further investigation. Interestingly, we also identified significantly increased levels of EZH2 and G9a activity in FRDA human fibroblasts as compared to normal fibroblasts. This agrees with previous proposals that stalled RNAPII, during RNA:DNA hybrid formation, may be recruiting high levels of HMTases to methylate histones locally and reducing *FXN* gene transcription, as a defense mechanism (Yandim et al., 2013). Furthermore, following individual and combination treatment of BIX01294 and GSK126, the G9a and EZH2 levels were significantly reduced, respectively, in both the normal and FRDA human fibroblasts. This suggests that the drugs target and inhibit their corresponding HMTase activities in a non-disease specific manner. Moreover, significantly increased H3K9me3 and H3K27me3 levels, alongside decreased H3K9ac levels, were seen in the *FXN* 5′UTR promoter region in FRDA fibroblasts, as previously reported (De Biase et al., 2009; Sandi et al., 2014a). However, after combined treatment of BIX01294 and GSK126, a non-cell type specific reduction in H3K9me3 and H3K27me3, and an increase in H3K9ac was seen, which correlated well with the changes in G9a and EZH2 levels.

Since epigenetic therapies are likely to alter gene expression more widely, we selected a panel of endogenous control genes to assess whether BIX01294 and GSK126 exert significant off-target effects. Although our gene panel was limited and, of note, did not include any known cancer-related genes, we did not observe any off-target effects following combination treatment. Of the selection of genes investigated, TBP, USB1, and HPRT1 are known to have lower expression levels. ChIP-sequencing signals from ENCODE/SYDH in UCSE Genome Browser[1] reveal that generally these genes have higher histone acetylation marks near the promoter region, with elevated H3K36me3 enrichment alongside lower H3K9me3 and H3K27me3 enrichments throughout the gene (Kent et al., 2002). However, no studies have reported that these genes can be affected by HMTase inhibitors.

Overall, our results indicated that a combination treatment of BIX01294 and GSK126 may be effective in increasing the *FXN* gene expression levels in FRDA, by simultaneously targeting H3K9me3 and H3K27me3 repressive marks. However, based on our findings of frataxin protein levels after drug treatment, *in vivo* animal studies are not proposed at this stage. Compared to other epigenetic-based therapies, the use of HMTase inhibitors is still highly underexplored in FRDA. Since larger expanded GAA repeats are highly associated with heterochromatin mediated *FXN* gene silencing, it is crucial to carry out future *in vitro* studies using patient-derived cells with higher GAA repeats, and possibly different cell culture systems (Sandi et al., 2014b). Nevertheless, HMTase inhibitors should still be pursued for further preclinical studies, perhaps with other synergistic epigenetic-based compounds, such as HDAC inhibitors and DNMT inhibitors. Similar to HMTase inhibitors, HDAC inhibitors could potentially reduce epigenetic silencing of an affected gene by targeting the heterochromatin state. In FRDA, the HDAC inhibitors 109/RG2833 and nicotinamide (vitamin B3) have shown the most promising results in restoring frataxin to normal levels by increasing histone acetylation at the *FXN* locus (Nageshwaran and Festenstein, 2015; Burk, 2017). Moreover, alongside abnormal histone modification, numerous studies have reported an increase in DNA methylation levels in the pathogenic *FXN* alleles. Thus far, no studies have reported the effects of DNA demethylation agents in treating FRDA. Recent reports investigating the TNR disorder fragile X syndrome (FXS), have shown promising results using the DNMT inhibitor, 5-aza-CdR, either alone or in combination with HDAC inhibitors (Chiurazzi et al., 1999) or with HMTase inhibitors (Kumari and Usdin, 2016) to effectively reduce the FMR1 promoter hypermethylation and reinstating mRNA and protein levels to normal in FXS patient cells. Therefore, it would be interesting to investigate the synergistic effects of HMTase inhibitors with HDAC inhibitor compounds and/or DNMT inhibitors in the reactivation of *FXN* gene transcription *in vitro* and subsequently in FRDA mouse models (Anjomani Virmouni et al., 2014, 2015; Sandi et al., 2014b).

In conclusion, the evaluation of therapeutic agents for FRDA has rapidly advanced in the last few decades, with the finding of numerous pharmacological agents at different stages of development. Our study encourages the use of simultaneous administration of two or more epigenetic-based drugs for further preliminary studies to improve disease phenotype in FRDA.

DATA AVAILABILITY STATEMENT

All datasets generated for this study are included in the article/**Supplementary Material**.

AUTHOR CONTRIBUTIONS

SA-M, AV, MP, and SA conceived and designed the study. MS, SA-M, NP, AV, MP, and SA wrote the manuscript. All authors performed the experiments and read and approved the manuscript.

FUNDING

This work was supported by funding from Friedreich's Ataxia Research Alliance (FARA) and Takeda Pharmaceutical Limited Cambridge. The funders were not involved in the study design, collection, analysis, interpretation of data, the writing of this article, or the decision to submit it for publication. Part of the data presented in this manuscript contributed to the doctoral thesis of MS (Sherzai, 2018).

SUPPLEMENTARY MATERIAL

The Supplementary Material for this article can be found online at: https://www.frontiersin.org/articles/10.3389/fgene.2020.00584/full#supplementary-material

[1] genome.ucsc.edu

REFERENCES

Al-Mahdawi, S., Pinto, R. M., Ismail, O., Varshney, D., Lymperi, S., Sandi, C., et al. (2008). The Friedreich ataxia GAA repeat expansion mutation induces comparable epigenetic changes in human and transgenic mouse brain and heart tissues. *Hum. Mol. Genet.* 17, 735–746. doi: 10.1093/hmg/ddm346

Anjomani Virmouni, S., Ezzatizadeh, V., Sandi, C., Sandi, M., Al-Mahdawi, S., Chutake, Y., et al. (2015). A novel GAA-repeat-expansion-based mouse model of Friedreich's ataxia. *Dis. Model. Mech.* 8, 225–235. doi: 10.1242/dmm.018952

Anjomani Virmouni, S., Sandi, C., Al-Mahdawi, S., and Pook, M. A. (2014). Cellular, molecular and functional characterisation of YAC transgenic mouse models of Friedreich ataxia. *PLoS One* 9:e107416. doi: 10.1371/journal.pone.0107416

Burk, K. (2017). Friedreich Ataxia: current status and future prospects. *Cereb. Ataxias* 4:2017. doi: 10.1186/s40673-017-0062-x

Campuzano, V., Montermini, L., Lutz, Y., Cova, L., Hindelang, C., Jiralerspong, S., et al. (1997). Frataxin is reduced in Friedreich ataxia patients and is associated with mitochondrial membranes. *Hum. Mol. Genet.* 6, 1771–1780. doi: 10.1093/hmg/6.11.1771

Campuzano, V., Montermini, L., Molto, M. D., Pianese, L., Cossee, M., Cavalcanti, F., et al. (1996). Friedreich's ataxia: autosomal recessive disease caused by an intronic GAA triplet repeat expansion. *Science* 271, 1423–1427.

Chan, P. K., Torres, R., Yandim, C., Law, P. P., Khadayate, S., Mauri, M., et al. (2013). Heterochromatinization induced by GAA-repeat hyperexpansion in Friedreich's ataxia can be reduced upon HDAC inhibition by vitamin B3. *Hum. Mol. Genet.* 22, 2662–2675. doi: 10.1093/hmg/ddt115

Chiurazzi, P., Pomponi, M. G., Pietrobono, R., Bakker, C. E., Neri, G., and Oostra, B. A. (1999). Synergistic effect of histone hyperacetylation and DNA demethylation in the reactivation of the FMR1 gene. *Hum. Mol. Genet.* 8, 2317–2323. doi: 10.1093/hmg/8.12.2317

Chutake, Y. K., Lam, C. C., Costello, W. N., Anderson, M. P., and Bidichandani, S. I. (2016). Reversal of epigenetic promoter silencing in Friedreich ataxia by a class I histone deacetylase inhibitor. *Nucleic Acids Res.* 44, 5095–5104. doi: 10.1093/nar/gkw107

Cnop, M., Igoillo-Esteve, M., Rai, M., Begu, A., Serroukh, Y., Depondt, C., et al. (2012). Central role and mechanisms of beta-cell dysfunction and death in friedreich ataxia-associated diabetes. *Ann. Neurol.* 72, 971–982. doi: 10.1002/ana.23698

De Biase, I., Chutake, Y. K., Rindler, P. M., and Bidichandani, S. I. (2009). Epigenetic silencing in Friedreich ataxia is associated with depletion of CTCF (CCCTC-binding factor) and antisense transcription. *PLoS One* 4:e7914. doi: 10.1371/journal.pone.0007914

Festenstein, R. (2006). Breaking the silence in Friedreich's ataxia. *Nat. Chem. Biol.* 2, 512–513. doi: 10.1038/nchembio1006-512

Gottesfeld, J. M., Rusche, J. R., and Pandolfo, M. (2013). Increasing frataxin gene expression with histone deacetylase inhibitors as a therapeutic approach for Friedreich's ataxia. *J. Neurochem.* 126(Suppl. 1), 147–154. doi: 10.1111/jnc.12302

Greene, E., Mahishi, L., Entezam, A., Kumari, D., and Usdin, K. (2007). Repeat-induced epigenetic changes in intron 1 of the frataxin gene and its consequences in Friedreich ataxia. *Nucleic Acids Res.* 35, 3383–3390. doi: 10.1093/nar/gkm271

Herman, D., Jenssen, K., Burnett, R., Soragni, E., Perlman, S. L., and Gottesfeld, J. M. (2006). Histone deacetylase inhibitors reverse gene silencing in Friedreich's ataxia. *Nat. Chem. Biol.* 2, 551–558. doi: 10.1038/nchembio815

Jenuwein, T. (2006). The epigenetic magic of histone lysine methylation. *FEBS J.* 273, 3121–3135. doi: 10.1111/j.1742-4658.2006.05343.x

Kearney, M., Orrell, R. W., Fahey, M., and Pandolfo, M. (2012). Antioxidants and other pharmacological treatments for Friedreich ataxia. *Cochrane Database Syst. Rev.* 4:CD007791. doi: 10.1002/14651858.CD007791.pub3

Kent, W. J., Sugnet, C. W., Furey, T. S., Roskin, K. M., Pringle, T. H., Zahler, A. M., et al. (2002). The human genome browser at UCSC. *Genome Res.* 12, 996–1006. doi: 10.1101/gr.229102

Koeppen, A. H. (2011). Friedreich's ataxia: pathology, pathogenesis, and molecular genetics. *J. Neurol. Sci.* 303, 1–12. doi: 10.1016/j.jns.2011.01.010

Kourmouli, N., Jeppesen, P., Mahadevhaiah, S., Burgoyne, P., Wu, R., Gilbert, D. M., et al. (2004). Heterochromatin and tri-methylated lysine 20 of histone H4 in animals. *J. Cell. Sci.* 117, 2491–2501. doi: 10.1242/jcs.01238

Kouzarides, T. (2007). Chromatin modifications and their function. *Cell* 128, 693–705. doi: 10.1016/j.cell.2007.02.005

Kubicek, S., O'Sullivan, R. J., August, E. M., Hickey, E. R., Zhang, Q., Teodoro, M. L., et al. (2007). Reversal of H3K9me2 by a small-molecule inhibitor for the G9a histone methyltransferase. *Mol. Cell* 25, 473–481. doi: 10.1016/j.molcel.2007.01.017

Kumari, D., and Usdin, K. (2016). Sustained expression of FMR1 mRNA from reactivated fragile X syndrome alleles after treatment with small molecules that prevent trimethylation of H3K27. *Hum. Mol. Genet.* 25, 3689–3698. doi: 10.1093/hmg/ddw215

Lagedrost, S. J., Sutton, M. S., Cohen, M. S., Satou, G. M., Kaufman, B. D., Perlman, S. L., et al. (2011). Idebenone in *Friedreich ataxia* cardiomyopathy-results from a 6-month phase III study (IONIA). *Am. Heart J.* 161, 639.e–645.e. doi: 10.1016/j.ahj.2010.10.038

Lynch, D. R., Perlman, S. L., and Meier, T. (2010). A phase 3, double-blind, placebo-controlled trial of idebenone in friedreich ataxia. *Arch. Neurol.* 67, 941–947. doi: 10.1001/archneurol.2010.168

Mariotti, C., Solari, A., Torta, D., Marano, L., Fiorentini, C., and Di Donato, S. (2003). Idebenone treatment in Friedreich patients: one-year-long randomized placebo-controlled trial. *Neurology* 60, 1676–1679. doi: 10.1212/01.wnl.0000055872.50364.fc

Martin, C., and Zhang, Y. (2005). The diverse functions of histone lysine methylation. *Nat. Rev. Mol. Cell Biol.* 6, 838–849. doi: 10.1038/nrm1761

McCabe, M. T., Ott, H. M., Ganji, G., Korenchuk, S., Thompson, C., Van Aller, G. S., et al. (2012). EZH2 inhibition as a therapeutic strategy for lymphoma with EZH2-activating mutations. *Nature* 492, 108–112. doi: 10.1038/nature11606

Nageshwaran, S., and Festenstein, R. (2015). Epigenetics and triplet-repeat neurological diseases. *Front. Neurol.* 6:262. doi: 10.3389/fneur.2015.00262

Pandolfo, M. (2009). Friedreich ataxia: the clinical picture. *J. Neurol.* 256(Suppl. 1), 3–8. doi: 10.1007/s00415-009-1002-3

Peters, A. H., Kubicek, S., Mechtler, K., O'Sullivan, R. J., Derijck, A. A., Perez-Burgos, L., et al. (2003). Partitioning and plasticity of repressive histone methylation states in mammalian chromatin. *Mol. Cell* 12, 1577–1589. doi: 10.1016/s1097-2765(03)00477-5

Punga, T., and Buhler, M. (2010). Long intronic GAA repeats causing Friedreich ataxia impede transcription elongation. *EMBO Mol. Med.* 2, 120–129. doi: 10.1002/emmm.201000064

Sandi, C., Al-Mahdawi, S., and Pook, M. A. (2013). Epigenetics in Friedreich's ataxia: challenges and opportunities for therapy. *Genet. Res. Int.* 2013:852080. doi: 10.1155/2013/852080

Sandi, C., Pinto, R. M., Al-Mahdawi, S., Ezzatizadeh, V., Barnes, G., Jones, S., et al. (2011). Prolonged treatment with pimelic o-aminobenzamide HDAC inhibitors ameliorates the disease phenotype of a Friedreich ataxia mouse model. *Neurobiol. Dis.* 42, 496–505. doi: 10.1016/j.nbd.2011.02.016

Sandi, C., Sandi, M., Anjomani Virmouni, S., Al-Mahdawi, S., and Pook, M. A. (2014a). Epigenetic-based therapies for Friedreich ataxia. *Front. Genet.* 5:165. doi: 10.3389/fgene.2014.00165

Sandi, C., Sandi, M., Jassal, H., Ezzatizadeh, V., Anjomani-Virmouni, S., Al-Mahdawi, S., et al. (2014b). Generation and characterisation of Friedreich ataxia YG8R mouse fibroblast and neural stem cell models. *PLoS One* 9:e89488. doi: 10.1371/journal.pone.0089488

Saveliev, A., Everett, C., Sharpe, T., Webster, Z., and Festenstein, R. (2003). DNA triplet repeats mediate heterochromatin-protein-1-sensitive variegated gene silencing. *Nature* 422, 909–913. doi: 10.1038/nature01596

Schulz, J. B., Boesch, S., Burk, K., Durr, A., Giunti, P., Mariotti, C., et al. (2009). Diagnosis and treatment of Friedreich ataxia: a European perspective. *Nat. Rev. Neurol.* 5, 222–234. doi: 10.1038/nrneurol.2009.26

Sherzai, S. (2018). *Investigating Novel Therapies for Frieidriech's Ataxia*. PhD thesis, Brunel University London, Uxbridge.

Soragni, E., Miao, W., Iudicello, M., Jacoby, D., De Mercanti, S., Clerico, M., et al. (2014). Epigenetic therapy for Friedreich ataxia. *Ann. Neurol.* 76, 489–508. doi: 10.1002/ana.24260

Wang, Z., and Liu, H. (2019). Lysine methylation regulates nervous system diseases. *Neuropeptides* 76:101929. doi: 10.1016/j.npep.2019.04.004

Willis, J. H., Isaya, G., Gakh, O., Capaldi, R. A., and Marusich, M. F. (2008). Lateral-flow immunoassay for the frataxin protein in Friedreich's ataxia patients and carriers. *Mol. Genet. Metab.* 94, 491–497. doi: 10.1016/j.ymgme.2008.03.019

Yandim, C., Natisvili, T., and Festenstein, R. (2013). Gene regulation and epigenetics in Friedreich's ataxia. *J. Neurochem.* 126(Suppl. 1), 21–42. doi: 10.1111/jnc.12254

Ziemka-Nalecz, M., Jaworska, J., Sypecka, J., and Zalewska, T. (2018). Histone deacetylase inhibitors: a therapeutic key in neurological disorders? *J. Neuropathol. Exp. Neurol.* 77, 855–870. doi: 10.1093/jnen/nly073

Conflict of Interest: The authors declare that the research was conducted in the absence of any commercial or financial relationships that could be construed as a potential conflict of interest.

frontiers in Genetics

OPINION
published: 09 June 2020
doi: 10.3389/fgene.2020.00528

Prime Editing: Genome Editing for Rare Genetic Diseases Without Double-Strand Breaks or Donor DNA

Ianis G. Matsoukas [1,2]*

[1] School of Medicine, University of Bolton, Bolton, United Kingdom, [2] René Descartes College, Athens, Greece

Keywords: CRISPR, genome editing, human therapeutics, prime editing, rare disease

An article published in Nature (Anzalone et al., 2019) reports the development of a genome editing experimental approach that mediates all possible base-to-base conversions, "indels," and combinations in human genome without the need of double-strand breaks (DSBs) or donor DNA (dDNA) templates. Prime editing, the novel method of genome editing, exploits a longer-than-usual single guide RNA (gRNA), known as prime editing gRNA (pegRNA), and a fusion protein consisting of Cas9 H840A nickase fused to an engineered reverse transcriptase (RT) enzyme. Described as "search-and-replace" base-editing technology, prime editing supplies the desired genetic construct in an extension to the gRNA, which is then converted to DNA using the RT enzyme. The new approach eliminates the need for co-delivery of a corrective DNA template, performs all possible nucleotide substitutions (including those for a sizeable proportion of genetic disorders), resolves frameshifts induced by indels and confers fewer off-target edits when compared with conventional CRISPR-Cas devices. Prime editing is an exciting new complement to existing CRISPR editing systems and may even be an improvement in many cases. However, prime editing introduces new challenges. Overcoming these obstacles and applying prime editing *in vivo*, will give rise to new genome editing therapies for rare genetic diseases.

OPEN ACCESS

Edited by:
Sascha Meyer,
Saarland University Hospital, Germany

Reviewed by:
Jernej Kovac,
University Medical Centre
Ljubljana, Slovenia

***Correspondence:**
Ianis G. Matsoukas
i.matsoukas@cnam.gr

Specialty section:
This article was submitted to Genetic Disorders, a section of the journal Frontiers in Genetics

Received: *15 January 2020*
Accepted: *01 May 2020*
Published: *09 June 2020*

Citation:
Matsoukas IG (2020) Prime Editing: Genome Editing for Rare Genetic Diseases Without Double-Strand Breaks or Donor DNA. Front. Genet. 11:528. doi: 10.3389/fgene.2020.00528

INTRODUCTION: PROGRAMMABLE GENOME EDITING TECHNOLOGIES

Precision genome editing is a versatile and powerful gene therapy tool. Since the development of CRISPR/Cas systems for genome editing (**Figure 1A**), the field has been subject to continuous improvements (Charpentier and Doudna, 2013; Doudna and Charpentier, 2014; Hsu et al., 2014; Sternberg and Doudna, 2015; Komor et al., 2017). The new biotechnology involves the formation of a site-specific DSB followed by two major types of repair mechanisms: non-homologous end-joining (NHEJ; Davis and Chen, 2013) and homology-directed repair (HDR; Li and Heyer, 2008). The activated type of the molecular repair mechanism depends on the genome, cellular heterogeneity and cell-division cycle (Hsu et al., 2014; Komor et al., 2017).

Therefore, the induction of a precise mutation conferred by a genome editing tool, is heavily depends on HDR occurring at the DSB *locus* via the dDNA template harboring the desired construct (Yang et al., 2014; Song and Stieger, 2017; Bollen et al., 2018). Although CRISPR/Cas systems can efficiently confer a DSB at a specific genomic sequence (Cong et al., 2013; Jinek et al., 2013; Savic et al., 2018), HDR in mammalian cells is inefficient or unsuitable due to the low innate rate of HDR and obstacles in onsite delivery of dDNA (Cong et al., 2013; Mali et al., 2013). The correction rates of the conventional genome-editing tools are 0.1–5%, and, typically, they introduce a plenty of random indels at the target genomic sequence resulting from the cellular response to DSBs (Cox et al., 2015; Hilton and Gersbach, 2015). Recently, CRISPR/Cas-mediated base editing tools have

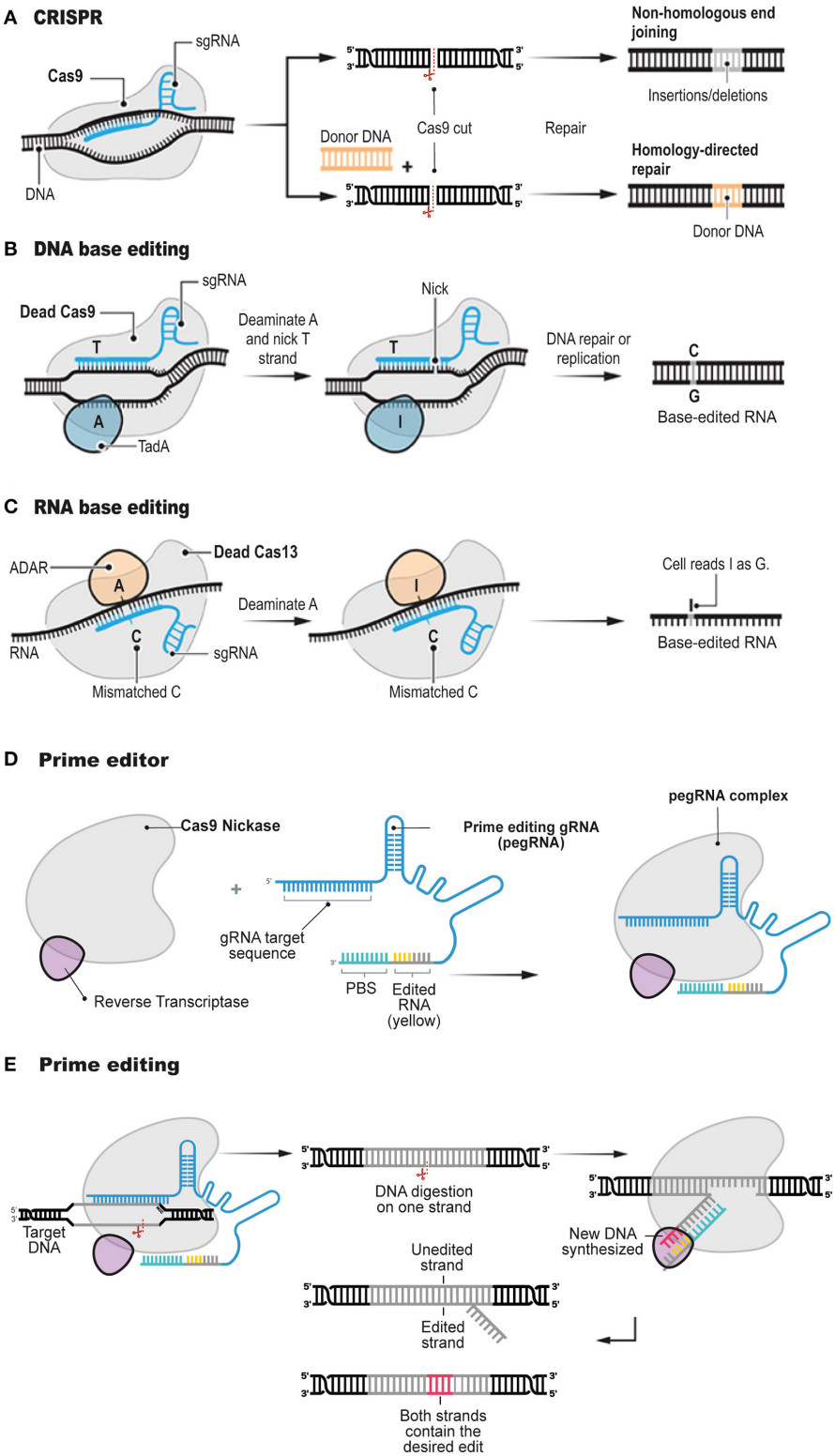

FIGURE 1 | Structure and function of prime editor. The conventional CRISPR DNA editor **(A)**. CRISPR relies on the ability of CRISPR gRNAs to target the Cas9 endonuclease to precise genomic locations, where Cas9 introduces DSBs. Base editors do not digest the double strand, but instead they chemically alter single bases with deaminase enzymes such as TadA (**B**, DNA base editor) and ADAR (**C**, RNA base editor). Prime editor **(D)** involves a longer-than-usual gRNA, known as pegRNA, and a fusion protein consisting of Cas9 H840A nickase fused to a modified RT enzyme. The Cas9 element of the prime editor digest the genomic DNA and the RT element polymerises DNA onto the nicked strand based on the pegRNA sequence **(E)**. Adapted from Anzalone et al. (2019) and Matsoukas (2018a).

been developed to circumvent these constraints (**Figures 1B,C**; Komor et al., 2016; Nishida et al., 2016; Kim et al., 2017; Gehrke et al., 2018; Li et al., 2018; Sharon et al., 2018; Wang et al., 2018). Several excellent review articles have been published on the different types of customizable base editors (Rees and Liu, 2018; Molla and Yang, 2019; Yang et al., 2019). Hence, these base-editing tools will not be described in great detail here.

Briefly, base editors generate mutations at single-base resolution. All four transition mutations, C→T, G→A, A→G, and T→C, can be introduced in the genome with the already described CRISPR/Cas base editors. The cytosine base editors (Komor et al., 2016; Nishida et al., 2016; Kim et al., 2017; Gehrke et al., 2018; Li et al., 2018; Matsoukas, 2018a; Wang et al., 2018) can establish a C-G to T-A mutation, while the adenine base editors (Gaudelli et al., 2017; Kim et al., 2019) can modify an A-T base dyad into a G-C dyad. In RNA, conversion of Adenine to Inosine is also possible with an RNA base editor (**Figure 1C**; Cox et al., 2017; Matsoukas, 2018b). Since many genetic diseases and disorders arise from nucleotide substitutions and nucleotide additions or deletions, base editing has important implications in the study of human pathogenesis.

However, base editors cannot install all transversion mutations. For example the currently reported base editors cannot introduce the eight transversion mutations (C→A, C→G, G→C, G→T, A→C, A→T, T→A, and T→G), such as the T·A-to-A·T mutation required to precisely correct the most common etiology of sickle cell disease (SCD). SCD, a homozygous mutation (from A → T) in the sixth codon (E6V) of the human b-globin (HBB) gene, converts a glutamate to a valine which synthesizes defective b-globin proteins and results in abnormal red blood cells (Vakulskas et al., 2018). It is postulated that HDR-mediated HBB gene correction in autologous hematopoietic stem and progenitor cells, would be a safe and effective gene therapy approach for SCD.

In addition, no DSB-free experimental approach has been reported to confer targeted deletions, such as the removal of the 4-base duplication that causes Tay-Sachs disease (HEXA 1278+TATC; McGinniss et al., 2002), or targeted insertions, such as the 3-base insertion needed to precisely correct the most common etiology of cystic fibrosis (cf. Lukacs and Verkman, 2012). In regard to CF, the deletion of the phenylalanine residue at position ΔF508, is present in one or both alleles in ∼90% of CF patients. Interestingly, these challenges drive the development of novel and state-of-the-art precision genome editing technologies.

This article describes prime editing, a novel genome editing tool which has been developed to expand the scope and capabilities of the existing CRISPR/Cas-based therapies for rare genetic diseases. The article also discusses the new challenges that the new biotechnology introduces and suggests possible directions for future research.

PRIME EDITORS: EXPANDING THE GENOME-EDITING TOOLBOX

Targeted transversions, insertions and deletions are problematic to induce or repair efficiently and without excess by-products in most cellular types, even though they collectively account for most known pathogenic alleles. Interestingly, a paper recently published in Nature (Anzalone et al., 2019) reports a tool developed to address the base-editing limitations described above. Prime editing, the most recent base-editing tool, employs the same mechanism as conventional CRISPR/Cas systems mediating all 12 possible base-to-base conversions, and combinations, but without conferring DSBs in the target sequence or exploiting a dDNA template. Prime editing involves a longer-than-usual gRNA, known as pegRNA, and a fusion protein consisting of Cas9 H840A nickase fused to an engineered RT enzyme (**Figure 1D**).

This article (Anzalone et al., 2019) follows other important publications (Gaudelli et al., 2017; Kim et al., 2017) by the same research group, which described the first base-editing molecular devices. In the latest article, Anzalone et al. (2019) tested whether gRNA could be extended to include extra nucleotides. Some of these extra nucleotides would serve as a template for synthesis of a new DNA sequence, while others would bind to the DNA strand, opposite from the expected gRNA binding site, to use that genomic *locus* as a primer for the RT initiation. With the construction of the extended pegRNA, Anzalone et al. (2019) was able not only to guide Cas9 enzyme variants to the appropriate *locus* but also to install the desired edit and prime the RT enzyme (**Figure 1E**).

This novel experimental approach was enhanced by the construction of three incremental devices. The first molecular device (PE1) was created by a fusion of Cas9 H840A nickase and wild-type (WT) Maloney murine leukemia virus RT enzyme. In this construct, the Cas9 H840A nickase domain of the prime editing fusion protein (PEFP) nicks only one of the polynucleotide strands for subsequent restoration, whereas the RT domain generates complementary DNA (cDNA) by copying the pegRNA (carrying the desired construct) to reinstate a segment of the nicked DNA strand. In this device, Anzalone et al. (2019) also increased the length of the pegRNA site that binds the primer section of the DNA. The application of the PE1 device led to minor but still detectable genome edits.

In the PE2 device, Anzalone et al. (2019) improved the thermostability, processivity, and DNA-RNA substrate affinity of the RT component of the PEFP by introducing five specific mutations. This pentamutant RT enzyme incorporated into PE1, creating the PE2 device. The PE2 device led to a 5.1-fold improvement in prime editing point mutation efficiency and conferred targeted insertions and deletions more methodically than PE1.

In the third molecular device (PE3), Anzalone et al. (2019) introduced a second gRNA, in addition to the pegRNA. The additional gRNA was a standard gRNA directing the Cas9 H840A nickase element of the PEFP to nick the genomic DNA at a nearby site, but on the opposite strand as the original nick. They applied this approach due to a concern that efficient editing of one strand, as observed with PE2 device, might be repressed due to a mismatch between the engineered and non-engineered DNA strands. By installing a nick on the non-engineered DNA strand, Anzalone et al. (2019) reasoned that the DNA repair machinery might replace the original *locus* with the desired

segment. Interestingly, PE3 device was more efficient when the additional gRNA constructed to match the newly-edited sequence introduced by the pegRNA. The PE3 device with the new characteristic of gRNA was labeled PE3b. The group also observed improved efficiencies when they designed the pegRNA to mutate the original protospacer adjacent motif (PAM).

DNA base editors have consistently proven forceful for installing precise point mutations in the genome of a wide variety of model systems [reviewed in (Sharon et al., 2018; Molla and Yang, 2019)]. In the article published by Anzalone et al. (2019), PE2, PE3, and PE3b devices were compared with cytidine/adenine base editors and with an HDR system. Interestingly, it was shown that that PE devices function in a complementary fashion to the base editor systems, depending on the desired *locus*. Also, prime editing compared favorably, in its specific abilities, to HDR. As with all genome editing technologies, base editors have the potential to operate on DNA at off-target genomic *loci*. However, it was shown that prime editing introduces much lower off-target editing than Cas9 at known Cas9 off-target *loci*.

PRIME EDITING THERAPEUTICS

Anzalone et al. (2019) tested the ability of prime editing to install and then to correct several pathogenic mutations, including the mutations known to cause SCD and Tay-Sachs diseases. In case of SCD, they exploited the PE3 device to install the HBB E6V mutation in HEK293T cell line. This approach resulted with 44% efficiency and 4.8% indels. To correct the HBB E6V allele back to WT HBB, they treated homozygous HBB E6V HEK293T cells with PE3 and a pegRNA programmed to directly revert the HBB E6V mutation to WT HBB phenotype. All tested pegRNAs devices mediated efficient correction of HBB E6V to WT HBB (26–52% efficiency), and 2.8 $\pm$ 0.70% indels. In addition, installation of a PAM-modifying silent mutation in PE3 device, improved editing efficiency and product purity to 58% correction rate, with 1.4% indels.

In regard to Tay-Sachs disease, they created the mutant phenotype by exploiting the PE3 device to install a 4-bp insertion into *HEXA,* with 31% efficiency and 0.8% indels. To recreate the WT phenotype, application of the PE3 device resulted in $\geq$20% editing, whereas application of the PE3b device resulted 33% efficiency with 0.32% indels.

Anzalone et al. (2019) also succeeded in introducing a mutation that imparts resistance to prion disease in humans (Mead et al., 2009) and mice (Asante et al., 2015). The PE3 device was used to install a protective G·C-to-T·A transversion into *PRION PROTEIN* in HEK293T cell line, creating a G127V mutant allele that confers the resistance to prion disease. The most effective pegRNA, by using the PE3 device, resulted in 53% installation of G127V with 1.7% indels.

The findings were further enhanced by introducing prime editing into mouse murine primary cortical neurons, using a lentiviral delivery system. To determine if prime editing is feasible in post-mitotic, terminally differentiated primary cells, they transduced primary cortical neurons from E18.5 mice with a PE3 lentiviral delivery system, in which PE2 protein components were expressed from the neuron-specific synapsin promoter along with a green fluorescence protein biomarker (Kügler et al., 2003). It was shown that the PE3 device was more efficient (7.1%), generated fewer by-products and with lower off-target editing, compared to conventional CRISPR/Cas9 genome editing systems. This indicates that post-mitotic, terminally differentiated primary cells, can tolerate prime editing.

DISCUSSION

The development of prime editing is a significant addition to the genome editing toolbox. Prime editing is the most recent of the tools developed to address CRISPR/Cas limitations and calibrate the genome editing process. For academic use, the technology can be currently obtained by the Addgene repository (Kamens, 2015).

Just as prime editors, cytidine base editors and adenine base editors can install transition mutations efficiently and with few indels. Arguably, there are particular cases where conventional base editors are more desired. For instance, if the target *locus* is positioned within the canonical base editing window, base editing has higher efficiency and fewer indels than prime editing. However, the application of base editing can be limited by unwanted bystander edits from the presence of multiple cytidine or adenine bases, or by the absence of a PAM positioned $\sim$15 $\pm$ 2 nt from the target *locus*. On the other hand, prime editing eliminates the need for co-delivery of a corrective DNA construct, a factor that can magnify standard challenges in the delivery of genome editing machinery.

However, prime editing introduces new challenges. Prime editors may not be able to confer the large DNA insertions or deletions that conventional CRISPR/Cas9 systems are capable of. Also, the fact that the desired sequence has to be encoded in an extensive RNA molecule, raises concerns regarding its stability; the longer the RNA strand gets, the more likely it is to be affected by intracellular RNA-degrading enzymes. In addition, due to presence of the RT in the molecular device, random cDNAs could be potentially incorporated in the genome. Furthermore, as the protein constructs involved are too large, this might affect the delivery of a full-length therapeutic protein by a single adeno-associated viral vector.

Therefore, more work remains before prime editors can be used to treat patients with rare genetic disorders. This includes approaches for optimizing prime editors, maximizing its efficiency in different cell types, and examining potential effects of prime editing on different cell lines. Furthermore, additional experimentation with rare disease models and mechanisms at cellular and organismal level and exploring novel delivery mechanisms in animal model systems to provide potential approaches for human therapeutic applications, are required. In conclusion, undoubtedly, prime editing is another double-edged sword on offer in the field of genome editing therapies for rare genetic diseases, offering more precise base editing ability and efficiency.

AUTHOR CONTRIBUTIONS

The author confirms being the sole contributor of this work and has approved it for publication.

FUNDING

Research in the Laboratory of IM is supported by a Jenkinson TIRI Award, the University of Bolton, UK, and René Descartes College, GR.

REFERENCES

Anzalone, A. V., Randolph, P. B., Davis, J. R., Sousa, A. A., Koblan, L. W., Levy, J. M., et al. (2019). Search-and-replace genome editing without double-strand breaks or donor DNA. *Nature* 576, 149–157. doi: 10.1038/s41586-019-1711-4

Asante, E. A., Smidak, M., Grimshaw, A., Houghton, R., Tomlinson, A., Jeelani, A., et al. (2015). A naturally occurring variant of the human prion protein completely prevents prion disease. *Nature* 522, 478–481. doi: 10.1038/nature14510

Bollen, Y., Post, J., Koo, B. K., and Snippert, H. J. G. (2018). How to create state-of-the-art genetic model systems: strategies for optimal CRISPR-mediated genome editing. *Nucleic Acids Res.* 46, 6435–6454. doi: 10.1093/nar/gky571

Charpentier, E., and Doudna, J. A. (2013). Rewriting a genome. *Nature* 495:50–51. doi: 10.1038/495050a

Cong, L., Ran, F. A., Cox, D., Lin, S., Barretto, R., Habib, N., et al. (2013). Multiplex genome engineering using CRISPR/Cas systems. *Science* 339, 819–823. doi: 10.1126/science.1231143

Cox, D. B. T., Gootenberg, J. S., Abudayyeh, O. O., Franklin, B., Kellner, M. J., Joung, J., et al. (2017). RNA editing with CRISPR-Cas13. *Science* 358, 1019–1027. doi: 10.1126/science.aaq0180

Cox, D. B. T., Platt, R. J., and Zhang, F. (2015). Therapeutic genome editing: Prospects and challenges. *Nat. Med.* 21, 121–131. doi: 10.1038/nm.3793

Davis, A. J., and Chen, D. J. (2013). DNA double strand break repair via non-homologous end-joining. *Transl. Cancer Res.* 2, 130–143. doi: 10.3978/j.issn.2218-676X.2013.04.02

Doudna, J. A., and Charpentier, E. (2014). The new frontier of genome engineering with CRISPR-Cas9. *Science* 346:1258096.doi: 10.1126/science.1258096

Gaudelli, N. M., Komor, A. C., Rees, H. A., Packer, M. S., Badran, A. H., Bryson, D. I., et al. (2017). Programmable base editing of T to G C in genomic DNA without DNA cleavage. *Nature* 551, 464–471. doi: 10.1038/nature24644

Gehrke, J. M., Cervantes, O., Clement, M. K., Wu, Y., Zeng, J., Bauer, D. E., et al. (2018). An apobec3a-cas9 base editor with minimized bystander and off-target activities. *Nat. Biotechnol.* 36, 77–982. doi: 10.1038/nbt.4199

Hilton, I. B., and Gersbach, C. A. (2015). Enabling functional genomics with genome engineering. *Genome Res.* 25, 1442–1455. doi: 10.1101/gr.190124.115

Hsu, P. D., Lander, E. S., and Zhang, F. (2014). Development and applications of CRISPR-Cas9 for genome engineering. *Cell* 157, 1262–1278. doi: 10.1016/j.cell.2014.05.010

Jinek, M., East, A., Cheng, A., Lin, S., Ma, E., and Doudna, J. (2013). RNA-programmed genome editing in human cells. *Elife.* 2:e00471. doi: 10.7554/eLife.00471

Kamens, J. (2015). The addgene repository: an international nonprofit plasmid and data resource. *Nucleic Acids Res.* 43:D1152–D1157. doi: 10.1093/nar/gku893

Kim, H. S., Jeong, Y. K., Hur, J. K., Kim, J.-S., and Bae, S. (2019). Adenine base editors catalyze cytosine conversions in human cells. *Nat. Biotechnol.* 37, 1145–1148. doi: 10.1038/s41587-019-0254-4

Kim, Y. B., Komor, A. C., Levy, J. M., Packer, M. S., Zhao, K. T., and Liu, D. R. (2017). Increasing the genome-targeting scope and precision of base editing with engineered Cas9-cytidine deaminase fusions. *Nat. Biotechnol.* 35, 371–376. doi: 10.1038/nbt.3803

Komor, A. C., Kim, Y. B., Packer, M. S., Zuris, J. A., and Liu, D. R. (2016). Programmable editing of a target base in genomic DNA without double-stranded DNA cleavage. *Nature* 533, 420–424. doi: 10.1038/nature17946

Komor, A. C., Zhao, K. T., Packer, M. S., Gaudelli, N. M., Waterbury, A. L., Koblan, L. W., et al. (2017). Improved base excision repair inhibition and bacteriophage Mu Gam protein yields C:G-to-T: a base editors with higher efficiency and product purity. *Sci. Adv.* 3:eaao4774. doi: 10.1126/sciadv.aao4774

Kügler, S., Kilic, E., and Bähr, M. (2003). Human synapsin 1 gene promoter confers highly neuron-specific long-term transgene expression from an adenoviral vector in the adult rat brain depending on the transduced area. *Gene Ther.* 10, 337–347. doi: 10.1038/sj.gt.3301905

Li, X., and Heyer, W. D. (2008). Homologous recombination in DNA repair and DNA damage tolerance. *Cell Res.* 18, 99–113. doi: 10.1038/cr.2008.1

Li, X., Wang, Y., Liu, Y., Yang, B., Wang, X., Wei, J., et al. (2018). Base editing with a Cpf1-cytidine deaminase fusion. *Nat. Biotechnol.* 36, 324–327.doi: 10.1038/nbt.4102

Lukacs, G. L., and Verkman, A. S. (2012). CFTR: folding, misfolding and correcting the ΔF508 conformational defect. *Trends Mol. Med.* 18, 81–91. doi: 10.1016/j.molmed.2011.10.003

Mali, P., Yang, L., Esvelt, K. M., Aach, J., Guell, M., DiCarlo, J. E., et al. (2013). RNA-guided human genome engineering via Cas9. *Science* 339, 823–826. doi: 10.1126/science.1232033

Matsoukas, I. G. (2018a). Commentary: programmable base editing of A·T to G·C in genomic DNA without DNA cleavage. *Front. Genet.* 9:21. doi: 10.3389/fgene.2018.00021

Matsoukas, I. G. (2018b). Commentary: RNA editing with CRISPR-Cas13. *Front. Genet.* 9:134. doi: 10.3389/fgene.2018.00134

McGinniss, M. J., Brown, D. H., Fulwiler, A., Marten, M., Lim-Steele, J. S. T., and Kaback, M. M. (2002). Eight novel mutations in the HEXA gene. *Genet. Med.* 4, 158–161. doi: 10.1097/00125817-200205000-00010

Mead, S., Whitfield, J., Poulter, M., Shah, P., Uphill, J., Campbell, T., et al. (2009). A novel protective prion protein variant that colocalizes with kuru exposure. *N. Engl. J. Med.* 361, 2056–2065. doi: 10.1056/NEJMoa0809716

Molla, K. A., and Yang, Y. (2019). CRISPR/Cas-mediated base editing: technical considerations and practical applications. *Trends Biotechnol.* 37, 1121–1142. doi: 10.1016/j.tibtech.2019.03.008

Nishida, K., Arazoe, T., Yachie, N., Banno, S., Kakimoto, M., Tabata, M., et al. (2016). Targeted nucleotide editing using hybrid prokaryotic and vertebrate adaptive immune systems. *Science* 353:aaf8729. doi: 10.1126/science.aaf8729

Rees, H. A., and Liu, D. R. (2018). *Base* editing: precision chemistry on the genome and transcriptome of living cells. *Nat. Rev. Genet.* 19, 770–788. doi: 10.1038/s41576-018-0059-1

Savic, N., Ringnalda, F. C. A. S., Lindsay, H., Berk, C., Bargsten, K., Li, Y., et al. (2018). Covalent linkage of the DNA repair template to the CRISPR-Cas9 nuclease enhances homology-directed repair. *Elife.* 7:e33761. doi: 10.7554/eLife.33761

Sharon, E., Chen, S. A. A., Khosla, N. M., Smith, J. D., Pritchard, J. K., and Fraser, H. B. (2018). Functional genetic variants revealed by massively parallel precise genome editing. *Cell* 175, 544–557.e16. doi: 10.1016/j.cell.2018.08.057

Song, F., and Stieger, K. (2017). Optimizing the DNA donor template for homology-directed repair of double-strand breaks. *Mol. Ther. Nucleic Acids.* 7, 53–60. doi: 10.1016/j.omtn.2017.02.006

Sternberg, S. H., and Doudna, J. A. (2015). Expanding the biologist's toolkit with CRISPR-Cas9. *Mol. Cell.* 58, 568–574. doi: 10.1016/j.molcel.2015.02.032

Vakulskas, C. A., Dever, D. P., Rettig, G. R., Turk, R., Jacobi, A. M., Collingwood, M. A., et al. (2018). A high-fidelity Cas9 mutant delivered as a ribonucleoprotein complex enables efficient gene editing in human

hematopoietic stem and progenitor cells. *Nat. Med.* 24, 1216–1224. doi: 10.1038/s41591-018-0137-0

Wang, X., Li, J., Wang, Y., Yang, B., Wei, J., Wu, J., et al. (2018). Efficient base editing in methylated regions with a human apobec3a-cas9 fusion. *Nat. Biotechnol.* 36, 946–949. doi: 10.1038/nbt.4198

Yang, B., Yang, L., and Chen, J. (2019). Development and application of base editors. *Cris. J.* 2, 91–104. doi: 10.1089/crispr.2019.0001

Yang, L., Yang, J. L., Byrne, S., Pan, J., and Church, G. M. (2014). CRISPR/Cas9-directed genome editing of cultured cells. *Curr. Protoc. Mol. Biol.* 107, 31.1.1-31.1.17. doi: 10.1002/0471142727.mb3101s107

Conflict of Interest: The author declares that the research was conducted in the absence of any commercial or financial relationships that could be construed as a potential conflict of interest.

frontiers in Pediatrics

REVIEW
published: 25 June 2020
doi: 10.3389/fped.2020.00339

Pediatric NMOSD: A Review and Position Statement on Approach to Work-Up and Diagnosis

Silvia Tenembaum[1], *E. Ann Yeh*[2]* *and The Guthy-Jackson Foundation International Clinical Consortium (GJCF-ICC)*[†]

[1] Department of Neurology, National Pediatric Hospital Dr. J. Garrahan, Buenos Aires, Argentina, [2] Division of Neurology, Department of Pediatrics, SickKids Research Institute, The Hospital for Sick Children, University of Toronto, Toronto, ON, Canada

OPEN ACCESS

Edited by:
Pasquale Striano,
University of Genoa, Italy

Reviewed by:
Stefano Sartori,
University of Padova, Italy
Tetsuya Akaishi,
Tohoku University, Japan
Nicolas Collongues,
Hôpitaux Universitaires de Strasbourg, France
Maria Margherita Mancardi,
Giannina Gaslini Institute (IRCCS), Italy

***Correspondence:**
E. Ann Yeh
ann.yeh@sickkids.ca

[†]See Appendix for complete list of active GJCF-ICC Members

Specialty section:
This article was submitted to Pediatric Neurology, a section of the journal Frontiers in Pediatrics

Received: 27 April 2020
Accepted: 21 May 2020
Published: 25 June 2020

Citation:
Tenembaum S, Yeh EA and The Guthy-Jackson Foundation International Clinical Consortium (GJCF-ICC) (2020) Pediatric NMOSD: A Review and Position Statement on Approach to Work-Up and Diagnosis. Front. Pediatr. 8:339. doi: 10.3389/fped.2020.00339

Neuromyelitis Optica Spectrum Disorder (NMOSD) is an inflammatory demyelinating disease of the central nervous system (CNS) primarily affecting the optic nerves and spinal cord, but also involving other regions of the CNS including the area postrema, periaqueductal gray matter, and hypothalamus. Knowledge related to pediatric manifestations of NMOSD has grown in recent years, particularly in light of newer information regarding the importance of not only antibodies to aquaporin 4 (AQP4-IgG) but also myelin oligodendrocyte glycoprotein (MOG-IgG) in children manifesting clinically with this syndrome. In this review, we describe the current state of the knowledge related to clinical manifestations, diagnosis, and chronic therapies for children with NMOSD, with emphasis on literature that has been published in the last 5 years. Following the review, we propose recommendations for the assessment/follow up clinical care, and treatment of this population.

Keywords: pediatric, neuroinflammation, NMOSD, MOG, treatment, diagnosis

INTRODUCTION

Neuromyelitis Optica Spectrum Disorder (NMOSD) is a chronic relapsing condition characterized by inflammatory episodes of the central nervous system, primarily affecting the optic nerves and spinal cord, but also involving other regions of the central nervous system including the area postrema, periaqueductal gray matter, and hypothalamus. Specific cases may also show a variety of abnormalities in the brain, involving the periependymal and subcortical white matter, the corpus callosum, corticospinal tracts and deep gray matter. Since the landmark description of a highly sensitive and specific antibody against the AQP4 channel—AQP4-IgG antibody—in 2004 (1), knowledge about this syndrome and its treatment has increased substantially.

While much work has focused on manifestations of the syndrome in the adult population, recent years have seen an exponential rise in knowledge regarding NMOSD in children. This has occurred together with the establishment of the clinical utility/relevance of another antibody that appears with great frequency in children with neuroinflammatory disorders, and which has been associated with a similar clinical syndrome, albeit with specific and distinct manifestations, antibodies to myelin oligodendrocyte glycoprotein (MOG) (2, 3).

In this review, we describe the current state of the knowledge related to clinical manifestations, diagnosis, and chronic therapies for children with NMOSD, with emphasis on literature that has been published in the last 5 years. We will not discuss treatment of acute relapses in this review. Following the review, we propose recommendations for the assessment/follow up clinical care, and treatment of this population.

REVIEW OF CURRENT KNOWLEDGE

Definitions

Diagnostic criteria for neuromyelitis optica (NMO) have evolved since the initial 1999 publication which described NMO as an inflammatory CNS syndrome distinct from MS. Initial criteria required the presence of optic neuritis, longitudinally extensive transverse myelitis, CSF pleocytosis >50 cells/mm^3, and the absence of brain MRI lesions or absence of lesions typical for MS (4). Since 1999, the criteria have undergone 2 more revisions. In 2006, the criteria saw the introduction of AQP4-IgG -positivity as a supportive criterion and loosening of the supportive criterion related to—*brain MRI abnormalities not meeting MS diagnostic criteria*. The diagnostic entity continued to be called NMO. Over the next decade, identification of the antibody and widespread availability of testing made it clear that a spectrum of clinical and MRI manifestations outside of optic neuritis and transverse myelitis should be included in this clinical entity, including specific focal abnormalities such as area postrema and hypothalamic involvement that might occur *in the absence of* optic nerve or spinal cord involvement. This led to a nosological change, to the current consensus criteria based entity of *Neuromyelitis Optica Spectrum Disorder* (NMOSD) (5). Core criteria include optic neuritis, acute myelitis, area postrema syndrome, acute brainstem syndrome, narcolepsy/acute diencephalic syndrome, and symptomatic cerebral syndrome with NMOSD-typical brain lesions. Importantly, for diagnosis, only one core criterion is necessary in the presence of AQP4-antibody. The criteria for making the diagnosis in seronegative patients or in the absence of access to AQP4-IgG testing included dissemination in space with the presence of two core clinical criteria and additional MRI requirements. The diagnosis is contingent on the absence of alternate reasons explaining the syndrome. These diagnostic criteria have been validated in the pediatric age group (6).

Demographics and Epidemiology

Previous epidemiologic studies have focused primarily on ***AQP4-IgG related NMOSD***, and have revealed that NMOSD prevalence varies by race, being higher in non-white than in white populations (7, 8). A study conducted in Australia and New Zealand showed that NMOSD was three times more prevalent in individuals with Asian ancestry than in the remaining population with predominantly European ancestry (9). In addition, the NMOSD/multiple sclerosis ratio has been reported to be higher in Asia than in Western countries (10). A recent study using data from a large international cohort of adult patients with NMOSD revealed that race affected the clinical phenotype, age at onset, and severity of attacks, but the overall clinical outcome was most dependent on early and effective immunosuppressive treatment initiation (11).

Although infrequent, NMOSD can occur in children and current data suggest that pediatric-onset NMOSD accounts for 3–5% of all NMOSD cases, depending on the diagnostic criteria and the inclusion of AQP4-antibody testing (12, 13). Median age of onset in a Chinese study was 14 (range 7–17 years) (14).

Demographic data from pediatric patients with NMOSD selected from different multinational publications are summarized in **Table 1**. These studies have focused primarily on AQP4-IgG related disease (6, 15–21). Overall, findings have been variable, but most studies suggest that NMOSD is more common in girls than boys, with F:M ratios ranging from 9:1 (UK) (18) to 1:1 (multinational) (19). One study from the US has noted variations in F:M ratio in different age groups, with children older than 11 years of age demonstrating a 3.5:1 ratio, and those younger than 11 a F:M ratio of 1.5:1 (6). Incidence and prevalence of pediatric-onset NMOSD are not well-characterized, but population-based studies from Europe, Asia, and South America suggest that the overall incidence of NMOSD in children and adults ranges from 0.05 to 4/100,000 per year, and the prevalence from 0.52 to 4.4/100,000 (22). In Japan, the incidence of pediatric NMOSD was reported to be 0.06 per 100,000 children (23).

In a retrospective study of the Catalonian population in Spain prevalence and incidence in children with NMOSD were 0.22/100,000 and 0.037/100,000, respectively. Of the 5 incident pediatric cases identified in this study, 2 were AQP4-IgG positive, 1 was MOG-IgG positive, and 2 were double seronegative (20). Further work is needed to clarify the incidence and prevalence of ***MOG-IgG related NMOSD in children***.

Clinical Manifestations

A recent study compared demographic and clinical characteristics of pediatric and adult patients with confirmed clinical diagnoses of NMOSD and found that pediatric patients were more likely to be evaluated by an ophthalmologist (88 vs. 21%; $p < 0.001$) and rheumatologist (44 vs. 7%; <0.001) within 6 months prior to or 6 months after their first clinical event. Children were also more likely to require hospitalization (94 vs. 55%; $p < 0.01$) and to undergo MRI of the orbits (44 vs. 11%; $p < 0.01$) within $\pm$ 30 days of their diagnosis (21). Notably, MOG-IgG antibodies are of great importance in NMOSD: in one study, 40% of individuals presenting with optic neuritis and transverse myelitis who were negative for AQP4-antibodies were found to be positive for MOG-IgG (24). In this section, we will describe features associated with either/both MOG-IgG and AQP4-IgG in children and specifically indicate which antibody these clinical features have been associated with.

Optic Neuritis and Transverse Myelitis

A first clinical event of optic neuritis (ON) occurred in 50–75% of patients and transverse myelitis in 30–50%, either alone or in combination according to different pediatric case series of NMOSD (6, 13, 18, 25). The frequency of AQP4-IgG seropositivity is much lower in pediatric-onset NMOSD compared with adults. In a pediatric cohort from UK, 12/24

TABLE 1 | Demographic data of pediatric NMOSD from eight published series.

Pediatric NMOSD population	German	French	Brazilian	UK	US network	Multinational	Catalonia (Spain)	US
	n = 7 (15)	*n* = 12 (16)	*n* = 29 (17)	*n* = 20 (18)	*n* = 38 (6)	*n* = 12 NMO, 33 limited forms (19)	*n* = 5 (20)	*n* = 16 (21)
Mean age at onset	9.6 (5–14)	14.5 (4–17.9)	13 (5–17)	10.5 (2.9–16.8)	10.2 ± 4.7	9 (0.75–17)	n/a	12 (1–15)
Female/Male ratio	2.5:1	3:1	2.6–1	9:1	<11 years = 1.5:1 >11 years = 3.25:1	1:1	1.5:1	3:1
AQP4-IgG positive	2/7	8/12	22/27	12/20	24/37	5/45	2/5	70%
MOG-IgG positive	–	–	–	–	–	25/45	1/5	–
Race	White = 6/7 Arabian = 1/7	White = 8/12 Asian = 2/12 Black = 1/12 American Indian 1/12	Caucasian = 41% Mixed = 52% African = 7%	n/a	White = 37% African American = 37% Asian = 11%	Caucasian = 91% Non-Caucasian = 9%	n/a	White = 31%
Ethnicity					Non-Hispanic/non-Latino = 37% Hispanic/ Latino = 13%			

(50%) of NMOSD patients had MOG- antibodies, while only 2 children had AQP4-IgG (26). In a recent study, 110 MOG-IgG positive patients with optic neuritis were evaluated comparing clinical characteristics and outcome according to the age of presentation: pediatric, young (18–46 years) and middle-aged (>46 years) adult patients (27). Overall, children showed better recovery of visual acuity, lower annual relapse rate, and more intracranial optic nerve involvement than the young and middle-aged groups (27). Two subsets of relapsing optic neuritis, one with discrete acute attacks named RION (recurrent isolated optic neuritis), and the other characterized by chronic relapsing inflammatory optic neuropathy with corticosteroid dependence, named CRION, seem to be associated with MOG-IgG antibodies (28) with high seropositivity rates: 7/7 children (29), 11/12 adults (30).

Area Postrema Syndrome

Area postrema syndrome is a core criterion of NMOSD diagnosis. Prolonged and intractable vomiting and hiccups may be the initial presentation of AQP4-IgG related NMOSD in adult and pediatric patients. Indeed, presentation with an isolated area postrema syndrome is more specific for AQP4-IgG positive NMOSD than longitudinally extensive spinal cord lesions extending to this area (31).

Acute Brainstem Syndromes

Diplopia, facial palsy, hearing loss, hypogeusia, pruritus, trigeminal neuralgia, vestibular ataxia, and dysarthria may be observed at similar frequencies in children (40%) and adult (33–39%) patients with AQP4-IgG seropositive NMOSD in the early stages of the disease (32, 33). Neurogenic respiratory dysfunction due to medullary respiratory center dysfunction is a possible brainstem symptom. Oscillopsia and different types of nystagmus and eye movement abnormalities may occur, due to involvement of eye movement nuclei and tracts within the brainstem.

Cerebral Syndromes

Hemiparesis, visual field involvement, and signs of encephalopathy may be associated with large cerebral hemispheric lesions in 16–32% of AQP4-seropositive children (6, 18). In a recently published pediatric cohort of 116 MOG-IgG seropositive patients, 4/6 children with an NMOSD phenotype had associated brain MRI findings, and 68 additional patients showed an encephalopathic presentation, including 64 with acute disseminated encephalomyelitis (ADEM) features and 22 satisfying criteria for autoimmune encephalitis without ADEM features (34).

Diencephalic Clinical Syndrome

The syndrome of inappropriate antidiuretic hormone secretion (SIADH) is a common presentation of AQP4-IgG related NMOSD (35, 36). Hypotension, hypersomnia, hypothermia, behavioral changes, amenorrhea galactorrhea syndrome, or narcolepsy, with anterior thalamic and hypothalamic MRI involvement should prompt a serum test for AQP4-IgG. This syndrome has been reported in a 12-year-old girl with AQP4-IgG positive NMOSD 3 months after presenting with paraparesis and lower cranial nerve dysfunction (19).

Coexisting Autoimmune Diseases

AQP4-IgG related NMOSD may coexist with other autoimmune diseases, including organ-specific disorders (e.g., myasthenia gravis, thyroid disease, celiac disease) and non-organ-specific disorders (systemic lupus erythematosus, Sjögren syndrome). Five pediatric patients exhibiting coexisting NMOSD and Sjögren syndrome have recently been described (37, 38). NMOSD may also coexist or be followed by NMDA-receptor antibody encephalitis or other autoimmune encephalitis (39–41).

Differential Diagnosis

Vision loss and severe myelopathy can be observed in patients suffering from a variety of disorders and may include metabolic, ischemic, infectious/post-infectious and other inflammatory disorders. One **metabolic** etiology that may be mistaken for NMOSD includes late-onset biotinidase deficiency. It is a treatable disorder that presents distinctly from the classical form of biotinidase deficiency (42). This challenging diagnosis has been reported in adult (43) and pediatric patients (44–46). Spinal cord infarct may present with sudden, painful acute and rapidly evolving weakness and sensory abnormalities. The clinical picture may therefore be difficult to distinguish from inflammatory spinal cord disease: in one series, 41/226 adult patients who received an initial diagnosis of idiopathic transverse myelitis were eventually diagnosed with a vascular myelopathy (47). Imaging is of utility, and will show pencillike hyperintensitities (100%) or a classical "owl eye" appearance (37.5%) in anterior spinal artery infarcts (48). Evidence for spinal growth dystrophy may be present in children with spinal cord infarct (49). **Inflammatory, post-infectious and systemic inflammatory** etiologies include entities such as sarcoidosis, flaccid myelitis, and SLE. Sarcoidosis can cause both optic neuritis and longitudinally extensive myelitis (50). The predilection for a posterior-dorsal subpial gadolinium enhancement in spinal cord sarcoidosis ("trident sign") may help distinguish this entity from NMOSD (51). Acute flaccid myelitis has been increasingly recognized in children presenting with rapidly progressive, asymmetric, and flaccid weakness frequently associated with enterovirus D68 (52–54). The syndrome is usually a pure motor syndrome. On MRI, brain imaging demonstrates dorsal pons involvement in many cases, and spinal cord involvement follows a predominantly gray matter (anterior horn cell) pattern. Optic nerve involvement does not occur in this entity (52, 53).

Systemic Lupus Erythematosus (SLE) may present with longitudinally extensive transverse myelitis which may co-occur with MS and with AQP4-IgG positive NMOSD or be a sign of lupus myelitis. Lupus Myelitis may be difficult to differentiate from SLE with NMOSD myelitis, thus evaluation of serum AQP4-IgG is essential in patients with lupus related myelitis (55). The area postrema syndrome, while suggestive of AQP4-IgG related NMOSD, may exist in other entities in children: an area postrema syndrome with intractable nausea and vomiting was recently described as the presenting symptoms of MS in a 10 year-old girl. MRI, together with laboratory testing and careful clinical evaluation, can provide important and conclusive information regarding diagnosis in cases like this (56).

Neuroimaging in AQP4-IgG and MOG-IgG Related NMOSD

Previous literature has documented the radiographic/MRI features associated with AQP4- IgG positive NMOSD, including longitudinally extensive transverse myelitis with central/gray matter predominance in the presence of hypothalamic and periventricular brainstem lesions, namely dorsal brainstem/area postrema lesions (5). Brain abnormalities are frequently seen and may also include lesions of the corpus callosum (12–40%)—located next to the lateral ventricles with unique features such as complete involvement of the splenium and extension into the cerebral hemispheres—and tumefactive lesions of the brain. Optic nerve involvement includes the presence of longitudinally extensive T2-weighted bright and T1-weighted gadolinium-enhancing lesions of the optic nerve, often bilateral (57). These lesions may be associated with increased diffusivity, suggesting the presence of vasogenic edema. Of note, MRI features of spinal cord lesions may change with time, with longitudinally extensive lesions taking on a patchy appearance or longitudinally extensive spinal cord atrophy at follow up (58).

These features, while associated with AQP4-IgG NMOSD in the adult population, do not distinguish AQP4-IgG positive NMOSD in children from those suffering from other neuroinflammatory disorders, however. LETM is a frequent occurrence across all pediatric neuroinflammatory conditions and is almost universally seen (88%) in children with monophasic transverse myelitis (59). Importantly, recent work on MOG antibody-associated syndromes suggests that this antibody is a more frequent association with LETM in children: one series reported that 11% of children presenting with NMO or limited forms (brainstem syndrome, bilateral ON, recurrent optic neuritis, LETM) were positive for the AQP4-antibody, while 58% were MOG-IgG positive (19). Conversely, in the adult population, over half of LETM patients are AQP4-IgG positive (60, 61).

MRI features of MOG-IgG -associated disease in children include brain lesions in the majority (67%), with subcortical white matter and brainstem lesions (62), which are noted to be large with indistinct borders (63), with complete resolution in over half (53%). Conflicting reports about corpus callosum involvement exist (64). Lesions of the cerebellar peduncle distinguish children with MOG-antibodies from those with AQP4-IgG (65). As for spinal cord lesions, one small study suggests that about half of children with MOG-antibodies may have spinal cord lesions, most of which are localized to the cervical spine (62, 66). Finally, children presenting with ON in the context of MOG-IgG positivity may present with involvement of any part of the optic nerve, but are more likely to have intracranial ON involvement than those who are seronegative (51.2 vs. 17.4%, $p = 0.009$) (67).

Visual Imaging in Pediatric MS and MOG-IgG and AQP4-IgG Related NMOSD: Optical Coherence Tomography

Imaging of the anterior visual pathway using optical coherence tomography may be of utility in distinguishing children with

NMOSD from others. In an older study, children with a history of CRION, an entity now known to be highly associated with MOG-IgG antibodies (28), were found to have a marked decrease in Average Retinal Nerve Fiber Layer Thickness (RNFLT) in comparison to MS patients (50 ± 2 microns in CRION vs. 83 ± 12 in MS ON affected eyes and 107 ± 12 in healthy controls), suggesting more severe injury of the optic nerve in this entity than MS (68). More recently, in a cross sectional study, Chen et al. compared children with new onset ON who were AQP4-IgG positive, MOG-IgG positive, or negative for both antibodies. Average RNFLT in affected eyes was similar between the MOG-IgG positive (58.03 ± 8.73 microns) and AQP4-IgG positive patients (64.34 ± 12.88 microns): those who were antibody positive differed from those who were antibody negative (69). By contrast, another group found almost normal RNFLT in AQP4-IgG positive patients, with similar results to the study above otherwise-−58 microns (range 34,97; IQR 23) in MOG-IgG-positive and 82.5 microns (range 32,116; IQR 36) in seronegative patients (70). In another Chinese study of 48 pediatric patients with acute ON, children seropositive for MOG-IgG had thicker peripapillary retinal nerve fiber layers overall and in the superior and inferior quadrants than patients seropositive for AQP4 -IgG ($p = 0.005$, $p = 0.002$l, and $p = 0.024$, respectively) (67).

Chronic Treatment Strategies: Relapse Prevention

AQP4-IgG associated NMOSD is a relapsing disorder with recurrent attacks of optic neuritis and myelitis if untreated, leading to significant morbidity from relapse-related disability (8, 71) AQP4-IgG seropositive patients have a greater than 50% risk of recurrence in the 12 months after diagnosis. AQP4-IgG seronegative patients likely represent individuals with both monophasic and relapsing inflammatory CNS disorders (72), including those with positive MOG-antibodies.

The clinical course of MOG-IgG related disease—including NMOSD and other clinical phenotypes – is less clear; although initially reported to be typically monophasic, cumulative experience now suggests that, depending on published series, 25% to almost 75% will relapse, and some data suggests that this is particularly true if the serum MOG-IgG persists (73).

Relapse prevention therapies are indicated to decrease the risk and severity of relapses and subsequent disability in patients with high risk of relapse, such as those with AQP4-IgG positive disease, in addition to patients with recurrent disease and persistent MOG- antibodies.

The current available treatment options, including the off-label use of Intravenous Immunoglobulin (IVIG), rituximab, mycophenolate mofetil, and azathioprine will be reviewed with special focus in their pediatric use. As the use of these agents has been reported in both AQP4-IgG positive patients and, in selected cases, MOG-IgG positive children with NMOSD, we will review the use of these agents together, but will specify the population of relevance under the agent being discussed. Following this section, in Position Subsection (below), we will provide suggested treatment recommendations based on available evidence by subtype (AQP4-IgG, MOG-IgG, no identified antibody).

Rituximab

Rituximab is an anti-CD20 chimeric monoclonal antibody that depletes B-cells that has been in off-label use for the treatment of NMOSD for more than 10 years in adult and pediatric patients (74). Various studies on children with AQP4-IgG positive NMOSD have demonstrated reduction in the annualized relapse rate (75) or a more robust response to rituximab with almost complete cessation of relapses (76).

Its use has also been described in relation to all subtypes of MOG-IgG related disease in children. In a recently published study, no new MRI lesions or clinical relapses were observed in 10/12 children with a relapsing MOG-IgG associated disorder while B-cells were suppressed on rituximab treatment, and 4/6 children had clinical relapses occurring in the context of B-cell repopulation (77). Another retrospective series reported a decrease in ARR in MOG-IgG positive children, from 2.12 to 0.67 ($n = 9$) while using rituximab (78). Notably, response to rituximab may be different in MOG-IgG and AQP4-IgG positive patients. A recent publication comparing seropositive adult NMOSD patients on rituximab showed reemergence of B cells in the majority of relapses associated with AQP4- antibodies (92.5%; 12/13) and only 20% (2/10) of relapses in those who were positive for MOG- antibodies (79).

Because there is no standard protocol for rituximab infusions, induction dosing in pediatric patients is variable among centers. Two different protocols may be used for the starting dosing: 375 mg/m^2/dose, weekly for 4 consecutive infusions, or 500 mg/m^2/dose (max 1 g), 2 infusions 2 weeks apart. Monitoring of B-cell counts is recommended 2–3 weeks after the last infusion to confirm CD19 suppression, and then monthly starting at 4 months, as one study has shown repopulation to occur as early as 4 months (75). We have seen B-cell repopulation occur earlier in rare cases and the 4 months recommendation may therefore not be suitable for all children. Considering the risk of relapses with B-cell repopulation, redosing regimen depends on the availability for frequent monitoring of CD19 cells and patient age: 500 or 750 mg/m^2/dose (1,000 mg maximum) when CD19 >1%, or every 6 months. Switching from six monthly infusions to B-cell-monitoring reduces cumulative rituximab dose without apparent loss of efficacy (80). Moreover, in contrast to total CD19+ cell detected with routine techniques, the addition of assessment of subpopulations of B cells using multicolor flow cytometry, namely CD19+ CD27+ memory B cells, have been shown to be a reliable marker that correlates with biological relapse. In this study, the authors found the reemergence of naïve B cells prior to the emergence of CD19+ CD27+ memory B cells in some cases, and that this reemergence did not correlate with total B cell emergence, allowing for a decrease in the frequency of rituximab infusions (81). Low dose rituximab regimens have been described by several groups (82–84), but notably, dosing may need to be more frequent with lower doses. In a recently published study performed in adult patients with NMOSD, similar to other previously published studies (82), recovery of CD19+ B-cells analyzed by linear regression was significantly faster in patients

who received low doses of rituximab (250 mg) compared to 500 mg and higher doses (85). Infusion doses of 1,000 mg yielded the longest interval before reinfusion, with a mean of 14.7 ± 6.6 months.

Safety data associated with the use of rituximab must be considered. In one study, infusion-associated adverse events were recorded in 18/144 (12.5%) children with a wide range of autoimmune and inflammatory CNS disorders, including 20 with NMOSD (74). In addition, 11 patients (7.6%) in this series developed an infectious complication during follow-up: severe (death) in two children with autoimmune encephalitis (cytomegalovirus colitis and staphylococcal toxic shock syndrome), and cytomegalovirus retinitis, pneumonia, bronchiectasis, salmonella enteritis, mastoiditis in the remaining children (74).

The risk of developing hypogammaglobulinemia appears to increase with repeated courses and long-term use of rituximab (86). Persistent hypogammaglobuninemia following rituximab use should alert the physician to the possibility of primary immune deficiency. In one pediatric series, one-third of children with autoimmune cytopenia had persistent hypogammaglobulinemia (>12 months) after treatment with rituximab, 53% (9/17) of whom later received a diagnosis of primary immune deficiency (87). Mild to serious sinopulmonary infections, urinary tract infections, and septicemia may occur associated with hypogammaglobulinemia (88, 89). To mitigate these potential side effects, we recommend pretreatment vaccinations, close B-cell monitoring to limit cumulative rituximab dose, and use of immunoglobulin replacement therapy in cases of symptomatic hypogammaglobulinemia only with IVIG at 0.4–0.6 g/kg/months, or with subcutaneous formulations (90).

Mycophenolate Mofetil

Mycophenolate mofetil (MMF), a prodrug of mycophenolic acid, has shown to be effective in adult and pediatric patients with NMOSD in a retrospective study of patients who were, for the most part AQP4-IgG positive (90%) (91). The median post-MMF annualized relapse rate and Expanded Disability Status Scale (EDSS) scores were significantly decreased, with 60% of patients being relapse free. Adverse events were observed in 24% of patients, including rash, amenorrhea, herpes zoster, cystitis, hypotension, fatigue, and mild hair loss. In addition, a retrospective series showed a reduction in ARR in relapsing MOG-IgG positive pediatric patients from 1.79 to 0.52 (n = 15), confirming safety and possible efficacy of this agent for this disorder (78).

Recommended dosing of MMF is 500–750 mg/m^2/dose, administered orally twice a day, with a maximum of 2,000 mg total/day. Although mycophenolic acid levels can be measured (area under the curve), its use in optimizing dose both in adults and in children with NMOSD remains to be evaluated. Considering that MMF may have a slow onset of efficacy in preventing clinical attacks, its use should initially overlap with another immune therapy, such as oral corticosteroids, for up to 6 months (92).

Slower up-titration is associated with better tolerability in children, starting at 250 mg once or twice a day, increasing the dose every 7 days until reaching the final goal dose (93).

Azathioprine

Azathioprine is a purine analog that interferes with DNA synthesis in proliferating cells, including T and B cells. It has been shown to be a modestly effective treatment for NMO in a large cohort of AQP4-IgG positive patients including adults and children (94). Although 89% experienced reductions in relapse rate and 61% remained relapse free at 18 months after treatment initiation, at last follow-up 46% had discontinued treatment due to side effects or because of ongoing disease activity. The therapeutic benefit of azathioprine over a 5-years period in a single child wrongly classified as pediatric MS, but with a clinical phenotype of relapsing MOG-IgG associated disorder, has been recently published (95). In another series, pediatric patients with MOG-IgG positive disease receiving azathioprine had an ARR reduction from 1.84 to 1.0 ($n = 20$) (78).

Reported side effects include nausea, elevated liver function tests, diarrhea, severe leukopenia, rash, and hypersensitivity reactions. Recommended pediatric dosing is 2–3 mg/kg/day. In the past, azathioprine was one of the most frequently used preventive treatments in NMOSD due to its wide availability, low cost, and oral route. However, the need of the chronic combination with steroids to sustain its modest efficacy has substantially reduced the use of this treatment.

IVIG

IVIG consists of polyclonal IgG pooled from the serum of thousands of donors, and is frequently used as an anti-inflammatory treatment in a number of neurological disorders, such as Guillain-Barré syndrome and myasthenia gravis. The mechanism of by which it exerts its anti-inflammatory effect in specific diseases is unknown and may be disease dependent: it may stem from both functional domains of the IgG molecule, the antigen binding fragment ($F(ab)_2$ and the fragment crystallizable region (Fc) (96).

In a retrospective series, the use of IVIG on a 2–3 monthly basis (1 g/kg/dose) was associated with reduction in relapses in adult NMOSD patients, of whom 4/6 were positive for AQP4-IgG (the remaining 2 did not have testing results available) (97). No reports of its use for chronic prevention in pediatric AQP4-IgG related NMOSD are available.

On the other hand, in MOG-IgG related NMOSD in pediatrics, several reports of use of IVIG for relapse prevention have been published. In a retrospective case series, 12 MOG-IgG positive relapsing patients receiving monthly IVIG experienced an improvement of ARR from 2.16 to 0.51 (78) In addition, a case report of a child previously diagnosed with MS and subsequently found to be MOG-IgG positive was treated with multiple therapies with ongoing breakthrough disease, including interferon and rituximab, received IVIG as monotherapy on a monthly basis for 24 months with excellent disease control (98). Dosing used in current practice is variable and ranges from 1 to 2 g/kg, with some recommending a 2 g/kg induction dose and 1 g/kg/dose monthly thereafter as maintenance.

TABLE 2 | Attack prevention treatment strategies for NMO/NMOSD.

Categories of immune therapies	
1- Non-cell-specific interference with DNA synthesis and interference with DNA repair (cytotoxic agents)	Cyclophosphamide
2- Cell-specific interference with DNA synthesis(anti-proliferative agents)	Azathioprine Mycophenolate mofetil
3- Depletion of B-cells	Rituximab (CD20) Ocrelizumab (CD20) Ofatumumab (CD20) Inebilizumab (CD19)
4- Different mechanisms	Tocilizumab (IL-6 receptor) Satralizumab (IL-6 receptor) Eculizumab (C5 complement)
5- MS therapies that should be avoided	IFN-beta Natalizumab Fingolimod Alemtuzumab

Adapted from (102).

Several retrospective analyses of IVIG related adverse events (AE) in pediatric populations have been published, with the majority of reported AEs being mild, including fever and headache (99, 100). The extent of the mild AEs may vary from center to center, and reported numbers may be as high as almost 40% (100). Other common and more serious associated AEs include aseptic meningitis, thrombosis and anaphylaxis (96).

Future Options

Several new therapies for NMOSD have been developed in the recent years and are currently undergoing clinical evaluation in patients with both AQP4-IgG positive and negative NMOSD (101). Notably, MOG-IgG patients, if included in these trials, were not identified, as testing for MOG-IgG was not performed on AQP4-IgG negative patients. These new agents have different mechanisms of action: Eculizumab inhibits complement C5, satralizumab and tocilizumab are monoclonal antibodies against IL-6 receptor, and inebilizumab is an anti-CD19 antibody designed to deplete B cells (**Table 2**). These new therapeutic monoclonal antibodies are listed in **Table 3** and described in more detail below.

Eculizumab

Eculizumab is a humanized monoclonal antibody that targets the complement protein C5, with consequent inhibition of the complement cascade that is responsible for forming membrane attack complex (MAC) attacking AQP4 expressing cells. Eculizumab has been recently approved by the FDA for the treatment of NMOSD in AQP4-IgG positive adult patients. This approval was based on results from a Phase 3 randomized, double-blind placebo-controlled study (PREVENT), with relapse free status in 98% of patients treated with eculizumab as an add-on to stable-dose immunosuppressive therapy, compared to 63% of patients receiving placebo (103). A clinical trial to evaluate safety in youth with NMOSD is currently underway.

While there is no published experience with eculizumab in children with NMOSD, this monoclonal antibody is approved in USA, EU, Japan and other countries as first-line therapy in atypical hemolytic uremic syndrome, for both adult and pediatric patients. In addition, a recently published study reported results of eculizumab treatment also in children with severe hemolytic uremic syndrome related to Shiga-toxin-secreting Escherichia coli infection (STEC-HUS), showing a trend toward a favorable outcome in patients with persistent complement blockade (104).

The most severe adverse event associated with eculizumab is the risk of serious infection with encapsulated organisms, as the MAC is important in the immune response to these organisms. A report from the Centers for Disease Control and prevention in the United States (CDC) identified 16 cases of meningococcal disease occurring in eculizumab-treated patients between 2008 and 2016, primarily meningococcal sepsis without meningitis (105). Another recent report described four children who developed Neisseria meningitidis serogroup B (MenB)-associated invasive meningococcal disease despite previous vaccination with a multicomponent vaccine against MenB; two of them had been previously treated with eculizumab (106). Therefore, the risk of severe and potentially fatal infection with these organisms remains a concern during eculizumab treatment. Meningococcal vaccination is mandatory prior to initiation of this therapy. Other reported adverse events with eculizumab are less severe and include headache and infusion-related reactions (101).

Tocilizumab

Tocilizumab is an IL-6 receptor-blocking humanized monoclonal antibody. The potential use of tocilizumab in patients with NMOSD is based on the success reported in two open label studies in adults (107, 108). In addition to the control of immunological disease activity, more than 50% of patients in these studies exhibited neuropathic pain reduction. Chronic neuropathic pain occurs frequently in adult NMOSD patients and usually requires treatment with a combination of symptomatic therapies (109).

Safety concerns described with tocilizumab treatment in adult patients with rheumatoid arthritis include the risk of cardiovascular disease and increase in cholesterol levels (101). Published experience of tocilizumab use in pediatric patients includes a 14-year-old boy suffering from NMOSD and Sjogren's syndrome and two female adolescents with AQP4 IgG positive NMOSD who relapsed during rituximab treatment (38, 110). In all of them, tocilizumab led to clinical stabilization without an increased frequency of infections, or the adverse events observed in adults. To mitigate potential risks associated with use of multiple monoclonal antibodies at once, we recommend recovery of B cells prior to initiation of tocilizumab if used after rituximab failure. Of note, both SC and IV options are available and are used in practice (111).

TABLE 3 | Immunosuppressive molecules for attack prevention in NMOSD.

	Monoclonal antibody	Mechanism	Route	Risk
Rituximab	Chimeric	CD20-B cell depletion	IV	Infections; Hepatitis B reactivation; Infusion-related reaction
Eculizumab	Humanized	C5 complement inhibitor	IV	Meningococcal infection; Possible PML risk; Infusion-related reaction
Satralizumab	Humanized recycling	IL-6 receptor blocker	SC	
Tocilizumab	Humanized	IL-6 receptor blocker	SC	Cardiovascular risk; Cholesterol levels
Inebelizumab	Humanized	CD19-B cell depletion	IV	Infections; Infusion-related reaction
Ofatumumab	Fully humanized	CD20-B cell depletion	SC	Infections; Infusion-related reaction; Hepatitis B reactivation
Ocrelizumab	Humanized	CD20-B cell depletion	IV	Infections; Infusion-related reaction; Hepatitis B reactivation

Satralizumab

Satralizumab (SA237), like tocilizumab, is a humanized recombinant monoclonal antibody targeting the IL-6 receptor with immunomodulatory potential that was designed to improve pharmacokinetics by applying an "antibody recycling technology." In a phase three trial, 83 patients with seropositive or seronegative AQP4-IgG-NMOSD, including seven adolescents aged 13–18 years, were randomly assigned to receive satralizumab at 120 mg administered subcutaneously or placebo as add on therapy. Satralizumab significantly reduced the risk of relapses with a better response in the seropositive cohort (112). Unlike observational studies of tocilizumab, pain reduction was not seen in this trial. Preparation for a pediatric clinical trial of this agent is underway.

Inebilizumab

Inebilizumab (MEDI-551) is a humanized anti-CD19 monoclonal antibody, an antigen that is broadly expressed by pro-B cells, pre-B cells, mature and memory B cells and plasmablasts. Thus, compared with rituximab, inebilizumab may provide broader depletion along the B cell lineage. Importantly, CD19 is expressed on the majority of plasmablasts in the bone marrow, blood, and secondary lymphoid organs: as such, inebilizumab could remove the plasmablasts that produce the AQP4-IgG with potential benefits toward mitigating the damage from these pathogenic antibodies (101).

In a multicentre, phase 3 study, 230 adult patients with an active NMOSD were randomly allocated to 300 mg inebilizumab administered intravenously or placebo, to evaluate safety and efficacy (113). The study group included patients who were seropositive (93%) or seronegative for AQP4-IgG. Overall, treatment with inebilizumab significantly reduced the risk of clinical relapses, disability worsening, MRI lesion activity, and requirement of hospitalizations compared with placebo (113). Adverse events were common in both groups, including urinary tract infections, arthralgia, and infusion-related reactions. No cases of malignancies were reported; however, the overall follow-up safety period of 12 months was too short to assess long-term risks of opportunistic infections, secondary malignancies, or hypogammaglobulinemia. There is no published experience on the use of inebilizumab in children with NMOSD yet.

Ofatumumab

Ofatumumab is a fully human monoclonal antibody targeting B cells that may provide an attractive alternative to rituximab since it can deplete rituximab-resistant cells that express low levels of CD20, possibly through targeting a different epitope of CD20 (114) or by increased complement-dependent cytotoxicity (115). Following the first ofatumumab clinical trial in refractory or relapsed chronic lymphocytic leukemia in 2008, it has been evaluated for various conditions including nephrotic syndrome, refractory follicular lymphoma, and MS.

There are limited case series reporting the off-label use of ofatumumab in pediatric-onset SLE, mainly in patients with severe infusion reactions to rituximab. In a retrospective review, nine patients with SLE who were treated with ofatumumab at a median age of 16 years (11–18 years) showed clinical improvement with a good safety profile (116). Additional successful pediatric exposure to ofatumumab has been recently published in two siblings with monogenic SLE before the age of 3 years (117). There is no published experience on the use of ofatumumab in children with NMOSD yet.

POSITION SUBSECTION

Recommendations for Routine Clinical Care

Given the rarity of NMOSD in the pediatric population, the potential for significant neurological deficits associated with this disorder and need for ongoing therapy and management, we recommend assessment and ongoing follow up of children suspected to have NMOSD at a pediatric facility by a child neurologist with training in neuroinflammatory disorders. We have outlined suggested routine baseline work up and follow up schedule and laboratory/imaging assessments on **Tables 4**, **5**.

Recommendations for the Initiation of Preventative/Chronic Therapies

Current available treatment options for patients with NMOSD have become increasingly complex regarding different treatment efficacy, treatment adherence, and side-effect profile, in addition to specific requirements and monitoring associated with pediatric immunosuppression. Management decisions to minimize treatment-related risks require comprehensive clinical, laboratory and MRI assessment at the time of the initial diagnostic evaluation. We recommend using a standardized

TABLE 4 | Recommendations for routine clinical care and workup in pediatric NMOSD.

A. Recommended baseline laboratory testing and imaging
a. BASELINE DIAGNOSTIC TESTS: see Table 5 (1)
b. BASELINE INVESTIGATION FOR ASSOCIATED AUTOIMMUNITY: See Table 5 (2)
B. Recommended clinical follow up laboratory testing and imaging
a. Complete neurological assessment at baseline and at follow up 3–6 months after presentation with routine follow up q6-12 months if asymptomatic.
b. Routine laboratory follow-up specific to preventative/immunosuppressive therapy used **Table 5.5**)
c. MRI brain, orbits, spine. Perform at baseline, 3 months after presentation, 6 months, 12 months then yearly thereafter, or at time of acute attack.
d. OCT and comprehensive visual evaluation: Complete visual battery at baseline (see in **Table 5.1**), 6 months after presentation if abnormalities detected at baseline then yearly follow up with visual battery thereafter. Visual battery also to be performed at the time of acute attack.
C. Subspecialty and other consultations
a. Subspecialty Consultation
i. Ophthalmology: all patients should receive ophthalmological assessment
ii. Urology as needed
iii. Rheumatology if concomitant systemic autoimmunity
iv. Psychiatry as needed
v. PICU/Respirology as needed during relapse
b. Rehabilitation: Physiatry, Physical Therapy, Occupational Therapy, Speech and Language Therapy. Baseline assessment suggested with follow up as needed.
c. Social work as needed.
d. Cognitive testing: Baseline cognitive testing 6 months after acute attack and every 2 years if possible, particularly in youth with cerebral involvement.

checklist which includes both practical measures and suggested evaluations (see **Table 4**). The optimal duration of treatment in this population of children is currently unknown and should be the subject of future studies.

Treatment of Pediatric AQP4-IgG Seropositive NMOSD

The detection of AQP4-IgG predicts relapses of myelitis and optic neuritis in adults and children with NMOSD, with cumulative neurological disability, justifying prompt initiation of immunosuppressive therapy (74) with currently available treatment options: rituximab, mycophenolate mofetil, and azathioprine (75, 76, 91, 94), until more experience and knowledge regarding safety in children is gained about newer agents such as eculizumab, satralizumab, and tocilizumab.

Treatment of AQP4-IgG Seronegative NMOSD

Current treatment strategies are essentially the same as for children with AQP4-IgG seropositive NMOSD. This recommendation may change if some of the investigational agents that target AQP4-IgG pathogenic mechanisms (anti-C5; anti-IL6) prove to be effective only in seropositive patients.

Treatment of Pediatric NMOSD Clinical Phenotype Associated With MOG-IgG

There is no consensus regarding preventive therapy for MOG-IgG-associated disease. Although it appears to be quite corticosteroid-responsive, we recommend avoiding the long-term use of oral corticosteroids and start steroid discontinuation without additional immunosuppression in children who present with a first CNS inflammatory attack and are found to be MOG-IgG seropositive. On serial serum follow-up, more than 50% of children who were seropositive at onset became MOG-IgG seronegative (64, 65, 73, 118, 119).

Persistent high titer of serum MOG-IgG has been associated with greater risk of clinical relapse. Thus, it is justifiable to consider initiation of preventive therapies in children showing persistent MOG-IgG seropositivity after a first attack or after developing a relapsing disease. Sustained remission during treatment with IVIG and with currently available immunosuppressants such as azathioprine, mycophenolate mofetil, or rituximab has been reported but the optimal drug and duration of therapy is not yet clear (77, 78, 95, 120).

CONCLUSION, GAPS, AND FUTURE DIRECTIONS

Here, we have reviewed recent literature detailing the distinct clinical, imaging and laboratory features of NMOSD in pediatric patients. The high prevalence of MOG-IgG antibodies in the pediatric population with an NMOSD phenotype contrasts with the adult population, where the majority of NMOSD patients are AQP4-IgG positive. We currently face the dilemma of whether to consider MOG-IgG and AQP4-IgG associated disorders separate entities or as two entities under the umbrella of NMOSD (3, 121).

MRI, structural/functional visual testing and antibody testing are of upmost importance in making this diagnosis and dictating treatment plans. Antibody testing alone appears to provide diagnostic information for the vast majority of pediatric patients presenting with NMOSD, although future studies will clarify the utility of repeated MOG-IgG antibody testing to predict relapsing disease in children. Studies have evaluated the significance of

TABLE 5 | Recommendations for routine baseline and risk mitigation checklist in pediatric immunosuppression.

1- BASELINE DIAGNOSTIC TESTS

- Brain, orbit, and spinal cord MRI, with and without gadolinium
- Visual battery as clinically indicated (High Contrast and Low Contrast Visual Acuity, Visual Evoked Potentials, Visual Fields, Optical Coherence Tomography, Color Vision)
- Full blood cell count – leukocytes / platelets
- Liver function tests, urea, creatinine
- Cholesterol, triglycerides
- Pregnancy test (in juvenile female patients)
- Immunoglobulin levels
- Lymphocyte subsets (CD19, CD20)
- Serum complement (C3, C4)
- Serum protein electrophoresis
- Vitamin D serum level
- AQP4-IgG test in serum (CBA)
- MOG-IgG test in serum (CBA)
- CSF analysis - cell count, cultures, IEF for oligoclonal bands in CSF and serum
- Infection screening

  a) HCV and HIV serology
  b) HBV serology: HBV surface antigen and core antibody
  c) TB tests: QuantiFERON or tuberculin skin testing and chest radiograph

2- BASELINE INVESTIGATION FOR ASSOCIATED AUTOIMMUNITY

- Antinuclear antibodies (ANA)
- Extractable nuclear antigen-antibodies (ENA)
- Anti-DNA antibodies
- Antithyroid antibodies and thyroid function tests (TSH, T3, Free T4, Total T4)
- Celiac disease

3- RISK MITIGATION FOR INFECTIOUS EVENT AT BASELINE

- Varicella zoster virus (VZV) serology
- HBV serology: surface antibody
- Vaccinations: complete immunization according to age (non-live vaccines >4 weeks, live vaccines >8 weeks prior to first infusion); complete pneumococcal vaccine
- Complete immunization if necessary, according to VZV and HBV serology

4- INFUSION DAY CHECKLIST FOR RITUXIMAB/OCRELIZUMAB

- **Evaluations:**
  - Clinical assessment to exclude active infection
  - Body weight, body temperature
  - Blood cell count and liver function tests
- **Pre-treatment regimen** (to reduce infusion-related reactions)
  a) Corticosteroids: Hydrocortisone, 1 mg/kg/dose
  b) Antihistamines: Diphenhydramine, 1 mg/kg/dose (Max 50 mg)
  c) Antipyretics: Acetaminophen, 10 mg/kg/dose

5- GENERAL ASPECTS OF MONITORING IMMUNOSUPPRESSION (specific requirements depending on the molecule)

- Clinical disease activity
- Repeat neuroimaging for new baseline: Brain, orbit, and spinal cord MRI (4–6 months)
- Blood

  a) Full blood cell count—leukopenia, lymphopenia
  b) Liver enzymes
  c) Urea, creatinine
  d) Cholesterol, triglycerides
  e) Lymphocyte subsets
  f) Serum complement
  g) Immunoglobulin levels
- Urine

  a) Infection;

  b) Renal dysfunction
- New associated autoimmunity

  a) Thyroid function tests and thyroid antibodies
  b) Antinuclear antibodies/ENA
  c) Celiac disease

early and transient MOG-IgG positivity vs. persistent MOG-IgG antibody positivity in indicating risk for recurrent disease: further knowledge related to need for and timing of follow up MOG-IgG antibody testing is needed (64). Access to antibody testing is of great importance, as are further studies in pediatrics delineating associations between children with antibody positive disease, treatments, and outcomes.

As demonstrated in several large studies of AQP4-IgG testing in the adult population, use of a fixed cell-based immunofluorescence assay (IFA) kit and live cell-based testing provided high and almost identical sensitivity and specificity (122). Performing live cell-based assays for MOG-IgG related disease has been limited to a small number of large centers around the world. The release of a fixed cell-based IFA kit has allowed for greater access around the world to this testing. Several related studies have examined this question and suggested relatively high sensitivity of the testing kit, but lower than live cell-based testing: in one study live cell based MOG-IgG demonstrated 96% agreement between 4 national testing centers, whereas fixed cell-based assay immunofluorescence showed 90% agreement (123–125). The high sensitivity and specificity of the testing kits, and their high diagnostic yield support a need for access to both AQP4-IgG and MOG-IgG testing in all settings in which children with NMOSD might present.

While the list of treatment options in adults with NMOSD have grown, only one randomized controlled trial of NMOSD has included children, and that trial included only children older than 12 years of age. Yet, as we have shown in this review, abundant literature suggests the presence of relapsing disease in children with NMOSD in need of treatment. Importantly, all trials in NMOSD to date have focused primarily on AQP4-IgG related disease, and trials in the adult population to date have shown the greatest benefit in those who are positive for the AQP4-IgG antibody. Notably, the majority of pediatric patients with an NMOSD phenotype have antibodies to MOG-IgG, emphasizing the urgent need for new trials evaluating therapies for this subgroup of patients. In addition to randomized clinical trials, future real-life studies with international cohorts evaluating therapy effectiveness in these children are needed.

AUTHOR CONTRIBUTIONS

EY and ST: drafting, conceptualization, and editing. All authors contributed to the article and approved the submitted version.

REFERENCES

1. Lennon VA, Wingerchuk DM, Kryzer TJ, Pittock SJ, Lucchinetti CF, Fujihara K, et al. A serum autoantibody marker of neuromyelitis optica: distinction from multiple sclerosis. *Lancet.* (2004) 364:2106–12. doi: 10.1016/S0140-6736(04)17551-X
2. Narayan R, Simpson A, Fritsche K, Salama S, Pardo S, Mealy M, et al. MOG antibody disease: a review of MOG antibody seropositive neuromyelitis optica spectrum disorder. *Mult Scler Relat Dis.* (2018) 25:66–72. doi: 10.1016/j.msard.2018.07.025
3. Zamvil SS, Slavin AJ. Does MOG Ig-positive AQP4-seronegative opticospinal inflammatory disease justify a diagnosis of NMO spectrum disorder? *Neurology.* (2015) 2:e62. doi: 10.1212/NXI.0000000000000062
4. Wingerchuk DM, Hogancamp WF, O'Brien PC, Weinshenker BG. The clinical course of neuromyelitis optica (Devic's syndrome). *Neurology.* (1999) 53:1107–1114. doi: 10.1212/WNL.53.5.1107
5. Wingerchuk DM, Banwell B, Bennett JL, Cabre P, Carroll W, Chitnis T, et al. International consensus diagnostic criteria for neuromyelitis optica spectrum disorders. *Neurology.* (2015) 85:177–89. doi: 10.1212/WNL.0000000000001729
6. Chitnis T, Ness J, Krupp L, Waubant E, Hunt T, Olsen CS, et al. Clinical features of neuromyelitis optica in children: US network of pediatric MS centers report. *Neurology.* (2016) 86:245–52. doi: 10.1212/WNL.0000000000002283
7. Mealy MA, Wingerchuk DM, Greenberg BM, Levy M. Epidemiology of neuromyelitis optica in the United States: a multicenter analysis. *Arch Neurol.* (2012) 69:1176–80. doi: 10.1001/archneurol.2012.314
8. Flanagan EP, Cabre P, Weinshenker BG, Sauver JS, Jacobson DJ, Majed M, et al. Epidemiology of aquaporin-4 autoimmunity and neuromyelitis optica spectrum. *Ann Neurol.* (2016) 79:775–83. doi: 10.1002/ana.24617
9. Bukhari W, Prain KM, Waters P, Woodhall M, O'Gorman CM, Clarke L, et al. Incidence and prevalence of NMOSD in Australia and New Zealand. *J Neurol Neurosurg Psychiatry.* (2017) 88:632–8. doi: 10.1136/jnnp-2016-314839
10. Kim SH, Kim HJ. Central nervous system neuroinflammatory disorders in Asian/Pacific regions. *Curr Opin Neurol.* (2016) 29:372–80. doi: 10.1097/WCO.0000000000000315
11. Kim SH, Mealy MA, Levy M, Schmidt F, Ruprecht K, Paul F, et al. Racial differences in neuromyelitis optica spectrum disorder. *Neurology.* (2018) 91:e2089–e99. doi: 10.1212/WNL.0000000000006574
12. Quek AM, McKeon A, Lennon VA, Mandrekar JN, Iorio R, Jiao Y, et al. Effects of age and sex on aquaporin-4 autoimmunity. *Arch Neurol.* (2012) 69:1039–43. doi: 10.1001/archneurol.2012.249
13. Tenembaum S, Chitnis T, Nakashima I, Collongues N, McKeon A, Levy M, et al. Neuromyelitis optica spectrum disorders in children and adolescents. *Neurology.* (2016) 87:S59–66. doi: 10.1212/WNL.0000000000002824
14. Zhou Y, Zhong X, Shu Y, Cui C, Wang J, Wang Y, et al. Clinical course, treatment responses and outcomes in Chinese paediatric neuromyelitis optica spectrum disorder. *Mult Scler Relat Dis.* (2019) 28:213–20. doi: 10.1016/j.msard.2018.12.038
15. Huppke P, Bluthner M, Bauer O, Stark W, Reinhardt K, Huppke B, et al. Neuromyelitis optica and NMO-IgG in European pediatric patients. *Neurology.* (2010) 75:1740–4. doi: 10.1212/WNL.0b013e3181fc2823
16. Collongues N, Marignier R, Zephir H, Papeix C, Blanc F, Ritleng C, et al. Neuromyelitis optica in France: a multicenter study of 125 patients. *Neurology.* (2010) 74:736–42. doi: 10.1212/WNL.0b013e3181d31e35
17. Fragoso YD, Ferreira ML, Oliveira EM, Domingues RB, Ribeiro TA, Brooks JB, et al. Neuromyelitis optica with onset in childhood and adolescence. *Pediatr Neurol.* (2014) 50:66–8. doi: 10.1016/j.pediatrneurol.2013.07.003
18. Absoud M, Lim MJ, Appleton R, Jacob A, Kitley J, Leite MI, et al. Paediatric neuromyelitis optica: clinical, MRI of the brain and prognostic features. *J Neurol Neurosurg Psychiatry.* (2015) 86:470–2. doi: 10.1136/jnnp-2014-308550
19. Lechner C, Baumann M, Hennes EM, Schanda K, Marquard K, Karenfort M, et al. Antibodies to MOG and AQP4 in children with neuromyelitis optica and limited forms of the disease. *J Neurol Neurosurg Psychiatry.* (2016) 87:897–905. doi: 10.1136/jnnp-2015-311743
20. Sepulveda M, Aldea M, Escudero D, Llufriu S, Arrambide G, Otero-Romero S, et al. Epidemiology of NMOSD in Catalonia: influence of the new 2015 criteria in incidence and prevalence estimates. *Mult Scler.* (2018) 24:1843–851. doi: 10.1177/1352458517735191
21. Gmuca S, Hardy DI, Narula S, Stoll S, Harris J, Zhao Y, et al. Validation of claims-based diagnoses of adult and pediatric neuromyelitis optica spectrum disorder and variations in diagnostic evaluation and treatment initiation. *Mult Scler Relat Dis.* (2020) 37:101488. doi: 10.1016/j.msard.2019.101488
22. Pandit L, Asgari N, Apiwattanakul M, Palace J, Paul F, Leite MI, et al. Demographic and clinical features of neuromyelitis optica: A review. *Mult Scler.* (2015) 21:845–53. doi: 10.1177/1352458515572406
23. Yamaguchi Y, Torisu H, Kira R, Ishizaki Y, Sakai Y, Sanefuji M, et al. A nationwide survey of pediatric acquired demyelinating syndromes in Japan. *Neurology.* (2016) 87:2006–15. doi: 10.1212/WNL.0000000000003318

24. Jarius S, Ruprecht K, Kleiter I, Borisow N, Asgari N, Pitarokoili K, et al. MOG-IgG in NMO and related disorders: a multicenter study of 50 patients. part 1: frequency, syndrome specificity, influence of disease activity, long-term course, association with AQP4-IgG, and origin. *J Neuroinflamm.* (2016) 13:279. doi: 10.1186/s12974-016-0717-1
25. Collongues N, Marignier R, Zephir H, Papeix C, Fontaine B, Blanc F, et al. Long-term follow-up of neuromyelitis optica with a pediatric onset. *Neurology.* (2010) 75:1084–8. doi: 10.1212/WNL.0b013e3181f39a66
26. Duignan S, Wright S, Rossor T, Cazabon J, Gilmour K, Ciccarelli O, et al. Myelin oligodendrocyte glycoprotein and aquaporin-4 antibodies are highly specific in children with acquired demyelinating syndromes. *Dev Med Child Neurol.* (2018) 60:958–62. doi: 10.1111/dmcn.13703
27. Song H, Zhou H, Yang M, Xu Q, Sun M, Wei S. Clinical characteristics and outcomes of myelin oligodendrocyte glycoprotein antibody-seropositive optic neuritis in varying age groups: a cohort study in China. *J Neurol Sci.* (2019) 400:83–9. doi: 10.1016/j.jns.2019.03.014
28. Petzold A, Woodhall M, Khaleeli Z, Tobin WO, Pittock SJ, Weinshenker BG, et al. Aquaporin-4 and myelin oligodendrocyte glycoprotein antibodies in immune-mediated optic neuritis at long-term follow-up. *J Neurol Neurosurg Psychiatry.* (2019) 90:1021–6. doi: 10.1136/jnnp-2019-320493
29. Mayer MC, Breithaupt C, Reindl M, Schanda K, Rostasy K, Berger T, et al. Distinction and temporal stability of conformational epitopes on myelin oligodendrocyte glycoprotein recognized by patients with different inflammatory central nervous system diseases. *J Immunol.* (2013) 191:3594–604. doi: 10.4049/jimmunol.1301296
30. Lee HJ, Kim B, Waters P, Woodhall M, Irani S, Ahn S, et al. Chronic relapsing inflammatory optic neuropathy (CRION): a manifestation of myelin oligodendrocyte glycoprotein antibodies. *J. Neuroinflammation.* (2018) 15:302. doi: 10.1186/s12974-018-1335-x
31. Dubey D, Pittock SJ, Krecke KN, Flanagan EP. Association of extension of cervical cord lesion and area postrema syndrome with neuromyelitis optica spectrum disorder. *JAMA neurology.* (2017) 74:359–61. doi: 10.1001/jamaneurol.2016.5441
32. Kremer L, Mealy M, Jacob A, Nakashima I, Cabre P, Bigi S, et al. Brainstem manifestations in neuromyelitis optica: a multicenter study of 258 patients. *Mult Scler.* (2014) 20:843–7. doi: 10.1177/1352458513507822
33. Baghbanian SM, Asgari N, Sahraian MA, Moghadasi AN. A comparison of pediatric and adult neuromyelitis optica spectrum disorders: a review of clinical manifestation, diagnosis, and treatment. *J Neurol Sci.* (2018) 388:222–31. doi: 10.1016/j.jns.2018.02.028
34. Armangue T, Olive-Cirera G, Martinez-Hernandez E, Sepulveda M, Ruiz-Garcia R, Munoz-Batista M, et al. Associations of paediatric demyelinating and encephalitic syndromes with myelin oligodendrocyte glycoprotein antibodies: a multicentre observational study. *Lancet Neurol.* (2020) 19:234–46. doi: 10.1016/S1474-4422(19)30488-0
35. Inoue K, Nakayama T, Kamisawa A, Saito J. Syndrome of inappropriate antidiuretic hormone accompanied by bilateral hypothalamic and anterior thalamic lesions with serum antiaquaporin 4 antibody. *BMJ Case Rep.* (2017) 2017:bcr2017219721. doi: 10.1136/bcr-2017-219721
36. Oh SJ, Ihm CG, Lee TW, Kim JS, Kim DR, Park EJ, et al. Syndrome of inappropriate antidiuretic hormone secretion associated with seronegative neuromyelitis optica spectrum disorder. *Kidney Res Clin Pract.* (2017) 36:100–4. doi: 10.23876/j.krcp.2017.36.1.100
37. Gmuca S, Lieberman SM, Mehta J. Pediatric neuromyelitis optica spectrum disorder and sjogren syndrome: more common than previously thought? *J Rheumatol.* (2017) 44:959–60. doi: 10.3899/jrheum.160978
38. Marino A, Narula S, Lerman MA. First pediatric patient with neuromyelitis optica and sjogren syndrome successfully treated with tocilizumab. *Pediatr Neurol.* (2017) 73:e5–e6. doi: 10.1016/j.pediatrneurol.2017.05.015
39. Yeh EA. White matter changes in childhood NMDA receptor encephalitis: bringing new light to an old phenotype. *Neurology.* (2014) 1:e3. doi: 10.1212/NXI.0000000000000003
40. Luo JJ, Lv H, Sun W, Zhao J, Hao HJ, Gao F, et al. Anti-N-methyl-d-aspartate receptor encephalitis in a patient with neuromyelitis optica spectrum disorders. *Mult Scler Relat Dis.* (2016) 8:74–77. doi: 10.1016/j.msard.2016.05.002
41. Nagata S, Nishimura Y, Mitsuo K. [A case of anti-myelin oligodendrocyte glycoprotein (MOG) and anti-N-methyl-D-aspartate (NMDA) receptor antibody-positive encephalitis with optic neuritis]. *Rinsho Shinkeigaku.* (2018) 58:636–41. doi: 10.5692/clinicalneurol.cn-001194
42. Wolf B. Biotinidase deficiency should be considered in individuals thought to have Mult Scler Relat Dis. *Mult Scler Relat Dis.* (2019) 28:26–30. doi: 10.1016/j.msard.2018.11.030
43. Bottin L, Prud'hon S, Guey S, Giannesini C, Wolf B, Pindolia K, et al. Biotinidase deficiency mimicking neuromyelitis optica: Initially exhibiting symptoms in adulthood. *Mult Scler.* (2015) 21:1604–7. doi: 10.1177/1352458515596457
44. Girard B, Bonnemains C, Schmitt E, Raffo E, Bilbault C. Biotinidase deficiency mimicking neuromyelitis optica beginning at the age of 4: a treatable disease. *Mult Scler.* (2017) 23:119–22. doi: 10.1177/1352458516646087
45. Yilmaz S, Serin M, Canda E, Eraslan C, Tekin H, Ucar SK, et al. A treatable cause of myelopathy and vision loss mimicking neuromyelitis optica spectrum disorder: late-onset biotinidase deficiency. *Metab Brain Dis.* (2017) 32:675–8. doi: 10.1007/s11011-017-9984-5
46. Yang Y, Li C, Qi Z, Xiao J, Zhang Y, Yamaguchi S, et al. Spinal cord demyelination associated with biotinidase deficiency in 3 Chinese patients. *J Child Neurol.* (2007) 22:156–60. doi: 10.1177/0883073807300307
47. Zalewski NL, Flanagan EP, Keegan BM. Evaluation of idiopathic transverse myelitis revealing specific myelopathy diagnoses. *Neurology.* (2018) 90:e96–e102. doi: 10.1212/WNL.0000000000004796
48. Yadav N, Pendharkar H, Kulkarni GB. Spinal cord infarction: clinical and radiological features. *J Stroke Cerebrovasc Dis.* (2018) 27:2810–21. doi: 10.1016/j.jstrokecerebrovasdis.2018.06.008
49. Bar C, Cheuret E, Bessou P, Pedespan JM. Childhood idiopathic spinal cord infarction: description of 7 cases and review of the literature. *Brain Dev.* (2017) 39:818–27. doi: 10.1016/j.braindev.2017.05.009
50. Kidd DP, Burton BJ, Graham EM, Plant GT. Optic neuropathy associated with systemic sarcoidosis. *Neurology.* (2016) 3:e270. doi: 10.1212/NXI.0000000000000270
51. Flanagan EP, Kaufmann TJ, Krecke KN, Aksamit AJ, Pittock SJ, Keegan BM, et al. Discriminating long myelitis of neuromyelitis optica from sarcoidosis. *Ann Neurol.* (2016) 79:437–47. doi: 10.1002/ana.24582
52. Yea C, Bitnun A, Robinson J, Mineyko A, Barton M, Mah JK, et al. Longitudinal outcomes in the 2014. acute flaccid paralysis cluster in Canada. *J Child Neurol.* (2017) 32:301–7. doi: 10.1177/0883073816680770
53. Bitnun A, Yeh EA. Acute flaccid paralysis and enteroviral infections. *Curr Infect Dis Rep.* (2018) 20:34. doi: 10.1007/s11908-018-0641-x
54. Mishra N, Ng TFF, Marine RL, Jain K, Ng J, Thakkar R, et al. Antibodies to enteroviruses in cerebrospinal fluid of patients with acute flaccid myelitis. *mBio.* (2019) 10:e01903-19. doi: 10.1128/mBio.01903-19
55. Williams JN, Speyer CB, Kreps DJ, Kimbrough DJ, Costenbader K, Bhattacharyya S. Spinal cord syndromes in patients with systemic lupus erythematosus: differentiating lupus myelitis, neuromyelitis optica, and multiple sclerosis. *Lupus.* (2019) 28:1656–62. doi: 10.1177/0961203319886103
56. Vila-Bedmar S, Ostos-Moliz F, Camacho-Salas A. Pediatric multiple sclerosis presenting as area postrema syndrome. *Pediatr Neurol.* (2017) 70:83–4. doi: 10.1016/j.pediatrneurol.2017.02.002
57. Mealy MA, Whetstone A, Orman G, Izbudak I, Calabresi PA, Levy M. Longitudinally extensive optic neuritis as an MRI biomarker distinguishes neuromyelitis optica from multiple sclerosis. *J Neurol Sci.* (2015) 355:59–63. doi: 10.1016/j.jns.2015.05.013
58. Kim HJ, Paul F, Lana-Peixoto MA, Tenembaum S, Asgari N, Palace J, et al. MRI characteristics of neuromyelitis optica spectrum disorder: an international update. *Neurology.* (2015) 84:1165–73. doi: 10.1212/WNL.0000000000001367
59. Thomas T, Branson HM, Verhey LH, Shroff M, Stephens D, Magalhaes S, et al. The demographic, clinical, and magnetic resonance imaging (MRI) features of transverse myelitis in children. *J Child Neurol.* (2012) 27:11–21. doi: 10.1177/0883073811420495
60. Kitley J, Leite MI, Kuker W, Quaghebeur G, George J, Waters P, et al. Longitudinally extensive transverse myelitis with and without aquaporin 4 antibodies. *JAMA Neurol.* (2013) 70:1375–81. doi: 10.1001/jamaneurol.2013.3890

61. Chang KH, Lyu RK, Chen CM, Wu YR, Chang HS, Huang CC, et al. Distinct features between longitudinally extensive transverse myelitis presenting with and without anti-aquaporin 4 antibodies. *Mult Scler.* (2013) 19:299–307. doi: 10.1177/1352458512451659
62. Konuskan B, Yildirim M, Gocmen R, Okur TD, Polat I, Kilic H, et al. Retrospective analysis of children with myelin oligodendrocyte glycoprotein antibody-related disorders. *Mult Scler Relat Dis.* (2018) 26:1–7. doi: 10.1016/j.msard.2018.07.022
63. Baumann M, Sahin K, Lechner C, Hennes EM, Schanda K, Mader S, et al. Clinical and neuroradiological differences of paediatric acute disseminating encephalomyelitis with and without antibodies to the myelin oligodendrocyte glycoprotein. *J Neurol Neurosurg Psychiatry.* (2015) 86:265–72. doi: 10.1136/jnnp-2014-308346
64. Waters P, Fadda G, Woodhall M, O'Mahony J, Brown RA, Castro DA, et al. Serial anti-myelin oligodendrocyte glycoprotein antibody analyses and outcomes in children with demyelinating syndromes. *JAMA Neurol.* (2019) 77:E1–E12. doi: 10.1001/jamaneurol.2019.2940
65. Hacohen Y, Mankad K, Chong WK, Barkhof F, Vincent A, Lim M, et al. Diagnostic algorithm for relapsing acquired demyelinating syndromes in children. *Neurology.* (2017) 89:269–78. doi: 10.1212/WNL.0000000000004117
66. Fernandez-Carbonell C, Vargas-Lowy D, Musallam A, Healy B, McLaughlin K, Wucherpfennig KW, et al. Clinical and MRI phenotype of children with MOG antibodies. *Mult Scler.* (2016) 22:174–84. doi: 10.1177/1352458515587751
67. Song H, Zhou H, Yang M, Tan S, Wang J, Xu Q, et al. Clinical characteristics and prognosis of myelin oligodendrocyte glycoprotein antibody-seropositive paediatric optic neuritis in China. *Br J Ophthalmol.* (2019) 103:831–6. doi: 10.1136/bjophthalmol-2018-312399
68. Yeh EA, Weinstock-Guttman B, Lincoff N, Reynolds J, Weinstock A, Madurai N, et al. Retinal nerve fiber thickness in inflammatory demyelinating diseases of childhood onset. *Mult Scler.* (2009) 15:802–10. doi: 10.1177/1352458509104586
69. Chen Q, Zhao G, Huang Y, Li Z, Sun X, Lu P, et al. Clinical characteristics of pediatric optic neuritis with myelin oligodendrocyte glycoprotein seropositive: a cohort study. *Pediatr Neurol.* (2018) 83:42–9. doi: 10.1016/j.pediatrneurol.2018.03.003
70. Narayan RN, McCreary M, Conger D, Wang C, Greenberg BM. Unique characteristics of optical coherence tomography (OCT) results and visual acuity testing in myelin oligodendrocyte glycoprotein (MOG) antibody positive pediatric patients. *Mult Scler Relat Dis.* (2019) 28:86–90. doi: 10.1016/j.msard.2018.11.026
71. Kitley J, Waters P, Woodhall M, Leite MI, Murchison A, George J, et al. Neuromyelitis optica spectrum disorders with aquaporin-4 and myelin-oligodendrocyte glycoprotein antibodies: a comparative study. *JAMA Neurol.* (2014) 71:276–83. doi: 10.1001/jamaneurol.2013.5857
72. Palace J, Lin DY, Zeng D, Majed M, Elsone L, Hamid S, et al. Outcome prediction models in AQP4-IgG positive neuromyelitis optica spectrum disorders. *Brain.* (2019) 142:1310–23. doi: 10.1093/brain/awz054
73. Hennes EM, Baumann M, Schanda K, Anlar B, Bajer-Kornek B, Blaschek A, et al. Prognostic relevance of MOG antibodies in children with an acquired demyelinating syndrome. *Neurology.* (2017) 89:900–8. doi: 10.1212/WNL.0000000000004312
74. Dale RC, Brilot F, Duffy LV, Twilt M, Waldman AT, Narula S, et al. Utility and safety of rituximab in pediatric autoimmune and inflammatory CNS disease. *Neurology.* (2014) 83:142–50. doi: 10.1212/WNL.0000000000000570
75. Nosadini M, Alper G, Riney CJ, Benson LA, Mohammad SS, Ramanathan S, et al. Rituximab monitoring and redosing in pediatric neuromyelitis optica spectrum disorder. *Neurol Neuroimmunol Neuroinflamm.* (2016) 3:e188. doi: 10.1212/NXI.0000000000000188
76. Longoni G, Banwell B, Filippi M, Yeh EA. Rituximab as a first-line preventive treatment in pediatric NMOSDs: preliminary results in 5 children. *Neurol Neuroimmunol Neuroinflamm.* (2014) 1:e46. doi: 10.1212/NXI.0000000000000046
77. Albassam F, Longoni G, Yea C, Wilbur C, Grover SA, Yeh EA. Rituximab in children with myelin oligodendrocyte glycoprotein antibody and relapsing neuroinflammatory disease. *Dev Med Child Neurol.* (2020) 62:390–5. doi: 10.1111/dmcn.14336
78. Hacohen Y, Wong YY, Lechner C, Jurynczyk M, Wright S, Konuskan B, et al. Disease course and treatment responses in children with relapsing myelin oligodendrocyte glycoprotein antibody-associated disease. *JAMA Neurol.* (2018) 75:478–87. doi: 10.1001/jamaneurol.2017.4601
79. Durozard P, Rico A, Boutiere C, Maarouf A, Lacroix R, Cointe S, et al. Comparison of the response to rituximab between myelin oligodendrocyte glycoprotein and aquaporin-4 antibody diseases. *Ann Neurol.* (2020) 87:256–66. doi: 10.1002/ana.25648
80. Cohen M, Romero G, Bas J, Ticchioni M, Rosenthal M, Lacroix R, et al. Monitoring CD27+ memory B-cells in neuromyelitis optica spectrum disorders patients treated with rituximab: results from a bicentric study. *J Neurol Sci.* (2017) 373:335–8. doi: 10.1016/j.jns.2017.01.025
81. Lebrun C, Cohen M, Rosenthal-Allieri MA, Bresch S, Benzaken S, Marignier R, et al. Only follow-up of memory B cells helps monitor rituximab administration to patients with neuromyelitis optica spectrum disorders. *Neurol Ther.* (2018) 7:373–83. doi: 10.1007/s40120-018-0101-4
82. Greenberg BM, Graves D, Remington G, Hardeman P, Mann M, Karandikar N, et al. Rituximab dosing and monitoring strategies in neuromyelitis optica patients: creating strategies for therapeutic success. *Mult Scler.* (2012) 18:1022–6. doi: 10.1177/1352458511432896
83. Zhang M, Zhang C, Bai P, Xue H, Wang G. Effectiveness of low dose of rituximab compared with azathioprine in Chinese patients with neuromyelitis optica: an over 2-year follow-up study. *Acta Neurol Belg.* (2017) 117:695–702. doi: 10.1007/s13760-017-0795-6
84. Yang CS, Yang L, Li T, Zhang DQ, Jin WN, Li MS, et al. Responsiveness to reduced dosage of rituximab in Chinese patients with neuromyelitis optica. *Neurology.* (2013) 81:710–3. doi: 10.1212/WNL.0b013e3182a1aac7
85. Ellrichmann G, Bolz J, Peschke M, Duscha A, Hellwig K, Lee DH, et al. Peripheral CD19(+) B-cell counts and infusion intervals as a surrogate for long-term B-cell depleting therapy in multiple sclerosis and neuromyelitis optica/neuromyelitis optica spectrum disorders. *J Neurol.* (2019) 266:57–67. doi: 10.1007/s00415-018-9092-4
86. Marcinno A, Marnetto F, Valentino P, Martire S, Balbo A, Drago A, et al. Rituximab-induced hypogammaglobulinemia in patients with neuromyelitis optica spectrum disorders. *Neurol Neuroimmunol neuroinflamm.* (2018) 5:e498. doi: 10.1212/NXI.0000000000000498
87. Ottaviano G, Marinoni M, Graziani S, Sibson K, Barzaghi F, Bertolini P, et al. Rituximab unveils hypogammaglobulinemia and immunodeficiency in children with autoimmune cytopenia. *J Allergy Clin Immunol Pract.* (2020) 8:273–282. doi: 10.1016/j.jaip.2019.07.032
88. Tallantyre EC, Whittam DH, Jolles S, Paling D, Constantinesecu C, Robertson NP, et al. Secondary antibody deficiency: a complication of anti-CD20 therapy for neuroinflammation. *J Neurol.* (2018) 265:1115–22. doi: 10.1007/s00415-018-8812-0
89. Radaelli M, Moiola L, Sangalli F, Esposito F, Barcella V, Ferre L, et al. Neuromyelitis optica spectrum disorders: long-term safety and efficacy of rituximab in Caucasian patients. *Mult Scler.* (2016) 22:511–9. doi: 10.1177/1352458515594042
90. Perez EE, Orange JS, Bonilla F, Chinen J, Chinn IK, Dorsey M, et al. Update on the use of immunoglobulin in human disease: a review of evidence. *J Allergy Clin Immunol.* (2017) 139:S1–S46. doi: 10.1016/j.jaci.2016.09.023
91. Huh SY, Kim SH, Hyun JW, Joung AR, Park MS, Kim BJ, et al. Mycophenolate mofetil in the treatment of neuromyelitis optica spectrum disorder. *JAMA Neurol.* (2014) 71:1372–8. doi: 10.1001/jamaneurol.2014.2057
92. Nosadini M, Gadian J, Lim M, Sartori S, Thomas T, Dale RC. Mycophenolate mofetil in paediatric autoimmune or immune-mediated diseases of the central nervous system: clinical experience and recommendations. *Dev Med Child Neurol.* (2019) 61:458–68. doi: 10.1111/dmcn.14020
93. Gombolay GY, Chitnis T. Pediatric neuromyelitis optica spectrum disorders. *Curr Treat Options Neurol.* (2018) 20:19. doi: 10.1007/s11940-018-0502-9
94. Elsone L, Kitley J, Luppe S, Lythgoe D, Mutch K, Jacob S, et al. Long-term efficacy, tolerability and retention rate of azathioprine in 103 aquaporin-4 antibody-positive neuromyelitis optica spectrum disorder patients: a multicentre retrospective observational study from the UK. *Mult Scler.* (2014) 20:1533–40. doi: 10.1177/1352458514525870

95. Zhou Y, Huang Q, Lu T, Sun X, Fang L, Lu Z, et al. Azathioprine therapy in a case of pediatric multiple sclerosis that was seropositive for MOG-IgG. *J Clin Neurosci.* (2017) 38:71–3. doi: 10.1016/j.jocn.2016.12.022
96. Lunemann JD, Nimmerjahn F, Dalakas MC. Intravenous immunoglobulin in neurology–mode of action and clinical efficacy. *Nat Rev Neurol.* (2015) 11:80–9. doi: 10.1038/nrneurol.2014.253
97. Viswanathan S, Wong AH, Quek AM, Yuki N. Intravenous immunoglobulin may reduce relapse frequency in neuromyelitis optica. *J Neuroimmunol.* (2015) 282:92–6. doi: 10.1016/j.jneuroim.2015.03.021
98. Tsantes E, Curti E, Siena E, Granella F. Successful intravenous immunoglobulin treatment in relapsing MOG-antibody-associated disease. *Mult Scler Relat Dis.* (2019) 32:27–9. doi: 10.1016/j.msard.2019.04.021
99. Elajez R, Ezzeldin A, Gaber H. Safety evaluation of intravenous immunoglobulin in pediatric patients: a retrospective, 1-year observational study. *Ther Adv Drug Saf.* (2019) 10:2042098619876736. doi: 10.1177/2042098619876736
100. Kubota J, Hamano SI, Daida A, Hiwatari E, Ikemoto S, Hirata Y, et al. Predictive factors of first dosage intravenous immunoglobulin-related adverse effects in children. *PloS One.* (2020) 15:e0227796. doi: 10.1371/journal.pone.0227796
101. Paul F, Murphy O, Pardo S, Levy M. Investigational drugs in development to prevent neuromyelitis optica relapses. *Expert Opin Investig Drugs.* (2018) 27:265–71. doi: 10.1080/13543784.2018.1443077
102. Klotz L, Havla J, Schwab N, Hohlfeld R, Barnett M, Reddel S, et al. Risks and risk management in modern multiple sclerosis immunotherapeutic treatment. *Ther Adv Neurol Disord.* (2019) 12:1–31. doi: 10.1177/1756286419836571
103. Pittock SJ, Berthele A, Fujihara K, Kim HJ, Levy M, Palace J, et al. Eculizumab in aquaporin-4-positive neuromyelitis optica spectrum disorder. *N Engl J Med.* (2019) 381:614–25. doi: 10.1056/NEJMoa1900866
104. Percheron L, Gramada R, Tellier S, Salomon R, Harambat J, Llanas B, et al. Eculizumab treatment in severe pediatric STEC-HUS: a multicenter retrospective study. *Pediatr Nephrol.* (2018) 33:1385–94. doi: 10.1007/s00467-018-3903-9
105. McNamara LA, Topaz N, Wang X, Hariri S, Fox L, MacNeil JR. High risk for invasive meningococcal disease among patients receiving eculizumab (soliris) despite receipt of meningococcal vaccine. *MMWR Morb Mortal Wkly Rep.* (2017) 66:734–7. doi: 10.15585/mmwr.mm6627e1
106. Soler-Garcia A, Fernandez de Sevilla M, Abad R, Esteva C, Alsina L, Vazquez J, et al. Meningococcal serogroup B disease in vaccinated children. *J Pediatric Infect Dis Soc.* (2019). doi: 10.1093/jpids/piz071. [Epub ahead of print].
107. Araki M, Matsuoka T, Miyamoto K, Kusunoki S, Okamoto T, Murata M, et al. Efficacy of the anti-IL-6 receptor antibody tocilizumab in neuromyelitis optica: a pilot study. *Neurology.* (2014) 82:1302–6. doi: 10.1212/WNL.0000000000000317
108. Ringelstein M, Ayzenberg I, Harmel J, Lauenstein AS, Lensch E, Stogbauer F, et al. Long-term therapy with interleukin 6 receptor blockade in highly active neuromyelitis optica spectrum disorder. *JAMA Neurol.* (2015) 72:756–63. doi: 10.1001/jamaneurol.2015.0533
109. Asseyer S, Schmidt F, Chien C, Scheel M, Ruprecht K, Bellmann-Strobl J, et al. Pain in AQP4-IgG-positive and MOG-IgG-positive neuromyelitis optica spectrum disorders. *Mult Scler J Exp Transl Clin.* (2018) 4:2055217318796684. doi: 10.26226/morressier.5b719e455aff74008ae4ccc0
110. Breu M, Glatter S, Hoftberger R, Freilinger M, Kircher K, Kasprian G, et al. Two cases of pediatric AQP4-antibody positive neuromyelitis optica spectrum disorder successfully treated with tocilizumab. *Neuropediatrics.* (2019) 50:193–6. doi: 10.1055/s-0039-1684004
111. Lotan I, Charlson RW, Ryerson LZ, Levy M, Kister I. Effectiveness of subcutaneous tocilizumab in neuromyelitis optica spectrum disorders. *Mult Scler Relat Dis.* (2019) 39:101920. doi: 10.1016/j.msard.2019.101920
112. Yamamura T, Kleiter I, Fujihara K, Palace J, Greenberg B, Zakrzewska-Pniewska B, et al. Trial of satralizumab in neuromyelitis optica spectrum disorder. *N Engl J Med.* (2019) 381:2114–24. doi: 10.1056/NEJMoa1901747
113. Cree BAC, Bennett JL, Kim HJ, Weinshenker BG, Pittock SJ, Wingerchuk DM, et al. Inebilizumab for the treatment of neuromyelitis optica spectrum disorder (N-MOmentum): a double-blind, randomised placebo-controlled phase 2/3 trial. *Lancet.* (2019). 394:1352–63. doi: 10.1016/S0140-6736(19)31817-3
114. Keating MJ, Dritselis A, Yasothan U, Kirkpatrick P. Ofatumumab. *Nat Rev Drug Discov.* (2010) 9:101–2. doi: 10.1038/nrd3100
115. Teeling JL, French RR, Cragg MS, van den Brakel J, Pluyter M, Huang H, et al. Characterization of new human CD20 monoclonal antibodies with potent cytolytic activity against non-Hodgkin lymphomas. *Blood.* (2004) 104:1793–800. doi: 10.1182/blood-2004-01-0039
116. Sagcal-Gironella AC, Muscal E, Ramirez AA, Marcus M, Gillispie M, Lapin WB, De Guzman MM, et al. Ofatumumab use in childhood-onset systemic lupus erythematosus: a single-center experience [abstract]. *Arthritis Rheumatol.* (2018) 70. Available online at: https://acrabstracts.org/abstract/ofatumumab-use-in-childhood-onset-systemic-lupus-erythematosus-a-single-center-experience/
117. Lei L, Muhammad S, Al-Obaidi M, Sebire N, Cheng IL, Eleftheriou D, et al. Successful use of ofatumumab in two cases of early-onset juvenile SLE with thrombocytopenia caused by a mutation in protein kinase C delta. *Pediatr Rheumatol Online J.* (2018) 16:61. doi: 10.1186/s12969-018-0278-1
118. Hino-Fukuyo N, Haginoya K, Takahashi T, Nakashima I, Fujihara K, Takai Y, et al. Long-term outcome of a group of Japanese children with myelin-oligodendrocyte glycoprotein encephalomyelitis without preventive immunosuppressive therapy. *Brain Dev.* (2019) 41:790–5. doi: 10.1016/j.braindev.2019.06.004
119. Lopez-Chiriboga AS, Majed M, Fryer J, Dubey D, McKeon A, Flanagan EP, et al. Association of MOG-IgG serostatus with relapse after acute disseminated encephalomyelitis and proposed diagnostic criteria for MOG-IgG-associated disorders. *JAMA Neurol.* (2018) 75:1355–63. doi: 10.1001/jamaneurol.2018.1814
120. Nagashima M, Osaka H, Ikeda T, Matsumoto A, Miyauchi A, Kaneko K, et al. Rituximab was effective for acute disseminated encephalomyelitis followed by recurrent optic neuritis with anti-myelin oligodendrocyte glycoprotein antibodies. *Brain Dev.* (2018) 40:607–11. doi: 10.1016/j.braindev.2018.03.011
121. Weinshenker BG, Wingerchuk DM. The two faces of neuromyelitis optica. *Neurology.* (2014) 82:466–7. doi: 10.1212/WNL.0000000000000114
122. Prain K, Woodhall M, Vincent A, Ramanathan S, Barnett MH, Bundell CS, et al. AQP4 antibody assay sensitivity comparison in the era of the 2015. diagnostic criteria for NMOSD. *Front Neurol.* (2019). 10:1028. doi: 10.3389/fneur.2019.01028
123. Reindl M, Schanda K, Woodhall M, Tea F, Ramanathan S, Sagen J, et al. International multicenter examination of MOG antibody assays. *Neurol Neuroimmunol Neuroinflamm.* (2020) 7:e674. doi: 10.1212/NXI.0000000000000674
124. Yeh EA, Nakashima I. Live-cell based assays are the gold standard for anti-MOG-Ab testing. *Neurology.* (2019) 92:501–2. doi: 10.1212/WNL.0000000000007077
125. Waters PJ, Komorowski L, Woodhall M, Lederer S, Majed M, Fryer J, et al. A multicenter comparison of MOG-IgG cell-based assays. *Neurology.* (2019) 92:e1250–e1255. doi: 10.1212/WNL.0000000000007096

Conflict of Interest: ST serves as a non-remunerated editorial board member of *Neurology: Neuroimmunology & Neuroinflammation* and *Frontiers in Neurology*. She has received speaker honoraria from Biogen-Idec Argentina, Merck Serono LATAM, Genzyme, Novartis Argentina, and Novartis Pharma Inc. She is member of the Genentech-Roche Inc. NMO Scientific Advisory Committee and Chair of the NMO Relapse Adjudication Committee, Alexion Pharmaceuticals Inc.

EY receives research funding from the NMSS, CMSC, OIRM, SCN, CBMH Chase-an-Idea, SickKids Foundation, MS Scientific Foundation (Canada), NIH, McLaughlin Center, Biogen MA Inc. She has served as a scientific advisor to Alexion and Hoffman-LaRoche. She has received speakers' honoraria from Excemed and MS at the Limits.

APPENDIX

Active Members of The Guthy-Jackson Charitable Foundation International Clinical Consortium (GJCF-ICC)

Hesham Abboud, Case Western Reserve University, Cleveland, OH, United States Orhan Aktas, Institute of Neuroimmunology, Duesseldorf, Germany Raed Alroughani, Amiri Hospital, Kuwait City, Kuwait Ayse Altintas, Koc University School of Medicine, Istanbul, Turkey Lilyana Amezcua, University of Southern California, Los Angeles, CA, United States Metha Apiwattanakul, Prasat Neurological Institute, Bangkok, Thailand Nasrin Asgari, University of Southern Denmark, Odense, Denmark Brenda Banwell, The Children's Hospital of Philadelphia, University of Pennsylvania, Philadelphia, PA, United States Jeffrey Bennett, University of Colorado, Denver, CO, United States Denis Bichuetti, Universidade Federal de São Paulo, São Paulo, Brazil Terrence F. Blaschke, Stanford University [Emeritus], Stanford, CA, United States James Bowen, Swedish Neuroscience Institute, Seattle, WA, United States Alexey Boyko, Prigov's Russian Scientific Research Medical University, Moscow, Russia Alexander Brandt, University of California, Irvine, Irvine, CA, United States Simon Broadley, Griffith University, Mount Gravatt, QLD, Australia Wolfgang Brück, University Medical Center Göttingen, Göttingen, Germany Edgar Carnero Contentti, Hospital Alemán, Buenos Aires, Argentina Robert Carruthers, University of British Columbia, Vancouver, BC, Canada Tanuja Chitnis, Brigham and Women's Hospital & Massachusetts General Hospital, Boston, MA, United States Jeffrey Cohen, Cleveland Clinic, Cleveland, OH, United States Guillermo Delgado-García, Instituto Nacional de Neurologia y Neurocirugia, Mexico City, Mexico Irena Dujmovic Basuroski, UNC School of Medicine, Chapel Hill, NC, United States Nikos Evangelou, University of Nottingham, Nottingham, United Kingdom Kazuo Fujihara, Tohoku University, Sendai, Japan Andrew Goodman, University of Rochester, Rochester, NY, United States Benjamin Greenberg, University of Texas Southwestern Medical Center at Dallas, Dallas, TX, United States Yael Hacohen, Great Ormond Street Hospital / UCL, London, United Kingdom May Han, Stanford University School of Medicine, Stanford, CA, United States Joachim Havla, Ludwig-Maximilians University, Munich, Germany Kerstin Hellwig, St. Josef Hospital Bochum, Bochum, Germany Jyh Yung Hor, Penang General Hospital, George Town, Malaysia Raffaele Iorio, Institute of Neurology, Catholic University of Sacred Heart, Rome, Italy Anu Jacob, Walton Centre, Liverpool, United Kingdom Sven Jarius, UniversitatKlinikum, Heidelberg, Germany Jorge Andres Jimenez Arango, Universidad de Antioquia, Medellin, Colombia Ilana Katz Sand, Icahn School of Medicine at Mount Sinai, New York, NY, United States Ho Jin Kim, National Cancer Center, Goyang-si, South Korea Sung Min Kim, Seoul National University Hospital, Seoul, South Korea Dorlan Kimbrough, Brigham and Women's Hospital & Massachusetts General Hospital, Boston, MA, United States Najib Kissani, Neurology Department, University Hospital, Marrakech, Morocco Eric Klawiter, Massachusetts General Hospital, Harvard Medical School, Boston, MA, United States Ingo Kleiter, Marianne-Strauß-Klinik, Berg, Germany Marco Lana-Peixoto, Universidade Federal de Minas Gerais, Belo Horizonte, Brazil Maria Isabel Leite, Oxford University Hospitals, Oxford, United Kingdom Michael Levy, Massachusetts General Hospital, Boston, MA, United States Yaou Liu, Xuanwu Hospital, Capital Medical University, Beijing, China Fred Lublin, Icahn School of Medicine at Mount Sinai, New York, NY, United States Youssoufa Maiga, Teaching Hospital Gabriel Touré, Bamako, Mali Yang Mao-Draayer, University of Michigan, Neurology Department, Ann Arbor, MI, United States Romain Marignier, CHU Lyon, Lyon, France Sara Mariotto, University of Verona, Italy Marcelo Matiello, Brigham and Women's Hospital & Mass General, Boston, MA, United States Maureen Mealy, Viela Bio, Baltimore, MD, United States Esther Melamed, UT Austin, Austin, TX, United States Callene Momtazee, University of California, Los Angeles, Los Angeles, CA, United States Ichiro Nakashima, Tohoku University, Sendai, Japan Jayne Ness, Children's of Alabama - Neurology, Birmingham, AL, United States Celia Oreja-Guevara, Hospital Clínico San Carlos, Madrid, Spain Jacqueline Palace, Oxford University Hospitals, Oxford, United Kingdom Lekha Pandit, K S Hegde Medical Academy, Mangalore, India Friedemann Paul, Charité University Medicine Berlin, Berlin, Germany Sarah Planchon Pope, Cleveland Clinic, Cleveland, OH, United States Anne-Katrin Pröbstel, Neurologic Clinic and Policlinic, University Hospital Basel & Department of Biomedicine, University of Basel, Basel, Switzerland Peiqing Qian, Swedish Neuroscience Institute, Seattle, WA, United States Chao Quan, Huashan Hospital, Shanghai, China Pavle Repovic, Swedish Neuroscience Institute, Seattle, WA, United States Claire Riley, Columbia University, New York, NY, United States Marius Ringelstein, Heinrich-Heine-University, Duesselforf, Germany Dalia Rotstein, St. Michael's Hospital, Toronto, ON, Canada Klemens Ruprecht, Charité University Medicine Berlin, Berlin, Germany Maria José Sá, Centro Hospitalar São João, Porto, Portugal Albert Saiz, IDIBAPS Hospital Clinic of Barcelona, Barcelona, Spain Douglas Sato, Brain Institute (InsCer) PUCRS, Porto Alegre, Brazil Ché Serguera, MIRCen INSERM/ CEA, Paris, France Eslam Shosha, Prince Sultan Military Medical City, Riyadh, Saudi Arabia Nancy Sicotte, Cedars Sinai, Los Angeles, CA, United States Sasitorn Siritho, Mahidol University, Bangkok, Thailand Aksel Siva, Istanbul University, Cerrahpaşa School of Medicine, Istanbul, Turkey Terry J. Smith, University of Michigan, Ann Arbor, MI, United States Ibis Soto de Castillo, Hospital Universitario de Maracaibo, Maracaibo, Venezuela Silva Tenembaum, Hospital de Pediatria, Buenos-Aires, Argentina Leticia Tornes, University of Miami, Coral Gables, FL, United States Pablo Villoslada, Stanford University School of Medicine, Stanford, CA, United States Dean Wingerchuk, Mayo Clinic, Scottsdale, AZ, United States Jens Wüfel, MIAC AG, Basel, Switzerland Bassem Yamout, American University of Beirut Medical Center, Beirut, Lebanon Michael R. Yeaman, University of California, Los Angeles, Los Angeles, CA, United States E. Ann Yeh, Hospital for Sick Children, University of Toronto, Toronto, ON, Canada Scott Zamvil, University of California, San Francisco, San Francisco, CA, United States.

frontiers in Pediatrics

CORRECTION
published: 15 February 2021
doi: 10.3389/fped.2020.642203

Corrigendum: Pediatric NMOSD: A Review and Position Statement on Approach to Work-Up and Diagnosis

Silvia Tenembaum[1], *E. Ann Yeh*[2]* *and The Guthy-Jackson Foundation International Clinical Consortium (GJCF-ICC)*[†]

[1] Department of Neurology, National Pediatric Hospital Dr. J. Garrahan, Buenos Aires, Argentina, [2] Division of Neurology, Department of Pediatrics, SickKids Research Institute, The Hospital for Sick Children, University of Toronto, Toronto, ON, Canada

Keywords: pediatric, neuroinflammation, NMOSD, MOG, treatment, diagnosis

Approved by:
Frontiers Editorial Office, Frontiers Media SA, Switzerland

***Correspondence:**
E. Ann Yeh
ann.yeh@sickkids.ca

[†]*See Appendix for complete list of active GJCF-ICC Members*

Specialty section:
This article was submitted to Pediatric Neurology, a section of the journal Frontiers in Pediatrics

Received: *15 December 2020*
Accepted: *16 December 2020*
Published: *15 February 2021*

Citation:
Tenembaum S, Yeh EA and The Guthy-Jackson Foundation International Clinical Consortium (GJCF-ICC) (2021) Corrigendum: Pediatric NMOSD: A Review and Position Statement on Approach to Work-Up and Diagnosis. Front. Pediatr. 8:642203. doi: 10.3389/fped.2020.642203

A Corrigendum on

Pediatric NMOSD: A Review and Position Statement on Approach to Work-Up and Diagnosis
by Tenembaum, S., Yeh, E. A., and The Guthy-Jackson Foundation International Clinical Consortium (GJCF-ICC) (2020). Front. Pediatr. 8:339. doi: 10.3389/fped.2020.00339

In the original article, there was a mistake in **Table 3** as published. The administration form of satralizumab is "SC" not "IV." The corrected **Table 3** appears below.

The authors apologize for this error and state that this does not change the scientific conclusions of the article in any way. The original article has been updated.

TABLE 3 | Immunosuppressive molecules for attack prevention in NMOSD.

	Monoclonal antibody	Mechanism	Route	Risk
Rituximab	Chimeric	CD20-B cell depletion	IV	Infections; Hepatitis B reactivation; Infusion-related reaction
Eculizumab	Humanized	C5 complement inhibitor	IV	Meningococcal infection; Possible PML risk; Infusion-related reaction
Satralizumab	Humanized recycling	IL-6 receptor blocker	SC	
Tocilizumab	Humanized	IL-6 receptor blocker	SC	Cardiovascular risk; Cholesterol levels
Inebelizumab	Humanized	CD19-B cell depletion	IV	Infections; Infusion-related reaction
Ofatumumab	Fully humanized	CD20-B cell depletion	SC	Infections; Infusion-related reaction; Hepatitis B reactivation
Ocrelizumab	Humanized	CD20-B cell depletion	IV	Infections; Infusion-related reaction; Hepatitis B reactivation

frontiers in Pediatrics

CASE REPORT
published: 05 August 2020
doi: 10.3389/fped.2020.00443

High-Throughput Sequencing Reveals the Loss-of-Function Mutations in *GALT* Cause Recessive Classical Galactosemia

Lulu Li[1†], Li Ma[2†], Min Sun[2], Jiancheng Jiao[2], Yudong Zhang[2], Yue Tang[1], Nan Yang[1] and Yuanyuan Kong[1]*

[1] Department of Newborn Screening Center, Beijing Obstetrics and Gynecology Hospital, Capital Medical University, Beijing Maternal and Child Health Care Hospital, Beijing, China, [2] Department of Neonatology, Hebei Provincial Children's Hospital, Shijiazhuang, China

Background: Classical Galactosemia (CG) is a rare autosomal recessive metabolic disease caused by mutations in the galactose-1-phosphate uridyl transferase (*GALT*) gene. This study aim to identify pathogenic mutations underlying classic galactosemia in two Chinese families.

Methods: We collected blood samples from two Chinese families and extracted genomic DNA. High-throughput sequencing, sanger sequencing, and bioinformatics analysis were used to investigate the molecular cause of manifestations in the two Chinese families.

Results: We found compound heterozygous mutations (c.396C>G; p.His132Gln and c.974C>T; p.Pro325Leu) in family 1 and a homozygous missense variant (c.974C>T; p.Pro325Leu) in family 2. Bioinformatics and Sanger sequencing were performed to verify the identified variants.

Conclusion: The present study identified the *GALT* mutations as a genetic etiology in the two Chinese families with classic galactosemia and expanded the phenotypic and mutational spectrum of *GALT.* Our findings could be useful in providing evidence for prenatal interventions and more precise pharmacological treatments to patients. High-throughput sequencing conducted in our study is a convenient and useful tool for clinical diagnosis of galactosemia and other associated genetic disorders.

Keywords: classical galactosemia (CG), high-throughput sequencing, *GATL*, gene mutation, hepatomegaly, autosomal recessive (AR), Chinese patient, mutation spectrum

OPEN ACCESS

Edited by:
Sascha Meyer,
Saarland University Hospital, Germany

Reviewed by:
Rita Selvatici,
University of Ferrara, Italy
Fan Jin,
Zhejiang University, China

***Correspondence:**
Yuanyuan Kong
kongyuanyuan1971@163.com

[†] These authors have contributed equally to this work

Specialty section:
This article was submitted to Genetics of Common and Rare Diseases, a section of the journal Frontiers in Pediatrics

Received: *22 May 2020*
Accepted: *26 June 2020*
Published: *05 August 2020*

Citation:
Li L, Ma L, Sun M, Jiao J, Zhang Y, Tang Y, Yang N and Kong Y (2020) High-Throughput Sequencing Reveals the Loss-of-Function Mutations in GALT Cause Recessive Classical Galactosemia. Front. Pediatr. 8:443. doi: 10.3389/fped.2020.00443

INTRODUCTION

Classical Galactosemia (CG) (Type I galactosemia OMIM # 230400) is a rare autosomal recessive inborn error of galactose metabolism, It is caused by galactose-1-phosphate uridylyltransferase (GALT, EC 2.7.7.12) enzyme deficiency (1, 2). The action of the GALT enzyme is to convert galactose-1-phosphate and uridine diphosphate glucose into glucose-1-phosphate and uridine diphosphate-galactose (3). The incidence rates of CG has been reported as 1/16–1/60,000 individuals in various global populations (4, 5). Clinical features associated with CG are feeding difficulty, diarrhea, jaundice, liver and renal complications, muscular hypotonia, cataract, and low intelligence level (1, 6). CG disease caused by the failure to metabolize galactose is potentially life-threatening. With the benefit of early diagnosis by newborn screening, the acute

presentation of CG can be prevented. The advent of high-throughput sequencing technology in the field of genetics has provided an unprecedented opportunity for the identification of rare pathogenic variants causing Mendelian disorders.

In this article, we demonstrate two Chinese families with hallmark features of CG. By high throughput sequencing technology we identified novel compound heterozygous and homozygous mutations in the *GALT* gene in family 1 and 2, respectively.

METHODS AND MATERIALS

Family Recruitment and Ethical Sight

This study was approved by the Ethics Committee of Beijing Obstetrics and Gynecology Hospital affiliated to Capital Medical University, and family members (or guardians) all signed informed consent.

Blood Samples Collection and DNA Extraction

Blood sample was drawn from the affected and normal individuals. Genomic DNA was extracted using phenol chloroform method and was quantified using Nanodrop-2000 by standard methods.

High-Throughput Sequencing

One to three micrograms of genomic DNA from each sample was sheared into fragments of about 200 bp using the Bioruptor NGS sonication device (Diagenode, Seraing, Belgium). The fragments were purified with Agencourt AMPure XP Kit (Beckman Coulter, Indianapolis, IN). An adenine base was added to the end-repaired DNA fragments followed by ligation to paired-end adapters, amplification for the adapter-ligated library, and quality examination of the amplified library. Nimblegen SeqCap EZ Exome Plus Kit (Roche, Basel, Switzerland) was utilized to hybridize the sample and SeqCap EZ libraries. The capture beads were prepared using Invitrogen Dynabeads M-280 Streptavidin (Thermo Fisher Scientific) and were washed after DNA binding. Captured DNA was amplified via ligation-mediated PCR before purification of the amplified captured multiplex DNA sample. After inspection of reading quality, the captured library was subject to sequencing on the HiSeq 2500 System (Illumina, San Diego, CA).

Bioinformatics Analysis

Sequencing data was analyzed, filtered, and compared with the human genome reference sequence hg19 (GRCh37/hg19). To identify plausible pathogenic mutations, we mainly focused on non-synonymous homozygous or compound heterozygous variants with a minor allele frequency of 1% (dbSNP142 or ExAC) were retained. The variants were cross-checked in the Human Gene Mutation Database (HGMD; http://www.hgmd.cf.ac.uk/ac/index.php) to see if the identified variants are novel or already reported.

Primer Designing and Mutation Confirmation

Primer 5.0 primer software was used to design the specific PCR primers (*GALT*-exon 5-F/R: 5′-GTAGCACAGCCAAGCCCTAC-3′/5′-CCCAGAACCAAAGCTTCATC-3′; *GALT*-exon10-F/R: 5′-CAGATACCTGGTTGGGTTTG-3′/5′-GACGCCAGACTGTTCTGAGT-3′). Target region was amplified by polymerase chain reaction (PCR) machine (Takara/Clontech). The PCR reaction was commenced with an initial 3-min denaturation step at 95°C, followed by 38 cycles of denaturation (94°C) for 30 s, annealing (56–61°C) for 30 s, and extension (72°C) for 50 s, and ended with a final extension step at 72°C for 8 min.

Bioinformatics Analysis

Different bioinformatics softwares including Mutation Taster (http://www.mutationtaster.org/), Polyphen-2 (http://genetics.bwh.harvard.edu/pph2), and Sorting Intolerant From Tolerant (SIFT, http://provean.jcvi.org/index.php), were used for functional effect prediction**.** Finally, for the interpretation of variants, the American College of Medical Genetics and Genomics (ACMG) 2015 guidelines were used.

RESULTS

Detailed Clinical Features of the Patient

Family 1

Case 1 (**Figure 1A**, II-1) female subject, 15 days old at the initial diagnosis, was admitted to the Department of Newborn Screening Center, Beijing Obstetrics and Gynecology Hospital, Capital Medical University for reexamination of "increased blood phenylalanine level in neonatal screening." She was a full-term normal baby, and her mother (gravidity 1, parity 1) experienced a smooth pregnancy this time. For the baby, symptoms of jaundice occurred and recurred in 3rd and 10th day of life. The physical and mental reaction were minor, the full body skin was dark yellow, abdominal distention, abdominal wall vein filling (**Figure 1B**), hepatomegaly, spleen was not touched. Laboratory examinations showed elevated liver enzymes, total bilirubin, mainly direct bilirubin, accompanied by elevated bile acids (**Supplementary Table 1**); AFP $>$ 1,000 μg/L; abnormal coagulation function (**Supplementary Table 2**); serum arginine, citrulline, and tyrosine increased to varying degrees (**Supplementary Table 3**); urine lactic acid, phenyllactic acid, 4-hydroxyphenyllactic acid increased. Abdominal B-ultrasound showed that: 3.3 cm below the liver ribs and 2.9 cm under the sword, the echo of liver parenchyma was enhanced, the sheath of grissen's was thickened, free ascites was found in the abdominal cavity, the depth was about 4.6 cm; Brain MRI showed that—the echo of brain white matter was slightly strong, and the ventricles were not expanded. The child died after 2 months—due to severe liver failure. There was no family history was seen of Classical Galactosemia.

Family 2

Case 2 (**Figure 2A**, II-1): female subject, 12 days old at the initial diagnosis, who was hospitalized in the department of

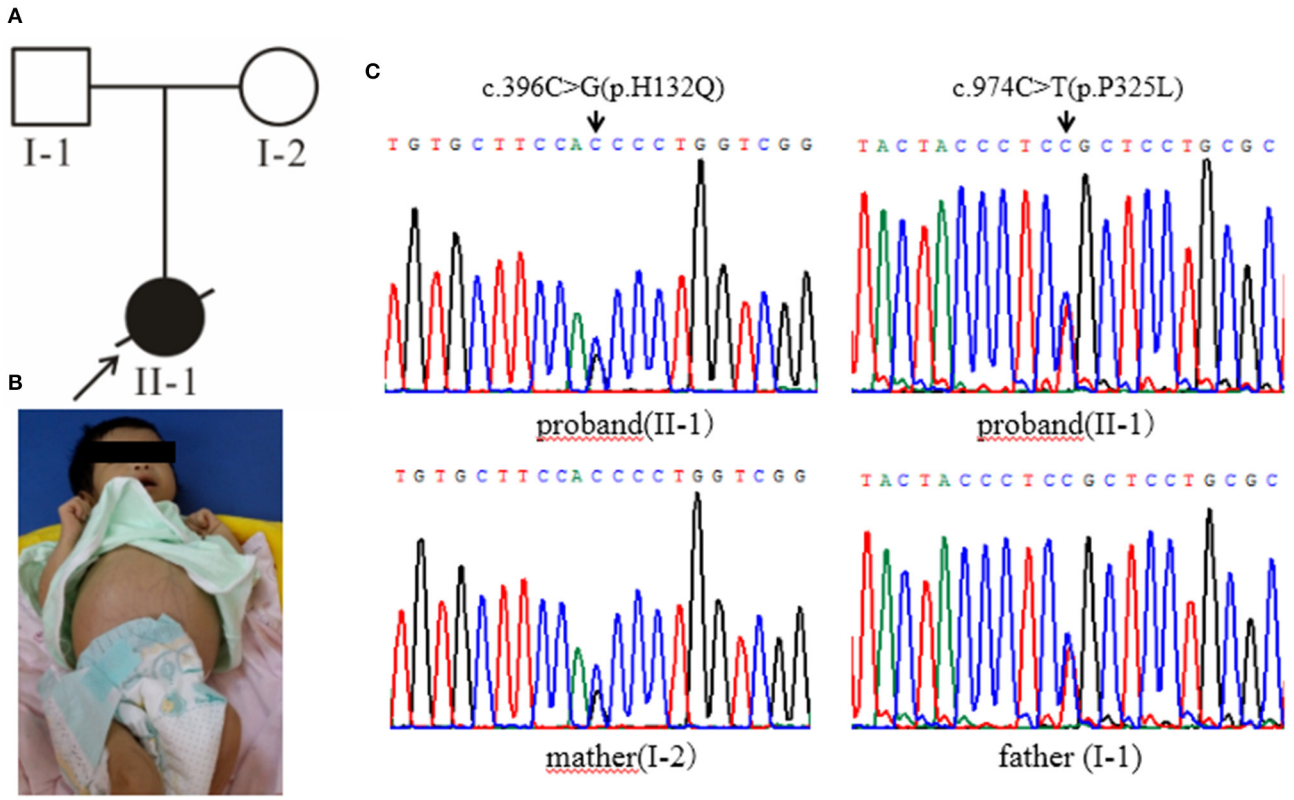

FIGURE 1 | (A) The black arrow indicates the proband, and the slash indicates the proband has died. **(B)** The clinical manifestations of the proband: yellow skin, dark yellow color, abdominal distention, and abdominal wall vein filling. **(C)** Gene sequencing results: the proband carries the GALT gene c.396C>G (p.His132Gln) and c.974C>T (p.Pro325Leu) complex heterozygous mutation, c.396C>G (p.His132Gln) from the maternal source, and c.974C>T (p.Pro325Leu) from the paternal source.

Neonatology, Hebei Provincial Children's Hospital for half a day due to "less milk intake and fever." She was a full-term normal baby, birth weight 3,200 g and her mother (gravidity 2, parity 2) experienced a smooth pregnancy this time. After the birth of breast-feeding, early self-feeding was good, and then gradually reduced the amount of milk, yellow paste stool, and frequency. Twelve days after birth (half-day before admission) after contact with fever patients (the mother of the child), with the maximum temperature of 38.0°C. The yellow skin stain was found on the 3rd day of birth, but it did not subside. The body weight was 2,970 g (230 g lower than birth), the face was painful, the skin was sallow and flowery, the abdomen was swollen, the veins of the abdominal wall were full, 6.0 cm under the liver rib, 6.0 cm under the sword, 4.0 cm under the spleen rib, soft. In the laboratory, The total bilirubin was significantly increased, mainly the direct bilirubin and the bile acid (**Supplementary Table 1**); the coagulation function was abnormal (**Supplementary Table 2**); there was no obvious abnormality in the blood metabolism screening, and urine 4-hydroxyphenyllactate increased; the blood culture was positive for *Escherichia coli*. B-ultrasonography of abdomen showed that the echo of liver parenchyma was enhanced and thickened, the point-like strong echo in the wall of the intestinal tract, and the peritoneal effusion; brain MRI showed that left intracerebral hemorrhage with ventricular enlargement. After admission, the patient was given anti infection and symptomatic treatment. The general condition improved, but there were still gastrointestinal symptoms with poor weight growth. Considering the presence of genetic metabolic diseases, the patient was finally diagnosed by genetic testing. After 3 months of birth, the follow-up showed that there was no vomiting and diarrhea after feeding milk powder without lactose, the mental reaction was good (**Figure 2B**), the liver function was obviously improved. The parents married without close relatives, there was no family history was seen of Classical Galactosemia.

Molecular Analysis

High-throughput sequencing data were processed to identify pathogenic mutations in the CG families. Proband from both families (1 and 2) and their parents were selected for high-throughput sequencing. After data analysis and filtrations, homozygous or compound heterozygous non-synonymous variants were selected having MAF >0.1% in different databases including dbSNP, ExAC, and gnomAD, etc. An identified mutation was further verified by Sanger sequencing using ABI3730 Automated Sequencer (PE Biosystems, Foster

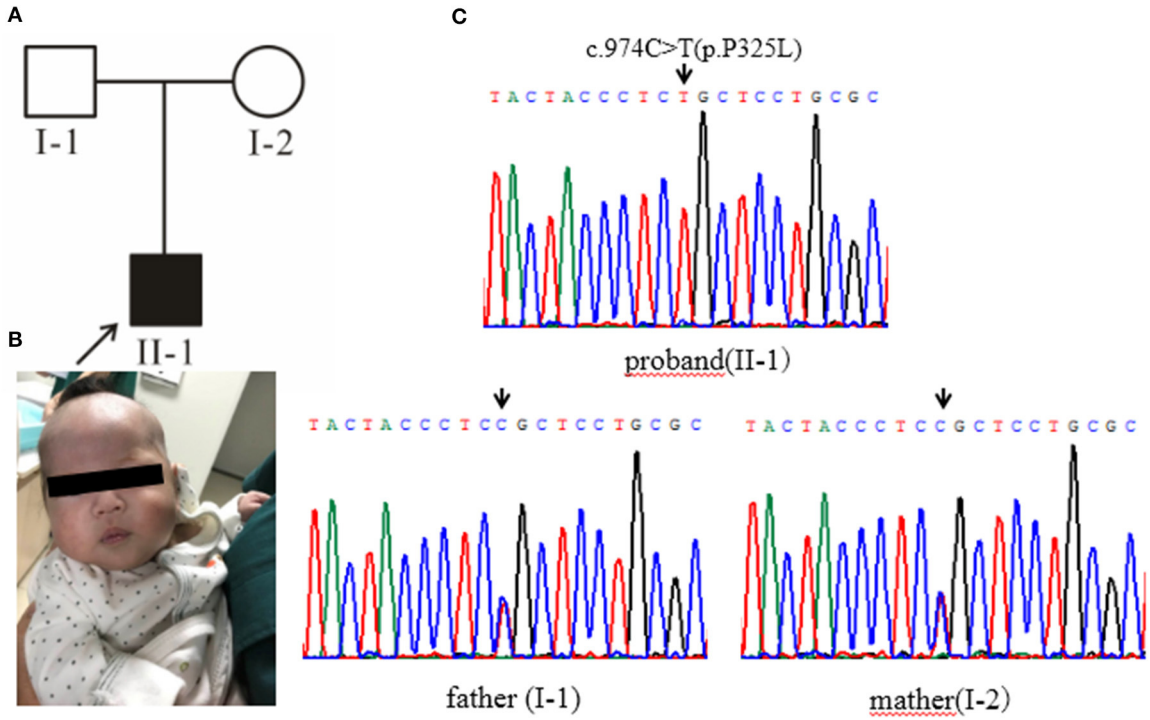

FIGURE 2 | (A) Pedigree chart, black arrow indicates the proband. **(B)** The proband's condition improves after being fed milk powder without lactose. **(C)** Gene sequencing results: the proband of pedigree 2 carries the homozygous mutation of GALT gene c.974C>T (p.Pro325Leu) and the parents are all carriers of the mutation.

City, CA). We identified compound heterozygous mutation (c.396C>G; p.His132Gln and c.974C>T; p.Pro325Leu) in family 1 (**Figure 1C**) and a homozygous missense mutation (c.974C>T; p.Pro325Leu) in family 2 (**Figure 2C**) respectively. Finally, the identified variants were confirmed by different bioinformatics tools such as Polymorphism Phenotyping v2 (Polyphen-2), Sorting Intolerant from Tolerant (SIFT) and Mutation Taster (**Table 1**). The prediction results were also supported by the extremely low allele frequencies of the two mutations (**Table 1**).

DISCUSSION

Classic Galactosemia (CG) is a rare autosomal recessive disorder of galactose metabolism. It caused by mutations in the galactose-1-phosphate uridyl transferase (GALT) gene located on chromosome 9p13.3 and has a total length of 4.3kb (7). GALT consists of 11 exons and encodes 379 amino acids expressed highly in liver, red blood cells (RBCs), and other tissues of the body. CG disease caused by the inability to digest galactose, is life-threatening but its pathophysiology has not been clearly defined.

Depending on the enzyme that is deficient (GALK, GALT, or GALE), there are three types of diseases (8). Classic Galactosemia type 1 represents the most severe form of the disease which is caused by the deficiency of GALT. Most of the children at perinatal period, presenting with vomiting, diarrhea, drowsiness, and other neurological symptoms, followed by jaundice, hepatomegaly, hypoglycemia, renal dysfunction, coagulation, and other abnormalities (9, 10). If not treated on time, the symptoms will be aggravated, and finally, death may occur (11, 12). Type II and type III are rare forms of galactosemia caused by GALK and Gale deficiency, respectively. The main clinical feature associate with Type II galactosemia is cataract (1). Due to the poor specificity of the clinical manifestations of gale patients, it is difficult to diagnose the disease. Therefore, it is very important for the rapid diagnosis and treatment of the disease to explore the genetic causes of gale patients through high-throughput sequencing technology, combined with conventional differential diagnosis. GALT gene presents high allelic heterogeneity and more than 100 mutations have been identified in human gene mutation database (HGMD: http://www.hgmd.org). The most common mutations in various populations identified in GALT are the Gln188Arg, Lys 285Asn, Ser135Leu, and Asn314Asp (13–15).

Here, we report two families with CG who were detected during a neonatal screening in China. Clinical investigation of family 1 showed full abdominal vein, hepatomegaly (**Figure 1B**), elevated level of serum arginine, methionine, citrulline, and tyrosine (**Supplementary Table 3**), and the level of lactate and phenylactate in urine were increased. In family 2, there were symptoms including fever, hepatosplenomegaly, intrauterine infection, and hematologic disorders. Molecular study of both families (1 and 2) revealed compound heterozygous (c.396C>G; p.His132Gln and c.974C>T; p.Pro325Leu) (**Figure 1C**) and homozygous missense (c.974C>T; p.Pro325Leu) (**Figure 2C**) mutations in GALT gene in family 1 and 2 respectively. Through

TABLE 1 | Bioinformatic analysis of *GALT* variants.

	ExACALL	1,000 g 2015 Aug all	GnomAD ALL	SIFT score	SIFT pred	Polyphen2 score	Polyphen2 pred	Mutation Taster score	Mutation Taster pred
c.396C>G (p.H132Q)	–	–	–	0.028	D	0.991	D	1	D
c.974C>T (p.P325L)	–	0.000008237	0.00003232	0	D	1	D	1	D

D, Damaging; P, Possibly Pathogenic.

molecular simulation prediction, it is suggested that p.His132Gln indirectly destroys the active site of the enzyme, decrease GALT enzymatic activity, and finally effects protein translation and /or protein stability (16). Although the mutation c.396C>G has not been previously reported, it leads to the same amino acid substitution (p.His132Gln) as the mutation c.396C>A which has been previously reported and included in the Clinvar database (16). Given that the effects of this substitution has been well-studied, it is reasonable to determine the pathogenicity of this missense mutation. The homozygous missense mutation c.974C>T; p.Pro325Leu changes the proline to leucine at 325th amino acid lead to CG phenotypes. *In silico* analysis, it is predicted that the mutations were pathogenic that lead to CG. Although c.974C>T (p. p.Pro325Leu) is a known mutation (17), but it is the first found in the Chinese population. This study verifies the pathogenicity of the mutation again. The clinically features observed in our patients were jaundice and hepatomegaly, which accorded with the typical characteristics of galactosemia in infancy (6).

The conventional differential diagnosis methods of gal are enzymatic diagnosis and chemical diagnosis (8, 13). Enzymology diagnosis is easy to be interfered by external environmental factors, temperature, and humidity are too high to cause false negative or false positive. Chemical diagnosis can only get positive results when the disease attacks and is greatly affected by diet, which can only be used as a means of screening, not as a basis for diagnosis. At the same time, the study found that neonatal intrahepatic cholestasis caused by citrin deficiency (NICCD) is very similar to galactosemia in clinical manifestations and experimental examination, but there is a large difference in later treatment (14, 15). Meanwhile, the case 2, began to "fever" treatment, for hepatosplenomegaly, initially suspected of intrauterine infection, blood system disease, hemophagocytic syndrome, or congenital genetic metabolic disease? After a series of clinical examinations, no diagnosis was made. Therefore, it is very important to find an accurate and effective clinical differential diagnosis method for patients' prognosis, clinical treatment, and genetic consultation. With the rapid development of high-throughput sequencing technology, the target gene can be accurately captured and the disease species with high genetic heterogeneity can be comprehensively analyzed (18). Not only the operation cost is low, the flux is high, and the operation speed is fast, but also the results are reliable and stable. At present, it has been successfully applied to the diagnosis of multiple genetic metabolic diseases such as methylmalonic acidemia, maple syrup uremia, ornithine carbamylase deficiency, etc. (19).

In conclusion, use of high-throughput sequencing technology, can identify the cause of disease and improve the efficiency of disease diagnosis. In particular, we should pay more attention to gene detection in children with persistent jaundice and abnormal liver function. Achieving early detection early diagnosis and early treatment can provide effective genetic consultation and prenatal diagnosis for patients' families.

DATA AVAILABILITY STATEMENT

The raw data supporting the conclusions of this article will be made available by the authors, without undue reservation.

ETHICS STATEMENT

The studies involving human participants were reviewed and approved by Ethics Committee of Beijing Obstetrics and Gynecology Hospital affiliated to Capital Medical University. Written informed consent to participate in this study was provided by the participants' legal guardian/next of kin. Written informed consent was obtained from the individual(s), and minor(s)' legal guardian/next of kin, for the publication of any potentially identifiable images or data included in this article.

AUTHOR CONTRIBUTIONS

LL and LM performed the sequencing analysis, and wrote the manuscript. MS, JJ, and YZ conducted data collection as well as data analysis. YT and NY helped with recruiting patients and YT helped to discuss the data. All authors performed critical reading and approved the final version of manuscript. YK conceived the study and supervised this research.

ACKNOWLEDGMENTS

The authors thank the participants described in this report for their consent and support to publish this manuscript.

SUPPLEMENTARY MATERIAL

The Supplementary Material for this article can be found online at: https://www.frontiersin.org/articles/10.3389/fped.2020.00443/full#supplementary-material

REFERENCES

1. Demirbas D, Coelho AI, Rubio-Gozalbo ME, Berry GT. Hereditary galactosemia. *Metabolism.* (2018) 83:188–96. doi: 10.1016/j.metabol.2018.01.025
2. Calderon FR, Phansalkar AR, Crockett DK, Miller M, Mao R. Mutation database for the galactose-1-phosphate uridyltransferase (GALT) gene. *Hum Mutat.* (2007) 28:939–43. doi: 10.1002/humu.20544
3. Holden HM, Rayment I, Thoden JB. Structure and function of enzymes of the leloir pathway for galactose metabolism. *J Biol Chem.* (2003) 278:43885–8. doi: 10.1074/jbc.R300025200
4. Garcia DF, Camelo JS Jr, Molfetta GA, Turcato M, Souza CFM, Porta G, et al. Clinical profile and molecular characterization of galactosemia in brazil: identification of seven novel mutations. *BMC Med Genet.* (2016) 17:39. doi: 10.1186/s12881-016-0300-8
5. Choi R, Jo KI, Ko D-H, Lee DH, Song J, Jin D-K, et al. Novel GALT variations and mutation spectrum in the Korean population with decreased galactose-1-phosphate uridyltransferase activity. *BMC Med Genet.* (2014) 15:94. doi: 10.1186/s12881-014-0094-5
6. Timson DJ. The molecular basis of galactosemia - past, present and future. *Gene.* (2016) 589:133–141. doi: 10.1016/j.gene.2015.06.077
7. De Lucca M, Barba C, Casique L. A novel splicing mutation in GALT gene causing Galactosemia in Ecuadorian family. *Clin Chim Acta.* (2017) 470:20–3. doi: 10.1016/j.cca.2017.04.021
8. Holton JB, Walter JH, Tyfield LA. *The Metabolic and Molecular Basis of Inherited Disease*. New York: McGraw-Hill (2001).
9. Welling L, Boelen A, Derks TG, Schielen PC, de Vries M, Williams M, et al. Nine years of newborn screening for classical galactosemia in the Netherlands: effectiveness of screening methods, and identification of patients with previously unreported phenotypes. *Mol Genet Metab.* (2017) 120:223–8. doi: 10.1016/j.ymgme.2016.12.012
10. Bosch AM. Classical galactosaemia revisited. *J Inherit Metab Dis.* (2006) 29:516–25. doi: 10.1007/s10545-006-0382-0
11. Holton JB. Galactosaemia: pathogenesis and treatment. *J Inherit Metab Dis.* (1996) 19:3–7. doi: 10.1007/BF01799341
12. Potter NL, Nievergelt Y, Shriberg LD. Motor and speech disorders in classic galactosemia. *JIMD Rep.* (2013) 11:31–41. doi: 10.1007/8904_2013_219
13. Viggiano E, Marabotti A, Burlina AP, Cazzorla C, D'Apice MR, Giordano L, et al. Clinical and molecular spectra in galactosemic patients from neonatal screening in northeastern Italy: Structural and functional characterization of new variations in the galactose-1-phosphate uridyltransferase (GALT) gene. *Gene.* (2015) 559:112–8. doi: 10.1016/j.gene.2015.01.013
14. Seyrantepe V, Ozguc M, Coskun T, Ozalp I, Reichardt JK. Identification of mutations in the galactose-1-phosphate uridyltransferase (GALT) gene in 16 Turkish patients with galactosemia, including a novel mutation of F294Y. *Hum Mutat.* (1999) 13:339. doi: 10.1002/(SICI)1098-1004(1999)13:4<339::AID-HUMU17>3.0.CO;2-V
15. Schulpis K, Papakonstantinou ED, Michelakakis H, Podskarbi T, Patsouras A, Shin Y. Screening for galactosemia in Greece. *Paediatr Perinat Epidemiol.* (1997) 11:436–440. doi: 10.1046/j.1365-3016.1997.d01-31.x
16. Tang M, Facchiano A, Rachamadugu R, Calderon F, Mao R, Milanesi L, et al. Correlation assessment among clinical phenotypes, expression analysis and molecular modeling of 14 novel variations in the human galactose-1-phosphate uridylyltransferase gene. *Hum Mutat.* (2012) 33:1107–15. doi: 10.1002/humu.22093
17. Greber-Platzer S, Guldberg P, Scheibenreiter S, Item C, Schuller E, Patel N, et al. Molecular heterogeneity of classical and duarte galactosemia: mutation analysis by denaturing gradient gel electrophoresis. *Hum Mutat.* (1997) 10:49–57. doi: 10.1002/(SICI)1098-1004(1997)10:1<49::AID-HUMU7>3.0.CO;2-H
18. Li L, Zhao J-Q, Wang C, Yang N, Gong L-F, Yang H-H, et al. Whole-exome sequencing as a powerful tool for identifying genetic causes in a patient with POLG-related disorders and phenylketonuria. *J Int Med Res.* (2019) 47:1387–94. doi: 10.1177/0300060518823096
19. Tong W, Wang Y, Lu Y, Ye T, Song C, Xu Y, et al. Whole-exome sequencing helps the diagnosis and treatment in children with neurodevelopmental delay accompanied unexplained dyspnea. *Sci Rep.* (2018) 8:5214. doi: 10.1038/s41598-018-23503-2

Conflict of Interest: The authors declare that the research was conducted in the absence of any commercial or financial relationships that could be construed as a potential conflict of interest.

frontiers in Genetics

PERSPECTIVE
published: 14 October 2020
doi: 10.3389/fgene.2020.583932

The Value of Mouse Models of Rare Diseases: A Spanish Experience

Silvia Murillo-Cuesta[1,2,3], Rafael Artuch[1,4], Fernando Asensio[5], Pedro de la Villa[6], Mara Dierssen[1,7,8], Jose Antonio Enríquez[9,10], Cristina Fillat[1,11], Stéphane Fourcade[1,12], Borja Ibáñez[9,13,14], Lluis Montoliu[1,15], Eduardo Oliver[9,13], Aurora Pujol[1,12,16], Eduardo Salido[1,17], Mario Vallejo[2,18] and Isabel Varela-Nieto[1,2,3]* for/on behalf of the, Working Group on Animal Models of Rare Diseases, Biomedical Research and Networking Center for Rare Diseases (CIBERER), Institute of Health Carlos III*

[1] Biomedical Research Networking Center on Rare Diseases (CIBERER), Institute of Health Carlos III, Madrid, Spain, [2] Instituto de Investigaciones Biomédicas Alberto Sols (IIBM), Consejo Superior de Investigaciones Científicas/Universidad Autónoma de Madrid, Madrid, Spain, [3] Hospital La Paz Institute for Health Research (IdiPAZ), Madrid, Spain, [4] Institut de Recerca Sant Joan de Déu (IRSJD), Barcelona, Spain, [5] Gregorio Marañón Institute for Health Research (IISGM), Madrid, Spain, [6] Faculty of Medicine, University of Alcalá (UAH), Alcalá de Henares, Spain, [7] Centre for Genomic Regulation (CRG), Barcelona Institute of Science and Technology (BIST), Barcelona, Spain, [8] Universitat Pompeu Fabra (UPF), Barcelona, Spain, [9] Spanish National Center for Cardiovascular Research (CNIC), Institute of Health Carlos III, Madrid, Spain, [10] Biomedical Research Networking Center on Frailty and Healthy Ageing (CIBERFES), Institute of Health Carlos III, Madrid, Spain, [11] Institut d'Investigacions Biomèdiques August Pi i Sunyer (IDIBAPS), Barcelona, Spain, [12] Bellvitge Biomedical Research Institute (IDIBELL), L'Hospitalet de Llobregat, Barcelona, Spain, [13] Biomedical Research Networking Center on Cardiovascular Diseases (CIBERCV), Institute of Health Carlos III, Madrid, Spain, [14] Cardiology Department, Fundación Jiménez Díaz University Hospital Health Research Institute (IIS-FJD), Madrid, Spain, [15] National Center for Biotechnology (CNB), Spanish National Research Council, Madrid, Spain, [16] Catalan Institution of Research and Advanced Studies (ICREA), Barcelona, Spain, [17] Unidad de Investigación, Hospital Universitario de Canarias, Instituto de Tecnologías Biomédicas (ITB), La Laguna, Spain, [18] Biomedical Research Networking Center on Diabetes and Metabolic Diseases (CIBERDEM), Institute of Health Carlos III, Madrid, Spain

Animal models are invaluable for biomedical research, especially in the context of rare diseases, which have a very low prevalence and are often complex. Concretely mouse models provide key information on rare disease mechanisms and therapeutic strategies that cannot be obtained by using only alternative methods, and greatly contribute to accelerate the development of new therapeutic options for rare diseases. Despite this, the use of experimental animals remains controversial. The combination of respectful management, ethical laws and transparency regarding animal experimentation contributes to improve society's opinion about biomedical research and positively impacts on research quality, which eventually also benefits patients. Here we present examples of current advances in preclinical research in rare diseases using mouse models, together with our perspective on future directions and challenges.

Keywords: orphan diseases, animal models, preclinical research, novel therapies, ethics, transparency

OPEN ACCESS

Edited by:
E. Ann Yeh,
Hospital for Sick Children, Canada

Reviewed by:
Rameshwar Nath Koul Bamezai,
Jawaharlal Nehru University, India
Nicolina Cristina Sorrentino,
Telethon Institute of Genetics and Medicine (TIGEM), Italy

****Correspondence:***
Silvia Murillo-Cuesta
smurillo@iib.uam.es
Isabel Varela-Nieto
i.varela.nieto@csic.es

Specialty section:
This article was submitted to Genetics of Common and Rare Diseases, a section of the journal Frontiers in Genetics

Received: *15 July 2020*
Accepted: *14 September 2020*
Published: *14 October 2020*

Citation:
Murillo-Cuesta S, Artuch R, Asensio F, de la Villa P, Dierssen M, Enríquez JA, Fillat C, Fourcade S, Ibáñez B, Montoliu L, Oliver E, Pujol A, Salido E, Vallejo M and Varela-Nieto I (2020) The Value of Mouse Models of Rare Diseases: A Spanish Experience. Front. Genet. 11:583932. doi: 10.3389/fgene.2020.583932

INTRODUCTION

Animal research has contributed greatly to advance human health and quality of life. The use of laboratory animals increased exponentially in the 20th century and they are currently employed in almost every field of biomedical research. Animal models reproduce many aspects of human biological and pathological processes, and provide key information on the molecular pathophysiology of human diseases. Non-animal approaches based mainly on cell or tissue/organ

culture, and computational methods like data mining/generation, may help to predict clinical outcomes and reduce animal use (Cronin, 2016), but they cannot mimic the complexity of human biology. Animals remain the best model–however imperfect–to predict and characterize disease activity in patients (Garattini and Grignaschi, 2017).

Choosing a suitable animal model is a critical step in basic and preclinical research, and is usually based on a number of criteria, including species similarities to humans (the greater the phylogenetic closeness, the more similar is the genetic composition, anatomy, and physiology), genetic homogeneity, previous knowledge of the model, cost, availability, translatability of the results, ease of manipulation, and ethical implications, among others (National Research Council, 1998). Thus, the laboratory mouse is the most widely used mammalian animal in biomedical research, representing more than 60% of the total number of animals used in the EU (European Commission, 2019).

Genome manipulation and phenotype characterization is a common strategy for studying human pathology in animals, and particularly, in mice. In the last few years, CRISPR-Cas9-based genome editing has transformed the field and greatly expanded the repertoire of animal/cell systems available for disease modeling (Ahmad and Amiji, 2018). Gene homology between mouse and man is an essential prerequisite for pursuing this genotype-to-phenotype approach. Homogenization of the genetic background by inbreeding is also an important factor to reduce experimental variability. In this context, the International Mouse Phenotyping Consortium has generated, phenotyped and archived more than 6000 knockout mice on the C57BL/6 background, the most well-known and widely used inbred mouse strain (Cacheiro et al., 2019). Complete catalogs of genetically modified mouse models are available online at the International Phenotype Mouse Consortium and The Jackson Laboratory webpages (**Table 1**).

ANIMAL MODELS FOR RARE DISEASE RESEARCH

The definition of a rare disease (RD) in Europe is a disease with a prevalence of <1 in 2000, whereas *ultra*-RDs affect <1 in 50,000. RDs comprise more than 7000 different conditions (Orphadata, **Table 1**), usually severe, clinically complex and chronic, affecting 3.5–5.9% of the world's population (Nguengang Wakap et al., 2020), most of whom are children. The fact that each RD affects a relatively small number of patients has resulted in limited knowledge of RDs at the clinical level, which often delays an early and accurate diagnosis–patients can wait 8 years before receiving a diagnosis–and a potential therapy. Alarmingly, 95% of RDs have no approved or effective treatments, in part because RDs are underserved by pharmaceutical companies. Accordingly, RDs are considered a public health priority and specific research programs as the International Rare Diseases Research Consortium (IRDiRC) (**Table 1**) have been established to foster knowledge development (Gahl et al., 2016; European Commission, 2017).

Animal models are indispensable to identify the genetic bases and molecular mechanisms of RDs, as well as to understand their physiopathology, clinical heterogeneity and genotype-phenotype correlations. Indeed, RDs are excellent candidates for animal models, particularly in the context of genetically modified mice, as most RDs involve mutations in a single gene (Institute of Medicine, 2010). Due to the scarcity of available information on RD models, however, one of the major issues hindering translational research is the (incorrect) choice of model in preclinical studies. To address this and other issues some initiatives have been recently launched to generate and register RD mouse models. For instance, the Jackson Laboratory Rare and Orphan Disease Center (**Table 1**) has generated animal models for Friedreich's ataxia, Rett syndrome and spinal muscular atrophy. Likewise, the Infrafrontier platform provides access to 670 mouse strains that are related to nearly 1200 distinct RDs. Information about RD mouse models can also be obtained from the governmental agencies responsible for the evaluation of orphan medicinal product designation applications from pharmaceutical companies. In this context, Vaquer et al. (2013) compiled a list of 57 mammalian animal models for metabolic, neuromuscular, and ophthalmological orphan-designated conditions, based on information gathered by the European Medicines Agency (EMA). Additionally, some countries have developed specific national plans to prioritize RD research. For example, in Spain, the Biomedical Research Center Network for RDs (CIBERER) of the Carlos III Health Institute has contributed to the advancement of RD research by (i) developing new animal models, (ii) performing preclinical assays of novel therapeutics, and (iii) creating a mouse model phenotyping unit and a working group to register model information.

Here, we discuss some representative examples of RD mouse models under investigation at CIBERER (**Table 2**), which serve to illustrate the phenotypic variability of RDs and the possibilities offered by animal modeling to fill the knowledge gaps regarding in this area, and to contribute to the IRDiRC's goal of accelerating diagnosis and approving 1000 new therapies for RDs by 2027.

Metabolic RDs

They encompass a large and heterogeneous group of RDs caused by mutations affecting the function of enzymes, transporters, receptors, or hormones involved in metabolizing and transporting small (e.g., amino acids or neurotransmitters) or complex (i.e., glycogens or lipids) molecules, and defects in mitochondrial energy metabolism. One of the most extensively investigated is phenylketonuria, which severely affects the brain by interfering with dopamine and serotonin metabolism (Winn et al., 2018). $Pah^{enu2/enu2}$ and $Pah^{enu3/enu3}$ mice mimic human phenylketonuria pathophysiology and have aided in discovering mechanisms and therapies based on phenylalanine-restricted diets (Winn et al., 2018). Similarly, aromatic amino acid decarboxylase deficiency is a defect in dopamine and serotonin synthesis that also causes devastating central nervous system degeneration. $Ddc^{TM1.1Nwlh}$ mutant mice have been used to study the disease (Lee et al., 2013) and to evaluate adeno-associated viral gene therapy, which improved both survival and brain

TABLE 1 | Reference online resources on RDs, mouse models, legislation, and recommendations on animal experimentation.

Online resource	Description	URL
International Rare Diseases Research Consortium (IRDiRC)	International consortium of national and international governmental and non-profit funding bodies, companies, umbrella patient advocacy organizations, and scientific researchers to accelerate diagnosis and contribute to the development of new therapies for RDs	https://irdirc.org/
Orphanet	European website providing information about orphan drugs and rare diseases. It contains content both for physicians and for patients	https://www.orpha.net
Orphadata	Comprehensive, quality data sets related to RDs and orphan drugs from the Orphanet knowledge base, in reusable formats.	http://www.orphadata.org
Biomedical Research Center Network for RDs (CIBERER)	Spanish network cooperative structure of basic and clinical research groups with the purpose of (1) generating new scientific knowledge on the causes and mechanisms of RDs, and (2) developing new treatments and diagnostic procedures for these illnesses.	https://www.ciberer.es/en
Committee for Orphan Medicinal Products (COMP)	Committee of the European Medicines Agency (EMA) responsible for recommending orphan designation of medicines for rare diseases.	https://www.ema.europa.eu/en/committees/committee-orphan-medicinal-products-comp
The Jackson Laboratory	Independent, non-profit organization focusing on mammalian genetics research to advance human health	https://www.jax.org
Jackson Laboratory Rare and Orphan Disease Center	Jackson Lab center focused in the generation of mouse models for rare disease research.	https://www.jax.org/research-and-faculty/research-centers/rare-and-orphan-disease-center
International Phenotype Mouse Consortium	International consortium of research institutions to identify the function of every protein-coding gene in the mouse genome.	https://www.mousephenotype.org
International Mouse Phenotyping Resource of Standardized Screens (IMPReSS)	Standardized phenotyping protocols which are essential for the characterization of mouse phenotypes.	https://www.mousephenotype.org/impress/
European Commission	European legislation for the protection of animals used for scientific purpose 2010/63/EU directive	https://ec.europa.eu/environment/chemicals/lab_animals/legislation_en.htm http://data.europa.eu/eli/dir/2010/63/oj
Animal Research Reporting of *In Vivo* Experiments (ARRIVE) guidelines	Gold Standard publication Checklist reporting Guidelines	https://arriveguidelines.org/
European Quality in Preclinical Data (EQIPD) Consortium		https://quality-preclinical-data.eu/

TABLE 2 | Rare disease mouse models.

ORPHA number	Allelic symbol	Allele name	Genotype	MGI number	References
Adrenoleukodystrophies					
43	*Abcd2*^{tm1Apuj}	ATP-binding cassette, sub-family D (ALD), member 2; targeted mutation 1, Aurora Pujol	Homozygous	3617308	Pujol et al., 2002, 2004; Fourcade et al., 2008; Lopez-Erauskin et al., 2011, 2012; Schluter et al., 2012; Ruiz et al., 2015
	Abcd1^{tm1Kds}	ATP-binding cassette, sub-family D (ALD), member 1; targeted mutation 1, Kirby D Smith	Homozygous	2446588, 2680904	
Rare aminoacidurias and hyperoxalurias					
2195	*Slc7a8*^{tm1Gen}	Solute carrier family 7 (cationic amino acid transporter, y+ system), member 8; targeted mutation 1, Genoway	Homozygous	6323258, 6323255	Vilches et al., 2018
			Heterozygous	6323256	
1032	*Slc16a10*^{m1Ingm}	Solute carrier family 16 (monocarboxylic acid transporters), member 10; mutation 1, Ingenium Pharmaceuticals	Homozygous	5544309	
93598	*Agxt*^{tm1Ull}	Alanine-glyoxylate aminotransferase; targeted mutation 1, Eduardo C Salido	Homozygous	3717654, 5314652	Salido et al., 2006; Knight et al., 2012
93600	*Grhpr*$^{Gt(OST383093)Lex}$	Glyoxylate reductase/hydroxypyruvate reductase; gene trap OST383093, Lexicon Genetics.	Homozygous	5314653	Knight et al., 2012
Rare cardiomiopathies					
247	*AAV-PCSK9*^{DY} *ApoE*$^{-/-}$ *AAV-PCSK9*^{DY}	AAV-based vector for targeted transfer of the *PCSK9(DY)* gene			Cruz et al., 2015; Roche-Molina et al., 2015
Rare deafness					
90635	*Tecta*$^{tm3.1Gpr}$	Tectorin alpha; targeted mutation 3.1, Guy P Richardson	Homozygous	5527172	Legan et al., 2014
			Heterozygous	5527171	
90635	*Tecta*$^{tm4.1Gpr}$	Tectorin alpha; targeted mutation 4.1, Guy P Richardson	Homozygous	5527174	Legan et al., 2014
			Heterozygous	5527173	
90635	*Tecta*$^{tm5.1Gpr}$	Tectorin alpha; targeted mutation 5.1, Guy P Richardson	Homozygous	5527176	Legan et al., 2014
			Heterozygous	5527175	

(Continued)

TABLE 2 | Continued

ORPHA number	Allelic symbol	Allele name	Genotype	MGI number	References
90636	*Gjb2*^{tm1Ugds} *Tg(Otog-cre)1Ugds* *Gjb2*^{tm1Ugds} *Tg(Sox10-cre)1Wdr*	Gap junction protein, beta 2; targeted mutation 1, Unite de Genetique des Deficits Sensoriels	Homozygous conditional Homozygous conditional	3588875 5571190	Cohen-Salmon et al., 2002 Takada et al., 2014
9063	*Mpzl2*$^{tm1.1Jczp}$	Myelin protein zero-like 2; targeted mutation 1.1, Juan Carlos Zuniga-Pflucker	Homozygous	6358214	Wesdorp et al., 2018
73272	*Igf1*^{tm1Arge}	Insulin-like growth factor 1; targeted mutation 1, Argiris Efstratiadis	Homozygous	3688508	Liu et al., 1993; Camarero et al., 2001, 2002; Cediel et al., 2006; Fuentes-Santamaria et al., 2016, 2019
Albinism					
79431	*Tg(Tyr-Th,-Gch1)6775 Lmon*	Transgene insertion 6775, Lluis Montoliu		4443311 (EM: 02610)	Lavado et al., 2006; Murillo-Cuesta et al., 2010
79431	*Tg(Tyr)1999 Lmon*	Transgene insertion 1999, Lluis Montoliu		5787939 (EM: 03096)	Lavado et al., 2006; Murillo-Cuesta et al., 2010

Representative examples of mouse models developed or studied in the CIBER consortium to increase knowledge, provide diagnosis, and explore advanced therapies in RDs, identified by their ORPHA number. Rare Disease Database at Orphanet website (https://www.orphanet.com) and Mouse Genome Database (MGD) at the Mouse Genome Informatics (MGI) website, The Jackson Laboratory, Bar Harbor, Maine (http://www.informatics.jax.org) (June 2020).

levels of dopamine and serotonin (Lee et al., 2016). A clinical trial using this approach is ongoing with encouraging results (Chien et al., 2017).

X-linked adrenoleukodystrophy (X-ALD) is another severe neurometabolic disease characterized by progressive central demyelination, adrenal insufficiency and accumulation of saturated very long-chain fatty acids, and caused by loss of function of the ABCD1 peroxisomal transporter (Ferrer et al., 2010). To date, no pharmacological treatment has been proven to be beneficial and current therapeutic options are unsatisfactory and restricted to bone marrow transplants and hematopoietic stem cell gene therapy, but most patients remain untreated. Mouse models uncovered the factors that account for genotype-phenotype correlation in human disease variants. The *Abcd1*$^{-}$ mutant mouse exhibits late-onset axonal degeneration of the spinal cord corticospinal tracts and microglial and astroglial activation, compatible with chronic low-level stimulation of the innate immune response, and constitutes a good model for ALD (Pujol et al., 2002; Ruiz et al., 2015). The *Abcd2* gene product shares physiological and biochemical functions with that of *Abcd1* (Pujol et al., 2004), and the *Abcd1*$^{-}$*/Abcd2*$^{-/-}$ double mutant presents with an earlier and more severe axonal degenerative phenotype, constituting a more useful model for preclinical evaluation (Pujol et al., 2004). These mouse models revealed that X-ALD shares pathogenic processes with other neurodegenerative disorders (Galea et al., 2012), including redox dyshomeostasis, mitochondrial dysfunction, and proteostasis malfunction (Fourcade et al., 2015). Encouraging preclinical results with neurotrophic factors and antioxidants (Pujol, 2016) have paved the way for the launch of three phase II/III clinical trials for ALD (Casasnovas et al., 2019), and the approval of two orphan drug designations.

Defects in glyoxylate and hydroxyproline hepatic metabolism result in the hepatic overproduction of oxalate and primary hyperoxaluria (PH) – an *ultra*-RD with a prevalence of 1–3 in 10^6 individuals (Cochat and Rumsby, 2013). PH1, the most common and severe form, is caused by *AGXT* mutations (Milliner et al., 1993), whereas PH2 and PH3 are caused by mutations in *GRHPR* and *HOGA1*, respectively. Loss of function mutations in any of these genes results in impaired detoxification of glyoxylate, which is converted into oxalate. PH patients present elevated oxalate concentrations in plasma and urine, oxalate deposition in multiple organs, recurrent kidney stone episodes and chronic renal failure, which results in end-stage renal disease. Current therapies include large daily fluid intake and medications to reduce oxalate production (Cochat et al., 2012), but they do not eliminate recurring stones and renal disease. Combined liver and kidney transplantation is the only curative treatment available, but is associated with significant morbi-mortality and problems related to donor organ shortage and life-long immunosuppressive treatment.

The *Agxt*^{TM1Ull} mouse reproduces the main PH1 features (Salido et al., 2006) and has been used to evaluate promising experimental therapies (Martin-Higueras et al., 2017). Regulation of oxalate transepithelial flux in the gut following intestinal colonization with *Oxalobacter* (Hatch et al., 2011) has received an innovative new drug designation by the United States Food

and Drug Administration and is in clinical trials. Similarly, gene therapy with adeno-associated vectors carrying human *AGXT* under the control of a liver-specific promoter achieved a long-term metabolic correction (Salido et al., 2011), and was granted an EMA orphan drug designation. Deletion of the glycolate oxidase gene, inhibition of its enzymatic product or suppressing its expression with short-interfering RNA (siRNA) resulted in a substantial reversal of the hyperoxaluric phenotype (Martin-Higueras et al., 2016), the latter is currently being evaluated in a clinical trial with encouraging preliminary results. Therapies based on *in vivo* CRISPR-Cas9 technology are also a potential strategy for curing PH1 by substrate reduction with the administration of AAV-mediated glycolate oxidase-targeted guide RNAs (Zabaleta et al., 2018). We have generated a *Grhpr* knockout mouse for PH2 (Knight et al., 2012), and both *Agxt* and *Grhpr* mutant mice have been used to test the potential of inhibiting hepatic lactate dehydrogenase with siRNA to treat PH (Lai et al., 2018), which has moved to a clinical trial. In contrast to the models for PH1 and PH2, the mouse model for PH3 generated by the International Knockout Mouse Consortium (*Hoga1*$^{TM2a(KOMP)Wtsi}$, MGI:4419886) does not have the expected phenotype and it is currently being used to investigate differences in mouse and human glyoxylate metabolism. This example highlights a key point, which is that the understanding of the differences in the metabolic interactome between species is fundamental for the efficient transfer of the knowledge from experimental models to clinical practice.

Rare aminoacidurias caused by defects in amino acid transporters are being studied with murine models, which emerge as a promising tool to design evidence-based therapies to halt the progression of the disease. Using the *Slc16a10*$^{-/-}$ *Slc7a8*$^{-/-}$ mouse and a targeted metabolomics approach, it was confirmed that both transporters functionally cooperate *in vivo*. This approach also uncovered compensation mechanisms that explain the lack of human basolateral neutral aminoacidurias (Vilches et al., 2018). Similarly, the *Slc7a7*$^{-/-}$ model of lysinuric protein intolerance resembles the human phenotype, including malabsorption and impaired reabsorption of cationic amino acids, hypoargininemia, and hyperammonemia, and importantly, responses to citrulline treatment, which improved the metabolic derangement and survival (Bodoy et al., 2019).

Rare Cardiac Diseases

Arrhythmogenic right ventricular cardiomyopathy is a severe disease characterized by ventricular fibrofatty replacement of cardiomyocytes, contractile defects, and high risk for developing malignant arrhythmias, which can ultimately lead to sudden cardiac death especially in young athletes (Gandjbakhch et al., 2018). More than 50% of the 380 mutations identified lie within *PKP2*, which encodes the desmosomal protein plakoglobin-2, a major component of cell-to-cell junctions (van Tintelen et al., 2006). Given the complexity of developing multiple transgenic animals, a novel approach was developed by delivering genes encoding mutated proteins into wild-type mice using adeno-associated viruses (Roche-Molina et al., 2015). Using this strategy, C57BL6/J mice stably expressed the R735X version of *PKP2*, a dominant-negative mutant, driven by a cardiac-specific promoter, resulting in development of an arrhythmogenic right ventricular cardiomyopathy phenotype following exercise (Cruz et al., 2015). Although no evidence of myocardial fibrosis or fibrofatty cardiomyocyte replacement was observed, a miss localization of the gap-junction protein connexion-43 was evident. This model provides a versatile and accessible tool for investigating this devastating disease.

Albinism

Murine models have been central to understand this rare genetic condition primarily associated with severe visual deficits and variable hypopigmentation, and caused by mutations in at least twenty genes (Montoliu and Marks, 2017). Vision and hearing deficits have been characterized in the *Tyr* mutant mouse, a model for human oculocutaneous albinism 1 (Lavado et al., 2006; Murillo-Cuesta et al., 2010). Additional mouse models have been generated using CRISPR-Cas9 tools, including those addressing the role of non-coding DNA of regulatory elements in *Tyr* gene expression (Seruggia et al., 2015).

Sensorineural Hearing Loss

Approximately half of all cases of both non-syndromic and syndromic human hearing loss (HL) are due to rare mutations. TECTA-based human deafness is an example of autosomal dominant non-syndromic HL, in which domain-specific alterations in the glycoprotein Tecta, leading to changes in the tectorial membrane of the cochlea, have been studied using *Tecta* mutant mice (Legan et al., 2014). Autosomal recessive non-syndromic HL, which in the majority of cases is caused by mutations in *GJB2* and *GJB6*, encoding the gap junction proteins connexin 26 and 30, respectively, has been studied using conditional mutant mice. Thus, *Gjb2*^{TM1Ugds} mouse shows a decrease in *Cx26* expression, extensive loss of cochlear epithelial cells and an increase in hearing thresholds (Cohen-Salmon et al., 2002; Crispino et al., 2017).

Syndromic HL is a common condition in many RDs including insulin-like growth factor I (IGF-1) deficiency, an *ultra*-RD caused by homozygous mutations in *IGF1* and associated with growth retardation, intellectual deficit, and HL (Varela-Nieto et al., 2013). The use of experimental models is practically the only way to investigate the pathology of *ultra*-RDs. In this respect, the *Igf1*$^{TM1Arge/tm1Arge}$ mouse (Liu et al., 1993) recapitulates the human phenotype, and presents with severe deafness, neural loss (Cediel et al., 2006) and alterations in the auditory central pathway (Fuentes-Santamaria et al., 2016; Fuentes-Santamaria et al., 2019), offering a unique window into the role of the IGF-1 in human hearing.

DISCUSSION

Animal experimentation is essential for understanding the pathogenic mechanisms of RDs and developing new, safe and effective treatments (Garattini and Grignaschi, 2017). This is especially true for RDs whose low prevalence is associated with

a lack of knowledge, delays in diagnosis, and absence of effective treatments in most cases (European Commission, 2017). Non-animal experimental approaches provide valuable information, but they are far from reproducing the complexities and interactions in a living organism (Cronin, 2016). Rather than an alternative, non-animal methods are a useful complementary approach that helps to reduce the number of specimens used in biomedical research (European Commission, 2018).

The mouse is currently the most commonly used species due to its genetic tractability, relative ease of genome editing and cost-efficient management (European Commission, 2019). During the last 20 years, public and private initiatives have made a strong effort to generate and phenotype many hundreds of genetically modified strains (Cacheiro et al., 2019). However, it has been only recently that special attention has been paid to RDs (Institute of Medicine, 2010; Gahl et al., 2016). Information on RD mouse models is limited and scattered across different databases, which could hamper the preclinical testing of new therapeutic approaches. It would be useful to gather all the data from already existing mutant mouse databases with those from the orphan drug evaluation committees in international agencies (Vaquer et al., 2013) and from national initiatives for RDs research. As an example, the Spanish CIBERER consortium has generated mouse models for some RDs that have been shown to be effective for preclinical testing of new drugs (**Table 2**).

The usefulness of mouse models to advance RD research should not make us forget the importance of the ethical aspects and transparency in animal research. The use of animals in biomedical research remains a contentious issue in society (Matthews, 2008). Citizens demand treatments that require preclinical safety and efficacy testing, but they are increasingly concerned by animal welfare and demand the elimination of pain, and ultimately, of animal experimentation. Authorities and the scientific community are devoted to protect public health and the environment, and require the testing of new medicines, chemicals, and food products in animal models. But they are also fully committed to animal welfare and to the progressive reduction of animal testing (European Commission, 2018), as stated in the current legislation. There is a large body of laws and regulations regarding the use of animals for scientific research and educational purposes. The 2010/63/EU directive (**Table 1**) states that: (i) animal experimentation can be carried out only after a number of independent evaluations, and authorization from the competent authority; (ii) researchers must reasonably justify the use of experimental animals over alternative methods; (iii) experiments involving animals can only be conducted by competent and experienced professionals in authorized facilities; (iv) the 3Rs principle (reduction, refinement, and replacement) has always to be considered (Mocho, 2020). However, it is critical to improve communication with the general public to convey the fact that animal experimentation is necessary not only to protect human health, but also to protect animals and the environment.

Society also demands transparency regarding animal experimentation. Modern science is now so complex that citizens are often unaware of the gaps in knowledge still existing and wrongly assume that the use of animals is no longer necessary. It is essential that researchers take a stand and clearly explain their position with regard to the use of animals (Van Zutphen, 2002). To fill these gaps, some initiatives have arisen from scientific organizations addressing the requirement for transparency (Montoliu, 2018). The scientific community hopes that society will soon better understand the benefits of the use of animals in research and will provide greater support for animal experimentation, resolving the current controversies. In addition, initiatives like the Animal Research Reporting of *In Vivo* Experiments (ARRIVE) guidelines and the European Quality in Preclinical Data (EQIPD) have arose to solve challenges with regard to the robustness, rigor, and validity of research data, which often impact the transition from preclinical to clinical testing.

Ethics and transparency in this context will undoubtedly enhance the quality of biomedical research and societal engagement (Van Zutphen, 2002; Montoliu, 2018).

AUTHOR CONTRIBUTIONS

SM-C, IV-N, RA, LM, SF, AP, BI, EO, and ES wrote the manuscript. All the co-authors revised and approved the manuscript.

FUNDING

This work was supported by a grant from the Center for Biomedical Research on Rare Diseases (CIBERER) (ER18GDT761) to SM-C. Additional support came from: Multi Target and View FEDER/CM-B2017/BMD-3688 and MINECO/FEDER SAF2017-86107-R grants to SM-C and IV-N; CERCA Program/Generalitat de Catalunya, Autonomous Government of Catalonia (2017SGR1206), and CIBERER (ACCI18-27) to AP; Miguel Servet program CPII16/00016 (Instituto de Salud Carlos III co-funded by European Social Fund ESF) to SF; CNIC (ISCIII, Ministerio de Ciencia, Innovación y Universidades), Pro CNIC Foundation, Severo Ochoa Center of Excellence (SEV-2015-0505) to BI and EO; Generalitat de Catalunya (Grups consolidats 2017 SGR 926) to MD. EO was beneficiary of a grant from "Programa de Atracción de Talento" of Comunidad de Madrid (2017-T1/BMD-5185). SM-C holds a ISCiii CIBER postdoctoral researcher contract. The work at CRG was supported by grants from the Spanish Ministry of Science and Innovation to the EMBL partnership, the Centro de Excelencia Severo Ochoa and the CERCA Programme/Generalitat de Catalunya.

ACKNOWLEDGMENTS

We appreciate the helpful discussion and support by our research groups and CIBER colleagues. We acknowledge support of the publication fee by the CSIC Open Access Publication Support Initiative through its Unit of Information Resources for Research (URICI).

REFERENCES

Ahmad, G., and Amiji, M. (2018). Use of CRISPR/Cas9 gene-editing tools for developing models in drug discovery. *Drug Discov. Today* 23, 519–533. doi: 10.1016/j.drudis.2018.01.014

Bodoy, S., Sotillo, F., Espino-Guarch, M., Sperandeo, M. P., Ormazabal, A., Zorzano, A., et al. (2019). Inducible Slc7a7 knockout mouse model recapitulates lysinuric protein intolerance disease. *Int. J. Mol. Sci.* 20:5294. doi: 10.3390/ijms20215294

Cacheiro, P., Haendel, M. A., Smedley, D., International Mouse Phenotyping Consortium, and The Monarch Initiative (2019). New models for human disease from the International mouse phenotyping consortium. *Mamm. Genome* 30, 143–150. doi: 10.1007/s00335-019-09804-5

Camarero, G., Avendano, C., Fernandez-Moreno, C., Villar, A., Contreras, J., De Pablo, F., et al. (2001). Delayed inner ear maturation and neuronal loss in postnatal Igf-1-deficient mice. *J. Neurosci.* 21, 7630–7641. doi: 10.1523/jneurosci.21-19-07630.2001

Camarero, G., Villar, M. A., Contreras, J., Fernandez-Moreno, C., Pichel, J. G., Avendano, C., et al. (2002). Cochlear abnormalities in insulin-like growth factor-1 mouse mutants. *Hear. Res.* 170, 2–11. doi: 10.1016/s0378-5955(02)00447-1

Casasnovas, C., Ruiz, M., Schluter, A., Naudi, A., Fourcade, S., Veciana, M., et al. (2019). Biomarker identification, safety, and efficacy of high-dose antioxidants for adrenomyeloneuropathy: a phase II pilot study. *Neurotherapeutics* 16, 1167–1182. doi: 10.1007/s13311-019-00735-2

Cediel, R., Riquelme, R., Contreras, J., Diaz, A., and Varela-Nieto, I. (2006). Sensorineural hearing loss in insulin-like growth factor I-null mice: a new model of human deafness. *Eur. J. Neurosci.* 23, 587–590. doi: 10.1111/j.1460-9568.2005.04584.x

Chien, Y. H., Lee, N. C., Tseng, S. H., Tai, C. H., Muramatsu, S. I., Byrne, B. J., et al. (2017). Efficacy and safety of AAV2 gene therapy in children with aromatic L-amino acid decarboxylase deficiency: an open-label, phase 1/2 trial. *Lancet Child Adolesc. Health* 1, 265–273. doi: 10.1016/s2352-4642(17)30125-6

Cochat, P., Hulton, S. A., Acquaviva, C., Danpure, C. J., Daudon, M., and De Marchi, M. (2012). Primary hyperoxaluria Type 1: indications for screening and guidance for diagnosis and treatment. *Nephrol. Dial. Transplant.* 27, 1729–1736. doi: 10.1093/ndt/gfs078

Cochat, P., and Rumsby, G. (2013). Primary hyperoxaluria. *N. Engl. J. Med.* 369, 649–658.

Cohen-Salmon, M., Ott, T., Michel, V., Hardelin, J. P., Perfettini, I., Eybalin, M., et al. (2002). Targeted ablation of connexin26 in the inner ear epithelial gap junction network causes hearing impairment and cell death. *Curr. Biol.* 12, 1106–1111. doi: 10.1016/s0960-9822(02)00904-1

Crispino, G., Galindo Ramirez, F., Campioni, M., Zorzi, V., Praetorius, M., Di Pasquale, G., et al. (2017). In vivo genetic manipulation of inner ear connexin expression by bovine adeno-associated viral vectors. *Sci. Rep.* 7:6567.

Cronin, M. (2016). *Non-Animal Approaches: The Way Forward*. Brussels: European Commission.

Cruz, F. M., Sanz-Rosa, D., Roche-Molina, M., Garcia-Prieto, J., Garcia-Ruiz, J. M., Pizarro, G., et al. (2015). Exercise triggers ARVC phenotype in mice expressing a disease-causing mutated version of human plakophilin-2. *J. Am. Coll. Cardiol.* 65, 1438–1450. doi: 10.1016/j.jacc.2015.01.045

European Commission (2017). *Rare Diseases: A Major Unmet Medical Need*. Brussels: European Commission.

European Commission (2018). *Commission replies to "Stop Vivisection" European Citizens' Initiative*. Brussels: European Commission.

European Commission (2019). *2019 Report on The Statistics on the Use of Animals for Scientific Purposes in the Member States of the European Union in 2015-2017, Report From The Commission To The European Parliament And The Council*. Brussels: European Commission.

Ferrer, I., Aubourg, P., and Pujol, A. (2010). General aspects and neuropathology of X-linked adrenoleukodystrophy. *Brain Pathol.* 20, 817–830. doi: 10.1111/j.1750-3639.2010.00390.x

Fourcade, S., Ferrer, I., and Pujol, A. (2015). Oxidative stress, mitochondrial and proteostasis malfunction in adrenoleukodystrophy: a paradigm for axonal degeneration. *Free Radic. Biol. Med.* 88, 18–29. doi: 10.1016/j.freeradbiomed.2015.05.041

Fourcade, S., Lopez-Erauskin, J., Galino, J., Duval, C., Naudi, A., Jove, M., et al. (2008). Early oxidative damage underlying neurodegeneration in X-adrenoleukodystrophy. *Hum. Mol. Genet.* 17, 1762–1773. doi: 10.1093/hmg/ddn085

Fuentes-Santamaria, V., Alvarado, J. C., Rodriguez-De La Rosa, L., Juiz, J. M., and Varela-Nieto, I. (2019). Neuroglial Involvement in Abnormal Glutamate Transport in the Cochlear Nuclei of the Igf1 (-/-) Mouse. *Front. Cell. Neurosci.* 13:67. doi: 10.3389/fncel.2019.00067

Fuentes-Santamaria, V., Alvarado, J. C., Rodriguez-De La Rosa, L., Murillo-Cuesta, S., Contreras, J., Juiz, J. M., et al. (2016). IGF-1 deficiency causes atrophic changes associated with upregulation of VGluT1 and downregulation of MEF2 transcription factors in the mouse cochlear nuclei. *Brain Struct. Funct.* 221, 709–734. doi: 10.1007/s00429-014-0934-2

Gahl, W. A., Mulvihill, J. J., Toro, C., Markello, T. C., Wise, A. L., and Ramoni, R. B. (2016). The NIH undiagnosed diseases program and network: applications to modern medicine. *Mol. Genet. Metab.* 117, 393–400. doi: 10.1016/j.ymgme.2016.01.007

Galea, E., Launay, N., Portero-Otin, M., Ruiz, M., Pamplona, R., Aubourg, P., et al. (2012). Oxidative stress underlying axonal degeneration in adrenoleukodystrophy: a paradigm for multifactorial neurodegenerative diseases? *Biochim. Biophys. Acta* 1822, 1475–1488. doi: 10.1016/j.bbadis.2012.02.005

Gandjbakhch, E., Redheuil, A., Pousset, F., Charron, P., and Frank, R. (2018). Clinical diagnosis, imaging, and genetics of arrhythmogenic right ventricular cardiomyopathy/dysplasia: JACC state-of-the-art review. *J. Am. Coll. Cardiol.* 72, 784–804.

Garattini, S., and Grignaschi, G. (2017). Animal testing is still the best way to find new treatments for patients. *Eur. J. Intern. Med.* 39, 32–35. doi: 10.1016/j.ejim.2016.11.013

Hatch, M., Gjymishka, A., Salido, E. C., Allison, M. J., and Freel, R. W. (2011). Enteric oxalate elimination is induced and oxalate is normalized in a mouse model of primary hyperoxaluria following intestinal colonization with Oxalobacter. *Am. J. Physiol. Gastrointest. Liver Physiol.* 300, G461–G469.

Knight, J., Holmes, R. P., Cramer, S. D., Takayama, T., and Salido, E. (2012). Hydroxyproline metabolism in mouse models of primary hyperoxaluria. *Am. J. Physiol. Renal Physiol.* 302, F688–F693.

Lai, C., Pursell, N., Gierut, J., Saxena, U., Zhou, W., Dills, M., et al. (2018). Specific inhibition of hepatic lactate dehydrogenase reduces oxalate production in mouse models of primary hyperoxaluria. *Mol. Ther.* 26, 1983–1995. doi: 10.1016/j.ymthe.2018.05.016

Lavado, A., Jeffery, G., Tovar, V., De La Villa, P., and Montoliu, L. (2006). Ectopic expression of tyrosine hydroxylase in the pigmented epithelium rescues the retinal abnormalities and visual function common in albinos in the absence of melanin. *J. Neurochem.* 96, 1201–1211. doi: 10.1111/j.1471-4159.2006.03657.x

Lee, N. C., Lee, Y. M., Chen, P. W., Byrne, B. J., and Hwu, W. L. (2016). Mutation-adapted U1 snRNA corrects a splicing error of the dopa decarboxylase gene. *Hum. Mol. Genet.* 25, 5142–5147.

Lee, N. C., Shieh, Y. D., Chien, Y. H., Tzen, K. Y., Yu, I. S., Chen, P. W., et al. (2013). Regulation of the dopaminergic system in a murine model of aromatic L-amino acid decarboxylase deficiency. *Neurobiol. Dis.* 52, 177–190. doi: 10.1016/j.nbd.2012.12.005

Legan, P. K., Goodyear, R. J., Morin, M., Mencia, A., Pollard, H., Olavarrieta, L., et al. (2014). Three deaf mice: mouse models for TECTA-based human hereditary deafness reveal domain-specific structural phenotypes in the tectorial membrane. *Hum. Mol. Genet.* 23, 2551–2568. doi: 10.1093/hmg/ddt646

Liu, J. P., Baker, J., Perkins, A. S., Robertson, E. J., and Efstratiadis, A. (1993). Mice carrying null mutations of the genes encoding insulin-like growth factor I (Igf-1) and type 1 IGF receptor (Igf1r). *Cell* 75, 59–72. doi: 10.1016/s0092-8674(05)80084-4

Lopez-Erauskin, J., Fourcade, S., Galino, J., Ruiz, M., Schluter, A., Naudi, A., et al. (2011). Antioxidants halt axonal degeneration in a mouse model of X-adrenoleukodystrophy. *Ann. Neurol.* 70, 84–92. doi: 10.1002/ana.22363

Lopez-Erauskin, J., Galino, J., Bianchi, P., Fourcade, S., Andreu, A. L., Ferrer, I., et al. (2012). Oxidative stress modulates mitochondrial failure and cyclophilin D function in X-linked adrenoleukodystrophy. *Brain* 135, 3584–3598. doi: 10.1093/brain/aws292

Martin-Higueras, C., Luis-Lima, S., and Salido, E. (2016). Glycolate oxidase is a safe and efficient target for substrate reduction therapy in a mouse model of primary hyperoxaluria type I. *Mol. Ther.* 24, 719–725. doi: 10.1038/mt.2015.224

Martin-Higueras, C., Torres, A., and Salido, E. (2017). Molecular therapy of primary hyperoxaluria. *J. Inherit. Metab. Dis.* 40, 481–489.

Matthews, R. A. (2008). Medical progress depends on animal models - doesn't it? *J. R. Soc. Med.* 101, 95–98. doi: 10.1258/jrsm.2007.070164

Milliner, D. S., Harris, P. C., Cogal, A. G., and Lieske, J. C. (1993). "Primary hyperoxaluria type 1," in *GeneReviews((R))*, eds M. P. Adam, H. H. Ardinger, R. A. Pagon, S. E. Wallace, L. J. H. Bean, K. Stephens, et al. (Seattle, WA: NIH).

Mocho, J. P. (2020). 3Rs - reduce reuse recycle. *Lab. Anim.* 54:194. doi: 10.1177/0023677220909272

Montoliu, L. (2018). *Transparency in Animal Experimentation [Online]*. Available online at: https://network.febs.org/users/104011-lluis-montoliu/posts/32348-transparency-in-animal-experimentation (accessed May 7, 2018).

Montoliu, L., and Marks, M. S. (2017). A new type of syndromic albinism associated with mutations in AP3D1. *Pigment Cell. Melanoma Res.* 30, 5–7. doi: 10.1111/pcmr.12543

Murillo-Cuesta, S., Contreras, J., Zurita, E., Cediel, R., Cantero, M., Varela-Nieto, I., et al. (2010). Melanin precursors prevent premature age-related and noise-induced hearing loss in albino mice. *Pigment Cell. Melanoma Res.* 23, 72–83. doi: 10.1111/j.1755-148x.2009.00646.x

Institute of Medicine (2010). *Rare Diseases and Orphan Products: Accelerating Research and Development*. Washington, DC: The National Academies Press. doi: 10.17226/12953

National Research Council (1998). *Biomedical Models and Resources: Current Needs and Future Opportunities*. Washington, DC: National Research Council.

Nguengang Wakap, S., Lambert, D. M., Olry, A., Rodwell, C., Gueydan, C., Lanneau, V., et al. (2020). Estimating cumulative point prevalence of rare diseases: analysis of the Orphanet database. *Eur. J. Hum. Genet.* 28, 165–173. doi: 10.1038/s41431-019-0508-0

Pujol, A. (2016). Novel therapeutic targets and drug candidates for modifying disease progression in adrenoleukodystrophy. *Endocr. Dev.* 30, 147–160. doi: 10.1159/000439340

Pujol, A., Ferrer, I., Camps, C., Metzger, E., Hindelang, C., Callizot, N., et al. (2004). Functional overlap between ABCD1 (ALD) and ABCD2 (ALDR) transporters: a therapeutic target for X-adrenoleukodystrophy. *Hum. Mol. Genet.* 13, 2997–3006. doi: 10.1093/hmg/ddh323

Pujol, A., Hindelang, C., Callizot, N., Bartsch, U., Schachner, M., and Mandel, J. L. (2002). Late onset neurological phenotype of the X-ALD gene inactivation in mice: a mouse model for adrenomyeloneuropathy. *Hum. Mol. Genet.* 11, 499–505. doi: 10.1093/hmg/11.5.499

Roche-Molina, M., Sanz-Rosa, D., Cruz, F. M., Garcia-Prieto, J., Lopez, S., Abia, R., et al. (2015). Induction of sustained hypercholesterolemia by single adeno-associated virus-mediated gene transfer of mutant hPCSK9. *Arterioscler. Thromb. Vasc. Biol.* 35, 50–59. doi: 10.1161/atvbaha.114.303617

Ruiz, M., Jove, M., Schluter, A., Casasnovas, C., Villarroya, F., Guilera, C., et al. (2015). Altered glycolipid and glycerophospholipid signaling drive inflammatory cascades in adrenomyeloneuropathy. *Hum. Mol. Genet.* 24, 6861–6876.

Salido, E., Rodriguez-Pena, M., Santana, A., Beattie, S. G., Petry, H., and Torres, A. (2011). Phenotypic correction of a mouse model for primary hyperoxaluria with adeno-associated virus gene transfer. *Mol. Ther.* 19, 870–875. doi: 10.1038/mt.2010.270

Salido, E. C., Li, X. M., Lu, Y., Wang, X., Santana, A., Roy-Chowdhury, N., et al. (2006). Alanine-glyoxylate aminotransferase-deficient mice, a model for primary hyperoxaluria that responds to adenoviral gene transfer. *Proc. Natl. Acad. Sci. U.S.A.* 103, 18249–18254. doi: 10.1073/pnas.0607218103

Schluter, A., Espinosa, L., Fourcade, S., Galino, J., Lopez, E., Ilieva, E., et al. (2012). Functional genomic analysis unravels a metabolic-inflammatory interplay in adrenoleukodystrophy. *Hum. Mol. Genet.* 21, 1062–1077. doi: 10.1093/hmg/ddr536

Seruggia, D., Fernandez, A., Cantero, M., Pelczar, P., and Montoliu, L. (2015). Functional validation of mouse tyrosinase non-coding regulatory DNA elements by CRISPR-Cas9-mediated mutagenesis. *Nucleic Acids Res.* 43, 4855–4867. doi: 10.1093/nar/gkv375

Takada, Y., Beyer, L. A., Swiderski, D. L., O'neal, A. L., Prieskorn, D. M., Shivatzki, S., et al. (2014). Connexin 26 null mice exhibit spiral ganglion degeneration that can be blocked by BDNF gene therapy. *Hear. Res.* 309, 124–135. doi: 10.1016/j.heares.2013.11.009

van Tintelen, J. P., Entius, M. M., Bhuiyan, Z. A., Jongbloed, R., Wiesfeld, A. C., Wilde, A. A., et al. (2006). Plakophilin-2 mutations are the major determinant of familial arrhythmogenic right ventricular dysplasia/cardiomyopathy. *Circulation* 113, 1650–1658. doi: 10.1161/circulationaha.105.609719

Van Zutphen, L. F. (2002). Use of animals in research: a science - society controversy? The European perspective. *Altex* 19, 140–144.

Vaquer, G., Riviere, F., Mavris, M., Bignami, F., Llinares-Garcia, J., Westermark, K., et al. (2013). Animal models for metabolic, neuromuscular and ophthalmological rare diseases. *Nat. Rev. Drug Discov.* 12, 287–305. doi: 10.1038/nrd3831

Varela-Nieto, I., Murillo-Cuesta, S., Rodriguez-De La Rosa, L., Lassatetta, L., and Contreras, J. (2013). IGF-I deficiency and hearing loss: molecular clues and clinical implications. *Pediatr. Endocrinol. Rev.* 10, 460–472.

Vilches, C., Boiadjieva-Knopfel, E., Bodoy, S., Camargo, S., Lopez De Heredia, M., Prat, E., et al. (2018). Cooperation of antiporter LAT2/CD98hc with uniporter TAT1 for renal reabsorption of neutral amino acids. *J. Am. Soc. Nephrol.* 29, 1624–1635. doi: 10.1681/asn.2017111205

Wesdorp, M., Murillo-Cuesta, S., Peters, T., Celaya, A. M., Oonk, A., Schraders, M., et al. (2018). MPZL2, encoding the epithelial junctional protein myelin protein zero-like 2, is essential for hearing in man and mouse. *Am. J. Hum. Genet.* 103, 74–88. doi: 10.1016/j.ajhg.2018.05.011

Winn, S. R., Scherer, T., Thony, B., Ying, M., Martinez, A., Weber, S., et al. (2018). Blood phenylalanine reduction corrects CNS dopamine and serotonin deficiencies and partially improves behavioral performance in adult phenylketonuric mice. *Mol. Genet. Metab.* 123, 6–20. doi: 10.1016/j.ymgme.2017.10.009

Zabaleta, N., Barberia, M., Martin-Higueras, C., Zapata-Linares, N., Betancor, I., Rodriguez, S., et al. (2018). CRISPR/Cas9-mediated glycolate oxidase disruption is an efficacious and safe treatment for primary hyperoxaluria type I. *Nat. Commun.* 9:5454.

Conflict of Interest: The authors declare that the research was conducted in the absence of any commercial or financial relationships that could be construed as a potential conflict of interest.

frontiers in Pediatrics

CASE REPORT
published: 30 October 2020
doi: 10.3389/fped.2020.585646

Late-Onset Carnitine–Acylcarnitine Translocase Deficiency With *SLC25A20* c.199-10T>G Variation: Case Report and Pathologic Analysis of Liver Biopsy

Min Chen†, *Yao Cai*†, *Sitao Li, Hui Xiong, Mengxian Liu, Fei Ma, Xin Xiao** and *Hu Hao**

Department of Pediatrics, The Sixth Affiliated Hospital of Sun Yat-sen University, Guangzhou, China

OPEN ACCESS

Edited by:
Oliver Semler, University Hospital of Cologne, Germany

Reviewed by:
Lara Console, University of Calabria, Italy
Ronald Wanders, University of Amsterdam, Netherlands
Cesare Indiveri, University of Calabria, Italy

***Correspondence:**
Hu Hao
haohu@mail.sysu.edu.cn
Xin Xiao
xiaoxin2@mail.sysu.edu.cn

†*These authors have contributed equally to this work*

Specialty section:
This article was submitted to Genetics of Common and Rare Diseases, a section of the journal Frontiers in Pediatrics

Received: *21 July 2020*
Accepted: *23 September 2020*
Published: *30 October 2020*

Citation:
Chen M, Cai Y, Li S, Xiong H, Liu M, Ma F, Xiao X and Hao H (2020) Late-Onset Carnitine–Acylcarnitine Translocase Deficiency With SLC25A20 c.199-10T>G Variation: Case Report and Pathologic Analysis of Liver Biopsy. Front. Pediatr. 8:585646. doi: 10.3389/fped.2020.585646

Introduction: Carnitine–acylcarnitine translocase deficiency (CACTD) is a rare and life-threatening autosomal recessive disorder of mitochondrial fatty acid oxidation caused by variation of the Solute carrier family 25 member 20 (*SLC25A20*) gene. Carnitine–acylcarnitine translocase is one of the crucial transport proteins in the oxidation process of mitochondrial fatty acids. In Asia, the c.199-10T>G splice site variation is the most frequently reported variant of *SLC25A20*. Patients with CACTD with c.199-10T>G variation usually present with a severe clinical phenotype.

Materials and Methods: Herein, we report a neonatal case of late-onset CACTD in mainland China. Symptoms emerged 61 days after birth; the patient presented with a severe metabolic crisis, and her clinical condition rapidly deteriorated, and she died of respiratory insufficiency and cardiac arrest at 61 days. We present the clinical and biochemical features of this patient and briefly review previously reported CACTD cases with c.199-10T>G variation.

Results: Acylcarnitine profiling by tandem mass spectrometry and high-throughput sequencing revealed that our patient was homozygous for the c.199-10T>G variation, confirming the diagnosis of CACTD. Histopathologic analysis of the liver by Prussian blue staining showed focal iron deposition in hepatocytes, and electron microscopy analysis revealed a large number of lipid droplet vacuoles in diffusely distributed hepatocytes.

Conclusion: The development of CACTD in our patient 61 days after birth is the latest reported onset for CACTD with *SLC25A20* c.199-10T>G variation. Early recognition of symptoms and timely and appropriate treatment are critical for improving the outcome of this highly lethal disorder. Death from late-onset CACTD may be caused by the accumulation of long-chain fatty acids as well as iron deposition in the heart leading to heart failure.

Keywords: carnitine-acylcarnitine translocase deficiency, late-onset CACTD, *SLC25A20* gene, liver biopsy, steatosis, iron deposition

INTRODUCTION

Carnitine–acylcarnitine translocase deficiency (CACTD) (Online Mendelian Inheritance in Man #212138) is a rare and life-threatening autosomal recessive disorder of mitochondrial fatty acid oxidation (FAO) resulting from variation of the Solute carrier family 25 member 20 (*SLC25A20*) gene. Carnitine–acylcarnitine translocase (CACT) is one of the crucial transport proteins in the oxidation process of mitochondrial fatty acids. It mainly catalyzes the exchange of acylcarnitine and free carnitine on both sides of the mitochondrial inner membrane and plays an important role in the transport of long-chain (LC) acylcarnitine into mitochondria. The classic phenotype of CACTD includes neonatal hypoketotic hypoglycemia, hyperammonemia, cardiomyopathy, hepatopathy, and myopathy (1). The estimated incidence of CACTD is 1/60,000 in Hong Kong (2) and 1/76,894 in Hunan, China (3). The majority of reported CACTD cases have resulted in unexplained sudden death during the neonatal period (4, 5).

The *SLC25A20* gene is located on 3p21.31 and contains nine exons (6). To date, at least 42 different pathogenic or possibly pathogenic variants of *SLC25A20* have been identified that cause CACTD (Human Genome Mutation Database [HGMD] Professional 2018.4), including 20 missense or nonsense variations, 10 small deletions, 2 small insertions, 1 small indel, 4 gross deletions, and 5 splice site variations. In Asia, the c.199-10T>G splice site variation is the most frequently reported variant; patients harboring this variation typically present with a severe clinical phenotype (3).

In most cases, the c.199-10T>G variation affects children within a few days after birth. Here, we present the case of a female patient who developed symptoms of the disease 61 days after birth, which is the latest reported manifestation for this variant of *SLC25A20*. We describe the clinical, biochemical, histopathologic, and molecular characteristics of this patient and briefly review other cases of CACTD with the *SLC25A20* c.199-10T>G variation that have been reported in the literature.

MATERIALS AND METHODS

Case Description

The female infant was the fourth fetus and third delivery for the mother and was born by cesarean section at 36 weeks gestation, with a birth weight of 2.2 kg. Her amniotic fluid was clean at birth, and she was breastfed after birth. The father was healthy, and the mother was a carrier of chronic hepatitis B virus, and they were not close relatives. The mother's first child was aborted for personal reasons; the second child, a boy, died on the day of birth of an unknown cause. The third child, a 5-year-old girl, is in good health. The family pedigree is shown in **Figure 4**. After birth, the child was diagnosed as a premature infant and hospitalized for 13 days. When discharged from the hospital, the child's general condition was good, and she showed good feeding behavior and reflexes. However, weight gain was not ideal, and the child's body mass was only 3.66 kg at 2 months. At 61 days, she was admitted to another hospital for 1 day due to fever; her responses deteriorated, and she was transferred to our hospital for further treatment. A physical examination conducted upon admission revealed poor response, lethargy, shortness of breath, and low muscle strength and tone in the extremities. Routine laboratory tests showed that the patient had hypoglycemia (glucose: 0.28 mmol/L) and elevated myocardial enzymes [creatine kinase (CK): 569 U/L; CK-MB: 136 U/L] and transaminases (alanine aminotransferase: 169 U/L; aspartate aminotransferase: 239 U/L). Even after symptomatic treatments such as increasing blood sugar, nourishment of the heart, and protection of the liver, the patient's condition gradually deteriorated. Five hours after admission, apnea and cardiac arrest occurred, accompanied by low peripheral capillary oxygen saturation (70%); several resuscitation attempts failed, and the patient died.

Heel blood and urine samples were collected for tandem mass spectrometry (MS/MS) and gas chromatography–mass spectrometry analyses. All mass spectrometry experiments were performed on a Waters TQD mass spectrometer (Waters, Milford, Massachusetts, USA). Data were acquired and analyzed with Waters MassLynx v4.1 software. The urine samples were treated with urea removal, internal standard add, protein removal, vacuum drying, and trimethylsilyl derivatization and then analyzed by JMS-Q1000GC GC-MS (JEOL, Japan) for such as organic acids, amino acids, carbohydrate, polyols, purines, and pyrimidines in the urine. After the child died, we immediately biopsied her liver with the consent of her parents. Liver tissues were fixed in 4% paraformaldehyde, embedded in paraffin, and sectioned at 5 μm. Hematoxylin, eosin, Prussian blue, reticular fiber, masson, and picrosirius red staining were performed according to standard procedures.

Genetic Testing

This study was approved by the ethics committee of the Sixth Affiliated Hospital of Sun Yat-sen University (approval no.

TABLE 1 | Tandem mass spectrometry results at the onset of carnitine–acylcarnitine translocase deficiency.

Species	Concentration (μmol/L)	Reference range
Gln	26.8	2.0–20.0
His	246.3	10.0–200.0
Met	42.8	8.0–38.0
Orn	86.4	5.0–50.0
Glu	55	60.0–200.0
C0	3.3	14.0–55.0
C2	2.6	6.0–30.0
C3	0.19	0.30–3.00
C4-OH	0.02	0.03–0.18
C5	0.05	0.06–0.30
C8	0.02	0.03–0.30
C16	4.3	0.5–2.5
C18	0.85	0.20-1.40
C20	0.12	0.02-0.12
C22	0.18	0.03–0.16
C24	0.27	0.02–0.12

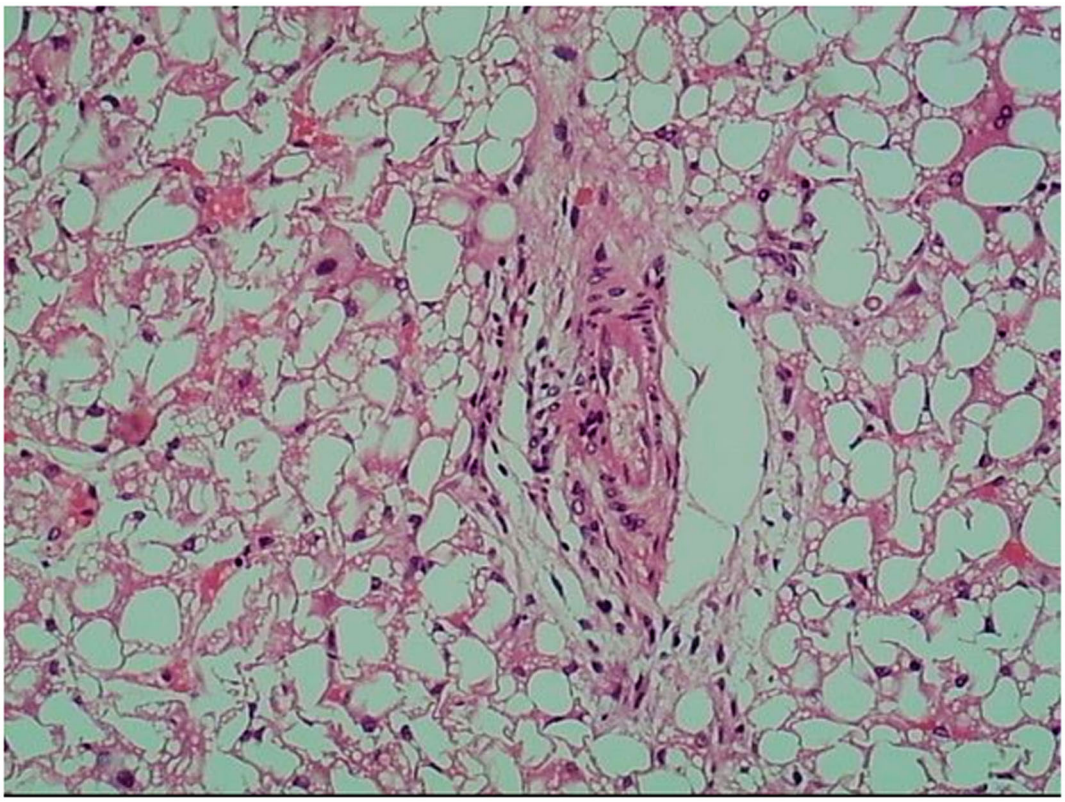

FIGURE 1 | Hematoxylin and eosin staining of liver tissue from patient with CACTD. Extensive vacuolar degeneration was observed (100× magnification).

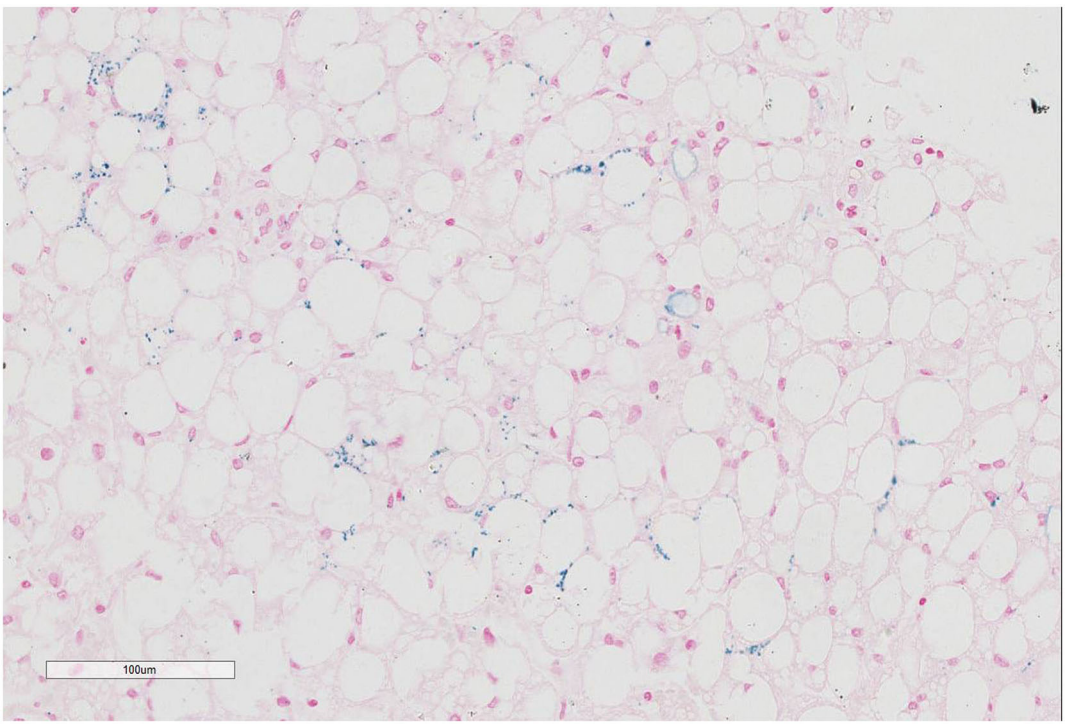

FIGURE 2 | Prussian blue staining of liver tissue from patient with CACTD. Iron deposition was visible in liver cells (100× magnification).

2017ZSLYEC-105) and carried out after obtaining informed consent from the parents of the patient. Peripheral venous blood samples were obtained from the patient and her parents in 3-ml ethylenediaminetetraacetic acid anticoagulant tubes, and genomic DNA was extracted using the Solpure Blood DNA kit (Magen Biotechnology, Guangzhou, China). After DNA fragmentation, end-repair, amplification, and purification, the genomic library was established. Target genes were captured with the Clinical 4000 Pathogenic Gene Package (Guangzhou Jia-Jian Medical Testing, Guangzhou, China). The detection interval of the gene package for this syndrome included 4,047 related genes, and the 55,698 coding regions contained a total of 11,781,176 bases with an average coverage depth of 227 ± 143x, accounting for 99.6% of the coverage interval >10× and 99.5% of the coverage interval >20×. High-throughput sequencing was performed on a Nextseq 500 sequencing platform (Illumina, San Diego, CA, USA). Bioinformatics methods analyzed the sequencing results, and Sanger sequencing was performed to verify the positive loci of the patient, her parents, and her older sister. The reference human genome was hg19 (February 2009; University of California at Santa Cruz, Santa Cruz, CA, USA), and the data were interpreted according to the American College of Medical Genetics and Genomics guidelines.

RESULTS

Tandem Mass Spectrometry and Gas Chromatography–Mass Spectrometry

At the time of symptom emergence, the results of the MS/MS analysis revealed elevated levels of Gln, His, Met, Orn, C16, C22, and C24 and reduced levels of Glu, C0, C2, C3, C4-OH, C5, and C8 in the blood (**Table 1**). Gas chromatography–mass spectrometry analysis of the urine sample showed increased concentrations of several amino acids, 4-hydroxyphenyllactic acid, and pyrimidines.

Liver Pathology

Prussian blue staining showed focal iron deposition in hepatocytes, and examination of liver tissue by electron microscopy revealed many lipid droplet vacuoles in diffusely distributed hepatocytes containing round, square, and irregularly shaped crystals, consistent with fatty liver disease (**Figures 1**–**3**). Masson and Picrosirius red staining showed no proliferation of fibrous tissue; reticular fiber staining showed the preservation of the reticular scaffold of hepatocytes.

Results of Gene Sequencing

A homozygous c.199-10T>G splice site variation was detected in the *SLC25A20* gene of the patient by high-throughput sequencing. Combined with the clinical manifestations, the child was diagnosed with CACTD. Both parents were heterozygous carriers of the variation and had no clinical symptoms. The c.199-10T>G variation was confirmed in all subjects by Sanger sequencing, which showed that the older sister of the patient was also a carrier (**Figures 4**, **5**).

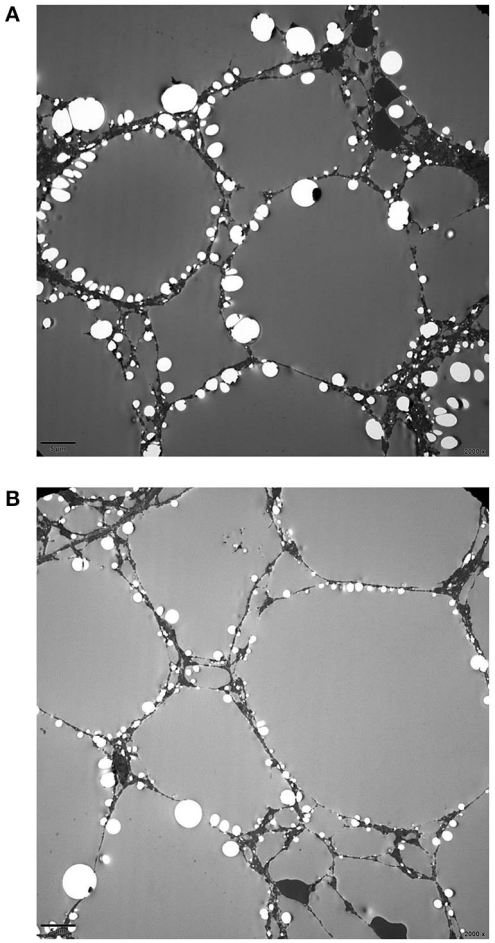

FIGURE 3 | Electron micrograph of the liver from patient with CACTD. **(A,B)** A large number of lipid droplet vacuoles were observed in diffusely distributed hepatocytes (2,000× magnification).

Literature Search Results

Using "Carnitine-acylcarnitine translocase deficiency," "CACTD," "*SLC25A20* gene," and "c.199-10T>G" as keywords, we searched the Online Mendelian Inheritance in Man database and PubMed HGMD up to May 2020 and found 12 reports on CACTD with the c.199-10T>G variation. The clinical features and prognosis of the 25 patients are shown in **Table 2**. Most of the patients developed symptoms within 3 days after birth. The most common symptoms were hypoglycemia and cardiac arrest. The case fatality rate was 96% (25/26). Clinical symptoms in our patient appeared at 61 days, which is the latest onset that has been reported to date for this variant of *SLC25A20*. The disease is mainly manifested as abnormal liver function and sudden cardiac arrest. The severe steatosis observed by histopathologic analysis of the liver suggests that our patient may have had an abnormal liver function before 61 days, masked by compensatory mechanisms. As the patient did not show obvious hypoglycemia, jaundice, or feeding intolerance, her parents did not bring her to the hospital for examination; therefore, the

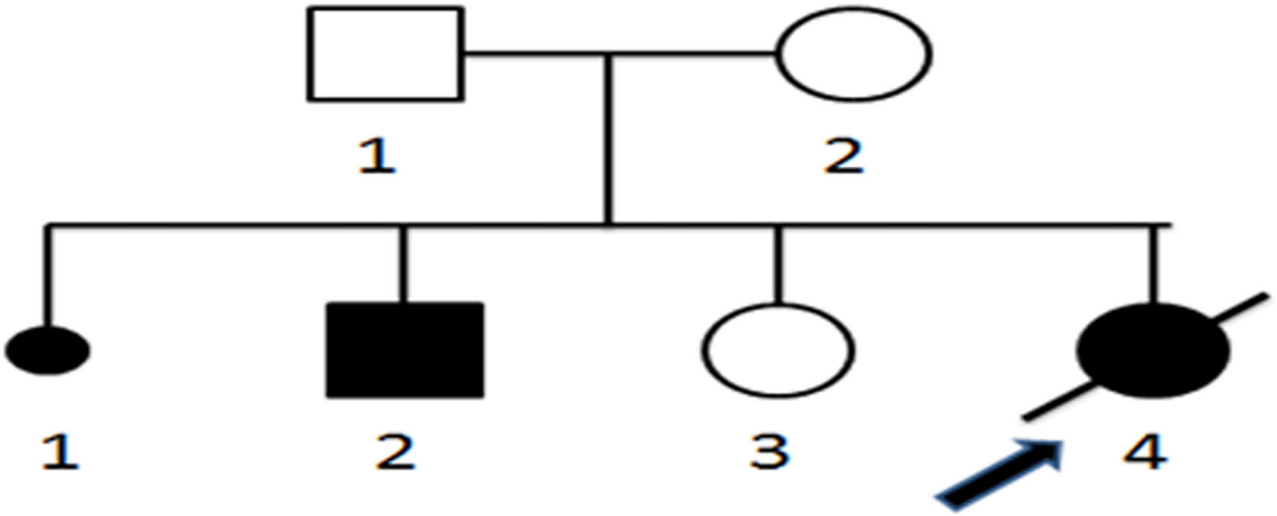

FIGURE 4 | Pedigree of neonatal sudden death carnitine–acylcarnitine translocase deficiency. 1–4, Order of family members; □ normal male; ○, normal female; ■ male patient; •, female patient; , patient who died of CACTD; , stillbirth or abortion; , proband.

specific disease onset time could not be determined. One study examining the effect of the *SLC25A20* c.199-10T>G variation on messenger RNA products found that it disrupted the second and third transmembrane domains of the protein, resulting in loss of translocase activity (17), which could explain the severe phenotype and high mortality associated with this variant.

DISCUSSION

CACTD is a rare autosomal recessive genetic disease characterized by LC FAO disorder. Five cases of CACTD were identified in ∼500,000 newborns in Guangzhou, China, between 2016 and 2017, for an estimated incidence of at least 1:100,000 (18). The first case of CACTD was described in 1992, and only 55 cases have been reported worldwide in the two decades since (3). The first three cases of CACTD in the Chinese population were reported in Hong Kong (13). Two more cases were identified in 153,789 newborns screened over a 3-year period from 2015 to 2017 in Hunan province, China (3). To date, there have been 20 cases of CACTD in China, all with the c.199-10T>G variation. Children usually develop symptoms after a long period of starvation or infection; patients who develop symptoms in the neonatal period have a high fatality rate, whereas those who develop symptoms, later on have a good prognosis (19). In most reported cases, patients developed symptoms in the neonatal period, and their condition rapidly deteriorated, resulting in death; this was especially true in cases with the c.199-10T>G variation. In our patient, the disease developed slowly and manifested as sudden hypoglycemia, respiratory insufficiency, and cardiac arrest before death.

The causative gene of CACTD is *SLC25A20*, which is located on chromosome 3p21.31 and contains nine exons encoding 301 amino acids. To date, at least 42 different pathogenic or possibly pathogenic variations have been identified for CACTD (HGMD Professional 2018.4). The most common are the c.199-10T>G splice site variation, which is observed in patients from East Asia (Japan, China, and Vietnam), and the c.713A>G missense variation, which has been detected in patients of Middle Eastern origin. The c.199-10T>G variation is located in a protective lasso branching sequence of *SLC25A20* intron 2 (6); according to the Exome Aggregation Consortium, it is a common hot spot variation in Asian populations that is detected at a frequency of 0.4‰. However, one study identified 11 carriers in sequencing data of 2,184 people in Guangxi Zhuang Autonomous Region, corresponding to a frequency of 5‰ (14), which is much higher than that in the Exome Aggregation Consortium database.

Routine biochemical tests of CACTD patients typically reveal hypoglycemia and elevated CK and liver enzymes, with a lack of specific diagnostic indicators. Early detection of the disease is mainly through neonatal genetic screening for metabolic diseases. The MS/MS results showed that extremely LC acylcarnitine (i.e., C16, C18, C16:1, C16:1-OH, C18:2, C18:1) accompanied by decreased or normal levels of C0 are indicative of CACTD. However, as the clinical manifestations of severe neonatal and infant carnitine palmityl transferase deficiency are similar to those of CACTD—including acylcarnitine changes in the MS/MS profile—genetic testing or enzymatic analysis is required for definitive diagnosis.

The main principles underlying the treatment of children with CACTD are to avoid malnutrition, prevent infection, and adhere to a high-carbohydrate/low-fat diet (18, 20). During the acute onset of CACTD, continuous high-speed intravenous infusion of glucose solution should be carried out in addition to the reduction of blood ammonia and the administration of other symptomatic and supportive treatments. Long-term treatment should be based on diet control, with supplementation of essential amino acids and fatty acids and the restriction

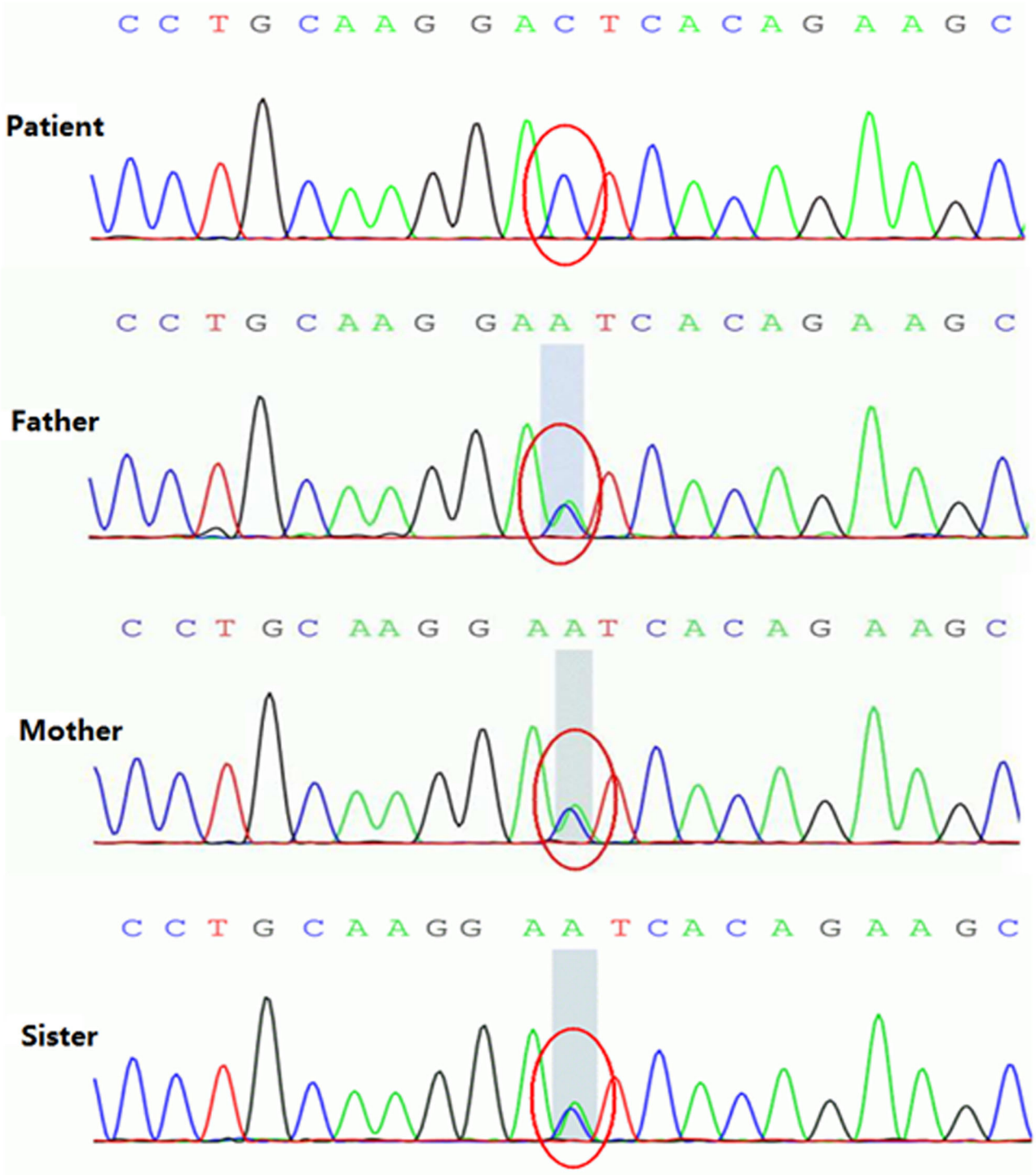

FIGURE 5 | Homozygous variant of the c.199-10T>G splice site in the *SLC25A20* gene of patient with CACTD. Both parents and older sister were heterozygous carriers of the mutation.

of long-chain fatty acid (LCFA) intake. Screening for neonatal genetic and metabolic diseases can detect CACTD early on; however, although early treatment can improve survival, the prognosis of most children is extremely poor. Therefore, for carriers of an identified variation, a prenatal diagnosis should be performed when pregnancy is confirmed to prevent the birth of

TABLE 2 | Characteristics of patients with carnitine–acylcarnitine translocase deficiency with c.199-10T>G mutation.

Patient	Sex	Country	Gene variant	Age of onset	Symptom	Outcome	References
1	F	China	c.199-10T>G Homozygous variant	61 days	Hepatic dysfunction and hypoglycemia	Died of respiratory insufficiency and cardiac arrest 61 days after birth	This report
2	M	China	c.199-10T>G+c.120delT Heterozygous variant	36 h	Seizures and respiratory insufficiency	Died of respiratory failure at 37 months	Stanley et al. (7)
3	F	China	c.199-10T>G+c.326delG Heterozygous variant	27 h	Lethargy, feeding difficulties	Died 31 h after birth	Chalmers et al. (8)
4	F	Vietnam	c.199-10T>G Homozygous variant	2 days	Hypoglycemia	Died of respiratory arrest 6 months after birth	Hammond et al. (9) Costa et al. (10)
5	M	Vietnam	c.199-10T>G Homozygous variant	Within 3 days	Hypoglycemia and hypopnea	Sudden death (unknown time)	Costa et al. (10)
6	M	Vietnam	c.199-10T>G Homozygous variant	Within 3 days	Unknown	Sudden death 2 months after birth	Costa et al. (10)
7	M	Japan	c.199-10T>G+c.576G>A Heterozygous variant	2 days	Respiratory insufficiency	Died at 33 months after birth	Fukushima et al. (11)
8	M	Hong Kong, China	c.199-10T>G Homozygous variant	41 h	Cardiac arrest	Died of cardiac arrest 3 days after birth	Lam et al. (12) Lee et al. (13)
9	F	Hong Kong, China	c.199-10T>G Homozygous variant	32 h	Cardiac arrest	Still alive and followed up for 32 months after birth	Lee et al. (13)
10	M	Hong Kong, China	c.199-10T>G Homozygous variant	28 h	Respiratory insufficiency and cardiomyopathy	Died of cardiac arrest 38 h after birth	Lee et al. (13)
11	M	Thailand	c.199-10T>G Homozygous variant	10 h	Hypothermia followed by cardiac arrest 60 h after birth	Died of upper gastrointestinal bleeding and metabolic disorders at the age of 2 years and 8 months	Vatanavicharn et al. (6)
12	F	Thailand	c.199-10T>G Homozygous variant	2 days	Lethargy, difficulty feeding, and cardiac arrest	Died of cardiac arrest 4 months after birth	Vatanavicharn et al. (6)
13	M	China	c.199-10T>G Homozygous variant	25 min	Hypoglycemia, apnea, and seizures	Died of cardiac arrest 78 h after birth	Yan et al. (3)
14	F	China	c.199-10T>G+C.1A>G	52 h	Hypoglycemia and hypotension	Died of heart failure 6 days after birth	Yan et al. (3)
15	M	China	c.199-10T>G Homozygous variant	2 days	Hypoglycemia	Died of heart failure 3 days after birth	Fan et al. (14)
16	M	China	c.199-10T>G Homozygous variant	1.5 days	Hypoglycemia, seizures, and apnea	Died of heart failure 2 days after birth	Fan et al. (14)
17	M	China	c.199-10T>G Homozygous variant	3 days	Hypoglycemia	Sudden death 4 days after birth	Fan et al. (14)
18	F	China	c.199-10T>G Homozygous variant	30 days	Hypoglycemia	Sudden death 30 days after birth	Fan et al. (14)
19	M	China	c.199-10T>G/c.719-8_c.719-1dupCCCCACAG	1 days	Hypoglycemia	Died 3 days after birth from cardiogenic shock with malignant ventricular arrhythmia and pulmonary hemorrhage	Fan et al. (14)
20	F	China	c.199-10T>G/c.719-8_c.719-1dupCCCCACAG	1 day	Hypoglycemia	Died of cardiac arrest 8 days after birth	Tang et al. (15)
21	M	China	c.199-10T>G Homozygous variant	3 days	Hypoglycemia	Sudden death 2 months after birth	Tang et al. (15)
22	F	China	c.199-10T>G Homozygous variant	2 days	Lethargy	Died of cardiac arrest 3 days after birth	Tang et al. (15)
23	M	China	c.199-10T>G Homozygous variant	2 days	Lethargy and hypotonia	Died of respiratory distress and arrhythmia	Tang et al. (15)
24	F	China	c.199-10T>G Homozygous variant	2 days	Lethargy and hypoglycemia	Died of cardiac arrest 3 days after birth	Tang et al. (15)
25	M	China	c.199-10T>G Homozygous variant	2 days	Hypoglycemia, lethargy, and hypotonia	Died of heart failure 4 days after birth	Liu et al. (16)
26	M	China	c.199-10T>G Homozygous variant	3 days	Lethargy and cyanosis	Died of arrhythmia and heart failure 3 days after birth	Liu et al. (16)

F, female; M, male.

a fetus with the variation, which is essential for preventing and reducing the incidence of CACTD.

Our patient harbored the homozygous c.199-10T>G variation of the *SLC25A20* gene, which generates a truncated protein, causing severe clinical phenotypes, including neonatal death (15). Mitochondrial FAO is a major source of energy during prolonged fasting and cardiac and skeletal muscle during long-term exercise (21). The carnitine cycle transfers LCFAs such as acylcarnitine from the cytosol into the intramitochondrial space where mitochondrial FAO occurs (1, 22). When fat is broken down under conditions of starvation, CACT deficiency can lead to the accumulation of toxic LC acylcarnitine in the heart, liver, or skeletal muscle, leading to heart failure, arrhythmia, and cardiac arrest (3). Newborns lacking CACT are particularly vulnerable in the first few postnatal days because of their low oral intake of nutrients and low glycogen reserves. Our patient survived for 2 months after birth, possibly because of frequent breastfeeding by her mother. Nonetheless, toxic LC acylcarnitine slowly accumulated in the patient's liver and heart, and the postmortem examination revealed iron deposition and severe steatosis in the liver.

Chronic liver disease can lead to iron metabolism disorder and excessive iron deposition in the body (23), which is associated with fatal complications such as cirrhosis and heart failure (24–26). Death from late-onset CACTD may be caused not only by the accumulation of LCFAs but also by iron deposits that lead to heart failure. We did not measure serum iron and ferritin levels or perform a histopathologic examination of the heart in our patient; therefore, the precise cause of death is unclear. The contribution of iron deposition to the pathogenesis of late-onset CACTD warrants further study, as it may provide insight into potential treatment strategies for late-onset CACTD.

DATA AVAILABILITY STATEMENT

The datasets presented in this study can be found in online repositories. The names of the repository/repositories and accession number(s) can be found in the article/supplementary material.

ETHICS STATEMENT

The studies involving human participants were reviewed and approved by the Ethics Committee of the Sixth Affiliated Hospital of Sun Yat-sen University (approval number: 2017ZSLYEC-105). Written informed consent to participate in this study was provided by the participants' legal guardian/next of kin.

AUTHOR CONTRIBUTIONS

All authors listed have made a substantial, direct and intellectual contribution to the work, and approved it for publication.

FUNDING

This work was supported by the Science and Technology Foundation of Guangzhou, China (201604020154 and 201704020230).

REFERENCES

1. Rubio-Gozalbo ME, Bakker JA, Waterham HR, Wanders RJA. Carnitine-acylcarnitine translocase deficiency, clinical, biochemical and genetic aspects. *Mol Asp Med.* (2004) 25:521–32. doi: 10.1016/j.mam.2004.06.007
2. Hui J, Tang NL, Li CK, Law LK, To KF, Yau P, et al. Inherited metabolic diseases in the Southern Chinese population: spectrum of diseases and estimated incidence from recurrent mutations. *Pathology.* (2014) 46:375–82. doi: 10.1097/PAT.0000000000000140
3. Yan HM, Hu H, Ahmed A, Feng BB, Liu J, Jia ZJ, et al. Carnitine-acylcarnitine translocase deficiency with c.199-10 T>G and novel c.1A>G mutation: two case reports and brief literature review. *Medicine.* (2017) 96:e8549. doi: 10.1097/MD.0000000000008549
4. Korman SH, Pitt JJ, Boneh A, Dweikat I, Zater M, Meiner V, et al. A novel SLC25A20 splicing mutation in patients of different ethnic origin with neonatally lethal carnitine-acylcarnitine translocase (CACT) deficiency. *Mol Genet Metab.* (2006) 89:332–8. doi: 10.1016/j.ymgme.2006.06.009
5. Lopriore E, Gemke RJ, Verhoeven NM, Jakobs C, Wanders RJ, Roeleveld-Versteeg AB, et al. Carnitine-acylcarnitine translocase deficiency: phenotype, residual enzyme activity and outcome. *Eur J Pediatr.* (2001) 160:101–4. doi: 10.1007/s004310000644
6. Vatanavicharn N, Yamada K, Aoyama Y, Fukao T, Densupsoontorn N, Jirapinyo P, et al. Carnitine -acylcarnitine translocase deficiency: two neonatal cases with common splicing mutation and in vitro bezafibrate response. *Brain Dev.* (2015) 37:698–703. doi: 10.1016/j.braindev.2014.10.005
7. Stanley CA, Hale DE, Berry GT, Deleeuw S, Boxer J, Bonnefont JP. Brief report: a deficiency of carnitine -acylcarnitine translocase in the inner mitochondrial membrane. *N Engl J Med.* (1992) 327:19–23. doi: 10.1056/NEJM199207023270104
8. Chalmers RA, Stanley CA, English N, Wigglesworth JS. Mitochondrial carnitine acylcarnitine translocate deficiency presenting as sudden neonatal death. *J Pediatr.* (1997) 131:220–25. doi: 10.1016/S0022-3476(97)70157-4
9. Hammond JW, Sim KG, Trenholm A, Stanley T, Wilcken B. Sudden death in infancy: Two New Zealand cases of carnitine/acylcarnitine translocate deficiency. *J Inherit Metab Dis.* (1998) 21:60.
10. Costa C, Costa JM, Slama A, Boutron A, Vequaud C, Legrand A, et al. Mutational spectrum and DNA-based prenatal diagnosis in carnitine-acylcarnitine translocase deficiency. *Mol Genet Metab.* (2003) 78:68–73. doi: 10.1016/S1096-7192(02)00205-6
11. Fukushima T, Kaneoka H, Yasuno T, Sasaguri Y, Tokuyasu T, Tokoro K, et al. Three novel mutations in the carnitine - acylcarnitine translocase (CACT) genein patients with CACT deficiency and in healthy individual. *J Hum Genet.* (2013) 58:788–93. doi: 10.1038/jhg.2013.103
12. Lam CW, Lai CK, Chow CB, Tong SF, Yuen YP, Mak YF, et al. Ethnic-specific splicing mutation of the carnitine-acylcarnitine translocase gene in a Chinese neonate presenting with sudden unexpected death. *Chin Med J.* (2003) 116:1110–2.
13. Lee RS, Lam CW, Lai CK, Yuen YP, Chan KY, Shek CC, et al. Carnitine-acylcarnitinetranslocase deficiency in three neonates presenting with rapid deterioration and cardiac arrest. *Hong Kong Med J.* (2007) 13:66–8.
14. Fan X, Xie BB, Zhang Q, Yi S, Geng GX, Yang Q, et al. Analysis of four carnitine-acylcarnitine translocase deficiency cases caused by homozygous mutation of SLC25A20 c.199-10T>G. *Zhonghua Er Ke Za Zhi.* (2018) 56:545–9. doi: 10.3760/cma.j.issn.0578-1310.2018.07.014
15. Tang C, Liu S, Wu M, Lin S, Lin Y, Su L, et al. Clinical and molecular characteristics of carnitine-acylcarnitine translocase deficiency: experience with six patients in Guangdong China. *Clin Chim Acta.* (2019) 495:476–80. doi: 10.1016/j.cca.2019.05.018

16. Liu M, Li S, Liang Y, Gu X, Yang Q, Cai Y, et al. Clinical feature and gene mutation analysis of neonatal sudden death type carnitine-acylcarnitine translocase deficiency. *Chin J Appl Clin Pediatr.* (2019) 34:1496–9. doi: 10.3760/cma.j.issn.2095-428x.2019.19.014
17. Hsu BY, Iacobazzi V, Wang Z, Harvie H, Chalmers RA, Saudubray JM, et al. Aberrant mRNA splicing associated with coding region mutations in children with carnitine-acylcarnitine translocase deficiency. *Mol Genet Metab.* (2001) 74:248–55. doi: 10.1006/mgme.2001.3235
18. Spiekerkoetter U, Lindner M, Santer R, Grotzke M, Baumgartner MR, Boehles H, et al. Treatment recommendations in long-chain fatty acid oxidation defects: consensus from a workshop. *J Inherit Metabo Dis.* (2009) 32:498–505. doi: 10.1007/s10545-009-1126-8
19. Vitoria I, Martín-Hernández E, Peña-Quintana L, Bueno M, Quijada-Fraile P, Dalmau J, et al. Carnitine-acylcarnitine translocase deficiency: experience with four cases in Spain and review of the literature. *JIMD Rep.* (2015) 20:11–20. doi: 10.1007/8904_2014_382
20. Mahapatra S, Ananth A, Baugh N, Damian M, Enns GM. Triheptanoin: a rescue therapy for cardiogenic shock in carnitine-acylcarnitine translocase deficiency. *JIMD Rep.* (2018) 39:19–23. doi: 10.1007/8904_2017_36
21. Iacobazzi V, Invernizzi F, Baratta S, Pons R, Chung W, Garavaglia B, et al. Molecular and functional analysis of SLC25A20 mutations causing carnitine-acylcarnitine translocase deficiency. *Hum Mutat.* (2004) 24:312–20. doi: 10.1002/humu.20085
22. Indiveri C, Iacobazzi V, Tonazzi A, Giangregorio N, Infantino V, Convertini P, et al. The mitochondrial carnitine/acylcarnitine carrier: function, structure and physiopathology. *Mol Aspects Med.* (2011) 32:223–33. doi: 10.1016/j.mam.2011.10.008
23. Bacon BR, Adams PC, Kowdley KV, Powell LW, Tavill AS, American Association for the Study of Liver Diseases. Diagnosis and management of hemochromatosis: 2011 practice guideline by the American association for the study of liver diseases. *Hepatology*. (2011) 54:328–43. doi: 10.1002/hep.24330
24. Sukumaran A, Chang J, Han M, Mintri S, Khaw BA, Kim J. Iron overload exacerbates age-associated cardiac hypertrophy in a mouse model of hemochromatosis. *Sci Rep*. (2017) 7:5756. doi: 10.1038/s41598-017-05810-2
25. Zhabyeyev P, Das SK, Basu R, Shen M, Patel VB, Kassiri Z, et al. TIMP3 deficiency exacerbates iron overload-mediated cardiomyopathy and liver disease. *Am J Physiol Heart Circ Physiol.* (2018) 314:H978–90. doi: 10.1152/ajpheart.00597.2017
26. Murphy CJ, Oudit GY. Iron-overload cardiomyopathy: pathophysiology, diagnosis, and treatment. *J Card Fail.* (2010) 16:888–900. doi: 10.1016/j.cardfail.2010.05.009

Conflict of Interest: The authors declare that the research was conducted in the absence of any commercial or financial relationships that could be construed as a potential conflict of interest.

frontiers in Pediatrics

REVIEW
published: 23 November 2020
doi: 10.3389/fped.2020.583877

New Therapeutics Options for Pediatric Neuromuscular Disorders

Marina Flotats-Bastardas[1]* *and Andreas Hahn*[2]

[1] Department of Pediatric Neurology, Saarland University Hospital, Homburg, Germany, [2] Department of Child Neurology, University of Giessen, Giessen, Germany

Neuromuscular disorders (NMDs) of Childhood onset are a genetically heterogeneous group of diseases affecting the anterior horn cell, the peripheral nerve, the neuromuscular junction, or the muscle. For many decades, treatment of NMDs has been exclusively symptomatic. But this has changed fundamentally in recent years due to the development of new drugs attempting either to ameliorate secondary pathophysiologic consequences or to modify the underlying genetic defect itself. While the effects on the course of disease are still modest in some NMDs (e.g., Duchenne muscular dystrophy), new therapies have substantially prolonged life expectancy and improved motor function in others (e.g., spinal muscular atrophy and infantile onset Pompe disease). This review summarizes recently approved medicaments and provides an outlook for new therapies that are on the horizon in this field.

Keywords: Duchenne and Becker muscular dystrophies, spinal muscular atrophies, Pompe disease, Zolgensma, Spinraza, AAV (adeno-associated virus)

OPEN ACCESS

Edited by:
E. Ann Yeh,
Hospital for Sick Children, Canada

Reviewed by:
Chiara Fiorillo,
University of Genoa, Italy
Hernan Dario Gonorazky,
Hospital for Sick Children, Canada

***Correspondence:**
Marina Flotats-Bastardas
marina.flotats-bastardas@uks.eu

Specialty section:
This article was submitted to Pediatric Neurology, a section of the journal Frontiers in Pediatrics

Received: *15 July 2020*
Accepted: *22 October 2020*
Published: *23 November 2020*

Citation:
Flotats-Bastardas M and Hahn A (2020) New Therapeutics Options for Pediatric Neuromuscular Disorders. Front. Pediatr. 8:583877. doi: 10.3389/fped.2020.583877

INTRODUCTION

Neuromuscular disorders (NMDs) include conditions affecting the anterior horn cell (e.g., Spinal muscular atrophy = SMA), the peripheral nerve (e.g., Charcot-Marie-Tooth disease = CMT), the neuromuscular junction (e.g., Congenital myasthenia), or the muscle itself (e.g., Duchenne muscular dystrophy = DMD). In general, NMDs are progressive, impair motor function, and often reduce life expectancy as well as quality of life. Most of the more prevalent NMDs have been first described at the end of the nineteenth century. Although the genetic basis of these disorders has been unraveled during the last century, treatment remained symptomatic or even palliative for many decades. The vast majority of NMDs manifesting in childhood have a genetic basis. Therapeutic agents targeting to treat these conditions can either attempt correcting the genetic defect, or try mitigating the pathophysiological consequences that originate from the genetic error.

NMDs as a whole are not infrequent, but every single one is a rare or orphan disease (prevalence <1 per 1,500 persons in the U.S. and <1 per 2,000 persons in Europe) (1–3). An orphan drug is a pharmaceutical agent developed to treat medical conditions which, because they are so rare, would not be profitable to produce without government assistance (4). Acknowledging the need for better care of patients with rare diseases has led to legislations in the U.S. and in Europe that resulted in tax incentives, enhanced patent protection and marketing rights, and research subsidies, encouraging pharmaceutical companies to develop orphan drugs (4).

These measures together with recent progress in the understanding of pathophysiological mechanisms underlying specific NMDs and in genetic engineering, has resulted in the development of several highly innovative pharmaceutical agents for children with NMDs. This short review gives an overview about recently approved drugs and promising therapeutic agents currently investigated in pre-clinical and clinical trials by focussing on more prevalent pediatric NMDs (**Table 1**).

DISEASES OF THE ANTERIOR HORN CELL/SPINAL MUSCULAR ATROPHIES (SMAs)

Spinal muscular atrophies are characterized by premature degeneration of the second motor neuron. 5q-associated SMA is by far the most common form with an incidence of about one in 6,000 to 10,000 live births. The phenotype is broad and ranges from infants dying within the first year of life due to respiratory insufficiency to patients showing first symptoms of mild proximal muscle weakness beyond the age of 18 years. The disease is caused by biallelic mutations in the *Survival Motor Neuron* (*SMN1*) gene. *SMN1* encodes the SMN protein that is ubiquitously expressed and essential for proper function of the anterior horn cells in spinal cord and brainstem. About 95% of patients carry homozygous *SMN1* deletions of exon 7 or exons 7 and 8, resulting in a truncated and unstable SMN protein. Humans have 1–8 copies of a paralogous gene, *SMN2*, located next to *SMN1* that differs by five nucleotides. This results in a splicing defect diminishing the SMN protein produced by one copy of *SMN2* to ∼10% of the normal value (5, 6). Based on age at onset of clinical symptoms and best motor function 3–5 SMA subtypes (SMA 0, 1, 2, 3 + 4) are distinguished. While biallelic mutations in *SMN1* cause SMA, disease severity is related to the number of *SMN2* copies.

The Food and Drug Administration (FDA) in 2017 and the European Medical Agency (EMA) in 2018 approved nusinersen (Spinraza®), an antisense oligonucleotide that modifies the splicing process of *SMN2*, thereby enhancing the production of stable and functional SMN-protein, for all patients with 5q-associated SMA. Since nusinersen does not pass the blood brain barrier, it has to be administered intrathecally every 4 months following 4 loading doses within the first 2 months. A multicentre placebo-controlled phase 3 study including 121 SMA 1 patients demonstrated that significantly more nusinersen treated subjects were alive and that they had better motor functions at the end of the trial than untreated individuals (7). Similarly, a study with 126 SMA 2 patients aging 2–9 years displayed that subjects receiving nusinersen had significant and clinically meaningful improvement in motor function compared to untreated patients (8). Finally, an observational study with 19 adult SMA 3 patients receiving nusinersen for 10 months showed motor and respiratory improvement (9).

Onasemnogene abeparvovec (Zolgensma®) is a AAV9 vector based gene therapy approved in 2019 by the FDA for children with SMA under the age of 2 years (10), and by the EMA in 2020 for SMA 1 patients and for all SMA subjects with up to 3 *SMN2* copies regardless of their age and weight (11). The Adeno-associated virus subtype 9 (AAV9) is able to cross the blood-brain and to transfect motor neurons. The vector contains a single strain copy of the *SMN1* gene that persists in the cell nucleus as an extrachromosomal episome. The drug is given as an one-time intravenous infusion over 60 minutes. An open-label study including 15 SMA 1 patients showed that all patients were alive and without permanent ventilation by the age of 20 months compared to only 8% of patients from a natural history cohort

TABLE 1 | Current status of new therapeutic approaches in pediatric neuromuscular disorders.

Disease	Therapeutic approach	Status of development
SMA		
	Gene replacement therapy	
	Onasemnogene abeparvovec	Approved
	Splicing modification	
	Nusinersen	Approved
	Risdiplam	Approved*
	Other mode of action	
	SRK-015	Phase 3
CMT1A		
	Gene replacement therapy	
	AAV1	Phase 2
	Splicing modification	
	ASOs	Preclinical
	Other mode of action	
	PXT3003	Phase 3
	L-Serine	Phase 2
CMS		
	Increasing acetylcholine	
	Pyridostigmine	Approved
	3,4-Diaminonpyridine	Approved
	Modulating channel opening	
	Fluoxetine	Approved
	Quinidine	Approved
	Unknown	
	Salbutamol	Approved
DM1		
	Splicing modification	
	Metformin	Phase 2
	Other mode of action	
	Tideglusib	Phase 2
	Small molecule	Preclinical
DMD		
	Gene replacement therapy	
	AAVrh74	Phase 1
	Splicing modification	
	Ataluren	Approved*
	Eteplirsen	Approved*
	Golodirsen	Approved*
	Arbekacin	Phase 2
	Gentamycin	Phase 1
	Reducing inflammation	
	Prednisone	Approved
	Vamorolone	Phase 3
	Edasalonexent	Phase 3
	Targeting Cardiomyopathy	
	ACE inhibitors	Approved
	Angiotensin receptor antagonists	Approved
	Beta-blockers	Approved
	Other mode of action	
	Idebenone	Phase 3
	ACE-031	Phase 2
LGMD		
	Gene replacement therapy	
	AAVrh7 beta-sarcoglycan	Phase 2
	AAVrh74 alpha-sarcoglycan	Phase 2

(Continued)

TABLE 1 | Continued

Disease	Therapeutic approach	Status of development
	AAV1 gamma-sarcoglycan	Phase 1
	dual AAVrh74 dysferlin	Phase 1
Congenital myopathies		
	Gene replacement therapy	
	AAV8 Myotubular myopathy	Phase 2
	Splicing modification	
	DYN10 Dynamin-2 centronuclear myopathy	Phase 2
Lamin A/C related muscle disease		
	Splicing modification	
	Exon Skipping	Preclincial
Pompe		
	Gene replacement therapy	
	AAV	Preclinical/Phase 1
	Enzyme replacement therapy	
	Lumizyme/Myozyme	Approved
	Neo-GAA	Phase 3
	ATB200	Phase 4
	Other mode of action	
	Albuterol	Phase 1/2

*SMA, spinal muscular atrophy; CMT1A, Charcot-Marie-tooth 1A; CMS, congenital myasthenic syndromes; DM1, myotonic dystrophy 1; DMD, Duchenne muscular dystrophy; LGMD, limb-girdle muscle dystrophies. *Approved only by the FDA or EMA.*

(12). Moreover, some patients gained motor milestones such as sitting and standing not attained by any patient in the untreated cohort (13). A clinical trial evaluating the safety of intrathecal administration in patients with 3 *SMN2* copies (NCT03381729) is on hold at the time of writing (July, 2020) because of dorsal root ganglia damage observed in non-human primates (14).

Risdiplam (Evrysdi®) is a small molecule also modifying pre-mRNA splicing of *SMN2*. The drug is studied in patients with SMA 1–3 and in pre-symptomatic SMA 1 patients (NCT02908685, NCT02913482, NCT03779334) (15). Risdiplam can be given orally since it penetrates the blood brain barrier (16). Preliminary data from clinical trials in SMA 1 patients and from studies with children and young adults with SMA 2 indicate improved survival and motor function compared to untreated patients (17). Based on these data, Risdiplam has been recently approved by the FDA and is available in Europe in the scope of a compassionate use program for SMA 1 and 2 patients deemed as not suitable for treatment with nusinersen or onasemnogene abeparvovec.

Currently, many SMA 1 patients start treatment with one of the above-mentioned therapeutic agents after they have been diagnosed on clinical grounds. Although the efficacy of these new drugs has been well-documented in clinical trials, improvement of motor function is often modest, and swallowing and respiration remain substantially compromised (7, 18). This stands in sharp contrast to the results of studies with nusinersen and onasemnogene abeparvovec in pre-symptomatic SMA 1 patients, showing that many of them achieve walking, learn to speak, and remain ventilator-free at least within the first years of life (19, 20). These data strongly support inclusion of SMA into new-born screening programs (21–24).

No head-to-head studies comparing the efficacy of nusinersen and onasemnogene abeparvovec are available. An indirect unanchored comparison of the two pivotal trials (7, 12) among symptomatic SMA type 1 infants suggested that onasemnogene abeparvovec may have an efficacy advantage relative to nusinersen (25), but this study has been criticized because of substantial methodological shortcomings (26). The availability of these very expensive new drugs raises many ethical questions such as access to treatment, and start or termination of therapy in patients with advanced disease. Unfortunately, guidelines defining standards of care have been updated for the last time shortly before these new therapies have been approved (27).

Besides these already licensed gene expression modifying drugs, muscle enhancing therapies have been studied. Myostatin is a negative regulator of muscle growth. SRK-015, a monoclonal antibody selectively inhibiting myostatin, has been shown to promote muscle cells growth and differentiation, thereby ameliorating muscle force in SMA mice (28). Safety and tolerability of this approach has been confirmed in a phase I trial (NCT02644777), and a phase II study (NCT03921528) including 58 SMA 2 and 3 children is still ongoing. Preliminary results are expected at the end of this year (29).

PERIPHERAL NERVE DISEASES/CHARCOT-MARIE-TOOTH DISORDERS (CMTs)

CMTs are a heterogeneous group of hereditary motor and sensory neuropathies with a prevalence of 1:2,500 (30). Age at onset varies from the neonatal period to adulthood. Clinically, patients have sensory deficits and usually show a slowly progressive distal muscle weakness, and foot and hand deformities. Axonal and demyelinating forms are distinguished, and currently mutations in more than 90 genes are known to be involved (31).

CMT1A is the most frequent form, accounting for about 60% of cases. The disease is caused by a duplication of the *PMP22* gene. Peripheral myelin protein 22 kDa (PMP22) is produced by Schwann cells and has an important role in proliferation and differentiation of myelin. Overexpression of PMP22 protein leads to demyelination and abnormal re-myelination with slowing of nerve conduction velocity, and over time, causes secondary axonal degeneration (32, 33). Different therapeutic approaches are currently under investigation, attempting to regulate PMP22 expression or enhancing myelination (30).

PXT3003 is a combination preparation of three medicaments (3 mg baclofen, 0.35 mg naltrexone, and 105 mg sorbitol) with the aim to reduce the expression of PMP22. A phase 2 placebo-controlled study over 1 year was conducted in 80 patients with CMT1A. Patients in the high-dose arm demonstrated improvement in motor conduction velocities and in the overall neuropathy limitations scale (ONLS) (34). Similarly, a phase 3 study with 323 patients ranging in age from 16 to 65 years taking PXT3003 for 15 months showed an improvement in the

10-m walking test as well as in ONLS in patients receiving the higher dose (NCT02579759) (35). Due to a temporary treatment interruption, the FDA requested an additional pivotal phase 3 trial expected to start in 2021.

Antisense oligonucleotides (ASOs) have been found to effectively suppress PMP22 mRNA in affected nerves in 2 murine CMT1A models. Initiation of ASO treatment restored impressively myelination, motor nerve conduction velocity and compound muscle action potentials almost to levels seen in wild type animals (36). These data demonstrate that strategies to reduce PMP22 have potential as effective therapeutic approaches for CMT1A (37).

Neurotrophin 3 (NT-3) is implicated in the support, survival, and growth of Schwann cells and regeneration of peripheral nerves (38). Preclinical studies with human recombinant NT-3 showed improved axonal regeneration and myelination, which resulted in a subsequent placebo-controlled phase 1/2 study including eight adult patients for 6 months. Patients who received NT-3 subcutaneously experienced a clinical improvement as measured with the Mayo Clinic Neuropathy Score and showed improved regeneration of myelinated fibers in nerve biopsies (39). Because of the limited half-life of subcutaneously administered NT-3 a preclinical AAV mediated NT-3 gene study was conducted in animals, showing improvements in motor function, compound muscle action potentials, and nerve biopsy findings (40). Moreover, a phase 1/2 trial is ongoing with nine patients aging 15 to 35 years treated with intramuscular injections in both legs of AAV1.tMCK.NTF3 (NCT03520751). Results are expected in 2023.

While treatment of CMT1A is still symptomatic and classic pharmacological options have been disappointing (41), a recent randomized trial with L-serine in 18 adults with hereditary sensory autonomic neuropathy (HSAN) showed that the CMT neuropathy score improved significantly in the treated group (42).

DISORDERS OF THE NEUROMUSCULAR JUNCTION/CONGENITAL MYASTHENIC SYNDROMES (CMS)

CMS include a group of currently 30 genetically distinct entities all sharing the symptoms of fatigable muscle weakness and impaired neurotransmission (43). Application of next generation sequencing techniques has resulted not only in identification of new genes and proteins, but also in a better understanding of the pathophysiology of the neuromuscular junction. This has enabled a more tailored therapeutic approach (44). While drugs like pyridostigmine, an acetylcholine (ACh) esterase inhibitor, often used in tandem with 3,4-diaminonpyridine, a potassium channel blocker increasing ACh release, are more or less effective in some of these conditions, they may worsen symptoms in slow-channel forms, in which prolonged ACh receptor-gated channel opening causes deleterious entry of Ca2+ into the postsynaptic region and consecutive degeneration of post-synaptic structures (43, 44). In addition, treatment with sympathomimetics like salbutamol has been shown to be beneficial in subjects refractory to cholinesterase inhibitors (43). Moreover, ACh receptor open channel blockers, for example, fluoxetine and quinidine, have been shown to be effective in some of the slow channel syndromes (44).

PRIMARY DISEASES OF THE SKELETAL MUSCLE

Myotonic Dystrophies

Myotonic dystrophy type 1 and 2 are dominantly inherited, progressive diseases affecting multiple tissues due to unstable repeats in untranslated DNA. Myotonic dystrophy type 1 (DM1) is the most prevalent neuromuscular disorder in adults and has a broad phenotype ranging from onset of myotonia and mild muscle weakness in adulthood to congenital forms characterized by severe muscular hypotonia, generalized muscle weakness, and respiratory failure in neonates due to aggravation of disease severity through successive generations (anticipation) (45). DM1 is caused by an expansion of a CTG repeat sequence in the 3′-UTR of the myotonic dystrophy kinase protein (DMPK) gene. This results in DMPK transcripts with expanded CUG repeats that are retained in the nucleus and form multiple discrete RNA foci, triggering a cascade of toxic effects. Tideglusib is an inhibitor of glycogen synthase kinase 3 beta that has been shown to reduce the amount of toxic CUG-containing RNA in DM1-mice (46). A phase 1/2 study including 16 adolescents and younger adults with DM1 has already been completed, but results are not yet available (NCT02858908), and a double-blind placebo-controlled study assessing safety and efficacy in a smaller group of children with a congenital form is planned (NCT03692312). Metformin is an antidiabetic drug modifying RNA splicing, autophagy, insulin sensitivity, and glycogen synthesis that has been found to have positive effects on mobility and motor function in a small-scale monocentric phase II study (47). The pathophysiology of DM1 is extremely complex, and a bundle of small molecule compounds such as up-regulators of the muscleblind-like (MBNL) splicing factor family, H-RAS pathway inhibitors, transcription inhibitors, and protein kinase modulators has been shown to mitigate DM1 pathogenesis in different experimental systems (48), giving hope that more clinical trials will start in the nearer future (45).

Duchenne Muscular Dystrophy (DMD)

DMD is caused by mutations in the dystrophin gene, located on Xp21. The dystrophin gene is one of the largest human genes and has 79 exons. The incidence of DMD is 1:3,000 to 1:5,000 male births and the prevalence is 1.3–1.8:10,000 boys. Rarely female carriers with skewed X-inactivation may also develop symptoms (49). Boys typically present with hyperCKemia, motor or global developmental delay, proximal muscle weakness and calf pseudohypertrophy before the age of 5 years. Most patients become wheelchair bound until age 12 years. Scoliosis, dilative cardiomyopathy, and respiratory failure evolve thereafter and result in premature death without assisted ventilation around 20 years of age (50). Recommendations for standards of care have been published (49, 51) and their transformation into

clinical practice (e.g., steroid treatment, spinal surgery, non-invasive ventilation) has delayed age at loss of ambulation and substantially increased life expectancy (50, 52, 53).

Dystrophin is part of a protein complex linking the cytoskeleton to the basal lamina, thereby stabilizing the muscle cell membrane. Dystrophin deficiency makes the muscle cell more vulnerable to microtraumas that trigger a cascade of pathophysiological reactions including inflammation, mitochondrial dysfunction, and calcium influx, finally resulting in cell death. Large deletions disrupting the reading frame account for ∼65% of mutations, and about 10% of patients carry nonsense mutations resulting in premature termination of the protein synthesis (54). Steroids were the first drugs that have been shown to improve muscle strength and pulmonary function (51, 55). It is supposed that prednisone reduces the inflammatory process as result of the cell membrane breakage, but other effects like enhancing dystrophin expression or lowering calcium influx are also discussed (55). Vamorolone is a synthetic variant of cortisol specifically developed to avoid the side effects of glucocorticoids (56). A phase 3 clinical trial showed that a dosage of 2 mg/kg/die given for 24 weeks was well-tolerated and improved time function tests without negative effects on bone, metabolic, or adrenal function (57). Vamorolone recently received a priority review approval by the FDA. Edasalonexent (CAT-1004) is a small molecule inhibiting the transcription factor NF-κB, which is enhancing muscle degeneration. A phase 1 trial including 17 children has shown good tolerability and reduced expression of NF-kB (NCT02439216) (58). There is an ongoing placebo-controlled phase 3 study to evaluate efficacy and safety of Edasalonexent in 131 pediatric patients (NCT03703882).

There is cumulating evidence that angiotensin converting enzyme inhibitors (ACE inhibitors) reduce the progression rate of dilative cardiomyopathy when initiated early, that is, prior to decline of left ventricular ejection fraction. Similarly, it has been found that the combination of ACE inhibitors or angiotensin receptor antagonists with beta-blockers improves the outcome of patients with established cardiomyopathy (59). Current clinical guidelines recommend an early use of ACE-inhibitors (or angiotensin receptor antagonists for those not tolerating ACE inhibitors) in asymptomatic patients by the age of 10 years (51).

Ataluren (Translarna®) is approved by the EMA, but not yet by the FDA, for treatment of ambulant DMD patients older than age 2 years with nonsense mutations in the dystrophin gene (60). Ataluren is a small molecule acting at the ribosome, that is assumed to read through stop codons and in this way enhances the rate of full-length dystrophin transcripts. The drug is given orally three times a day. A phase 3 study with 115 ambulatory patients treated with ataluren for 48 weeks vs. 115 patients receiving placebo found no significant differences in the 6-min walking test (6MWT), and thus failed the primary endpoint. But a pre-specified analysis in a subgroup of patients with a walking distance of 300–400 m in the 6MWT at baseline demonstrated a significantly lower decline in the walking distance in treated patients (61). Preliminary results of an ongoing prospective study matching the data of 181 DMD patients treated with ataluren for on average 2 years with those of a natural history cohort, suggest a statistically relevant later loss of ambulation in the ataluren group (11 vs. 14.5 years) (62). Further substances assumed to improve read through that have been investigated in phase I and II studies are arbekacin and gentamycin (NCT01918384, NCT00451074).

Exon skipping therapies aim to restore the reading frame in DMD patients with deletions. This allows production of a shortened and defective, but still functional dystrophin protein (63). Among boys with deletions, about 20% patients are amenable to skipping of exon 51, 13% to skipping of exon 53, 12% to skipping of exon 45, and 11% to skipping of exon 44. Eteplirsen (Exondys51®) received an accelerated approval by the FDA in 2016 for the treatment of DMD patients with mutations amenable to skipping of exon 51. The drug is an antisense oligonucleotide that binds to the dystrophin pre-mRNA and supresses correct splicing of exon 51. Results of a phase 2 study showed an increase of dystrophin in muscle biopsies as well as a significantly lower decline in the 6MWT when given to 12 patients for 48 weeks and compared to a placebo group (63). Following up these patients for 3 years and matching their data with those of a natural history cohort also revealed a significant difference in the 6MWT in favor of the eteplirsen group (64). The drug is given intravenously over 30–60 min. Golodirsen (Vyondys53®) has also been approved in December 2019 by the FDA for treatment of DMD patients amenable to skipping of exon 53 (65) after a phase 1/2 clinical trial showed an ∼16-fold improvement in dystrophin production (66). The phase 2 and 3 studies are still ongoing (NCT02310906 and NCT02500381). As eteplirsen golodirsen is infused once a week (65). Both drugs are yet not approved by the EMA.

Systemic gene therapy is a promising way to treat DMD. But the size of the dystrophin gene is a major hurdle, since it exceeds the packaging capacity of the AAV vector (67). To overcome this problem different highly abbreviated micro-dystrophins have been invented, and several independent systemic AAV vector mediated gene phase I therapy trials are conducted (NCT03368742, NCT03375164, NCT03362502, NCT03333590). Recently published data on four young DMD patients followed-up for 12 months after a rAAVrh74.MHCK7.micro-dystrophin gene transfer showed that this treatment was well-tolerated, and was associated with robust micro-dystrophin expression, reduced serum CK levels, and functional improvement as measured by the North Star Ambulatory Assessment (68).

Idebenone is an antioxidant that is assumed to improve mitochondrial energy production. In a phase 3 randomized controlled study (DELOS) in DMD patients 10–18 years of age idebenone reduced significantly the loss of respiratory function over a 1-year period, and a *post-hoc* analysis suggested that more patients in the placebo group compared to the idebenone group experienced bronchopulmonary adverse events (69, 70). In addition, the reduced decline of the pulmonary function assessed in a retrospective cohort study (SYROS) from 18 patients was maintained for several years (71). Despite these promising results, the drug has not yet been approved neither by the FDA nor by the EMA.

Preclinical studies exploring myostatin inhibition have shown increased muscle growth as well as reduced fibrosis. ACE-031 is a fusion protein that inhibits myostatin. In a phase 2 clinical

trial ACE-031 was injected subcutaneously in 24 patients. This study was stopped because of safety concerns (epistaxis and telangiectasia), but preliminary results showed positive trends concerning distance in the 6MWT and increase of lean body mass (NCT01099761) (72).

Further therapeutic concepts studied in DMD are utrophin upregulation, anti-fibrotic substances, neuronal nitric oxide synthase upregulation and other anti-inflammatory medications (73).

Limb-Girdle Muscle Dystrophies (LGMDs)

LGMDs are a heterogeneous group of diseases characterized by progressive proximal weakness of the pelvic and/or shoulder muscles. Disease onset is usually after the age of 2 years and the estimated prevalence is 1:100,000 (74). CK concentrations vary from slightly to highly elevated, while muscle biopsy findings range from mildly abnormal to severely dystrophic. Autosomal dominant (LGMD D) and recessive (LGMD R) forms are distinguished. Currently, more than 30 genetically different types are known. Sarcoglycans are proteins that form a tetrameric complex at the muscle cell plasma membrane. This complex stabilizes the association of dystrophin with the dystroglycans and contributes to the stability of the plasma membrane cytoskeleton. Dysferlin or dystrophy-associated fer-1-like protein is encoded by *DYSF*. Several lines of evidence indicate that dysferlin is linked with muscle cell membrane repair. *DYSF* defects can result in different forms of neuromuscular disorders such as Miyoshi myopathy (MM), limb-girdle muscular dystrophy type R2 and Distal myopathy (DM) (75).

LGMD R4 (Beta-Sarcoglycanopathy)

Preclinical studies in ß-sarcoglycan deficient mice treated with AAVrh7 containing a β-sarcoglycan transgene targeting to treat skeletal, diaphragm and cardiac muscles demonstrated functional and biochemical improvements (76). Currently, there is an ongoing phase 1/2 clinical trial with six patients ranging in age from 4 to 15 years (NCT03652259). Results from an interim analysis in three patients after 9 months displayed improvement in motor function, reduction of CK, and increase of beta-sarcoglycan expression in the muscle (77). Final results are expected in 2021.

LGMD R3 (Alpha-Sarcoglycanopathy)

Preclinical studies in α-sarcoglycan deficient mice treated with systemic AAV containing α-sarcoglycan using a muscle specific promoter showed histological improvement, correction of pseudohypertrophy as well as increase of global activity (78). This prompted a phase 1/2 study that included 3 non-ambulatory patients aging 12 to 14 years, who received an intramuscular injection of AAVrh74 containing an alpha-sarcoglycan transgene. All patients showed a positive gene expression in muscle biopsies performed on week 6, and 3 and 6 months (NCT00494195) (79). Similar results were obtained in two of three patients aging 23 to 43 years old, in whom muscle biopsies were taken 6 months after gene delivery (80). It was supposed that the negative results in the third patient were caused by pre-existing immunity against the used vector (60).

LGMD R5 (Gamma-Sarcoglycanopathy)

Preclinical trials in γ-sarcoglycan deficient mice treated with intramuscular AAV containing γ-sarcoglycan with a muscle specific promoter showed histological improvement mainly in those muscles that did not show significant fibrosis (81). In a consecutive phase 1 study 8 out of 9 non-ambulatory patients ranging in age from 12–14 years who received an intramuscular AAV1 injection with a gamma-sarcoglycan transgene showed a positive gene expression in muscle biopsies performed 1 month after application (NCT01344798) (82).

LGMD R2 (Dysferlinopathy)

Studies in dysferlin deficient mice treated with systemic dual adeno-associated virus vectors AAVrh74 showed histological and radiological improvement (83). Since *DYSF* is a large gene (55 exons) it has been splintered into two fragments that are packaged into separate AAVrh74 vectors. Both fragments have a 1 kb overlap region that allows the recombination of the two cDNA segments after systemic co-injection (84). Currently, there is an ongoing phase 1 clinical study that includes non-ambulatory adults with LGMDR2 who received intramuscular delivery of AAVrh74 with the aim to explore gene expression after 3 and 6 months (NCT02710500).

Congenital Myopathies

Myotubular Myopathy

X-linked Myotubular Myopathy (XLMTM) is a rare congenital myopathy characterized by severe muscle weakness, respiratory failure and early death. Mortality rate is estimated to be 50% in the first 18 months of life. The disease is caused by mutations in the *MTM1* gene that lead to absence or dysfunction of myotubularin, a protein that is necessary for normal development, maturation, and function of skeletal muscle cells. The disease affects ∼1 in 50,000 new-born males. In a study with XLMTM dogs, intravenous administration of a recombinant AAV8 vector expressing canine myotubularin at 10 weeks of age demonstrated impressively that this treatment was well-tolerated, prolonged lifespan, and corrected the skeletal muscle phenotype in a dose-dependent manner. This prompted a phase 1/2 study (NCT03199469) in children with XLMTM ranging in age from 0–5 years. While the first six patients dosed at 1×10^{14} genome copies/kg also showed very encouraging results, all 3 patients administered a 3-fold higher dose (3×10^{14}) experienced severe hepatotoxicity and two of them died (85). Further development of this product is currently on hold pending further evaluation of these serious adverse events (86).

Dynamin-2 Related Centronuclear Myopathy

Mutations in *DNM2* encoding dynamin-2 cause autosomal dominant centronuclear myopathy, which is associated with variable muscle weakness and wasting (87). In *DNM2*-mutated mice, weekly intrapleural injections of ASOs targeting DNM2 for 5 weeks corrected muscle mass, histopathology, and muscle ultrastructure (88). These findings prompted an ongoing phase 1/2 study with DYN101, a synthetically manufactured constrained ethyl gapmer ASO directed against DNM2 pre-mRNA in 18 adolescents and young adults (NCT04033159).

Lamin A/C Related Muscle Disease

LMNA-related disorders are caused by mutations in the LMNA gene, encoding the nuclear envelope proteins lamin A and C by alternative splicing. LMNA mutations are linked with a wide range of disease phenotypes such as neuromuscular, cardiac and metabolic disorders to premature aging syndromes. Neuromuscular phenotypes include LMNA-related muscular dystrophy, autosomal dominant Emery-Dreifuss muscular dystrophy, and congenital muscular dystrophy. Apart from symptomatic treatment including the use of steroids amelioration of pathogenesis by exon skipping has been proposed as a potential treatment strategy (89).

Pompe Disease

Pompe disease (glycogen storage disease type 2) is caused by biallelic mutations of the acid alpha-glucosidase (GAA) gene. This results in deficiency of the lysosomal enzyme GAA and impaired autophagy. Severity of disease depends on the amount of residual enzyme activity. Two types are distinguished, infantile and late onset Pompe disease (IOPD/LOPD). The incidence of IOPD is about 1:140,000 and that of all types amounts to ∼1:40,000 in Europe. In classic IOPD, GAA activity is <1%. Contrary to milder forms with later onset that are characterized mainly by a progressive proximal myopathy with early respiratory involvement, this causes marked accumulation of glycogen not only in skeletal muscle, but also in heart and other tissues. Affected patients present with CK elevation, hypertrophic cardiomyopathy, failure to thrive, muscular hypotonia and axial muscle weakness during the first 6 months of life. IOPD is rapidly progressive and the majority of untreated subjects die within the first year of life due to a combination of ventilatory and cardiac failure without achieving any motor mile stone such as turning, sitting, or standing. Survival beyond the age of 18 months is exceptional. Although GAA activity is <1% in all IOPD patients, two groups have to be differentiated. Patients may synthesize a non-functional form of GAA or are completely unable to form any kind of native enzyme. The former patients are designated as cross-reactive immunological material (CRIM)-positive, whereas the latter are classified as CRIM-negative (90–92).

An enzyme replacement therapy (ERT) with recombinant human alpha-glucosidase (Lumizyme®/Myozyme®) was approved in 2006 by the FDA and the EMA. The recombinant enzyme has to be administered intravenously every 2 weeks over about 4 h. In the pivotal phase 3 study including 18 infants diagnosed before 6 months of age, all patients were alive and seven walked independently after 12 months of ERT (93). In a follow-up extension study over 3 years 13 patients were still alive and 6 remained able to walk (94). In addition, a placebo-controlled phase 3 study was performed in 90 ambulant LOPD patients about 18 months. This showed that treated patients had significantly better motor function (measured by the 6MWT) as well as stabilized pulmonary function (95).

The positive results of the pivotal IOPD trials have been confirmed by several real world studies, but it has been recognized over the years that the response to ERT is imperfect and that patients respond differently. A beginning of ERT as early as possible and immunomodulation in CRIM-negative subjects to avoid antibody formation against the recombinant enzyme have been identified as important factors to improve outcome, but morbidity and mortality are still high. Moreover, prolonged survival of IOPD patients has resulted in a new phenotype with variable residual muscle weakness and worsening of motor function after some years of ERT, hearing impairment, oropharyngeal and facial weakness causing speech and swallowing difficulties as well as neurocognitive, respiratory and orthopedic problems (96, 97). Strategies to further improve outcome in IOPD and also LOPD focus on manufacturing improved enzyme versions that allow a better uptake into the muscle cell, and developing gene therapies. Neo-GAA (avalglucosidasa alfa), a modified recombinant human GAA with higher affinity to the mannose-6-phosphate (M6P) receptor, is currently tested in a phase 3 study and final results are expected soon (NCT02782741). ATB200 is another rhGAA with a higher content of M6P and bis-M6P glycan residues that is tested in a clinical trial in association with a pharmacological chaperone. Albuterol has also been investigated as an add-on therapy which may enhance the lysosomal uptake of hrGAA (98). Moreover, there are several pre-clinical and early clinical *ex-vivo* and *in-vivo* gene therapy trials targeting different tissues with variable transgenes (for review see Ronzitti et al. ATM 2019) (99). To date, it is not clear which approach will finally be best suited for this complex disease.

CONCLUSIONS

Several new therapeutic options have become available for the treatment of pediatric NMDs in the last years, and multiple others are currently studied in pre-clinical and clinical trials. While some diseases have now become principally treatable, many others are still waiting for the major breakthrough. The new therapeutic options in SMA 1 and IOPD are examples for drugs that have transformed rapidly progressive lethal diseases into more chronic conditions. But it has to be kept in mind that patients treated this way are not cured. Moreover, both conditions show that success and efficacy of these new therapies depend on the time point of their application and the clinical status of the patients. Pompe disease was the first NMD that became principally treatable. One lesson to be learned from the use of ERT in IOPD since almost 15 years is that problems emerged totally unexpected before. It does not take a crystal ball to see that similar things will happen in other diseases. Nevertheless, the development of new, highly innovative drugs has heralded a new era in the treatment of pediatric NMDs.

AUTHOR CONTRIBUTIONS

MF-B conceived and designed the work and draft the article. AH designed the work and performed a critical revision of the article. All authors contributed to the final manuscript.

FUNDING

We acknowledge support by the Deutsche Forschungsgemeinschaft (DFG, German Research Foundation) and Saarland University within the funding programme Open Access Publishing.

REFERENCES

1. European Union. *Regulation (EC) N° 141/2000 of the European Parliament and of the Council of 16 December 1999 on Orphan Medicinal Products*. (2000). Available online at: http://data.europa.eu/eli/reg/2000/141/oj (access October 10, 2020).
2. Baldovino S, Moliner AM, Taruscio D, Daina E, Roccatello D. Rare diseases in Europe: from a wide to a local perspective. *Isr Med Assoc J.* (2016) 18:359–63.
3. Deenen JCW, Horlings CGC, Verschuuren JJGM, Verbeek ALM, van Engelen BGM. The epidemiology of neuromuscular disorders: a comprehensive overview of the literature. *J Neuromuscul Dis.* (2015) 2:73–85. doi: 10.3233/JND-140045
4. Giannuzzi V, Conte R, Landi A, Ottomano SA, Bonifazi D, Baiardi P, et al. Orphan medicinal products in Europe and United States to cover needs of patients with rare diseases: an increased common effort is to be foreseen. *Orphanet J Rare Dis.* (2017) 12:64. doi: 10.1186/s13023-017-0617-1
5. Lunn MR, Wang CH. Spinal muscular atrophy. *Lancet.* (2008) 371:2120–33. doi: 10.1016/S0140-6736(08)60921-6
6. Pechmann A, Kirschner J. Diagnosis and new treatment avenues in spinal muscular atrophy. *Neuropediatrics.* (2017) 48:273–81. doi: 10.1055/s-0037-1603517
7. Finkel RS, Mercuri E, Darras BT, Connolly AM, Kuntz NL, Kirschner J, et al. Nusinersen versus sham control in infantile-onset spinal muscular atrophy. *N Engl J Med.* (2017) 377:1723–32. doi: 10.1056/NEJMoa1702752
8. Mercuri E, Darras BT, Chiriboga CA, Day JW, Campbell C, Connolly AM, et al. Nusinersen versus sham control in later-onset spinal muscular atrophy. *N Engl J Med.* (2018) 378:625–35. doi: 10.1056/NEJMoa1710504
9. Walter MC, Wenninger S, Thiele S, Stauber J, Hiebeler M, Greckl E, et al. Safety and treatment effects of nusinersen in longstanding adult 5q-SMA type 3—a prospective observational study. *J Neuromuscul Dis.* (2019) 6:453–65. doi: 10.3233/JND-190416
10. Hoy SM. Onasemnogene abeparvovec: first global approval. *Drugs.* (2019) 79:1255–62. doi: 10.1007/s40265-019-01162-5
11. Buckingham L. *New Gene Therapy to Treat Spinal Muscular Atrophy* (corrected) (2020). *European Medicines Agency* [zitiert 2. Mai 2020]. Available online at: https://www.ema.europa.eu/en/news/new-gene-therapy-treat-spinal-muscular-atrophy-corrected (access October 10, 2020).
12. Mendell JR, Al-Zaidy S, Shell R, Arnold WD, Rodino-Klapac LR, Prior TW, et al. Single-dose gene-replacement therapy for spinal muscular atrophy. *N Engl J Med.* (2017) 377:1713–22. doi: 10.1056/NEJMoa1706198
13. Al-Zaidy SA, Kolb SJ, Lowes L, Alfano LN, Shell R, Church KR, et al. AVXS-101 (Onasemnogene Abeparvovec) for SMA1: comparative study with a prospective natural history cohort. *J Neuromuscul Dis.* (2019) 6:307–17. doi: 10.3233/JND-190403
14. Kirschner J, Butoianu N, Goemans N, Haberlova J, Kostera-Pruszczyk A, Mercuri E, et al. European ad-hoc consensus statement on gene replacement therapy for spinal muscular atrophy. *Eur J Paediatr Neurol.* (2020) 28:38–43. doi: 10.1016/j.ejpn.2020.07.001
15. Sturm S, Günther A, Jaber B, Jordan P, Al Kotbi N, Parkar N, et al. A phase 1 healthy male volunteer single escalating dose study of the pharmacokinetics and pharmacodynamics of risdiplam (RG7916, RO7034067), a SMN2 splicing modifier. *Br J Clin Pharmacol.* (2019) 85:181–93. doi: 10.1111/bcp.13786
16. Poirier A, Weetall M, Heinig K, Bucheli F, Schoenlein K, Alsenz J, et al. Risdiplam distributes and increases SMN protein in both the central nervous system and peripheral organs. *Pharmacol Res Perspect.* (2018) 6:e00447. doi: 10.1002/prp2.447
17. Baranello G, Servais L, Day J, Deconinck N, Mercuri E, Klein A, et al. P.353FIREFISH Part 1: 16-month safety and exploratory outcomes of risdiplam (RG7916) treatment in infants with type 1 spinal muscular atrophy. *Neuromuscul Disord.* (2019) 29:S184. doi: 10.1016/j.nmd.2019.06.515
18. Day J, Chiriboga C, Darras B, Finkel R, Connolly A, Iannacconne S, et al. Onasemnogene Abeparvovec-xioi gene-replacement therapy for spinal muscular atrophy type 1 (SMA1): phase 3 US study (STR1VE) update (1828). *Neurology.* (2020) 94(Suppl. 15).
19. De Vivo DC, Bertini E, Swoboda KJ, Hwu W-L, Crawford TO, Finkel RS, et al. Nusinersen initiated in infants during the presymptomatic stage of spinal muscular atrophy: interim efficacy and safety results from the phase 2 nurture study. *Neuromuscul Disord.* (2019) 29:842–56. doi: 10.1016/j.nmd.2019.09.007
20. Lowes LP, Alfano LN, Arnold WD, Shell R, Prior TW, McColly M, et al. Impact of age and motor function in a phase 1/2a study of infants with SMA type 1 receiving single-dose gene replacement therapy. *Pediatr Neurol.* (2019) 98:39–45. doi: 10.1016/j.pediatrneurol.2019.05.005
21. Boemer F, Caberg J-H, Dideberg V, Dardenne D, Bours V, Hiligsmann M, et al. Newborn screening for SMA in Southern Belgium. *Neuromuscul Disord.* (2019) 29:343–9. doi: 10.1016/j.nmd.2019.02.003
22. Glascock J, Sampson J, Haidet-Phillips A, Connolly A, Darras B, Day J, et al. Treatment algorithm for infants diagnosed with spinal muscular atrophy through newborn screening. *J Neuromuscul Dis.* (2018) 5:145–58. doi: 10.3233/JND-180304
23. Vill K, Kölbel H, Schwartz O, Blaschek A, Olgemöller B, Harms E, et al. One year of newborn screening for SMA—results of a German pilot project. *J Neuromuscul Dis.* (2019) 6:503–15. doi: 10.3233/JND-190428
24. Govoni A, Gagliardi D, Comi GP, Corti S. Time is motor neuron: therapeutic window and its correlation with pathogenetic mechanisms in spinal muscular atrophy. *Mol Neurobiol.* (2018) 55:6307–18. doi: 10.1007/s12035-017-0831-9
25. Dabbous O, Maru B, Jansen JP, Lorenzi M, Cloutier M, Guérin A, et al. Survival, motor function, and motor milestones: comparison of AVXS-101 relative to nusinersen for the treatment of infants with spinal muscular atrophy type 1. *Adv Ther.* (2019) 36:1164–76. doi: 10.1007/s12325-019-00923-8
26. Sandrock AW, Farwell W. Comparisons between separately conducted clinical trials: letter to the editor regarding Dabbous O, Maru B, Jansen JP, Lorenzi M, Cloutier M, Guérin A, et al. *Adv Ther.* (2019) 36:1164–76. doi: 10.1007/s12325-019-01087-1
27. Finkel RS, Mercuri E, Meyer OH, Simonds AK, Schroth MK, Graham RJ, et al. Diagnosis and management of spinal muscular atrophy: part 2: pulmonary and acute care; medications, supplements and immunizations; other organ systems; and ethics. *Neuromuscul Disord.* (2018) 28:197–207. doi: 10.1016/j.nmd.2017.11.004
28. Long KK, O'Shea KM, Khairallah RJ, Howell K, Paushkin S, Chen KS, et al. Specific inhibition of myostatin activation is beneficial in mouse models of SMA therapy. *Hum Mol Genet.* (2019) 28:1076–89. doi: 10.1093/hmg/ddy382
29. Messina S, Sframeli M. New treatments in spinal muscular atrophy: positive results and new challenges. *J Clin Med.* (2020) 9:2222. doi: 10.3390/jcm9072222
30. Morena J, Gupta A, Hoyle JC. Charcot-Marie-tooth: from molecules to therapy. *Int J Mol Sci.* (2019) 20:3419. doi: 10.3390/ijms20143419
31. Mathis S, Goizet C, Tazir M, Magdelaine C, Lia A-S, Magy L, et al. Charcot–Marie–tooth diseases: an update and some new proposals for the classification. *J Med Genet.* (2015) 52:681. doi: 10.1136/jmedgenet-2015-103272
32. van Paassen BW, van der Kooi AJ, van Spaendonck-Zwarts KY, Verhamme C, Baas F, de Visser M. PMP22 related neuropathies: Charcot-Marie-tooth disease type 1A and hereditary neuropathy with liability to Pressure Palsies. *Orphanet J Rare Dis.* (2014) 9:38. doi: 10.1186/1750-1172-9-38
33. Watila MM, Balarabe SA. Molecular and clinical features of inherited neuropathies due to PMP22 duplication. *J Neurol Sci.* (2015) 355:18–24. doi: 10.1016/j.jns.2015.05.037
34. Attarian S, Vallat J-M, Magy L, Funalot B, Gonnaud P-M, Lacour A, et al. An exploratory randomised double-blind and placebo-controlled phase 2 study of a combination of baclofen, naltrexone and sorbitol (PXT3003) in patients with Charcot-Marie-Tooth disease type 1A. *Orphanet J Rare Dis.* (2014) 9:199. doi: 10.1186/s13023-014-0199-0
35. Thomas F, Boutalbi Y, Fitoussi S, Rinaudo P, Bertrand V, Hajj R, et al. Efficacy ANS safety of PXT3003 in patients with Charcot-Marie-tooth disease type1A: results of Pleo-Charcot–Marie–tooth: an international pivotal phase III trial. *Muscle Nerve.* (2019) 60(S1):S46.
36. Zhao HT, Damle S, Ikeda-Lee K, Kuntz S, Li J, Mohan A, et al. PMP22 antisense oligonucleotides reverse Charcot-Marie-tooth disease type 1A features in rodent models. *J Clin Invest.* (2018) 128:359–68. doi: 10.1172/JCI96499
37. Shy ME. Antisense oligonucleotides offer hope to patients with Charcot-Marie-tooth disease type 1A. *J Clin Invest.* (2018) 128:110–2. doi: 10.1172/JCI98617
38. Sahenk Z. Neurotrophins and peripheral neuropathies. *Brain Pathol.* (2006) 16:311–9. doi: 10.1111/j.1750-3639.2006.00038.x

39. Sahenk Z, Nagaraja HN, McCracken BS, King WM, Freimer ML, Cedarbaum JM, et al. NT-3 promotes nerve regeneration and sensory improvement in CMT1A mouse models and in patients. *Neurology.* (2005) 65:681–9. doi: 10.1212/01.WNL.0000171978.70849.c5
40. Sahenk Z, Galloway G, Clark KR, Malik V, Rodino-Klapac LR, Kaspar BK, et al. AAV1.NT-3 gene therapy for Charcot–Marie–tooth neuropathy. *Mol Ther.* (2014) 22:511–21. doi: 10.1038/mt.2013.250
41. Boutary S, Echaniz-Laguna A, Adams D, Loisel-Duwattez J, Schumacher M, Massaad C, et al. Treating PMP22 gene duplication-related Charcot-Marie-Tooth disease: the past, the present and the future. *Transl Res.* (2020) S1931–5244:30175–4. doi: 10.1016/j.trsl.2020.07.006
42. Fridman V, Suriyanarayanan S, Novak P, David W, Macklin EA, McKenna-Yasek D, et al. Randomized trial of l-serine in patients with hereditary sensory and autonomic neuropathy type 1. *Neurology.* (2019) 92:e359–70. doi: 10.1212/WNL.0000000000006811
43. Nicole S, Azuma Y, Bauché S, Eymard B, Lochmüller H, Slater C. Congenital myasthenic syndromes or inherited disorders of neuromuscular transmission: recent discoveries and open questions. *J Neuromuscul Dis.* (2017) 4:269–84. doi: 10.3233/JND-170257
44. Vanhaesebrouck AE, Beeson D. The congenital myasthenic syndromes: expanding genetic and phenotypic spectrums and refining treatment strategies. *Curr Opin Neurol.* (2019) 32:696–703. doi: 10.1097/WCO.0000000000000736
45. Turner C, Hilton-Jones D. Myotonic dystrophy: diagnosis, management and new therapies. *Curr Opin Neurol.* (2014) 27:599–606. doi: 10.1097/WCO.0000000000000128
46. Timchenko L. Correction of RNA-binding protein CUGBP1 and GSK3β signaling as therapeutic approach for congenital and adult myotonic dystrophy type 1. *Int J Mol Sci.* (2019) 21:94. doi: 10.3390/ijms21010094
47. Bassez G, Audureau E, Hogrel J-Y, Arrouasse R, Baghdoyan S, Bhugaloo H, et al. Improved mobility with metformin in patients with myotonic dystrophy type 1: a randomized controlled trial. *Brain.* (2018) 141:2855–65. doi: 10.1093/brain/awy231
48. López-Morató M, Brook JD, Wojciechowska M. Small molecules which improve pathogenesis of myotonic dystrophy type 1. *Front Neurol.* (2018) 9:349. doi: 10.3389/fneur.2018.00349
49. Bushby K, Finkel R, Birnkrant DJ, Case LE, Clemens PR, Cripe L, et al. Diagnosis and management of Duchenne muscular dystrophy, part 1: diagnosis, and pharmacological and psychosocial management. *Lancet Neurol.* (2010) 9:77–93. doi: 10.1016/S1474-4422(09)70271-6
50. McDonald CM, Henricson EK, Abresch RT, Han JJ, Escolar DM, Florence JM, et al. The cooperative international neuromuscular research group Duchenne natural history study—a longitudinal investigation in the era of glucocorticoid therapy: design of protocol and the methods used. *Muscle Nerve.* (2013) 48:32–54. doi: 10.1002/mus.23807
51. Birnkrant DJ, Bushby K, Bann CM, Apkon SD, Blackwell A, Brumbaugh D, et al. Diagnosis and management of Duchenne muscular dystrophy, part 1: diagnosis, and neuromuscular, rehabilitation, endocrine, and gastrointestinal and nutritional management. *Lancet Neurol.* (2018) 17:251–67. doi: 10.1016/S1474-4422(18)30024-3
52. Landfeldt E, Thompson R, Sejersen T, McMillan HJ, Kirschner J, Lochmüller H. Life expectancy at birth in Duchenne muscular dystrophy: a systematic review and meta-analysis. *Eur J Epidemiol.* (2020) 35:643–53. doi: 10.1007/s10654-020-00613-8
53. McDonald CM, Henricson EK, Abresch RT, Duong T, Joyce NC, Hu F, et al. Long-term effects of glucocorticoids on function, quality of life, and survival in patients with Duchenne muscular dystrophy: a prospective cohort study. *Lancet.* (2018) 391:451–61. doi: 10.1016/S0140-6736(17)32160-8
54. Aartsma-Rus A, Ginjaar IB, Bushby K. The importance of genetic diagnosis for Duchenne muscular dystrophy. *J Med Genet.* (2016) 53:145–51. doi: 10.1136/jmedgenet-2015-103387
55. Moxley RT, Ashwal S, Pandya S, Connolly A, Florence J, Mathews K, et al. Practice parameter: corticosteroid treatment of Duchenne dystrophy: report of the Quality Standards Subcommittee of the American Academy of Neurology and the Practice Committee of the Child Neurology Society. *Neurology.* (2005) 64:13–20. doi: 10.1212/01.WNL.0000148485.00049.B7
56. Hoffman EP, Riddle V, Siegler MA, Dickerson D, Backonja M, Kramer WG, et sl. Phase 1 trial of vamorolone, a first-in-class steroid, shows improvements in side effects via biomarkers bridged to clinical outcomes. *Steroids.* (2018) 134:43–52. doi: 10.1016/j.steroids.2018.02.010
57. Hoffman EP, Schwartz BD, Mengle-Gaw LJ, Smith EC, Castro D, Mah JK, et al. Vamorolone trial in Duchenne muscular dystrophy shows dose-related improvement of muscle function. *Neurology.* (2019) 93:e1312–23. doi: 10.1212/WNL.0000000000008168
58. Finanger E, Vandenborne K, Finkel RS, Lee Sweeney H, Tennekoon G, Yum S, et al. Phase 1 study of edasalonexent (CAT-1004), an oral NF-κB inhibitor, in pediatric patients with Duchenne muscular dystrophy. *J Neuromuscul Dis.* (2019) 6:43–54. doi: 10.3233/JND-180341
59. El-Aloul B, Altamirano-Diaz L, Zapata-Aldana E, Rodrigues R, Malvankar-Mehta MS, Nguyen C-T, et al. Pharmacological therapy for the prevention and management of cardiomyopathy in Duchenne muscular dystrophy: a systematic review. *Neuromuscul Disord.* (2017) 27:4–14. doi: 10.1016/j.nmd.2016.09.019
60. Ryan NJ. Ataluren: first global approval. *Drugs.* (2014) 74:1709–14. doi: 10.1007/s40265-014-0287-4
61. McDonald CM, Campbell C, Torricelli RE, Finkel RS, Flanigan KM, Goemans N, et al. Ataluren in patients with nonsense mutation Duchenne muscular dystrophy (ACT DMD): a multicentre, randomised, double-blind, placebo-controlled, phase 3 trial. *Lancet.* (2017) 390:1489–98. doi: 10.1016/S0140-6736(17)31611-2
62. Mercuri E, Muntoni F, Osorio AN, Tulinius M, Buccella F, Morgenroth LP, et al. Safety and effectiveness of ataluren: comparison of results from the STRIDE Registry and CINRG DMD natural history study. *J Comp Eff Res.* (2020) 9:341–60. doi: 10.2217/cer-2019-0171
63. Mendell JR, Rodino-Klapac LR, Sahenk Z, Roush K, Bird L, Lowes LP, et al. Eteplirsen for the treatment of Duchenne muscular dystrophy. *Ann Neurol.* (2013) 74:637–47. doi: 10.1002/ana.23982
64. Mendell JR, Goemans N, Lowes LP, Alfano LN, Berry K, Shao J, et al. Longitudinal effect of eteplirsen versus historical control on ambulation in Duchenne muscular dystrophy. *Ann Neurol.* (2016) 79:257–71. doi: 10.1002/ana.24555
65. Heo Y-A. Golodirsen: first approval. *Drugs.* (2020) 80:329–33. doi: 10.1007/s40265-020-01267-2
66. Frank DE, Schnell FJ, Akana C, El-Husayni SH, Desjardins CA, Morgan J, et al. Increased dystrophin production with golodirsen in patients with Duchenne muscular dystrophy. *Neurology.* (2020) 94:e2270–82. doi: 10.1212/WNL.0000000000009233
67. Duan D. Systemic AAV micro-dystrophin gene therapy for Duchenne muscular dystrophy. *Mol Ther.* (2018) 26:2337–56. doi: 10.1016/j.ymthe.2018.07.011
68. Mendell JR, Sahenk Z, Lehman K, Nease C, Lowes LP, Miller NF, et al. Assessment of systemic delivery of rAAVrh74.MHCK7.micro-dystrophin in children with Duchenne muscular dystrophy: a nonrandomized controlled trial. *JAMA Neurol.* (2020) 77:1–10. doi: 10.1001/jamaneurol.2020.1484
69. Buyse GM, Goemans N, van den Hauwe M, Thijs D, de Groot IJM, Schara U, et al. Idebenone as a novel, therapeutic approach for Duchenne muscular dystrophy: results from a 12 month, double-blind, randomized placebo-controlled trial. *Neuromuscul Disord.* (2011) 21:396–405. doi: 10.1016/j.nmd.2011.02.016
70. McDonald CM, Meier T, Voit T, Schara U, Straathof CSM, D'Angelo MG, et al. Idebenone reduces respiratory complications in patients with Duchenne muscular dystrophy. *Neuromuscul Disord.* (2016) 26:473–80. doi: 10.1016/j.nmd.2016.06.257
71. Servais L, Straathof CSM, Schara U, Klein A, Leinonen M, Hasham S, et al. Long-term data with idebenone on respiratory function outcomes in patients with Duchenne muscular dystrophy. *Neuromuscul Disord.* (2020) 30:5–16. doi: 10.1016/j.nmd.2019.10.008
72. Campbell C, McMillan HJ, Mah JK, Tarnopolsky M, Selby K, McClure T, et al. Myostatin inhibitor ACE-031 treatment of ambulatory boys with Duchenne muscular dystrophy: results of a randomized, placebo-controlled clinical trial. *Muscle Nerve.* (2017) 55:458–64. doi: 10.1002/mus.25268
73. Dowling JJ, D Gonorazky H, Cohn RD, Campbell C. Treating pediatric neuromuscular disorders: the future is now. *Am J Med Genet A.* (2018) 176:804–41. doi: 10.1002/ajmg.a.38418
74. Liewluck T, Milone M. Untangling the complexity of limb-girdle muscular dystrophies. *Muscle Nerve.* (2018) 58:167–77. doi: 10.1002/mus.26077

75. Fanin M, Angelini C. Progress and challenges in diagnosis of dysferlinopathy. *Muscle Nerve.* (2016) 54:821–35. doi: 10.1002/mus.25367
76. Pozsgai ER, Griffin DA, Heller KN, Mendell JR, Rodino-Klapac LR. Systemic AAV-mediated β-sarcoglycan delivery targeting cardiac and skeletal muscle ameliorates histological and functional deficits in LGMD2E mice. *Mol Ther.* (2017) 25:855–69. doi: 10.1016/j.ymthe.2017.02.013
77. Estepan I. *Sarepta Therapeutics Announces Positive Functional Results from the SRP-9003 (MYO-101) Gene Therapy Trial to Treat Limb-Girdle Muscular Dystrophy Type 2E, or Beta-Sarcoglycanopathy | Sarepta Therapeutics, Inc. Investorrelations*. (2019). Available online at: https://investorrelations.sarepta.com/news-releases/news-release-details/sarepta-therapeutics-announces-positive-functional-results-srp (accessed June 13, 2020).
78. Fougerousse F, Bartoli M, Poupiot J, Arandel L, Durand M, Guerchet N, et al. Phenotypic correction of α-sarcoglycan deficiency by intra-arterial injection of a muscle-specific serotype 1 rAAV vector. *Mol Ther.* (2007) 15:53–61. doi: 10.1038/sj.mt.6300022
79. Mendell JR, Rodino-Klapac LR, Rosales-Quintero X, Kota J, Coley BD, Galloway G, et al. Limb-girdle muscular dystrophy type 2D gene therapy restores alpha-sarcoglycan and associated proteins. *Ann Neurol.* (2009) 66:290–7. doi: 10.1002/ana.21732
80. Mendell JR, Rodino-Klapac LR, Rosales XQ, Coley BD, Galloway G, Lewis S, et al. Sustained alpha-sarcoglycan gene expression after gene transfer in limb-girdle muscular dystrophy, type 2D. *Ann Neurol.* (2010) 68:629–38. doi: 10.1002/ana.22251
81. Cordier L, Hack AA, Scott MO, Barton-Davis ER, Gao G, Wilson JM, et al. Rescue of skeletal muscles of gamma-sarcoglycan-deficient mice with adeno-associated virus-mediated gene transfer. *Mol Ther.* (2000) 1:119–29. doi: 10.1006/mthe.1999.0019
82. Herson S, Hentati F, Rigolet A, Behin A, Romero NB, Leturcq F, et al. A phase I trial of adeno-associated virus serotype 1-γ-sarcoglycan gene therapy for limb girdle muscular dystrophy type 2C. *Brain.* (2012) 135(Pt 2):483–92. doi: 10.1093/brain/awr342
83. Potter RA, Griffin DA, Sondergaard PC, Johnson RW, Pozsgai ER, Heller KN, et al. Systemic delivery of dysferlin overlap vectors provides long-term gene expression and functional improvement for dysferlinopathy. *Hum Gene Ther.* (2018) 29:749–62. doi: 10.1089/hum.2017.062
84. Sondergaard PC, Griffin DA, Pozsgai ER, Johnson RW, Grose WE, Heller KN, et al. AAV.Dysferlin overlap vectors restore function in dysferlinopathy animal models. *Ann Clin Transl Neurol.* (2015) 2:256–70. doi: 10.1002/acn3.172
85. Annoussamy M, Lilien C, Gidaro T, Gargaun E, Chê V, Schara U, et al. X-linked myotubular myopathy: a prospective international natural history study. *Neurology.* (2019) 92:e1852–67. doi: 10.1212/WNL.0000000000007319
86. Wilson JM, Flotte TR. Moving forward after two deaths in a gene therapy trial of myotubular myopathy. *Hum Gene Ther.* (2020) 31:695–6. doi: 10.1089/hum.2020.182
87. Zhao M, Maani N, Dowling JJ. Dynamin 2 (DNM2) as cause of, and modifier for, human neuromuscular disease. *Neurotherapeutics.* (2018) 15:966–75. doi: 10.1007/s13311-018-00686-0
88. Buono S, Ross JA, Tasfaout H, Levy Y, Kretz C, Tayefeh L, et al. Reducing dynamin 2 (DNM2) rescues DNM2-related dominant centronuclear myopathy. *Proc Natl Acad Sci USA.* (2018) 115:11066–71. doi: 10.1073/pnas.1808170115
89. Scharner J, Figeac N, Ellis JA, Zammit PS. Ameliorating pathogenesis by removing an exon containing a missense mutation: a potential exon-skipping therapy for laminopathies. *Gene Ther.* (2015) 22:503–15. doi: 10.1038/gt.2015.8
90. American Association of Neuromuscular & Electrodiagnostic Medicine. Diagnostic criteria for late-onset (childhood and adult) Pompe disease. *Muscle Nerve.* (2009) 40:149–60. doi: 10.1002/mus.21393
91. Cupler EJ, Berger KI, Leshner RT, Wolfe GI, Han JJ, Barohn RJ, et al. Consensus treatment recommendations for late-onset Pompe disease. *Muscle Nerve.* (2012) 45:319–33. doi: 10.1002/mus.22329
92. van der Ploeg AT, Reuser AJJ. Pompe's disease. *Lancet.* (2008) 372:1342–53. doi: 10.1016/S0140-6736(08)61555-X
93. Kishnani PS, Corzo D, Nicolino M, Byrne B, Mandel H, Hwu WL, et al. Recombinant human acid [alpha]-glucosidase: major clinical benefits in infantile-onset Pompe disease. *Neurology.* (2007) 68:99–109. doi: 10.1212/01.wnl.0000251268.41188.04
94. Kishnani PS, Corzo D, Leslie ND, Gruskin D, Van der Ploeg A, Clancy JP, et al. Early treatment with alglucosidase alpha prolongs long-term survival of infants with Pompe disease. *Pediatr Res.* (2009) 66:329–35. doi: 10.1203/PDR.0b013e3181b24e94
95. van der Ploeg AT, Clemens PR, Corzo D, Escolar DM, Florence J, Groeneveld GJ, et al. A randomized study of alglucosidase alfa in late-onset Pompe's disease. *N Engl J Med.* (2010) 362:1396–406. doi: 10.1056/NEJMoa0909859
96. Kohler L, Puertollano R, Raben N. Pompe disease: from basic science to therapy. *Neurotherapeutics.* (2018) 15:928–42. doi: 10.1007/s13311-018-0655-y
97. Hahn A, Schänzer A. Long-term outcome and unmet needs in infantile-onset Pompe disease. *Ann Transl Med.* (2019) 7:283. doi: 10.21037/atm.2019.04.70
98. Koeberl DD, Case LE, Desai A, Smith EC, Walters C, Han S-O, et al. Improved muscle function in a phase I/II clinical trial of albuterol in Pompe disease. *Mol Genet Metab.* (2020) 129:67–72. doi: 10.1016/j.ymgme.2019.12.008
99. Ronzitti G, Collaud F, Laforet P, Mingozzi F. Progress and challenges of gene therapy for Pompe disease. *Ann Transl Med.* (2019) 7:287. doi: 10.21037/atm.2019.04.67

Conflict of Interest: MF-B received honoraria for participation in advisory boards and consultancy fees from Biogen, Roche, and PTC.

The remaining author declares that the research was conducted in the absence of any commercial or financial relationships that could be construed as a potential conflict of interest.

frontiers in Genetics

ORIGINAL RESEARCH
published: 20 January 2021
doi: 10.3389/fgene.2020.590924

Characteristics of Genetic Variations Associated With Lennox-Gastaut Syndrome in Korean Families

Jin Ok Yang[1,2†], Min-Hyuk Choi[3,4†], Ji-Yong Yoon[3], Jeong-Ju Lee[3], Sang Ook Nam[5], Soo Young Jun[3], Hyeok Hee Kwon[6], Sohyun Yun[3], Su-Jin Jeon[3,4], Iksu Byeon[1], Debasish Halder[3], Juhyun Kong[5], Byungwook Lee[1], Jeehun Lee[7], Joon-Won Kang[8] and Nam-Soon Kim[3,4]**

[1] Korea BioInformation Center, Korea Research Institute of Bioscience and Biotechnology, Daejeon, South Korea, [2] Department of Bio and Brain Engineering, Korea Advanced Institute of Science and Technology, Daejeon, South Korea, [3] Rare-Disease Research Center, Korea Research Institute of Bioscience and Biotechnology, Daejeon, South Korea, [4] Department of Functional Genomics, Korea University of Science and Technology, Daejeon, South Korea, [5] Department of Pediatrics, Pusan National University Children's Hospital, Pusan National University School of Medicine, Yangsan, South Korea, [6] Department of Medical Science and Anatomy, Chungnam National University, Daejeon, South Korea, [7] Department of Pediatrics, Samsung Medical Center, Sungkyunkwan University School of Medicine, Seoul, South Korea, [8] Department of Pediatrics and Medical Science, Chungnam National University Hospital, College of Medicine, Chungnam National University, Daejeon, South Korea

OPEN ACCESS

Edited by:
Oliver Semler,
University Hospital of Cologne, Germany

Reviewed by:
Pasquale Striano,
University of Genoa, Italy
Aglaia Vignoli,
University of Milan, Italy

***Correspondence:**
Nam-Soon Kim
nskim37@kribb.re.kr
Joon-Won Kang
childlove@cnu.ac.kr

[†] These authors have contributed equally to this work

Specialty section:
This article was submitted to Genetics of Common and Rare Diseases, a section of the journal Frontiers in Genetics

Received: 03 August 2020
Accepted: 31 December 2020
Published: 20 January 2021

Citation:
Yang JO, Choi M-H, Yoon J-Y, Lee J-J, Nam SO, Jun SY, Kwon HH, Yun S, Jeon S-J, Byeon I, Halder D, Kong J, Lee B, Lee J, Kang J-W and Kim N-S (2021) Characteristics of Genetic Variations Associated With Lennox-Gastaut Syndrome in Korean Families. Front. Genet. 11:590924. doi: 10.3389/fgene.2020.590924

Lennox-Gastaut syndrome (LGS) is a severe type of childhood-onset epilepsy characterized by multiple types of seizures, specific discharges on electroencephalography, and intellectual disability. Most patients with LGS do not respond well to drug treatment and show poor long-term prognosis. Approximately 30% of patients without brain abnormalities have unidentifiable causes. Therefore, accurate diagnosis and treatment of LGS remain challenging. To identify causative mutations of LGS, we analyzed the whole-exome sequencing data of 17 unrelated Korean families, including patients with LGS and LGS-like epilepsy without brain abnormalities, using the Genome Analysis Toolkit. We identified 14 mutations in 14 genes as causes of LGS or LGS-like epilepsy. 64 percent of the identified genes were reported as LGS or epilepsy-related genes. Many of these variations were novel and considered as pathogenic or likely pathogenic. Network analysis was performed to classify the identified genes into two network clusters: neuronal signal transmission or neuronal development. Additionally, knockdown of two candidate genes with insufficient evidence of neuronal functions, *SLC25A39* and *TBC1D8*, decreased neurite outgrowth and the expression level of *MAP2*, a neuronal marker. These results expand the spectrum of genetic variations and may aid the diagnosis and management of individuals with LGS.

Keywords: Lennox-Gastaut syndrome, epilepsy, whole-exome sequencing, genetic variation, Rare-diseases

INTRODUCTION

Lennox-Gastaut syndrome (LGS) is a severe form of childhood-onset epilepsy with a heterogeneous etiology, and epileptiform abnormalities may contribute to progressive dysfunction (Lund et al., 2014; Asadi-Pooya, 2018). The primary features of LGS are multiple types of seizures (generalized tonic, atonic, and atypical absence), generalized slow spike-and-wave or generalized paroxysmal

fast activity discharges on electroencephalography, and intellectual disabilities (Camfield, 2011; Asadi-Pooya, 2018). In approximately 70% of patients with LGS, this disease is caused by brain damage, infection, and brain malformation. Thirty percent of LGS patients do not present abnormalities in brain imaging, and thus the cause of their condition is unclear (Asadi-Pooya, 2018). Functional magnetic resonance imaging studies showed that abnormal network connectivity in subcortical structures causes LGS (Pedersen et al., 2015). Hence, several researchers have focused on screening genetic risk factors from patients with LGS without abnormalities by next-generation sequencing.

Recently, several causative genetic variations related to LGS and epilepsy, which play important roles in the development of these syndromes, have been detected by whole-exome sequencing (WES; Allen et al., 2013, 2015; Lund et al., 2013; Terrone et al., 2014; Zerem et al., 2016; Wang et al., 2017; Asadi-Pooya, 2018; Dunn et al., 2018; Tumiene et al., 2018). Nevertheless, effective treatments and an understanding of the genetic basis of LGS are lacking because the biological mechanisms of LGS are not well-understood. The seizure frequency is either controlled by administering anti-epileptic medicine to patients or stimulating the vagus nerve. Therefore, comprehensive information from LGS-related genetic variations and networks is required to identify markers influencing LGS.

In this study, we examined novel candidate genetic variations and networks associated with LGS without brain abnormalities as genetic markers. First, we collected 58 WES datasets from 17 Korean families with a clinical history of LGS or LGS-like epilepsy without brain abnormalities. We investigated the causative variations in each family and relationships among genes and these variations, and then estimated the genetic risk factors for LGS. We found that these variations contained 14 mutations, including *de novo*, autosomal recessive (AR), and X-linked mutations. Several genes showed novel variations and were found to be associated with LGS or epilepsy. Depletion of two candidate genes with insufficient evidence of neuronal functions decreased neurite outgrowth in the SH-SY5Y cell line. This finding provides a more informative resource for LGS-related genetic variations and may contribute to the diagnosis of and therapeutic platform development for LGS and LGS-like epilepsy.

MATERIALS AND METHODS

Clinical Specimens of Korean Patients With LGS

We collected 58 samples from 17 affected individuals and 41 unaffected individuals. These subjects were from 17 unrelated Korean families containing either 10 patients with LGS or 7 patients with LGS-like epilepsy (**Figure 2**). Patients with an incomplete phenotype of LGS were categorized as having LGS-like epilepsy. The magnetic resonance imaging results were normal (15 patients) or showed non-epileptogenic abnormalities (2 patients), including arachnoid cyst, posterior fossa, and brain atrophy. The mean age at seizure onset was 3.3 years (range 0.16–12 years). All patients diagnosed with LGS or LGS-like epilepsy were older than 3 years. Affected individuals presented with various seizure types: tonic (16/17), atonic (6/17), generalized tonic-clonic (4/17), myoclonic (4/17), and atypical absence (8/17; **Table 1**). All patients underwent neurologic and genetic evaluations based on the clinical criteria of LGS by an experienced neurologist (Camfield, 2011). LGS is characterized by: (1) a clinical triad of various types of generalized seizures, including generalized tonic, atonic, myoclonic, atypical absence seizures, and epileptic spasms; (2) generalized slow spikes and waves and/or generalized paroxysmal rapid activity for electroencephalography; and (3) progressive developmental regression after seizure onset. LGS-like epilepsy is broadly defined to result in at least two types of generalized seizures, including tonic seizures, or a combination of atonic and atypical absence seizures, learning disabilities, resistance to treatment, and bilateral synchronous epileptic discharges. Ethical approval for the study was obtained from the Institutional Review Board and Ethics Committee at the Chungnam National University Hospitals and Korea Research Institute of Bioscience and Biotechnology. Written informed consent was obtained from all participants or their legal representatives. Available clinical information on these patients is shown in **Table 1**.

Analysis of Genetic Variations and Annotation

We obtained high-throughput WES data from all participants by HiSeq 2500 (Illumina, San Diego, CA, United States). All sequencing reads were mapped to the human reference genome GRCh38/hg38 by using Burrows-Wheeler Aligner software (v0.7.17). Variant calling and functional annotation were performed using the Genome Analysis Toolkit (GATK4, Broad Institute, MA, United States) and ANNOVAR (Version 2018Apr16), respectively, (McKenna et al., 2010; Wang et al., 2010). For the rare-disease study, mutations with less than 5% minor allele frequency in our data were selected using genetic variation data in the Single Nucleotide Polymorphism Database (dbSNP, https://www.ncbi.nlm.nih.gov/snp/), NHLBI Grand Opportunity Exome Sequencing Project database (ESP6500, https://evs.gs.washington.edu/EVS/), and 1000 Genomes Project[1]. We also examined the allele frequency of candidate genetic variations using the Exome Aggregation Consortium (ExAC, http://exac.broadinstitute.org/) and Genome Aggregation Database (gnomAD, https://gnomad.broadinstitute.org/), and ethnic mutations were removed by referencing 1,055 healthy Korean WES data (KOVA v1, http://kobic.re.kr/kova/). To validate these genetic variants, we carried out Sanger sequencing using an ABI3730XL DNA sequencer (Applied Biosystems, Foster City, CA, United States). We also identified copy number variations (CNVs) by CODEX, which is based on a multi-sample normalization model (Jiang et al., 2015). It includes terms that specifically remove biases due to GC content, exon length, and targeting and amplification efficiency. We normalized the WES read count data of each patient with LGS and LGS-like epilepsy based on the read depth of unaffected individuals, after which we derived *de novo* CNVs. CNVs were validated by array-based SNP analysis (Illumina

[1]https://www.internationalgenome.org/

TABLE 1 | Clinical features of patients with LGS and LGS-like epilepsy.

Family/Patient number (Gender)	Seizure onset	Seizure types	AEDs	Response to therapy	EEG	Brain MRI	Epileptic syndrome	Additional symptom	Phenotypes in unaffected individuals
1 (M)	9 y	Tonic, atonic, atypical absence	Valproic acid, Rufinamide	Intractable	GPFA, GSSW	Normal	LGS	DD	None
2 (F)	4 m	Tonic, atypical absence	Valproic acid, Clobazam, Rufinamide, Levetiracetam	Intractable	GPFA, GSSW	Normal	LGS	DD	None
3 (M)	12 y	Tonic, atonic	Valproic acid, Lamotrigine, Rufinamide, Levetiracetam, Lacosamide	Intractable	GPFA, GSSW	Normal	LGS	DD	None
4 (F)	2 y	Tonic, atypical absence	Valproic acid, Rufinamide	Intractable	GPFA, GSSW	Normal	LGS	DD	None
5 (M)	7 y	Tonic, atonic	Rufinamide, Valproic acid, Oxcarbazepine, Topiramate, Levetiracetam, Clobazam	Intractable	GPFA, GSSW	Normal	LGS	DD	None
6 (M)	1 y	Tonic, atonic, atypical absence	Valproic acid, Levetiracetam, Zonisamide, Clobazam	Intractable	GPFA, GSSW	Normal	LGS	DD	Mild ID (Maternal grandmother, mother)
7 (M)	4 m	Tonic, myoclonic	Topiramate, Valproic acid, Clobazam, Lamotrigine, Perampanel	Intractable	GPFA, GSSW	Normal	LGS	Infantile spasms	None
8 (M)	6 m	Tonic, atypical absence	Clobazam, Vigabatrin, Rufinamide, Levetiracetam	Intractable	GPFA, GSSW	Arachnoid cyst, posterior fossa	LGS	Infantile spasms	None
9 (M)	19 m	Generalized tonic-clonic, tonic, atypical absence, myoclonic	Vigabatrin, Clobazam, Zonisamide	Intractable	GPFA, GSSW	Normal	LGS	DD, ID	None
10 (M)	7 m	Generalized tonic-clonic, tonic, myoclonic	Valproic acid, Phenobarbital, Lacosamide, Oxcarbazepine, Rufinamide	Intractable	GPFA, GSSW	Normal	LGS	DD, ID	None
11 (F)	4 y	Tonic, atonic	Valproic acid	Good	GSSW	Normal	LGS-like	DD	None
12 (M)	2 y	Tonic	Valproic acid, Clobazam, Rufinamide	Good	GPFA, GSSW	Normal	LGS-like	DD	None
13 (M)	3 y	Tonic, atonic	Levetiracetam	Good	GSSW	Normal	LGS-like	DD	None
14 (M)	3 y	Tonic, atypical absence	Valproic acid	Intractable	GSSW	Normal	LGS-like	ID	None
15 (F)	3 m	Tonic, myoclonic, partial	Topiramate, Valproic acid, Clobazam, Levetiracetam, Vigabatrin, Zonisamide	Intractable	GPFA	Normal	LGS-like	DD, ID	None
16 (M)	10 y	Generalized tonic-clonic, atypical absence	Topiramate, Lamotrigine, Valproic acid, Clobazam, Perampanel	Intractable	GSSW	Normal	LGS-like	DD, ID	None
17 (M)	2 m	Generalized tonic-clonic, tonic	Topiramate, Valproic acid, Clobazam, Vigabatrin, Levetiracetam, Phenobarbital	Intractable	GPFA	Brain atrophy	LGS-like	DD, ID	None

Abbreviations: y, year; m, month; AEDs, Anti-epileptic drugs; EEG, Electroencephalography; GPFA, Generalized paroxysmal fast activity; GSSW, Generalized slow spike-and-wave; DD, Developmental delay; ID, Intellectual disability; and MRI, Magnetic resonance imaging.

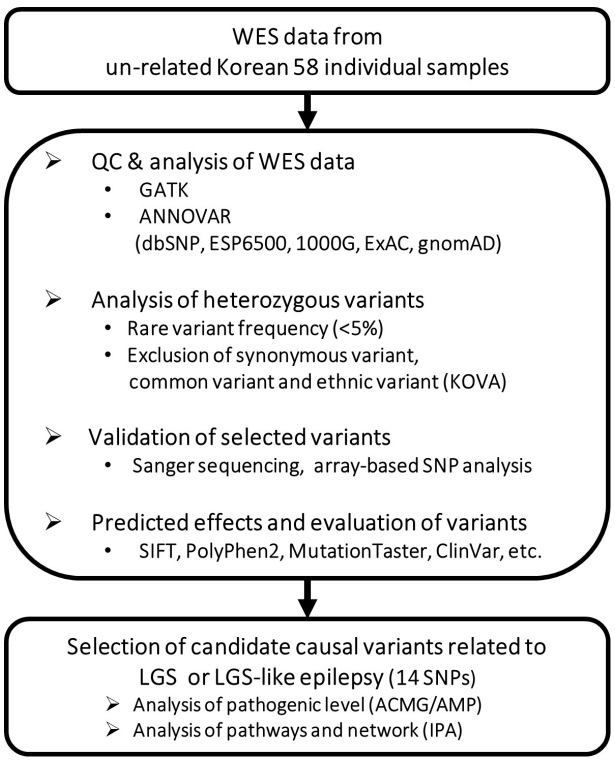

FIGURE 1 | Workflow for identifying potential causative genetic variants related to LGS or LGS-like epilepsy.

Infinium Omni2.5-8 BeadChip; **Supplementary Methods**). The family dataset without candidate markers was excluded. The summarized workflow is shown in **Figure 1**.

Pathogenicity Prediction and Pathway Analysis

We investigated the pathogenicity of all mutations using the ClinVar database and prediction algorithms in ANNOVAR (PolyPhen2, SIFT, LRT, and MutationTaster; Chun and Fay, 2009; Adzhubei et al., 2010; Schwarz et al., 2010; Sim et al., 2012). Additionally, we evaluated pathogenicity using criteria described in the American College of Medical Genetics and Association for Molecular Pathology guidelines, after which we selected genes with damaging, possibly damaging, pathogenic, or likely pathogenic mutations as candidate genes of LGS and LGS-like epilepsy (Richards et al., 2015).

We performed Ingenuity Pathway Analysis (QIAGEN, Hilden, Germany) to explore the pathways and networks associated with selected candidate gene sets, and classified genes according to their functions by using Database for Annotation, Visualization and Integrated Discovery (DAVID, https://david.ncifcrf.gov).

Neurite Outgrowth Assay

Human SH-SY5Y neuroblastoma cells were transfected with target siRNAs for 24 h and then treated with retinoic acid for 48 h. Cells were then fixed in 4% paraformaldehyde for 1 h at room temperature (RT), permeabilized with 0.1% Triton X-100 in PBS for 15 min, and incubated in blocking reagent (5% normal fetal bovine serum in PBS) for 1 h. Cells were incubated with primary antibody against MAP2, a neuronal marker (Mouse Anti-MAP2, Abcam, Cambridge, United Kingdom), at 4°C overnight, followed by incubation with a secondary antibody (Alexa Fluor 488, Goat anti-mouse, Life Technologies, California, United States) at RT for 1 h. For nuclear counterstaining, the cells were incubated with DAPI solution (300 nM in PBS) for 5 min at RT and then observed with a fluorescence microscope (Eclipse Ti-S, Nikon, Tokyo, Japan). To measure neurite length in SH-SY5Y cells, neurite length was calculated as the longest neurite distance from the cell body (direct path to the soma) on each neuron showing MAP2 (green) using ImageJ software (10 calculated cells per group). The mRNA expression levels of target genes and MAP2 were analyzed by real-time PCR.

RESULTS

Annotation of Genetic Variations as Candidates for LGS and LGS-Like Epilepsy

We identified 14 mutations as candidates for causing LGS and LGS-like epilepsy. Two mutations were in the splicing site and 12 mutations were in the coding region. Among the coding region mutations, there was one frameshift deletion, one non-frameshift insertion, and 10 single-nucleotide variations (**Table 2** and **Supplementary Figure 1**).

CACNA1A, *CHD2*, *IQSEC2*, and *SCN10A* were LGS-related genes. *DNAJC5*, *FRRS1L*, *SHANK3*, *SYN1*, and *SYN2* were epilepsy-related genes. *MAGI1*, *NRG2*, *SLC25A39*, *SSPO*, and *TBC1D8* were functionally related to neurons or brain-expressed ion channels (**Figure 3A** and **Table 2**). Except for mutations in *FRRS1L*, *NRG2*, *SHANK3*, *SLC25A39*, *SSPO*, *SYN1*, and *SYN2*, the remaining mutations were novel.

Mendelian Inheritance Pattern

Among the 17 families, one family contained members with mild intellectual disability, whereas disorders were not present in members of the other 16 families (**Figure 2** and **Table 1**). We identified three AR (21%), one X-linked inherited (7%), five *de novo* (36%), and five potentially *de novo* mutations (36%; **Figure 3B**). Remarkably, as shown in **Table 2**, mutations in *CACNA1A*, *FRRS1L*, and *SSPO* were detected as AR in families 9, 10, and 11, in which unaffected parents possessed heterozygous mutations and the patients had homozygous mutations. The *IQSEC2* mutation was inherited as X-linked in family 6, in which the maternal grandmother and mother of the patient had mild intellectual disability with heterozygous mutations, whereas the male patient had hemizygous mutations. Genes such as *CHD2*, *DNAJC5*, *NRG2*, *SLC25A39*, and *TBC1D8* showed *de novo* mutations. *MAGI1*, *SCN10A*, *SHANK3*, *SYN1*, and *SYN2* were considered as unknown, potentially *de novo* mutations,

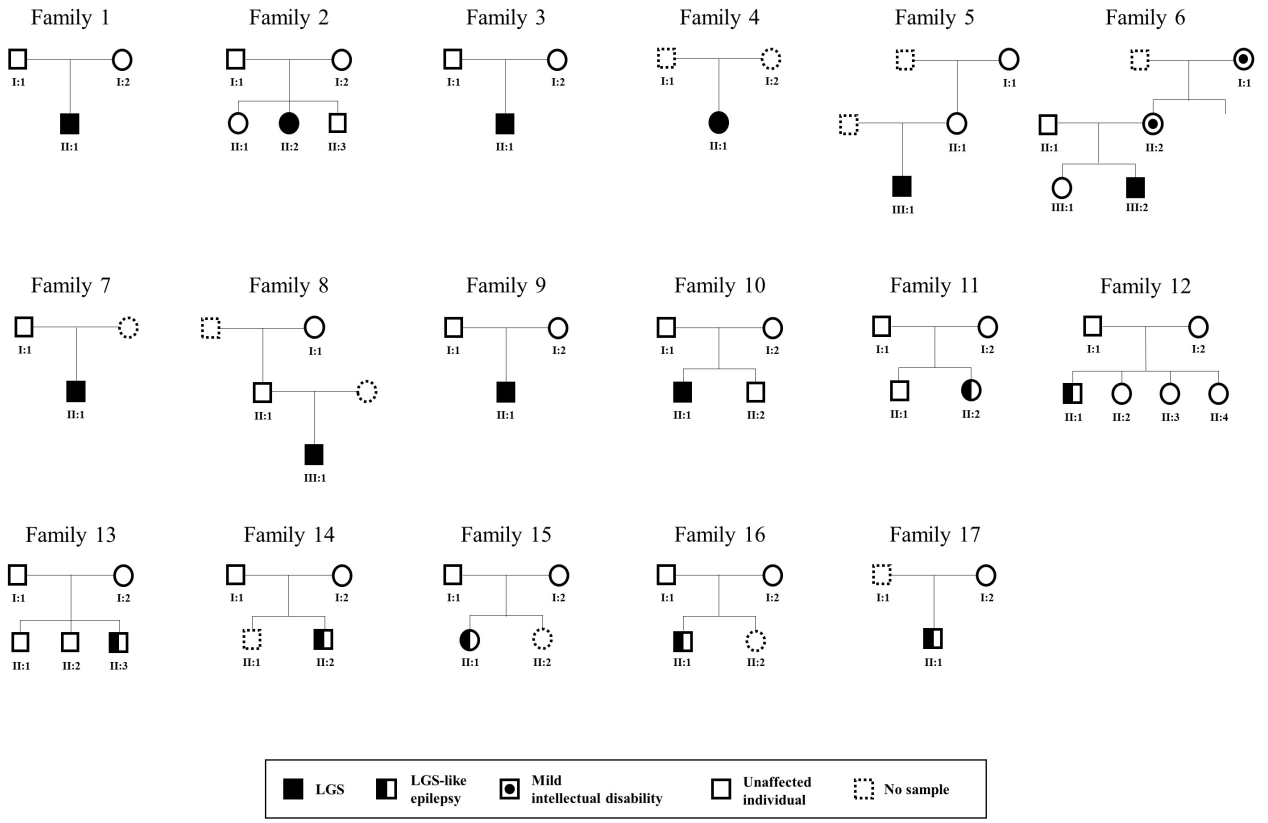

FIGURE 2 | Pedigree of LGS or LGS-like epilepsy families. Males and females are represented as squares and circles, respectively. Patients with LGS are indicated as completely filled symbols, and those with LGS-like epilepsy are indicated as half-filled symbols. The circle with dots indicates females with mild intellectual disabilities.

TABLE 2 | Potential causative genetic variations in patients with LGS or LGS-like epilepsy.

Patient	Inheritance	Gene name	NT, AA change	dbSNP ID	Description	ACMG/AMP	
						Criteria	Classification
1	*De novo*	*SLC25A39*	c.C112T, p.R38C	rs757102633	Neuron-related	PM2, PP3	Uncertain significance
3	*De novo*	*TBC1D8*	c.T1547G, p.L516R	None	Neuron-related	PM2, PP3	Uncertain significance
4	Unknown	*SYN1*	c.C1666T, p.R556C	rs1441575488	Epilepsy-related	PM1, PM2, PM6, PP3	Likely pathogenic
5	Unknown	*SHANK3*	c.C3746T, p.P1249L	rs757572910	Epilepsy-related	PM6, PP3	Uncertain significance
6	X-linked	*IQSEC2*	c.G1048A, p.A350T	None	LGS-related	PM1,PM2,PM5, PP3	Likely pathogenic
7	Unknown	*SYN2*	c.A1379G, p.Q460R	rs2289706	Epilepsy-related	PM2, PM6, PP3	Uncertain significance
8	Unknown	*MAGI1*	c.T2475G, p.F825L	None	Neuron-related	PM2, PP3	Uncertain significance
9	AR	*CACNA1A*	c.6975_ 6976ins CAGCAGCAGCAG, p.Q2325_ A2326ins QQQQ	None	LGS- related	PM3	Uncertain significance
10	AR	*FRRS1L*	c.G615T[#], p.M205I	rs750750976	Epilepsy-related	PVS1, PM1, PM2, PM3, PP3	Pathogenic
11	AR	*SSPO*	c.12608delC, p.Q4204Rfs*41	rs11353848	Neuron-related	PM3, PM4	Uncertain significance
12	*De novo*	*CHD2*	c.443 + 1G > A	None	LGS-related	PVS1, PS2, PM2, PP3	Pathogenic
14	*De novo*	*NRG2*	c.C835T, p.R279C	rs1226659673	Neuron-related	PM2, PP3	Uncertain significance
15	*De novo*	*DNAJC5*	c.C141A, p.N47K	None	Epilepsy-related	PS2, PM2, PP3	Likely pathogenic
17	Unknown	*SCN10A*	c.389 + 2T > C	None	LGS-related	PVS1,PM2,PP3	Pathogenic

[#]*This variation exists in the last nucleotide of exon 3 and is predicted to affect splicing.*

Abbreviations: AR, Autosomal recessive; NT, Nucleotide; AA, Amino acid; NA, Not available; and Unknown indicates potentially de novo.

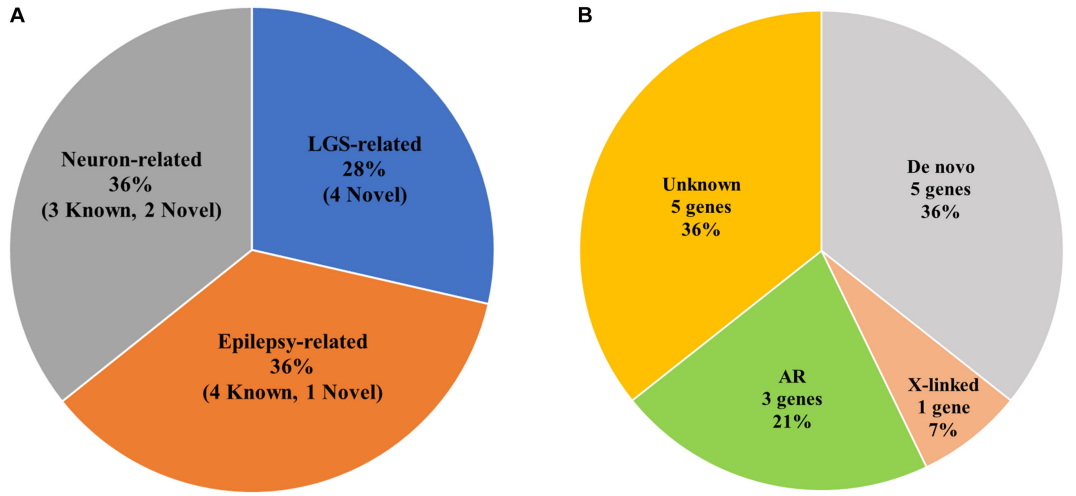

FIGURE 3 | Statistics of genetic variations in candidate genes of LGS or LGS-like epilepsy. **(A)** Pie chart of the frequency of LGS, epilepsy, or neuron-related genes. () indicates the number of genetic variations in candidate genes. **(B)** Ratio of Mendelian inheritance patterns of candidate genes.

as they were found in patients from single-parent or adoptive families (**Figure 3B**).

Pathogenicity Validation for Genetic Variations

Mutations in *FRRS1L*, *NRG2*, *SHANK3*, *SLC25A39*, *SSPO*, *SYN1*, and *SYN2* have been reported previously but their functional significance was not determined by ClinVar. In addition, other mutations were not reported in databases such as dbSNP, ClinVar, ExAC, ESP6500, gnomAD, and the 1000 Genomes Project. According to PolyPhen2, SIFT, LRT, and MutationTaster, damaging mutations were found in *DNAJC5*, *FRRS1L*, and *IQSEC2* in all pathogenicity prediction results, with the remaining mutations classified as possibly damaging or of unknown pathogenicity. According to the American College of Medical Genetics/Association for Molecular Pathology guidelines, the *CHD2*, *DNAJC5*, *FRRS1L*, *IQSEC2*, *SCN10A*, and *SYN1* mutations were sorted into pathogenic or likely pathogenic groups. Particularly, the *FRRS1L* mutation (c.615G > *T*, p.205M > *I*) at the last nucleotide of exon 3 may affect splicing. *FRRS1L* is related to epileptic encephalopathy, and its pathogenic variants have been reported previously (Madeo et al., 2016; Han et al., 2017). Based on these findings, the *FRRS1L* mutation was assigned to PVS1. The detailed criteria and classification results are presented in **Table 2** and **Supplementary Table 1**.

Systematic Analysis of Candidate Genes

We examined gene interaction networks and functional annotations to comprehensively understand the relationships among the candidate genes of LGS and LGS-like epilepsy. Based on gene ontology annotations by DAVID, these gene sets were enriched in biological functions including synaptic transmission, ion transport, MAPK cascade, and transcription (**Table 3**). Ingenuity Pathway Analysis revealed that the candidate genes were divided into two clusters. The first cluster comprised 11 genes (*CACNA1A*, *DNAJC5*, *FRRS1L*, *IQSEC2*, *MAGI1*, *NRG2*, *SHANK3*, *SLC25A39*, *SSPO*, *SYN1*, and *SYN2*), which functionally belong to synaptogenesis signaling, calcium signaling, and AMPA signaling. This gene set was associated with neurotransmission (**Figure 4A**). Another cluster, consisting of three genes (*CHD2*, *SCN10A*, and *TBC1D8*), was associated with cellular assembly and organization, nervous system development and function, and ion channels, as well as neurological disease, skeletal and muscular disorders, and behavioral disorders (**Figure 4B**). These data indicate that the candidate genes play important roles in LGS development.

Neurite Alteration in *SLC25A39* and *TBC1D8* Knockdown Cell Lines

Among neuron-related genes, the direct neuronal functions of *SLC25A39* and *TBC1D8* have not been reported: *Shawn*, the *Drosophila* homolog of *SLC25A39* and *SLC25A40*, reportedly plays a role in neurotransmitter release (Slabbaert et al., 2016) and *TBC1D24*, a member of the protein family of *TBC1D8*, regulates neuronal migration (Riazuddin et al., 2017). To examine the effects of *SLC25A39* and *TBC1D8* on neuronal function, we depleted *SLC25A39* and *TBC1D8* from the SH-SY5Y neuroblastoma cell line and examined neurite outgrowth. siRNA treatment of target genes decreased *SLC25A39* and *TBC1D8* expression by approximately 40%. Under retinoic acid-induced neuronal differentiation conditions, the mRNA level of *MAP2* was significantly decreased in *SLC25A39* or *TBC1D8* knockdown cells (**Figure 5A**). Additionally, the neurite length was reduced by 30% in the *TBC1D8* knockdown group and by 40% in the *SLC25A39* knockdown group compared to in the control, indicating impaired neuronal development (**Figures 5B,C**). These results suggest that *SLC25A39* and *TBC1D8* are involved in the neurite extension of neuronal cells.

TABLE 3 | Gene ontology results of candidate genes of LGS or LGS-like epilepsy.

Gene symbol	Description	GO term	Function	Related pathway
FRRS1L	Ferric chelate reductase 1 like	GO:0005886	Plasma membrane	AMPA receptor biogenesis
IQSEC2	IQ motif and Sec7 domain 2	GO:0030036	Actin cytoskeleton organization	AMPA receptor regulation
SSPO	SCO-spondin	GO:0007155	Cell adhesion	Central nerve system formation
CHD2	Chromodomain helicase DNA binding protein 2	GO:0006351	Transcription	Chromatin remodeling
SLC25A39	Solute carrier family 25 member 39	GO:0006412	Translation	Heme biosynthesis
CACNA1A	Calcium voltage-gated channel subunit alpha1 A	GO:0000096	Sulfur amino acid metabolic process	Ion channel
SCN10A	Sodium voltage-gated channel alpha subunit 10	GO:0002027	Regulation of heart rate	Ion channel
MAGI1	Membrane associated guanylate kinase, WW and PDZ domain containing 1	GO:0006461	Protein complex assembly	Neurite outgrowth
SHANK3	SH3 and multiple ankyrin repeat domains 3	GO:0000165	MAPK cascade	Neurotransmission
SYN1	Synapsin I	GO:0007268	Chemical synaptic transmission	Neurotransmitter release cycle
SYN2	Synapsin II	GO:0007268	Chemical synaptic transmission	Neurotransmitter release cycle
DNAJC5	Dnaj heat shock protein family (Hsp40) member C5	GO:0006887	Exocytosis	Protein folding
NRG2	Neuregulin 2	GO:0000165	MAPK cascade	Regulates neurite outgrowth and neuron cell survival
TBC1D8	TBC1 domain family member 8	GO:0006886	Intracellular protein transport	Vesicle-mediated transport

Abbreviation: GO, Gene ontology.

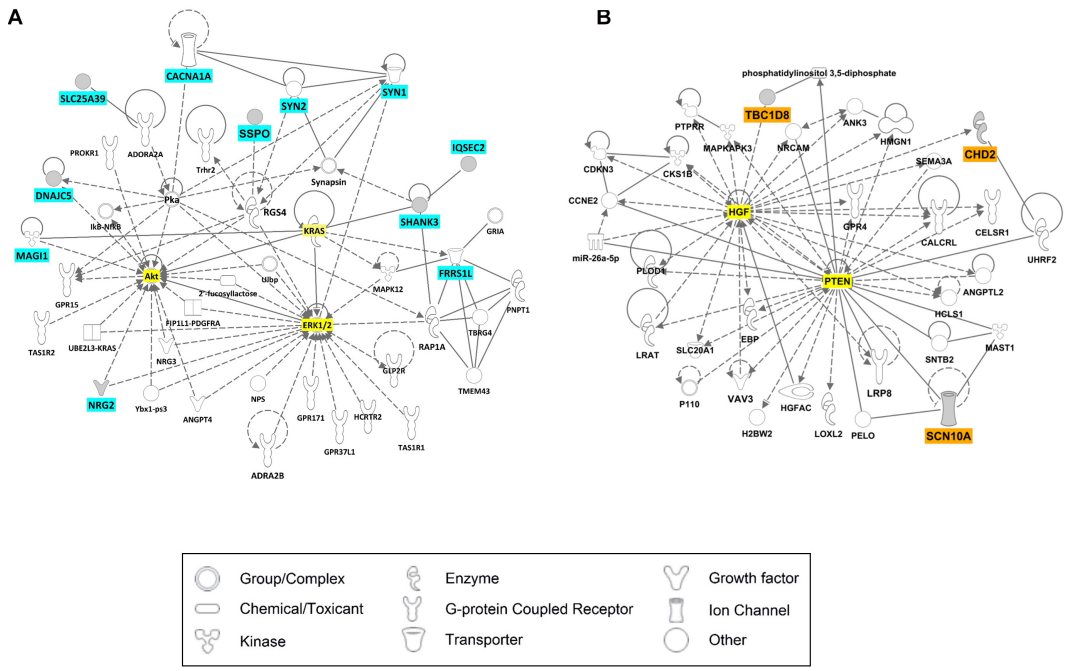

FIGURE 4 | Ingenuity Pathway Analysis (IPA) results for candidate genes of LGS or LGS-like epilepsy. The genes with cyan or orange colors indicate candidate genes selected in this study. The genes with yellow color represent those most relevant to the candidate genes. **(A)** Cell signaling network. **(B)** Neurological disease network.

DISCUSSION

Genetic variations play an important role in the development of epileptic syndromes, including LGS without brain abnormalities, by altering neurotransmission or neuronal development (Falace et al., 2014; Lund et al., 2014; Fedele et al., 2018). In this study, we identified 14 candidate genes and genetic variations related to neuronal development or neurotransmission as biomarkers of LGS and LGS-like epilepsy with unknown causes. Of these, seven mutations were novel. In addition, two genes showed insufficient evidence for epilepsy or neuronal functions; however, we demonstrated that these genes affect neurite outgrowth in a human neuroblastoma cell line.

Pathogenicity evaluation of genetic variations in our candidate genes, with probability used as a risk factor for LGS and LGS-like epilepsy, revealed that several variations were pathogenic

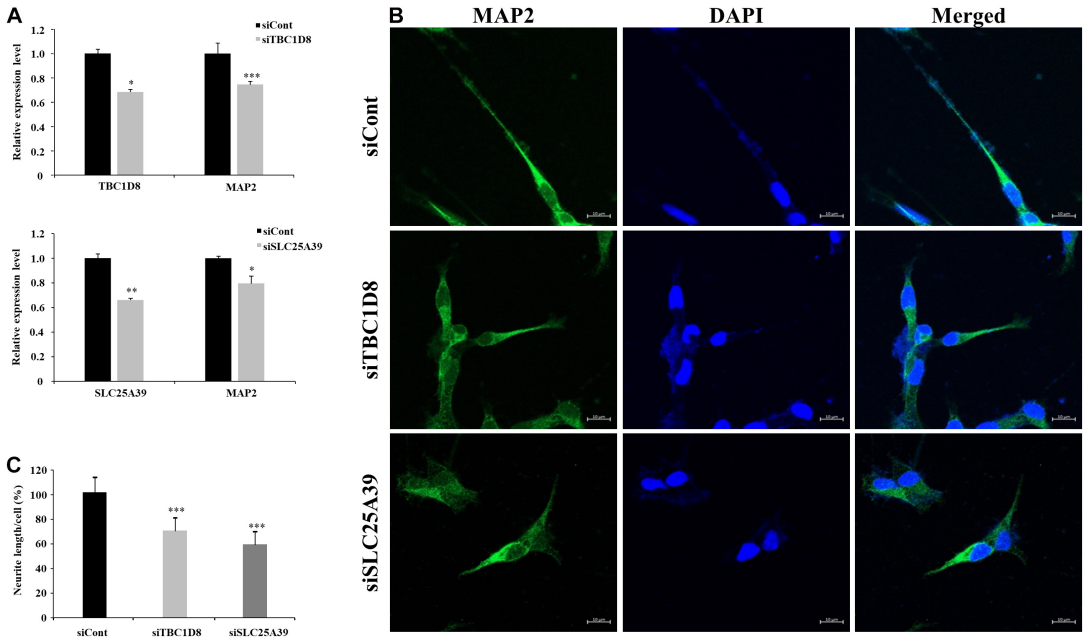

FIGURE 5 | Neurite length analysis by knockdown of candidate genes in neuronal cells. Human SH-SY5Y neuroblastoma cells were transfected with siRNA for *TBC1D8* and *SLC25A39* on day 3 *in vitro* (DIV 3). *MAP2* was used as a neuronal marker. **(A)** Expression levels of *TBC1D8*, *SLC25A39*, and *MAP2* were analyzed by RT-PCR ($n = 3$). **(B)** After retinoic acid stimulation for 48 h, the cells were stained for *MAP2* (green) and nuclei (blue). Scale bars: 30 μm. **(C)** Neurite length was measured in more than 10 cells in three independent experiments. $^{*}p < 0.05$, $^{**}p < 0.01$, $^{***}p < 0.001$, and Student's *t*-test compared with the control group.

or likely pathogenic. In addition, variations reported in four genes, *IQSEC2*, *SYN1*, *SYN2*, and *FRRSIL*, were in a domain position similar to those in the candidate genes and classified as pathogenic or of uncertain significance according to ClinVar classification (**Supplementary Table 2**). Furthermore, the protein stability of the 10 candidate genes was altered by isoelectric point changes via side chain modifications of amino acids by genetic variations, implicating the effect of protein function (**Supplementary Table 3**). Collectively, these results indicate that our variations are associated with LGS and LGS-like epilepsy. However, genotype-phenotype data and gene-specific mutation rates for our candidate genes were not provided because these variants were rare.

Among the genes with 14 genetic variations, including seven novel mutations, *MAGI1*, *NRG2*, *SSPO*, *SLC25A39*, and *TBC1D8* were not associated with LGS or epilepsy. However, they were selected as candidate genes because of their roles in neuronal development. *MAGI1*, *NRG2*, and *SSPO* exert neuron-related functions. *MAGI1* plays a role in regulating neurite outgrowth (Ito et al., 2012). *SSPO* promotes neuronal survival and differentiation and is required during early brain development (Goncalves-Mendes et al., 2004; Vera et al., 2013). *NRG2* promotes neuronal survival and neurite extension (Nakano et al., 2016). *SLC25A39* resides in susceptibility loci for epilepsy with heterogeneous phenotypes but not as an epilepsy-related gene because its variant has not been identified in families with epilepsy (Siren et al., 2010). However, a variant of *SLC25A39* was identified in our LGS data, and depletion of *SLC25A39* decreased neurite outgrowth in human neuroblastoma cells. These data suggest a relationship between LGS and epilepsy with *SLC25A39*. These findings are also supported by previous studies in which mutations in *Shawn*, the *Drosophila* homolog of *SLC25A39* and *SLC25A40*, increase neurotransmitter release (Slabbaert et al., 2016). *TBC1D24*, a member of the same protein family as *TBC1D8*, regulates neuronal migration and its epilepsy-related mutation is in the Rab-GAP TBC domain, which is the same domain containing the mutation evaluated in our study (Falace et al., 2014; Banuelos et al., 2017). Alternatively, mutations in *TBC1D8* have been detected in patients with intellectual disability without an epilepsy phenotype (Riazuddin et al., 2017). However, our data revealed mutations of *TBC1D8* in Korean patients with LGS as well as decreased neurite outgrowth in human neuroblastoma cells by depletion of *TBC1D8*, suggesting that *TBC1D8* is a candidate gene for LGS or epilepsy. Epileptic seizure is defined as the transient occurrence of signs and/or symptoms because of abnormal excessive or synchronous neutral activity in the brain. Previous studies showed that epilepsy or LGS phenotypes may occur when neurotransmission and neuronal development in the brain are disrupted (Hermann et al., 2002; Staley, 2015; Fukata and Fukata, 2017; Falco-Walter et al., 2018; Jahngir et al., 2018). Collectively, these findings indicate that mutations in these five genes can trigger the LGS phenotype by disrupting neuronal development.

The results of network analysis revealed that the 11 genes *CACNA1A*, *DNAJC5*, *FRRS1L*, *IQSEC2*, *MAGI1*, *NRG2*, *SHANK3*, *SLC25A39*, *SSPO*, *SYN1*, and *SYN2* are directly or indirectly associated with *ERK1/2*, *AKT*, and *KRAS*, which play important roles in neuronal survival, neural stem cell

proliferation, and neurotransmission by α-amino-3-hydroxy-5-methyl-4-isoxazolepropionic acid (AMPA) and N-methyl-d-aspartate receptors (Nateri et al., 2007; Subramaniam and Unsicker, 2010; Bender et al., 2015). Therefore, genetic variations in genes from this group can induce seizure phenotypes of LGS because of both disrupted neuronal development and neurotransmission via ion channels in the brain. Another group of genes, *CHD2*, *SCN10A*, and *TBC1D8*, was associated with *HGF* and *PTEN*; these two genes are related to synaptic plasticity, neuronal cell survival, and CNS development, as well as related to epilepsy (Bae et al., 2010; Tonges et al., 2011; Sperow et al., 2012; Knafo and Esteban, 2017; Godale and Danzer, 2018). These results indicate that variations within candidate genes can impair protein function, directly or indirectly affect neurotransmission or neuronal development pathways, and subsequently induce LGS or LGS-like epilepsy. Our results are in accordance with a previous study in which homozygous mutations in *STXBP1* were identified in two siblings diagnosed with LGS. The mutations resulted in impairment of protein stability leading to reduced synaptic transmission (Lammertse et al., 2020).

Children with LGS have a high percentage of severe injuries as well as other comorbidities, with a potential increased risk of death (Autry et al., 2010). These children were 14-fold more likely than those of the general population to die, indicating that the genetic variation causing LGS is difficult to detect in the next generation. This is likely because there was no LGS family with AD in our study. In addition, the two patients with *SYN2* and *MAGI1* variations in our datasets experienced infantile spasms. The variations may have been responsible for these effects and subsequently led to LGS, as 30% of LGS patients can gradually progress from infantile spasms (Cross et al., 2017).

In summary, we identified mutations in 14 genes as potential causative markers of both LGS and LGS-like epilepsy. Many of these candidate genes are generally pathogenic and are associated with neurotransmission or neuronal function. These results expand the spectrum of variations in LGS and LGS-like epilepsy and are crucial for understanding their biological mechanisms for patient-specific therapeutic development. Further animal model studies are required to determine whether these genetic variations can disrupt neuronal function and cause the LGS phenotype.

DATA AVAILABILITY STATEMENT

The dataset generated for this study was submitted to the Seqeuence Read Archive (SRA) and can be accessed by searching the BioProject ID PRJNA601231 on the NCBI website (https://www.ncbi.nlm.nih.gov/bioproject/PRJNA601231).

ETHICS STATEMENT

The studies involving human participants were reviewed and approved by Institutional Review Board and Ethics Committe at the Chungnam National University Hospitals and the Korea Research Institute of Bioscience and Biotechnology (KRIBB). Written informed consent to participate in this study was provided by the participants' legal guardian/next of kin. Written informed consent was obtained from the individual(s), and minor(s)' legal guardian/next of kin, for the publication of any potentially identifiable images or data included in this article.

AUTHOR CONTRIBUTIONS

N-SK and J-WK conceived and designed the study. JY, M-HC, J-YY, and N-SK drafted the manuscript. JY performed breakpoints verification. JY, M-HC, J-YY, J-JL, and JL participated in the data analysis. SY, S-JJ, SJ, IB, DH, and BL reviewed and edited the manuscript and contributed to the discussions. SN, JK, HK, and JL participated in clinical data collection. N-SK supervised the study. All authors reviewed and approved this submission.

FUNDING

This study was supported by the Basic Science Research Program of the National Research Foundation of Korea (NRF) funded by the Ministry of Science and ICT (NRF-2014M3A9A5034157, 2014M3C9A2064619, and 2020R1A2C2006752) and the KRIBB Research Initiative Program.

ACKNOWLEDGMENTS

We would like to thank the patients and their families for participating in our research.

SUPPLEMENTARY MATERIAL

The Supplementary Material for this article can be found online at: https://www.frontiersin.org/articles/10.3389/fgene.2020.590924/full#supplementary-material

REFERENCES

Adzhubei, I. A., Schmidt, S., Peshkin, L., Ramensky, V. E., Gerasimova, A., Bork, P., et al. (2010). A method and server for predicting damaging missense mutations. *Nat. Methods* 7, 248–249. doi: 10.1038/nmeth0410-248

Allen, A. S., Berkovic, S. F., Coe, B. P., Cook, J., Cossette, P., Delanty, N., et al. (2015). Copy number variant analysis from exome data in 349 patients with epileptic encephalopathy. *Ann. Neurol.* 78, 323–328. doi: 10.1002/ana.24457

Allen, A. S., Berkovic, S. F., Cossette, P., Delanty, N., Dlugos, D., Eichler, E. E., et al. (2013). De novo mutations in epileptic encephalopathies. *Nature* 501, 217–221. doi: 10.1038/nature12439

Asadi-Pooya, A. A. (2018). Lennox-Gastaut syndrome: a comprehensive review. *Neurol. Sci.* 39, 403–414. doi: 10.1007/s10072-017-3188-y

Autry, A. R., Trevathan, E., Van Naarden Braun, K., and Yeargin-Allsopp, M. (2010). Increased risk of death among children with Lennox-Gastaut syndrome and infantile spasms. *J. Child Neurol.* 25, 441–447. doi: 10.1177/0883073809348355

Bae, M. H., Bissonette, G. B., Mars, W. M., Michalopoulos, G. K., Achim, C. L., Depireux, D. A., et al. (2010). Hepatocyte growth factor (HGF) modulates GABAergic inhibition and seizure susceptibility. *Exp. Neurol.* 221, 129–135. doi: 10.1016/j.expneurol.2009.10.011

Banuelos, E., Ramsey, K., Belnap, N., Krishnan, M., Balak, C., Szelinger, S., et al. (2017). Case Report: Novel mutations in TBC1D24 are associated with autosomal dominant tonic-clonic and myoclonic epilepsy and recessive Parkinsonism, psychosis, and intellectual disability. *F1000Res* 6:553. doi: 10.12688/f1000research.10588.1

Bender, R. H., Haigis, K. M., and Gutmann, D. H. (2015). Activated k-ras, but not h-ras or N-ras, regulates brain neural stem cell proliferation in a raf/rb-dependent manner. *Stem Cells* 33, 1998–2010. doi: 10.1002/stem.1990

Camfield, P. R. (2011). Definition and natural history of Lennox-Gastaut syndrome. *Epilepsia* 52(Suppl. 5), 3–9. doi: 10.1111/j.1528-1167.2011.03177.x

Chun, S., and Fay, J. C. (2009). Identification of deleterious mutations within three human genomes. *Genome Res.* 19, 1553–1561. doi: 10.1101/gr.092619.109

Cross, J. H., Auvin, S., Falip, M., Striano, P., and Arzimanoglou, A. (2017). Expert Opinion on the Management of Lennox-Gastaut Syndrome: Treatment Algorithms and Practical Considerations. *Front. Neurol.* 8:505. doi: 10.3389/fneur.2017.00505

Dunn, P., Albury, C. L., Maksemous, N., Benton, M. C., Sutherland, H. G., Smith, R. A., et al. (2018). Next Generation Sequencing Methods for Diagnosis of Epilepsy Syndromes. *Front. Genet.* 9:20. doi: 10.3389/fgene.2018.00020

Falace, A., Buhler, E., Fadda, M., Watrin, F., Lippiello, P., Pallesi-Pocachard, E., et al. (2014). TBC1D24 regulates neuronal migration and maturation through modulation of the ARF6-dependent pathway. *Proc. Natl. Acad. Sci. U S A.* 111, 2337–2342. doi: 10.1073/pnas.1316294111

Falco-Walter, J. J., Scheffer, I. E., and Fisher, R. S. (2018). The new definition and classification of seizures and epilepsy. *Epilepsy Res.* 139, 73–79. doi: 10.1016/j.eplepsyres.2017.11.015

Fedele, L., Newcombe, J., Topf, M., Gibb, A., Harvey, R. J., and Smart, T. G. (2018). Disease-associated missense mutations in GluN2B subunit alter NMDA receptor ligand binding and ion channel properties. *Nat. Commun.* 9:957. doi: 10.1038/s41467-018-02927-4

Fukata, Y., and Fukata, M. (2017). Epilepsy and synaptic proteins. *Curr. Opin. Neurobiol.* 45, 1–8. doi: 10.1016/j.conb.2017.02.001

Godale, C. M., and Danzer, S. C. (2018). Signaling Pathways and Cellular Mechanisms Regulating Mossy Fiber Sprouting in the Development of Epilepsy. *Front. Neurol.* 9:298. doi: 10.3389/fneur.2018.00298

Goncalves-Mendes, N., Blanchon, L., Meiniel, A., Dastugue, B., and Sapin, V. (2004). Placental expression of SCO-spondin during mouse and human development. *Gene Expr. Patterns* 4, 309–314. doi: 10.1016/j.modgep.2003.10.004

Han, W., Wang, H., Li, J., Zhang, S., and Lu, W. (2017). Ferric Chelate Reductase 1 Like Protein (FRRS1L) Associates with Dynein Vesicles and Regulates Glutamatergic Synaptic Transmission. *Front. Mol. Neurosci.* 10:402. doi: 10.3389/fnmol.2017.00402

Hermann, B., Seidenberg, M., Bell, B., Rutecki, P., Sheth, R., Ruggles, K., et al. (2002). The neurodevelopmental impact of childhood-onset temporal lobe epilepsy on brain structure and function. *Epilepsia* 43, 1062–1071.

Ito, H., Morishita, R., Sudo, K., Nishimura, Y. V., Inaguma, Y., Iwamoto, I., et al. (2012). Biochemical and morphological characterization of MAGI-1 in neuronal tissue. *J. Neurosci. Res.* 90, 1776–1781. doi: 10.1002/jnr.23074

Jahngir, M. U., Ahmad, M. Q., and Jahangir, M. (2018). Lennox-Gastaut Syndrome: In a Nutshell. *Cureus* 10:e3134. doi: 10.7759/cureus.3134

Jiang, Y., Oldridge, D. A., Diskin, S. J., and Zhang, N. R. (2015). CODEX: a normalization and copy number variation detection method for whole exome sequencing. *Nucleic Acids Res.* 43:e39. doi: 10.1093/nar/gku1363

Knafo, S., and Esteban, J. A. (2017). PTEN: Local and Global Modulation of Neuronal Function in Health and Disease. *Trends Neurosci.* 40, 83–91. doi: 10.1016/j.tins.2016.11.008

Lammertse, H. C. A., van Berkel, A. A., Iacomino, M., Toonen, R. F., Striano, P., Gambardella, A., et al. (2020). Homozygous STXBP1 variant causes encephalopathy and gain-of-function in synaptic transmission. *Brain* 143, 441–451. doi: 10.1093/brain/awz391

Lund, C., Brodtkorb, E., Oye, A. M., Rosby, O., and Selmer, K. K. (2014). CHD2 mutations in Lennox-Gastaut syndrome. *Epilepsy Behav.* 33, 18–21. doi: 10.1016/j.yebeh.2014.02.005

Lund, C., Brodtkorb, E., Rosby, O., Rodningen, O. K., and Selmer, K. K. (2013). Copy number variants in adult patients with Lennox-Gastaut syndrome features. *Epilepsy Res.* 105, 110–117. doi: 10.1016/j.eplepsyres.2013.01.009

Madeo, M., Stewart, M., Sun, Y., Sahir, N., Wiethoff, S., Chandrasekar, I., et al. (2016). Loss-of-Function Mutations in FRRS1L Lead to an Epileptic-Dyskinetic Encephalopathy. *Am. J. Hum. Genet.* 98, 1249–1255. doi: 10.1016/j.ajhg.2016.04.008

McKenna, A., Hanna, M., Banks, E., Sivachenko, A., Cibulskis, K., Kernytsky, A., et al. (2010). The Genome Analysis Toolkit: a MapReduce framework for analyzing next-generation DNA sequencing data. *Genome Res.* 20, 1297–1303. doi: 10.1101/gr.107524.110

Nakano, N., Kanekiyo, K., Nakagawa, T., Asahi, M., and Ide, C. (2016). NTAK/neuregulin-2 secreted by astrocytes promotes survival and neurite outgrowth of neurons via ErbB3. *Neurosci. Lett.* 622, 88–94. doi: 10.1016/j.neulet.2016.04.050

Nateri, A. S., Raivich, G., Gebhardt, C., Da Costa, C., Naumann, H., Vreugdenhil, M., et al. (2007). ERK activation causes epilepsy by stimulating NMDA receptor activity. *EMBO J.* 26, 4891–4901. doi: 10.1038/sj.emboj.7601911

Pedersen, M., Curwood, E. K., Archer, J. S., Abbott, D. F., and Jackson, G. D. (2015). Brain regions with abnormal network properties in severe epilepsy of Lennox-Gastaut phenotype: Multivariate analysis of task-free fMRI. *Epilepsia* 56, 1767–1773. doi: 10.1111/epi.13135

Riazuddin, S., Hussain, M., Razzaq, A., Iqbal, Z., Shahzad, M., Polla, D. L., et al. (2017). Exome sequencing of Pakistani consanguineous families identifies 30 novel candidate genes for recessive intellectual disability. *Mol. Psychiatry* 22, 1604–1614. doi: 10.1038/mp.2016.109

Richards, S., Aziz, N., Bale, S., Bick, D., Das, S., Gastier-Foster, J., et al. (2015). Standards and guidelines for the interpretation of sequence variants: a joint consensus recommendation of the American College of Medical Genetics and Genomics and the Association for Molecular Pathology. *Genet. Med.* 17, 405–424. doi: 10.1038/gim.2015.30

Schwarz, J. M., Rodelsperger, C., Schuelke, M., and Seelow, D. (2010). MutationTaster evaluates disease-causing potential of sequence alterations. *Nat. Methods* 7, 575–576. doi: 10.1038/nmeth0810-575

Sim, N. L., Kumar, P., Hu, J., Henikoff, S., Schneider, G., and Ng, P. C. (2012). SIFT web server: predicting effects of amino acid substitutions on proteins. *Nucl. Acids Res.* 40, W452–W457. doi: 10.1093/nar/gks539

Siren, A., Polvi, A., Chahine, L., Labuda, M., Bourgoin, S., Anttonen, A. K., et al. (2010). Suggestive evidence for a new locus for epilepsy with heterogeneous phenotypes on chromosome 17q. *Epilepsy Res.* 88, 65–75. doi: 10.1016/j.eplepsyres.2009.09.022

Slabbaert, J. R., Kuenen, S., Swerts, J., Maes, I., Uytterhoeven, V., Kasprowicz, J., et al. (2016). Shawn, the Drosophila Homolog of SLC25A39/40, Is a Mitochondrial Carrier That Promotes Neuronal Survival. *J. Neurosci.* 36, 1914–1929. doi: 10.1523/JNEUROSCI.3432-15.2016

Sperow, M., Berry, R. B., Bayazitov, I. T., Zhu, G., Baker, S. J., and Zakharenko, S. S. (2012). Phosphatase and tensin homologue (PTEN) regulates synaptic plasticity independently of its effect on neuronal morphology and migration. *J. Physiol.* 590, 777–792. doi: 10.1113/jphysiol.2011.220236

Staley, K. (2015). Molecular mechanisms of epilepsy. *Nat. Neurosci.* 18, 367–372. doi: 10.1038/nn.3947

Subramaniam, S., and Unsicker, K. (2010). ERK and cell death: ERK1/2 in neuronal death. *FEBS J.* 277, 22–29. doi: 10.1111/j.1742-4658.2009.07367.x

Terrone, G., Bienvenu, T., Germanaud, D., Barthez-Carpentier, M. A., Diebold, B., Delanoe, C., et al. (2014). A case of Lennox-Gastaut syndrome in a patient with FOXG1-related disorder. *Epilepsia* 55, 116–119e. doi: 10.1111/epi.12800

Tonges, L., Ostendorf, T., Lamballe, F., Genestine, M., Dono, R., Koch, J. C., et al. (2011). Hepatocyte growth factor protects retinal ganglion cells by increasing neuronal survival and axonal regeneration in vitro and in vivo. *J. Neurochem.* 117, 892–903. doi: 10.1111/j.1471-4159.2011.07257.x

Tumiene, B., Maver, A., Writzl, K., Hodzic, A., Cuturilo, G., Kuzmanic-Samija, R., et al. (2018). Diagnostic exome sequencing of syndromic epilepsy patients in clinical practice. *Clin. Genet.* 93, 1057–1062. doi: 10.1111/cge.13203

Vera, A., Stanic, K., Montecinos, H., Torrejon, M., Marcellini, S., and Caprile, T. (2013). SCO-spondin from embryonic cerebrospinal fluid is required for

neurogenesis during early brain development. *Front. Cell Neurosci.* 7:80. doi: 10.3389/fncel.2013.00080

Wang, J., Lin, Z. J., Liu, L., Xu, H. Q., Shi, Y. W., Yi, Y. H., et al. (2017). Epilepsy-associated genes. *Seizure* 44, 11–20. doi: 10.1016/j.seizure.2016.11.030

Wang, K., Li, M., and Hakonarson, H. (2010). ANNOVAR: functional annotation of genetic variants from high-throughput sequencing data. *Nucl. Acids Res.* 38:e164. doi: 10.1093/nar/gkq603

Zerem, A., Haginoya, K., Lev, D., Blumkin, L., Kivity, S., Linder, I., et al. (2016). The molecular and phenotypic spectrum of IQSEC2-related epilepsy. *Epilepsia* 57, 1858–1869. doi: 10.1111/epi.13560

Conflict of Interest: The authors declare that the research was conducted in the absence of any commercial or financial relationships that could be construed as a potential conflict of interest.

frontiers in Genetics

CORRECTION
published: 05 March 2021
doi: 10.3389/fgene.2021.669107

Corrigendum: Characteristics of Genetic Variations Associated With Lennox-Gastaut Syndrome in Korean Families

Jin Ok Yang[1,2†], Min-Hyuk Choi[3,4†], Ji-Yong Yoon[3], Jeong-Ju Lee[3], Sang Ook Nam[5], Soo Young Jun[3], Hyeok Hee Kwon[6], Sohyun Yun[3], Su-Jin Jeon[3,4], Iksu Byeon[1], Debasish Halder[3], Juhyun Kong[5], Byungwook Lee[1], Jeehun Lee[7], Joon-Won Kang[8] and Nam-Soon Kim[3,4*]*

[1] Korea BioInformation Center, Korea Research Institute of Bioscience and Biotechnology, Daejeon, South Korea, [2] Department of Bio and Brain Engineering, Korea Advanced Institute of Science and Technology, Daejeon, South Korea, [3] Rare-Disease Research Center, Korea Research Institute of Bioscience and Biotechnology, Daejeon, South Korea, [4] Department of Functional Genomics, Korea University of Science and Technology, Daejeon, South Korea, [5] Department of Pediatrics, Pusan National University Children's Hospital, Pusan National University School of Medicine, Yangsan, South Korea, [6] Department of Medical Science and Anatomy, Chungnam National University, Daejeon, South Korea, [7] Department of Pediatrics, Samsung Medical Center, Sungkyunkwan University School of Medicine, Seoul, South Korea, [8] Department of Pediatrics and Medical Science, Chungnam National University Hospital, College of Medicine, Chungnam National University, Daejeon, South Korea

Keywords: Lennox-Gastaut syndrome, epilepsy, whole-exome sequencing, genetic variation, Rare-diseases

OPEN ACCESS

Approved by:
Frontiers Editorial Office, Frontiers Media SA, Switzerland

***Correspondence:**
Nam-Soon Kim
nskim37@kribb.re.kr
Joon-Won Kang
childlove@cnu.ac.kr

† These authors have contributed equally to this work

Specialty section:
This article was submitted to Genetics of Common and Rare Diseases, a section of the journal Frontiers in Genetics

Received: *18 February 2021*
Accepted: *19 February 2021*
Published: *05 March 2021*

Citation:
Yang JO, Choi M-H, Yoon J-Y, Lee J-J, Nam SO, Jun SY, Kwon HH, Yun S, Jeon S-J, Byeon I, Halder D, Kong J, Lee B, Lee J, Kang J-W and Kim N-S (2021) Corrigendum: Characteristics of Genetic Variations Associated With Lennox-Gastaut Syndrome in Korean Families. Front. Genet. 12:669107. doi: 10.3389/fgene.2021.669107

A Corrigendum on

Characteristics of Genetic Variations Associated With Lennox-Gastaut Syndrome in Korean Families

by Yang JO, Choi M-H, Yoon J-Y, Lee J-J, Nam SO, Jun SY, et al. (2021). Front. Genet. 11:590924. doi: 10.3389/fgene.2020.590924

In the published article, there were errors in affiliations for authors "Iksu Byeo" and "Byungwook Lee." Instead of "Department of Bio and Brain Engineering, Korea Advanced Institute of Science and Technology, Daejeon, South Korea", it should be "Korea BioInformation Center, Korea Research Institute of Bioscience and Biotechnology, Daejeon, South Korea" for both the authors.

The authors apologize for this error and state that this does not change the scientific conclusions of the article in any way. The original article has been updated.

frontiers in Pediatrics

MINI REVIEW
published: 19 February 2021
doi: 10.3389/fped.2021.633822

Liver Transplantation for Glycogen Storage Disease Type IV

Min Liu[1,2] *and Li-Ying Sun*[1,2,3]*

[1] Department of Liver Transplantation Center, Beijing Friendship Hospital, Capital Medical University, Beijing, China, [2] National Clinical Research Centre for Digestive Diseases, Beijing Friendship Hospital, Capital Medical University, Beijing, China, [3] Department of Intensive Care Unit, Beijing Friendship Hospital, Capital Medical University, Beijing, China

Glycogen storage disease type IV (GSD IV) is a rare autosomal recessive disorder caused by glycogen–branching enzyme (GBE) deficiency, leading to accumulation of amylopectin–like glycogen that may damage affected tissues. The clinical manifestations of GSD IV are heterogeneous; one of which is the classic manifestation of progressive hepatic fibrosis. There is no specific treatment available for GSD IV. Currently, liver transplantation is an option. It is crucial to evaluate long–term outcomes of liver transplantation. We reviewed the published literature for GSD IV patients undergoing liver transplantation. To date, some successful liver transplantations have increased the quantity and quality of life in patients. Although the extrahepatic manifestations of GSD IV may still progress after transplantation, especially cardiomyopathy. Patients with cardiac involvement are candidates for cardiac transplantation. Liver transplantation remains the only effective therapeutic option for treatment of GSD IV. However, liver transplantation may not alter the extrahepatic progression of GSD IV. Patients should be carefully assessed before liver transplantation.

Keywords: glycogen storage disease type IV, glycogen branching enzyme, Andersen disease, liver transplantation, metabolism

OPEN ACCESS

Edited by:
Andrea Gropman, Children's National Hospital, United States

Reviewed by:
Priya Kishnani, Duke University, United States
Nicolina Cristina Sorrentino, Telethon Institute of Genetics and Medicine (TIGEM), Italy

***Correspondence:**
Li-Ying Sun
sunxlx@outlook.com

Specialty section:
This article was submitted to Genetics of Common and Rare Diseases, a section of the journal Frontiers in Pediatrics

Received: *26 November 2020*
Accepted: *02 February 2021*
Published: *19 February 2021*

Citation:
Liu M and Sun L-Y (2021) Liver Transplantation for Glycogen Storage Disease Type IV. Front. Pediatr. 9:633822. doi: 10.3389/fped.2021.633822

INTRODUCTION

Glycogen storage disease type IV (GSD IV, Andersen disease, amylopectinosis, OMIM:232500) is an autosomal recessive disorder of glycogen metabolism (1). GSD IV is estimated to occur in 1 in 600 000 to 800 000 individuals worldwide (2). GSD IV is caused by deficiency of glycogen-branching enzyme (GBE), encoded by *GBE1* gene, leading to accumulation of amylopectin-like glycogen (polyglucosan) in affected tissues (3–6). More than 40 mutations in the *GBE1* gene have been found to cause GSD IV. *GBE1* is located on chromosome 3p14 and encodes a 702-amino-acid protein (7–9).

GSD IV is a rare form of glycogen storage disease that accounts for ∼3% of glycogenosis (2). The accumulation of abnormal branched glycogen results in tissue damage. The clinical manifestations of GSD IV are heterogeneous with variable age of onset, severity and involvement of the liver, cardiac muscle neuromuscular system (3). The progressive hepatic type is the most common and classic form of GSD IV and is characterized by hepatomegaly that rapidly progresses to liver cirrhosis. Patients ultimately die from liver failure by 5 years of age, unless liver transplantation is performed (10, 11). Patients with a rare non-progressive hepatic form do not develop cirrhosis and survive to adulthood without liver transplantation (12–14). The neuromuscular form of GSD IV varies in onset (from fetal to adult age) and severity (4, 7, 15), which present with symptoms of

myopathy, cardiomyopathy, and central and peripheral nervous system dysfunction (7, 16).The fatal infantile neuromuscular type is the most severe form of GSD IV (17, 18). Patients with the congenital neuromuscular form have severe muscle wasting, hypotonia, cardiomyopathy, respiratory distress, neuronal involvement and death in early infancy (19, 20). Neurological adult forms can present as isolated myopathy or as widespread upper and lower motor neuron lesions (adult polyglucosan body disease, APBD) (21). Liver biopsies have confirmed signs of cirrhosis and cells with periodic acid-Schiff (PAS) –stained, diastase-resistant inclusions, consistent with GSD IV. There is no specific treatment for GSD IV. Prognosis is unfavorable for patients with severe cardiomyopathy, associated neurological dysfunction and classic forms who do not undergo liver transplantation.

As there is no treatment to compensate for the deficient enzyme activity, additionally, the classic form of GSD IV usually leads to liver failure, and liver transplantation is the only effective treatment presently available for GSD IV with progressive liver disease (22). Since the first successful liver transplant for GSD IV in September 1984 (23), it has been increasingly used to treat GSD IV cases with liver failure and has improved survival. It is important to know the long–term outcomes of this therapeutic option. In this article, we review all GSD IV patients who underwent liver transplantation to explore the effectiveness and outcomes of liver transplantation for GSD IV.

METHODOLOGY

The English–language literature about GSD IV patients undergoing liver transplantation was systematically reviewed in PubMed and in the references of relevant publications. The key words used included glycogen storage disease type IV, Andersen disease, amylopectinosis, type IV glycogenosis, glycogen-branching enzyme deficiency, and liver transplantation. Indications for liver transplantation, age at transplantation, follow-up period and complications were reviewed. Liver function post–transplantation, extrahepatic manifestations after transplantations, and clinical outcomes were analyzed to better clarify the clinical value of liver transplantation for GSD IV.

RESULTS

We summarized the characteristics and results of 24 patients with GSD IV who underwent liver transplantation between 1984 and 2017 (**Table 1**). There were 19 male patients with two sets of brothers (cases 7 and12, 8 and 11) and five female patients. The youngest was transplanted at 10 months of age and the oldest at 23 years. Two patients required a second liver transplantation: one for nonfunction of the graft 2 d after the first liver transplant, and one for antibody–mediated rejection due to ABO–incompatible live donor graft 6.2 mo after the first transplant. A living related transplantation was performed in seven patients. The indication for liver transplantation was based on the occurrence of progressive liver cirrhosis with evidence of portal hypertension in most cases; for one patient, liver cirrhosis was associated with liver adenoma, and for another, it was heart failure.

On myocardial biopsy, PAS–positive deposits in the myocardium were found in 10 patients with GSD IV, including five postmortem specimens (**Table 2**). All myocardial biopsies were performed postoperatively, except for biopsy of the first patient. Death was reported in nine (37.5%) patients because of: sepsis following bowel perforation 7 d after transplantation ($n = 1$); meningococcal sepsis ($n = 1$); sepsis 1 mo after second liver transplantation ($n = 1$); respiratory and circulatory failure secondary to sepsis 0.3 years post-transplantation ($n = 1$); terminal heart failure and Gram-positive bacterial sepsis 76 mo after liver transplantation ($n = 1$); cardiomyopathy ($n = 3$); and hepatic artery thrombosis 1 mo post–liver transplantation ($n = 1$). Five patients died < 1 year after transplantation;two of whom died < 30 d after liver transplantation. Four patients died > 1-year post–transplant. All other patients were alive at time of follow–up (range several months to 13.5 years after transplantation). In all identified survivors, liver function was normal and portal hypertension was decompressed via the new liver. Catch–up growth was reported in eight patients.

Cardiomyopathy was the most frequent and serious complication, eventually leading to heart failure. Cardiomyopathy developed in six (25%) patients, including one with pre-transplantation heart failure. None of these individuals had undergone combined liver–heart transplantation. Transplant–related complications were seen in eight (33.3%) patients and included portal vein thrombosis ($n = 1$), hepatic artery thrombosis ($n = 1$), rejection ($n = 2$), sepsis ($n = 4$) and non-function of graft ($n = 1$). One of the eight patients had both rejection and sepsis. Of the 15 (62.5%) survivors, one presented at birth with severe hypotonia and flexion contractures of the hips and articulus. He was reported to have symptomatic improvement with mild hypotonia and arthrogryposis 3 years post–transplantation. Thirteen survivors had no neuromuscular or heart complications during follow-up for as long as 13.5 years. Notably, there was a marked reduction in the amount of amylopectin on myocardial biopsy in one of these patients after transplantation (case 12, **Table 1**). The patient who underwent liver transplantation for heart failure had not experienced any symptoms of cardiac failure at 6 mo after transplantation (case 1, **Table 1**).

DISCUSSION

Our review shows that liver transplantation corrects the primary hepatic enzyme defect, so the graft does not accumulate polyglucosan. Liver transplantation normalized the liver function of all the patients with GSD IV except case 3, thereby improving the survival rate and quality of life of patients. Since then, liver transplantation has improved patients' outcome because metabolic sequelae, such as cardiomyopathy and skeletal myopathy, have not developed post–transplantation in most cases. Most remarkable, eight patients were reported to had retarded growth pre–transplantation, but developed well with normal growth,

TABLE 1 | Patients with GSD IV who underwent liver transplantation.

References	Case	Sex	Age at LT (yr.)	Indications for LT	Complications	Follow-up/survival (yr.)	Liver function post-LT	Cardio-/myo-/neuropathy
Aksu et al. (3)	1	F	23	HF LC	None	0.5	NA	cardiomyopathy
Choi et al. (24)	2	M	0.8	LF	None	1	normal	None
Willot et al. (25)	3	M	0.9	LF	Death[a]	6.3	abnormal	cardiomyopathy
	4	M	0.9	LF	Death[b]	1	normal	Cardiomyopathy myopathy
Sokal et al. (26)	5	M	1.2	LF	Death[b]	0.9	normal	Cardiomyopathy
Ban et al. (27)	6	F	2.3	LF	None	0.5	normal	NA
Selby et al. (23, 28)	7	M	2.6	LF	NA	13.2	normal	None
	8	M	0.9	LF	Death[c]	[7 days]		
	9	M	3.0	LF	Death[d]	0.1		
	10	M	3.8	LT	NA	11.9	normal	None
	11	M	1.8	LF	Death[e]	5.4	normal	
	12	M	1.7	LF	NA	8.8	normal	None
	13	M	2.8	LF	NA	8.7	normal	None
Dhawan et al. (29)	14	M	12	LF	Non-function of graft			None
				Re-transplant (2 days after 1st LT)[f]	NA	3.9		
Alshak et al. (30) Rosenthal et al. (31)	15	M	0.9	LF HA	Rejection Death[b]	2.5	normal	cardiomyopathy
Bruno et al. (7)	16	M	3	LF	mild hypotonia Arthrogryposis	3	normal	myopathy
Magoulas et al. (2)	17	F	0.8	LF	Sepsis Death[g]	0.3	normal	cardiomyopathy
Morioka et al. (32)	18	M	3.7	LF	Rejection			
				Re-transplant (6.2 months after 1st LT)	Sepsis Death[h]	0.6		
	19	M	NA	NA	NA	NA	NA	NA
	20	F	NA	NA	NA	NA	NA	NA
Matern et al. (33)	21	M	1.3	LF	None	13.5	NA	None
	22	M	3.7	LF	None	5.5	NA	None
	23	M	5.5	LF	PVT	9.9	NA	None
Troisi et al. (34)	24	F	2	NA	None	0.8	normal	None

LF, liver failure; HA, hepatic adenomas; HF, heart failure; LC, liver cirrhosis; PVT, portal vein thrombosis; LT, liver transplantation; HAT, hepatic artery thrombosis; M, male; F, female; NA, not available.

[a] *Death due to terminal heart failure and Gram-positive bacterial sepsis.*

[b] *Death due to heart failure.*

[c] *Death 7 days post-LT due to sepsis following bowel perforation.*

[d] *Death at 1 month post-LT following hepatic artery thrombosis.*

[e] *Death due to meningococcal sepsis.*

[f] *Due to non-functioning 1st donor liver.*

[g] *Death 0.3 years post LT due to respiratory and circulatory failure secondary to sepsis.*

[h] *Death 1 month after the second LT due to sepsis.*

after liver transplantation (25, 27, 28). As there is no way to compensate for the insufficient enzyme activity, liver transplantation remains the only effective treatment for patients with the progressive hepatic subtype of GSD IV who develop liver failure.

The clinical onset frequently in patients with classical GSD IV is earlier than in atypical individuals (23). We identified that most patients did not develop cardiomyopathy or neuromuscular complications during follow–up of up to 13.5 years (11). Seven of these patients received liver transplantation from living donors, which included five heterozygous and three ABO–incompatible donors, and no mortality or morbidity associated with heterozygosity has yet been observed (3, 24, 27, 32, 34). One of these patents was a 3.7-year-old boy with GSD IV (case 18, **Table 1**), who underwent first liver transplantation using an ABO–incompatible liver graft from his mother, which led to graft

TABLE 2 | PAS-positive inclusion deposits in the myocardium of ten patients with GSD IV pre-or-post liver transplantation.

References	Case	Time sample (months posttransplant)	Mean % area occupied by inclusions	No of inclusions per 3.6 × 10^5 μm^2	Mean size of inclusions (μm^2)
Aksu et al. (3)	1	Pretransplant	–	–	–
Willot et al. (25)	3	76.0 (Autopsy)	–	–	–
	4	11 (Autopsy)	50%	–	–
Sokal et al. (26)	5	9.0	–	–	–
Selby et al. (23, 28)	7	54.0	0.5%	24	140
	9	1.2 (Autopsy)	2%	46	141
	12	0.9	13 %	332	146
		14.0	5.9%	129	164
	13	1.0		Too few to quantitate	
		11.0		Too few to quantitate	
Alshak et al. (30) Rosenthal et al. (31)	15	30.0 (Autopsy)	–	–	–
Magoulas et al. (2)	17	4.0 (Autopsy)	–	–	–

failure due to ABO-incompatibility and was replaced by an ABO–incompatible liver graft from his father 6.2 mo after the first liver transplant. In one patient who underwent liver transplantation for heart failure due to cardiomyopathy, and her heart failure was restored during 6 mo follow–up (3). Remarkably, there was resorption of amylopectin on myocardial biopsy in one patient after liver transplantation (35). The mechanism of this decrease of abnormal glycogen remains unclear (11). It may have been due to migration of donor cells from the liver allograft to the recipient heart and microchimerism (5, 35).

However, the prognosis is grave when extrahepatic manifestations of GSD IV develop, especially cardiomyopathy (36). Accordingly, it is a major concern that liver transplantation may only improve the hepatic function of individuals with GSD IV, and extrahepatic manifestations might develop post–transplantation and result in poor prognosis. Amylopectin is not soluble, and the enzyme defect is present in other affected organs such as muscle, heart or nervous system. Amylopectin accumulation in other affected tissues might progress after transplantation. Postoperative extrahepatic progression of the disease caused by amylopectin accumulation in other affected tissues might be a potential risk for these individuals. Cardiac amylopectionosis was the most common postoperative complication in GSD IV patients (6/24) and four of those died from heart failure. We identified only one patient with heart failure before transplantation. The evaluation of pretransplant cardiac function is not a predicting factor of poor outcome in this situation. Of the four patients who died of cardiac failure after liver transplantation, all preoperative heart function was normal, but they developed cardiac amylopectionosis, attributed to accumulation of amylopectin in cardiac muscle. The patients died 2.55 years (range: 0.9–6.3years) after transplantation (25, 26, 31). In three of those four patients, autopsy showed that cardiomyocytes contained massive PAS–positive, diastase-resistant inclusions (25, 31). In the fourth patient, postoperative myocardial biopsy showed PAS–positive, amylase–resistant deposits in cardiomyocytes up to 9 mo following liver transplantation (26). In another patient, cardiomyopathy was discovered by postmortem examination after he died from respiratory and circulatory failure secondary to sepsis (2). Myocardial biopsy is a potential predictor of cardiac functional prognosis after transplantation, but the number of amylopectin–like deposits related to progressive fatal cardiac failure needs to be defined. Further, long-term follow-up is necessary to evaluate possible cardiac or neuromuscular complications (24). To further evaluate this risk, patients with GSD IV need careful assessment of heart, liver, and muscle before and after liver transplantation.

Heart transplantation has been suggested in cases with severe cardiac involvement. Patients with progressive cardiomyopathy and myocardial involvement confirmed by myocardial biopsy secondary to GSD IV may be candidates for cardiac transplantation. The experience with cardiac transplantation for GSD IV is insufficient. Only three patients are known to have undergone cardiac transplantation for extrahepatic progression related to GSD IV (37–39). Two patients were transplanted successfully and in good condition during follow–up. The third one died due to infectious complications after orthoptic heart transplantation. Evaluation of the genotype–phenotype correlation in GSD IV may be helpful, which may provide valuable information in decision-making and help us to better understand the outcome of liver transplantation (6, 33).

CONCLUSION

Liver transplantation remains the only therapeutic option for treatment of hepatic manifestation of GSD IV. Our review shows that all GSD IV patients who survived had normal liver function after liver transplantation. Selection of patients with GSD IV for liver transplantation should be alert to extrahepatic progression, as the cardiomyopathy may lead to fatal complications. Consideration of combined liver–heart transplantation and careful assessment of

cardiac function even in the absence of evidence of clinical decompensation appears warranted for patients with GSD IV. Histopathological studies of myocardial tissues and evaluation of the correlation between genotype–phenotype and the condition may predict the degree of severity and assist with treatment decisions.

AUTHOR CONTRIBUTIONS

ML identified all the cases to be included, analyzed and interpreted the data and drafted the manuscript. L-YS reviewed the manuscript. Both authors read and approved the final manuscript.

REFERENCES

1. Andersen DH. Familial cirrhosis of the liver with storage of abnormal glycogen. *Lab Invest*. (1956)5:11–20.
2. Magoulas PL, El-Hattab AW, Roy A, Bali DS, Finegold MJ, Craigen WJ. Diffuse reticuloendothelial system involvement in type IV glycogen storage disease with a novel GBE1 mutation: a case report and review. *Hum Pathol*. (2012) 43:943–51. doi: 10.1016/j.humpath.2011.10.001
3. Aksu T, Colak A, Tufekcioglu O. Cardiac involvement in glycogen storage disease type iv: two cases and the two ends of a spectrum. *Case Rep Med*. (2012)2012:764286. doi: 10.1155/2012/764286
4. Fernandez C, Halbert C, De Paula AM, Lacroze V, Froissart R, Figarella-Branger D, et al. Non-lethal neonatal neuromuscular variant of glycogenosis type IV with novel GBE1 mutations. *Muscle Nerve*. (2010) 41:269–71. doi: 10.1002/mus.21499
5. Dainese L, Adam N, Boudjemaa S, Hadid K, Rosenblatt J, Jouannic JM, et al. Glycogen storage disease type IV and early implantation defect: early trophoblastic involvement associated with a New GBE1 mutation. *Pediatr Dev Pathol*. (2016) 19:512–5. doi: 10.2350/14-09-1557-CR.1
6. Moses SW, Parvari R. The variable presentations of glycogen storage disease type IV: a review of clinical, enzymatic and molecular studies. *Curr Mol Med*. (2002) 2:177–88. doi: 10.2174/1566524024605815
7. Bruno C, van Diggelen OP, Cassandrini D, Gimpelev M, Giuffre B, Donati MA, et al. Clinical and genetic heterogeneity of branching enzyme deficiency (glycogenosis type IV). *Neurology*. (2004) 63:1053–8. doi: 10.1212/01.wnl.0000138429.11433.0d
8. Lamperti C, Salani S, Lucchiari S, Bordoni A, Ripolone M, Fagiolari G, et al. Neuropathological study of skeletal muscle, heart, liver, and brain in a neonatal form of glycogen storage disease type IV associated with a new mutation in GBE1 gene. *J Inherit Metab Dis*. (2009) 32(Suppl 1):S161–8. doi: 10.1007/s10545-009-1134-8
9. Shin YS. Glycogen storage disease: clinical, biochemical, and molecular heterogeneity. *Semin Pediatr Neurol*. (2006) 13:115–20. doi: 10.1016/j.spen.2006.06.007
10. Cenacchi G, Papa V, Costa R, Pegoraro V, Marozzo R, Fanin M, et al. Update on polyglucosan storage diseases. *Virchows Arch*. (2019) 475:671–86. doi: 10.1007/s00428-019-02633-6
11. Davis MK, Weinstein DA. Liver transplantation in children with glycogen storage disease: controversies and evaluation of the risk/benefit of this procedure. *Pediatr Transplant*. (2008) 12:137–45. doi: 10.1111/j.1399-3046.2007.00803.x
12. Bao Y, Kishnani P, Wu JY, Chen YT. Hepatic and neuromuscular forms of glycogen storage disease type IV caused by mutations in the same glycogen-branching enzyme gene. *J Clin Invest*. (1996) 97:941–8. doi: 10.1172/JCI118517
13. Greene HL, Brown BI, McClenathan DT, Agostini RJ, Taylor SR. A new variant of type IV glycogenosis: deficiency of branching enzyme activity without apparent progressive liver disease. *Hepatology*. (1988) 8:302–6. doi: 10.1002/hep.1840080219
14. McConkie-Rosell A, Wilson C, Piccoli DA, Boyle J, DeClue T, Kishnani P, et al. Clinical and laboratory findings in four patients with the non-progressive hepatic form of type IV glycogen storage disease. *J Inherit Metab Dis*. (1996) 19:51–8. doi: 10.1007/BF01799348
15. Radhakrishnan P, Moirangthem A, Nayak SS, Shukla A, Mathew M, Girisha KM. Novel pathogenic variants in GBE1 causing fetal akinesia deformation sequence and severe neuromuscular form of glycogen storage disease type IV. *Clin Dysmorphol*. (2019) 28:17–21. doi: 10.1097/MCD.0000000000000248
16. Tay SK, Akman HO, Chung WK, Pike MG, Muntoni F, Hays AP, et al. Fatal infantile neuromuscular presentation of glycogen storage disease type IV. *Neuromuscul Disord*. (2004) 14:253–60. doi: 10.1016/j.nmd.2003.12.006
17. Assereto S, van Diggelen OP, Diogo L, Morava E, Cassandrini D, Carreira I, et al. Null mutations and lethal congenital form of glycogen storage disease type IV. *Biochem Biophys Res Commun*. (2007) 361:445–50. doi: 10.1016/j.bbrc.2007.07.074
18. Yu W, Brundler MA, Wright JJ. Polyglucosan bodies in placental extravillious trophoblast for the diagnosis of fatal perinatal neuromuscular-type glycogen storage disease type IV. *Pediatr Dev Pathol*. (2018) 21:423–7. doi: 10.1177/1093526617707852
19. Nolte KW, Janecke AR, Vorgerd M, Weis J, Schroder JM. Congenital type IV glycogenosis: the spectrum of pleomorphic polyglucosan bodies in muscle, nerve, and spinal cord with two novel mutations in the GBE1 gene. *Acta Neuropathol*. (2008) 116:491–506. doi: 10.1007/s00401-008-0417-8
20. Taratuto AL, Akman HO, Saccoliti M, Riudavets M, Arakaki N, Mesa L, et al. Branching enzyme deficiency/glycogenosis storage disease type IV presenting as a severe congenital hypotonia: muscle biopsy and autopsy findings, biochemical and molecular genetic studies. *Neuromuscul Disord*. (2010) 20:783–90. doi: 10.1016/j.nmd.2010.07.275
21. Bruno C, Cassandrini D, Assereto S, Akman HO, Minetti C, Di Mauro S. Neuromuscular forms of glycogen branching enzyme deficiency. *Acta Myol*. (2007)26:75–8.
22. Kido J, Nakamura K, Matsumoto S, Mitsubuchi H, Ohura T, Shigematsu Y, et al. Current status of hepatic glycogen storage disease in Japan: clinical manifestations, treatments and long-term outcomes. *J Hum Genet*. (2013) 58:285–92. doi: 10.1038/jhg.2013.17
23. Selby R, Starzl TE, Yunis E, Todo S, Tzakis AG, Brown BI, et al. Liver transplantation for type I and type IV glycogen storage disease. *Eur J Pediatr*. (1993) 152(Suppl 1):S71–6. doi: 10.1007/BF02072093
24. Choi SY, Kang B, Choe JY, Lee Y, Jang HJ, Park HD, et al. A case of glycogen storage disease iv with rare homozygous mutations in the glycogen branching enzyme gene. *Pediatr Gastroenterol Hepatol Nutr*. (2018) 21:365–8. doi: 10.5223/pghn.2018.21.4.365
25. Willot S, Marchand V, Rasquin A, Alvarez F, Martin SR. Systemic progression of type IV glycogen storage disease after liver transplantation. *J Pediatr Gastroenterol Nutr*. (2010) 51:661–4. doi: 10.1097/MPG.0b013e3181d29780
26. Sokal EM, Van Hoof F, Alberti D, de Ville DGJ, de Barsy T, Otte JB. Progressive cardiac failure following orthotopic liver transplantation for type IV glycogenosis. *Eur J Pediatr*. (1992) 151:200–3. doi: 10.1007/BF01954384
27. Ban HR, Kim KM, Jang JY, Kim GH, You HW, Kim K, et al. Living donor liver transplantation in a korean child with glycogen storage disease type IV and a GBE1 mutation. *Gut Liver*. (2009)3:60–3. doi: 10.5009/gnl.2009.3.1.60
28. Selby R, Starzl TE, Yunis E, Brown BI, Kendall RS, Tzakis A. Liver transplantation for type IV glycogen storage disease. *N Engl J Med*. (1991) 324:39–42. doi: 10.1056/NEJM199101033240107
29. Dhawan A, Tan KC, Portmann B, Mowat AP. Glycogenosis type IV: liver transplant at 12 years. *Arch Dis Child*. (1994) 71:450–1. doi: 10.1136/adc.71.5.450
30. Alshak NS, Cocjin J, Podesta L, van de Velde R, Makowka L, Rosenthal P, et al. Hepatocellular adenoma in glycogen storage disease type IV. *Arch Pathol Lab Med*. (1994)118:88–91.
31. Rosenthal P, Podesta L, Grier R, Said JW, Sher L, Cocjin J, et al. Failure of liver transplantation to diminish cardiac deposits of amylopectin and leukocyte inclusions in type IV glycogen storage disease. *Liver Transpl Surg*. (1995) 1:373–6. doi: 10.1002/lt.500010607
32. Morioka D, Kasahara M, Takada Y, Corrales JP, Yoshizawa A, Sakamoto S, et al. Living donor liver transplantation for pediatric patients with

inheritable metabolic disorders. *Am J Transplant*. (2005) 5:2754–63. doi: 10.1111/j.1600-6143.2005.01084.x
33. Matern D, Starzl TE, Arnaout W, Barnard J, Bynon JS, Dhawan A, et al. Liver transplantation for glycogen storage disease types I, III, and IV. *Eur J Pediatr*. (1999) 158(Suppl 2):S43–8. doi: 10.1007/pl00014320
34. Troisi RI, Elsheikh YM, Shagrani MA, Broering D. First fully laparoscopic donor hepatectomy for pediatric liver transplantation using the indocyanine green near-infrared fluorescence imaging in the Middle East: a case report. *Ann Saudi Med*. (2014) 34:354–7. doi: 10.5144/0256-4947.2014.354
35. Starzl TE, Demetris AJ, Trucco M, Ricordi C, Ildstad S, Terasaki PI, et al. Chimerism after liver transplantation for type IV glycogen storage disease and type 1 Gaucher's disease. *N Engl J Med*. (1993) 328:745–9. doi: 10.1056/NEJM199303183281101
36. Maheshwari A, Rankin R, Segev DL, Thuluvath PJ. Outcomes of liver transplantation for glycogen storage disease: a matched-control study and a review of literature. *Clin Transplant*. (2012) 26:432–6. doi: 10.1111/j.1399-0012.2011.01549.x
37. de La Blanchardière A, Vayssier C, Duboc D, Jacquemin IE, Eymard B, Fardeau M, et al. [Severe cardiomyopathy revealing amylopectinosis. Two cases in adolescents from the same family]. *Presse Med*. (1994) 23:1124–7.
38. Ewert R, Gulijew A, Wensel R, Dandel M, Hummel M, Vogel M, et al. [Glycogenosis type IV as a seldom cause of cardiomyopathy - report about a successful heart transplantation]. *Z Kardiol*. (1999) 88:850–6. doi: 10.1007/s003920050361
39. Ndugga-Kabuye MK, Maleszewski J, Chanprasert S, Smith KD. Glycogen storage disease type IV: dilated cardiomyopathy as the isolated initial presentation in an adult patient. *BMJ Case Rep*. (2019) 12:e230068. doi: 10.1136/bcr-2019-230068

Conflict of Interest: The authors declare that the research was conducted in the absence of any commercial or financial relationships that could be construed as a potential conflict of interest.

frontiers in Genetics

CASE REPORT
published: 04 March 2021
doi: 10.3389/fgene.2021.609040

Case Report: A Novel *PAX3* Mutation Associated With Waardenburg Syndrome Type 1

Qiuming Hu[1], *Huazhong Ma*[2], *Jiawei Shen*[3†], *Zongming Zhuang*[1,4], *Jianqiang Li*[4], *Xinlan Huang*[4], *Xian Li*[5*†] and *Haoyu Li*[1,4*†]

[1] Department of Ophthalmology, The First Affiliated Hospital of Guangxi Medical University, Nanning, China, [2] Department of Ophthalmology, Pingguo People's Hospital, Baise, China, [3] Department of Stomatology, The Affiliated Hospital of Medical School, Ningbo University, Ningbo, China, [4] Department of Retina and Vitreous, Jingliang Eye Hospital, Guangxi Medical University, Nanning, China, [5] Division of Pharmacy and Optometry, Faculty of Biology, Medicine and Health, University of Manchester, Manchester, United Kingdom

OPEN ACCESS

Edited by:
Sascha Meyer,
Saarland University Hospital, Germany

Reviewed by:
Chiara Di Resta,
Vita-Salute San Raffaele University, Italy
Monkol Lek,
Yale University, United States

***Correspondence:**
Xian Li
xian.li-2@postgrad.manchester.ac.uk
Haoyu Li
med.dr.lihy@gmail.com

†ORCID:
Jiawei Shen
orcid.org/0000-0002-8780-2553
Xian Li
orcid.org/0000-0001-8410-1586
Haoyu Li
orcid.org/0000-0002-9826-181X

Specialty section:
This article was submitted to Genetics of Common and Rare Diseases, a section of the journal Frontiers in Genetics

Received: 22 September 2020
Accepted: 12 February 2021
Published: 04 March 2021

Citation:
Hu Q, Ma H, Shen J, Zhuang Z, Li J, Huang X, Li X and Li H (2021) Case Report: A Novel PAX3 Mutation Associated With Waardenburg Syndrome Type 1. Front. Genet. 12:609040. doi: 10.3389/fgene.2021.609040

Background: Waardenburg Syndrome Type 1 (WS1) is a rare hereditary disease, which is usually caused by the mutations of *PAX3* (*paired box 3*). Here, we reported a pedigree with WS1, which was caused by a novel mutation in *PAX3*.

Case Report: In this present report, a 10-year-old boy and his twin sister from a Han Chinese family presented with iris pigmentary abnormality, synophrys, and broad and high nasal root. Their father presented premature whitening of the hair, but no iris pigmentary abnormality. Their aunts presented the same clinical characteristics with the twins and premature graying of hair. However, none of the patients reported hearing loss. The clinical diagnosis of the four patients from this pedigree was WS1. The whole exome sequencing (WES) revealed a novel mutation (c.959-5T>G) in the *PAX3* gene, which could be responsible for the observed pathogenic of WS1 in this pedigree. The genetic test confirmed the diagnosis of WS1 in the four patients from the studied pedigree.

Conclusion: This present study demonstrated that genetic test based on WES, an effective alternative to regular clinical examinations, helps diagnose WS1. The newly identified *PAX3* gene mutation can expand the understanding of WS1.

Keywords: Waardenburg Syndrome Type 1, Heterochromia iridis, *PAX3* gene, whole exome sequencing, case report

INTRODUCTION

Waardenburg Syndrome (WS), also named auditory-pigmentary syndrome, is one of the most common causes of syndromic deafness, contributing to 2–5% of congenital deafness cases. This syndrome is mainly caused by monogenetic variants that are mostly inherited through autosomal dominance with incomplete penetrance (Read and Newton, 1997). In China, WS patients account for about 1% of the deaf population (Chen et al., 2020). WS can be classified into four types (WS1, OMIM# 193500; WS2, OMIM# 193510; WS3, OMIM# 148820, and WS4, OMIM# 277580) according to different clinical characteristics, and WS1 and WS2 are the most common types (Pingault et al., 2010). The first WS case was described as a syndrome of a disorder combining anomalies of the eyelids, eyebrows, and nasal root with congenital deafness, which is now known as WS1 (Waardenburg, 1951). WS2 is similar to WS1, but hearing loss is more common in the former, and widely spaced eyes occur more common in the latter (Arias, 1971). WS3, also known

as Klein-Waardenburg syndrome, often exhibits all the clinical features of WS1 and upper limb deformity. WS4, also known as Waardenburg-Hirschsprung disease, often exhibits all the clinical characteristics of WS2 in addition to megacolon or gastrointestinal atresia (Ma et al., 2019). WS is usually caused by mutations of the following six genes (Pingault et al., 2010): *PAX3* (*paired box 3*), *EDN3* (*endothelin 3*), *EDNRB* (*endothelin receptor type B*), *MITF* (*microphthalmia-associated transcription factor*), *SOX10* (*SRY Box10*), and *SNAI2* (*snail homolog 2*). *PAX3* gene mutations are the common genetic causes of WS1 and WS3 (Li et al., 2020).

WS is often described as an autosomal dominantly inherited disorder of neural crest (NC) cells. *PAX3* protein contains two highly conserved DNA binding domains (Apuzzo and Gros, 2007): a pairing domain (PD, Amino acids at position 33–160) and a homologous domain (HD, Amino acids at position 219-276). Genes, including *PAX3*, play a vital role in the development and differentiation of melanocytes derived from embryonic NC cells. The corresponding protein function will be affected, if a mutation occurs in the functional region, which will cause WS (Liu et al., 2020). Until now, over 150 mutations of the *PAX3* gene associated with WS have been reported (Li et al., 2020), and most of them are located at exons 2–6 (Pingault et al., 2010). In this report, a novel mutation (c.959-5T>G) of the *PAX3* gene was detected in a Chinese family with WS1. The discovery of this study may provide valuable information for genetic counseling of WS1 families.

CASE PRESENTATION

In the studied family, a 10-year-old boy (the proband, III-1), his father (II-1), aunts (II-8 and II-10), and twin sister (III-2) presented with iris pigmentary abnormality, synophrys, and broad and high nasal root (**Figure 1**). This studied family members were Han Chinese and had no history of medication use, infectious disease, severe constipation, blockage of the intestine, or abnormalities or limits of mobility in the limbs. The iris pigmentary abnormality, synophrys, and broad and high nasal root of the proband were observed, the iris color in his right eye was off-white, and the color in his left eye was brown (**Figure 2**). Like the proband, patient III-2 was with the same clinical features, the iris color in her left eye was off-white, and the color in her right eye was brown (**Figure 2**). Based on iris pigmentary abnormality, synophrys, and broad and high nasal root, both II-8 and II-10 had premature whitening of hair. However, there was only premature whitening of the hair but no iris pigmentary abnormality in II-1. Notably, none of the patients in this pedigree complained of hearing loss, and they refused pure-tone audiometry. The clinical features are summarized in **Supplementary Table 1**. The patients III-1 and III-2 received a comprehensive ophthalmological examination, which included comprehensive medical optometry, anterior

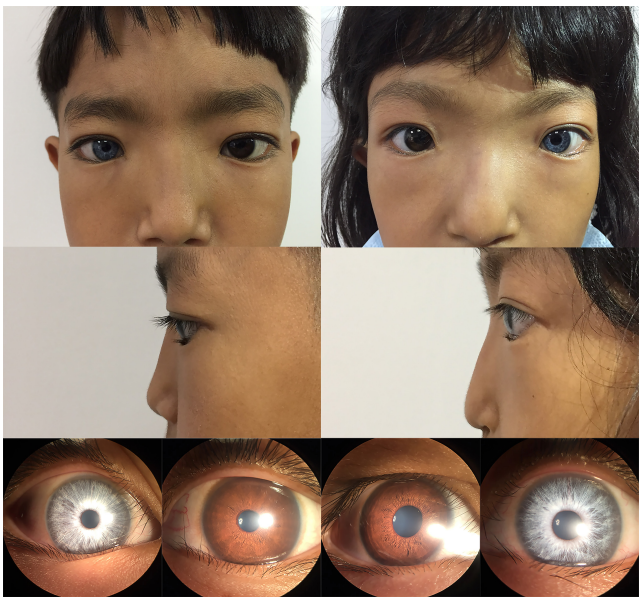

FIGURE 2 | Photographic features of appearance and iris pigment in III-1 and III-2. Synophrys, and broad, and high nasal root without forehead white hair can be observed in III-1 (proband) and III-2. The iris color in the right eye of III-1 is off-white and the left eye is brown. The iris color in the right eye of III-2 is brown and the left eye is off-white.

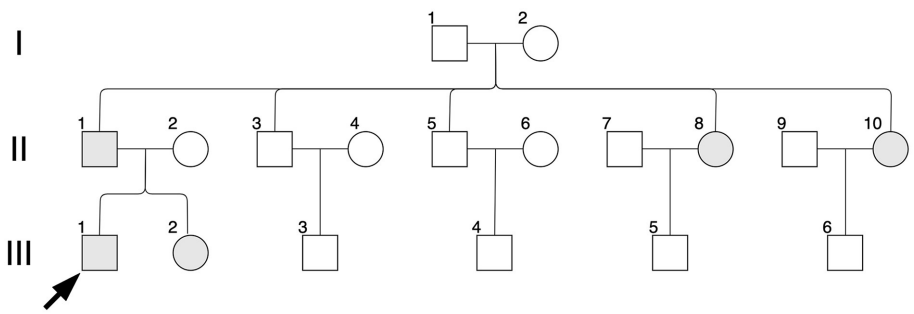

FIGURE 1 | Pedigree diagram. Black arrow indicates the proband, II-1; shapes in gray indicate affected individuals, II-1, II-8, II-10, III-1 and III-2.

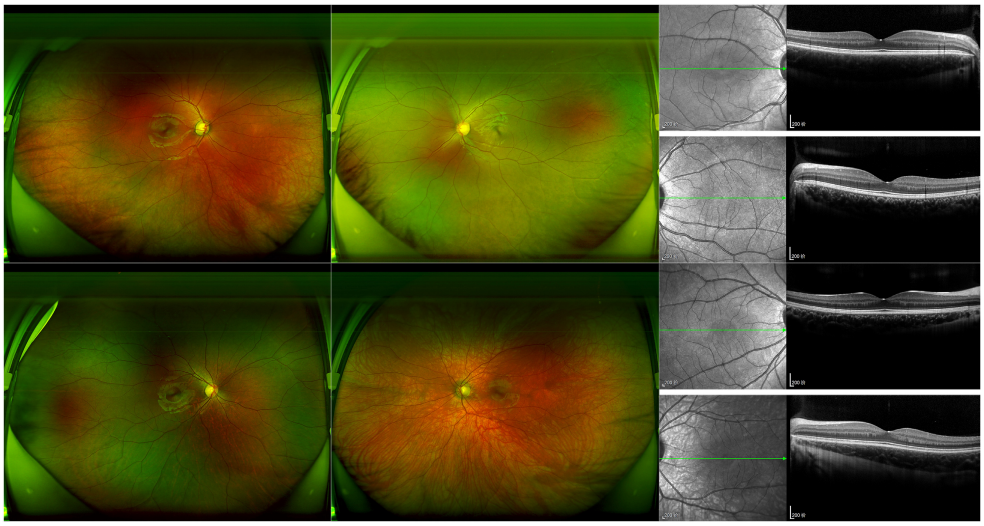

FIGURE 3 | Photographic features of fundus in III-1 and III-2. Ultra-widefield laser scanning image and B-scan results of optical coherence tomography of III-1 (proband) and III-2 are shown. The hypopigmented fundus on the same side as the depigmentation of the iris can be observed.

TABLE 1 | Summary of the six candidate variants of five genes in the Waardenburg Syndrome Type 1 pedigree.

Gene	PAX3 (NM_181457.4)	COL5A1 (NM_000093.5)	UBE3B (NM_130466.4)	WDR73 (NM_032856.4)	ZNF469 (NM_001367624.2)	ZNF469 (NM_001367624.2)
Genomic position	chr2:223085078	chr9:137619155	chr12:109972466	chr15:85186903	chr16:88495541	chr16:88498788
Position in cDNA	c.959-5T>G	c.698C>G	c.3086G>A	c.935G>A	c.1663G>A	c.4910G>A
III-1	Heterozygous	Heterozygous	Heterozygous	Heterozygous	Heterozygous	Heterozygous
II-1	Heterozygous	Heterozygous	Heterozygous	Heterozygous	Heterozygous	Wild type
II-2	Wild type	Wild type	Wild type	Wild type	Wild type	Heterozygous
II-8	Heterozygous	NA	NA	NA	NA	NA
II-10	Heterozygous	NA	NA	NA	NA	NA
III-2	Heterozygous	Heterozygous	Wild type	Wild type	Wild type	Heterozygous

NA, not applicable; Human genome reference: GRCh37/hg19.

segment photography, optical coherence tomography, and ultra-widefield laser scanning imaging. Except for abnormal iris color and fundus depigmentation in the corresponding eye, no other abnormalities or refractive errors were found (**Figure 3**).

In addition to clinical examinations, analysis of mutations *via* whole exome sequencing (WES) using peripheral blood was performed for II-1, II-2, II-8, II-10, III-1, and III-2, which was conducted by Aegicare Technology Co., Ltd. (Shenzhen, China). The DNA was extracted from the patients' blood sample, and 20,000 exons and the region about 20 bps upstream and downstream were sequenced. The reference genome GRCh37 was used for sequence alignment. The Aegicare's Weaver algorithm was used to detect copy number variations at the exon level. The sequencing depth was over 30× average depth. Then the sequencing results were verified through Sanger sequencing. In this study, the most major mutation associated with the clinical features located at *PAX3* (c.959-5T>G). The c.959-5T>G mutation was a novel mutation of NO. 959-5 nucleotide from thymine to guanine, which occurred in intron 6 of the *PAX3* gene. Other mutations identified in this study included *COL5A1* (c.698C>G, p.Ala233Gly), *UBE3B* (c.3086G>A, p.Arg1029His), *WDR73* (c.935G>A, p.Arg312Gln) and *ZNF469* (c.1663G>A, p.Asp555Asn and c.4910G>A, p.Arg1637Gln). The candidate variants are summarized in **Table 1**, and the results of Sanger sequencing are shown in **Supplementary Figure 1**. The identified mutation of the *PAX3* gene was found in II-1, II-8, II-10, III-1, and III-2, while II-2 (the mother of the proband) had the wild-type *PAX3*. Therefore, the *PAX3* mutation of the twins was from their father.

In addition to the previous publication, this *PAX3* mutation was not recorded in gnomAD_exome, gnoAD_gnome, ExAc, or 1000 Genomes Project database. A series of prediction tools were used to evaluate the possible functional impacts of mutations in this study (Ng and Henikoff, 2003; Reva et al., 2007; Chun and Fay, 2009; Schwarz et al., 2010; Shihab et al., 2013; Choi and Chan, 2015). The results of the prediction are summarized in **Supplementary Table 2**. According to the prediction results of SpliceAI [DS_AL (acceptor loss) score =

0.5457] (Jaganathan et al., 2019), the detected mutation has a greater possibility of affecting the splicing. A DS_AL score >2 indicates a possibility of affecting the splicing; a score >5 indicates a possibility to cause a splicing-related disease. Splice variants frequently give rise to alternative splicing and affect protein coding. Consistent with the results, the mutations identified in Ehlers-Danlos-syndrome-related gene *COL5A1* (Tuna et al., 2019; Angwin et al., 2020) and Kaufman-Oculocerebrofacial-syndrome-related gene *UBE3B* (Cheon et al., 2019; Ambrozkiewicz et al., 2020) also had a higher risk of disease. However, no results of the *PAX3* mutation were available through the prediction tools. The American College of Medical Genetics and Genomics (ACMG) guidelines were used for the interpretation of variants (Richards et al., 2015).

DISCUSSION

Diagnosis of WS is often established by clinical features. For WS1, the diagnosis requires two major criteria or one major plus two minor criteria (Farrer et al., 1992; Saleem, 2019). There are five major criteria: (1) congenital sensorineural hearing loss; (2) white forelock; (3) abnormal iris pigment; (4) dystopia canthorum; and (5) affected first-degree relative. The five minor criteria are (1) cutaneous hypopigmentation; (2) synophrys or medial eyebrow flare; (3) broad/high nasal root or low columella; (4) hypoplastic nasal alae; and (5) premature gray hair. In this studied family, all the patients met the criteria of WS1 diagnosis, although they presented different clinical characteristics. According to previous research, congenital sensorineural hearing loss is the most frequent clinical feature of WS1 patients (Oysu et al., 2000); however, none of the patients in this family presented this feature. In addition to hearing loss, dystopia canthorum is still considered the most reliable part for WS1, although it is a controversial diagnostic criterion (Sun et al., 2016; Minami et al., 2019). According to the Waardenburg consortium, dystopia canthorum should be evaluated by the W index. In this study, all the patients could be diagnosed with WS1 without considering this unagreeable indicator, the W index. Consistent with the previous research (Shields et al., 2013), the ocular features of III-1 and III-2 were described in this report that abnormal iris color and fundus depigmentation in the corresponding eye.

The sensorineural hearing loss is one of the typical phenotypes of WS1; however, none of the patients in this family complained of hearing loss. The rough hearing test also showed no abnormalities. Regretful, they refused the pure-tone audiometry. We deduced that the patients' hearing is generally normal, or the damage is too slight to detect.

The melanocyte, one of the cells affected by WS1, is derived from the NC. The NC can produce a series of cells and tissues, including melanocytes, neurons, the enteric nervous system, the facial skeleton, and other structures (Mica et al., 2013). Melanocytes exist in human skin, eyes, and cochlea. Melanocytes in the epidermis and iris contribute to skin and eye color variation, respectively (Lin and Fisher, 2007; Shields et al., 2013); melanocytes in the stria vascularis of the inner ear contribute to normal hearing (Tachibana, 2001). The biological activities of melanocytes are mediated by a series of genes, including *MITF*, *PAX3*, and other genes (Tachibana et al., 1996). MITF protein is essential for the survival and function of melanocytes, while transcription factors, such as *PAX3*, regulate *MITF* expression *via* extracellular signaling (Hou and Pavan, 2008). Additionally, *PAX3* is broadly expressed in several other lineages of NC cells, and early expression of *PAX3* is critical for developing melanocytes, craniofacial structure, and formation of the upper limbs (Wildhardt et al., 2013). Therefore, it is not difficult to understand that the abnormal expression of *MITF* or its regulatory genes can lead to WS characterized by depigmentation. In this study, the *PAX3* gene mutation (c.959-5T>G) was identified through WES and Sanger sequencing, and it was considered the cause of WS1.

In this study, several mutations were discovered. According to ACMG guidelines and clinical manifestations, mutations with lower risk or inconsistent characteristics were excluded. Consistent with the clinical phenotypes and genetic traits, the proband's *PAX3* conversion came from his father and was inherited autosomal dominantly. However, this novel mutation of *PAX3* was rare, and due to the low frequency of population database and the mutation was co-segregated with the disease in multiple family members, according to the ACMG guidelines, it was classified as a variant of uncertain significance (VUS). Further study is needed to verify our results.

Comprehensive management of patients is required. As WS1 is a high-risk indicator for hearing loss, hearing screening and auditory diagnostic assessments are needed. In addition to the auditory system, wearing contact lenses or sunglasses to relieve photophobia and appropriate integumentary system protection and treatments are necessary. A previous study indicated that the pathogenic *PAX3* alleles might increase the risk of severe neural tube defects in the patients' offspring, associated with folate-response (Hart and Miriyala, 2017). Thus, daily folic acid supplementation is recommended to all childbearing age women (Saleem, 2019).

In conclusion, this present study reports a novel mutation, c.959-5T>G of the *PAX3* gene in a Han Chinese family with WS1. Discovering and reporting novel WS1-associated mutations facilitate the analysis of correlations between WS genotypes and phenotypes, helping further genetic consultation and diagnosis. Besides, our results showed that WES is a useful approach for congenital disease diagnosis and is of great benefit to disease screening, genetic diagnosis, and counseling.

DATA AVAILABILITY STATEMENT

The datasets for this report are not publicly available due to concerns regarding participant anonymity. The datasets generated for this study can be available on request to the corresponding author.

ETHICS STATEMENT

The studies involving human participants were reviewed and approved by The Ethics Committee of Jingliang

Eye Hospital Affiliated to Guangxi Medical University. Written informed consent was obtained from the minor(s)' legal guardian/next of kin for the publication of any potentially identifiable images or data included in this article.

AUTHOR CONTRIBUTIONS

HM, JL, XH, and ZZ cared for the patients and performed medical examinations. QH took the lead in writing the manuscript. HM, JS, XL, and HL revised the manuscript. XL and HL designed the present research and guided the entire essay. All authors reviewed the manuscript and provided critical feedback and agreed on the final manuscript.

ACKNOWLEDGMENTS

The authors would like to express their gratitude to the family for their participation in this study. The authors also sincerely thank Aegicare (Shenzhen) Technology Co., Ltd. (Shenzhen, China) for technical support.

SUPPLEMENTARY MATERIAL

The Supplementary Material for this article can be found online at: https://www.frontiersin.org/articles/10.3389/fgene.2021.609040/full#supplementary-material

Supplementary Figure 1 | The c.959-5T>G mutation in the PAX3 gene, which is identified in III-1 (proband), II-1, II-8, II-10 and III-2. The wild type is identified in II-2.

REFERENCES

Ambrozkiewicz, M. C., Borisova, E., Schwark, M., Ripamonti, S., Schaub, T., Smorodchenko, A., et al. (2020). The murine ortholog of Kaufman oculocerebrofacial syndrome protein Ube3b regulates synapse number by ubiquitinating Ppp3cc. *Mol. Psychiatry*. doi: 10.1038/s41380-020-0714-8. [Epub ahead of print].

Angwin, C., Brady, A. F., Pope, F. M., Vandersteen, A., Baker, D., Cheema, H., et al. (2020). Arterial complications in classical Ehlers-Danlos syndrome: a case series. *J. Med. Genet*. 57, 769–776. doi: 10.1136/jmedgenet-2019-106689

Apuzzo, S., and Gros, P. (2007). Cooperative interactions between the two DNA binding domains of Pax3: helix 2 of the paired domain is in the proximity of the amino terminus of the homeodomain. *Biochemistry* 46, 2984–2993. doi: 10.1021/bi062107q

Arias, S. (1971). Genetic heterogeneity in the Waardenburg syndrome. *Birth Defects Orig. Artic. Ser.* 7, 87–101.

Chen, S., Jin, Y., Xie, L., Xie, W., Xu, K., Qiu, Y., et al. (2020). A novel spontaneous mutation of the SOX10 gene associated with Waardenburg Syndrome Type II. *Neural. Plast.* 2020:9260807. doi: 10.1155/2020/9260807

Cheon, S., Kaur, K., Nijem, N., Tuncay, I. O., Kumar, P., Dean, M., et al. (2019). The ubiquitin ligase UBE3B, disrupted in intellectual disability and absent speech, regulates metabolic pathways by targeting BCKDK. *Proc. Natl. Acad. Sci. U.S.A.* 116, 3662–3667. doi: 10.1073/pnas.1818751116

Choi, Y., and Chan, A. P. (2015). PROVEAN web server: a tool to predict the functional effect of amino acid substitutions and indels. *Bioinformatics* 31, 2745–2747. doi: 10.1093/bioinformatics/btv195

Chun, S., and Fay, J. C. (2009). Identification of deleterious mutations within three human genomes. *Genome Res.* 19, 1553–1561. doi: 10.1101/gr.092619.109

Farrer, L. A., Grundfast, K. M., Amos, J., Arnos, K. S., Asher, J. H., Jr., et al. (1992). Waardenburg syndrome (WS) type I is caused by defects at multiple loci, one of which is near ALPP on chromosome 2: first report of the WS consortium. *Am. J. Hum. Genet.* 50, 902–913.

Hart, J., and Miriyala, K. (2017). Neural tube defects in Waardenburg syndrome: a case report and review of the literature. *Am. J. Med. Genet. A* 173, 2472–2477. doi: 10.1002/ajmg.a.38325

Hou, L., and Pavan, W. J. (2008). Transcriptional and signaling regulation in neural crest stem cell-derived melanocyte development: do all roads lead to Mitf? *Cell Res.* 18, 1163–1176. doi: 10.1038/cr.2008.303

Jaganathan, K., Kyriazopoulou Panagiotopoulou, S., McRae, J. F., Darbandi, S. F., Knowles, D., Li, Y. I., et al. (2019). Predicting splicing from primary sequence with deep learning. *Cell* 176, 535–548 e524. doi: 10.1016/j.cell.2018.12.015

Li, S., Guo, M., Ruan, B., Liu, Y., Cui, X., Han, W., et al. (2020). A Novel PAX3 Mutation in a Chinese family with Waardenburg Syndrome Type 1. *Genet. Test. Mol. Biomarkers* 24, 249–255. doi: 10.1089/gtmb.2019.0231

Lin, J. Y., and Fisher, D. E. (2007). Melanocyte biology and skin pigmentation. *Nature* 445, 843–850. doi: 10.1038/nature05660

Liu, Q., Cheng, J., Lu, Y., Zhou, J., Wang, L., Yang, C., et al. (2020). The clinical and genetic research of Waardenburg syndrome type I and II in Chinese families. *Int. J. Pediatr. Otorhinolaryngol.* 130:109806. doi: 10.1016/j.ijporl.2019.109806

Ma, J., Lin, K., Jiang, H. C., Yang, Y., Zhang, Y., Yang, G., et al. (2019). A novel mutation of the PAX3 gene in a Chinese family with Waardenburg Syndrome Type I. *Mol. Genet. Genomic Med.* 7:e00798. doi: 10.1002/mgg3.798

Mica, Y., Lee, G., Chambers, S. M., Tomishima, M. J., and Studer, L. (2013). Modeling neural crest induction, melanocyte specification, and disease-related pigmentation defects in hESCs and patient-specific iPSCs. *Cell. Rep.* 3, 1140–1152. doi: 10.1016/j.celrep.2013.03.025

Minami, S. B., Nara, K., Mutai, H., Morimoto, N., Sakamoto, H., Takiguchi, T., et al. (2019). A clinical and genetic study of 16 Japanese families with Waardenburg syndrome. *Gene* 704, 86–90. doi: 10.1016/j.gene.2019.04.023

Ng, P. C., and Henikoff, S. (2003). SIFT: Predicting amino acid changes that affect protein function. *Nucleic Acids Res.* 31, 3812–3814. doi: 10.1093/nar/gkg509

Oysu, C., Baserer, N., and Tinaz, M. (2000). Audiometric manifestations of Waardenburg's syndrome. *Ear Nose Throat. J.* 79, 704–709. doi: 10.1177/014556130007900909

Pingault, V., Ente, D., Dastot-Le Moal, F., Goossens, M., Marlin, S., and Bondurand, N. (2010). Review and update of mutations causing Waardenburg syndrome. *Hum. Mutat.* 31, 391–406. doi: 10.1002/humu.21211

Read, A. P., and Newton, V. E. (1997). Waardenburg syndrome. *J. Med. Genet.* 34, 656–665. doi: 10.1136/jmg.34.8.656

Reva, B., Antipin, Y., and Sander, C. (2007). Determinants of protein function revealed by combinatorial entropy optimization. *Genome Biol.* 8:R232. doi: 10.1186/gb-2007-8-11-r232

Richards, S., Aziz, N., Bale, S., Bick, D., Das, S., Gastier-Foster, J., et al. (2015). Standards and guidelines for the interpretation of sequence variants: a joint consensus recommendation of the American College of Medical Genetics and Genomics and the Association for Molecular Pathology. *Genet. Med.* 17, 405–424. doi: 10.1038/gim.2015.30

Saleem, M. D. (2019). Biology of human melanocyte development, Piebaldism, and Waardenburg syndrome. *Pediatr. Dermatol.* 36, 72–84. doi: 10.1111/pde.13713

Schwarz, J. M., Rodelsperger, C., Schuelke, M., and Seelow, D. (2010). MutationTaster evaluates disease-causing potential of sequence alterations. *Nat. Methods* 7, 575–576. doi: 10.1038/nmeth0810-575

Shields, C. L., Nickerson, S. J., Al-Dahmash, S., and Shields, J. A. (2013). Waardenburg Syndrome: iris and choroidal hypopigmentation: findings on anterior and posterior segment imaging. *JAMA Ophthalmol.* 131, 1167–1173. doi: 10.1001/jamaophthalmol.2013.4190

Shihab, H. A., Gough, J., Cooper, D. N., Stenson, P. D., Barker, G. L., Edwards, K. J., et al. (2013). Predicting the functional, molecular, and phenotypic consequences of amino acid substitutions using hidden Markov models. *Hum. Mutat.* 34, 57–65. doi: 10.1002/humu.22225

Sun, L., Li, X., Shi, J., Pang, X., Hu, Y., Wang, X., et al. (2016). Molecular etiology and genotype-phenotype correlation of Chinese Han deaf patients with type I and type II Waardenburg Syndrome. *Sci. Rep.* 6:35498. doi: 10.1038/srep35498

Tachibana, M. (2001). Cochlear melanocytes and MITF signaling. *J. Investig. Dermatol. Symp. Proc.* 6, 95–98. doi: 10.1046/j.0022-202x.2001.00017.x

Tachibana, M., Takeda, K., Nobukuni, Y., Urabe, K., Long, J. E., Meyers, K. A., et al. (1996). Ectopic expression of MITF, a gene for Waardenburg syndrome type 2, converts fibroblasts to cells with melanocyte characteristics. *Nat. Genet.* 14, 50–54. doi: 10.1038/ng0996-50

Tuna, F., Doganlar, Z. B., Özdemir, H., Demirbag Kabayel, D., and Doganlar, O. (2019). Ehlers-Danlos syndrome-related genes and serum strontium, zinc, and lithium levels in generalized joint hypermobility: a case-control study. *Connect. Tissue Res.* 62, 215–225. doi: 10.1080/03008207.2019.1675648

Waardenburg, P. J. (1951). A new syndrome combining developmental anomalies of the eyelids, eyebrows and nose root with pigmentary defects of the iris and head hair and with congenital deafness. *Am. J. Hum. Genet.* 3, 195–253.

Wildhardt, G., Zirn, B., Graul-Neumann, L. M., Wechtenbruch, J., Suckfüll, M., Buske, A., et al. (2013). Spectrum of novel mutations found in Waardenburg Syndrome Types 1 and 2: implications for molecular genetic diagnostics. *BMJ Open* 3: 001917. doi: 10.1136/bmjopen-2012-001917

Conflict of Interest: The authors declare that the research was conducted in the absence of any commercial or financial relationships that could be construed as a potential conflict of interest.

frontiers in Pediatrics

BRIEF RESEARCH REPORT
published: 04 March 2021
doi: 10.3389/fped.2021.638190

Novel Gross Deletion Mutations in *NTRK1* Gene Associated With Congenital Insensitivity to Pain With Anhidrosis

Lulu Li[1†], *Chao Jia*[2†], *Yue Tang*[1], *Yuanyuan Kong*[1], *Yaofang Xia*[2] *and Li Ma*[2*]

[1] Department of Newborn Screening Center, Beijing Obstetrics and Gynecology Hospital, Capital Medical University, Beijing Maternal and Child Health Care Hospital, Beijing, China, [2] Department of Neonatology, Hebei Provincial Children's Hospital, Shijiazhuang, China

Background: Congenital insensitivity to pain with anhidrosis (CIPA) is a rare inherited autosomal recessive disorder characterized by insensitivity to noxious stimuli, anhidrosis, recurrent fever, and intellectual disability. CIPA is mainly caused by mutations in the neurotrophic tyrosine kinase receptor type 1 gene (*NTRK1*). This study aims to identify pathogenic mutations underlying CIPA in two unrelated Chinese families.

Methods: DNA was extracted from blood samples of patients and their available family members and subjected to whole exome sequencing (WES). Real-time PCR (qPCR), Gap-PCR, and Sanger sequencing were applied to verify the identified variants.

Result: We found novel compound gross deletion mutations [exon1-6 del (g.1-1258_10169del); exon5-7 del (g.6995_11999del)] of *NTRK1* (MIM 191315) gene in family 1 and the compound heterozygous mutations [c.851-33T>A; exon5-7 del (g.6995_11999del)] in family 2. Interestingly, we discovered the intragenic novel gross deletion [exon5-7 del (g.6995_11999del)] mediated by recombination between Alu elements.

Conclusions: The present study highlights two rare gross deletion mutations in the *NTRK1* gene associated with CIPA in two unrelated Chinese families. The deletion of exon1-6 (g.1-1258_10169del) is thought to be the largest *NTRK1* deletion reported to date. Our findings expand the mutation spectrum of *NTRK1* mutations in the Chinese and could be useful for prenatal interventions and more precise pharmacological treatments to patients. WES conducted in our study is a convenient and useful tool for clinical diagnosis of CIPA and other associated disorders.

Keywords: Chinese families, HSAN, whole exome sequencing, mutations, CIPA, NTRK1

OPEN ACCESS

Edited by:
Sascha Meyer,
Saarland University Hospital, Germany

Reviewed by:
Muhammad Imran Naseer,
King Abdulaziz University, Saudi Arabia
Chunhua Zeng,
Guangzhou Women and Children's Medical Center, China

***Correspondence:**
Li Ma
18503292173@163.com

These authors have contributed equally to this work

Specialty section:
This article was submitted to Genetics of Common and Rare Diseases, a section of the journal Frontiers in Pediatrics

Received: *05 December 2020*
Accepted: *20 January 2021*
Published: *04 March 2021*

Citation:
Li L, Jia C, Tang Y, Kong Y, Xia Y and Ma L (2021) Novel Gross Deletion Mutations in NTRK1 Gene Associated With Congenital Insensitivity to Pain With Anhidrosis. Front. Pediatr. 9:638190. doi: 10.3389/fped.2021.638190

INTRODUCTION

Congenital insensitivity to pain with anhidrosis (CIPA; MIM 256800) or hereditary sensory and autonomic neuropathy type IV (HSAN-IV) is a rare autosomal recessive disease characterized by a loss of pain sensation, anhidrosis (inability to sweat), irregular body temperature, growth retardation, and progressive central nervous system defects (1–3). The HSAN affects both sexes

and has been classified into five distinct types proposed by Dyck and Ohta (4). These are sensory radicular neuropathy type I (HSAN I), congenital sensory neuropathy type II (HSAN II), familial dysautonomia (FD III), congenital insensitivity to pain with anhidrosis type IV (HSAN IV), and congenital indifference to pain associated with intellectual disability type V (HSAN V) (5). Each HSAN disorder is caused by different genetic factors that affect specific aspects of small fiber neurodevelopment, which results in variable phenotypic expression, and it is predominantly inherited as an autosomal recessive and dominant manner (6). HSAN type I is caused by the *SPTLC1* gene located on chromosomes 9q22.1–22.3, inherited as autosomal dominant form (7). However, HSAN type-II, HSAN type-III, HSAN type-IV, and HSAN type-V are inherited in an autosomal recessive manner caused by different genetic factors (4, 5).

CIPA was first described in 1963 by Swanson (8). It is caused by recessive loss-of-function mutations in neurotrophic tyrosine kinase receptor type 1 gene (*NTRK1*; MIM 191315) (9, 10). The gene *NTRK1* encodes tropomyosin receptor kinase A (TrkA) protein, which has a high affinity for nerve growth factor (NGF) receptor (11). NGF/TrkA signal is affected by *NTRK1* gene mutation (12). In recent years, with the enrichment of clinical experience and the development of sequencing technology, numerous CIPA cases have been reported, having homozygous or compound heterozygous mutations in *NTRK1* (13–15).

Here, we describe two unrelated Chinese families having HSAN type IV (CIPA) phenotype. Using whole exome sequencing (WES), we identified novel gross deletion mutations [exon1-6 del(g.1-1258_10169del) and exon5-7 del (g.6995_11999del)] in the *NTRK1* gene.

MATERIALS AND METHODS

Ethical Sight

The study design and protocol was approved by the Ethical Review Committee (ERC) Department of Newborn Screening Center, Beijing Obstetrics and Gynecology Hospital, Capital Medical University. Signed informed consent for the genetic analysis and publication of data was obtained from the patient's legal guardians. Pedigree was drawn (**Figures 1A**, **2A**), and the affected individuals were thoroughly examined by a local geneticist and physiologist.

Blood Sample Collection and DNA Extraction

Fresh blood sample was drawn from the affected and normal individuals. Genomic DNA was extracted using phenol chloroform method and was quantified by Nanodrop-2000 spectrophotometer.

Whole Exome Sequencing and Data Analysis

The two probands were subjected to whole exome sequencing (WES) at Beijing MyGenostics Technology Co., Ltd. WES libraries were prepared following the manufacturer's recommendations. Paired-end sequencing was performed on a NextSeq 500 sequencer (Illumina, San Diego, CA). After sequencing, the raw data were saved as a fastq format. After quality control, the clean reads were mapped to the UCSC hg19 human reference genome using BWA(0.7.12) software (http://bio-bwa.sourceforge.net/). The fastq file was converted to the bam file, and then to vcf file. The ANNOVAR software (http://annovar.openbioinformatics.org/en/latest/) was used to annotate the variants (**Supplementary Table 1**). We mainly focused on protein-altering variants such as missense, non-sense, splice site variants, and coding indels, with alternative allele frequencies <0.005 in the Exome Variant Server (EVS, https://evs.gs.washington.edu/EVS/), Genome Aggregation Database (gnomAD https://gnomad.broadinstitute.org/), 1000 Genomes (http://www.1000genomes.org/), dbSNP (http://www.ncbi.nlm.nih.gov/SNP/), and in the Exome Aggregation Consortium (ExAC, http://www.exac.broadinstitute.org) and an internal exome database including ∼200 exomes (16). To identify potential causal variants, we further filtered the variants based on a recessive and dominant mode of inheritance. Different bioinformatics software including Mutation Taster (http://www.mutationtaster.org/), Polyphen-2 (http://genetics.bwh.harvard.edu/pph2), and Sorting Intolerant From Tolerant (SIFT, http://www.sift.jcvi.org/) were used for functional effect prediction. The Human Gene Mutation Database (HGMD; http: //www. hgmd.cf.ac.uk/ac/index.php) was used to search for identified variant novelty. Finally, in the assessment of variant interpretations and pathogenicity, the American College of Medical Genetics and Genomics (ACMG) 2015 guidelines were used (17).

CNV Analysis

The CNV analysis was performed at Beijing MyGenostics Technology Co., Ltd. The Cnvkit software (https://cnvkit.readthedocs.io/en/stable/index.html) was used to analyze the samples captured in the same pool. The read depth of target region and non-target region was counted, and then the depth was homogenized and corrected in the sample, and compared with the control set, and the copy number information was obtained. Multiple samples to establish reference for error correction of reads-depth were used. Discrete copy number fragments were calculated through the built-in segmentation algorithm of the software. A ratio below 0.7 was speculated as putative deletions, and the ratio that rose above 1.3 was considered as putative duplications (18).

Real-Time Quantitative Polymerase Chain Reaction

The genomic DNA or cDNA reference sequences of *NTRK1* (hg19, NC_000001.10 and NM_001012331.1) were obtained from the University of California, Santa Cruz (UCSC) Genome browser database (https://genome.ucsc.edu/). Primer 5.0 primer software was used to design the specific PCR primers (**Supplementary Table 2**). Real-time quantitative PCR (Q-PCR) reaction was carried out using the CFX96 Touch Real-Time PCR Detection System (Bio-Rad, Hercules, CA, USA). SYBR Green I (TaKaRa) was used as the fluorescent label. The total reaction system is a 10-μl final volume; each assay was performed in quadruplicate. The reactions were carried out by the following

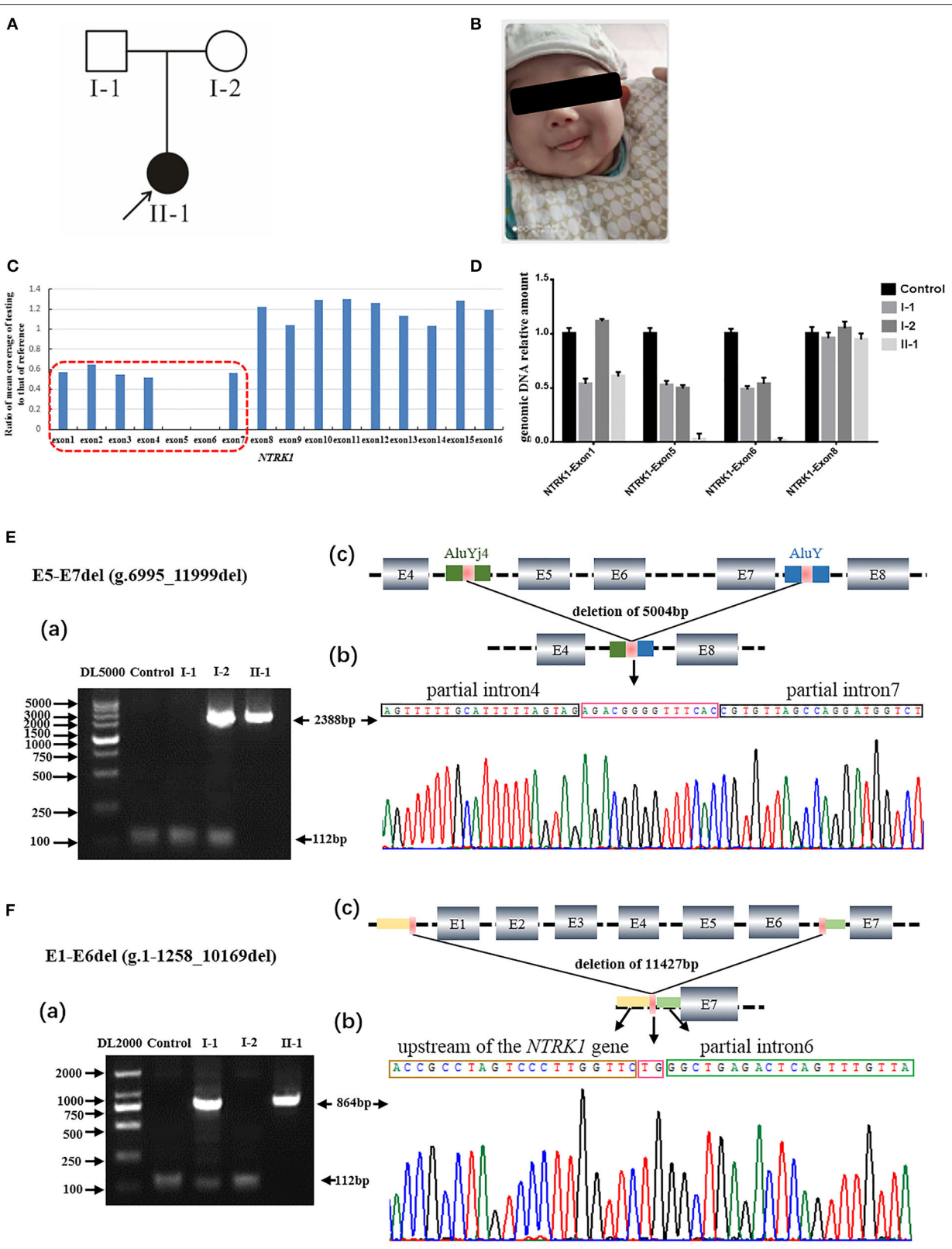

FIGURE 1 | Identification of compound heterozygous gross deletion mutations of neurotrophic tyrosine kinase receptor type 1 *(NTRK1)* in family 1. **(A)** Pedigree chart of family1, black arrow indicates the proband. **(B)** Current situation of patient 1. **(C)** The result of whole exome sequencing (WES), the blue bar chart Means coverage

(Continued)

FIGURE 1 | of each exon of *NTRK1* gene. Bar chart of readcount showing a suspicious area of CNVs (red squares) of *NTRK1*. It indicates the mutation conclude deletion of exon1-6 and the deletion of exon6-7. **(D)** The real-time quantitative PCR result (right) verified the compound heterozygous deletion. Deletion of exon1-6 derived from the father and deletion of exon6-7 derived from the mother. **(E)** Identification of the gross deletion E6-E7del (g.6995_11999del): (a) Gap-PCR products about 2,388 bp, the forward primer in exon4 and the reverse primer in exon8, proband and his mother amplified the products. Except for the patient 1, the other three people could amplify the internal reference fragment (112 bp); (b) DNA sequencing of the Gap-PCR products unveiled a deletion of 5,004 bp, and the breakpoint junction was located within two Alu repetitive elements with 14 bp common fusion; (c) The schematic map of gross deletion: E5-E7del (g.6995_11999del), gross deletion covering exons5, exon6, exon7, and introns in *NTRK1*. **(F)** Identification of the gross deletion E1-E6del (g.1-1258_10169del): (a) Gap-PCR products about 864 bp, the forward primer in upstream of the *NTRK1* gene, and the reverse primer in exon7, proband and his father amplified the products. The internal reference fragment (112 bp) only found between the control and the parents; (b) DNA sequencing of the Gap-PCR products unveiled a deletion of 11,427 bp, and the breakpoint junction with 2 bp common fusion; (c) The schematic map of gross deletion:E1-E6del (g.1-1258_10169del) gross deletion covering exon1-6, upstream of the *NTRK1* gene, and introns in *NTRK1*.

program: 95°C for 30 s followed by 40 cycles of 95°C for 10 s, 62°C for 15 s, and 72°C for 20 s.

Mutation Validation

Primer 5.0 primer software was used to design the Gap-PCR primers and internal reference primer of exon6 in the deleted fragment (**Supplementary Table 2**). The PCR reaction was commenced with an initial 3-min denaturation step at 95 °C, followed by 38 cycles of denaturation (94 °C) for 30 s, annealing (60 °C) for 30 s, and extension (72 °C) for 50 s, and ended with a final extension step at 72 °C for 8 min. The PCR products were purified and subjected to Sanger sequencing using an ABI3700 automated sequencer (PE Bio systems, Foster City, CA). The Sanger sequencing results were examined and compared with the help of visual software such as Chromas Lite and Codon Code Aligner. Sanger DNA sequencing was further used to identify the break-points of gross deletions.

RESULTS

Clinical Investigation

In this study, we recruited two Chinese families (family 1 and family 2) affected by CIPA due to variants *NRKT1*, which were identified by WES technology. Both families were visited at the Department of Newborn Screening Center, Beijing Obstetrics and Gynecology Hospital, Capital Medical University. Normal elders or guardians were interviewed to record the history of the disease, marriage type, affected and non-affected subjects, and disease status, and to generate the family tree (**Figures 1A**, **2A**).

Family 1

The members of family 1 (**Figure 1A**) live in Hebei Province of China. Family 1 has 1 affected individual (II-1) having typical features of autosomal recessive CIPA (**Figure 1A**). The family's medical history, pregnancy, and delivery were uneventful. Parents of the affected individuals were physically and mentally normal and healthy. The proband (II-1) showed intermittent fever with abnormal body temperature. Her clinical features include loss of pain sensation, anhidrosis, irregular body temperature, and dry skin (**Table 1**). There was no family history of CIPA seen in this family. Other clinical features such as intelligent quotient (IQ), height, cardiac, respiratory, skeletal, and hair were observed as normal (**Figure 1B**).

Family 2

Family 2 (**Figure 2A**) also originates from Hebei Province of China. The family comprises one affected male individual (II-3), indicating an autosomal recessive inheritance. The parents married without close relatives, and there was no family history of CIPA. The patient had congenital CIPA phenotype (**Figure 2B**): absence of normal responses to painful stimuli, anhidrosis, and recurrent fever. Last clinical examination, at 1 year and 3 months of age (**Figure 2Ba**) revealed fracture of the left humerus (**Figure 2Bb**), self-harm and biting of hands (**Figure 2Bc**), peeling fingers, dry and cracked skin, and growth retardation was observed. Other anomalies such as cardiac, respiratory, skeletal, hearing anomalies were seen normal. Detailed clinical information of the affected individuals is summarized in **Table 1**.

Mutation Identification and Confirmation

WES was performed for two affected individuals as described previously (16). Filtration of the identified variants was performed considering all patterns of inheritances. We focused only on pathogenic, likely pathogenic, VUS, non-synonymous (NS) variants causing missense, non-sense, frame-shift, splice site variants (SS), coding insertions, or deletions (indel). We identified gross novel deletion mutations in the two unrelated CIPA Chinese families (**Figures 1C**, **2C**). The pathogenic variants of the proband were detected in both alleles of *NTRK1*; their parents carries one pathogenic allele (**Table 1**).

Q-PCR analysis showed that patient 1 and her father had the same exon1 deletion, and patient 1 carries the homozygous deletion of exon5 and exon6 (**Figure 1D**). The result of Q-PCR verified that patient 2 carries the heterozygous deletion of exon5 and exon6, and the mutation of gross deletion was derived from the mother (**Figure 2D**).

Agarose gel electrophoresis indicated that patient 1 and his mother had the same 2,388-bp products (**Figure 1E**a). By gap-PCR and Sanger sequencing, we found a 5,004-bp (g.6995_11999del) deletion including exon5-7 (**Figure 1E**b). We made the schematic map of this gross deletion: the breakpoints were found in introns 4 and 7, and the junction of breakpoints was located within two Alu repetitive elements, which share a 14-bp common fusion sequence (**Figure 1E**c). This same gross deletion was detected in family 2 (**Figure 2E**). In the Sanger sequencing of the 864-bp Gap-PCR products (**Figure 1F**a), we found that patient 1 and his father had the deleted 11,427-bp (g.1-1258_10169del) fragments (**Figure 1F**b), and the

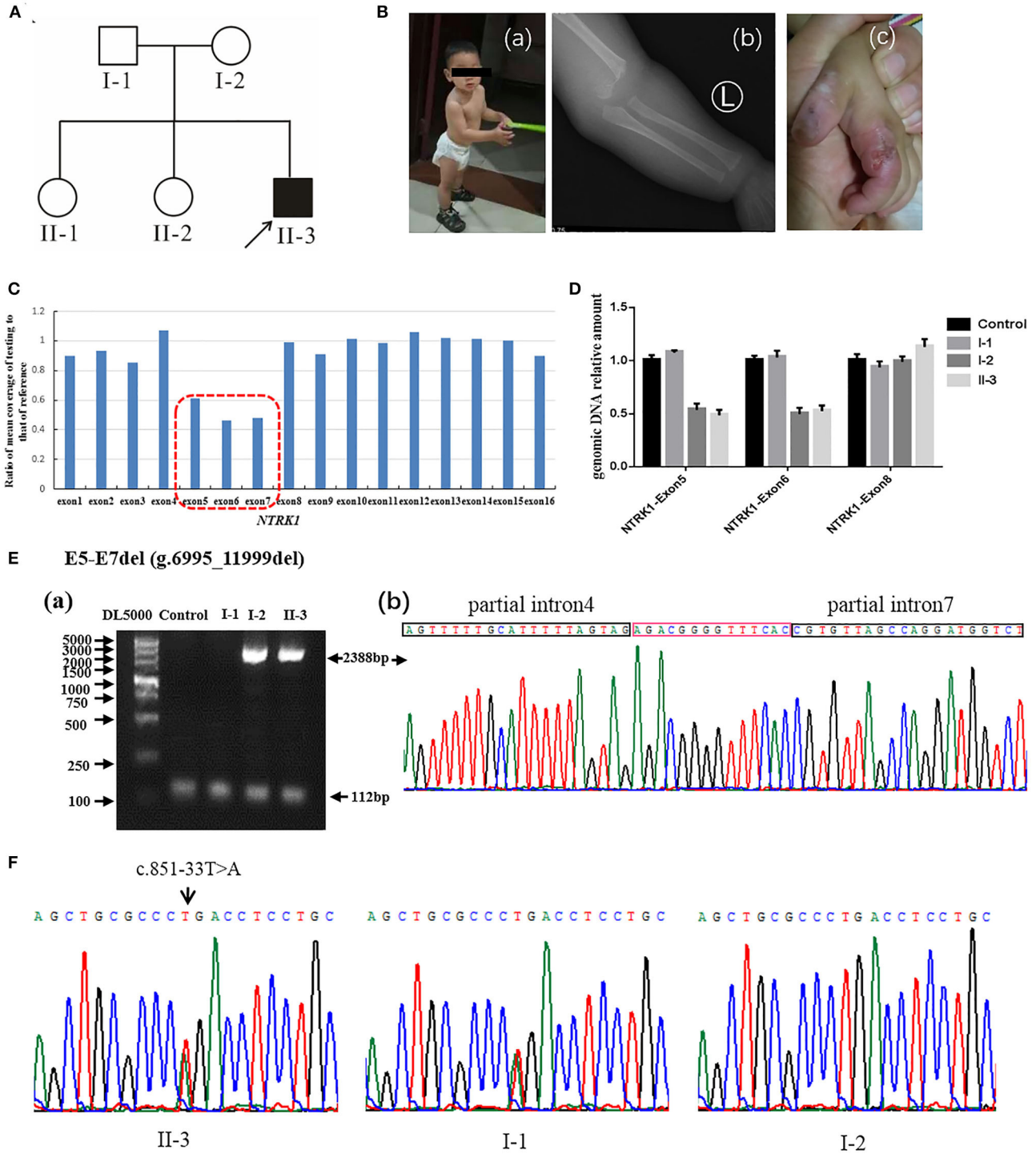

FIGURE 2 | Identification of compound heterozygous mutations of *NTRK1* in family 2. **(A)** Pedigree chart of family 2, black arrow indicates the proband. **(B)** The clinical manifestations of the proband: (a) current situation of patient 2 (b) damaged hand; (c) X-ray image showing a humeral fracture. **(C)** The result of whole exome sequencing (WES), the blue bar chart means coverage of each exon of *NTRK1* gene. Bar chart of readcount showing a suspicious area of CNVs (red squares) of *NTRK1*. It indicates the heterozygous gross deletion mutation from exon5 to exon7. **(D)** The real-time quantitative PCR result verified the gross deletion, and the heterozygous mutation of deletion derived from the mother. **(E)** Identification of the gross deletion: E6-E7del (g.6995_11999del): (a) Gap-PCR products about 2,388 bp, proband, and his mother amplified the products; the internal reference fragments (112 bp) can be amplified in all samples; (b) DNA sequencing of the Gap-PCR products, the breakpoint junction was located within intron4 and intron7. **(F)** Gene sequencing results: the proband carries heterozygous splicing mutation of *NTRK1* gene c.851-33T>A, and the mutation derived from the father.

TABLE 1 | Mutations of the CIPA patients recruited in this study.

Patient	Gene	Zygote type	Allele origin	Variant location	Nucleotide (amino acid) change	Novel variant
1	*NTRK1*	C-het	P	E1–E6	exon1-6 del (g.1-1258_10169del)	Yes
			M	E5–E7	exon5-7 del (g.6995_11999del)	Yes
2	*NTRK1*	C-het	P	I7	c.851- 33T>A	No
			M	E5–E7	exon5-7 del (g.6995_11999del)	Yes

C-het, compound heterozygote; P, paternal; M, maternal; E, exon; I, intron.

breakpoints were found in intron 6 and upstream of *NTRK1* (**Figures 1F**b,c). Meanwhile, except for patient 1, the other three people could amplify the internal reference fragment (112 bp) to verify the homozygous deletion of exon6 (**Figures 1E**a,**1F**a). Patient 2 carries the gross deletion mutation (g.6995_11999del) derived from the mother (**Figure 2E**a; **Supplementary Figure 1**). Through the gel image, we can see that all samples can amplify the internal reference fragments (112 bp), confirming that patient 2 is a heterozygous carrier of the mutation (**Figure 2E**a). By Sanger sequencing, we found that patient 2 carries heterozygous splicing mutation of the *NTRK1* gene c.851-33T>A and the mutation derived from the father (**Figure 2F**, **Supplementary Figure 1**).

DISCUSSION

The *NTRK1* is also known as *MTC*, *TRK*, *TRK1*, *TRKA*, *Trk-A*, and *p140-TrkA*, respectively. It is located on chromosome number 1q23.1 and covers about 20 kb of DNA. It has 17 exons and encodes 790/796 amino acid *NTRK1* enzymes (9, 10). The TrkA receptor has three functional domains: the extracellular domain, transmembrane domain, and intracellular tyrosine kinase domain (11, 12). To date, 128 different types of *NTRK1* gene mutations have been described in the human gene mutation database (HGMD, version Professional 2020.6; http://www.hgmd.org) causing CIPA phenotypes (**Supplementary Table 3**). The most reported mutations were in the intracellular tyrosine kinase domain. However, there is no clear correlation between the genotype and phenotype of CIPA patients (2, 19). Among 128 different mutations, we found that only four reports about gross deletion mutations (2, 20–23); the largest deletion range was about 1,403 bp, which included exon5-6 (**Supplementary Table 3**). It affects the extracellular domain (2).

In this study, we investigated two Chinese families (A and B) with CIPA. The two patients exhibited the common clinical characteristic symptoms of CIPA (24, 25): insensitivity to pain, anhidrosis, recurrent fever, and xerosis cutis, chapped (**Table 2**). Patient 2 have shown bone fracture, intellectual disability, and self-mutilation symptoms, but are not found in patient 1. We suspect that patient 1 is still in infancy. She has no teeth, and she does not have the ability to move independently. So some phenotypes have not yet appeared.

In family 1, we identified compound novel gross deletion mutations [exon1-6 del (g.1-1258_10169del) and exon5-7 del (g.6995_11999del)] of the *NTRK1* gene in patient 1. Both mutations are located in the extracellular domain. To our knowledge, the mutation [exon1-6 del] is the first reported and the largest *NTRK1* deletion of *NTRK1* in CIPA. The gross deletion contains the upstream of *NTRK1* gene, so it may cause the promoter to not be recognized, and the normal transcription of the gene is affected. Mutation [exon5-7 del (g.6995_11999del)] may lead to a premature termination of translation. By checking the UCSC Genome Browser (https://genome.ucsc.edu/), we found that the breakpoint was located within Alu elements. The breakpoint in intron 4 was within the AluYj4 region (chr1:156867686-156867934); the genomic size of AluYj4 element is about 249 bp. The breakpoint in intron 7 was within the AluY (chr1:156872676-156872976) region, the genomic size of AluY element is about 301 bp.

Based on the difference in key diagnostic nucleotides, the main Alu lineages are divided into AluJ, AluS, and AluY (26). AluYj was an AluY subfamily member, and it is classified as AluYj3 and AluYj4 (27). Alu element accounts for 10% of the human genome, due to the high similarity and richness of these Alu elements, it often participates in the rearrangement of the genome, thereby affecting gene expression and leading to the occurrence of diseases (28, 29). At present, about 515 cases of Alu-mediated deletion events have been reported, mainly through Alu insertion-mediated deletion (AIMD) or Alu recombination-mediated deletion (ARMD). Among them, the ARMD event was mainly caused by the recombination of Alu elements in different subfamilies (26, 30, 31). Although the AluJ subfamily is more abundant than the AluY subfamily, the AluY subfamily has higher sequence homology. Therefore, the ARMD event is closely related to the AluY subfamily (32). By using the NCBI Blast (https://blast.ncbi.nlm.nih.gov/Blast.cgi), we found that the similarity of these two Alu elements is as high as 89%. Our researches confirm once again (2) that Alu elements may be an important reason for *NTRK1* intragenic deletions.

In family 2, affected individuals revealed compound heterozygous mutations [c.851-33T>A and exon5-7 del (g.6995_11999del)]. The mutation c.851- 33T>A has been reported repeatedly at home and abroad (33, 34), which is the most common hot spot mutation in the CIPA population in Asia c.851-33T>A was first found by Miura et al. (35). The mini-gene

TABLE 2 | Clinical manifestations of the CIPA patients recruited in this study.

Patient	Affected patients number in family	Age at first visit (day)	Gender (M&F)	Insensitivity to pain	Anhidrosis	Recurrent fever	Bone fractures/times	Osteomyelitis	Intellectual disability	Self-mutilation	Irascibility	Xerosis cutis, chapped
1	1	16d	F	Y	Y	Y	N	N	N/A	N	N/A	Y
2	1	18d	M	Y	Y	Y	Y/1	N	Y	Y	N/A	Y

F, female; M, male; Y, yes; N, no; N/A, not available.

assay showed that the mutation resulted in the formation of a branching site, which was re-identified as an Ag signal and led to the insertion of 137 bp at the 3′ end of intron 7. The mutation exon5-7 del (g.6995_11999del) is the same as the mutation of patient 1.

Next-generation sequencing (NGS) technology includes WES, WGS, and Panel. It has expanded in the last decades with significant improvements in the reliability, sequencing chemistry, pipeline analyses, data interpretation, and costs. Such advances make the use of NGS feasible in clinical practice today for diagnostic evaluation of patients with suspected genetic disorders. Geng et al. (2) examined the *NTRK1* mutation spectrum and prevalence among 36 patients with CIPA in the Chinese population and described that there is no obvious correlation between genotype and phenotype relationship with *NTRK1* mutation. They performed NGS technology and found gross deletion and deep intronic mutation in the *NTRK1* gene (2). Zhao et al. (33) recruited 21 patients with CIPA and identified multiple forms of variants responsible for CIPA. By using WES technology, they identified gross deletion mutation in the deep intron, and they found a rough boundary of uniparental homodisomy (33). More interestingly, we found that Martin Farr et al. (36) used the NGS technology to detect the Alu-medicated exon duplication for Fabry disease.

CIPA is rare and rarely reported at home and abroad (1–3). The main clinical manifestation of CIPA is recurrent fever without obvious regularity (24). Many clinicians do not fully understand the disease and often misdiagnose it as infectious fever. At the same time, children with CIPA have lack of pain and may have self-mutilation behaviors such as tongue biting and hand biting, and are prone to accidental injuries such as fractures and burns (25). At present, there is no effective treatment for the disease, which mainly adopts cooling and active anti-infection symptomatic treatment. Therefore, high-throughput sequencing technology is used to detect and diagnose early, and effective protective treatment is carried out for children, to reduce the disability of children and ensure a better prognosis.

CONCLUSION

In conclusion, we identified the pathogenic mutations in two CIPA families and found two novel gross deletion mutations. It enriches the pathogenic mechanism of the *NTRK1* gene. The data will be helpful in diagnosing and predicting CIPA, and continued study of *NTRK1* gene mutations will be valuable for identification of affected newborns or gene carriers in families with an identified mutation. WES is not only convenient and fast but also can be used for rare deep intron variation and gross deletion.

DATA AVAILABILITY STATEMENT

The datasets presented in this study can be found in online repositories. The name of the repository and accession number can be found at: National Center for Biotechnology

Information (NCBI) GenBank, https://www.ncbi.nlm.nih.gov/genbank/, MW467564.

ETHICS STATEMENT

Signed informed consent for the genetic analysis and publication of data was obtained from the patient's legal guardians.

AUTHOR CONTRIBUTIONS

LL and CJ performed the sequencing analysis and wrote the manuscript. YT conducted the data collection as well as data analysis. YK and YX helped with recruiting patients. LM conceived the study and supervised this research. All authors performed critical reading and approved the final version of the manuscript.

FUNDING

This study was supported by grants from Beijing Obstetrics and Gynecology Hospital Specialized Youth Foundation Project (FCYYQN-202002).

ACKNOWLEDGMENTS

The authors thank the participants described in this report for their consent and support to publish this manuscript.

SUPPLEMENTARY MATERIAL

The Supplementary Material for this article can be found online at: https://www.frontiersin.org/articles/10.3389/fped.2021.638190/full#supplementary-material

REFERENCES

1. Indo Y, Tsuruta M, Hayashida Y, Karim MA, Ohta K, Kawano T, et al. Mutations in the TRKA/NGF receptor gene in patients with congenital insensitivity to pain with anhidrosis. *Nat Genet.* (1996) 4:485–8. doi: 10.1038/ng0896-485
2. Geng X, Liu Y, Ren X, Guan Y, Wang Y, Mao B, et al. Novel NTRK1 mutations in Chinese patients with congenital insensitivity to pain with anhidrosis. *Mol Pain.* (2018) 14:1744806918781140. doi: 10.1177/1744806918781140
3. Indo Y. NGF-dependent neurons and neurobiology of emotions and feelings: lessons from congenital insensitivity to pain with anhidrosis. *Neurosci Biobehav Rev*. (2018) 87:1–16. doi: 10.1016/j.neubiorev.2018.01.013
4. Axelrod FB, Gold-von Simson G. Hereditary sensory and autonomic neuropathies: types II, III, and IV. *Orphanet J Rare Dis.* (2007) 2:39. doi: 10.1186/1750-1172-2-39
5. Auer-Grumbach M, Mauko B, Auer-Grumbach P, Pieber TR. Molecular genetics of hereditary sensory neuropathies. *Neuromol Med.* (2006) 8:147–58. doi: 10.1385/NMM:8:1-2:147
6. Reyes-Reali J, Mendoza-Ramos MI, Garrido-Guerrero E, Méndez-Catalá CF, Méndez-Cruz AR, Pozo-Molina G. Hypohidrotic ectodermal dysplasia: clinical and molecular review. *Int J Dermatol.* (2018) 57:965–72. doi: 10.1111/ijd.14048
7. Auer-Grumbach M. Hereditary sensory neuropathy type I. *Orphanet J Rare Dis.* (2008) 3:7. doi: 10.1186/1750-1172-3-7
8. Swanson AG. Congenital insensitivity to pain with anhydrosis. A unique syndrome in two male siblings. *Arch Neurol.* (1963) 8:299–306. doi: 10.1001/archneur.1963.00460030083008
9. Mardy S, Miura Y, Endo F, Matsuda I, Sztriha L, Frossard P, et al. Congenital insensitivity to pain with anhidrosis: novel mutations in the TRKA (NTRK1) gene encoding a high-affinity receptor for nerve growth factor. *Am J Hum Genet.* (1999) 64:1570–9. doi: 10.1086/302422
10. Indo Y. Nerve growth factor, pain, itch and inflammation: lessons from congenital insensitivity to pain with anhidrosis. *Expert Rev Neurother.* (2010) 10:1707–24. doi: 10.1586/ern.10.154
11. Luberg K, Park R, Aleksejeva E, Timmusk T. Novel transcripts reveal a complex structure of the human TRKA gene and imply the presence of multiple protein isoforms. *BMC Neurosci.* (2015) 16:78. doi: 10.1186/s12868-015-0215-x
12. Smeyne RJ, Klein R, Schnapp A, Long LK, Bryant S, Lewin A, et al. Severe sensory and sympathetic neuropathies in mice carrying a disrupted Trk/NGF receptor gene. *Nature.* (1994) 368:246–9. doi: 10.1038/368246a0
13. Algahtani H, Naseer MI, Al-Qahtani M, Abdulrahman SA, Boker F, Shirah B. Congenital insensitivity to pain with anhidrosis: a report of two siblings with a novel mutation in (TrkA) NTRK1 gene in a Saudi family. *J Neurol Sci.* (2016) 370:35–8. doi: 10.1016/j.jns.2016.09.016
14. Masri A, Shboul M, Khasawneh A, Jadallah R, ALmustafa A, Escande-Beillard N, et al. Congenital insensitivity to pain with anhidrosis syndrome: a series from Jordan. *Clin Neurol Neurosurg.* (2020) 189:105636. doi: 10.1016/j.clineuro.2019.105636
15. López-Cortés A, Zambrano AK, Guevara-Ramírez P, Echeverría BA, Guerrero S, Cabascango E, et al. Clinical, genomics and networking analyses of a high-altitude native American Ecuadorian patient with congenital insensitivity to pain with anhidrosis: a case report. *BMC Med Genomics.* (2020) 13:113. doi: 10.1186/s12920-020-00764-3
16. Li L, Mao B, Li S, Xiao J, Wang H, Zhang J, et al. Genotypic and phenotypic characterization of Chinese patients with osteogenesis imperfecta. *Hum Mutat.* (2019) 40:588–600. doi: 10.1002/humu.23718
17. Richards S, Aziz N, Bale S, Bick D, Das S, Gastier-Foster J, et al. Standards and guidelines for the interpretation of sequence variants: a joint consensus recommendation of the American College of Medical Genetics and Genomics and the Association for Molecular Pathology. *Genet Med.* (2015) 17:405–24. doi: 10.1038/gim.2015.30
18. Sun T, Xu K, Ren Y, Xie Y, Zhang X, Tian L, et al. Comprehensive molecular screening in Chinese usher syndrome patients. *Invest Ophthalmol Vis Sci.* (2018) 59:1229–37. doi: 10.1167/iovs.17-23312
19. Li N, Guo S, Wang Q, Duan G, Sun J, Liu Y, et al. Heterogeneity of clinical features and mutation analysis of NTRK1 in Han Chinese patients with congenital insensitivity to pain with anhidrosis. *J Pain Res.* (2019) 12:453–65. doi: 10.2147/JPR.S188566
20. Xue XM, Liu YQ, Pang P, Sun CF. Congenital loss of permanent teeth in a patient with congenital insensitivity to pain with anhidrosis due to 2 novel mutations in the NTRK1 gene. *J Oral Maxillofac Surg.* (2018) 76:2582.e1–9. doi: 10.1016/j.joms.2018.06.170
21. Amin S, Forrester N, Norman A, Lux A, Vijayakumar K. Novel 9 amino acid in-frame deletion in the NTRK1 tyrosine kinase domain in a patient with congenital insensitivity to pain with anhydrosis. *Clin Genet.* (2017) 92:559–60. doi: 10.1111/cge.13064
22. Huehne K, Zweier C, Raab K, Odent S, Bonnaure-Mallet M, Sixou JL, et al. Novel missense, insertion and deletion mutations in the neurotrophic tyrosine kinase receptor type 1 gene (NTRK1) associated with congenital insensitivity to pain with anhidrosis. *Neuromuscul Disord.* (2008) 18:159–66. doi: 10.1016/j.nmd.2007.10.005
23. Li B, Zhang Z, Wu X, Chen W, Chen J, Lyu Q, et al. Mutation analysis of NTRK1 gene in a family affected with congenital insensitivity to pain with anhidrosis. *J Med Genet.* (2017) 34:646–9. doi: 10.3760/cma.j.issn.1003-9406.2017.05.005
24. Shaikh SS, Chen YC, Halsall SA, Nahorski MS, Omoto K, Young GT, et al. A comprehensive functional analysis of NTRK1 missense mutations causing hereditary sensory and autonomic neuropathy type IV (HSAN IV). *Hum Mutat.* (2017) 8:55–63. doi: 10.1002/humu.23123

25. Nabiyev V, Kara A, Aksoy MC. Multidisciplinary assessment of congenital insensitivity to pain syndrome. *Childs Nerv Syst.* (2016) 32:1741–4. doi: 10.1007/s00381-016-3059-5
26. Kim S, Cho CS, Han K, Lee J. Structural variation of Alu element and human disease. *Genomics Inform.* (2016) 14:70–7. doi: 10.5808/GI.2016.14.3.70
27. Park ES, Huh JW, Kim TH, Kwak KD, Kim W, Kim HS. Analysis of newly identified low copy AluYj subfamily. *Genes Genet Syst.* (2005) 80:415–22. doi: 10.1266/ggs.80.415
28. Sen SK, Han K, Wang J, Lee J, Wang H, Callinan PA, et al. Human genomic deletions mediated by recombination between Alu elements. *Am J Hum Genet.* (2006) 79:41–53. doi: 10.1086/504600
29. Callinan PA, Wang J, Herke SW, Garber RK, Liang P, Batzer MA. Alu retrotransposition-mediated deletion. *J Mol Biol.* (2005) 348:791–800. doi: 10.1016/j.jmb.2005.02.043
30. Rüdiger NS, Gregersen N, Kielland-Brandt MC. One short well conserved region of Alu-sequences is involved in human gene rearrangements and has homology with prokaryotic chi. *Nucleic Acids Res.* (1995) 3:256–60. doi: 10.1093/nar/23.2.256
31. Gu W, Zhang F, Lupski JR. Mechanisms for human genomic rearrangements. *Pathogenetics.* (2008) 1:4. doi: 10.1186/1755-8417-1-4
32. Ade C, Roy-Engel AM, Deininger PL. Alu elements: an intrinsic source of human genome instability. *Curr Opin Virol.* (2013) 3:639–45. doi: 10.1016/j.coviro.2013.09.002
33. Zhao F, Mao B, Geng X, Ren X, Wang Y, Guan Y, et al. Molecular genetic analysis in 21 Chinese families with congenital insensitivity to pain with or without anhidrosis. *Eur J Neurol.* (2020) 27:1697–705. doi: 10.1111/ene.14234
34. Liu Z, Liu J, Liu G, Cao W, Liu S, Chen Y, et al. Phenotypic heterogeneity of intellectual disability in patients with congenital insensitivity to pain with anhidrosis: a case report and literature review. *J Int Med Res.* (2018) 46:2445–57. doi: 10.1177/0300060517747164
35. Miura Y, Mardy S, Awaya Y, Nihei K, Endo F, Matsuda I, et al. Mutation and polymorphism analysis of the TRKA (NTRK1) gene encoding a high-affinity receptor for nerve growth factor in congenital insensitivity to pain with anhidrosis (CIPA) families. *Hum Genet.* (2000) 106:116–24. doi: 10.1007/s004399900205
36. Farr M, Ferreira S, Al-Dilaimi A, Bögeholz S, Goesmann A, Kalinowski J, et al. Fabry disease: detection of Alu-mediated exon duplication by NGS. *Mol Cell Probes.* (2019) 45:79–83. doi: 10.1016/j.mcp.2019.03.008

Conflict of Interest: The authors declare that the research was conducted in the absence of any commercial or financial relationships that could be construed as a potential conflict of interest.

frontiers in Genetics

ORIGINAL RESEARCH
published: 29 April 2021
doi: 10.3389/fgene.2021.636934

Identification of Hub Genes and MicroRNAs Associated With Idiopathic Pulmonary Arterial Hypertension by Integrated Bioinformatics Analyses

*Xue Qiu[1], Jinyan Lin[2], Bixiao Liang[2], Yanbing Chen[2], Guoqun Liu[2] and Jing Zheng[1]**

[1] Department of Cardiology, The First Affiliated Hospital of Guangxi Medical University, Nanning, China, [2] The First Clinical Medical School, Guangxi Medical University, Nanning, China

Objective: The aim of this study is the identification of hub genes associated with idiopathic pulmonary arterial hypertension (IPAH).

Materials and Methods: GSE15197 gene expression data was downloaded from the Gene Expression Omnibus (GEO) database. Differentially expressed genes (DEGs) were identified by screening IPAH patients and controls. The 5,000 genes with the greatest variances were analyzed using a weighted gene co-expression network analysis (WGCNA). Modules with the strongest correlation with IPAH were chosen, followed by a functional enrichment analysis. Protein–protein interaction (PPI) networks were constructed to identify hub gene candidates using calculated degrees. Real hub genes were found from the overlap of DEGs and candidate hub genes. microRNAs (miRNAs) targeting real hub genes were found by screening miRNet 2.0. The most important IPAH miRNAs were identified.

Results: There were 4,395 DEGs identified. WGCNA indicated that green and brown modules associated most strongly with IPAH. Functional enrichment analysis showed that green and brown module genes were mainly involved in protein digestion and absorption and proteoglycans in cancer, respectively. The top ten candidate hub genes in green and brown modules were identified, respectively. After overlapping with DEGs, 11 real hub genes were identified: *EP300*, *MMP2*, *CDH2*, *CDK2*, *GNG10*, *ALB*, *SMC2*, *DHX15*, *CUL3*, *BTBD1*, and *LTN1*. These genes were expressed with significant differences in IPAH versus controls, indicating a high diagnostic ability. The miRNA–gene network showed that hsa-mir-1-3p could associate with IPAH.

Conclusion: *EP300*, *MMP2*, *CDH2*, *CDK2*, *GNG10*, *ALB*, *SMC2*, *DHX15*, *CUL3*, *BTBD1*, and *LTN1* may play essential roles in IPAH. Predicted miRNA hsa-mir-1-3p could regulate gene expression in IPAH. Such hub genes may contribute to the pathology and progression in IPAH, providing potential diagnostic and therapeutic opportunities for IPAH patients.

Keywords: idiopathic pulmonary arterial hypertension, differentially expressed genes, functional enrichment analysis, weighted gene co-expression network analysis, hub genes

OPEN ACCESS

Edited by:
Sascha Meyer, Saarland University Hospital, Germany

Reviewed by:
Duy Ngoc Do, Dalhousie University, Canada
Maria Do Carmo Costa, University of Michigan, United States

****Correspondence:***
Jing Zheng
z2003jing@163.com

Specialty section:
This article was submitted to Genetics of Common and Rare Diseases, a section of the journal Frontiers in Genetics

Received: *02 December 2020*
Accepted: *22 March 2021*
Published: *29 April 2021*

Citation:
Qiu X, Lin J, Liang B, Chen Y, Liu G and Zheng J (2021) Identification of Hub Genes and MicroRNAs Associated With Idiopathic Pulmonary Arterial Hypertension by Integrated Bioinformatics Analyses. Front. Genet. 12:667406. doi: 10.3389/fgene.2021.636934

INTRODUCTION

Idiopathic pulmonary arterial hypertension (IPAH) is a pulmonary proliferative vasculopathy (Gallo de Moraes et al., 2016). Pathological changes including plexiform lesions, cellular proliferation, fibrosis, *in situ* thrombosis of the small pulmonary arteries and arterioles, and angiogenic dysfunction, leading to increased pulmonary vascular resistance, result in IPAH (Barnes et al., 2019). The incidence of IPAH is approximately four to six per million globally. When left untreated, IPAH eventually leads to right heart failure and death (Pahal and Sharma, 2020). IPAH remains intractable, with a 51% 5-year survival rate (Barnes et al., 2019). In the last 20 years, new therapies have been developed, improving hemodynamics and long-term prognosis (Wang Y. et al., 2019). For those not sensitive to therapy, surgery such as atrial septostomy and lung transplantation are options, although the prognosis is poor (Pahal and Sharma, 2020).

Many genes and microRNAs (miRNAs) have been shown to be involved in IPAH. A meta-analysis suggested the serotonin transporter (*SERT*) is associated with IPAH risk, and those with long genotypes have greater incidence of IPAH than those with short genotypes (Zhang et al., 2013). Mutations in the human bone morphogenetic protein 9 (*BMP9*) gene reduced anti-apoptosis in pulmonary arterial endothelial cells (Wang X. J. et al., 2019). A greater expression of miR-199b-5p accelerated hemodynamics and pulmonary vascular remodeling (Wu et al., 2016). Silencing of miR23a increased the expression of PGC1α, leading to IPAH progression (Sarrion et al., 2015). However, the genetic mechanisms underlying IPAH pathology remain unclear. More studies are required to explore the pathogenesis, potential drug targets, and diagnostic biomarkers of IPAH.

A systems biology analysis of gene expression and regulation has become an effective method for exploring disease pathogenesis. A weighted gene co-expression network analysis (WGCNA) can identify correlations between genes and microarray samples (Wang T. et al., 2019). Clustering genes with similar expression profiles can identify the association of genes and clinical traits. Thus, WGCNA can be used to find hub genes associated with a specific disease, including cardiovascular disease (Zheng et al., 2020) and cancer (Hu et al., 2020; Shi et al., 2021).

Although cardiovascular disease is well studied, there are few bioinformatics analyses of IPAH. Here, a co-expression network was constructed to identify genes related to IPAH pathogenesis, providing new routes to diagnose and treat IPAH. This study should provide novel biomarkers associated with IPAH pathogenesis and progression, which may be useful as potential therapeutic targets in IPAH. The flow diagram of the work is shown in **Figure 1**.

MATERIALS AND METHODS

Data Sources

Microarray expression data (GSE15197) was downloaded from the Gene Expression Omnibus (GEO)[1] database, representing a GPL6480 Agilent-014850 Whole Human Genome Microarray 4 × 44K G4112F (Probe Name version). GSE15197 includes 31 lung tissue specimens from 18 IPAH patients and 13 normal controls. Subject characteristics are presented in **Supplementary Table 1**. Platform information and probe annotation were extracted for additional analysis.

Data Preprocessing and Differentially Expressed Genes Screening

The downloaded gene expression data (GSE15197.txt) was preprocessed using k-nearest neighbor (KNN) to supplement missing values. Expression levels were then normalized using a log2 transformation. When multiple probes map to the same gene, the average value was retained as the expression level. After pooling unmatched probes, 17,540 mRNAs were accessed. These samples were divided between IPAH and control groups. Differently expressed mRNAs (DEmRNAs) were screened using the limma package in R3.5.3 (Ritchie et al., 2015). A false discovery rate and the Benjamini–Hochberg method (Fu et al., 2014) were used to calculate fold changes (FC). $|\mathrm{Log_2FC}| > 0.5$ and adjusted p-value < 0.05 were used as thresholds.

Weighted Gene Co-expression Network Analysis

To maintain sample diversity, the top 5,000 genes with the greatest variance between IPAH and normal controls were used to construct a co-expression network using the WGCNA package in R3.5.3 (Li et al., 2020; Tutorials for Wgcna R package, 2020; Zhang and Horvath, 2005). The "hclust" function was used for sample cluster analysis. Samples with heights over 115 were regarded as outliers. Other samples were used for calculating Pearson's correlation coefficients. Scale independence and mean connectivity were calculated using the gradient method, with power values between 1 and 20. An appropriate soft threshold power of β was selected to meet the standard of a scale-free network (scale-free $R2 \geq 0.80$) (Langfelder and Horvath, 2008) and ensure the network with enough information. The adjacency matrix was transformed into a topological overlap measure (TOM) matrix, which helped estimate the connectivity properties of the network (Iancu et al., 2015). Subsequently, the dynamic branch-cutting method was used to identify gene modules. Genes with similar gene expression profiles were placed in the same module. Each module contained genes with a minimum size of 30. The correlation between module eigengenes and clinical traits was analyzed and displayed as a heatmap. Modules that correlated most significantly with disease status were treated as key modules of IPAH. Gene significance (GS) represented the association between gene expression and each trait. Module membership (MM) was the correlation between gene expression and each module eigengene. The correlation between MM and GS was calculated using Pearson correlation analysis to validate module–trait associations (Zhang and Horvath, 2005).

Functional Enrichment Analysis of Genes in the Key Module

Key modules showing the strongest correlations with IPAH were chosen for further analysis. The gene complement of each

[1]https://www.ncbi.nlm.nih.gov/geo/

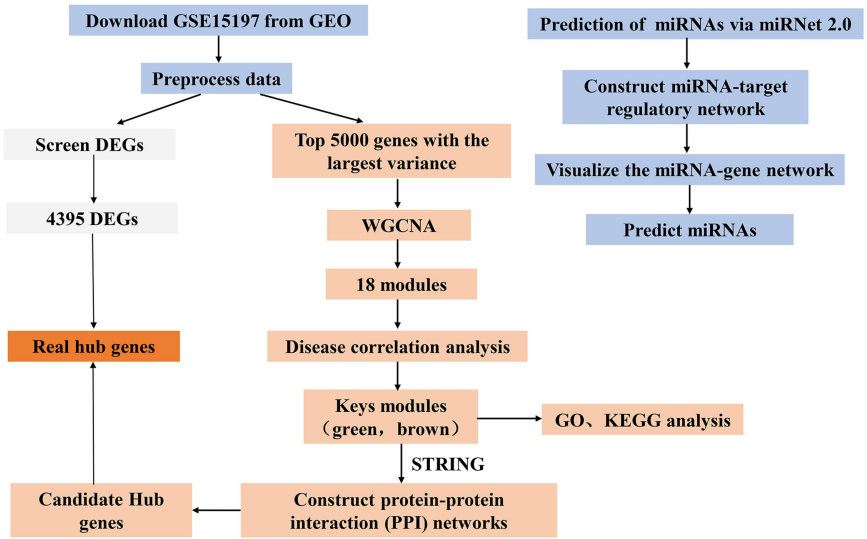

FIGURE 1 | Flow chart for this study. miRNA, microRNA.

key module was examined using Gene Ontology (GO) and the Kyoto Encyclopedia of Genes and Genomes (KEGG) pathway enrichment analysis using the GEne SeT Analysis Toolkit[2]. The GO analysis annotates gene function at three levels: biological process (BP), cellular component (CC), and molecular function (MF). $P < 0.05$ was taken as statistically significant. The top 10 enriched items from each GO category and from KEGG were displayed using bubble charts.

Identification of Protein–Protein Interaction Networks

To explore the potential roles of hub genes in the pathogenesis of IPAH, we used genes from all key modules to construct protein–protein interaction (PPI) networks using the STRING database[3] (version 11.0). Cytoscape3.6.1 software was used for visualization and analysis (Shannon et al., 2003). Nodes represent proteins. Edges between nodes indicate the evidence of the supposed relationship between distinct nodes. The more and stronger connections a node has, the more likely it is to have an important role in IPAH pathogenesis. Cytoscape3.6.1 provides 11 methods for calculating the connections between nodes. Degree was chosen to represent connections between nodes. Genes with the top 10 degree in key modules were considered candidate hub genes.

Identification of Real Hub Genes and Statistical Analysis

To increase the biological significance of candidate hub genes, we sought overlaps between candidates and differentially expressed genes (DEGs) to find real hub genes. Student's *t*-tests were used to assess expression differences of 11 hub genes between IPAH and controls. Receiver operating characteristic (ROC) curves were used to evaluate the diagnostic ability of hub genes, with the area under the curve (AUC) representing sensitivity and specificity. All *P*-values were two sided. $P < 0.05$ was taken as statistically significant. Statistical analysis was performed using GraphPad Prism 8.0 (GraphPad Statistics Guide, 2020) and MedCalc 19.5.1 (Schoonjans et al., 1995).

Construction of Potential miRNA-Target Regulatory Networks

We used miRNet 2.0[4] to search for miRNAs targeting real hub genes and visualized the miRNA-target regulatory network (Fan et al., 2016). miRNAs with degrees 3 or above are shown.

RESULTS

DEGs Screening

There were 4,395 differently expressed genes between IPAH and controls. This included 2,529 upregulated and 1,866 downregulated genes. The top 20 DEGs are listed in **Supplementary Table 2**.

Construction and Analysis of Co-expression Network

The top 5,000 genes were selected for construction of a co-expression network. Results of the cluster analysis are shown in **Figure 2A**. After clustering, GSM379320 was identified as an outlier, so has been excluded. The other 30 samples were used to construct a WGCNA network. To ensure a scale-free network and greater mean connectivity, a power of $\beta = 6$ was chosen (**Figure 2B**). As shown in **Figure 2C**, 18 gene modules were

[2]http://www.webgestalt.org/

[3]https://string-db.org

[4]https://www.mirnet.ca/

identified using the dynamic branch-cutting approach, with a merge cut height of 0.25. Genes in the same module had similar expression profiles. From the module–trait relationships analysis (**Figure 2D**), we found that the green (r = 0.74, p < 0.001), blue (r = 0.59, p < 0.001), black (r = 0.58, p < 0.001), and brown modules (r = −0.60, p < 0.001) were strongly related to the IPAH disease status. The green module had the strongest positive relation with IPAH, and the brown module had the strongest negative relation. We considered these two modules as the key IPAH modules, selecting them for further analysis. Associations between MM and GS for disease status were calculated. Significant correlations between MM and GS for IPAH in the green and brown modules are presented in **Figures 3A,B**.

Functional Enrichment Analysis of Genes in the Green and Brown Modules

Genes in the green and brown modules were analyzed using GO and KEGG enrichment analysis. As shown in **Figure 4**, the results of GO analysis indicated that the green module

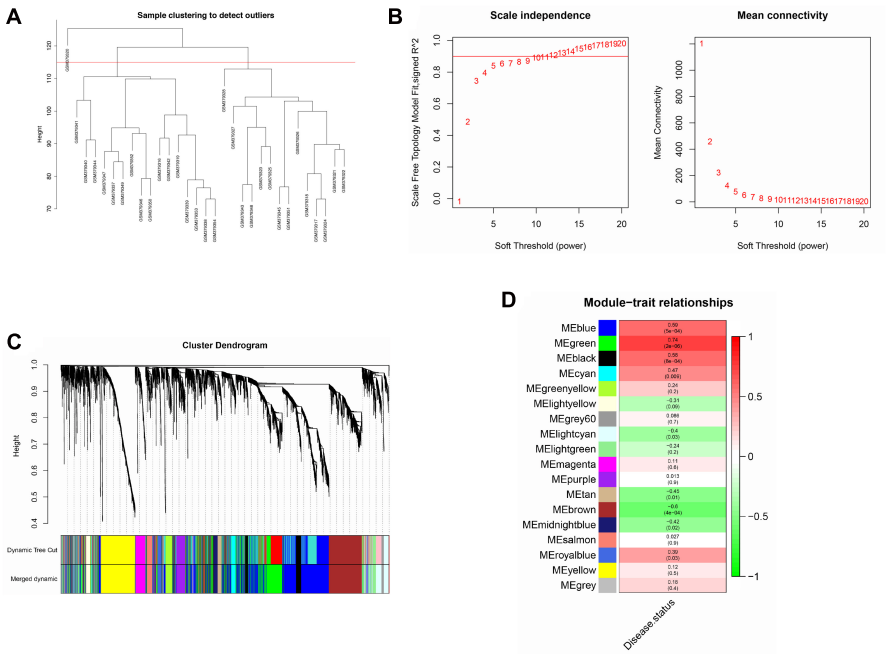

FIGURE 2 | Construction of co-expression network. **(A)** Sample clustering analysis based on GSE15197. **(B)** Analysis of network topology for various soft-thresholding powers. **(C)** Clustering dendrogram of genes. Genes with similar expression patterns divided into same module. Each line of hierarchical clustering represents one gene. **(D)** Module–trait associations. Each cell contains the corresponding correlation and *P*-value.

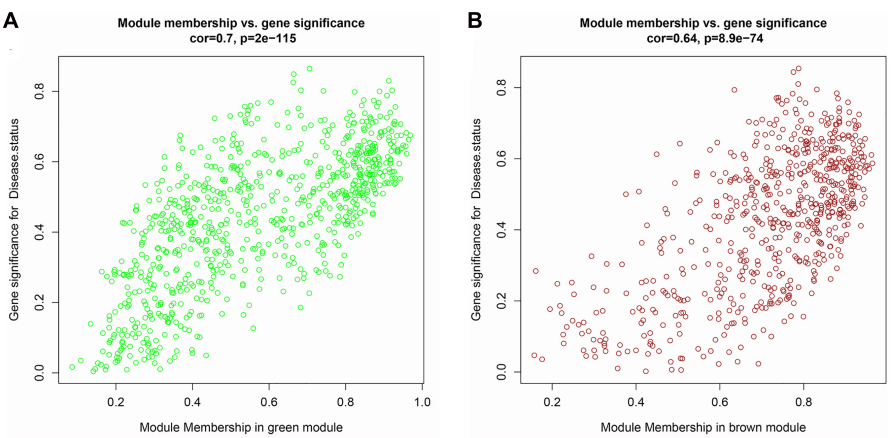

FIGURE 3 | Scatter plot of module membership (MM) vs. gene significance (GS) in **(A)** green and **(B)** brown modules. MM presents the correlation between gene expression and each module eigengene. GS represents the association between gene expression and each trait. In both modules, GS and MM have a high correlation.

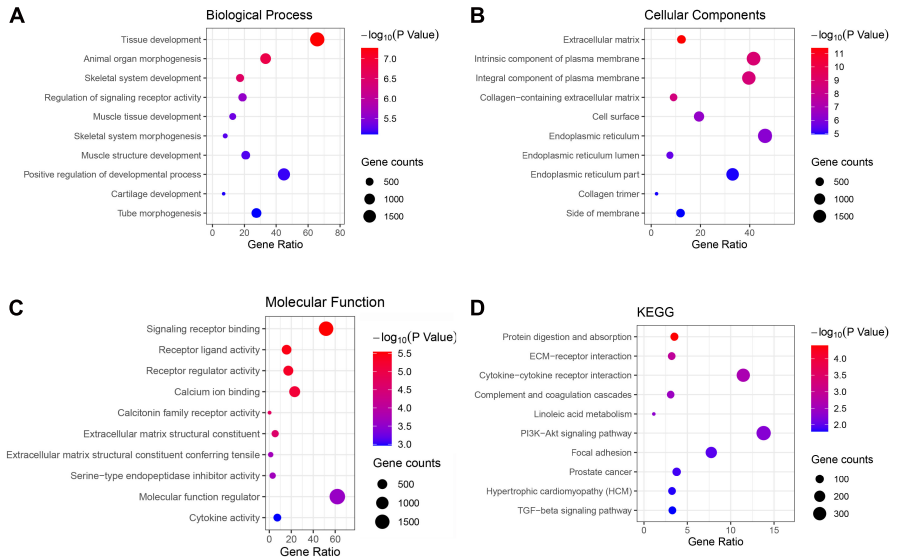

FIGURE 4 | Gene Ontology (GO) terms in **(A)** biological process, **(B)** cellular component, **(C)** molecular function, and **(D)** the Kyoto Encyclopedia of Genes and Genomes (KEGG) pathway of genes in the green module.

genes were primarily associated with tissue development, extracellular matrix, and signaling receptor binding. KEGG analysis suggested that the green module genes were mainly enriched with protein digestion and absorption. GO enrichment results indicated that the brown module genes were significantly associated with kinetochore organization, the perinuclear region of the cytoplasm, and DNA-binding transcription factor activity. Moreover, KEGG analysis suggested that the brown module genes were mainly enriched in proteoglycans in cancer (**Figure 5**).

PPI Network Analysis of Genes in the Green and Brown Modules

Green and brown module genes were used to construct a PPI network using the STRING database. The combined score was > 0.4. The top 100 genes from the green and brown modules as ranked by degree were visualized using Cytoscape3.6.1 (**Figure 6**). The 10 genes with the highest degree from each module were considered candidate IPAH hub genes.

In the green module, candidate hub genes were as follows: E1A binding protein p300 (*EP300*, degree 51); androgen receptor (*AR*, degree 39); matrix metallopeptidase 2 (*MMP2*, degree 36); cadherin 2 (*CDH2*, degree 35); brain-derived neurotrophic factor (*BDNF*, degree 33); leptin (*LEP*, degree 32); secreted phosphoprotein 1 (*SPP1*, degree 30); cyclin-dependent kinase 2 (*CDK2*, degree 27); G protein subunit gamma 10 (*GNG10*, degree 27); and CD34 (*CD34*, degree 26).

In the brown module, the candidate hub genes included the following: albumin (*ALB*, degree 37), structural maintenance of chromosomes 2 (*SMC2*, degree 24); DEAH-box helicase 15 (*DHX15*, degree 22); cullin 3 (*CUL3*, degree 21); F-box and leucine rich repeat protein 3 (*FBXL3*, degree 21); kelch repeat and BTB domain containing 8 (*KBTBD8*, degree 20); structural maintenance of chromosomes 4 (*SMC4*, degree 20); cullin 2 (*CUL2*, degree 19); BTB domain containing 1 (*BTBD1*, degree 18); and listerin E3 ubiquitin protein ligase 1 (*LTN1*,degree 18).

Identification and Verification of Real Hub Gene Expression and ROC Curve Analysis

After overlapping with DEGs, we selected 11 real hub genes: *EP300*, *MMP2*, *CDH2*, *CDK2*, *GNG10*, *ALB*, *SMC2*, *DHX15*, *CUL3*, *BTBD1*, and *LTN1* (see **Supplementary Table 3**). As shown in **Figure 7**, the expression level differences in real hub genes were statistically significant. *EP300* and *CDH2* were highly expressed in IPAH patients. Other hub genes showed a greater expression in controls. ROC curve analysis indicated that 11 real hub genes discriminated strongly between IPAH patients and controls (**Figure 8**). Real hub genes might have important roles in IPAH pathogenesis and development.

Prediction of Potential miRNA-Target Regulatory Networks

We searched for miRNAs targeting real hub genes using the miRNet 2.0 database. The resulting miRNA-target network was visualized using miRNet 2.0 (**Figure 9**). Only miRNAs with a degree of 3 or over were displayed. We found that hsa-mir-1-3p had the highest degree (degree 8). We speculated that hsa-mir-1-3p could be the most crucial miRNA in IPAH pathogenesis and development.

DISCUSSION

IPAH is a rare but severe cardiopulmonary disease associated with progressive deterioration. There are many molecular

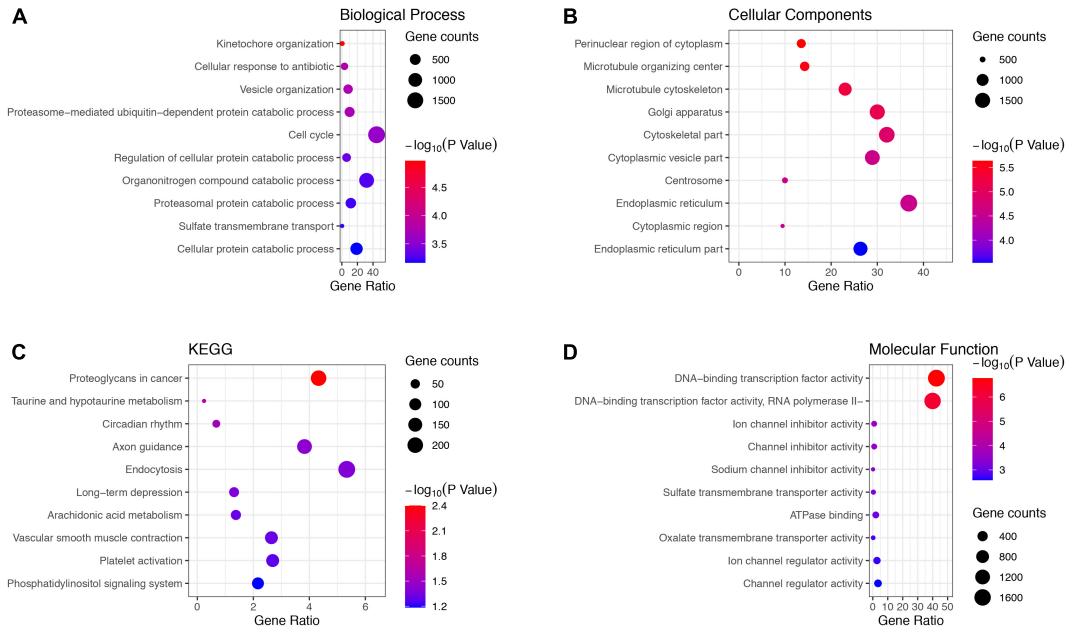

FIGURE 5 | Gene Ontology terms in **(A)** biological process, **(B)** cellular component, **(C)** molecular function and, **(D)** KEGG pathway of genes in the brown module.

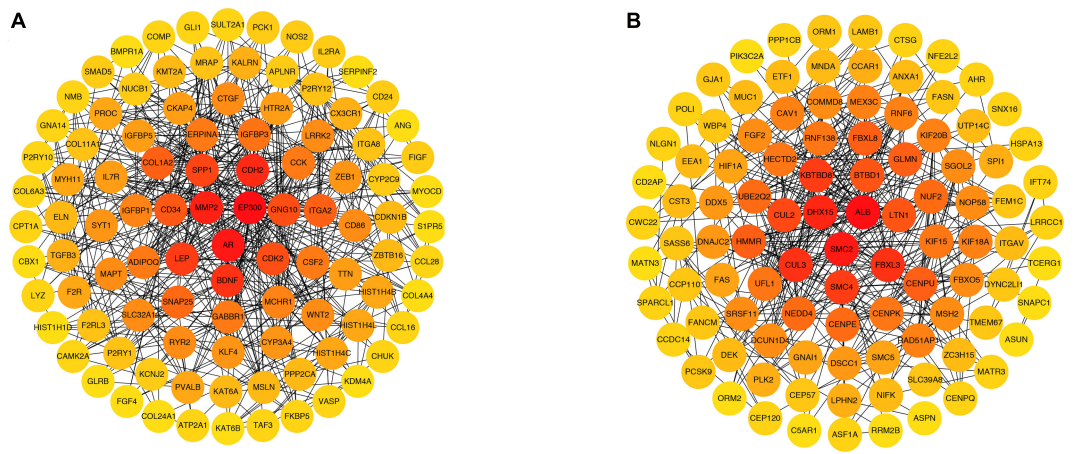

FIGURE 6 | Protein–protein interaction networks of genes in **(A)** green and **(B)** brown modules. Each node represents a gene, and each node is connected by a degree. The color changes from red to yellow as one moves from the inside toward the outside, and the degree decreases from red to yellow. The genes with top 100 degrees and genes with the same degrees as the 100th gene were also presented.

mechanisms underlying IPAH, and extant treatments for IPAH are limited (Yanai et al., 2017). To find new targets or therapies, it is essential to explore IPAH hub genes. Bioinformatics analysis of microarray data has been used widely to identify disease-associated hub genes (Yin et al., 2018).

In this study, DEGs from GSE15197 were analyzed. There were 4,395 significantly differentially expressed genes identified in IPAH and normal lung tissue. These DEGs may play important biological roles. We undertook WGCNA on GSE15197, identifying the green and brown modules as key modules. We also conducted GO and KEGG analyses of these modules. The GO analysis showed that the green and brown module genes were enriched, respectively, in tissue development and kinetochore organization. The KEGG analysis indicated that the green and brown modules genes were involved, respectively, in protein digestion and absorption and proteoglycans in cancer. By overlapping DEGs and candidate hub genes obtained from WGCNA, we found 11 real hub genes associated with IPAH: *EP300*, *MMP2*, *CDH2*, *CDK2*, *GNG10*, *ALB*, *SMC2*, *DHX15*, *CUL3*, *BTBD1*, and *LTN1*.

Among the 11 hub genes, *EP300* and *CDH2* are upregulated hub genes. *EP300* encodes histone acetyltransferase, which regulates gene transcription by binding chromatin in the cell nucleus (Sen et al., 2019). It has been linked to arterial

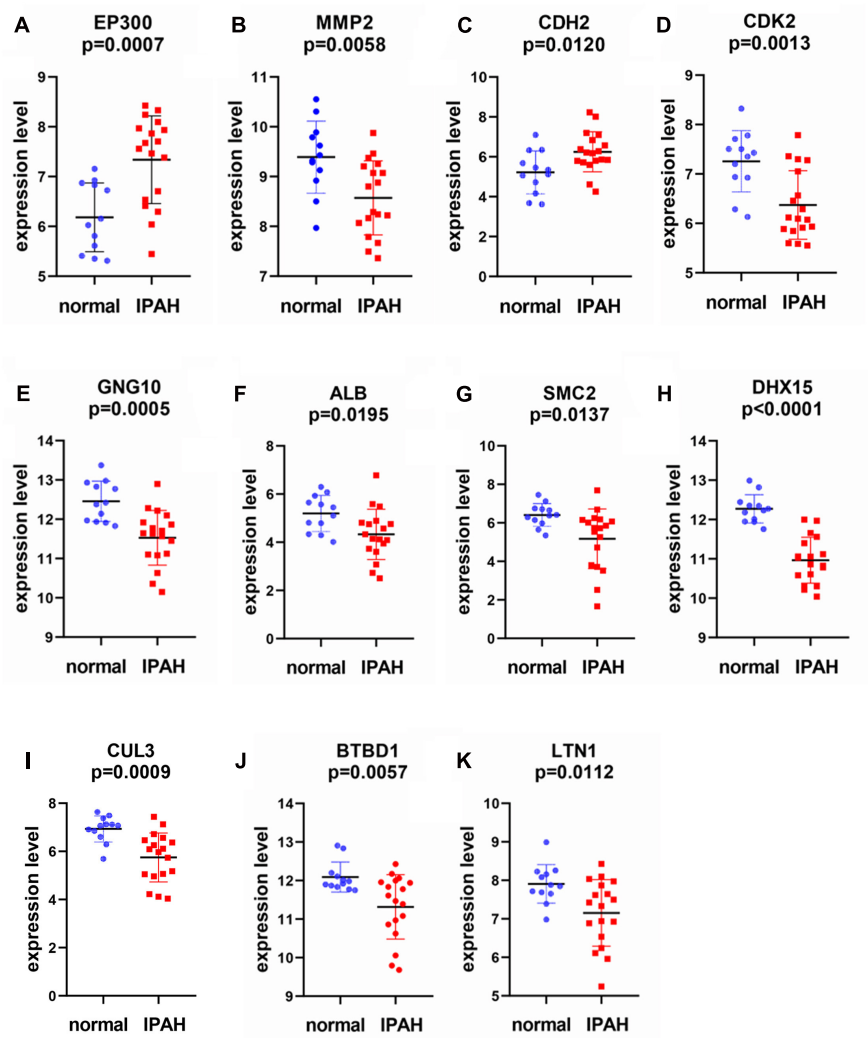

FIGURE 7 | Scatter diagrams for the expressions of real hub genes in GSE15197. **(A)** *EP300*, **(B)** *MMP2*, **(C)** *CDH2*, **(D)** *CDK2*, **(E)** *GNG10*, **(F)** *ALB*, **(G)** *SMC2*, **(H)** *DHX15*, **(I)** *CUL3*, **(J)** *BTBD1*, and **(K)** *LTN1*. Each point represents a sample. In GSE15197, there are 18 IPAH samples and 12 normal samples. *EP300*, E1A binding protein p300; *MMP2*, matrix metallopeptidase 2; *CDH2*, cadherin 2; *CDK2*, cyclin-dependent kinase 2; *GNG10*, G protein subunit gamma 10; *ALB*, albumin; *SMC2*, structural maintenance of chromosomes 2; *DHX15*, DEAH-box helicase 15; *CUL3*, cullin 3; *BTBD1*, BTB domain containing 1; *LTN1*, listerin E3 ubiquitin protein ligase 1.

stiffness prior to hypertension, increase of pulse pressure, and structural vessel wall changes (Herrera et al., 2014). *EP300* can function as a regulatory factor during vascular endothelial growth factor A-induced angiogenesis (Sacilotto et al., 2016). The overexpression of *EP300* increases lung fibrotic hallmarks in a bleomycin mouse model (Rubio et al., 2019). Cardiac miR-133a overexpression in diabetes inhibits *EP300*, preventing early cardiac fibrosis (Chen et al., 2014). We reason that *EP300* may promote IPAH development. Although much evidence supports a role for *EP300* in vascular disease, its mechanism in IPAH remains unclear. Further studies are required to explore how *EP300* participates in IPAH progression.

CDH2 encodes cadherin 2 or N-cadherin (Mayosi et al., 2017). Significant *CDH2* expression promotes endothelial cell proliferation and vascular smooth muscle cell migration (Lyon et al., 2010; Zhuo et al., 2019), causing intimal thickening, and could drive vascular remodeling in IPAH. Moreover, *CDH2* mutations are associated with arrhythmogenic cardiomyopathy (Mayosi et al., 2017; Ghidoni et al., 2021).

MMP2 is a proteolytic enzyme that contributes to vascular protein degradation and aortic wall destruction (Longo et al., 2002; Li et al., 2019). Much evidence suggest that *MMP2* is associated with an increased risk of cardiovascular diseases, such as myocardial infarction (Alp et al., 2011) and degenerative mitral valve disease (Balistreri et al., 2016). Rat vascular smooth muscle cell migration can be inhibited by the *c-Myc/MMP2* and *ROCK/JNK* signaling pathways (Luo et al., 2019). Higher ratios of *MMP2/TIMP4* in plasma predict a significantly higher risk of death or clinical deterioration in IPAH patients (Wetzl et al., 2017). Activation of *MMP2* is increased in smooth muscle cells of

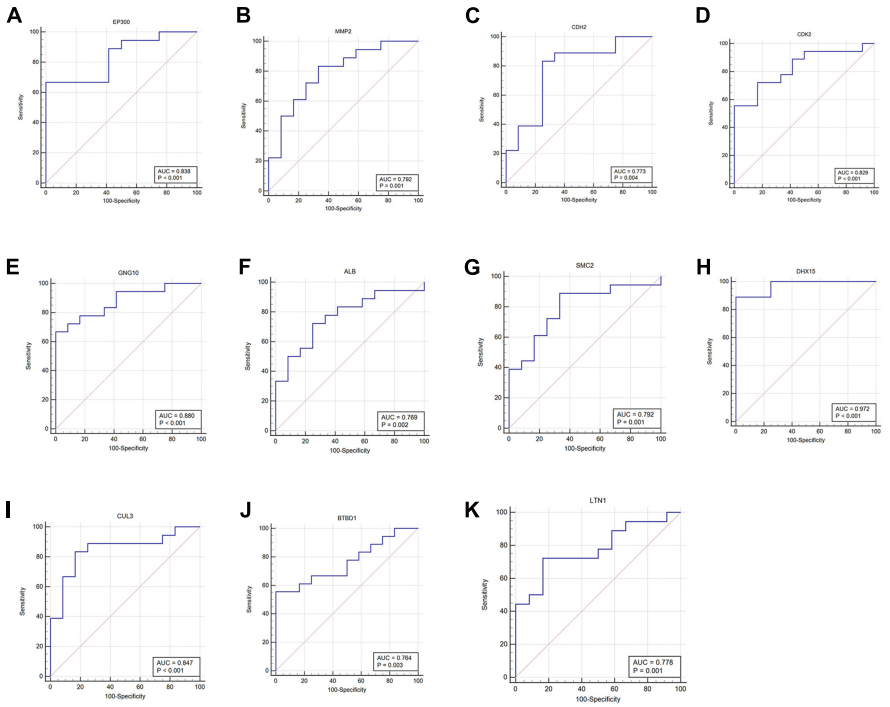

FIGURE 8 | ROC curves of the hub genes. **(A)** *EP300*, **(B)** *MMP2*, **(C)** *CDH2*, **(D)** *CDK2*, **(E)** *GNG10*, **(F)** *ALB*, **(G)** *SMC2*, **(H)** *DHX15*, **(I)** *CUL3*, **(J)** *BTBD1*, and **(K)** *LTN1*. ROC, receiver operating characteristic; *EP300*, E1A binding protein p300; *MMP2*, matrix metallopeptidase 2; *CDH2*, cadherin 2; *CDK2*, cyclin-dependent kinase 2; *GNG10*, G protein subunit gamma 10; *ALB*, albumin; *SMC2*, structural maintenance of chromosomes 2; *DHX15*, DEAH-box helicase 15; *CUL3*, cullin 3; *BTBD1*, BTB domain containing 1; *LTN1*, listerin E3 ubiquitin protein ligase 1.

IPAH patients, contributing to smooth muscle cell migration and proliferation (Lepetit et al., 2005).

CDK2 encodes a form of protein-dependent kinases (Nathans et al., 2021), involved in cell cycle regulation, with a critical role during the G1 to S phase transition. Decreased *CDK2* expression can block cell cycle progression and inhibit the proliferation of pulmonary artery smooth muscle cells. Proliferative PASMCs exist in PAH patients and are closely related to vascular remodeling (Yue et al., 2020).

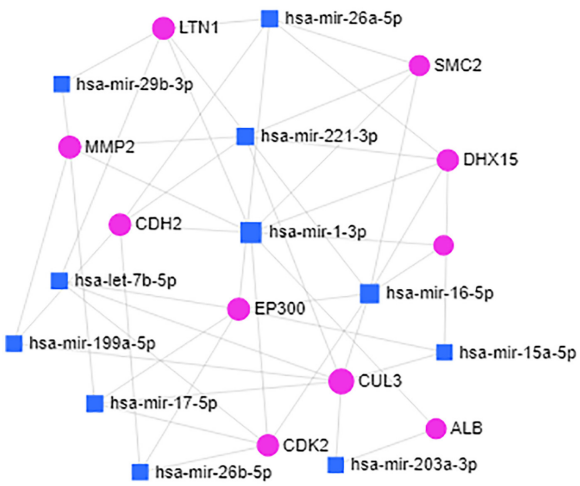

FIGURE 9 | miRNA–target regulatory network. The blue square represents miRNAs targeting the real hub genes, and the red circle represents the real hub genes. The bigger the circle or square, the higher the degree.

ALB encodes albumin, the most abundant protein in human blood, which plays a key role in regulating blood plasma colloid osmotic pressure. In IPAH, pulmonary vascular pressure is considerably elevated, leading to endothelial dysfunction and capillary leakage easily. In turn, this leads to loss of plasma proteins including serum albumin levels. Lower albumin levels may reflect disease progression and predict worse survival rates (Snipelisky et al., 2018).

CUL3 encodes cullin 3, a cullin protein family member, critical to maintaining the integrity of the endothelial barrier (Kovačević et al., 2018). Decreased expression of *CUL3* may occur in IPAH, resulting in the destruction of blood vessel architecture, cell proliferation, and vascular remodeling (Sakaue et al., 2017). Rats with *CUL3* mutations exhibit arterial hypertension, while patients with *CUL3* mutations present severe early-onset hypertension, vascular dysfunction, and arterial stiffness due to deficiency of vascular smooth muscle (Abdel Khalek et al., 2019).

GNG10 encodes a subtype of the G-protein γ subunit involved in suppressing heart rate (Senarath et al., 2018) and regulating the cell cycle (Clapham and Neer, 1997). The protein encoded by *SMC2* belongs to the condensin complex, which maintains chromosome stability (Feng et al., 2019). *DHX15*, a member of

the DEAH-box RNA helicase family, participates in modulating pre-mRNA splicing (Jing et al., 2018). *BTBD1* encodes a 482-amino-acid protein involved in protein–protein interactions. The expression of *BTBD1* in the heart is enhanced (Carim-Todd et al., 2001; Xu et al., 2002). *LTN1* encodes listerin E3 ubiquitin protein ligase 1, which functions as an E3 ubiquitin ligase (Chu et al., 2009). However, there is no research indicating a relationship between these five genes and IPAH. We propose that these genes are novel genes related to IPAH, suggesting the need for future study.

miRNAs represent novel potential therapeutic targets for many diseases including heart failure (Akat et al., 2014), acute myocardial infarction (Gupta et al., 2016), arrhythmias (den Hoed et al., 2013), and pulmonary hypertension (Zhou et al., 2018). We created a miRNA-target network to explore potential miRNAs in IPAH. The network suggested that hsa-mir-1-3p might regulate gene expression in IPAH. Previous studies have shown elevated hsa-mir-1-3p in perioperative myocardial injury patients (May et al., 2020). Further research is needed to verify the mechanism linking hsa-mir-1-3p to IPAH.

We also examined expression levels in IPAH versus controls and the diagnostic power of the 11 identified hub genes using the ROC curve analysis. The expression of the 11 hub genes showed significant differences between IPAH and controls. A previous work has identified diagnostic IPAH biomarkers in plasma (Wang T. et al., 2019). Here, we used lung microarray data, not plasma, to identify hub genes using WGCNA. We consider that this result is more reliable for spatial specificity of gene expression. The 11 genes may all have a considerable diagnostic ability and be better candidate targets, although lung tissues cannot be obtained as easily as plasma samples.

The principal limitation of our study is the lack of independent experimental validation. Although 11 hub genes were identified, their involvement in IPAH pathogenesis has not been experimentally validated using *in vivo* or *in vitro* experimentation, and their possible mechanisms of action remain unclear. Further research is needed to validate our results and to explore the specific mechanisms of action for each gene.

CONCLUSION

In conclusion, our results indicate that the 11 real hub genes may play critical roles in IPAH. *EP300* and *CDH2* are the upregulated hub genes, while *MMP2*, *CDK2*, *GNG10*, *ALB*, *SMC2*, *DHX15*, *CUL3*, *BTBD1*, and *LTN1* are the downregulated hub genes. Predicted miRNA hsa-mir-1-3p might regulate gene expression in IPAH. These hub genes could contribute to the pathology and progression of IPAH and may be candidate targets for IPAH treatment.

DATA AVAILABILITY STATEMENT

Publicly available datasets were analyzed in this study. This data can be found here: GSE15197.

AUTHOR CONTRIBUTIONS

XQ, JL, and JZ designed the research, analyzed the data, and wrote the manuscript. BL, YC, and GL participated in data preparation, analysis of data, and figures preparation. JZ revised the manuscript. All authors read and approved the manuscript for publication.

ACKNOWLEDGMENTS

We acknowledge the GEO database for providing the platform and the contributors for uploading their meaningful datasets.

SUPPLEMENTARY MATERIAL

The Supplementary Material for this article can be found online at: https://www.frontiersin.org/articles/10.3389/fgene.2021.636934/full#supplementary-material

REFERENCES

Abdel Khalek, W., Rafael, C., Loisel-Ferreira, I., Kouranti, I., Clauser, E., Hadchouel, J., et al. (2019). Severe arterial hypertension from cullin 3 mutations is caused by both renal and vascular effects. *J. Am. Soc. Nephrol.* 30, 811–823. doi: 10.1681/asn.2017121307

Akat, K. M., Moore-McGriff, D., Morozov, P., Brown, M., Gogakos, T., Correa Da Rosa, J., et al. (2014). Comparative RNA-sequencing analysis of myocardial and circulating small RNAs in human heart failure and their utility as biomarkers. *Proc. Natl. Acad. Sci. U.S.A.* 111, 11151–11156. doi: 10.1073/pnas.1401724111

Alp, E., Menevse, S., Tulmac, M., Yilmaz, A., Yalcin, R., and Cengel, A. (2011). The role of matrix metalloproteinase-2 promoter polymorphisms in coronary artery disease and myocardial infarction. *Genet. Test. Mol. Biomarkers.* 15, 193–202. doi: 10.1089/gtmb.2010.0113

Balistreri, C. R., Allegra, A., Crapanzano, F., Pisano, C., Triolo, O. F., Argano, V., et al. (2016). Associations of rs3918242 and rs2285053 MMP-9 and MMP-2 polymorphisms with the risk, severity, and short- and long-term complications of degenerative mitral valve diseases: a 4.8-year prospective cohort study. *Cardiovasc. Pathol.: Off. J. Soc. Cardiovasc. Pathol.* 25, 362–370. doi: 10.1016/j.carpath.2016.05.004

Barnes, J. W., Tian, L., Krick, S., Helton, E. S., Denson, R. S., Comhair, S. A. A., et al. (2019). O-GlcNAc transferase regulates angiogenesis in idiopathic pulmonary arterial hypertension. *Int. J. Mol. Sci.* 20:6299. doi: 10.3390/ijms20246299

Carim-Todd, L., Sumoy, L., Andreu, N., Estivill, X., and Escarceller, M. (2001). Identification and characterization of BTBD1, a novel BTB domain containing gene on human chromosome 15q24. *Gene* 262, 275–281. doi: 10.1016/s0378-1119(00)00513-8

Chen, S., Puthanveetil, P., Feng, B., Matkovich, S. J., Dorn, G. W. 2nd, and Chakrabarti, S. (2014). Cardiac miR-133a overexpression prevents early cardiac fibrosis in diabetes. *J. Cell. Mol. Med.* 18, 415–421. doi: 10.1111/jcmm.12218

Chu, J., Hong, N. A., Masuda, C. A., Jenkins, B. V., Nelms, K. A., Goodnow, C. C., et al. (2009). A mouse forward genetics screen identifies LISTERIN as an E3 ubiquitin ligase involved in neurodegeneration. *Proc. Natl. Acad. Sci. U.S.A.* 106, 2097–2103. doi: 10.1073/pnas.0812819106

Clapham, D. E., and Neer, E. J. (1997). G protein beta gamma subunits. *Annu. Rev. Pharmacol. Toxicol.* 37, 167–203.

den Hoed, M., Eijgelsheim, M., Esko, T., Brundel, B. J., Peal, D. S., Evans, D. M., et al. (2013). Identification of heart rate-associated loci and their effects on cardiac conduction and rhythm disorders. *Nat. Genet.* 45, 621–631.

Fan, Y., Siklenka, K., Arora, S. K., Ribeiro, P., Kimmins, S., and Xia, J. (2016). miRNet - dissecting miRNA-target interactions and functional associations through network-based visual analysis. *Nucleic Acids Res.* 44, W135–W141.

Feng, Y., Liu, H., Duan, B., Liu, Z., Abbruzzese, J., Walsh, K. M., et al. (2019). Potential functional variants in SMC2 and TP53 in the AURORA pathway genes and risk of pancreatic cancer. *Carcinogenesis* 40, 521–528. doi: 10.1093/carcin/bgz029

Fu, G., Saunders, G., and Stevens, J. (2014). Holm multiple correction for large-scale gene-shape association mapping. *BMC Genet.* 15(Suppl. 1):S5. doi: 10.1186/1471-2156-15-S1-S5

Gallo de Moraes, A., Vakil, A., and Moua, T. (2016). Patent foramen ovale in idiopathic pulmonary arterial hypertension: long-term risk and morbidity. *Respiratory Med.* 118, 53–57. doi: 10.1016/j.rmed.2016.07.007

Ghidoni, A., Elliott, P. M., Syrris, P., Calkins, H., James, C. A., Judge, D. P., et al. (2021). Cadherin 2-Related arrhythmogenic cardiomyopathy: prevalence and clinical features. *Circ. Genom. Precis Med.* doi: 10.1161/CIRCGEN.120.003097 [Epub ahead of print].

GraphPad Statistics Guide. (2020). *GraphPad Statistics Guide*. Available online at: http://www.graphpad.com/guides/prism/8/statistics/index.htm (accessed November 30, 2020).

Gupta, S. K., Foinquinos, A., Thum, S., Remke, J., Zimmer, K., Bauters, C., et al. (2016). Preclinical development of a MicroRNA-Based therapy for elderly patients with myocardial infarction. *J. Am. College Cardiol.* 68, 1557–1571. doi: 10.1016/j.jacc.2016.07.739

Herrera, V. L., Decano, J. L., Giordano, N., Moran, A. M., and Ruiz-Opazo, N. (2014). Aortic and carotid arterial stiffness and epigenetic regulator gene expression changes precede blood pressure rise in stroke-prone Dahl salt-sensitive hypertensive rats. *PLoS One* 9:e107888. doi: 10.1371/journal.pone.0107888

Hu, X., Bao, M., Huang, J., Zhou, L., and Zheng, S. (2020). Identification and validation of novel biomarkers for diagnosis and prognosis of hepatocellular carcinoma. *Front. Oncol.* 10:541479. doi: 10.3389/fonc.2020.541479

Iancu, O. D., Colville, A., Oberbeck, D., Darakjian, P., McWeeney, S. K., and Hitzemann, R. (2015). Cosplicing network analysis of mammalian brain RNA-Seq data utilizing WGCNA and Mantel correlations. *Front. Genet.* 6:174. doi: 10.3389/fgene.2015.00174

Jing, Y., Nguyen, M. M., Wang, D., Pascal, L. E., Guo, W., Xu, Y., et al. (2018). DHX15 promotes prostate cancer progression by stimulating Siah2-mediated ubiquitination of androgen receptor. *Oncogene* 37, 638–650. doi: 10.1038/onc.2017.371

Kovačević, I., Sakaue, T., Majoleé, J., Pronk, M. C., Maekawa, M., Geerts, D., et al. (2018). The Cullin-3-Rbx1-KCTD10 complex controls endothelial barrier function via K63 ubiquitination of RhoB. *J. Cell. Biol.* 217, 1015–1032. doi: 10.1083/jcb.201606055

Langfelder, P., and Horvath, S. (2008). WGCNA: an R package for weighted correlation network analysis. *BMC Bioinform.* 9:559. doi: 10.1186/1471-2105-9-559

Lepetit, H., Eddahibi, S., Fadel, E., Frisdal, E., Munaut, C., Noel, A., et al. (2005). Smooth muscle cell matrix metalloproteinases in idiopathic pulmonary arterial hypertension. *Eur. Respiratory J.* 25, 834–842. doi: 10.1183/09031936.05.00072504

Li, T., Jing, J., Sun, L., Jiang, B., Xin, S., Yang, J., et al. (2019). TLR4 and MMP2 polymorphisms and their associations with cardiovascular risk factors in susceptibility to aortic aneurysmal diseases. *Biosci. Rep.* 39:BSR20181591.

Li, W., Wang, L., Wu, Y., Yuan, Z., and Zhou, J. (2020). Weighted gene coexpression network analysis to identify key modules and hub genes associated with atrial fibrillation. *Int. J. Mol. Med.* 45, 401–416.

Longo, G. M., Xiong, W., Greiner, T. C., Zhao, Y., Fiotti, N., and Baxter, B. T. (2002). Matrix metalloproteinases 2 and 9 work in concert to produce aortic aneurysms. *J. Clin. Investigation.* 110, 625–632. doi: 10.1172/jci0215334

Luo, Z., Deng, H., Fang, Z., Zeng, A., Chen, Y., Zhang, W., et al. (2019). Ligustilide inhibited rat vascular smooth muscle cells migration via c-Myc/MMP2 and ROCK/JNK signaling pathway. *J. Food Sci.* 84, 3573–3583. doi: 10.1111/1750-3841.14936

Lyon, C. A., Koutsouki, E., Aguilera, C. M., Blaschuk, O. W., and George, S. J. (2010). Inhibition of N-cadherin retards smooth muscle cell migration and intimal thickening via induction of apoptosis. *J. Vasc. Surg.* 52, 1301–1309. doi: 10.1016/j.jvs.2010.05.096

May, S. M., Abbott, T. E. F., Del Arroyo, A. G., Reyes, A., Martir, G., Stephens, R. C. M., et al. (2020). MicroRNA signatures of perioperative myocardial injury after elective noncardiac surgery: a prospective observational mechanistic cohort study. *Br. J. Anaesth.* 125, 661–671. doi: 10.1016/j.bja.2020.05.066

Mayosi, B. M., Fish, M., Shaboodien, G., Mastantuono, E., Kraus, S., Wieland, T., et al. (2017). Identification of cadherin 2 (CDH2) mutations in arrhythmogenic right ventricular cardiomyopathy. *Circ. Cardiovasc. Genet.* 10:e001605.

Nathans, J. F., Cornwell, J. A., Afifi, M. M., Paul, D., and Cappell, S. D. (2021). Cell cycle inertia underlies a bifurcation in cell fates after DNA damage. *Sci. Adv.* 7:eabe3882. doi: 10.1126/sciadv.abe3882

Pahal, P., and Sharma, S. (2020). *Idiopathic Pulmonary Artery Hypertension. StatPearls*. Treasure Island, FL: StatPearls Publishing Copyright © .

Ritchie, M. E., Phipson, B., Wu, D., Hu, Y., Law, C. W., Shi, W., et al. (2015). limma powers differential expression analyses for RNA-sequencing and microarray studies. *Nucleic Acids Res.* 43:e47. doi: 10.1093/nar/gkv007

Rubio, K., Singh, I., Dobersch, S., Sarvari, P., Günther, S., Cordero, J., et al. (2019). Inactivation of nuclear histone deacetylases by EP300 disrupts the MiCEE complex in idiopathic pulmonary fibrosis. *Nat. Commun.* 10:2229.

Sacilotto, N., Chouliaras, K. M., Nikitenko, L. L., Lu, Y. W., Fritzsche, M., Wallace, M. D., et al. (2016). MEF2 transcription factors are key regulators of sprouting angiogenesis. *Genes Dev.* 30, 2297–2309. doi: 10.1101/gad.290619.116

Sakaue, T., Maekawa, M., Nakayama, H., and Higashiyama, S. (2017). Prospect of divergent roles for the CUL3 system in vascular endothelial cell function and angiogenesis. *J. Biochem.* 162, 237–245.

Sarrion, I., Milian, L., Juan, G., Ramon, M., Furest, I., Carda, C., et al. (2015). Role of circulating miRNAs as biomarkers in idiopathic pulmonary arterial hypertension: possible relevance of miR-23a. *Oxid Med. Cell Longev.* 2015:792846.

Schoonjans, F., Zalata, A., Depuydt, C. E., and Comhaire, F. H. (1995). MedCalc: a new computer program for medical statistics. *Comput. Methods Programs Biomed.* 48, 257–262. doi: 10.1016/0169-2607(95)01703-8

Sen, P., Lan, Y., Li, C. Y., Sidoli, S., Donahue, G., Dou, Z., et al. (2019). Histone acetyltransferase p300 induces de novo super-enhancers to drive cellular senescence. *Mol. Cell.* 73, 684.e8–698.e8.

Senarath, K., Kankanamge, D., Samaradivakara, S., Ratnayake, K., Tennakoon, M., and Karunarathne, A. (2018). Regulation of G protein betagamma Signaling. *Int. Rev. Cell. Mol. Biol.* 339, 133–191.

Shannon, P., Markiel, A., Ozier, O., Baliga, N. S., Wang, J. T., Ramage, D., et al. (2003). Cytoscape: a software environment for integrated models of biomolecular interaction networks. *Genome Res.* 13, 2498–2504. doi: 10.1101/gr.1239303

Shi, M., Dai, W. Q., Jia, R. R., Zhang, Q. H., Wei, J., Wang, Y. G., et al. (2021). APC(CDC20)-mediated degradation of PHD3 stabilizes HIF-1a and promotes tumorigenesis in hepatocellular carcinoma. *Cancer Lett.* 496, 144–155. doi: 10.1016/j.canlet.2020.10.011

Snipelisky, D., Jentzer, J., Batal, O., Dardari, Z., and Mathier, M. (2018). Serum albumin concentration as an independent prognostic indicator in patients with pulmonary arterial hypertension. *Clin. Cardiol.* 41, 782–787. doi: 10.1002/clc.22954

Tutorials for Wgcna R package. (2020). *Tutorials for WGCNA R Package*. Available online at: https://labs.genetics.ucla.edu/horvath/CoexpressionNetwork/Rpackages/WGCNA/Tutorials/ (accessed November 1, 2020).

Wang, T., Zheng, X., Li, R., Liu, X., Wu, J., Zhong, X., et al. (2019). Integrated bioinformatic analysis reveals YWHAB as a novel diagnostic biomarker for idiopathic pulmonary arterial hypertension. *J. Cell. Physiol.* 234, 6449–6462. doi: 10.1002/jcp.27381

Wang, X. J., Lian, T. Y., Jiang, X., Liu, S. F., Li, S. Q., Jiang, R., et al. (2019). Germline BMP9 mutation causes idiopathic pulmonary arterial hypertension. *Eur. Respiratory J.* 53:1801609. doi: 10.1183/13993003.01609-2018

Wang, Y., Chen, S., and Du, J. (2019). Bosentan for treatment of pediatric idiopathic pulmonary arterial hypertension: state-of-the-art. *Front. Pediatr.* 7:302. doi: 10.3389/fped.2019.00302

Wetzl, V., Tiede, S. L., Faerber, L., Weissmann, N., Schermuly, R. T., Ghofrani, H. A., et al. (2017). Plasma MMP2/TIMP4 ratio at follow-up assessment predicts disease progression of idiopathic pulmonary arterial hypertension. *Lung* 195, 489–496. doi: 10.1007/s00408-017-0014-5

Wu, D., Talbot, C. C. Jr., Liu, Q., Jing, Z. C., Damico, R. L., Tuder, R., et al. (2016). Identifying microRNAs targeting Wnt/beta-catenin pathway in end-stage idiopathic pulmonary arterial hypertension. *J. Mol. Med. (Berl).* 94, 875–885. doi: 10.1007/s00109-016-1426-z

Xu, L., Yang, L., Hashimoto, K., Anderson, M., Kohlhagen, G., Pommier, Y., et al. (2002). Characterization of BTBD1 and BTBD2, two similar BTB-domain-containing Kelch-like proteins that interact with Topoisomerase I. *BMC Genomics* 3:1. doi: 10.1186/1471-2164-3-1

Yanai, S., Wakayama, M., Nakayama, H., Shinozaki, M., Tsukuma, H., Tochigi, N., et al. (2017). Implication of overexpression of dishevelled-associated activator of morphogenesis 1 (Daam-1) for the pathogenesis of human Idiopathic Pulmonary Arterial Hypertension (IPAH). *Diagnostic Pathol.* 12:25.

Yin, L., Cai, Z., Zhu, B., and Xu, C. (2018). Identification of key pathways and genes in the dynamic progression of HCC based on WGCNA. *Genes* 9:92. doi: 10.3390/genes9020092

Yue, Y., Li, Y. Q., Fu, S., Wu, Y. T., Zhu, L., Hua, L., et al. (2020). Osthole inhibits cell proliferation by regulating the TGF-beta1/Smad/p38 signaling pathways in pulmonary arterial smooth muscle cells. *Biomed. Pharmacother.* 121:109640. doi: 10.1016/j.biopha.2019.109640

Zhang, B., and Horvath, S. (2005). A general framework for weighted gene co-expression network analysis. *Stat. Appl. Genet. Mol. Biol.* 4:17.

Zhang, H., Xu, M., Xia, J., and Qin, R. Y. (2013). Association between serotonin transporter (SERT) gene polymorphism and idiopathic pulmonary arterial hypertension: a meta-analysis and review of the literature. *Metabolism* 62, 1867–1875. doi: 10.1016/j.metabol.2013.08.012

Zheng, J. N., Li, Y., Yan, Y. M., Shi, H., Zou, T. T., Shao, W. Q., et al. (2020). Identification and validation of key genes associated with systemic sclerosis-related pulmonary hypertension. *Front. Genet.* 11:816. doi: 10.3389/fgene.2020.00816

Zhou, S. S., Jin, J. P., Wang, J. Q., Zhang, Z. G., Freedman, J. H., Zheng, Y., et al. (2018). miRNAS in cardiovascular diseases: potential biomarkers, therapeutic targets and challenges. *Acta Pharmacologica Sinica.* 39, 1073–1084. doi: 10.1038/aps.2018.30

Zhuo, H., Zhao, Y., Cheng, X., Xu, M., Wang, L., Lin, L., et al. (2019). Tumor endothelial cell-derived cadherin-2 promotes angiogenesis and has prognostic significance for lung adenocarcinoma. *Mol. Cancer* 18:34.

Conflict of Interest: The authors declare that the research was conducted in the absence of any commercial or financial relationships that could be construed as a potential conflict of interest.

frontiers in Pediatrics

CASE REPORT
published: 10 June 2021
doi: 10.3389/fped.2021.606905

Case Report: Cerebral Revascularization in a Child With Mucopolysaccharidosis Type I

*Nathan Grant[1], J. Michael Taylor[2], Zach Plummer[1], Kasiani Myers[3], Thomas Burrow[4], Lori Luchtman-Jones[3], Anna Byars[2], Adrienne Hammill[3], Katie Wusick[3], Edward Smith[5], James Leach[6] and Sudhakar Vadivelu[1,6]**

[1] Division of Pediatric Neurosurgery, Cincinnati Children's Hospital Medical Center, Cincinnati, OH, United States, [2] Division of Neurology, Cincinnati Children's Hospital Medical Center, Cincinnati, OH, United States, [3] Division of Hematology – Oncology, Cincinnati Children's Hospital Medical Center, Cincinnati, OH, United States, [4] Division of Human Genetics, Cincinnati Children's Hospital Medical Center, Cincinnati, OH, United States, [5] Department of Neurosurgery, Boston Children's Hospital, Boston, MA, United States, [6] Department of Radiology, Cincinnati Children's Hospital Medical Center, Cincinnati, OH, United States

OPEN ACCESS

Edited by:
Andrea Gropman, Children's National Hospital, United States

Reviewed by:
Emanuele Micaglio, IRCCS Policlinico San Donato, Italy
Nicolina Cristina Sorrentino, Telethon Institute of Genetics and Medicine (TIGEM), Italy

***Correspondence:**
Sudhakar Vadivelu
sudhakar.vadivelu@cchmc.org

Specialty section:
This article was submitted to Genetics of Common and Rare Diseases, a section of the journal Frontiers in Pediatrics

Received: 16 September 2020
Accepted: 16 April 2021
Published: 10 June 2021

Citation:
Grant N, Taylor JM, Plummer Z, Myers K, Burrow T, Luchtman-Jones L, Byars A, Hammill A, Wusick K, Smith E, Leach J and Vadivelu S (2021) Case Report: Cerebral Revascularization in a Child With Mucopolysaccharidosis Type I. Front. Pediatr. 9:606905. doi: 10.3389/fped.2021.606905

Mucopolysaccharidosis (MPS) type I is a rare lysosomal storage disorder caused by an accumulation of glycosaminoglycans (GAGs) resulting in multisystem disease. Neurological morbidity includes hydrocephalus, spinal cord compression, and cognitive decline. While many neurological symptoms have been described, stroke is not a widely-recognized manifestation of MPS I. Accordingly, patients with MPS I are not routinely evaluated for stroke, and there are no guidelines for managing stroke in patients with this disease. We report the case of a child diagnosed with MPS I who presented with overt stroke and repeated neurological symptoms with imaging findings for severe ventriculomegaly, infarction, and bilateral terminal carotid artery stenosis. Direct intracranial pressure evaluation proved negative for hydrocephalus. The patient was subsequently treated with cerebral revascularization and at a 3-year follow-up, the patient reported no further neurological events or new ischemia on cerebral imaging. Cerebral arteriopathy in patients with MPS I may be associated with GAG accumulation within the cerebrovascular system and may predispose patients to recurrent strokes. However, further studies are required to elucidate the etiology of cerebrovascular arteriopathy in the setting of MPS I. Although the natural history of steno-occlusive arteriopathy in patients with MPS I remains unclear, our findings suggest that cerebral revascularization is a safe treatment option that may mitigate the risk of future strokes and should be strongly considered within the overall management guidelines for patients with MPS I.

Keywords: mucopolysaccharidosis I, stroke, cerebral arteriopathy, ventriculomegaly, pial synangiosis, cerebral revascularization

INTRODUCTION

Mucopolysaccharidosis (MPS) type I is a rare, autosomal recessive, lysosomal storage disorder caused by a deficiency of the enzyme alpha-L-iduronidase with resultant accumulation of glycosaminoglycans (GAGs) within the lysosomes (1, 2). MPS I is classified into two clinical entities based on disease severity: severe [Hurler syndrome (OMIM #607014)]

and attenuated [Hurler-Scheie (OMIM #607015) and Scheie syndromes (OMIM #607016)]. Clinical features include coarse facial appearance, corneal clouding, hepatosplenomegaly, hearing loss, hydrocephalus, cardiac valvular disease, airway obstruction, spinal cord compression, dysostosis multiplex, and cognitive decline (2). Without treatment, individuals with severe MPS I may die within the first decade of life, usually from cardiorespiratory failure or progressive neurological disease (2, 3). Currently, short-term administration of enzyme replacement therapy (ERT) in combination with hematopoietic stem cell transplantation (HSCT) is recommended for patients with severe MPS I and is associated with improved mortality and engraftment rates, reduced urinary GAG excretions, regression of cerebral ventriculomegaly, and stabilization of cardiac ventricular dysfunction (4–7). ERT, however, does not cross the blood-brain barrier in sufficient quantities to address neurological disease (2, 8, 9). Accordingly, the natural history of MPS I may be characterized by progressive neurological morbidity (2, 8–11).

Stroke is not a widely recognized manifestation of MPS I (2, 12, 13). Accordingly, patients with MPS I are not routinely screened for stroke and there are no established guidelines for managing stroke in this population. We report the first case of a 17-month-old male with MPS I who developed an acute ischemic stroke secondary to progressive multifocal cerebral arteriopathy. Cerebral revascularization was performed and long-term follow-up indicated successful engraftment and protection from further stroke. Our findings indicate that cerebral revascularization can be considered an appropriate treatment option for patients with MPS I at risk of stroke.

CASE DESCRIPTION

History and Presentation

The patient was born at 40 weeks to non-consanguineous parents who are carriers of MPS I. At 9 months, the patient developed dysostosis multiplex, kyphosis, macrocephaly, and coarse facial features. Enzyme analysis revealing abnormally low alpha-L-iduronidase activity and elevated GAG levels confirmed the diagnosis of MPS I (Hurler syndrome) (14). The patient commenced the recommended treatment for MPS I with 8 weeks of ERT followed by HSCT (5, 6). He experienced graft failure following his first HSCT; however, a second round of this combinatorial therapy resulted in successful donor engraftment.

Subsequent urinary analysis demonstrated GAG-level reduction consistent with the treatment protocol (4). There was no evidence of graft-versus-host disease, thrombotic microangiopathy, or adverse events related to treatment with ERT and HSCT. Prior to the patient's second HSCT, neuroimaging was obtained for macrocephaly and findings were consistent (15) with MPS I (**Figure 1**). However, the patient showed no clinical evidence of neurological symptoms at this time.

One month after his second HSCT, at 17 months of age, the patient reported new right-sided weakness, emesis, and a decrease in appetite that were concerning for stroke. Brain MRI revealed an acute left middle cerebral artery (MCA) territory infarct and right cerebral ischemia. MR and CT angiography demonstrated complete absence of blood flow into the distal left MCA segments and bilateral carotid terminus narrowing (**Figure 2**). The patient was given 81 mg aspirin daily.

Serial follow-up MR imaging >6 months post stroke demonstrated continued stroke evolution and bilateral internal carotid artery stenoses (**Figure 3**, upper panel). Digital subtraction angiography was not performed because of the patient's abdominal aortic aneurysm and renal artery stenosis. Cardiac echocardiograms demonstrated mild mitral regurgitation without evidence of vegetation and EKG, thrombophilia, and platelet function testing were unremarkable. The patient subsequently underwent direct intracranial pressure measurement and therapeutic drainage trials, which revealed normal intracranial pressures without clinical or ventricular improvement. Hydration and hemoglobin status remained stable. Therefore, a diagnosis of bilateral intracranial steno-occlusive arteriopathy was established in the setting of MPS I.

Surgical Treatment

To our knowledge, there is no literature describing surgical outcomes for steno-occlusive cerebrovascular disease in patients with MPS I. Accordingly, a multidisciplinary review in our Cerebrovascular Center at Cincinnati Children's Hospital and a secondary review with Boston Children's Hospital were convened to discuss treatment options. Given the patient's repetitive presentations of arm weakness and irritability, right steno-occlusive disease, and absence of elevated ICP, we collectively recommended right cerebral revascularization. Left cerebral revascularization was not recommended due to the patient's large-territory, completed stroke.

The patient underwent right-sided indirect revascularization with pial synangiosis and dural inversion, which was well-tolerated without post-operative complication (16, 17). A 2-year postoperative MRI demonstrated increased cortical vascularity without progressive ischemic changes (**Figure 3**, Lower panel). At a 3-year follow-up, the patient was clinically well with resolution of paresis and without recurrent symptoms.

DISCUSSION

For the first time, we describe a child with MPS I who presented with an acute ischemic stroke and underlying cerebral arteriopathy. Although strokes have been reported in patients with MPS I (12, 13, 18–20), stroke is not a widely-recognized clinical manifestation of MPS I and there are no reviews or guidelines for managing stroke in patients with this disease (2, 12, 13). This report, to our knowledge, is the first clinical description of the development of progressive cerebral arteriopathy treated via revascularization

Abbreviations: ERT, enzyme replacement therapy; GAGs, glycosaminoglycans; HSCT, hematopoietic stem cell transplantation; ICP, intracranial pressure; IONM, intraoperative neurophysiologic monitoring; MCA, middle cerebral artery; MMA, middle meningeal artery; MPS, mucopolysaccharidosis; rtPA, recombinant tissue plasminogen activator; STA, superficial temporal artery.

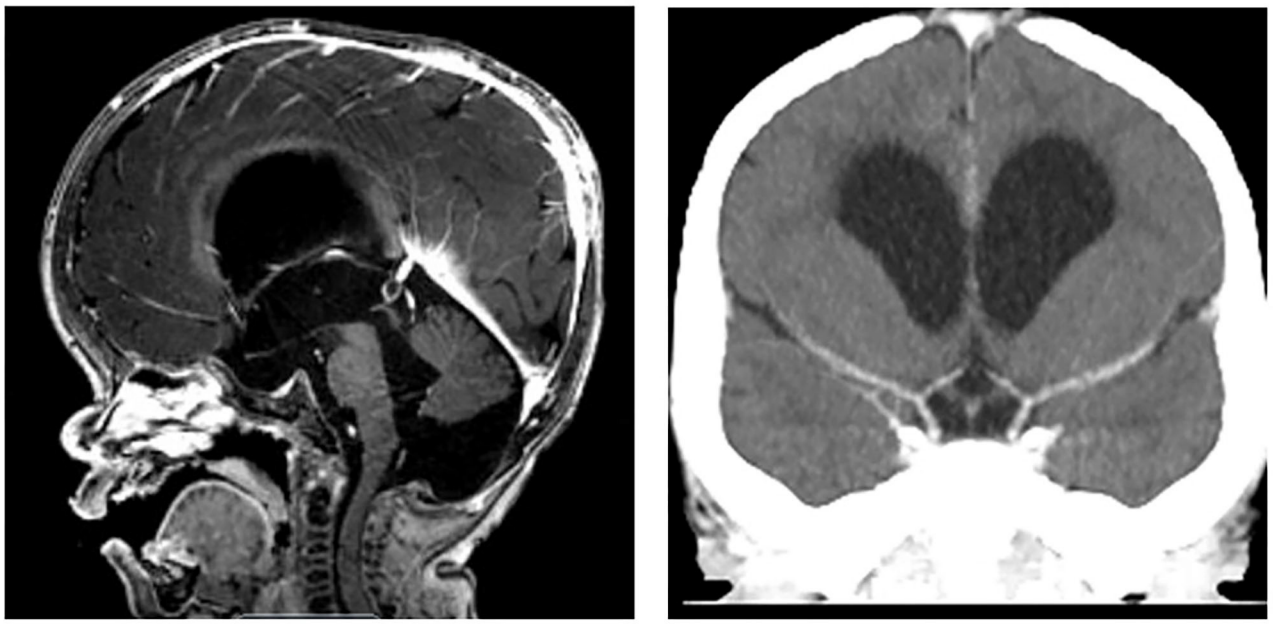

FIGURE 1 | MPS I prior to stroke. **(Left)** MRI Head demonstrating imaging findings of macrocephaly, ventriculomegaly, small foramen magnum, and mild narrowing of cervical spine without cord compression. **(Right)** CT Head with contrast demonstrating bilateral internal carotid termini without stenosis.

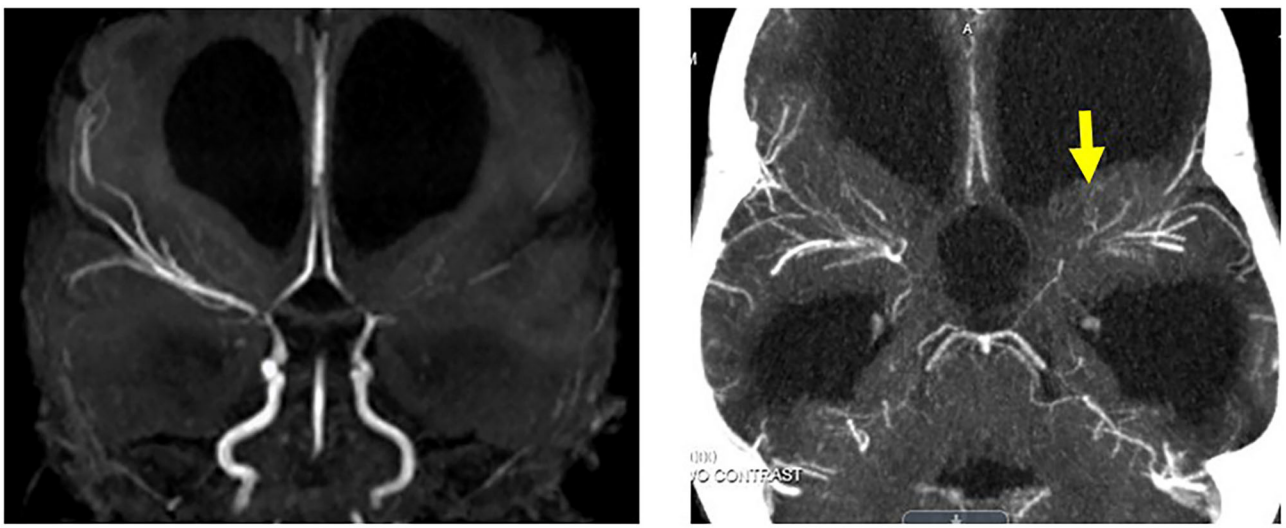

FIGURE 2 | MPS I arteriopathy after left cerebral stroke. **(Left)** MR angiogram 8 weeks after stroke with left MCA occlusion and bilateral ICA termini steno-occlusive disease. **(Right)** New left arm weakness episodes 3 months after overt stroke with persisting bilateral steno-occlusive disease and adjacent irregular collaterals identified on CT angiogram (yellow arrow).

surgery in a patient with MPS I. Our findings suggest that cerebral revascularization is a safe treatment option that may mitigate future stroke risk and should be considered within the overall management guidelines for patients with MPS I.

Stroke in MPS I

Neurological manifestations of MPS I include hydrocephalus, spinal cord compression, and cognitive decline (2, 10, 11, 21). Cardiac manifestations include hypertension, arrhythmia, valvular disease, and coronary artery disease (2, 7, 22). Stroke

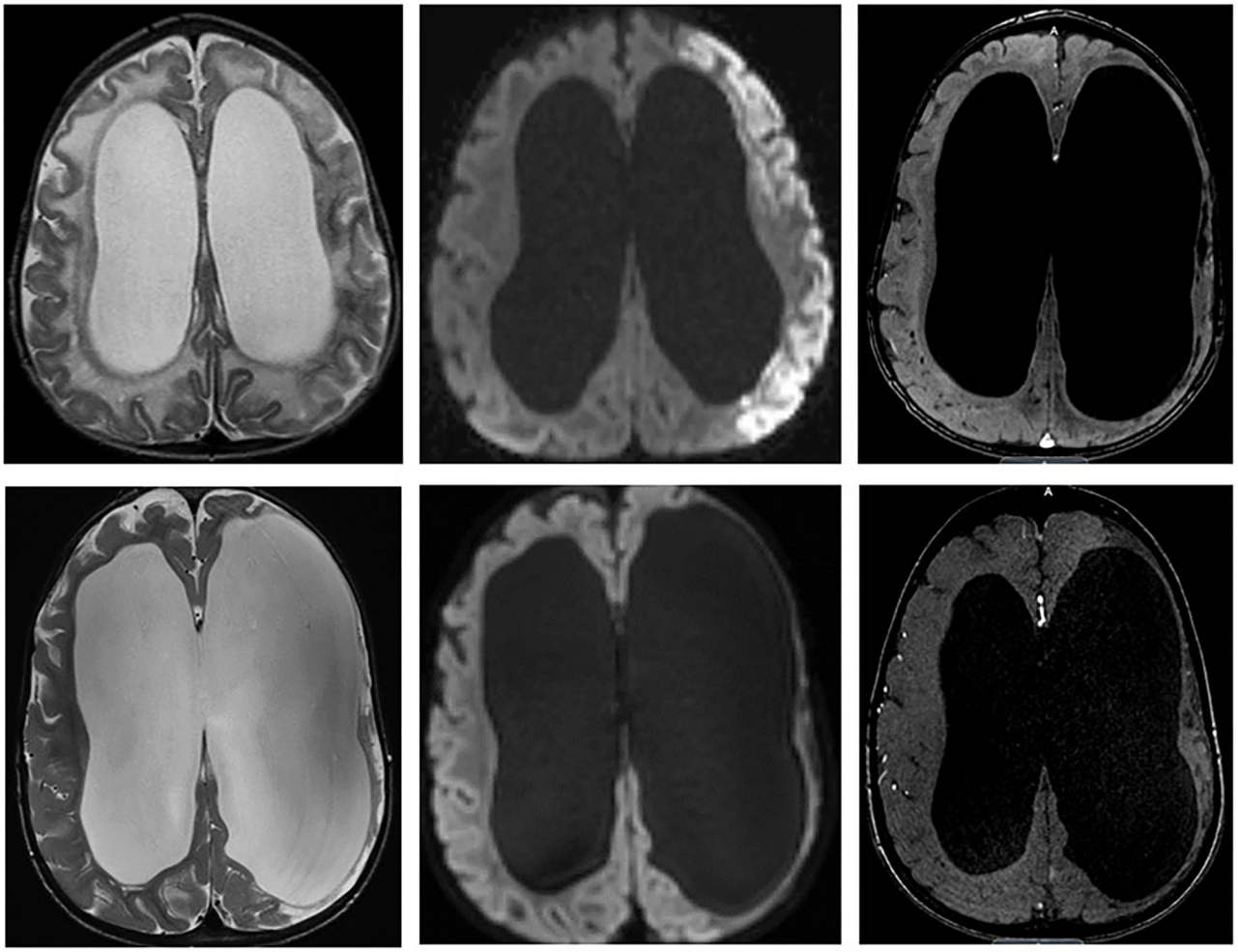

FIGURE 3 | (Upper) Initial MRI of left MCA overt stroke identified on T2, diffusion, and MRA. **(Lower)** Two years after right cerebral revascularization demonstrating no new ischemic or infarcted territories and increased right cerebral cortical vascularity.

is not a widely recognized manifestation of MPS I, and patients with MPS I are not routinely evaluated for stroke (2, 12, 13). However, a few cases of stroke have been reported in patients with this disease (**Table 1**) (12, 13, 18–20). A cardioembolic infarction disrupting the left internal carotid artery was the reported cause of stroke in a 41-year-old female with MPS I. After treatment with a recombinant tissue plasminogen activator (rtPA), this patient demonstrated signs of clinical improvement with recanalization of the left internal carotid artery (12). Another child with MPS I presented with an MCA territory occlusion and was treated with 7 days of heparinization, though no neurological changes were observed (13). Along with our current report, these studies indicate that stroke occurs in MPS I; however, it is uncertain whether rtPA therapy and anticoagulants will mitigate the risk of future strokes in patients with this disease. More research into the pathophysiological cause of stroke in MPS I and long-term treatment outcomes can help develop guidelines for managing stroke in this population.

Diagnostic Evaluation and Stroke Management

The patient described in this report was diagnosed with MPS I at 9 months and presented with a stroke at 17 months of age. The patient's symptoms and imaging are indicative of cerebral arteriopathy with bilateral internal carotid artery stenosis and left MCA occlusion. MRI examinations also demonstrated significant cerebral ventriculomegaly. The possibility of hydrocephalus-related vascular compression was evaluated through repeat lumbar punctures and intracranial pressure monitoring; however, all procedures confirmed normal intracranial pressure. The patient's cerebral ventriculomegaly was therefore consistent with *ex vacuo* changes of ischemic stroke rather than hydrocephalus.

Although the patient's stroke in association with bilateral internal carotid artery stenosis resembled moyamoya, we could not perform a conventional digital subtraction cerebral arteriogram in this patient to diagnose moyamoya (23). Nevertheless, the patient exhibited critical stenoses and distal

TABLE 1 | Stroke reported in patients with mucopolysaccharidosis (MPS) type I.

Study	Year	Country	*N*	Patient Characteristics	MPS I subtype	Clinical presentation	Imaging: imaging results	Diagnosis	Treatment	Follow-up (time after treatment)
Belani et al. (18)	1993	United States	1[a]	18-month-old patient (sex not specified)	Hurler syndrome	Intraoperative stroke during Leonard catheter placement	Not specified	Stroke (etiology not specified)	Not specified	Authors report patient showed partial recovery (time not specified)
Souillet et al. (19)	2003	France	1[b]	6-year-old male	Hurler-Scheie syndrome	Not specified	MRI: imaging findings not specified	Stroke (etiology not specified)	Not specified	Not specified
Fujii et al. (12)	2012	Japan	1	41-year-old female	Scheie syndrome	Acute onset dysarthria, right upper limb weakness, right central facial paralysis, mild right hemiparesis	MRI: subtle high signal lesions in left corona radiata and posterior limb of internal capsule MRA: disruption of left internal carotid artery Echocardiogram: mild aortic regurgitation	Stroke from cardioembolic infarction	Intravenous rtPA therapy with 0.6 mg/kg alteplase Commenced treatment with warfarin	Right arm weakness improved, MRA showed recanalization of left internal carotid artery (13 h) No further progression (22 months)
Hill and Preminger (20)	2014	United States	1[c]	9-month-old male	Hurler syndrome	Patent foramen ovale, new onset seizures	MRI: infarct affecting the left MCA territory	Stroke from paradoxical embolism	Percutaneous device closure of patent foramen ovale	No stroke-like symptoms (∼14 months)
Olgac et al. (13)	2018	Turkey	1	3-year-old female	Severity not specified	Left hemiplegia, right-sided central facial paralysis, increased deep tendon reflexes	MRI: restricted diffusion in right temporoparietal lobe MRA: right MCA occlusion Transthoracic echocardiography: moderate mitral and aortic valve regurgitation, high carotid intima-media thickness	Stroke from right MCA occlusion	Low-molecular-weight heparin therapy	No change in neurological condition (7 days)
Grant et al.	Current Report	United States	1	17-month-old male	Hurler syndrome	Right-sided weakness, emesis, decrease in appetite	MRI: left MCA infarction MRA: bilateral terminal internal carotid artery stenosis	Stroke from steno-occlusive cerebral arteriopathy	Right indirect cerebral revascularization	No complications during surgery Increased cortical vascularity, no new ischemic changes, near total resolution of right-sided weakness (3 years)

ERT, enzyme replacement therapy; MCA, middle cerebral artery; MPS, mucopolysaccharidosis; MRA, magnetic resonance angiography; MRI, magnetic resonance imaging; rtPA, recombinant tissue plasminogen activator.

[a] *Reported in a case series of 30 patients with MPS I, II, III, IV, and VI, of whom one patient who had MPS I presented with stroke.*

[b] *Reported in a chart review of 27 patients with MPS I who collectively received 30 hematopoietic stem cell transplants between 1986 and 2001; 1 patient presented with stroke.*

[c] *Case series of 2 identical twin boys with MPS I, of whom one presented with stroke.*

ischemia on MRI with waxing and waning clinical presentation. It is unlikely the serial MRAs overestimated the high degree of steno-occlusive arteriopathy given the patient's stable hydration and hemoglobin status. Furthermore, there was no evidence for cerebral vasculitis or cardiac abnormalities indicative of cardioembolic stroke. Therefore, a multidisciplinary team was convened to discuss treatment options for this patient. Continued clinical surveillance amid repetitive stroke-like presentations was considered of great risk; thus, cerebral revascularization was collectively recommended to mitigate the risk for recurrent stroke.

Potential Etiology

Our findings are consistent with a steno-occlusive disease, although the exact etiology of cerebral arteriopathy in patients with MPS I remains unclear. GAG accumulation is common in patients with MPS disorders and has been associated with many neurological and cardiac manifestations of MPS I (12, 21, 24). It is possible that an accumulation of GAGs contributed to this patient's cerebral arteriopathy, ultimately resulting in stroke. Proteoglycan imbalance may affect the arterial smooth muscle cell proliferation rate during MPS I elastogenesis (25), which may be like other intracranial steno-occlusive diseases (26). As we cannot demonstrate a molecular pathway for causation here, further studies will be necessary to determine the exact etiology of cerebral arteriopathy and stroke in patients with MPS I.

Treatment Recommendations and Outcomes

As cerebral arteriopathy predisposes patients to stroke, treatment is needed to mitigate the risk of recurrent strokes in MPS I. Surgical revascularization prevents further ischemic injury by increasing collateral blood flow to areas of insufficient perfusion due to arteriopathy using external circulation as a donor supply (17, 23, 27). Indirect cerebral revascularization is considered safe and effective for revascularizing the pediatric brain and preventing future stroke (17, 27, 28). While revascularization surgery has been documented in one patient with MPS I, this finding is listed in a large cohort study without clinical presentation, imaging results, and postoperative outcomes (29). The lack of MPS I revascularization evidence made management challenging, necessitating multidisciplinary review. Our findings demonstrate that cerebral revascularization is a safe and effective treatment option to mitigate the risk of recurrent stroke in children with MPS I. Cerebral revascularization should be considered within the overall management of this disease.

CONCLUSION

This report provides two important new findings. First, we demonstrate that patients with MPS I are at risk of significant overt stroke secondary to cerebral arteriopathy. As symptoms of MPS I typically emerge in early childhood (2, 11), pediatric providers should consider screening for stroke in children with this disease. Second, this is the first clinical description of cerebral revascularization in a patient with MPS I, supported by long-term follow-up that confirmed favorable tolerance of surgery without any transient or neurological stroke events. Further investigation will help establish guidelines for identifying and treating stroke in patients with MPS I.

DATA AVAILABILITY STATEMENT

The original contributions presented in the study are included in the article/**Supplementary Material**, further inquiries can be directed to the corresponding author/s.

ETHICS STATEMENT

Ethical review and approval was not required for the study on human participants in accordance with the local legislation and institutional requirements. Written informed consent to participate in this study was provided by the participants' legal guardian/next of kin. Written informed consent was obtained from the minor(s)' legal guardian/next of kin for the publication of any potentially identifiable images or data included in this article. Informed consent was obtained from the patient for being included in this case report.

AUTHOR CONTRIBUTIONS

NG collected data, analyzed and interpreted the data, drafted the initial manuscript, reviewed, and revised the manuscript. JT conceptualized and organized the case report, analyzed and interpreted the data, and critically revised the manuscript for important intellectual content. ZP, KM, TB, LL-J, AB, AH, KW, and ES analyzed and interpreted the data and critically revised the manuscript for important intellectual content. JL and SV conceptualized and organized the case report, analyzed and interpreted the data, drafted the initial manuscript, and critically revised the manuscript for important intellectual content. All authors have approved the final manuscript and agree to be accountable for all aspects of the work.

SUPPLEMENTARY MATERIAL

The Supplementary Material for this article can be found online at: https://www.frontiersin.org/articles/10.3389/fped.2021.606905/full#supplementary-material

REFERENCES

1. Bach G, Friedman R, Weissmann B, Neufeld EF. The defect in the Hurler and Scheie syndromes: deficiency of α-L-Iduronidase. *Proc Natl Acad Sci USA*. (1972) 69:2048–51. doi: 10.1073/pnas.69.8.2048

2. Muenzer J, Wraith JE, Clarke LA, the International Consensus Panel on the Management Treatment of Mucopolysaccharidosis I. Mucopolysaccharidosis I: management and treatment guidelines. *Pediatrics*. (2009) 123:19–29. doi: 10.1542/peds.2008-0416

3. Neufeld EF, Muenzer J. The mucopolysaccharidoses. In: Scriver C, Beaudet A, Sly W, Valle D, Childs R, Kinzler KW, eds. *The Metabolic and Molecular Bases of Inherited Disease*. New York, NY: McGraw Hill (2001) p. 3421–52.
4. Grewal SS, Wynn R, Abdenur JE, Burton BK, Gharib M, Haase C, et al. Safety and efficacy of enzyme replacement therapy in combination with hematopoietic stem cell transplantation in Hurler syndrome. *Genet Med.* (2005) 7:143–6. doi: 10.1097/01.GIM.0000154299.22120.6A
5. Tolar J, Grewal SS, Bjoraker KJ, Whitley CB, Shapiro EG, Charnas L, et al. Combination of enzyme replacement and hematopoietic stem cell transplantation as therapy for Hurler syndrome. *Bone Marrow Transplant.* (2008) 41:531–5. doi: 10.1038/sj.bmt.1705934
6. Ghosh A, Miller W, Orchard PJ, Jones SA, Mercer J, Church HJ, et al. Enzyme replacement therapy prior to haematopoietic stem cell transplantation in mucopolysaccharidosis type I: 10 year combined experience of 2 centres. *Mol Genet Metab.* (2016) 117:373–7. doi: 10.1016/j.ymgme.2016.01.011
7. Braunlin EA, Harmatz PR, Scarpa M, Furlanetto B, Kampmann C, Loehr JP, et al. Cardiac disease in patients with mucopolysaccharidosis: presentation, diagnosis, and management. *J Inherit Metab Dis.* (2011) 34:1183–97. doi: 10.1007/s10545-011-9359-8
8. Tokic V, Barisic I, Huzjak N, Petkovic G, Fumic K, Paschke E. Enzyme replacement therapy in two patients with an advanced severe (Hurler) phenotype of mucopolysaccharidosis I. *Eur J Pediatri.* (2007) 166:727–32. doi: 10.1007/s00431-006-0316-8
9. Concolino D, Deodato F, Parini R. Enzyme replacement therapy: efficacy and limitations. *Ital J Pediatr.* (2018) 44:120. doi: 10.1186/s13052-018-0562-1
10. Shapiro EG, Nestrasil I, Rudser K, Delaney K, Kovac V, Ahmed A, et al. Neurocognition across the spectrum of mucopolysaccharidosis type I: age severity, and treatment. *Mol Genet Metab.* (2015) 116:61–8. doi: 10.1016/j.ymgme.2015.06.002
11. Grosse SD, Lam WKK, Wiggins LD, Kemper AR. Cognitive outcomes and age of detection of severe mucopolysaccharidosis type I. *Genet Med.* (2017) 19:975–82. doi: 10.1038/gim.2016.223
12. Fujii D, Manabe Y, Tanaka T, Kono S, Sakai Y, Narai H, et al. Scheie syndrome diagnosed after cerebral infarction. *J Stroke Cerebrovasc Dis.* (2012) 21:330–2. doi: 10.1016/j.jstrokecerebrovasdis.2010.09.006
13. Olgac A, Tumer L, Damar Ç, Hasanoglu A, Ezgü F. Acute stroke in a patient with mucopolysaccharidosis type I with increased carotid intima-media thickness. *EJMO.* (2018) 2:114–6. doi: 10.14744/ejmo.2018.51523
14. Johnson BA, Dajnoki A, Bodamer OA. Diagnosing lysosomal storage disorders: mucopolysaccharidosis type I. *Curr Protoc Hum Genet.* (2015) 84:17.17.1–8. doi: 10.1002/0471142905.hg1717s84
15. Matheus MG, Castillo M, Smith JK, Armao D, Towle D, Muenzer J. Brain MRI findings in patients with mucopolysaccharidosis types I and II and mild clinical presentation. *Neuroradiology.* (2004) 46:666–72. doi: 10.1007/s00234-004-1215-1
16. Adelson PD, Scott RM. Pial synangiosis for moyamoya syndrome in children. *Pediatr Neurosurg.* (1995) 23:26–33. doi: 10.1159/000120932
17. Smith ER, Scott RM. Surgical management of moyamoya syndrome. *Skull Base.* (2005) 15:15–26. doi: 10.1055/s-2005-868160
18. Belani KG, Krivit W, Carpenter BL, Braunlin E, Buckley JJ, Liao JC, et al. Children with mucopolysaccharidosis:perioperative care, morbidity, mortality, and new findings. *J Pediatr Surg.* (1993) 28:403–10. doi: 10.1016/0022-3468(93)90240-L
19. Souillet G, Guffon N, Maire I, Pujol M, Taylor P, Sevin F, et al. Outcome of 27 patients with Hurler's syndrome transplanted from either related or unrelated haematopoietic stem cell sources. *Bone Marrow Transplant.* (2003) 31:1105–17. doi: 10.1038/sj.bmt.1704105
20. Hill J, Preminger T. Percutaneous PFO closure for paradoxical stroke in 8-kg twins. *Catheter Cardiovasc Interv.* (2014) 84:110–3. doi: 10.1002/ccd.25183
21. Dalla Corte A, de Souza CFM, Anés M, Giugliani R. Hydrocephalus and mucopolysaccharidoses: what do we know and what do we not know? *Childs Nerv Syst.* (2017) 33:1073–80. doi: 10.1007/s00381-017-3476-0
22. Mohan UR, Hay AA, Cleary MA, Wraith JE, Patel RG. Cardiovascular changes in children with mucopolysaccharide disorders. *Acta Paediatr.* (2002) 91:799–804. doi: 10.1111/j.1651-2227.2002.tb03330.x
23. Scott RM, Smith ER. Moyamoya disease and moyamoya syndrome. *N Engl J Med.* (2009) 360:1226–37. doi: 10.1056/NEJMra0804622
24. Cabrera GH, Fernández I, Dominguez M, Clarke LA. Left ventricular aneurysm in an adult patient with mucopolysaccharidosis type I: comment on pathogenesis of a novel complication. *Mol Genet Metab.* (2012) 106:470–3. doi: 10.1016/j.ymgme.2012.06.001
25. Hinek A, Wilson SE. Impaired elastogenesis in Hurler disease: dermatan sulfate accumulation linked to deficiency in elastin-binding protein and elastic fiber assembly. *Am J Pathol.* (2000) 156:925–38. doi: 10.1016/S0002-9440(10)64961-9
26. Milewicz DM, Kwartler CS, Papke CL, Regalado ES, Cao J, Reid AJ. Genetic variants promoting smooth muscle cell proliferation can result in diffuse and diverse vascular diseases: evidence for a hyperplastic vasculomyopathy. *Genet Med.* (2010) 12:196–203. doi: 10.1097/GIM.0b013e3181cdd687
27. Ellis MJ, Armstrong D, Dirks PB. Large vascular malformation in a child presenting with vascular steal phenomenon managed with pial synangiosis. *J Neurosurg Pediatr.* (2011) 7:15–21. doi: 10.3171/2010.10.PEDS10388
28. Scott RM, Smith JL, Robertson RL, Madsen JR, Soriano SG, Rockoff MA. Long-term outcome in children with moyamoya syndrome after cranial revascularization by pial synangiosis. *J Neurosurg.* (2004) 100:142–9. doi: 10.3171/ped.2004.100.2.0142
29. Guzman R, Lee M, Achrol A, Bell-Stephens T, Kelly M, Do HM, et al. Clinical outcome after 450 revascularization procedures for moyamoya disease. *J Neurosurg.* (2009) 111:927–35. doi: 10.3171/2009.4.JNS081649

Conflict of Interest: The authors declare that the research was conducted in the absence of any commercial or financial relationships that could be construed as a potential conflict of interest.

frontiers in Pediatrics

CASE REPORT
published: 18 August 2021
doi: 10.3389/fped.2021.710553

Case Report: *ISPD* Gene Mutation Leads to Dystroglycanopathies: Genotypic Phenotype Analysis and Treatment Exploration

*Haiyan Yang[1], Fang Cai[2], Hongmei Liao[1], Siyi Gan[3], Ting Xiao[3] and Liwen Wu[1]**

[1] Department of Neurology, Hunan Children's Hospital, Changsha, China, [2] Department of Neurology, Chenzhou No. 1 People's Hospital, Chenzhou, China, [3] Department of Pediatrics, Xiangya Hospital, Central South University, Changsha, China

ISPD gene mutation-related diseases have high clinical and genetic heterogeneity, and no studies have yet reported any effective treatments. We describe six patients with dystroglycanopathies caused by *ISPD* gene mutations and analyze their genotypes and phenotypes to explore possible effective treatments. Our results confirm that the phenotype of limb-girdle muscular dystrophies can be easily misdiagnosed as Duchenne muscular dystrophy and that exon deletions of *ISPD* gene are relatively common. Moreover, low-dose prednisone therapy can improve patients' exercise ability and prolong survival and may be a promising new avenue for *ISPD* therapy.

Keywords: *ISPD* gene, dystroglycanopathies, limb-girdle muscular dystrophies, Duchenne muscular dystrophy, pediatric

OPEN ACCESS

Edited by:
Juergen Brunner, Innsbruck Medical University, Austria

Reviewed by:
Stephanie Efthymiou, University College London, United Kingdom
Aleksandra Jezela-Stanek, National Institute of Tuberculosis and Lung Diseases, Poland

****Correspondence:***
Liwen Wu
wuliwen2020@sina.com

Specialty section:
This article was submitted to Pediatric Neurology, a section of the journal Frontiers in Pediatrics

Received: *16 May 2021*
Accepted: *21 July 2021*
Published: *18 August 2021*

Citation:
Yang H, Cai F, Liao H, Gan S, Xiao T and Wu L (2021) Case Report: ISPD Gene Mutation Leads to Dystroglycanopathies: Genotypic Phenotype Analysis and Treatment Exploration. Front. Pediatr. 9:710553. doi: 10.3389/fped.2021.710553

BACKGROUND

ISPD (MIM 614631, also named CDP-L-ribitol pyrophosphorylase A, *CRPPA*) gene, which maps to chromosome 7p21, has been associated with the loss of α-dystroglycan (α-DG) glycosylation (1–3). Defects in the post-translational modification of α-DG have been implicated in clinically distinct dystroglycanopathies that present as congenital muscular dystrophies with multisystem involvement, Walker–Warburg syndrome (MIM 614643), limb-girdle muscular dystrophies (LGMDs) (MIM 616052), or a spectrum of intermediate phenotypes (4). *ISPD* gene mutation-related diseases have high clinical and genetic heterogeneity (5). At present, there has been a lack of effective treatment for *ISPD* gene mutation-related diseases, and no studies have yet reported a possible effective treatment. Here, we report six patients with dystroglycanopathies caused by *ISPD* gene mutations and analyze their genotypes and phenotypes to explore possible effective treatments.

CASE PRESENTATION

Two siblings (case 1 and case 2) were reported in this family. The younger brother (case 1) was a 9-year-old male child who presented with a history of progressive weakness of the lower limbs since age 1.5 years. The results of laboratory testing revealed elevated creatine kinase (CK) (13,043.5 U/L) and elevated lactic acid (2.30 mmol/L) levels. Muscle biopsy showed myodystrophy changes. Muscle MRI showed different degrees of fatty infiltration with partial inflammation edema in each muscle group of the thigh (**Figures 1A–D**). The initial clinical diagnosis was considered Duchenne muscular dystrophy (DMD). The child has received prednisone (0.75 mg/kg/day) treatment

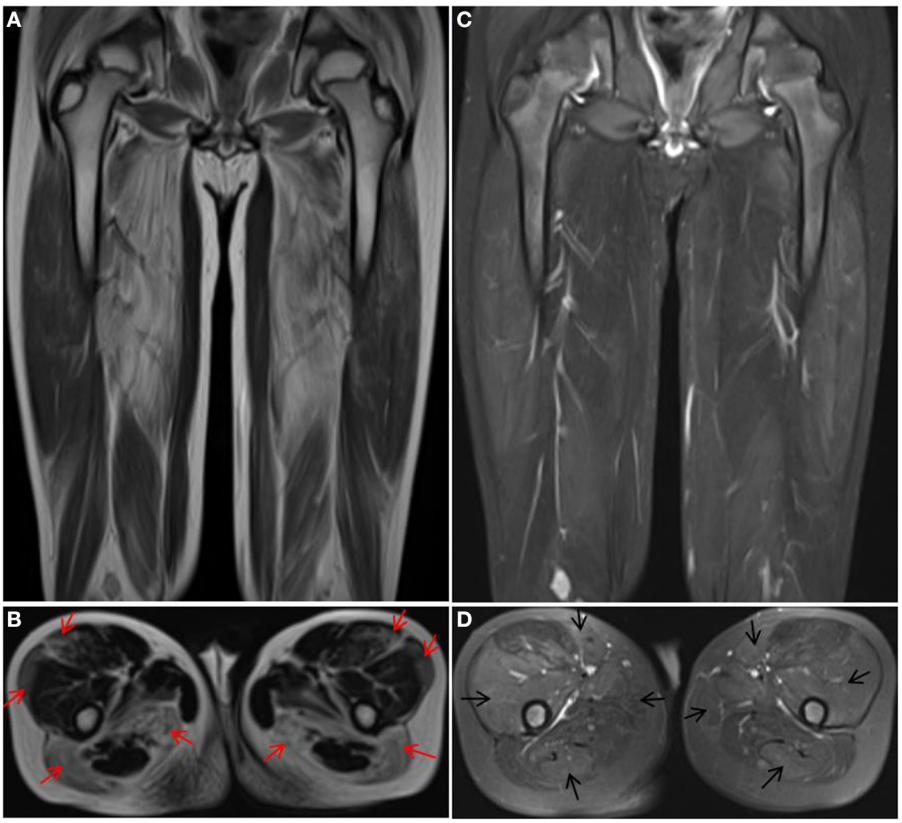

FIGURE 1 | Muscle MRI of case 1. T1 **(A,B)** showed obvious fat infiltration in thigh muscles, most notably in the vastus lateralis, rectus femoris, biceps femoris, and semimembranosus muscles (red arrow), but the fat infiltration in the vastus intermedius, sartorius, gracilis, and semitendinosus muscles was mild. T2 **(C,D)** showed obvious inflammation edema in the muscles with mild fat infiltration (black arrow).

since the age of 8, and the symptoms of muscle weakness have improved, along with a longer walking duration and less wrestling. After genetic diagnosis, the younger brother gradually stopped prednisone treatment plan. However, after prednisone reduction, the patient's motor function decreased, and the wrestling increased. The symptoms improved again when the child resumed prednisone therapy. The older sister (case 2) presented with a history of progressive weakness after birth and never gained the ability to walk independently. At the age of 3, a muscle biopsy showed myodystrophy changes; she did not receive special treatment and died at the age of 16.

Case 3 was a 16-year-old male patient who presented with a history of progressive weakness of the lower limbs from childhood. The results of laboratory testing revealed elevated CK levels (7,431.5 U/L), and muscle biopsy showed myodystrophy changes. The initial clinical diagnosis was considered DMD. The patient has received prednisone treatment (20 mg, gradually increased to 35 mg, Qd, 10-day regimen followed by a pause for 20 days) since the age of 12, and the symptoms of muscle weakness have improved. The child has no obvious Gowers' sign and can jump 2–3 cm off the ground with both feet but can barely jump off the ground with one foot.

Case 4 was a 10-year-old male child who presented with a history of progressive weakness of the lower limbs since age 1.3 years and the loss of ambulation at age 10. The results of laboratory testing revealed elevated CK (6,329.6 U/L). Muscle biopsy showed myodystrophy changes. The child was not treated with any medication.

Two sisters were also identified in this family. The proband (case 5) was 5 years old, was female, and had normal development, but she had slight weakness when climbing and running. Her CK level was between 2,400 and 5,600 U/L. She had a 3-year-old sister (case 6) with the same motor development features who suffered from retinoblastoma, and her CK was between 1,000 and 8,800 U/L. Their mother was 32 years old, presenting with intolerance of movement and an elevated CK level of 600–4,500 U/L. Muscle biopsy of the proband revealed atrophy in parts of the muscle fibers, mild hyperplasia of connective tissue, negative dystrophin-N staining in most muscle fibers, and decreased expression of dystrophin-C and dystrophin-R. Except for the younger sister of the proband, who underwent ophthalmectomy, the proband was not treated with any medication.

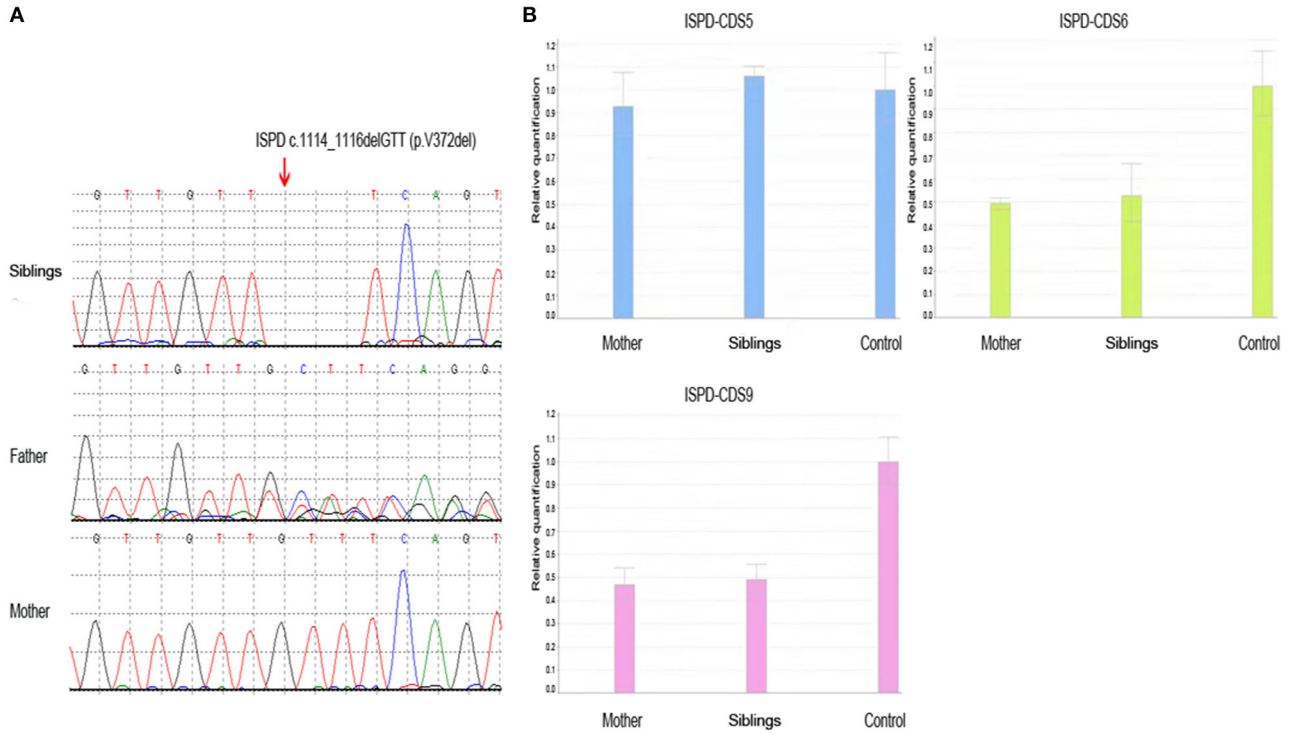

FIGURE 2 | The result of whole-exome sequencing of the siblings. **(A)** The siblings had *ISPD* c.1114_1116delGTT (p.V372del) mutation, which was inherited from the father, while the mother did not carry the mutation. **(B)** The siblings had *ISPD* exon 6–9 deletion, which was inherited from the mother.

METHODS

Written informed consent was obtained from the patients and their parents. This study was approved by the Medical Ethics Committee of Hunan Children's Hospital.

Genetic testing included the use of the multiplex ligation-dependent probe amplification (MLPA) method to screen for *DMD* gene duplication and deletion and next-generation sequencing methods to screen for other genes that might cause elevated CK and muscle weakness. All experiments and analyses were performed according to our previous research methods (6).

Sequence variants were annotated using population and literature databases, including 1,000 Genomes, dbSNP, GnomAD, Clinvar, HGMD, and OMIM. Variant interpretation was performed according to the American College of Medical Genetics and Genomics (ACMG) guidelines (7).

RESULTS

The detection for *DMD* gene from peripheral blood of the siblings (case 1 and case 2) was negative, including duplication and deletions, point mutations, and intron region mutations. Moreover, the possible RNA mutations of *DMD* gene were negative by detecting the muscle tissue of the siblings. These results were puzzling. Therefore, in September 2020, we reanalyzed the previous second-generation sequencing data and found that the siblings (case 1 and case 2) had *ISPD* c.1114_1116delGTT (p.V372del) mutation and exon 6–9 deletion (**Figures 2A,B**). The siblings (case 1 and case 2) were eventually diagnosed with LGMDs. The *DMD* gene duplication deletion, point mutation, and intron mutation test results of case 3 were all negative. Further next-generation sequencing revealed *ISPD* c.1114_1116delGTT (p.V372del) mutation, and the patient was eventually diagnosed as LGMDs. Case 4 had *ISPD* c.1114_1116delGTT (p.V372del) and *POMT1* c.979G>A (p.V327I) mutations. The sisters (case 5 and case 6) had *ISPD* c.984G>T (p.Q328H) and c.550C>T (p.R184X) compound heterozygous mutations and *DMD* c.130dupC mutation. Further details can be found in **Table 1**.

DISCUSSION

Relevant case reports from PubMed database since its establishment until December 2020 were searched with ISPD gene as the key word, and the variants and clinical phenotypes of ISPD gene were summarized. Currently, a total of 58 patients with *ISPD* gene mutations have been reported in nine literatures (2–5, 8–12) (**Table 2**). The reported clinical phenotypes include intrauterine growth restriction, gastroschisis, Walker–Warburg syndrome, LGMDs, cobblestone lissencephaly, and congenital muscular dystrophy with developmental delay. For LGMDs due

TABLE 1 | Genotype and phenotype analysis of the 6 patients with *ISPD* mutation.

Patient	Sex	Age	Muscle MRI	Muscle biopsy	Mutation	Inheritance	ACMG classification	Clinical feature	Effective treatment	Outcome
1	M	9 y	Fatty infiltration with partial inflammation edema in the thigh muscles	Myodystrophy	*ISPD*c.1114_1116delGTT (p.V372del)	Paternal	P	Limb-girdle muscular dystrophies	Prednisone	Survive
					Exons 6-9 deletion	Maternal	LP			
2	F	16 y	N/A	Myodystrophy	*ISPD* c.1114_1116delGTT (p.V372del)	Paternal	P	Limb-girdle muscular dystrophies	None	Died
					Exons 6-9 deletion	Maternal	LP			
3	M	16 y	N/A	Myodystrophy	*ISPD* c.1114_1116delGTT (p.V372del)	Paternal	P	Limb-girdle muscular dystrophies	Prednisone	Survive
4	M	10 y	N/A	Myodystrophy	*ISPD* c.1114_1116delGTT (p.V372del)	Paternal	P	Limb-girdle muscular dystrophies	None	Survive
					POMT1 c.979G>A (p.V327I)	Parental	Benign			
5	F	5 y	N/A	Myodystrophy	*ISPD* c.984G>T(p.Q328H)	Paternal	VUS	Limb-girdle muscular dystrophies	None	Survive
					c.550C>T(p.R184X)	Maternal	LP			
					DMD c.130dupC	Maternal	Benign			
6	F	3 y	N/A	N/A	*ISPD* c.984G>T(p.Q328H)	Paternal	VUS	Limb-girdle muscular dystrophies	None	Survive
					c.550C>T(p.R184X)	Maternal	LP			
					DMD c.130dupC	Maternal	Benign			

ACMG, American College of Medical Genetics; F, Female; LP, likely pathogenic; MRI, Magnetic resonance imaging; M, Male; N/A, Not available; P, pathogenic; VUS, variant of unknown significance; y, year.

to *ISPD* mutations, onset occurs in late childhood, adolescence, or adulthood (8). The main clinical manifestations of LGMDs include proximal muscle involvement of the upper and lower extremities, elevated CK, gastrocnemius hypertrophy, and Gowers' sign (13). Muscle biopsy and muscle MRI revealed changes indicative of myodystrophy, which is difficult to distinguish from DMD; and thus, these cases can be easily misdiagnosed (14).

At present, 48 variants of *ISPD* have been reported, of which point mutations account for 70.8% (34/48) and exon deletions account for 29.2% (14/48) (2–5, 8–12) (**Table 2**). Collectively, the literature and our experience with these patients indicate that exon deletion of *ISPD* gene is common. These microdeletions can be clinically difficult to detect by conventional second-generation sequencing methods. Therefore, for patients with LGMDs clinically excluded from DMD, in addition to routine screening for *ISPD* point mutations, we must carefully consider the possibility of *ISPD* exon deletion, which should be investigated during data analysis.

Among our patients, *ISPD* mutations were found to coexist with gene mutations of another myopathy. Compared with the other two male patients in this cohort who had only *ISPD* gene mutations, the male patient who had *ISPD* and *POMT1* gene mutations developed muscle weakness more quickly and lost walking ability at an earlier age. In the sisters with *ISPD* and *DMD* gene mutations, the degree of CK elevation was higher than that of their mother without synergistic *ISPD* pathogenic genes, and the symptoms of exercise intolerance appeared at an earlier age than their mother's. Therefore, whether *ISPD* mutation is synergistic with *DMD* or *POMT1* gene mutation should be carefully considered. These conditions increase the difficulty and complexity of prenatal diagnosis, so clinicians must be vigilant.

In our study, two patients (case 1 and case 3) were clinically diagnosed with DMD before genetic diagnosis and were offered the currently recommended low-dose prednisone therapy for DMD (15), which was unexpectedly found to be effective in improving the patient's motor function, prolonging the walking time and reducing the frequency of wrestling. The motor function of the two patients was improved compared with that before and after treatment and that of untreated case 4. After the genetic diagnosis, we also attempted to reduce and discontinue the hormone treatment for case 1. After the hormone treatment was discontinued, the patient's muscle weakness returned, and the frequency of wrestling increased significantly. After the hormone treatment was resumed, the symptoms improved again. Muscle MRI in case 1 showed significant inflammation edema changes before muscle atrophy, which further suggested that prednisone therapy could alleviate symptoms after improving inflammation edema.

TABLE 2 | Genotype and phenotype analysis of the *ISPD* gene reported in literature.

Mutation	Case (*n*)	Inheritance (*n*)	Sex (*n*)	Age (m)	Brain MRI (*n*)	Clinical feature	ACMG classification	Outcome
c.367G>A (p.G123A)	2	Parental (2)	F (1)	4.3 y	*N* (2)	Limb-girdle muscular dystrophies	LP	Survive (2)
			M (1)					
7p21.2p21.1 microdeletion	3	Maternal (3)	Fetus (3)	N/A	*A* (2)	Intrauterine growth restriction; Gastroschisis	P	Survive (1)
					N(1)			Died (2)
Exons 9 and 10 deletion	1	Paternal (1)	M(1)	13 months	*A* (1)	Walker-Warburg syndrome	P	Died (1)
c.614G>A (p.A205H)		Unknown (1)					P	
c.161G>C (p.G54A)	2	Maternal (2)	F (1)	50 y	*A* (2)	Limb-girdle muscular dystrophies	P	Survive (2)
			M (1)					
c.1114_1116delGTT (p.V372del)	6	Parental (3)	F (5)	32 y	*N* (4)	Limb-girdle muscular dystrophies	P	Survive (6)
		N/A (3)	N/A (1)		N/A (2)			
Exons 9 and 10 deletion	1	Parental (1)	N/A	N/A	N/A	Walker-Warburg syndrome	P	N/A
Exons 6–8 deletion	1	Parental (1)	N/A	N/A	N/A	Walker-Warburg syndrome	P	N/A
c.647C>A (p.A216A)	1	Parental (1)	N/A	N/A	N/A	Walker-Warburg syndrome	P	N/A
c.832A>T (p.Lys278*)	1	Parental (1)	N/A	N/A	N/A	Walker-Warburg syndrome	P	N/A
c.1186G>T (p.Glu396*)	1	Parental (1)	N/A	N/A	N/A	Walker-Warburg syndrome	P	N/A
c.53dupT (p.Ser19fs)	1	Paternal (1)	N/A	N/A	N/A	Walker-Warburg syndrome	P	N/A
c.377G>A (p.A126H)		Maternal (1)					P	
c.364G>C (p.A122P)	1	Maternal (1)	N/A	N/A	N/A	Walker-Warburg syndrome	P	N/A
c.802C>T (p.Arg268*)		Paternal (1)					P	
c.638T>G (p.M213A)	3	N/A	Fetus (3)	N/A	A (3)	Cobblestone-Lissencephaly	LP	N/A
exons 3 to 6 deletion		N/A					N/A	
c.466G>A (p.A156A)	2	N/A	Fetus (2)	N/A	A (2)	Cobblestone-Lissencephaly	LP	N/A
c.713C>T (p.T238I)	1	N/A	Fetus (1)	N/A	A (1)	Cobblestone-Lissencephaly	LP	N/A
c.256A>T (p.Arg86*)		N/A					N/A	
c.257+2T>G (*)	1	*De novo*	Fetus (1)	N/A	A (1)	Cobblestone-Lissencephaly	N/A	N/A
c.773C>A (p.Ser258)		N/A					N/A	
c.676T>C (p.T226H)	1	N/A	Fetus (1)	N/A	A (1)	Cobblestone-Lissencephaly	LP	N/A
Exons 4 to 6 deletion		N/A					N/A	
c.643C>T (p.Gln215*)	2	N/A (2)	F (1)	7 y	N/A	Walker-Warburg syndrome	N/A	N/A
Exons 9 and 10 deletion			N/A					
c.789+2T>G	2	N/A	N/A	N/A	N/A	Walker-Warburg syndrome	N/A	N/A
Exon 4 deletion								
c.277_279del ATT (p.Ile93del)	1	N/A	N/A	N/A	N/A	Walker-Warburg syndrome	N/A	N/A

(Continued)

TABLE 2 | Continued

Mutation	Case (*n*)	Inheritance (*n*)	Sex (*n*)	Age (m)	Brain MRI (*n*)	Clinical feature	ACMG classification	Outcome
c.1354T>A (p.*452Arg)	1	N/A	N/A	N/A	N/A	Walker-Warburg syndrome	N/A	N/A
c.1120-1G>T	1	N/A	N/A	N/A	N/A	Walker-Warburg syndrome	N/A	N/A
Exon 9 deletion								
c.550C>T (p.Arg184*)	1	N/A	N/A	N/A	N/A	Walker-Warburg syndrome	N/A	N/A
c.5A>T (p.G2V)	1	Maternal (1)	N/A	N/A	N/A	Walker-Warburg syndrome	P	N/A
c.505A>T (p.Lys169*)	1	Paternal (1)	N/A	N/A	N/A	Walker-Warburg syndrome	N/A	N/A
c.340C>G (p.H114A)	1	Maternal and Paternal (1)	N/A	N/A	N/A	Congenital muscular dystrophy	P	N/A
c.464A>G (p.H155A)	1	Paternal (1)	N/A	N/A	N/A	Congenital muscular dystrophy	P	N/A
c.712A>G (p.T238A)	1	Maternal (1)	N/A	N/A	N/A	Congenital muscular dystrophy	p	N/A
c.659A>T (p.A220V)	1	Maternal (1)	N/A	N/A	N/A	Congenital muscular dystrophy	P	N/A
c.1251G>A (p.Val374-Gln417del)	5	Paternal (1)	N/A	N/A	N/A	Congenital muscular dystrophy	N/A	N/A
c.990delC (p.Ile331Serfs*2)	1	Maternal (1)	N/A	N/A	N/A	Walker-Warburg syndrome	N/A	N/A
exons 6-9 deletion	1	Maternal (1)	N/A	N/A	N/A	Congenital muscular dystrophy with mental retardation	N/A	N/A
c.1026+1G>A	2	Parental (2)	N/A	N/A	N/A	Limb-girdle muscular dystrophies	N/A	N/A
c.1124A>G	1	Maternal (1)	N/A	N/A	N/A	Limb-girdle muscular dystrophies	N/A	N/A
c.1186G>T (p.Glu396*)	1	Parental (1)	N/A	N/A	N/A	Congenital muscular dystrophy with mental retardation	N/A	N/A
c.1183A>T (p.Arg395*)	2	N/A (2)	F (2)	14.5 y	N (2)	Limb-girdle muscular dystrophies	N/A	N/A
c.377G>A (p.A126H)	1	N/A	M (1)	6.5 y	A (1)	Limb-girdle muscular dystrophies	N/A	N/A
c.677A>G(p.T226C)	1	N/A	F (1)	10 y	N (1)	Limb-girdle muscular dystrophies with mental retardation	N/A	N/A

A, Abnormal; ACMG, American College of Medical Genetics; F, Female; MRI, Magnetic resonance imaging; M, Male; m, medium; N, Normal; N/A, Not available; n, number; p, pathogenic; y, year.

In conclusion, the genotypes and phenotypes of *ISPD* gene mutations represent a wide spectrum, and the phenotype of LGMDs is easily misdiagnosed as DMD. Exon deletions of *ISPD* gene are relatively common, so caution must be taken in the selection of gene testing methods and data analysis to avoid false-negative results. *ISPD* and other gene mutations coexist in some patients, so the possibility of synergistic pathogenesis needs to be confirmed by further large sample studies and functional verification. Our findings indicate that low-dose hormone therapy can improve patients' exercise ability and prolong survival and may be a promising new avenue for *ISPD* therapy.

DATA AVAILABILITY STATEMENT

The original contributions presented in the study are included in the article, further inquiries can be directed to the corresponding author/s.

ETHICS STATEMENT

The studies involving human participants were reviewed and approved by the Medical Ethics Committee of Hunan Children's Hospital. Written informed consent to participate in this study was provided by the participants' legal guardian/next of kin. Written informed consent was obtained from the minor(s)' legal guardian/next of kin for the publication of any potentially identifiable images or data included in this article.

AUTHOR CONTRIBUTIONS

HY conducted the literature review and drafted the manuscript. FC, HL, SG, and TX made substantial contributions to the conception and interpretation of data. LW was responsible for revising the manuscript critically and has given final approval of the version to be published. All authors read and approved the manuscript.

FUNDING

This work was supported by grants from the National Natural Science Foundation of China (No. 81671297). This work was supported by Provincial Technology Innovation Guidance Program Clinical Medical Technology Innovation Guidance (2017SK50704).

ACKNOWLEDGMENTS

We wish to thank the patients and their families for the participation in this study.

REFERENCES

1. Cirak S, Herrmann R, Ruthland P, Brokmann K, Korinthenberg R, Nurunberg P, et al. P097 A new locus for an autosomal recessive congenital muscular dystrophy without brain involvement maps to chromosome 7p21. *Eur J Paediatr Neurol.* (2009) 13(Suppl. 1):S51. doi: 10.1016/S1090-3798(09)70155-2
2. Willer T, Lee H, Lommel M, Yoshida-Moriguchi T, de Bernabe DB, Venzke D, et al. ISPD loss-of-function mutations disrupt dystroglycan O-mannosylation and cause Walker-Warburg syndrome. *Nat Genet.* (2012) 44:575–80. doi: 10.1038/ng.2252
3. Roscioli T, Kamsteeg EJ, Buysse K, Maystadt I, van Reeuwijk J, van den Elzen C, et al. Mutations in ISPD cause Walker-Warburg syndrome and defective glycosylation of α-dystroglycan. *Nat Genet.* (2012) 44:581–5. doi: 10.1038/ng.2253
4. Tasca G, Moro F, Aiello C, Cassandrini D, Fiorillo C, Bertini E, et al. Limb-girdle muscular dystrophy with alpha-dystroglycan deficiency and mutations in the ISPD gene. *Neurology.* (2013) 80:963–5. doi: 10.1212/WNL.0b013e3182840cbc
5. Cirak S, Foley AR, Herrmann R, Willer T, Yau S, Stevens E, et al. ISPD gene mutations are a common cause of congenital and limb-girdle muscular dystrophies. *Brain*. (2013) 136:269–81. doi: 10.1093/brain/aws312
6. Yang H, Yin F, Gan S, Pan Z, Xiao T, Kessi M, et al. The study of genetic susceptibility and mitochondrial dysfunction in mesial temporal lobe epilepsy. *Mol Neurobiol.* (2020) 57:3920–30. doi: 10.1007/s12035-020-01993-4
7. Richards S, Aziz N, Bale S, Bick D, Das S, Gastier-Foster J, et al. Standards and guidelines for the interpretation of sequence variants: a joint consensus recommendation of the American College of Medical Genetics and Genomics and the Association for Molecular Pathology. *Genet Med.* (2015) 17:405–24. doi: 10.1038/gim.2015.30
8. Song D, Fu X, Ge L, Chang X, Wei C, Liu J, et al. A splice site mutation c.1251G>A of ISPD gene is a common cause of congenital muscular dystrophy in Chinese patients. *Clin Genet.* (2020) 97:789–90. doi: 10.1111/cge.13695
9. Vuillaumier-Barrot S, Bouchet-Seraphin C, Chelbi M, Devisme L, Quentin S, Gazal S, et al. Identification of mutations in TMEM5 and ISPD as a cause of severe cobblestone lissencephaly. *Am J Hum Genet.* (2012) 91:1135–43. doi: 10.1016/j.ajhg.2012.10.009
10. Czeschik JC, Hehr U, Hartmann B, Lüdecke HJ, Rosenbaum T, Schweiger B, et al. 160 kb deletion in ISPD unmasking a recessive mutation in a patient with Walker-Warburg syndrome. *Eur J Med Genet.* (2013) 56:689–94. doi: 10.1016/j.ejmg.2013.09.014
11. Baranello G, Saredi S, Sansanelli S, Savadori P, Canioni E, Chipparini L, et al. A novel homozygous ISPD gene mutation causing phenotype variability in a consanguineous family. *Neuromuscul Disord.* (2015) 25:55–9. doi: 10.1016/j.nmd.2014.08.007
12. Trkova M, Krutilkova V, Smetanova D, Becvarova V, Hlavova E, Jencikova N, et al. ISPD gene homozygous deletion identified by SNP array confirms prenatal manifestation of Walker-Warburg syndrome. *Eur J Med Genet.* (2015) 58:372–5. doi: 10.1016/j.ejmg.2015.05.004
13. Sparks SE, Quijano-Roy S, Harper A, Rutkowski A, Gordon E, Hoffman EP, et al. Congenital muscular dystrophy overview - retired chapter, for historical reference only. (1993).
14. Alcantara-Ortigoza MA, Reyna-Fabian ME, Gonzalez-Del Angel A, Estandia-Ortega B, Bermúdez-López C, Cruz-Miranda GM, et al. Predominance of dystrophinopathy genotypes in mexican male patients presenting as muscular dystrophy with a normal multiplex polymerase chain reaction DMD gene result: a study including targeted next-generation sequencing. *Genes (Basel).* (2019) 10:856. doi: 10.3390/genes10110856
15. Vazquez-Cardenas NA, Ibarra-Hernandez F, Lopez-Hernandez LB, Escobar-Cedillo RE, Ruano-Calderón LA, Gómez-Díaz B, et al. Diagnosis and treatment with steroids for patients with Duchenne muscular dystrophy: experience and recommendations for Mexico. Administracion del Patrimonio de la Beneficencia Publica Asociacion de Distrofia Muscular de Occidente. *Rev Neurol.* (2013) 57:455–62. doi: 10.33588/rn.5710.2013380

Conflict of Interest: The authors declare that the research was conducted in the absence of any commercial or financial relationships that could be construed as a potential conflict of interest.

Publisher's Note: All claims expressed in this article are solely those of the authors and do not necessarily represent those of their affiliated organizations, or those of the publisher, the editors and the reviewers. Any product that may be evaluated in this article, or claim that may be made by its manufacturer, is not guaranteed or endorsed by the publisher.

frontiers in Pediatrics

ORIGINAL RESEARCH
published: 15 October 2021
doi: 10.3389/fped.2021.685497

Effect of Sirolimus on the Level of Peripheral Blood Lymphocyte Autophagy in Children With Systemic Lupus Erythematosus

*Xinliang Wang, Qingxiao Su, Zhiyan Dou, Xue Zhao, Naiqi Zhang, Bo Yu, Yuxue Wang and Zanhua Rong**

Department of Peadiatrics, The Second Hospital of HeBei Medical University, Shijiazhuang, China

Background: To observe the changes of autophagy-related protein levels in peripheral blood lymphocytes before and after sirolimus treatment in children with systemic lupus erythematosus (SLE).

Methods: Children with SLE were randomly divided into two groups, 28 in the traditional treatment group and 28 in the sirolimus group. Fifteen healthy children who were in the same period were collected as the normal control group. Clinical laboratory indexes, the percentage of routine lymphocytes, complement C3, complement C4, serum Anti-dsDNA and SLEDAI were detected.

Results: At 3 and 6 months after treatment, compared with the traditional treatment group, the percentage of routine lymphocytes in the sirolimus group increased ($P = 0.03$), SLEDAI score and positive rate of Anti-dsDNA decreased ($P = 0.01$). Compared with normal children, the expression of microtubule-associated protein 1 light chain 3 (LC3) protein in peripheral blood lymphocytes was significantly higher ($P = 0.006$); peripheral blood expression of P62/SQSTM1 (sequestosome 1) protein in lymphocytes decreased ($P = 0.02$).

Conclusion: Sirolimus can play a role in the treatment of systemic lupus erythematosus by regulating the level of autophagy.

Keywords: sirolimus, systemic lupus erythematosus, peripheral blood lymphocyte, autophagy, children

OPEN ACCESS

Edited by:
Oliver Semler, University Hospital of Cologne, Germany

Reviewed by:
Claudia Bracaglia, IRCCS Ospedale Pediatrico Bambino Gesù, Italy
Laurence Magder, University of Maryland, Baltimore, United States

****Correspondence:***
Zanhua Rong
rongzh_2021@21cn.com

Specialty section:
This article was submitted to Pediatric Immunology, a section of the journal Frontiers in Pediatrics

Received: *25 March 2021*
Accepted: *08 September 2021*
Published: *15 October 2021*

Citation:
Wang X, Su Q, Dou Z, Zhao X, Zhang N, Yu B, Wang Y and Rong Z (2021) Effect of Sirolimus on the Level of Peripheral Blood Lymphocyte Autophagy in Children With Systemic Lupus Erythematosus. Front. Pediatr. 9:685497. doi: 10.3389/fped.2021.685497

INTRODUCTION

Systemic lupus erythematosus (SLE) is an autoimmune disease with disordered immune system regulation. Autophagy refers to the process of using lysosomes to remove or reuse damaged organelles and metabolites in the cell under the conditions of starvation, hypoxia, infection, stress, etc. to help the cell maintain an effective energy cycle (1–5).

SLE patients have autophagy in the peripheral blood mononuclear cells, and the expression of Beclin-1 and LC3 mRNA is significantly higher than normal (6, 7). LC3 and p62/SQSTM1 (sequestosome 1) are often used as markers to detect autophagy. The study found that autophagy is associated with B lymphocytes in SLE patients. After comparing SLE patients with normal people, it was found that autophagy-related markers in B lymphocytes increased significantly. In the early stage of the onset of SLE, the LC3 expression level of lymphocytes was significantly increased,

the autophagy of B lymphocytes was excessively activated, a large number of autophagosomes appeared, and there was a positive correlation change with the disease activity of SLE (8). At the same time, the number of autophagosomes in T lymphocytes of SLE patients was also found to be higher than that of normal people, indicating that the upregulation of autophagy may be involved in the process of T lymphocyte differentiation, survival and function. Therefore, it is speculated that the incidence of systemic lupus erythematosus is related to the abnormality of lymphocyte autophagy.

Sirolimus is a mammalian target of rapamycin (mTOR) inhibitor, which exerts immunosuppressive function by acting on the mTOR pathway. The mTOR pathway plays a key role in inducing autophagy (9, 10). With the continuous understanding of the pathogenesis of rheumatic immune diseases and the mechanism of sirolimus, sirolimus, as a new, powerful and low-toxic macrolide immunosuppressive drug, is gradually recognized and familiarized by clinicians. And more and more are used in clinical treatment of rheumatic immune diseases. This experiment explores the relationship between autophagy and the onset of SLE, hoping to bring new ideas to the diagnosis and treatment of SLE.

TABLE 1 | Patients' characteristics.

Factor	Traditional treatment ($n = 28$)	Sirolimus ($n = 28$)	Normal control ($n = 15$)
Recipient age (*y*)	13 ± 1.5	13.4 ± 1.4	11.8 ± 2.4
Gender (male:female)	3:25	2:26	2:13
Fever	19	20	–
Asthenia	5	4	–
weight loss	4	3	–
Hypertension	8	11	–
Rash	24	23	–
light sensitivity	10	12	–
Mouth ulcers	8	7	–
Alopecia	11	9	–
24 h urinary protein ≥ 0.5 g/24 h	20	19	–
White blood cell count $< 4.0 \times 10^9$/L	9	10	–
Platelet count $<100 \times 10^9$/L	6	8	–
Hemoglobin <100 g/L	7	9	–
IgG (g/L) quartile	19 [14.25–25.75]	18 [14.25–24.75]	–
Anti-nuclear antibody	28	28	–

METHODS

Materials

Clinical Data

The data is collected from children diagnosed with SLE (56 cases) who were admitted to the pediatric outpatient and inpatient of the Second Hospital of Hebei Medical University from December 2016 to June 2018, and the diagnosis was in accordance with the SLE classification standard (11) revised by the American College of Rheumatology (ACR) in 1997 or the SLE classification standard revised by the ACR/Systemic Lupus International Collaborating Clinic (SLICC) in 2009 (12). Children with SLE who were not treated with sirolimus, hormones or other immunosuppressive agents before enrollment were randomly divided into two groups, the traditional treatment group and the combined sirolimus group (hereinafter referred to as sirolimus group), with 28 cases in each group. The traditional treatment group was composed of 3 males and 25 females with an average age of 13 ± 1.5 years (range 10–15), and the sirolimus group was composed of 2 males and 26 females with an average age of 13.4 ± 1.4 years (range 11–16). And 15 healthy children who were treated in the growth and development clinic of our hospital during the same period were selected as the normal control group, with an average age of 11.8 ± 2.4 years (range 8–15, male/female:2/13), as shown in **Table 1**. Clinical data and experimental data of children with SLE before and after treatment were collected and the SLEDAI score was calculated according to the systemic lupus erythematosus disease activity index (SLEDAI) (13).

Randomization

Randomization will be performed by an independent statistician using a randomization assignment procedure to generate a randomization sequence and randomly assign patients into two groups in a 1:1 ratio. The participant assignment table will be kept by an independent statistician until the end of the study.

Grouping Standards

Test Group

1) Twenty Eight cases in the traditional treatment group (Group A): oral prednisone 1 mg/kg/d, mycophenolate mofetil 600mg/m^2/bid, and the dosage was adjusted in the follow-up clinic.
2) Twenty Eight cases in the sirolimus group (Group B), oral drug: sirolimus capsule (specification 0.5 mg/capsule, manufacturer: North China Pharmaceutical Co., Ltd., approval number: National Pharmaceutical Standard H20100079) 1 mg/m^2/d, at the same time oral prednisone 1 mg/kg/d, mycophenolate mofetil 600 mg/m^2/bid, and the dosage was adjusted in the follow-up clinic.

Normal Control Group (Group C)

Fifteen healthy children who were treated in the growth and development clinic of our hospital during the same period were selected as the control group. Medical ethics were observed and permission from the children's guardians was obtained.

Exclusion Criteria

1) At the same time suffering from other autoimmune diseases, such as Sjogren syndrome, juvenile idiopathic arthritis, autoimmune liver disease, etc.;
2) At the same time suffering from other chronic diseases, such as parathyroid disease, diabetes, hypertension, acute and chronic infections or tumors;
3) Receive sirolimus, hormone and immunosuppressive therapy at least 6 months before enrollment;

4) Allergic reactions to the therapeutic drugs involved in the experiment.

Collection and Collation of Clinical Data

The collected contents include percentage of blood routine lymphocytes, complement C3, complement C4, serum Anti-dsDNA, triglyceride, total cholesterol and disease activity assessment (SLEDAI) of the enrolled children. After obtaining the children's guardians' informed consent, fill it out in the specified uniform format.

Experimental Reagents

Human peripheral blood lymphocyte separation solution (Tianjin Haoyang Biological Products Technology Co., Ltd.), Coomassie Brilliant Blue Protein Analysis Kit (Nanjing Jiancheng Bioengineering Research Institute), horseradish enzyme-labeled goat anti-rabbit IgG (imported packaging by Beijing Zhongshan Jinqiao Company), DAB coloring kit (imported packaging by Beijing Zhongshan Jinqiao Company), pre-stained protein molecular weight markers (American Thermo Scientific Company), PVDF membrane (Millipore Inc. USA), ECL enhanced chemiluminescence kit (Beijing TIANGEN Company), rabbit anti-actin polyclonal antibody (Proteintech, USA).

Experimental Equipment

DZ5-WS centrifuge (Shanghai Luxiangyi Centrifuge Instrument Co., Ltd.), high-pressure desktop sterilizer (Sai Strontium Krypton Shanghai Trading Co., Ltd.), fluorescence microscope (Beijing Shangguang Instrument Co., Ltd.), ultra-low temperature refrigerator (Qingdao Haier), vertical electrophoresis tank (Bio-Rad, USA), transfer electrophoresis (Bio-Rad, USA), transfer electrophoresis tank (Bio-Rad, USA), Odyssey FC imager (Li-COR Biosciences, USA), pressure steam sterilizer (Medical Equipment Factory of Boxun Industrial Co., Ltd.).

RESEARCH METHODS

Observation Indicators

Western blotting was used to detect the expression of LC3 and P62 in peripheral blood lymphocytes of children with SLE. Immunofluorescence was used to detect the expression of LC3 and P62.

Specimen Collection and Preparation

Peripheral blood lymphocyte protein collection: Collect 5 ml of fasting peripheral blood (venous blood) from the morning, use EDTA for anticoagulation, and isolate lymphocytes within 3 h by "human peripheral blood lymphocyte separation fluid." Add 500 ul of cell lysate to a 15 ml centrifuge tube containing lymphocytes, place it in a refrigerator at 4°C or on ice for 30 min, then transfer the supernatant to an EP tube and centrifuge (4°C, 12,000 rpm, 20 min) to extract the supernatant and obtain cellular proteins. Place the collected cellular proteins in the refrigerator at −80°C for later use. Or add a loading buffer to the protein sample solution according to the ratio of 100 ul lysate plus 20 μl 6X loading buffer, and denature the protein sample at high temperature (95°C, 5 min) and store at −20°C for later use.

Detection Methods

Human Peripheral Blood Lymphocyte Isolation

Use "Human Peripheral Blood Lymphocyte Separation Solution" to separate lymphocytes and follow the steps in the "Human Peripheral Blood Lymphocyte Separation Solution Instructions" (Tianjin Haoyang Biological Products Technology Co., Ltd.). The operation is carried out under the condition of 18–22°C.

Coomassie Brilliant Blue Reagent Method for Protein Quantification

Set blank tube, standard tube and sample tube in the experiment. Add 3 ml of Coomassie Blue Diluent to each tube, mix, let stand for 10 min, and then test under an ultraviolet spectrophotometer. The blank tube is reset to zero, and the absorbance value of the standard tube and the sample of each tube is measured separately. The protein sample concentration (mg/ml) = sample absorbance value/standard protein absorbance value × standard protein concentration.

Immunoblotting to Detect Protein Expression Levels

Primary antibodies include LC3 (1:1,000 dilution in 1% BSA), P62 (1:1,000 dilution in 1% BSA), β-actin (1:1,000 dilution in 1% BSA). The secondary antibody is horseradish peroxidase-labeled goat anti-rabbit or mouse IgG secondary antibody (diluted 1:5,000 in 1% BSA solution).

Cell Immunofluorescence Steps

1) Centrifuge the collected lymphocytes and add them to the slides and fix with 4% paraformaldehyde for 30 min.
2) Wash with PBS, 5 min/time, 3 times, Triton-100 (1:100) perforated, room temperature for 30 min.
3) Wash with PBS, 5 min/time, 3 times, block goat serum and incubate at 37°C for 30 min.
4) Add primary antibody and overnight at 4°C.
5) Re-warm for 30 min the next day, wash with PBS, 5 min/time, wash 3 times.
6) Add biomarker goat anti-rabbit IgG secondary antibody to the membrane and incubate at 37°C for 2 h.
7) Wash with PBS, 5 min/time, 3 times, stain with DAPI and seal for 30 min.
8) Observe and photograph the fluorescence result under a fluorescence microscope.

Formation of Autophagy Using GFP-LC3 Fusion Protein and GFP-P62 Fusion Protein Under the Fluorescent Microscope

The observation of the formation of autophagosomes under an electron microscope takes a long time, which is not conducive to the monitoring of autophagy. LC3 is a homolog of the yeast autophagy gene (Atg8) in mammals. People developed this technology by making use of the aggregation phenomenon that occurred during the autophagy of microtubule-associated protein 1 light chain 3 (LC3). This technology can be combined with a green fluorescent protein (GFP) to form GFP-LC3

TABLE 2 | Changes in clinical laboratory indicators at the end of 3 and 6 months in the traditional treatment group and sirolimus group.

	Traditional treatment group ($n = 28$)			Sirolimus group ($n = 28$)		
	0 month	3 months	6 months	0 month	3 months	6 months
Percentage of lymphocytes	13.91 ± 3.37	21.46 ± 2.64*	23.40 ± 4.46	13.97 ± 3.49	26.41 ± 3.58*#	41.36 ± 6.27#
SLEDAI	11.26 ± 3.49	9.46 ± 1.92*	4.53 ± 2.32	11.33 ± 2.46	6.26 ± 2.25*#	1.73 ± 1.48#
negative rate of anti-dsDNA	0 (0%)	4 (14.2%)	9 (32.1%)	0 (0%)	10 (36%)#	22 (78.6%)#
Positive rate of anti-dsDNA	28 (100%)	24 (85.8%)	19 (67.9%)	28 (100%)	18 (64.3%)#	6 (21.4%)#
Complement C3	0.62 ± 0.13	0.99 ± 0.15*	1.23 ± 0.10	0.66 ± 0.13	1.02 ± 0.19*	1.24 ± 0.22
Complement C4	0.08 ± 0.03	0.18 ± 0.04*	0.20 ± 0.05	0.10 ± 0.03	0.19 ± 0.05*	0.21 ± 0.06
Triglycerides	1.93 ± 0.63	2.03 ± 0.56*	2.94 ± 0.96	1.86 ± 0.66	2.41 ± 0.94*	2.99 ± 1.01
Total cholesterol	4.08 ± 1.22	4.87 ± 1.79*	4.99 ± 1.72	3.99 ± 1.03	4.52 ± 1.44*	5.17 ± 1.89
24 h urinary protein ≥ 0.5 g/24 h	20	0	0	19	0	0
White blood cell count < 4.0×10^9/L	9	4	1	10	5	2
Platelet count <100×10^9/L	6	0	0	8	0	0
Hemoglobin <100 g/L	7	1	0	9	3	1
IgG (g/L) quartile	20 [17–28]	14 [10–16]	9.9 [8.55–10.85]	18 [17–25]	16 [14–19]	14 [9.325–17.00]
Anti-nuclear antibody	28	26	25	28	25	25

*Compared with SLE before treatment, *P < 0.05; Compared with the traditional treatment group, #P < 0.05.*

to detect autophagosomes. When there is no autophagy, the GFP-LC3 fusion protein is dispersed in the cytoplasm; when autophagy occurs, the GFP-LC3 fusion protein is translocated to the autophagosome membrane, and multiple bright green fluorescent spots (puneta) are formed under a fluorescent microscope. A fluorescent spot is equivalent to an autophagosome, and the activity of autophagy can be evaluated by counting the fluorescent spots. P62 protein accumulates in the cytoplasm when autophagy is deficient, and is transferred to lysosomes for degradation when autophagy is activated. Therefore, the autophagy activity can be evaluated by counting the GFP-P62 in the cytoplasm.

STATISTICAL PROCESSING

SPSS22.0 statistical software was used for statistical processing. The normal distribution data was represented by mean ± standard deviation ($\bar{x} \pm s$). The comparison of the mean was by one-way analysis of variance and LSD-t (Least Significant Different-t) test; A repeated measurement analysis of variance was performed to compare the differences in clinical laboratory indicators at different time points before, during and after the interventions. the comparison between groups was by Mann-Whitney Test and count data using χ^2 test. $P < 0.05$ indicated statistical significance, and $P < 0.01$ were considered highly significant.

RESULTS

Changes of Clinical Laboratory Indexes in Children With Systemic Lupus Erythematosus

1) Compared with the traditional treatment group, the percentage of blood routine lymphocytes increased at the end of 3 months of treatment in the sirolimus group, which was statistically significant ($P = 0.03$). The percentage of blood routine lymphocytes increased at the end of 6 months of treatment, and the difference was statistically significant ($P = 0.002$) (see **Table 2**).
2) Compared with the traditional treatment group, the sirolimus group had a decrease in SLEDAI score at the end of 3 months of treatment, and the difference was statistically significant ($P = 0.01$). At the end of 6 months of treatment, the SLEDAI scores decreased, and the difference was statistically significant ($P = 0.001$). And the positive rate of Anti-dsDNA decreased at the end of 3 and 6 months of treatment, which was statistically significant compared with the traditional treatment group ($P = 0.02$) (see **Table 2**).
3) Comparing the sirolimus group with the traditional treatment group, complement C3, complement C4 triglyceride, and total cholesterol increased at the end of 3 months of treatment, and the difference was not statistically significant ($P = 0.08$). At the end of 6 months of treatment, complement C3, complement C4, triglyceride, and total cholesterol were increased, and the difference was not statistically significant ($P = 0.1$). (see **Table 2**).
4) Compared with before treatment, experimental indicators such as 24 h urinary protein ≥ 0.5 g/24 h and White blood cell count < 4.0 × 109/L in both groups were improved after treatment (see **Table 2**). As for side effects, one child in the Sirolimus group had transient nausea and abdominal pain on the 2nd day after oral administration.

Changes in Autophagy-Related Protein Levels

1) Compare the SLE group (Fifteen patients were randomly selected from the Traditional treatment group and the Sirolimus group and combined as the pre-treatment SLE

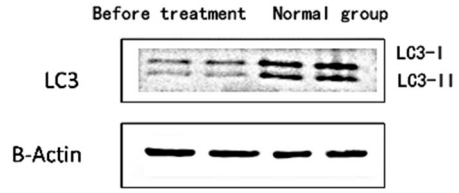

FIGURE 1 | The expression level of LC3 protein in peripheral blood lymphocytes of children with systemic lupus erythematosus and normal healthy children. Protein levels of LC3 I and LC3 II were detected by western blot analysis. Two columns on the left: before treatment; two columns on the right: normal children, β-Actin was used as the internal control for normalization.

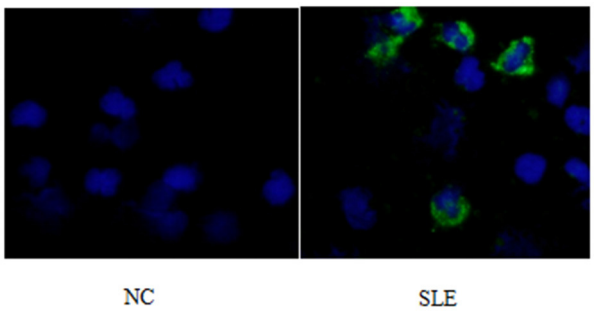

FIGURE 2 | LC3 immunofluorescence staining results of peripheral blood lymphocytes in systemic lupus erythematosus group and normal children (NC) before treatment. Left, NC; Right, SLE.

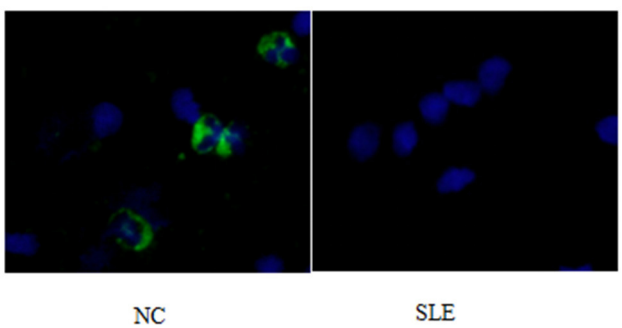

FIGURE 3 | P62 immunofluorescence staining results of peripheral blood lymphocytes in systemic lupus erythematosus group and normal children (NC) before treatment. Left, NC; Right, SLE.

group) before treatment with the normal children, the expression of LC3 protein in peripheral blood lymphocytes increased, with statistical significance ([0.3686 ± 0.0832] vs. [0.5175 ± 0.0721], $t = -5.428$, $P = 0.0003$); the expression of P62 protein in peripheral blood lymphocytes decreased, with statistical significance ([0.6005 ± 0.089] vs. [0.4965 ± 0.0731], $t = 3.456$, $P = 0.001$). Immunofluorescence was consistent with Western blotting results (see **Figures 1**–**3** and **Table 3**).

TABLE 3 | LC3 and P62 expression levels in peripheral blood lymphocytes of normal children (C), pre-treatment SEL (SLE), traditional treatment at the end of 6 months (A), sirolimus treatment at the end of 6 months (B) ($\bar{x} \pm s$).

Group	*n*	LC3 relative expression	p62 relative expression
Normal group	15	0.3686 686.0832	0.6005 005.0890
SLE	30	0.5175 175.0721	0.4965 965.0730
Traditional treatment group	28	0.5097 097.0911*	0.4942 942.0688*
Sirolimus group	28	0.6485 485.1314*#	0.4028 028.0765*#

*Compared with SLE before treatment, *P < 0.05; Compared with the traditional treatment group, #P < 0.05.*

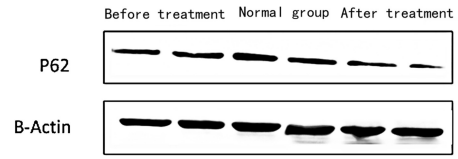

FIGURE 4 | The expression of P62 in peripheral blood lymphocytes of children with SEL in the traditional treatment group at the end of 6 months and in the sirolimus group at the end of 6 months and before treatment. Two columns on the left: traditional treatment group; two columns on the middle: before treatment, two columns on the right: sirolimus group, β-Actin was used as the internal control for normalization.

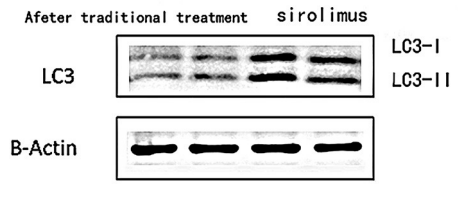

FIGURE 5 | The expression of LC3 in peripheral blood lymphocytes in the traditional treatment group and sirolimus group at the end of 6 months. Two columns on the left: traditional treatment group; two columns on the right: sirolimus group, β-Actin was used as the internal control for normalization.

2) Compare the SLE group before treatment with the traditional treatment group after 6 months of treatment, there was no significant difference in the expression of LC3 protein in peripheral blood lymphocytes, which was not statistically significant ([0.5175 ± 0.0721] vs. [0.5097 ± 0.0911], $t = 0.445$, $P = 0.2$). There was no significant difference in the expression of P62 protein in peripheral blood lymphocytes, which was not statistically significant ([0.4965 ± 0.0731] vs. [0.4942 ± 0.0688], $t = 0.086$, $P = 0.4$). Immunofluorescence was consistent with Western blotting results (see **Figure 4** and **Table 3**).
3) Compare the sirolimus group with the traditional treatment group after 6 months of treatment, the sirolimus group

showed increased expression of LC3 protein in peripheral blood lymphocytes, which was statistically significant ([0.6485 ± 0.1314] vs. [0.5097 ± 0.0911], $t = -3.245$, $P = 0.003$); the expression of P62 protein in peripheral blood lymphocytes decreased, with statistical significance ([0.4028 ± 0.0765] vs. [0.4942 ± 0.0688], $t = 3.068$, $P = 0.005$). Immunofluorescence was consistent with Western blotting results (see **Figure 5** and **Table 3**).

DISCUSSION

Abnormalities or regulatory disturbances in the process of autophagy are considered to be one of the main causes of abnormalities in the immune system of patients with systemic lupus erythematosus in recent years, and are closely related to the differentiation, proliferation and function of innate and adaptive immune cells. Obstruction of the autophagy process will lead to the untimely removal of dead cells, and the cleaning-up of DNA and RNA in the cells, and the long-term survival of T lymphocytes and B lymphocytes will be affected. As shown in **Figures 1**–**3**, compared with normal children, the level of autophagy in peripheral blood lymphocytes in children with systemic lupus erythematosus was significantly increased, as shown in **Table 2** for quantitative analysis of autophagy-related proteins, and compared with normal children, the increase of peripheral blood lymphocyte autophagy-related protein expression in children with systemic lupus erythematosus has statistical significance, indicating that abnormal autophagy is involved in the pathogenesis of systemic lupus erythematosus.

In systemic lupus erythematosus, the inappropriate activation and presence of T lymphocytes and B lymphocytes are very important factors that lead to the infiltration of multiple organ inflammatory factors and the continuous production of autoantibodies. Animal model studies have found that the survival rate of B lymphocytes in mice with the autophagy gene ATG7 knocked out is reduced, and B lymphocytes cannot effectively differentiate into plasma cells, indicating that autophagy activation can promote the survival and normal function of B lymphocytes. In addition, the density of freshly isolated mitochondria in B-lymphocytes of mice with the autophagy gene ATG7 knocked out was significantly higher than that in the control group. This study showed that impairment of mitochondrial clearance leads to the reduced survival rate of B lymphocytes. On the contrary, by promoting autophagy, it can effectively clear mitochondria, improve the survival of B lymphocytes, and contribute to its normal function. T lymphocytes in patients with systemic lupus erythematosus also have many abnormalities, including abnormal activation of T lymphocytes and prolonged survival of T lymphocytes. In the T lymphocytes of patients with systemic lupus erythematosus, the mTOR pathway is activated. Activation of the mTOR pathway can lead to lupus activity and recurrence, and sirolimus as an effective mTOR pathway inhibitor can effectively reduce disease activity, as shown in **Table 2**, at the end of 3 and 6 months of treatment, the sirolimus group showed a more significant decrease in SLEDAI than the traditional treatment group, and the anti-dsDNA positive rate was lower. It can be seen that the PI3K/Akt/mTOR pathway is generally activated under the pathological condition of lupus, which promotes the abnormal activation of T lymphocytes to a certain extent. A recent study analyzed LC3 conversion rate as an indicator of T lymphocyte autophagy activity in mouse models of lupus and human lupus patients (14). Most current studies suggest that autophagy is more likely to occur in systemic lupus erythematosus. Increased levels of LC3 in cells reflect the formation or accumulation of autophagosomes. Studies have found that compared with healthy people, patients with systemic lupus erythematosus have significantly higher levels of lymphocyte autophagy. Clarke et al. (7) also found that in the lymphocytes of patients with systemic lupus erythematosus, the level of autophagy was significantly higher than that of the normal control, which was consistent with the results of this test. In this study, sirolimus was used to treat children with systemic lupus erythematosus at the end of June to collect peripheral blood extracted lymphocytes to detect the expression of autophagy-related proteins. After treatment with sirolimus, the level of lymphocyte autophagy is greater than that in children with systemic lupus erythematosus than in healthy children and greater than that in the traditional treatment group. Combined with the clinical indicators of children in the same period as shown in **Table 2**, the SLEDAI decrease in the sirolimus treatment group at the end of June was significantly higher than that in the traditional treatment group, and the percentage of lymphocytes showed an increase compared to the traditional treatment group. As shown in **Table 2** the complement C3 and complement C4 shown in the two groups of children showed an increase, but there was no significant difference, and further analysis was needed for long-term observation. The increased autophagy level after sirolimus treatment may be due to increased autophagy induction or blocked autophagy pathway, but at this time the increase in autophagy level may just reset the autophagy disorder so that the homeostasis of the cell is re-established, as a result, patients recover from the disease. Comprehensive analysis of the research results and general conclusions of previous scholars at home and abroad leads to questions of whether the mTOR signaling pathway in lymphocytes of patients with systemic lupus erythematosus is not mainly involved in regulating the level of autophagy in lymphocytes, whether there is a regulatory defect in the mTOR signaling pathway in lymphocytes of patients with systemic lupus erythematosus, and whether there are more important signaling pathways involved in the regulation of lymphocyte autophagy in patients with systemic lupus erythematosus? The specific mechanism needs to be further studied.

There is also an in-depth study on the changes of peripheral blood T and B lymphocyte autophagy levels in patients with systemic lupus erythematosus before and after treatment with hormones and immunosuppressive agents. It was found that the autophagy level of T lymphocytes increased at the time of onset and decreased after treatment, and the level of autophagy was positively correlated with the SLEDAI score, while the level of autophagy of B lymphocytes decreased at the time of onset, and recovered after treatment, and was positively correlated with the complement level, and there was no correlation with

SLEDAI or serum Anti-dsDNA antibody titers (15). As shown in **Table 2**, the sirolimus treatment group is more effective than the traditional treatment group, but the autophagy level is not related to the clinical complement level, SLEDAI score, and Anti-dsDNA antibody level. It may be because peripheral blood mononuclear cells are known to contain multiple cell types, but this study did not further extract and classify lymphocytes, study the autophagy level of each type of cell separately, and how the autophagy level changes after treatment. These are the shortcomings of this test, which may lead to deviations in the results and need to be improved in future research.

The mechanism of autophagy involved in the pathogenesis of systemic lupus erythematosus also includes defects in the process of autophagy, which may cause the DNA and RNA in damaged or dead cells to be effectively degraded and reused, thus providing a permanent source of antigen. Pathological processes such as excessive production of type interferon (IFN) and the clearance obstacles of circulating immune complexes may involve autophagy defects. Theoretically, there may be a lot of invalid autophagy in the increase of autophagy level under pathological conditions. It is speculated that invalid autophagy can lead to the accumulation of damaged mitochondria and damaged or dead cells. Whether directly or after the formation of antigen-antibody complexes, a large number of DNA/RNA protein complexes of damaged or dead cells are involved in the destruction of self-tolerance and the initiation of autoimmune reactions, activating the innate immune system, which leads to the production of inflammatory cytokines. Therefore, after using sirolimus, the enhanced autophagy level measured in the test is shown in **Figures 4**, **5**, which may enhance the effective autophagy level, effectively remove damaged mitochondria and damaged or dead cells, effectively suppress the source of self-antigens, and reduce the production of autoantibodies and the production of inflammatory cytokines.

Although there has been a lot of research at home and abroad, the mechanism that causes the systemic lupus erythematosus to reduce its innate immune autophagy activity and increase the lymphocyte autophagy activity is still unclear, but the presence of disorder in the signal pathways involved in the regulation of lymphocyte proliferation, differentiation has been c determined to exist. The earliest guess and research about the involvement of autophagy in the pathogenesis of systemic lupus erythematosus is based on animal models and clinical treatments. Drugs for treating systemic lupus erythematosus, such as glucocorticoids, hydroxychloroquine, and sirolimus, all belong to mTOR inhibitors, which have beneficial effects. The comprehensive analysis found that the treatment of systemic lupus erythematosus focuses on resetting the flux of autophagy and keeping autophagy in a balanced state to regulate the growth and differentiation of body cells, so as to achieve the purpose of maintaining cell homeostasis.

In this experiment, we combined the clinical laboratory results to observe the efficacy of sirolimus in the treatment of systemic lupus erythematosus. For the 28 patients with systemic lupus erythematosus, after treatment with sirolimus, the percentage of lymphocytes increased, SLEDAI decreased, Anti-dsDNA positive rate decreased statistically, compared with the traditional treatment group. Complement levels increased, but there was no difference from the results of the traditional treatment group. Dyslipidemia is a common complication of GC treatment in children with systemic lupus erythematosus. As shown in **Table 2**, the changes in triglyceride and total cholesterol levels were observed. The application of sirolimus did not aggravate the occurrence of dyslipidemia. However, one child in the sirolimus group developed transient nausea with abdominal pain on the 2nd day after oral administration, symptom was mild, spontaneous remission did not recur, and the child was not withdrawn from the study.

This study also has some limitations. First of all, due to the small sample size, possible result bias and short observation time, the effect of mTOR inhibitors on the long-term prognosis of SLE was not observed in this study. Secondly, limited time to observe the clinical efficacy and side effects of the drug, and the lack of double-blind randomized controlled studies, which is the deficiency of this experiment. In the future, we will need more molecular biology, genomics, animal model tests, etc. to explore in detail the study of autophagy and its related pathways in the pathogenesis of systemic lupus erythematosus, as well as a larger sample of clinical trials to observe the efficacy and side effects of Sirolimus.

In conclusion, the pathogenesis of systemic lupus erythematosus is related to abnormal levels of peripheral blood lymphocyte autophagy. Compared with traditional treatment, sirolimus can increase the level of autophagy in peripheral blood lymphocytes, indicating that it may play a role in the treatment of systemic lupus erythematosus by regulating the level of autophagy. Compared with traditional treatment, sirolimus has faster recovery of clinical laboratory indicators, higher recovery percentage, and more significant effect.

DATA AVAILABILITY STATEMENT

The raw data supporting the conclusions of this article will be made available by the authors, without undue reservation.

ETHICS STATEMENT

The studies involving human participants were reviewed and approved by the Ethics Committee of Second Hospital of HeBei Medical University. Written informed consent to participate in this study was provided by the participants' legal guardian/next of kin.

AUTHOR CONTRIBUTIONS

XW and QS conceived of the study. ZD, XZ, and NZ participated in its design and coordination. BY, YW, and ZR helped to draft the manuscript. All authors read and approved the final manuscript.

REFERENCES

1. Wu Q, Gao C, Wang H, Zhang X, Li Q, Gu Z, et al. Mdivi-1 alleviates blood-brain barrier disruption and cell death in experimental traumatic brain injury by mitigating autophagy dysfunction and mitophagy activation. *Int J Biochem Cell Biol*. (2018) 94:44–55. doi: 10.1016/j.biocel.2017.11.007
2. Takahama M, Akira S, Saitoh T. Autophagy limits activation of the inflammasomes. *Immunol Rev*. (2018) 281:62–73. doi: 10.1111/imr.12613
3. Gatica D, Lahiri V, Klionsky DJ. Cargo recognition and degradation by selective autophagy. *Nat Cell Biol*. (2018) 20:233–42. doi: 10.1038/s41556-018-0037-z
4. Galluzzi L, Baehrecke EH, Ballabio A, Boya P, Bravo-San Pedro JM, Cecconi F, et al. Molecular definitions of autophagy and related processes. *EMBO J*. (2017) 36:1811–36. doi: 10.15252/embj.201796697
5. Kroemer G. Autophagy: a druggable process that is deregulated in aging and human disease. *J Clin Invest*. (2015) 125:1–4. doi: 10.1172/JCI78652
6. Zhou XJ, Lu XL, Lv JC, Yang HZ, Qin LX, Zhao MH, et al. Genetic association of PRDM1-ATG5 intergenic region and autophagy with systemic lupus erythematosus in a Chinese population. *Ann Rheum Dis*. (2011) 70:1330–7. doi: 10.1136/ard.2010.140111
7. Clarke AJ, Ellinghaus U, Cortini A, Stranks A, Simon AK, Botto M, et al. Autophagy is activated in systemic lupus erythema-tosus and required for plasmablast development. *Ann Rheum Dis*. (2015) 74:912–20. doi: 10.1136/annrheumdis-2013-204343
8. Bernard NJ. Connective tissue diseases: how do autoreactive B cells survive in SLE–autophagy? *Nat Rev Rheumatol*. (2014) 10:128. doi: 10.1038/nrrheum.2014.5
9. Kraig E, Linehan LA, Liang H, Romo TQ, Liu Q, Wu Y, et al. A randomized control trial to establish the feasibility and safety of rapamycin treatment in an older human cohort: immunological, physical performance, and cognitive effects. *Exp Gerontol*. (2018) 105:53–69. doi: 10.1016/j.exger.2017.12.026
10. Ozturk N, Ozturk D, Pala-Kara Z, Kaptan E, Sancar-Bas S, Ozsoy N, et al. The immune system as a chronotoxicity target of the anticancer mTOR inhibitor everolimus. *Chronobiol Int*. (2018) 35:705–18. doi: 10.1080/07420528.2018.1432632
11. Hochberg MC. Updating the American College of Rheumatology revised criteria forthe classification of systemic lupus erythematosus. *Arthritis Rheum*. (1997) 40:1725. doi: 10.1002/art.1780400928
12. Petri M, Orbai AM, Alarcón GS, Gordon C, Merrill JT, Fortin PR, et al. Derivation and validation of the systemic lupus international collaborating clinics classification criteria for systemic lupus erythematosus. *Arthritis Rheum*. (2012) 64:2677–86. doi: 10.1002/art.34473
13. Bombardier C, Gladman DD, Urowitz MB, Caron D, Chang CH. Derivation of the SLEDAI. A disease activity index for lupus patients. The Committee on Prognosis Studies in SLE. *Arthritis Rheum*. (1992) 35:630–40. doi: 10.1002/art.1780350606
14. Gros F, Arnold J, Page N, Décossas M, Korganow AS, Martin T, et al. Macroautophagy is deregulated in murine and human lupus T lymphocytes. *Autophagy*. (2012) 8:1113–23. doi: 10.4161/auto.20275
15. Chen YW, Wang C, Wang XG. Autophagy level of peripheral blood T and B cells in patients with systemic lupus erythematosus and its clinical significance. *Chin J Immunol*. (2015) 31:1380–38. doi: 10.3969/j.issn.1000-484X.2015.10.018

Conflict of Interest: The authors declare that the research was conducted in the absence of any commercial or financial relationships that could be construed as a potential conflict of interest.

Advantages of publishing in Frontiers

OPEN ACCESS
Articles are free to read for greatest visibility and readership

FAST PUBLICATION
Around 90 days from submission to decision

HIGH QUALITY PEER-REVIEW
Rigorous, collaborative, and constructive peer-review

TRANSPARENT PEER-REVIEW
Editors and reviewers acknowledged by name on published articles

Frontiers
Avenue du Tribunal-Fédéral 34
1005 Lausanne | Switzerland

Visit us: www.frontiersin.org
Contact us: frontiersin.org/about/contact

REPRODUCIBILITY OF RESEARCH
Support open data and methods to enhance research reproducibility

DIGITAL PUBLISHING
Articles designed for optimal readership across devices

FOLLOW US
@frontiersin

IMPACT METRICS
Advanced article metrics track visibility across digital media

EXTENSIVE PROMOTION
Marketing and promotion of impactful research

LOOP RESEARCH NETWORK
Our network increases your article's readership